Robert G. Maliva

Aquifer Characterization Techniques

Schlumberger Methods in Water Resources Evaluation Series No. 4

Schlumberger
Water Services

Springer

Springer Hydrogeology

The Springer Hydrogeology series seeks to publish a broad portfolio of scientific books, aiming at researchers, students, and everyone interested in hydrogeology. The series includes peer-reviewed monographs, edited volumes, textbooks, and conference proceedings. It covers the entire area of hydrogeology including, but not limited to, Isotope Hydrology, Groundwater models, Water Resources and Systems, and related subjects.

More information about this series at http://www.springer.com/series/10174

Robert G. Maliva

Aquifer Characterization Techniques

Schlumberger Methods in Water Resources
Evaluation Series No. 4

Robert G. Maliva
Schlumberger Water Services
Fort Myers, FL
USA

Preface

This book is an outgrowth of an investigation of the state of the art in aquifer characterization techniques. The focus is on what is possible and practical from an applied perspective. The word 'practical' is stressed in that the aquifer characterization and modeling approaches selected for a given project must be accommodated by project budgets and time frames. Leading-edge technologies developed in academia and government research laboratories are often not viable for applied projects, such as the assessment of a contaminated site, design of a managed aquifer recharge system, or impact assessment of proposed wellfield, because of their time requirements, costs, or the local unavailability of required specialized equipment and expertise. In the applied realm, the overriding objective is cost-effective solutions not technical wizardry. However, technologies are transferred into the applied realm to the extent that they are demonstrated to provide value by, for example, providing higher-quality data at a competitive cost to other more conventional options. For example, advanced borehole geophysical logs (e.g., nuclear magnetic resonance) developed for the oil and gas industry are relatively expensive to run, but can be justified for projects in which data are needed on fine-scale aquifer heterogeneity because they can provide detailed data on porosity and permeability at often a lesser cost than a coring program.

The objective is to have full toolbox of technologies available from which aquifer characterization tools are selected as appropriate for a given project. It is, therefore, incumbent on groundwater professionals to be familiar with all the available aquifer characterization tools, the types of information they provide, and their underlying assumptions and limitations. The goal of this book is to provide an overview of aquifer characterization techniques, focusing on aquifers in sediments and sedimentary rock. A brief primer on aquifer types, hydraulics, and heterogeneity is first provided. Next are chapters on the sedimentology and diagenesis of siliciclastic and carbonate aquifers, focusing on how they related to aquifer heterogeneity. The greatest part of the part of the book is a review of aquifer characterization technologies that are appropriate and have been used for the characterization of sedimentary aquifers. Finally, methods are presented as to how

the various data can be analyzed, processed, and incorporated into groundwater flow and solute-transport models.

In light of the enormous groundwater literature, any book on aquifer characterization must necessarily be cursory. Indeed, entire dedicated books have been written on the subjects of some chapters. Numerous references are, therefore, provided to key publications to allow the reader to further investigate each topic. It is important to recognize that some aquifer characterization techniques require a high level of technical expertise to properly perform and process the data, which necessitates inclusion of specialists in project teams. Practical experience can be invaluable towards insuring project success.

A state-of-the-art review is necessarily a snapshot of the technologies and methods available at one point in time. It is expected that with continued rapid development in the field, many new techniques will be developed and enter the applied hydrogeology realm.

Acknowledgments

Contents

About the Author

Dr. Robert G. Maliva has been a consulting hydrogeologist since 1992 and is currently a Principal Hydrogeologist with Schlumberger Water Services USA Inc. He is currently based in Fort Myers, Florida. Dr. Maliva specializes in groundwater resources development including alternative water supply, managed aquifer recharge, and desalination projects.

Robert G. Maliva completed his Ph.D. in Geology at Harvard University in 1988. He also has a masters degree from Indiana University (Bloomington) and a BA in Geological Sciences and Biological Sciences from the State University of New York at Binghamton. Upon completion of his doctorate degree, Dr. Maliva has held research positions in the Department of Earth Sciences at the University of Cambridge, England, and the Rosenstiel School of Marine and Atmospheric Science of the University of Miami, Florida. He grew up in New York City and attended Stuyvesant High School in Manhattan.

Dr. Maliva has also managed or performed numerous other types of water resources and hydrologic investigations including contamination assessments, environmental site assessments, water supply investigations, wellfield designs, and alternative water supply investigations. He has maintained his research interests and completed studies on such diverse topics Precambrian silica diagenesis, aquifer heterogeneity, precipitates in landfill leachate systems, carbonate diagenesis, and various aspects of the geology of Florida. Dr. Maliva gives frequent technical presentations and has numerous peer-reviewed papers and conference proceedings publications on ASR and injection well and water supply issues, hydrogeology, and carbonate geology and diagenesis. He coauthored the books, Aquifer Storage and Recovery and Managed Aquifer Recharge Using Wells: Planning, Hydrogeology, Design, and Operation and Arid Lands Water Evaluation and Management.

Chapter 1
Aquifer Characterization and Properties

Aquifer characterization is broadly defined as processes by which the three-dimensional structure, hydraulic and transport properties, and chemistry of aquifers are evaluated. Aquifer characterization provides the foundation for groundwater modeling, which is ubiquitously used to evaluate sedimentary aquifers. Detailed aquifer characterization is particularly important where solute transport is a concern, as aquifer heterogeneity has a much greater impact on groundwater flow direction and rates than it does on aquifer heads. An introduction to aquifer hydraulic and transport parameters and basic aquifer heterogeneity concepts is provided. Aquifer heterogeneity includes layered, lateral, and multiple-porosity systems. Aquifer characterization starts with an initial conceptual geological model development, followed by evaluations of the type and scale of aquifer heterogeneity and the values of petrophysical and hydraulic parameters, and finally, data analysis and synthesis, and groundwater flow and solute-transport modeling.

1.1 Introduction

Scarcity of freshwater is a serious challenge now facing many parts of the world. Water scarcity is expected to increase in the future because of the increasing demands associated with population growth and economic development. Climate change may also contribute to local water scarcity through changes in precipitation amounts and patterns and increased evapotranspiration. Fresh groundwater is a critical resource because of its often good quality, year-round availability, and oftentimes, location near areas of demand. In many places, fresh groundwater resources are being either depleted or contaminated (or both) as a result of over-pumping and other anthropogenic activities. Hitherto, unutilized brackish aquifers are also increasingly being turned to raw water sources for desalination systems and as storage zones for aquifer storage and recovery (ASR) systems. It is clear that

better management of groundwater resources is required in order to obtain the maximum value from these assets and to ensure that their use is sustainable.

Numerical groundwater modeling has become the fundamental tool for evaluating groundwater resources. The development of a variety of robust, efficient, and flexible model codes and user-friendly graphical user interfaces (GUIs), along with the exponential growth of computational power, has resulted in numerical modeling becoming an essential element in most groundwater investigations. Groundwater models are used to develop an understanding of historical and current conditions and to predict the response of aquifers to future stresses, which could be groundwater pumping, operation of groundwater remediation and aquifer recharge systems, and changes in natural recharge rates caused by climate change. However, the ability of a groundwater model to accurately simulate past, present, and future conditions depends upon the appropriateness of the underlying conceptual model of the groundwater system and the values of the aquifer hydraulic, transport, and water quality parameters incorporated into the model. The distribution of hydraulic conductivity, in particular, is critical for modeling groundwater flow and solute transport, but is a nontrivial parameter to measure directly. Direct measurements of hydraulic conductivity are often sparsely distributed or at an inappropriate scale for modeling the processes of interest (Slater 2007). Stochastic (probabilistic) modeling has been proposed as a means for addressing uncertainty in modeling caused by inadequacies in available hydrogeological data, but stochastic modeling, paradoxically, often has a greater data requirement than the traditional deterministic modeling approach (Phillips et al. 1989). Effective groundwater management thus requires a greater amount and quality of data on aquifer properties.

Aquifer characterization is analogous to reservoir characterization in the oil and gas industry, whose goal is to describe the spatial distribution of petrophysical properties (e.g., permeability and porosity) in three-dimensional space (Lucia 1995). Hydraulic conductivity, and its related parameters permeability and transmissivity, is of greatest importance in aquifer characterization because they both exert primary control on groundwater flow, and their values vary by many orders of magnitude in aquifer systems.

All aquifers are heterogeneous to some degree. Aquifer heterogeneity means that properties, such as hydraulic conductivity, spatially vary within a geologic formation. Heterogeneity occurs both within and between beds. Anisotropy refers to the condition where properties vary with direction. A fundamental question is how to best deal with this heterogeneous reality as we attempt to develop quantitative descriptions of flow in large-scale aquifer systems (Gelhar 1986). Heterogeneity occurs at various scales, and heterogeneities of different scales are often superimposed upon one another. A basic concern in aquifer characterization and groundwater modeling is deciding upon the degree to which aquifer heterogeneity needs to be considered in a given project and which approach or methods are most appropriate for characterizing the heterogeneity and incorporating it into groundwater models.

On a larger scale, aquifer heterogeneity in the form of high transmissivity flow zones can have a profound effect on regional groundwater flow, by affecting the flow rates and the magnitude and position of recharge and discharge zones (Freeze and Witherspoon

1966). On a smaller scale, aquifer heterogeneity can be the primary control on the direction and rate of solute transport, such as the migration of contaminants from their source area. Aquifer heterogeneity is also the primary cause of the spreading (dispersion) of solutes. Molz et al. (1983) observed that in modeling dispersion phenomena, it appears that a greater emphasis should be placed on field study and accurate determination of hydraulic conductivity variations and other inhomogeneities.

A key observation is that head variations due to aquifer heterogeneity tend to be small, whereas variations in velocity and travel time tend to be large (Poeter and Gaylord 1990; de Marsily et al. 2005). Groundwater models that closely reproduce hydraulic heads may lack detail to adequately stimulate fluid flow and solute transport (e.g., Fogg 1986). Projects involving the transport of contaminants and other solutes and particulate matter, in general, require a much greater understanding of aquifer heterogeneity than projects investigating only groundwater flow. For example, many remediation programs that rely on pumping contaminated water or injecting amendments may not be optimally working because of the reliance on inferior estimates of hydraulic conductivity and, more importantly, the lack of knowledge on site-specific heterogeneity that can influence contaminant transport (Berg and Illman 2013). Overarching lessons from several comprehensive and intensely monitored field laboratories are that aquifer heterogeneity is ever present, heterogeneity strongly influences contaminant plume evolution, and detailed and expensive site characterization may be required for reliable solute-transport models (Konikow 2011). Similarly, some ASR systems have failed or underperformed because of extreme aquifer heterogeneity that dominates the local groundwater flow and the mixing and movement of stored waters (Maliva and Missimer 2010).

Collection of more data does not necessarily result in an improved aquifer characterization. Feazel et al. (2004) observed that increasing the amount of data is not always better; it may just change the bias. Each of the elements of an aquifer characterization program should be capable of cost-effectively addressing the data need of a project. Correct use of data can have a greater impact than collecting more data. With respect to uncertainty analysis in hydrocarbon reservoirs, Ma (2011) observed that three basic questions need to be answered:

- How much do we need to know?
- How much can we know?
- How much should we try to know?

These questions integrate the value of information (VOI) with the cost of information (COI) paradigm. Further investigation is warranted, from an economic perspective, when the VOI is greater than the COI (Ma 2011). VOI, in turn, ties into risk, which is defined as the product of the probability of an adverse result and the consequences of an adverse result. Quantification of VOI is inherently difficult, but it is usually qualitatively understood that projects that involve greater risks require more thorough aquifer characterizations. High-risk projects include those in which a failed system could potentially cause great harm (e.g., underground nuclear waste depositories) or those in which failure to achieve performance targets could have

great economic consequences. The VOI thus includes the benefit of potentially avoiding adverse impacts resulting from having inadequate information.

Extensive data collection programs can lead to the charge that investigations have become 'science projects' in the sense that data are being collected for academic reasons beyond project requirements. Hence, it is important to have (and be able to convey) a complete understanding of project-specific data needs and the VOI of each element of an aquifer characterization program towards meeting those specific needs. Selection of the elements of aquifer characterization programs should consider their quality of information, reliability (i.e., likelihood they will provide the required data at a suitable accuracy), cost, and the local availability of technical resources.

1.2   Hydraulic Aquifer Types

An aquifer was defined by the U.S. Geological Survey (Lohman et al. 1972) as a

> formation, group of formations, or part of a formation that contains sufficient saturated permeable material to yield significant quantities of water to wells and springs.

Strata with distinctly lower hydraulic conductivity that are stratigraphically adjacent to aquifers are referred to as confining units and semiconfining units. Confining units or beds, which are also referred to as 'aquicludes', are strata that are impermeable in that they do not transmit significant quantities of water. Semiconfining units or beds, which are also referred to as 'aquitards', are strata that retard, but do not prevent, the flow of water to or from an adjacent aquifer. A semiconfining unit is considered to be a leaky confining unit.

The above definitions suffer from their imprecision. Strata with given hydraulic properties may be defined as either aquifers or semiconfining units depending upon circumstances, particularly the properties of adjacent units. The term 'significant' is subjective as there is no widely accepted quantitative threshold as to how much water a formation or part of a formation has to yield in order for it to be considered an aquifer. The significance of a water yield value is also tied to economics. A shallowly buried formation that can economically provide sufficient water to meet low-density, local household demands using self-supply wells would meet the criterion of significant yield. On the contrary, the same strata buried 1,000 m below land surface would not meet the criterion of significant yield because high well construction costs would make its use economically unviable. From an aquifer characterization perspective, the categorization or naming of strata is not especially relevant so long as the properties of the strata are adequately determined and modeled.

Aquifers differ in their degree of confinement and their relationship to the regional water table. There has been some variation in the terminology used for aquifer types. The main categories of aquifers in current use are unconfined, confined, and semiconfined (Fig. 1.1). Unconfined aquifers, which are also referred to as water-table aquifers, are characterized by their upper boundary being the water table. The water table is technically defined as the surface in a ground-water body
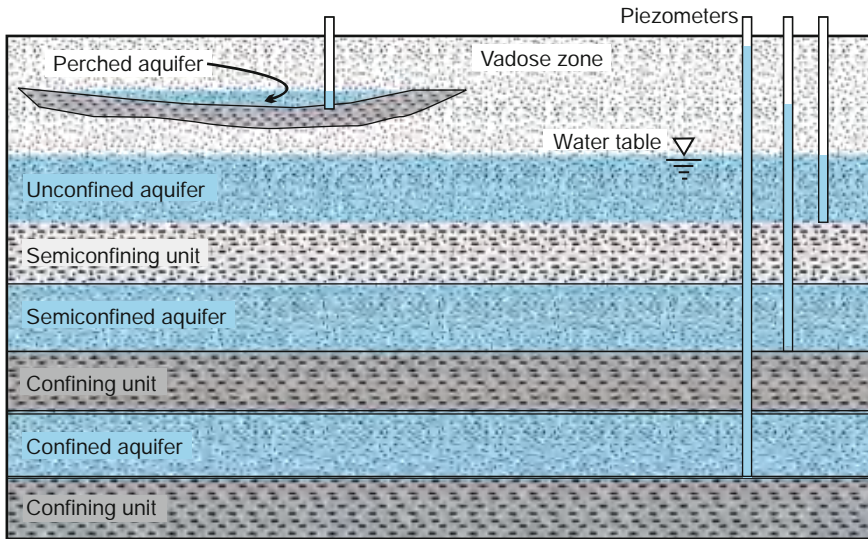
Fig. 1.1 Conceptual diagram of the main aquifer types and the relationship of their potentiometric surface elevations to the water table. The potentiometric surface of semiconfined and confined aquifers may be positioned alternatively below the water table, particularly where the aquifers are heavily exploited

that is at atmospheric pressure. The water table is the level at which water stands in wells that penetrate the water body just far enough to hold standing water (Lohman et al. 1972). The water table is commonly referred to as the upper boundary of the saturated zone, but this definition is technically incorrect because a capillary fringe that is fully saturated, but under lesser than atmospheric pressure, may be present above the water table. The water table is located at the base of the capillary fringe rather than its top. Groundwater is produced from unconfined aquifers largely by the drainage (dewatering) of water from pore spaces.

Potentiometric surface, which is defined by the levels at which water will rise in tightly cased wells, approximately corresponds to the water table in unconfined aquifers. The potentiometric surface elevation may vary from the water table in wells that penetrate greater depths in unconfined aquifers (not just the top), if an upward or downward component to groundwater flow exists (Lohman et al. 1972; Lohman 1979). Most unconfined aquifers fall into the 'semi-unconfined' type of Kruseman and de Ridder (1970) in that there is some natural degree of variation in sediment properties that creates a disparity in the flow of water between the vertical and horizontal directions. For example, the presence of clay-rich strata may substantially reduce the vertical hydraulic conductivity of an aquifer, creating a significant anisotropy ratio in hydraulic conductivity (horizontal hydraulic conductivity divided by vertical hydraulic conductivity), which can impact groundwater flow and solute transport.

In areas where the water table is located a large distance below land surface, permanent or temporary perched aquifers may occur. Perched groundwater is

unconfined groundwater separated from an underlying body of groundwater by an unsaturated zone. The top of a perched aquifer is a perched water table (Lohman et al. 1972), whose elevation is higher than that of the regional water table. Perched aquifers commonly occur where the regional water table is deep and low hydraulic conductivity strata are present that prevent or greatly retard the percolation of water to the regional water table.

Confined aquifers, by definition, are bounded above and below by essentially impervious confining units. The potentiometric surface of confined aquifers occurs above the top of the aquifer. Confined aquifers are also referred to as 'artesian' aquifers. Where wells flow naturally at land surface, the aquifers are referred to as flowing artesian aquifers. Water is produced from confined aquifers by the expansion of water and compression of the aquifer. The potentiometric surface in a confined aquifer during pumping continuously declines and does not reach an equilibrium condition.

A confined aquifer is an idealized end-member whose characteristic hydraulic conditions are rarely met, although they may be approached in some aquifers. Typically, 'confining' strata are not completely impermeable. In addition, some water may be produced from confining strata. Most aquifers below the surficial unconfined aquifer are more accurately described as semiconfined or leaky aquifers. Some leakage of water occurs through the strata that overlie or underlie (or both) the aquifer. The degree of confinement is directly related to the vertical hydraulic conductivity and the thickness of the bounding semiconfining units. The characteristic hydraulic units for semiconfined aquifers are transmissivity, storativity, and leakance, which is defined as the vertical hydraulic conductivity of the confining units divided by their thickness. When a semiconfined aquifer is pumped, the potentiometric surface declines, which induces leakage into the aquifer. The rate of leakage into the pumped aquifer eventually comes into equilibrium with the pumping rate, and no further decline of the potentiometric surface occurs (Hantush and Jacob 1955; Hantush 1960; Walton 1960).

1.3 Lithologic Aquifer Types

The ultimate control over the hydraulic properties of aquifers is the textures and fabrics of the sediments and rocks that comprise the aquifer. The 'texture' of sediments and sedimentary rocks refers to the shape, size, and orientation of the particles that constitute the sediment or sedimentary rock. The term 'fabric' refers to the three-dimensional arrangement of the components of a sediment or rock, particularly how individual grains are in contact with each other and whether the particles show any preferred orientation. Sedimentary rocks (other than chemical precipitates) have four main components: grains, matrix, cement, and pores. Grains and matrix are particles that are differentiated by their relative grain size; grains are coarser particles (commonly sand-sized and coarser) and matrix consists of fine-grained, silt- and clay-sized material that occurs between or surrounds grains. Cement is mineral material that precipitates in voids in the rock. Pores are open spaces, which, in aquifers, form the network in which water is stored and flows. An

additional component of some sedimentary rocks is mineral crystals that replaced grains, matrix, or cements.

Sedimentary aquifers can be divided into two broad categories based on whether the aquifer is composed predominantly of siliciclastic or carbonate sediment or rock. However, some aquifers are composed of intermixed or interbedded siliciclastic and carbonate rock. Clastic sedimentary rocks are composed of fragments (clasts) of pre-existing rock. Siliciclastic sedimentary rocks are composed predominantly of clasts of silicate minerals, of which quartz and feldspar are usually most common. The matrix of fine-grained siliciclastic sediments and rock commonly contains various clays minerals (e.g., illite, montmorillonite, kaolinite, chlorite) and silt-sized quartz.

Carbonate rocks, as the name implies, are composed predominantly of carbonate minerals, of which calcite ($CaCO_3$) and dolomite ($CaMg(CO_3)_2$) are most abundant by far. Carbonate rocks may be either clastic, in that they are composed of fragments of pre-existing carbonate rock (e.g., intraclasts and extraclasts) or shell (bioclasts), or they may form from local inorganic or biologically mediated precipitation. An example of the latter is reefal rock. Siliciclastic and carbonate rock usually differ in their initial texture and fabric and chemical reactivity.

Carbonate sediments are much more reactive under near-surface physicochemical conditions and thus are prone to a variety of alteration, dissolution, and precipitation processes that can change their porosity and hydraulic conductivity. The depositional environments (facies) and characteristics of siliciclastic and carbonate aquifers are discussed in Chaps. 3 and 4.

1.4   Groundwater Hydraulics Basics

Numerous introductory and advanced textbooks are available that provide solid introductions to basic groundwater hydraulics. Aquifers are hydraulically characterized by their ability to transmit water, which is quantified by their hydraulic conductivity and transmissivity, and to store water, which is expressed by their storativity. Groundwater flow velocity and solute transport are also controlled by effective porosity and dispersivity values. Bulk aquifer properties are often sufficient to evaluate the water level or pressure response of an aquifer to pumping. Accurate modeling of solute transport requires consideration of the spatial variations in aquifer parameters (i.e., aquifer heterogeneity).

1.4.1   Darcy's Law and Hydraulic Conductivity

The birth of quantitative hydrogeology can be traced to the publication in 1856 of Henry Darcy's famous text, "Les Fontaines Publiques de la Ville de Dijon" (The Public Fountains of the City of Dijon), which includes an equation relating the flow of water through a sand filter to the difference in water height and a coefficient that

depends on the permeability of the sand (Simmons 2008). Darcy's Law in one direction is generally expressed in differential form as

$$Q = -KA\left(\frac{dh}{dl}\right) \tag{1:1}$$

where
K   is a constant of proportionality referred to as 'hydraulic conductivity', which has the units of length over time (m/s)
Q   discharge (m^3/s)
dh/dl hydraulic gradient; change in head (h) with distance (l) (dimensionless)
A   the cross-sectional area of the flow path (m^2)

Discharge has the unit of volume over time. The specific discharge (q), which is the rate of flow through a unit cross-sectional area, has units of length over time. Specific discharge is obtained by dividing the discharge rate by the cross-sectional area

$$q = \frac{Q}{A} \tag{1:2}$$

Specific discharge is also referred to as Darcy velocity or Darcy flux. Although it has the unit of velocity (length/time), specific discharge is not equivalent to the actual flow velocity. Average linear flow velocity (v) is inversely proportional to effective porosity (n_e).

$$v = \frac{Q}{An_e} = \frac{q}{n_e} = -\frac{KA}{n_e}\left(\frac{dh}{dl}\right) \tag{1:3}$$

Effective porosity is the interconnected pore spaces through which water flows in a rock or sediment. Depending upon lithology, effective porosity may be significantly less than the total porosity. As porosity decreases, a correspondingly greater flow velocity is required for a given discharge rate (Q). Average linear velocity is important where solute transport and travel times and distances are of concern. For example, for a given hydraulic conductivity and hydraulic gradient, the travel time from a contamination source to a sensitive receptor will be shorter in rock that has a low effective porosity.

Hydraulic conductivity is an extrinsic property of a sediment or rock that depends upon the properties of the fluid. Permeability is an intrinsic property of a rock or sediment in that it is not dependent on other variables or conditions. The relationship between hydraulic conductivity (K) and intrinsic permeability (k) is

$$K = \frac{kqg}{l} \tag{1:4}$$

where
q density (kg/m^3)
g gravitation acceleration (9.807 m/s^2)
l dynamic viscosity (kg/(m s)

Dynamic viscosity is also expressed in units of Pascal-seconds (Pa s), which is equivalent to 1 kg m^{-1} s^{-1}, and in centipoise units (cP), which are equal to 1 × 10^{-3} kg/(m s). Permeability has unit of length squared, with the SI unit being m^2. The unit for permeability commonly used in the oil and gas industry is the millidarcy (mD), which is equivalent to 9.869 × 10^{-16} (≈1 × 10^{-15}) m^2 or 9.869 × 10^{-12} (≈1 × 10^{-11}) cm^2. At 20 °C, 1 D is equal to about 9.61 × 10^{-6} m/s (0.831 m/d).

In the groundwater field, hydraulic conductivity, rather than permeability, is normally used to quantify the ability of a material to conduct water because aquifers are usually a single-phase system, and the physical properties of water commonly have a low degree of variability within a given study area. However, the dynamic viscosity of water is sensitive to changes in temperature as expressed by the equation

$$l = 2.414 \times 10^{-5} \cdot 10^{\left(\frac{247.8}{T-140}\right)} \qquad (1.5)$$

where T is temperature in degree kelvin. For example, a decrease in temperature from 30 to 20°C results in an increase in dynamic viscosity of 25.6 %. The temperature effect on viscosity and hydraulic conductivity needs to be considered in systems in which there are significant temporal (e.g., seasonal) or spatial (e.g., depth-related) variations in temperature. The hydraulic conductivity of aquifers will be greater in the summer than in the winter. As a result, for example, infiltration rates into shallow aquifers will tend to be greatest in the summer. The temperature effect on viscosity, and thus hydraulic conductivity, may also be significant where cool water is injected into warm aquifers. Aquifer hydraulic conductivity (and transmissivity) values obtained by pumping tests under one temperature regime need to be temperature corrected if they are to be used to model the aquifer under different temperature conditions.

1.4.2 Transmissivity

Transmissivity (T) is defined as the volume of water that will flow through a unit width (e.g., 1 m or 1 ft) of the cross-sectional area of an aquifer under a unit hydraulic gradient. It is equivalent to the product of the average aquifer hydraulic conductivity (K′) and the aquifer thickness (b)

$$T = K'b \qquad (1.6)$$

For an aquifer divided into 'n' number of beds, the transmissivity calculated as

$$T = \sum_{i=1}^{n} K_i b_i \qquad\qquad (1{:}7)$$

where K_i and b_i are the thickness and average hydraulic conductivity of each bed. The standard units of transmissivity are length squared divided by time (m^2/d and ft^2/d). Transmissivity is also expressed in gallons per day per foot (gpd/ft), but this unit is now considered antiquated.

Transmissivity is a measure of the ability of an aquifer to transmit water. Higher transmissivities result in greater volumetric flow rates through an aquifer for a given hydraulic gradient. Aquifers with high transmissivities have lower drawdowns and injection pressures at a given pumping or injection rate. Transmissivity is a bulk property of aquifers that is typically measured by aquifer pumping tests (Chap. 7). Transmissivity is not directly related to the average linear flow velocity of water, which depends on the hydraulic conductivity and effective porosity of individual beds in the aquifer. As is the case for hydraulic conductivity, transmissivity is an extrinsic property of an aquifer and varies with temperature. In the unconfined aquifers, the reduction in the saturated thickness of an aquifer from drawdown during pumping results in a decrease in transmissivity. Thus, as unconfined aquifers are depleted, their transmissivity decreases and drawdown increases, even if pumping rates remain unchanged.

1.4.3   Storativity

Storativity (S) is defined as the volume of water that is released from a unit area of aquifer (e.g., 1 m^2) under a unit decline (e.g., 1 m) of hydraulic head. Storativity is thus a dimensionless parameter. Specific storage (S_s) is defined as the volume of water that is released from a unit volume of aquifer under a unit decline of hydraulic head. Specific storage has the units of the reciprocal length (e.g., m^{-1}). The storativity of a confined aquifer is the vertically integrated specific storage value, which for a homogeneous aquifer is the product of its specific storage and the thickness of the aquifer (b)

$$S = S_s b \qquad\qquad (1{:}8)$$

The storativity of unconfined aquifers is approximately equal to the specific yield (S_y), which is the amount of water that will gravitationally drain from a unit cross-sectional area of an aquifer per unit change in head. The water that is retained in the aquifer (i.e., does not drain) is referred to as specific retention (S_r). The sum of specific yield and specific retention is the total porosity of the rock or sediment.

The water released from storage in a confined aquifer by pumping is produced by a combination of compaction of the aquifer and expansion of the water, both of which are induced by a decrease in aquifer pore water pressure. The storativity values of confined aquifers, which are also referred to as their storage coefficients, are usually orders of magnitude less than the specific yields of the same rock or sediment types.

Specific yield is related to the effective (interconnected) porosity of the sediment or rock. The specific yield of porous granular sediments and rock are usually in the 0.05–0.4 range, whereas, storativity values are often on the order of 1×10^{-3} to 1×10^{-5}. Thus, a given drop in water level or pressure in an unconfined aquifer will result in the release of a much greater volume of water than in a confined aquifer. Similarly, a given rate of pumping will induce much greater drawdowns in a confined aquifer than in an unconfined aquifer. The rate of drawdown within a confined aquifer may decrease dramatically when the potentiometric surface falls below the top of an aquifer and the aquifer becomes unconfined.

The pressure response of aquifers to stresses (pumping or injection) is much more rapid than the rate of gravity drainage. Unconfined aquifers experience the delayed yield phenomenon in which the initial water production is largely from depressuring (similar to the case for confined aquifers), followed by production from drainage. In fine-grained sediments, the gravity drainage process can take months or years (Prill et al. 1965; Johnson 1967). Techniques used to measure specific yields are discussed in Sect. 14.3.

Storativity is an important parameter for transient simulations. Storativity is not relevant to steady-state simulations in which, by definition, hydraulic heads (water levels) are not changing. If hydraulic heads are not changing, then water is neither entering into or being released from storage.

1.4.4 Porosity and Permeability

Porosity is defined as the open space in a rock divided by the total rock volume. It is expressed as either a decimal fraction or as a percentage. Effective porosity consists of pore spaces that are connected and serve as the space through which water flows. Effective porosity excludes isolated pores and pore spaces occupied by water adsorbed on clay minerals or other grains. Effective porosity typically is less than total porosity and maybe only a small fraction of the total porosity in rocks in which most of the pores are not interconnected. Effective porosity is similar to, but not synonymous with, specific yield. Effective porosity relates to the flow of water in a saturated rock or sediment. Specific yield is related to the vertical drainage of water in what becomes unsaturated sediment or rock. The retained water includes capillary-bound water, in addition to water in isolated pores and adsorbed water.

Porosity can be subdivided into primary porosity and secondary porosity as described by Choquette and Pray (1970). Primary porosity is the original 'fabric' or pattern of pores that is present immediately after the sediments are deposited (Fig. 1.2). Primary porosity includes intergranular (interparticle) porosity, which is the space between the grains, and intragranular porosity, which is the pore spaces that occur within grains. The interior of a hollow shell (fossil) is an example of an intragranular pore.

Secondary porosity is pore space that forms after deposition, as sediments and rock undergo diagenesis. Diagenesis is defined as the physical, chemical, and biological

Fig. 1.2 Diagrams of
common pore type (yellow) in
sedimentary rock. Primary
pores are present in unaltered
sediments. Secondary pores
form after deposition as the
result of dissolution and
replacement processes.
Secondary pores may form
the dissolution of single
grains (moldic) or may be
much larger than the size of
grains (vuggy)

Primary Pore Types

Interparticle

Internal

Shelter

Secondary Pore Types

Moldic

Intercrystalline

Vuggy
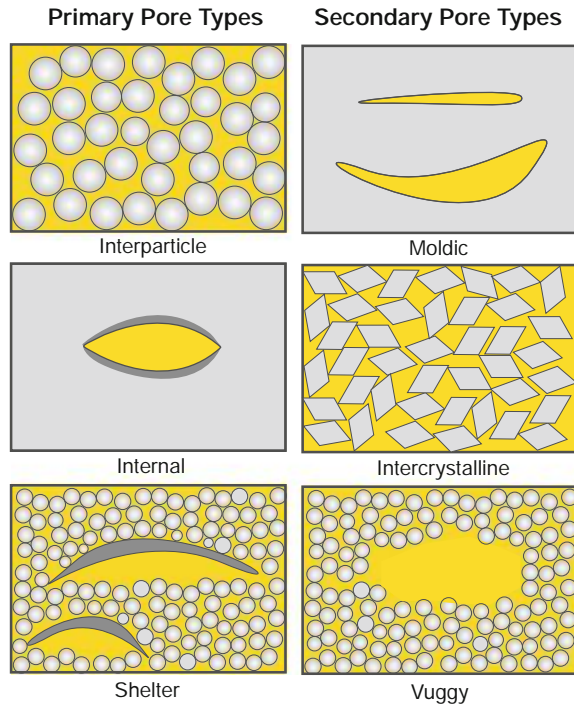
changes that take place in sediments and rock after they have been deposited, but before the rock enters the realm of metamorphism. The main diagenetic processes affecting porosity are mechanical compaction (consolidation), chemical compaction (intergranular pressure solution and stylolitization), dissolution, and cementation. Secondary pores include molds and vugs that are formed, respectively, by the dissolution of individual grains and larger volumes of rocks. Large secondary pores include fractures, which are tabular or more irregular pores that form by mechanical failure of rock, and conduits, which are elongated dissolution features that allow for the rapid (sometimes turbulent) flow of water. Intercrystalline porosity is the space present between crystals in a rock and is usually secondary.

The term 'matrix' is used in an aquifer hydraulic sense to denote the part of the aquifer that is not fracture or conduit porosity. The permeability of the matrix of sedimentary rocks is controlled by the characteristics of its porosity, which includes the total porosity, interconnected or effective porosity, pore size distribution, and pore-throat size distribution. A basic relationship in granular sediments and rocks (e.g., sands and sandstones) is that pore size, and thus permeability, generally increases as grain size increases (with consideration of sorting). Grain size distribution can be used to estimate the permeability and hydraulic conductivity of sediments (Sect. 9.5). Although permeability is correlated with grain and pore size, permeability is actually primarily controlled by the size of the pore throats that connect pores rather than the size of pores themselves. Pore throats are the

constrictions that connect adjoining pores through which water flows. Under a given pressure gradient, the diameter, length, and shape of the pore throats are the principal controls over water flow, as opposed to the size of the larger pores. As a generalization, fine-grained rocks have small pore sizes and, in turn, smaller diameter pore throats and lower permeabilities.

The porosity and permeability of sediments and sedimentary rocks are normally reduced through progressive burial due to compaction and cementation. Sediment types differ in their susceptibility to processes that result in reduction in porosity and hydraulic conductivity. Sediments composed of soft, clay-rich rock fragments may quickly lose nearly all of their effective porosity upon burial through mechanical compaction. Clean quartz sands, on the contrary, are much more resistant to mechanical compaction and usually lose porosity primarily through cementation.

1.4.5   Dispersivity

Hydrodynamic dispersion is the process by which solute 'particles' are spread out parallel and transverse to the direction of average fluid flow (Freeze and Cherry 1979). It includes two processes, molecular diffusion and mechanical dispersion. Molecular diffusion is velocity-independent flux of solute particles from areas of high to low concentrations. Mechanical dispersion is mixing caused by variations in fluid velocity. Variations in velocity are caused by (1) velocity differences within a pore due to drag exerted by the pore wall, (2) differences in pore sizes within the porous media, and (3) differences in length, branching, and interfingering of pore channels (i.e., tortuosity; Freeze and Cherry 1979).

The processes of molecular diffusion and mechanical dispersion cannot normally be separated in groundwater systems. Instead, the two parameters are combined into a single parameter called the hydrodynamic dispersion coefficient (D). There are actually three hydrodynamic dispersion coefficients based on the orientation with respect to the direction of groundwater flow. Longitudinal dispersion (D_L) occurs parallel to the direction of groundwater flow. Transverse or lateral dispersions (D_T) occurs perpendicular to the direction of flow on the horizontal plane, and vertical dispersion (D_V) occurs perpendicular to the direction of flow on the vertical plane.

Hydrodynamic dispersion coefficients are the sum of mechanical dispersion and coefficient of bulk diffusion (D^*), with the former being the product of the dispersivity value and average linear flow velocity in the principal direction of flow (t_i):

$$D_L = a_L t_i + D* \tag{1:9}$$

$$D_T = a_T t_i + D* \tag{1:10}$$

$$D_V = a_V t_i + D* \tag{1:11}$$

where a_L = the longitudinal dispersivity, a_T = the transverse dispersivity, and a_V = vertical dispersivity. Dispersivities have units of length (m or ft). Transverse and vertical dispersivities are typically an order of magnitude less than the longitudinal dispersivity.

From the above equations, it can be seen that hydrodynamic dispersion is dominated by diffusion as the flow velocity approaches zero. At high flow velocities, mechanical dispersion is the dominant process and diffusion can be ignored. The ratio of advective to diffusion transport is commonly expressed using the dimensionless Peclet number. Diffusion is generally insignificant relative to mechanical dispersion at flow rates of 1 m/yr or greater (Apello and Postma 2005).

Dispersivity is an important variable for solute transport, but has a high degree of uncertainty because it cannot be practically measured. Dispersivity values are also dependent upon scale, in addition to the geological material (Pickens and Grisak 1981; Molz et al. 1983; Gelhar 1986; Neumann 1990; Gelhar et al. 1992; Schulz-Makuch 2005). Scale refers to both the length of the flow path and to aquifer thickness. Full-aquifer dispersivity values are dependent upon the aquifer hydraulic conductivity distribution (i.e., degree of heterogeneity) and the effect and extent of transverse migration between layers in response to hydraulic and concentration gradients (Pickens and Grisak 1981). Variations in hydraulic conductivity between aquifer layers result in differences in tracer concentrations between juxtaposed layers, which cause increased dispersive and diffusive mixing.

In practice, dispersivity values used in models are usually initially estimated based on rock or sediment types. Dispersivity values needed to calibrate models depend upon the degree to which aquifer heterogeneity is incorporated into the model. If heterogeneity is not adequately represented, then erroneously large dispersivity values may be required for model calibration (Konikow 2011). The values are adjusted during the model calibration process, assuming there is a sufficient observational database. Dispersivity values can thus be considered to be a parameter that captures unmodeled features of a system (Barnett et al. 2012).

Solute-transport parameters are often evaluated by tracer testing (Chap. 13), which provides data on tracer concentrations versus time and location under controlled or closely monitored conditions. The best data on dispersion processes under natural conditions has come from tracer tests at massively instrumented (i.e., hundreds of observation point) test sites in Borden, Ontario (Canada; Freyburg 1986; Sudicky 1986), Cape Cod, Massachusetts (USA; Hess et al. 1992), and Columbus, Mississippi (USA; Adams and Gelhar 1992; Rehfeldt et al. 1992).

1.5 Aquifer Heterogeneity

1.5.1 Types and Scales of Aquifer Heterogeneity

Aquifer heterogeneity refers to spatial variation in hydraulic, transport, and geo-chemical properties within an aquifer system. The heterogeneity may be within or between beds (or both). Anisotropy refers to the condition where properties vary with direction. All aquifers are heterogeneous and the degree of heterogeneity varies with scale. A fundamental challenge in aquifer characterization is development of a data collection and modeling approach that captures the scale of heterogeneity relevant to a specific project. The ultimate relevant scale for petroleum reservoir and groundwater investigations is the practical size of the model grid blocks (Haldorsen 1986).

Aquifer heterogeneity can be caused by

- variations in the sediment composition and texture, such as grain size, shape, and sorting
- sediment composition
- depositional environment or facies
- diagenesis
- structural geological process.

Differences in permeability structure between depositional facies are primarily related to differing textures and bedding styles and enhancement of these hetero-geneities by diagenetic processes (Schatzinger and Tomtusa 1999).

Aquifer heterogeneity can be categorized in terms of its type and scale. An important type of heterogeneity in sedimentary aquifers is layered (i.e., interformational or stratigraphic), which is differences in aquifer properties between beds, bedsets, or formations. Layered heterogeneity occurs on multiple scales, and variations in properties may occur within a given layer. On a coarse scale, a stratigraphic succession may be divided into aquifer and (semi) confining strata, or an aquifer may be divided into several hydrostratigraphic zones with different transmissivities.

Intraformational heterogeneity refers to compositional and associated petrophysical variation within a given hydrostratigraphic unit. The heterogeneity may be the product of the three-dimensional interspersion of bodies of sediment or rock with different hydraulic properties within an aquifer or aquifer zone. Layered heterogeneity mainly refers to the variations in the properties in the vertical direction (between strata), whereas lateral heterogeneity mainly refers to the variations in the horizontal direction (within strata; Fig. 1.3). For investigations within a small geographic area (e.g., a contamination assessment of a gasoline service station site), a homogeneous 'layer cake' conceptualization may be sufficient, as strata may be continuous and may not have significant lateral variations in properties across the study site. As the scale of investigation increases, lateral heterogeneity becomes more important. In general, data on layered heterogeneity is more

Fig. 1.3 Conceptual diagram
of layered and lateral
heterogeneity. Lateral
heterogeneity may be due to
discontinuities of sediment
bodies or more gradual
changes in properties with an
aquifer layer. The data
requirements to characterize
lateral heterogeneity are much
greater than that needed for
layered heterogeneity

Layered heterogeneity

Medium K

High K

Low K

Lateral heterogeneity
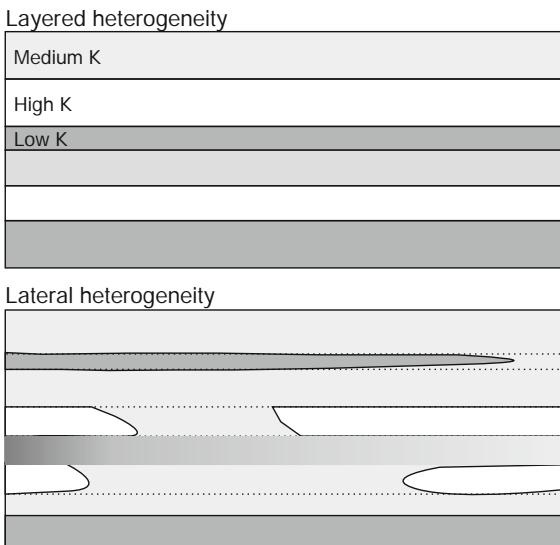
practicably obtainable, as it can be acquired from a single vertical well or borehole.
Evaluation of lateral heterogeneity is much more data intensive and, where con-
sidered, now commonly involves geostatistical methods (Chap. 20).

Dual-porosity or multiple-porosity conditions occur where a rock volume con-
tains more than one pore system with different properties. Typically, the rock
contains a matrix pore system, consisting of primary porosity modified by diage-
nesis to varying degrees, and a secondary pore system. The latter includes fractures
and solution conduits, which often have a high permeability relative to the matrix,
but make a very low contribution to the total porosity of the rock. Karstic lime-
stones (Fig. 1.4) are an extreme example of a dual-porosity system in which flow

Fig. 1.4 Karstic limestone
on Curacao. Secondary
porosity consists of isolated
vugs and larger continuous
conduits and caverns. The
tabular conduit (arrow) is
about 5 cm high

Table 1.1 Classification of aquifer heterogeneity scales

Scale	Description	Investigation methods
Microscopic	Scale of individual pores and sand grains	Thin section petrography
Mesoscopic	Scale of individual subfacies and bedding (e.g., bedsets within a point bar)	Conventional core plug, minipermeameter
Macroscopic	Heterogeneity on a sedimentary facies scale including stratification (e.g., individual point bar and lateral accretion units)	Borehole geophysical logs, drill stem/packer tests, slug tests
Megascopic	Scale of a wellfield and model grid blocks—addresses external geometric relationships of hydrostratigraphic units (e.g., meander belt)	Aquifer pumping tests
Gigascopic	Total formational or regional scale; scale of depositional systems and stratigraphic sequences	Multiple aquifer pumping tests, regional model calibration

may be dominated by caverns. Groundwater flow and solute transport are usually dominated by secondary porosity in karst systems, whereas the bulk of the water storage may occur in the matrix.

Aquifer heterogeneity can also be the result of structural geological features, such as folds and faults. The latter can result in a compartmentalization of an aquifer if the fault (fault gauge) acts as a permeability barrier or if displacement results in the juxtaposition of aquifer strata and confining strata. Faults and fracture zones may also be the loci of interformational groundwater flow. Dykes (dikes) are discordant, vertical or steeply dipping, tabular or sheet-like intruded bodies that cut across existing rocks. Depending on their properties, dykes can be barriers to groundwater flow.

Aquifer heterogeneity occurs at different scales and heterogeneities of different scales are often superimposed upon one another. Several classifications of heterogeneity scale have been proposed with some differences in definition between workers. A general scale classification is provided in Table 1.1, based on the categories proposed by Dagan (1986), Haldorsen (1986), and Galloway and Sharp (1998).

1.5.2   Anisotropy

Anisotropy in an aquifer is a directional difference in hydraulic conductivity or transmissivity. Stratified aquifers typically have large vertical (K_z) to horizontal (K_x) anisotropies because of differences in hydraulic conductivity between beds and finer-scale anisotropy within beds. Vertical to horizontal anisotropies, expressed as the K_z/K_x ratios are often 10 or greater and not uncommonly exceed 100. The effect of variations in hydraulic conductivity between beds on the K_z/K_x ratio of an aquifer is illustrated by a simple layered aquifer model (Fig. 1.5). For a given aquifer
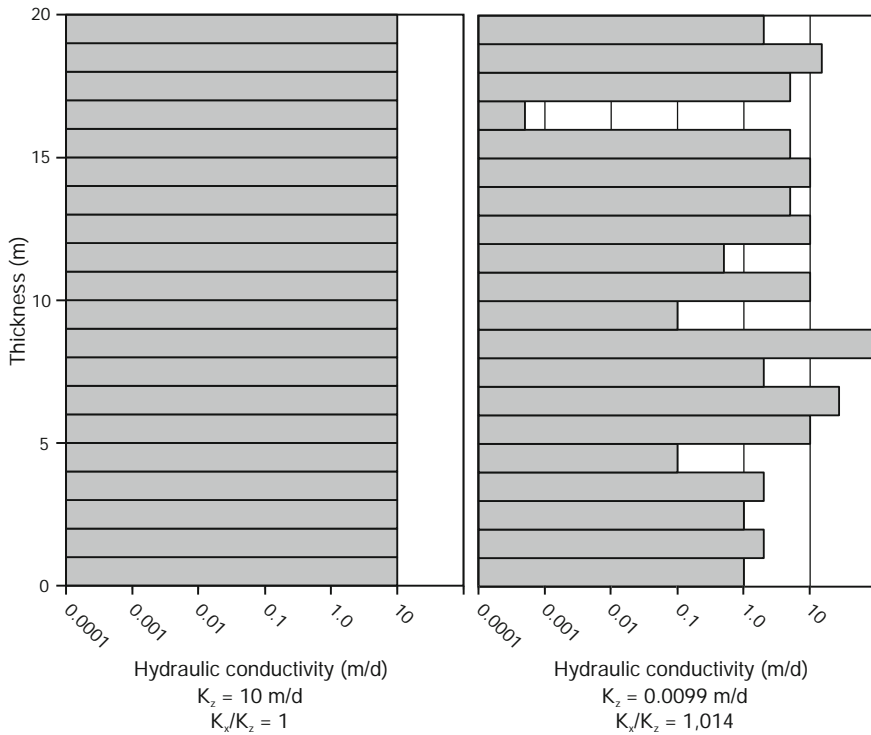
Fig. 1.5 Conceptual diagram comparing the equivalent vertical hydraulic conductivity (K_z) and anisotropy ratio (K_x/K_z) of a hypothetical homogeneous aquifer (left) and layered heterogeneous aquifer (right) that have the same transmissivity and average horizontal hydraulic conductivity

transmissivity, layered heterogeneity results in lower K_z values and higher anisotropy ratios.

The effective (average) horizontal and vertical hydraulic conductivity of a series of layers with a total thickness 'b' is calculated using the equations

$$K_x = \sum_{i=1}^{n} \frac{K_{xi}b_i}{b} \tag{1:12}$$

$$K_z = \frac{b}{\sum_{i=1}^{n}\left(\frac{b_i}{K_{zi}}\right)} \tag{1:13}$$

where b_i is thickness of layer 'i' and K_{xi} and K_{zi} are the horizontal and vertical hydraulic conductivity of layer 'i'. Effective horizontal hydraulic conductivity, and thus transmissivity, is controlled to a large degree by the most conductive beds, whereas, the effective vertical hydraulic conductivity is largely controlled by the vertical hydraulic conductivity of the least conductive beds. Indeed, studies have

shown that within aquitards, the greatest head decline may occur across a thin zone that provides most of the resistance to vertical flow (Bradbury et al. 2006). Vertical anisotropy thus is largely a function of the difference in hydraulic conductivity between the most and least conductive beds.

Horizontal anisotropy is directional differences in hydraulic conductivity within a bed or aquifer (i.e., K_x and K_y are not equal). There are multiple causes of horizontal anisotropy. Anisotropy can be due to deposition fabric such as the orientation and connectivity of relatively high permeability sediment bodies. For example, channel sand bodies (Sect. 3.2) usually have a preferred orientation parallel to the topographic slope at the time of deposition. The average hydraulic conductivity (and transmissivity) of the aquifer, thus, tends to be greatest in the general channel sand body direction and least perpendicular to the sand bodies. Fracturing can also cause horizontal anisotropy. If the fractures have high permeabilities, then the greatest aquifer transmissivity would be expected to occur parallel to the principal fracture direction.

Anisotropic aquifers are characterized with respect to transmissivity in terms of the principal directions (i.e., directions of maximum and minimum transmissivity) and the magnitude of anisotropy (ratio of maximum to minimum values). When a directional difference in hydraulic conductivity occurs, water will preferentially travel along the path with the least resistance (i.e., direction of higher conductivity). Anisotropy in the horizontal direction can cause the predominant flow direction to deviate from the direction of the hydraulic gradient.

Heterogeneity and anisotropy are related and both control groundwater flow and solute transport in addition to hydraulic gradients. In tracing contaminant pathways, the degree of contrast in hydraulic conductivity and the boundaries between discrete units determine whether or not the underlying geological structure constrains groundwater flow paths and, consequently, the location of greatest contaminant mass movement. As the contrast increases, the geological structure begins to exert more control on the paths and rates of fluid migration (Webb and Anderson 1996).

1.5.3   Connectivity

Interconnectedness of high-hydraulic conductivity units is of overriding importance in controlling groundwater flow and solute transport (Fogg 1986). For example, one or more well-connected sands, among a system of otherwise disconnected sands, can completely alter a groundwater flow velocity field (Ritzi et al. 1994). Isolated transmissive units, on the contrary, may be largely isolated from regional flow systems. However, significant transport connectivity may not require complete connection of all zones of relatively homogenous hydraulic conductivity (Bianchi et al. 2011). It has been documented that solutes can travel along preferential flow paths, leaking (jumping) from one hydraulic conductivity cluster to another, with transitions through low hydraulic conductivity zones (Bianchi et al. 2011).

Connectivity and associated aquifer heterogeneity also depend upon the presence and continuity of low-permeability strata. Laterally continuous, low-permeability strata (e.g., shale units) may vertically compartmentalize an aquifer. Boundary conditions between sedimentary rock units (packets) are important features in determining effective reservoir and aquifer characteristics. The effective permeability of sand packets, for example, will be determined largely by the lower permeabilities of the bounding units, which will control their ultimate through-flow capabilities (Pryor 1973).

Evaluation of connectivity is critical to quantifying heterogeneity for the purpose of hydrogeological investigations (Anderson 1997), and there is still the need to further develop and refine sedimentological techniques to identify and quantify connectivity among hydrofacies (Anderson et al. 1999). The challenge lies in extrapolating and interpolating one-dimensional facies or hydrofacies data from wells into a three-dimensional geological and numerical model (Webb and Anderson 1996).

1.6   Aquifer Characterization Approach

Aquifer characterization should start with an initial conceptual model of the groundwater system of interest. In the case of sedimentary aquifers, it is imperative to have a basic understanding of the geology and hydrogeology of the aquifer and confining strata including their depositional environment, main lithofacies and hydrofacies, and likely three-dimensional distribution. At this point in time, there are very few significant aquifers in the world in which at least some information on their geology is not available. Hence, all groundwater investigations should start with a literature review (i.e., desktop investigation). Insights into the likely degree, scale, and pattern of aquifer heterogeneity from the desktop investigation should then guide the development of a field data collection program whose purpose is to obtain additional data required for groundwater model development.

Aquifer characterization is a multi-step iterative process. The basic workflow includes four main elements as follows:

(1) conceptual geological model development
(2) evaluation of type and scale of aquifer heterogeneity
(3) petrophysical and hydraulic parameter evaluation
(4) data analysis and synthesis, and groundwater flow and solute-transport modeling

Aquifer characterization is an integrated process that involves feedback loops (Fogg 1989). It is also an iterative process in that simulation results may force a reevaluation of the conceptual model and flow and confining unit determinations, which may necessitate additional data collection and groundwater modeling.

The conceptual geologic model includes aspects of the study area such as aquifer boundaries, coarse-scale hydrostratigraphy (e.g., identification of aquifer and confining strata), identification of structural features that may affect groundwater flow

(e.g., folds, faults, fracture zones, stratal dip), and a general depositional model. Conceptual geological model development should start with data mining, which is a search for and a review of available information on the study area. The data may include published and unpublished reports by governmental agencies, academic researchers and consultants, geological and geophysical logs, well construction and testing reports, and other governmental databases.

The conceptual geological model should next be expanded upon to include an evaluation of type and scale of aquifer heterogeneity and its relevance to the project. The relevance of various types of aquifer heterogeneity depends upon project objectives. For example, bed-scale fracturing may not have to be explicitly considered in an investigation concerned only with groundwater flow and water levels, whereas it may have to be characterized and incorporated into models used to simulate local contaminant transport. For sedimentary aquifers, stratal architecture should be considered along with secondary porosity features that may affect groundwater flow. Stratal architecture may be investigated using geologic facies analysis and sequence stratigraphy. The evaluation of the type and scale of aquifer heterogeneity serves as a prelude to the field testing program by determining the data requirements for a project.

The petrophysical and hydraulic evaluation includes the actual field data collection, which is the primary focus of this book. A wide variety of tools are available that provide data on different scales. Professionals involved in projects need to choose the tools that can most effectively provide the required quantity and quality of data. It is necessary to understand the type of information a tool provides, its limitations, how obtained data are processed, and costs. The choice of aquifer characterization methods may also be constrained by the local availability of equipment and geological and borehole conditions.

The data analysis and groundwater flow and solute-transport task includes discretization and population of the model grid (deterministic and stochastic techniques) and performance of the actual simulations. Population of the model grid involves processing the data to the scale of the model grid (e.g., upscaling) and the extrapolation and interpolation of well data. Opportunities for improved aquifer characterization lie in the development and use of workflows that capture all of the available information and integrate it into numerical groundwater models. Finally, post-audits should be performed to evaluate the accuracy of model predictions. If a groundwater model proves to provide erroneous predictions, then the underlying conceptual model should be reevaluated.

References

Adams, E. E., & Gelhar, L.W. (1992) Field study of dispersion in a heterogeneous aquifer. 2. Spatial moment analysis. Water Resources Research, 28, 3293–3307.

Anderson, M. P. (1997) Characteriztion of geological heterogeneity. In G. Dagan, & S. P. Neuman (Eds.), Subsurface Flow and Transport: A Stochastic Approach (pp. 23–43). Cambridge: Cambridge University Press.

Anderson, M. P., Aiken, J. S., Webb, E. K., & Mickelson, D. M. (1999) Sedimentology and hydrogeology of two braided stream deposits. Sedimentary Geology, 129, 187–199.

Appelo, C. A. J., & Postma, D. (2005) Geochemistry, groundwater and pollution (2nd ed.). Leiden: AA Balkema.

Barnett, B., Townley, L. R., Post, V., Evans, R. E., Hunt, R. J., Peeters, L., Richardson S, Werner, A. D., Knapton, A., & Boronkay, A. (2012). Australian groundwater modelling guidelines. Waterlines reports series No. 82.

Berg, S. J., & Illman, W. A. (2013) Field study of subsurface heterogeneity with steady-state hydraulic tomography. Groundwater, 51, 29–40.

Bianchi, M., Zheng, C., Wilson, C., Tick, G. R., Liu, G., & Gorelick, S. M. (2011) Spatial connectivity in a highly heterogenous aquifer: From core to preferential flow paths. Water Resources Research, 47, W-5524.

Bradbury, K. R., Gotkowitz, M. G., Hart, D. J., Eaton, T. T., Cherry, J. A., Parker, B. L., & Borchardt, M. A. (2006) Contaminant transport through aquitards: Technical guidance for aquitard assessment. American Water Works Research Foundation, Denver.

Choquette, P. W., & Pray, L. C. (1970) Geologic nomenclature and classification of porosity in sedimentary carbonates. American Association of Petroleum Geologists Bulletin, 54, 207–250.

Dagan, G. (1986) Statistical theory of groundwater flow and transport: Pore to laboratory, laboratory to formation, and formation to regional scale. Water Resources Research, 22(9S), 120S-134S.

de Marsily, G., Delay, F., Goncalvès, J., Renard, Ph., Teles, V., & Violette, S. (2005) Dealing with spatial heterogeneity. Hydrogeology Journal, 13, 161–183.

Feazel, C. T., Byrnes, A. P., Honefenger, J. W., Leibrecht, R. J., Loucks, R. G., McCants, S., & Saller, A. H. (2004) Carbonate reservoir characterization and simulation: Report from the March 2004 Hedberg Research Symposium. American Association of Petroleum Geologists Bulletin, 88, 1467–1470.

Fogg, G. E. (1986) Groundwater flow and sand body interconnectedness in a thick multiple-aquifer system. Water Resources Research, 22, 679–694.

Fogg, G. E. (1989) Emergence of geological and stochastic approaches for characterization of heterogeneous aquifers. In Proceedings R.S. Kerr Environmental Research Lab (EPA) Conference on New Field Techniques for Quantifying the Physical and Chemical Properties of Heterogeneous Aquifers.

Freeze, R. A., & Cherry, J. A. (1979) Groundwater. Englewood Cliffs: Prentice-Hall.

Freeze, R. A., & Witherspoon, P. A. (1966) Theoretical analysis of regional groundwater flow. 2. Effect of water-table configuration and subsurface permeability variation. Water Resources Research, 3, 623–634.

Freyberg, D. L. (1986) A natural gradient experiment on solute transport in a sand aquifer: 2. Spatial moments and the advection and dispersion of nonreactive tracers. Water Resources Research, 22, 2031–2046.

Galloway, W. E., & Sharp, J. M., Jr. (1998) Characterizing aquifer heterogeneity within terrigenous clastic depositional systems. In G. S. Fraser, & J. M. Davis (Eds.), Hydrogeologic models of sedimentary aquifers, Concepts in hydrogeology and environmental geology, No. 1 (pp. 85–90): Tulsa: SEPM.

Gelhar, L. W. (1986) Stochastic subsurface hydrology from theory to applications. Water Resources Research, 22(9S),135S–145S.

Gelhar, L. W., Welty, C., & Rehfeldt, K. R. (1992) A critical review of data for field-scale dispersion in aquifers. Water Resources Research, 38, 1955–1974.

Haldorsen, H. H. (1986) Simulator parameter assignment and the problem of scale in reservoir engineering. In L. W. Leake, & H. B. Carroll, Jr., (Eds.), Reservoir characterization (pp. 293–340). Orlando: Academic Press.

Hantush, M. S. (1960) Modification of the theory of leaky aquifers. Journal of Geophysical Research, 65, 3713–3725.

Hantush, M. S., & Jacob, C. E. (1955) Nonsteady radial flow in an infinite leaky aquifer. Transactions of the American Geophysical Union, 36, 95–100.

Hess, K. M., Wolf, S. H., & Celia, M. A. (1992) Large-scale natural gradient tracer test in sand and gravel, Cape Cod, Massachusetts, 3. Hydraulic conductivity variability and calculated macrodispersivities. Water Resources Research, 28, 2011–2027.

Johnson, A. I. (1967) Specific yield - compilation of specific yields for various materials. U.S. Geological Survey Water Supply Paper 1662-D.

Konikow, L. F. (2011) The secret of successful solute-transport modeling. Ground Water, 49, 144–159.

Kruseman, G. P., & de Ridder, N. A. (1970) Analysis and evaluation of pumping test data. International Institute for Land Reclamation and Improvement, Bulletin 11, Wageningen, The Netherlands.

Lohman, S. W. (1979) Ground-water hydraulics. U.S. Geological Survey Professional Paper 708.

Lohman, S. W. et al. (1972) Definition of selected ground-water terms – revisions and conceptual refinements. U.S. Geological Survey Water-Supply Paper 1988.

Lucia, F. J. (1995) Rock-fabric/petrophysical classification of carbonate pore space for reservoir characterization. American Association Petroleum Geologists Bulletin, 79, 1275–1300.

Ma, Y. Z. (2011) Uncertainty analysis in reservoir characterization and management: How much should we know about what we don't know. In Y. Z. Ma & P. R. La Pointe (Eds.), Uncertainty analysis and reservoir modeling. Memoir 96 (pp. 1–15). Tulsa. American Association of Petroleum Geologists.

Maliva, R. G., & Missimer, T. M. (2010) Aquifer storage and recovery and managed aquifer recharge using wells: Planning, hydrogeology, design, and operation. Houston: Schlumberger Water Services.

Molz, F. J., Güven, O., & Melville, J. G. (1983) An examination of scale-dependent dispersion coefficients. Ground Water, 21, 715–725.

Neuman, S. P. (1990) Universal scaling of hydraulic conductivities and dispersivities in geologic media. Water Resources Research, 26, 1749–1758.

Phillips, F. M., Wilson, J. L., & Davis, J. M. (1989) Statistical analysis of hydraulic conductivity distributions: A qualitative geological approach. In Proceedings Conference of New Field Techniques for Quantifying the Physical and Chemical Properties of Heterogeneous Aquifers (pp. 19–31). Dublin, Ohio: National Water Well Association.

Pickens, J. F., & Grisak, G. E. (1981) Scale-dependent dispersion in a stratified granular aquifer. Water Resources Research, 17, 1191–1211.

Poeter, E., & Gaylord, D. R. (1990) Influence of aquifer heterogeneity on contaminant transport at the Hanford site. Ground Water, 28, 900–909.

Prill, R. C., Johnson, A. I., & Morris, D. A. (1965) Specific yield – Laboratory experiments showing the effect of time on column drainage. U.S. Geological Survey Water-Supply Paper 1662-B.

Pryor, W. A. (1973) Permeability-porosity patterns and variations in some Holocene sand bodies. American Association of Petroleum Geologists Bulletin, 57, 162–189.

Rehfeldt, K. R., Boggs, J. M., & Gelhar, L. W. (1992). Field study of dispersion in a heterogeneous aquifer: 3. Geostatistical analysis of hydraulic conductivity. Water Resources Research, 28, 3309–3324.

Ritzi, R. W., Jr., Jayne, D. F., Zahradnik, A. J., Jr., Field, A. A., & Fogg, G. E. (1994) Geostatistical modeling of heterogeneity in glaciofluvial, buried valley aquifers. Ground Water, 32, 666–674.

Schatzinger, R. A., & Tomutsa, L. (1999) Multiscale heterogeneity characterization of tidal channel, tidal delta and foreshore facies, Almond Formation outcrops, Rock Springs uplift, Wyoming. In R. Schatzinger, & J. Jordan (Eds.), Reservoir characterization – recent advances, Memoir 71 (pp. 45–56): Tulsa: American Association of Petroleum Geologists.

Schulze-Makuch, D. (2005) Longitudinal dispersivity data and implications for scaling behavior. Ground Water, 43, 433–456.

Simmons, C. T. (2008). Henry Darcy (1803–1858): Immortalised by his scientific legacy. Hydrogeology Journal, 16, 1023–1038.

Slater, L. (2007) Near surface electrical characterization of hydraulic conductivity: From petrophysical properties to aquifer geometries – A review. Surveys in Geophysics, 28, 169–197.

Sudicky, E. A. (1986) A natural gradient experiment on solute transport in a sand aquifer: Spatial variability of hydraulic conductivity and its role is dispersion processes. Water Resources Research, 22, 2069–2082.

Walton, W. C. (1960). Leaky artesian aquifer conditions in Illinois. Illinois State Water Survey Report of Investigation 39, Urbana.

Webb, E. K., & Anderson, M. P. (1996) Simulation of preferential flow in three-dimensional, heterogeneous conductivity fields with realistic internal architecture. Water Resources Research, 32, 533–545.

Chapter 2
Facies Analysis and Sequence Stratigraphy

The three-dimensional distribution of bodies of rock and sediments with different sedimentological properties and associated hydraulic properties is controlled to varying degrees by the depositional history of the strata of interest. Primary (depositional) variations in sediment textures and fabrics are modified by diagenetic processes, such as compaction, dissolution, and cement precipitation. A facies is a body of sedimentary rock with specified characteristics, which may include lithology (lithofacies), fossils (biofacies), and hydraulic properties (hydrofacies). Sedimentary facies analysis is based on the concept that facies transitions occur more commonly than would be expected if sedimentation processes were random. A facies model (or type model) is an idealized sequence of facies defined as a general summary of a specific sedimentary environment. Sequence stratigraphy is based on the concept that the sedimentary rock record can be divided into unconformity-bounded sequences, which reflect the sedimentological response to sea level changes, subsidence, and sediment supply. The value of facies analysis and sequence stratigraphy is that they can provide some predictability to the facies distribution between data points (i.e., wells). Where there is an underlying sedimentological control on the distribution of the hydraulic properties in aquifer systems, facies analysis can be used to better incorporate the underlying sedimentological fabric into groundwater models.

2.1 Introduction

A fundamental concept in the characterization of sedimentary rock aquifers is that the geometry and hydraulic properties of aquifers and confining units are related to sediment and rock types, which are, in turn, related to their depositional and diagenetic history. Geological heterogeneity is the product of complex yet discernable geological processes. Sedimentological studies can, therefore, provide valuable information towards quantifying the spatial structure of aquifers and reservoirs

(Davis et al. 1993). In particular, connectivity of bodies of sediment with high and low-hydraulic conductivity is a key feature in controlling groundwater flow and solute transport. Connected high-hydraulic conductivity zones act as flow conduits and connected low-hydraulic conductivity strata act as confining strata.

The spatial variability of textural and hydraulic parameters within sedimentary deposits has an element of predictability based on an understanding of depositional processes and environments. It has long been appreciated in the oil and gas industry that the vast data on modern and ancient sediments and sedimentary rocks from the sedimentology discipline can be invaluable for reservoir and aquifer characterization. Knowledge of the geometrical, compositional, and textural characteristics of sediment and rock types from different depositional environments, obtained from the vast sedimentological literature, can provide a valuable framework for determining the architecture of aquifers and groundwater basins. Indeed, the need for information on the geology of oil and gas reservoirs has been the ultimate primary driver for sedimentological research over the past 50 years. In terms of applied hydrogeology, the principal value of sedimentological data is that it can allow for more accurate interpolation and extrapolation of limited point data.

Tools such as facies analysis, sequence stratigraphy, and geostatistical analysis are used to evaluate the three-dimensional relationships among sedimentary strata and their relationships to aquifer hydraulic properties. An underlying assumption in characterizing reservoir or aquifer strata from outcrop studies is that the original framework of the sediments (i.e., grain-size distribution, texture, and fabric) determined by depositional processes still predominantly controls the permeability structure of the rock, although not necessarily the magnitude or even degree of contrast (Stalkup 1986).

Hydrogeologists would like to be able to use generic facies models to extrapolate limited field data and thereby avoid the expense and time involved in collecting more detailed site-specific information (Anderson 1989). Information on the depositional environment of aquifer and confining strata may allow hydrogeologists to better predict the expected spatial trends in hydraulic conductivity from limited site-specific information. Facies analysis is used in groundwater investigations in three main manners (Neton et al. 1994):

(1) deterministic prediction of trends in hydraulic conductivity from a limited number of point measurements
(2) assessment of the validity of stochastically determined distributions of hydraulic conductivity
(3) as a guide in well placement and the interpretation of aquifer test data.

It must be recognized that the hydraulic properties of sedimentary rocks can never be fully predictable. Every sedimentary formation has its unique features that cannot be predicted from general geological models. Additionally, primary textural differences may be overprinted by diagenesis, which, as a broad generalization, becomes more important with the burial history of the sediments. The interaction of diagenesis and depositional texture may be either a positive or negative feedback.

A positive feedback occurs when, for example, low-permeability clay-rich beds are preferentially compacted, further increasing the permeability contrast with clay-poor sands. In karstic carbonate systems, high permeability strata and fractured horizons are preferential loci for fluid flow and associated dissolution and permeability increase. A negative feedback would occur if high permeability sands are the preferential site of cementation due to enhanced solute transport associated with greater fluid flow rates.

2.2   Facies, Facies Sequences, and Facies Models

The sedimentary facies concept was reviewed by Middleton (1978), Walker (1984), Reading (1986a), Selley (1985; 2000), and many others. The most basic definition of a facies is a "body of rock with specified characteristics" (Reading 1986b, p. 4). Sedimentary facies are defined as areally restricted, three-dimensional bodies of rock or sediment that are distinguished from other bodies by their lithology, sedimentary structures, geometry, fossil content, and other attributes. Lithofacies are defined solely on the basis of their lithology. Similarly, biofacies are defined based on their fossil content. Ichnofacies are categorized based on their trace fossil assemblage.

The facies concept has been extended in some definitions to also reflect a particular depositional process or environment. For example, a purely descriptive lithofacies is a well-sorted, unfossiliferous, medium-grain quartz sand, whereas a corresponding genetic description might be a medium-grained quartz dune sand. Some have objected to the genetic definition of facies, in preference to retaining the original purely descriptive definition (e.g., Middleton 1978; Walker 1984; Selley 1985, 2000).

Anderton (1985) defined an interpretative (genetic) facies as a label summarizing the interpretation of the processes and environment of deposition of a certain unit of rock. Interpretative or genetic facies descriptions are commonly used. Anderton (1985) observed that there should be no objection to the use of interpretative facies so long as the distinction between descriptive and interpretative facies is clear from the context. It is normally obvious from the context whether the term facies is used in a descriptive or interpretative sense (Walker 2006).

Facies can be defined on a variety of scales depending upon (Walker 2006)

- the purpose of the study
- the time available to make the measurements
- the abundance of descriptive features in the studied strata.

For example, a ripple cross-laminated sand can be defined as a single facies, or constituent individual ripples or cross-laminated beds can be defined as a facies. Typically, in groundwater investigations, scales on the coarse end (decimeter to meter scale) of the spectrum are appropriate as the data will eventually have to be

upscaled to be incorporated into a large-scale (often kilometer or greater) groundwater model.

The principle value of facies analysis lies in that only a finite number of facies occurs repeatedly in rocks of different ages all over the world (Selley 1985). This provides important order in the analysis of sedimentary rock, which would not occur if each bed of rock were treated as a unique entity. However, facies have limited value when taken in isolation. A knowledge of the context and associations of facies is critical for environmental interpretations (Reading 1986b) and, in turn, realizing the predictive value of facies analysis.

Facies sequences are a series of facies whose transitions and relationships are geologically significant with respect to depositional environment (Walker 1984; Reading 1986b). The term 'sequence' had been co-opted in the sequence stratigraphy literature (Sect. 2.4) to have a more specific meaning. Hence, perhaps 'facies sequences' should now be referred to as 'facies successions'. Nevertheless, for the purpose of consistency with the historic literature, the original terminology is retained. A critical point is that where an individual facies may be ambiguous as to depositional environment, the sequence in which facies occur may contain much more information and be more diagnostic of depositional environment.

Depositional elements are facies sequences or associations that are easily defined and understood, and are characteristic of a specific depositional environment (Walker 2006). A depositional element (e.g., shoreface) may occur in several geographic settings. A similar concept is the architectural element of Miall (1985), which are defined in terms of geometry, scale, and lithofacies assemblages. Depositional or architectural elements are the recommended unit for sedimentological analysis for groundwater investigations because they are mappable units on a scale appropriate for groundwater models (Phillips et al. 1989; Davis et al. 1993; Hornung and Aigner 1999).

A facies model (or type model) is an idealized sequence of facies defined as a general summary of a specific sedimentary environment based on studies of both ancient rock and recent sediments (Walker 1984). Available information on a depositional environment is distilled to extract general information and generate an idealized environmental summary or sequence of facies. In addition to being a summary of the environment, a facies model should act as (Walker 1984)

- a norm for the purpose of comparison
- a framework and guide for future observations
- a predictor in new geological situations
- an integrated basis for interpretation of the environment of the system that it represents.

The fundamental assumption underlying facies models is that facies transitions occur more commonly than would be expected if the processes of deposition were random. Where the facies concept is particularly valuable is in sedimentary sequences where apparently similar facies are repeated many times over (Walker 1984).

A classic example of a facies model is the 'Bouma sequence' for the deposits of low-density turbidity currents (i.e., turbidites), which was described by Arnold Bouma (1962). A turbidity current is a rapid bottom-flowing sediment gravity (density) flow that is laden with suspended sediment. The Bouma sequence consists of five facies, designated A through E, from the base upwards (Fig. 2.1). The base of the classic Bouma sequence is an unconformity. Strata composed of turbidite deposits consist of stacked Bouma sequences. Not all of the five facies may be present in a given turbidite, but the general sequence pattern is usually retained. Turbidite strata thus can be described by a single facies model that contains five facies.

A limited amount of local information plus the guidance of a well-understood facies model allow for potentially important predictions about local depositional environments (Walker 1984). Given one or a limited number of pieces of information, it may be possible to assign the information to a particular model and, therefore, use the model to predict the rest of the system (Walker 2006). The basic procedure for building sedimentological models include (Walker 2006):

- recognition and definition of facies associations and depositional or architectural elements
- careful fitting of the elements into their three-dimensional framework, which involves determining both the elements that occur together and those that never occur together
- definition of the surfaces that separate elements
- interpretation of the elements as much as possible
- inferring a representative facies model (used as a norm).

Fig. 2.1 Conceptual diagram of the classic Bouma (1962) facies model of a turbidite sequence. All of the facies (A through E) may not be present in a given actual turbidite sequence
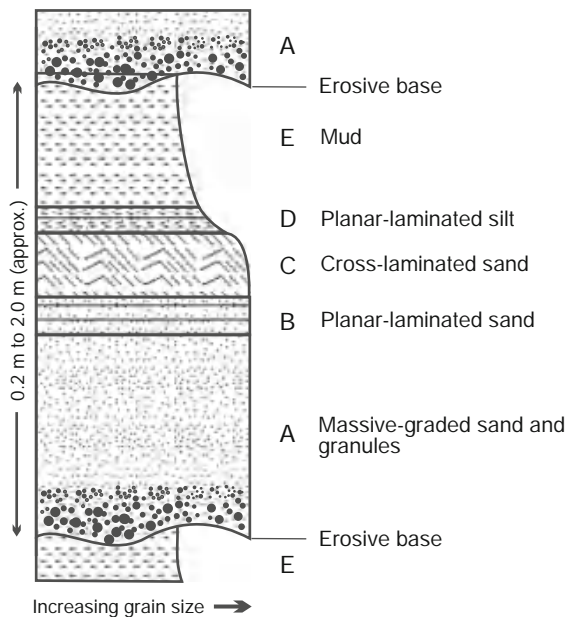
- evaluation of how the distribution of deposition or architectural elements in the studied strata conform to the model.

Genetic definitions have the advantage of potentially adding some predictability to the facies analysis because of sedimentological controls over the geometry of facies and genetic associations with other facies. For example, a meandering stream channel sand facies would be expected to be elongated in the direction of the paleo-stream gradient and be laterally and vertically associated with muddy floodplain deposits. Facies models can provide some insights into the likely geometry of individual elements.

Facies models were developed largely based on data from modern environments. However, the preservation potential of recent sediments is a critical issue when developing facies models from modern sediments. Most sediments are removed by erosion after deposition, and in many environments most sediment deposits have little chance for preservation (Reading 1986b). Sediment preservation potential is particularly low in depositional settings with limited accommodation space, such as shallow water and subaerial environments.

2.3 Limitation of Facies Models

The primary limitation of facies models is that facies characteristics and distributions are a complex function of the interaction of numerous variables within a depositional environment. Geological deposits have both apparently random and regular or predictable elements. With respect to fluvial deposits, Miall (1985) noted that numerous facies models have been proposed, which, in reality, reflect fixed points on a multidimensional continuum of variables. Sedimentary deposits, in general, are a continuum rather than consisting of a fixed number of discrete facies models (Anderton 1985). Walker (2006) countered that facies modeling is based on the recognition that there is system and order in nature, and geologists can identify and agree upon a limited number of depositional environments and systems. Indeed, facies models are general summaries of basic characteristics for which there is considerable variation in the details. Owing to the complexity of the heterogeneity and the subjective nature of geologic interpretation, estimated facies patterns are inherently characterized by a high degree of uncertainty (Fogg 1989).

Siliciclastic and carbonate facies models summarized in Chaps. 3 and 4 are conceptual-type models that illustrate characteristic features and patterns of sediments deposited in different depositional environments, which may be developed to varying degrees in actual deposits or may have been partially removed by subsequent erosional events. For siliciclastic sediments, the textures of a sediment are a function of not just the depositional environment, but also of its previous history (e.g., source of the sediment being transported into an environment) and subsequent diagenesis.

Miall (2006) noted with respect to fluvial deposits that important limitations of facies models are fragmentary preservation and variability. There can be a great

difference in modern facies assemblages and facies distribution and what is actually preserved in the geologic record. Earlier deposited sediments are subject to later partial or complete erosion and redeposition. Multiple factors control sediment deposition, which can result in a great variation in the physical character of sedimentary aquifers. Considerable uncertainty exists about the appropriateness of the analogs used for each specific case (Miall 2006). Large-scale facies trends can be deduced from facies models. Facies models are less useful for delineating small-scale heterogeneity within facies because small-scale spatial trends are dependent of local site-specific conditions (Anderson 1989).

Although a number of workers have identified limitations of facies analysis, the message is not that facies analysis has no value or is not worth the effort. The advised caution is more to avoid overinterpretation of data. Despite its limitations, facies modeling has been demonstrated to be an invaluable tool for the analysis of sedimentary deposits and ultimately aquifer characterization.

2.4   Sequence Stratigraphy

2.4.1   Introduction

Facies migrate over time due to global (eustatic) sea level change, variations in sediment supply, and subsidence. A basic limitation of standard facies analysis is that the predictive capacity of facies models is limited by their static view of time and relative sea level changes (Handford and Loucks 1993). Relative sea level changes are the sum of the rates of subsidence (or uplift) and eustatic sea level change. Sediment deposition is controlled to a large degree by sediment supply and accommodation, which is the amount of space that is available for sediments to fill up to base level. Base level is defined as the dynamic surface between erosion and deposition and is the highest level to which sedimentary successions can be built (Catuneanu et al. 2009). Base level in marine environments is approximately sea level. In nearshore environments, changes in water depth (and thus types of sediments deposited) and the position of the shoreline reflect the balance between sediment supply, the direction and rate of changes in sea level, and the subsidence rate. Depending upon the accommodation space, sediment supply, and magnitude and direction of relative change in sea level, sedimentary deposits may, in a predictable manner, shallow or deepen upwards, and individual facies may migrate either seawards (prograde) or landwards (retreat). Sequence stratigraphy integrates time and relative sea level changes to predict the migration and distribution of facies.

Sequence stratigraphy has arguably revolutionized stratigraphic analysis in the oil and gas industry, but to date, has had limited application in the evaluation and management of groundwater resources. The basic concept that the sedimentary rock record can be divided into unconformity-bounded sequences was recognized by Sloss (1963), who subdivided the North American cratonic deposits (Late Precambrian to the present) into six sequences. The seminal publication on

sequence stratigraphy was the American Association of Petroleum Geologists Memoir 26, "Seismic Stratigraphy—Application to Hydrocarbon Exploration", in which a depositional sequence was defined by Mitchum et al. (1977, p. 53) as a

> stratigraphic unit composed of a relatively conformable succession of genetically related strata and bounded at its top and based by unconformities or their correlated conformities.

The basic sequence stratigraphic approach involves dividing intervals of sedimentary rock strata into genetically related units bounded by surfaces with chronostratigraphic significance (Van Wagoner et al. 1988). A huge number of papers on various aspects of sequence stratigraphy has been published since Memoir 26 including dedicated books and review papers (e.g., Van Wagoner et al. 1988, 1990; Posamentier et al. 1993; Posamentier and James 1993; Posamentier and Allen 1999; Catuneanu 2006; Emery and Myers 2009; Miall 2010).

Sequence stratigraphy has been widely adopted in the oil and gas industry because it provides a powerful methodology for the analysis of time and rock relationships in sedimentary strata and a framework to predict facies relationships (Van Wagoner et al. 1988). The principal value of sequence stratigraphy is that it provides more predictability, particular where local or global sea level curves can be used to predict stratigraphic relationships in areas with minimal data (e.g., undrilled areas). What follows is a brief introduction into basic sequence stratigraphy concepts.

Depositional sequences are chronostratigraphically significant because they were deposited during an interval of geological time bounded by the ages of the sequence boundaries (Mitchum et al. 1977). Unconformities are surfaces of erosion or nondeposition that separate younger strata from older rocks and represent a significant hiatus. A hiatus is the total interval of geological time that is not represented by strata at a specific position along a stratigraphic surface (Mitchum et al. 1977). Conformities, on the contrary, have no evidence of erosion and nondeposition, and no significant hiatus is indicated. It is important to appreciate that sequences are chronostratigraphic units and that lithostratigrahic units may not coincide with chronostratigraphy as lithologic units may be time transgressive (Vail et al. 1977b). Inasmuch as hydrogeologic units often coincide with lithologic units, preferential flow (aquifer) and confining units may also not correspond to sequence stratigraphic units.

The definition of depositional sequence requires that the strata be 'genetically related'. A genetically related unit is deposited during a single episodic event, as opposed to being an arbitrary unit bounded by arbitrarily chosen unconformities (Mitchum et al. 1977). The key value of sequence stratigraphy lies in that sequence boundaries and depositional sequences can be related to local changes in relative sea level (i.e., changes in sea level relative to land surface) and global changes in absolute sea level (Vail et al. 1977a). Sequence stratigraphy is thus particularly useful for shallow-marine facies, whose deposition is partially controlled by sea level. Deep-marine facies are not directly controlled by sea level, and hinterland sequences are deposited independently of marine sequences (Vail et al. 1977a). However, sequence boundaries may also have non-eustatic (e.g., tectonic origins)

and may form gradually over finite intervals of geological time, rather than more or less instantaneously (Christie-Blick and Driscoll 1995).

The initial activity in sequence stratigraphic analysis is the identification and correlation of sequence boundaries and depositional sequences. Sequence boundaries are most readily identified by discordant (i.e., lapout) relationships in which strata terminate against a surface, as opposed to concordant relationships where strata parallel a surface (Mitchum et al. 1977). Basic discordant (lapout) relationships are illustrated in Fig. 2.2. The relationships between relative sea level change, sediment supply, and the transgression and regression of marine sediments were summarized by Vail et al. (1977a).

Sequence stratigraphy was originally based upon the interpretation of seismic reflection data. Lapout relationships, which are best observed on seismic profiles, are a key to the physical recognition of sequence stratigraphic surfaces (Catuneanu et al. 2009). However, sequence stratigraphy is also applied to the interpretation of field (outcrop) data and borehole data, when there is a sufficient density of wells. The relative low resolution of seismic reflection data relative to field and well data needs to be considered when comparing different data sources. As has been noted by a number of workers (e.g., Schlager 2005), features that appear as a surface in seismic reflection profiles may correspond to an actual transitional lithogical boundary of some thickness.

Multiple orders of global sea level change were documented by Vail et al. (1977b) and subsequently refined and expanded upon in numerous subsequent studies. Vail et al. (1977b) documented three orders of cycles (Table 2.1). Kerans and Tinker (1997) presented a five-order sequence classification (Table 2.2).
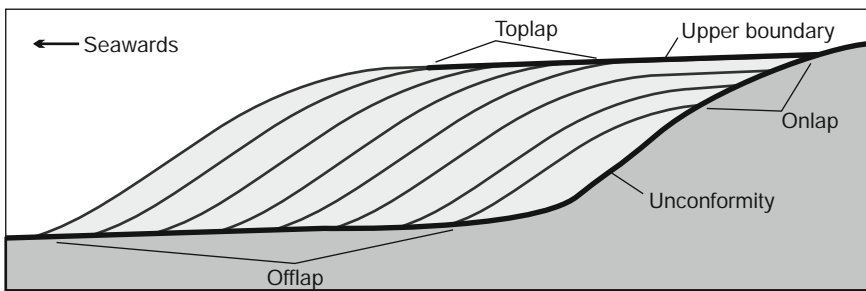
Fig. 2.2 Conceptual diagram of basic lapout relationships relevant to sequence stratigraphy

Table 2.1 Global sea level cycles of Vail et al. (1977b)

Order	Duration (million years)	Cycle type
1	225–300	Multiple period
2	10–80	Supercycles (1 or 2 per period)
3	1–10	Cycle (1 or more per epoch)

Table 2.2 Sequence classification system of Kerans and Tinker (1997)

Tectono-Eustatic cycle order	Sequence stratigraphic unit	Duration (million years)	Relative sea level amplitude (m)	Relative sea level change rate (cm/1000 yr)
First		>100		<1
Second	Supersequence	10–100	50–100	1–3
Third	Depositional sequence	1–10	50–100	1–10
Fourth	Parasequence and cycle set	0.1–1	1–150	40–500
Fifth	Parasequence, high-frequency cycle	0.01–0.1	1–150	60–700

There is inconsistency in the literature regarding the deposition significance of higher order sequences, the order assigned to a given type of unit, and the durations of unit types. Schlager (2005), for example, observed that although the principle of defining orders by duration has been almost universally followed, the actual values used in the definitions vary widely.

2.4.2 Sequence Stratigraphic Concepts and Definitions

The basic sequence stratigraphic concepts and key definitions with respect to siliciclastic sediments were overviewed by Van Wagoner et al. (1988) and are illustrated in Fig. 2.3 and summarized below. Parasequences and parasequence sets are the fundamental building blocks of sequences. A parasequence is a relatively conformable succession of genetically related beds or bedsets bounded by marine flooding surfaces. A marine flooding surface is a surface that separates younger from older strata, across which there is evidence for an abrupt increase in water depth. A parasequence set is a succession of genetically related parasequences, which form a distinctive stacking pattern that, in many cases, is bounded by major marine flooding surfaces. Depending upon the relationship between the rates of deposition and accommodation, parasequence sets may be either progradation (shallow upwards), retrogradation (deepening upwards), or aggradation (rate of deposition equals rate of accommodation). Systems tracts link contemporaneous depositional environments together. The three most important system tracts are the lowland systems tract (LST), transgressive systems tract (TST), and highstand systems tract (HST).

Lowstand systems tracts are prograding packages deposited at the early stage of base level rise when the sediment supply outpaces the base level rise. Strata downlap on the sequence boundary in a basinwards direction. LSTs are bounded above by the maximum regressive surface (MRS; maximum shoreline progradation), which is,
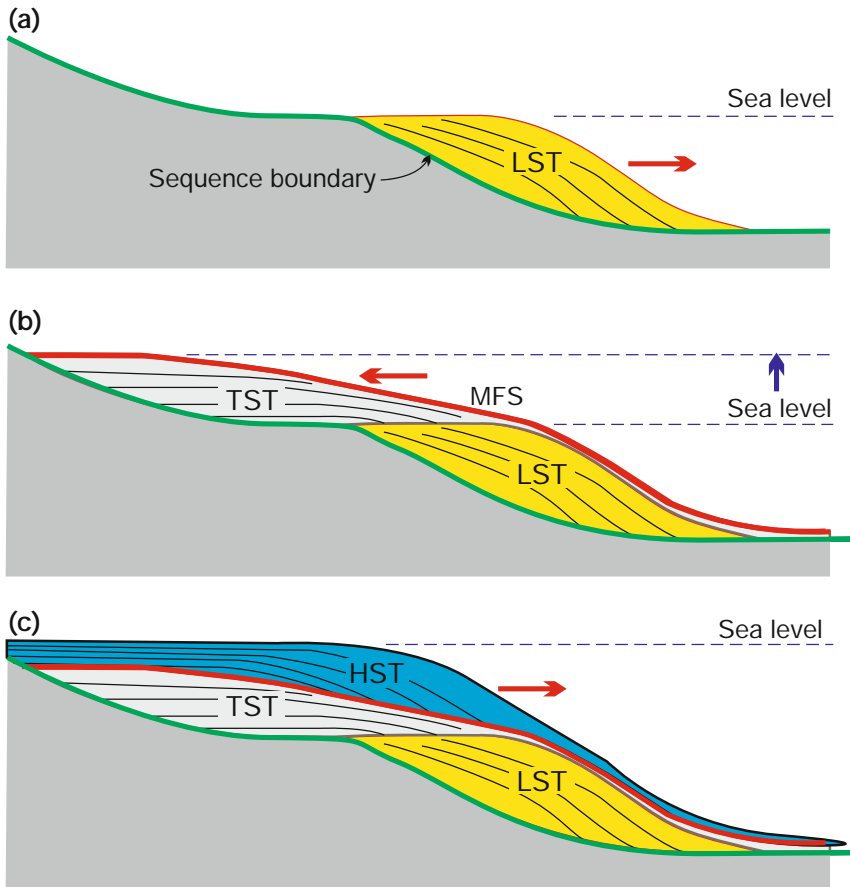
Fig. 2.3 Basic sequence stratigraphy diagram. a Lowstand system tract (LST) offlaps on the sequence boundary. b Transgressive system tract (TST) onlaps the sequence boundary. Its upper boundary is the maximum flooding surface (MFS), which is the surface of deposition at its maximum landward position (i.e., time of maximum transgression). c Highstand systems tract (HST) marks return of progradation with the offlap of strata on the MFS

subsequently, a transgressive surface. The MRS marks the initiation of transgression and is the first significant flooding surface across the shelf.

Transgressive systems tracts are deposited when base level rise outpaces sediment supply and, as a result, the shoreline and associated facies shifts landwards. Laterally extensive bodies of nearshore sediment (e.g., beach and deltaic sands and shallow water carbonates) are deposited as the loci of sediment deposition retreats with shoreline. Siliciclastic TSTs are characterized by one or more retrogradational parasequence sets and are bounded at the top by the maximum marine flood surface (MFS). The MFS marks the maximum transgression of sea level. It is the surface that marks the turn-around from landward-stepping to seaward-stepping strata.

Highstand systems tracts are deposited during the later stage of the progradation phase in which sediment supply once again outpaces base level rise and the shore starts to prograde again. HSTs are characterized by one or more aggradation parasequences that are succeeded by one or more progradational parasequence sets. HSTs are deposited during the latter part of a eustatic sea level rise, a eustatic standstill, or the early part of a eustatic fall. Some schemes subdivide the HST as also including a falling-stage systems tract (FSST), which consists of sediments that accumulated during a period of fall of relative sea. FSSTs are characterized by the seaward progradation of coastal deposits.

Classical sequence stratigraphy (Fig. 2.3) is best suited to the study of siliciclastic sedimentation at a differentially subsiding, passive continental margin with a well-defined shelf-slope break, and under conditions of fluctuating sea levels (Christie-Blick and Driscoll 1995). As is the case for facies models, sequence stratigraphic models represent general conditions, and it is important to appreciate the variability inherent in natural systems. Indeed, focusing on assigning strata to particular sequence types and subtypes tends to obscure that natural variability in sedimentary systems.

Catuneanu et al. (2009) noted that despite its widespread use, there is no standard code or guide for the application of sequence stratigraphy, particularly with respect to the classification of surfaces and nomenclature for sequence boundaries and system tracts. A basic sequence stratigraphic workflow was proposed, which includes four main elements (Catuneanu et al. 2009):

- observation of stacking trends and strata terminations
- delineation of sequence stratigraphic surfaces from stacking patterns and strata termination patterns
- identification of system tracts using surfaces, stacking patterns, and strata geometries
- definition of stratigraphic sequences using surfaces and system tracts.

2.4.3   Applications of Sequence Stratigraphy

Sequence stratigraphy is very widely used tool in the oil and gas industry for predicting the spatial distribution of lithofacies. It has proven to offer great value as a 'unifying framework' for analyzing and interpreting sedimentological (facies), lithostratigraphic, and chronostratigraphic data (Christie-Blick and Driscoll 1995). Sequence stratigraphy has been applied to a much lesser degree in groundwater projects, in which it is used mainly as an interpretative tool. The greatest potential value of high-resolution sequence stratigraphy in groundwater studies lies in improved interpolation between wells and extrapolation from wells. Proper correlation of lithofacies is critical for evaluating the connectivity of both aquifer and confining strata (Scharling et al. 2009). The true potential of sequence stratigraphy for predicting lithofacies and hydrofacies has yet to be realized.

It is important to emphasize that sequence stratigraphic analysis may be largely an academic exercise where the analysis either does not provide any new information or does not provide an improved understanding of the strata of interest. Stratigraphic correlations may still be made in groundwater studies without consideration of sequence stratigraphy. That an unconformity is a major sequence boundary may not have hydrogeologic significance if it does not impact groundwater flow. Sequence stratigraphy has greatest applications in studies involving large geographic areas in which there are significant lateral facies changes and in which the strata of interest contains multiple sequences. Sequence stratigraphy has limited value for local, small-scale groundwater investigations.

Sequence stratigraphy was used to evaluate the stratigraphic relationship of Pliocene to Holocene siliciclastic strata in the Dominguez Gap of Los Angeles County, California (Ponti et al. 2007; Edwards et al. 2009; Nishikawa et al. 2009). The Dominguez Gap is the location of saline-water intrusion into the Los Angeles Groundwater Basin. The sequence stratigraphic analysis (Fig. 2.4) provided insights into the relationships between transmissive sand strata that are avenues for saline-water flow and, in turn, can lead to more accurate solute-transport models.

A combination of sequence stratigraphy and facies analysis was used in a study of Miocene to Cretaceous aquifers of the Coastal Plain of New Jersey (Sugarman and Miller 1997; Sugarman et al. 2005). Well logs were used to trace sequence boundaries to core-hole control throughout the study region. The aquifer system consists of sand aquifers separated by semiconfining and confining clays and sands. The depositional environments include offshore marine, beach, deltaic and fluvial,
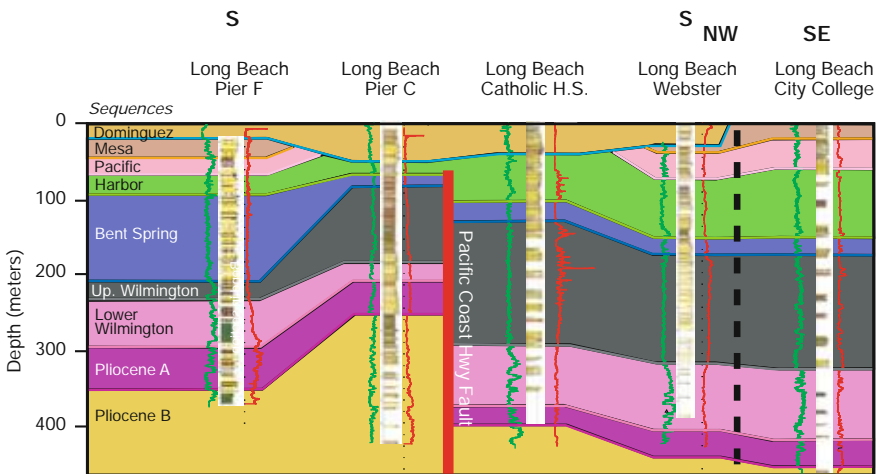
Fig. 2.4 Sequence stratigraphic interpretation of the Dominguez Gap at Long Beach, California by Ponti et al. (2007). The sequences in the approximately 8.3 km long cross-section are colored and resistivity (red) and natural gamma ray (green) logs are provided. Sequence stratigraphy has greatest potential values for large-scale investigations of geological complex sites such as the Dominguez Gap area

which result in the overall facies distribution being representative of historical sea level changes. Mapped sequences were found to be tied to global sea level changes. The principal value of utilizing sequence stratigraphy was that it allowed for more refined hydrostratigraphic correlations and predictions of the continuity of aquifers and confining units.

Houston (2004) applied high-resolution sequence stratigraphy to an investigation of groundwater resources in the Calama and Turi Basins of the Atacama Desert, northern Chile. Deposition in studied basins was controlled by episodic uplift and subsidence, which provided periodic accommodation space. Borehole geophysical logs and field observations were used to identify and correlate unconformity and sequence-bounded paleosols. The sequence stratigraphic analysis allowed for the development of a three-dimensional model of the basins, which helped delineate aquifer facies, low-permeability confining strata, and preferential flow paths.

Scharling et al. (2009) documented the application of sequence stratigraphy to an analysis of groundwater resources in Miocene strata at Jutland, Denmark. A descriptive sequence stratigraphic model was developed using existing seismic reflection data, lithologic and borehole geophysical logs (gamma ray), and biostratigraphic data. The borehole data in the study area was limited (<100 wells). Most of the wells in the region are shallow and do not penetrate the strata of interest. The final model had 23 surfaces including 10 sequence stratigraphic surfaces and 11 prominent lithofacies contact surfaces. The major benefit of the sequence stratigraphic analysis was an enhanced understanding of the distribution and connectivity of aquifers. Improper correlation of sand units (the main aquifer strata) and their connectivity could affect the flow regimes of groundwater models as groundwater is mainly transported in these units.

McFarlane et al. (1994) applied sequence stratigraphy to the analysis of the Dakota Aquifer of Kansas. Three sequences defined in the Front Range of Colorado were correlated to the study area, but the sequence stratigraphy was not an integral element of the data analysis.

Sequence stratigraphy was used main as a tool for stratigraphic interpretation of Tertiary carbonate and siliciclastic sediments in South Florida by Missimer (2001), Cunningham et al. (2001a, 2001b, 2003) and Ward et al. 2003). Cunningham et al. (2006) performed a sequence stratigraphic/cyclostratigraphic analysis of the Pleistocene limestones of the Biscayne Aquifer of southeastern Florida (Fig. 2.5). The analysis demonstrates that the stratigraphic section can be divided into high-frequency cycles, which can be correlated between wells. The strata were also divided into three porosity types that correlate with relatively permeability. The most permeable porosity type (Type I) contains touching vug porosity and thus conduit flow. The three porosity types occur in predictable vertical patterns in the cycles, which results in predictability in the presence of flow zones.
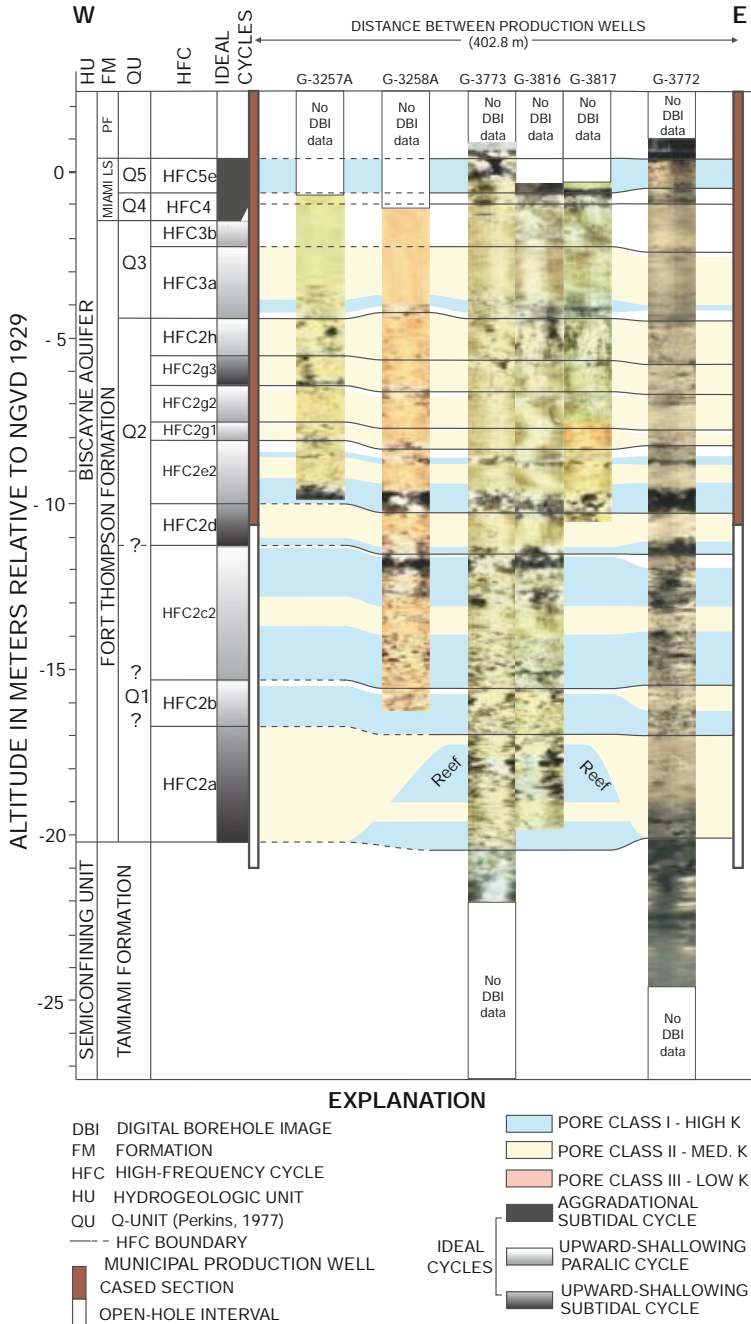
Fig. 2.5 Hydrostratigraphic correlation section from the Biscayne Aquifer (Miami-Dade County, Florida) including digital image logs by Cunningham et al. (2006). The stratigraphic section was divided into high-frequency cycles, which can be correlated between wells. A predictable vertical pattern of porosity and permeability was identified in the cycles. The highest permeabilities occur in porosity type I, which contains touching vug (conduit) porosity

2.5 Facies Modeling

The fundamental challenge in aquifer characterization is developing an acceptably accurate three-dimensional model of an aquifer system from scattered one-dimensional data from wells and boreholes. The term 'acceptably' recognizes that all models, by their nature, are imperfect (have inaccuracies), but still may be good enough to serve their intended purposes. A goal of aquifer characterization is to incrementally improve models through the collection of additional data and improved methods to process and interpret the data. It is useful to consider how facies data may be used to bridge the gaps between well data.

Facies analyses may be qualitatively used to develop conceptual models and to hydrogeologically interpret well data. Insights into the likely structure of an aquifer system may be derived from the knowledge of the depositional environment of the strata and the likely orientation, scale, and connectivity of aquifer and confining strata, which can be obtained from facies analysis and sequence stratigraphy.

The results of facies analyses can provide quantitative information on spatial correlation and can also be used as soft information or training images for geostatistical methods (Chap. 20). Geostatistics is a collection of numerical techniques used to characterize the spatial attributes of spatially dependent data. If data are random, then it is not possible to predict values between data points. Geostatistical techniques have multiple applications, but they are particularly useful for estimating or interpolating parameter values in spaces where sampling data are not available. The underlying concept is that, in general, things that are closer together tend to be more alike than things that are farther apart. For example, if a fluvial channel sand was identified at a given depth in a well, then there is a high probability that the sand will be located nearby at the same depth, particularly in the paleoflow direction. The degree of spatial correlation (i.e., probability that channel sand is present) decreases with increasing distance from the well. Data on spatial correlation of facies in the horizontal direction is sparse in most studies. Facies-specific general values may be used as default values in the absence of (or to supplement) site-specific data.

A more advanced technique is the development of models that can simulate the deposition of sedimentary rocks and thus facies distribution, which has been prompted to a large degree by the needs of oil and gas reservoir engineering. Synthetic depositional models have been developed based on factors (variables) such as sediment supply, rates of eustatic sea level change and subsidence, and hydraulic gradient (Allen 1978; Bridge and Leeder 1979; Leeder 1978; Flint and Bryant 1993; Webb 1994, 1995). There are two end-member modeling procedures (process and geometric methods), which were summarized by Webb and Anderson (1996).

Process-based models attempt to simulate the deposition of geological materials through the interaction of physical, chemical, and biological processes embodied in either theoretical or empirical relationships. Purely geometrical models attempt to produce spatial patterns similar to those observed in the field using empirically

derived geometric relationships. Most models incorporate aspects of both approaches (Webb and Anderson 1996).

Webb (1994, 1995), for example, developed the Braided Channel Simulator (BCS-3D), which can be used to simulate the three-dimensional internal geometry and relative distribution of facies of braided-stream deposits by simulating geomorphic surfaces associated with depositional processes. The simulations are performed on a scale appropriate for groundwater investigations; i.e., the architectural element scale of Miall (1985). The BCS-3D simulator can be used to model the three-dimensional shapes and spatial distribution of individual, recognizable sedimentary units. Webb (1994) noted it is relatively simple to adjust input parameters to match existing data in order to reproduce or simulate a well-described field setting. However, he also cautioned that it is rather difficult to determine these parameters a priori.

Webb and Anderson (1996) provide a good example of how facies simulations can be incorporated into groundwater models. The BCS-3D code was used to generate a three-dimensional realization of the internal structure (facies geometry) of the aquifer. The next step was to assign hydraulic conductivity values to each facies, which was performed using different methods:

- constant values were assigned to each facies unit.
- facies were combed into two groups (high and low-hydraulic conductivity), each of which was assigned a volumetrically weighted geometric mean value.
- each facies unit is assigned a value randomly sampled from a Gaussian hydraulic conductivity distribution assigned to that facies.

Sedimentological models have limited practical value because of the required level of calibration, the lack of resolution at scales relevant to many practical problems, and the impracticality of simulating the entire depositional history of an alluvial basin for a site investigation (Johnson 1995). Fluvial sedimentation, for example, is the product of simultaneous actions of various autogenic and allogenic sedimentary controls, and sufficient data would rarely be available to make computer modeling a practical tool (North 1996; Miall 2006). However sophisticated the statistical and numerical model used, ultimately these modeling efforts must resort to some means of determining the appropriate input data from the real world of actual fluvial systems (Miall 2006). Similar limitations occur in the modeling of other depositional systems.

2.6 Hydrofacies

The term 'hydrofacies' refers to hydrologically distinct lithofacies (Anderson 1989, Poeter and Gaylord 1990). The size, shape, and arrangement of lithofacies and erosional elements comprise the sedimentary architecture of a basin. Similarly, the arrangement of hydrofacies, consisting of both permeable and confining units,

determines the structure of the corresponding hydrogeological architecture of a groundwater basin. Aquifer characterization using the hydrofacies approach involves determination of the three-dimensional distribution of hydrofacies and their effective hydraulic properties.

The ultimate objective of hydrofacies analysis is to capture more of the three-dimensional hydrogeological structure or architecture of aquifer systems and create more realistic groundwater models that have a greater predictive capability. The fundamental challenge is interpolating and extrapolating spatially limited data to both develop conceptual models and populate numerical groundwater models. The facies approach recognizes that the distribution of sedimentary rock types is not random, but occurs in patterns that reflect processes within the depositional environment. Understanding facies and their internal variations and hydraulic properties of constituent elements is essential for characterizing the behavior of aquifer systems. Facies models thus provide some predictability in the distribution of sedimentary rock types and, in turn, hydrostratigraphic units.

Hydrofacies may correlate with lithofacies, facies associations, or architectural elements, where original sediment characteristics significantly influences current porosity and permeability. However, the correlation is often not one for one. A given hydrofacies may contain more than one sedimentological facies. The relationship between sedimentary facies and hydrofacies may be weak or nonexistent when porosity and permeability are largely controlled by diagenesis. Interconnectedness is the key to quantifying heterogeneity for the purpose of hydrogeological investigations (Anderson 1997).

Complete characterization of the subsurface would ideally yield a site-specific three-dimensional facies model that accurately incorporates the interconnectedness of both high- and low-connectivity zones (Anderson 1997). A basic approach to hydrofacies analysis is to perform a facies analysis in which the strata of the project area are assigned to depositional facies zones, based on knowledge of the basin depositional history, facies models, sequence stratigraphy, and available field and well data. The depositional facies are next assigned to hydrofacies. A given hydrofacies may include one or more depositional facies. Interpolation and extrapolation of facies or hydrofacies in areas without data can be performed by manual correlation or by using geostatistical methods in either a deterministic manner, in which a single realization is developed (e.g., using techniques such as kriging), or using a stochastic approach in which numerous realizations are generated (Chap. 20). Manual correlation should consider the overall depositional history of the basin such as the likely land surface or basin slope (and thus direction of sediment transport) and position of the paleo shoreline.

Hydraulic properties are then assigned to each hydrofacies based on available well and other data. Interfaces relationships (i.e., facies geometry) is discrete, while hydraulic conductivity distribution within facies may be described by a continuum (Anderson 1989). The hydrofacies data would next be upscaled (as needed) to populate the model grid. The values of hydraulic and solute-transported parameters in the hydrofacies-based model grid cells may be subsequently adjusted during the model calibration process.

McCloskey and Finnemore (1996) provide an example of the application of
the hydrofacies approach to a fault-bounded sedimentary basin in Santa Clara
County, California. The basin fill sediments consist predominantly of alluvial fan,
fluvial (braided stream), and lacustrine deposits. Using the basin sedimentary model
and standard alluvial fan and fluvial facies models, the strata were categorized as
having either high, medium, or low-hydraulic conductivity, and the distribution of
each strata type was mapped (Fig. 2.6). The expected high-hydraulic conductivity
strata are braided-stream fluvial deposits, which have the best sorting.
Low-hydraulic conductivity strata include fine-grained proximal fan deposits. The
facies model categorization of strata was supported by estimates of the sand to clay
ratio obtained from borehole geophysical logs. Transmissivity data were subse-
quently obtained from pumping test and specific capacity data. A good match was
observed between the distribution of hydraulic conductivity from the facies analysis
and well transmissivity data. For groundwater model development, facies model
and field hydraulic conductivity data would be combined to assign values to each
facies zone and thus cells in the model grid.

Fish and Stewart (1991) performed a hydrofacies analysis of the Surficial
Aquifer System in Miami-Dade County, Florida (USA). The studied strata included
the Biscayne Aquifer, which is the primary water source for the Miami-Fort
Lauderdale major metropolitan area. The hydrofacies approach involved catego-
rizing the strata from 34 test wells into a series of lithofacies. The lithofacies were
then each assigned to one of five hydraulic conductivity categories based on either
hydraulic testing data, published values relating hydraulic conductivity to grain size
and sorting, and hydrogeologic inferences based on inspection of samples. A series
of cross-sections were then generated by manual correlation between the test well
locations (Fig. 2.7)
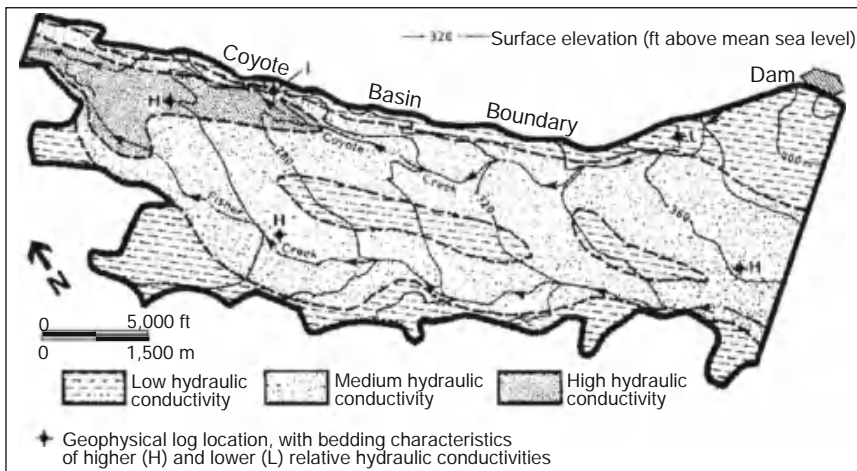
Fig. 2.6 Relative hydraulic conductivity map based on facies analysis for the Coyote Valley
basin, Santa Clara County, California (modified from McCloskey and Finnemore 1996)
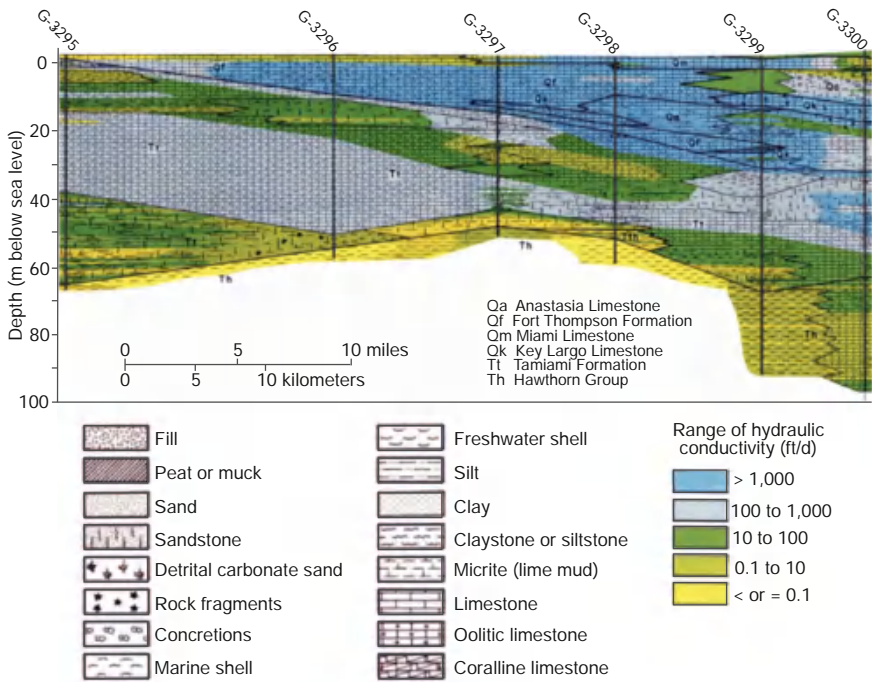
Fig. 2.7 Hydrofacies cross-section for the Surficial Aquifer System in Miami-Dade County, Florida (modified from Fish and Stewart 1991)

Surface geophysical data can be used to fill in the gaps between borehole data. In shallow aquifer systems, ground-penetrating radar (GPR) can be used to obtain data on aquifer structure, large-scale sedimentary features, and the position of the water table. Ezzy et al. (2006) implemented a high-resolution hydrofacies approach to a coastal plain alluvial aquifer located in the Bull Creek plain, north of Brisbane, Australia, which provides a good example of the application of surface geophysics in hydrofacies analysis. The study combined extensive well and core data with GPR surveys. GPR was particularly valuable for accurate definition of the boundary of narrow alluvial channels, which are significant conduits for shallow groundwater flow. Six hydrofacies were defined and the GPR data were used to develop a high-resolution map of alluvial aquifer thickness and interconnectivity and, in turn, hydrofacies distribution. Each of the hydrofacies were assigned values for hydraulic parameters based on testing results or commonly accepted literature values for the different materials. The values for the hydraulic parameters for the hydrofacies were refined through the model calibration process. Ezzy et al. (2006) noted that nonuniqueness in each hydrofacies zone remains an ill-posed problem and that the results of the model calibration is just one possible solution.

Facies and hydrofacies analyses are not a replacement for field data collection. Indeed, it requires the careful collection of higher-quality data. For example, well

cuttings need to be carefully described and analyzed along with borehole geo-physical logs and available existing data on the strata of interest in order to extract information on facies distributions. Facies and hydrofacies analyses should be approached as methods to maximize the value obtained from collected data. Facies analyses can allow for better constraint of numerical models by improving the differentiation between geologically plausible and implausible solutions. Where there is an underlying sedimentological control on the distribution of the hydraulic properties in aquifer systems, facies analysis can be used to better incorporate the underlying sedimentological fabric into models.

References

Allen, J. R. L. (1978) Studies of fluviatile sedimentation: An exploratory quantitative model for the architecture of avulsion-controlled alluvial suits. Sedimentary Geology, 21, 129–147.

Anderson, M. P. (1989) Hydrogeologic facies models to delineate large-scale spatial trends in glacial and glaciofluvial sediments. Geological Society of America Bulletin, 101, 501–511.

Anderson, M. P. (1997). Characterization of geological heterogeneity. In G. Dagan & S. O. Neuman (Eds.), Subsurface flow and transport: a stochastic approach (pp. 23–43). Cambridge: Cambridge University Press.

Anderton, R. (1985) Clastic facies models and facies analysis. Geological Society, London, Special Publication 18, 31–47.

Bouma, A. H. (1962). Sedimentology of some flysch deposits: A graphic approach to facies interpretation. Amsterdam: Elsevier.

Bridge, J. S., & Leeder, M. R. (1979) A simulation model of alluvial stratigraphy. Sedimentology, 26, 617–644.

Catuneanu, O. (2006). Principles of sequence stratigraphy. Amsterdam: Elsevier.

Catuneanu, O., Abreu, V., Bhattacharya, J. P., Blum, M. D., Dalrymple, R. W., Eriksson, P. G., & Winker, C. (2009). Towards the standardization of sequence stratigraphy. Earth-Science Reviews, 92(1), 1–33.

Christie-Blick, N., & Driscoll, N. W. (1995) Sequence Stratigraphy, Annual Reviews of Earth and Planetary Sciences, 23, 451–478.

Cunningham, K. J., Locker, S. D., Hine, A. C., Bukry, D., Barron, J. A., & Guertin, L.A. (2001a) Surface-geophysical characterization of ground-water systems of the Caloosahatchee River Basin, Southern Florida. U.S. Geological Survey Water-Resources Investigations Report 01–4084.

Cunningham, K. J., Bukry, D., Sato, T., Barron, J. A., Guertin, L. A., and Reese, R. S. (2001b) Sequence stratigraphy of a South Florida carbonate ramp and bounding siliciclastics (Late Miocene-Pliocene). In T. M. Missimer & T. M. Scott (Eds.), Geology and hydrogeology of Lee County, Florida. Florida Geological Special Publication 49 (pp. 35–66).

Cunningham, K. J., Locker, S. D., Hine, A. C., Bukry, D., Barron, J. A., & Guertin, L. A. (2003) Interplay of Late Cenozoic siliciclastic supply and carbonate response on the southeast Florida Platform. Journal of Sedimentary Research, 73, 31–46.

Cunningham, K. J., Renken, R. A., Wacker, M. A., Zygnerski, M. R., Robinson, E., Shapiro, A. M., & Wingard, G. L. (2006). Application of carbonate cyclostratigraphy and borehole geophysics to delineate porosity and preferential flow in the karst limestone of the Biscayne aquifer, SE Florida. In R. S. Harmon & C. M. Wicks (Eds.), Perspectives on karst geomorphology, hydrology, and geochemistry - A tribute volume to Derek C. Ford and William B. White. Special Paper 404 (pp. 191–208). Boulder: Geological Society of America.

Davis, J. M., Lohman, R. C., Phillips, F. M., Wilson, J. L., & Love, D. M. (1993) Architecture of the Sierra Ladrones Formation, central New Mexico: Depositional controls on the permeability correlation structure. Geological Society of America Bulletin, 105, 998–1007.

Edwards, B. D., Ehman, K. D., Ponti, D. J., Reichard, E. G., Tinsley, J. C., Rosenbauer, R. J., & Land, M. (2009). Stratigraphic controls on saltwater intrusion in the Dominguez Gap area of coastal Los Angeles. In H. J. Lee & W. R. Normak (Eds.), Earth science in the urban ocean: the southern California continental borderland. Special Paper 454 (pp. 375–395): Boulder: Geological Society of America.

Emery, D., & Myers, K. (Eds.). (2009). Sequence stratigraphy. Malden, MA: Wiley.

Ezzy, T. R., Cox, M. E., O'Rourke, A. J., & Huftile, G. J. (2006) Groundwater flow modeling within a coastal alluvial plain setting using a high-resolution hydrofacies approach, Bells Creek plain, Australia. Hydrogeology Journal, 14, 675–688.

Fish, J.E. and M. Stewart. 1991. Hydrogeology of the Surficial Aquifer System, Dade County, Florida. U.S. Geological Survey Water-Resources Investigations Report 90– 4108.

Flint, S. S., & Bryant, I. D., (Eds.) (1993) The geological modeling of hydrocarbon reservoirs and outcrop analogues: International Association of Sedimentologists Special Publication 15. Oxford: Blackwell Scientific Publications.

Fogg, G. E. (1989) Emergence of geological and stochastic approaches for characterization of heterogeneous aquifers. In Proceedings R.S. Kerr Environmental Research Lab (EPA) Conference on New Field Techniques for Quantifying the Physical and Chemical Properties of Heterogeneous Aquifers.

Handford, C. R. & Loucks, R. G. (1993) Carbonate depositional sequences and systems tracts - responses of carbonate platforms to relative sea-level changes. In, R. G. Loucks & G. F. Sarg (Eds.), Carbonate sequence stratigraphy. Memoir 57 (pp. 3–41). Tulsa: American Association of Petroleum Geologists.

Hornung, J., & Aigner, T. (1999) Reservoir and aquifer characterization of fluvial architectural elements: Stubensandstein, Upper Triassic, southwest Germany. Sedimentary Geology, 129, 215–280.

Houston, J. (2004) High-resolution sequence stratigraphy as a tool in hydrogeological exploration in the Atacama Desert. Quarterly Journal of Engineering Geology and Hydrogeology, v. 37, p. 7–17.

Johnson, N. M. (1995). Characterization of alluvial hydrostratigraphy with indicator semivariograms. Water Resources Research, 31(12), 3217–3227.

Kerans, C. & Tinker, S. (1997) Sequence stratigraphy and characterization of carbonate reservoirs. Short Course No. 40: Tulsa: SEPM: Society for Sedimentary Geology.

Leeder, M. R. (1978) A quantitative stratigraphic model for alluvium with special reference to channel deposit density and interconnectedness. In A. D. Miall (Ed.) Fluvial sedimentology, Memoir 5 (pp. 1–47). Calgary: Canadian Society Petroleum Geology.

McCloskey, T. F., & Finnemore, E. J. (1996). Estimating hydraulic conductivities in an alluvial basin from sediment facies models. Groundwater, 34(6), 1024–1032.

McFarlane, P. A., Doveton, J. H., Feldman, H. R., Butler, J. J., Jr., Combes, J. M. & Collins, D. R. (1994) Aquifer/aquitard units of the Dakota Aquifer Systems in Kansas: Methods of delineation and sedimentary architecture effects on ground water flow properties. Journal of Sedimentary Research, B64, 464–480.

Miall, A. D. (1985) Architectural-element analysis: A new method of facies analysis applied to fluvial deposits. Earth Science Reviews, 22, 261–308.

Miall, A. D. (2006) Reconstructing the architecture and sequence stratigraphy of the preserved fluvial record as a tool for reservoir development: a reality check. American Association of Petroleum Geologists Bulletin, 90, 989–1002.

Miall, A. D. (2010). The geology of stratigraphic sequences (2nd Ed.). Heidelberg: Springer.

Middleton, G. V. (1978) Facies. In R.W. Fairbridge, & J. Bourgeois (Eds.) Encyclopedia of sedimentology (p. 323–325). Stroudsburg, Pa: Dowden, Hutchinson and Ross.

Missimer, T. M. (2001) Late Paleogene and Neogene chronostratigraphy of Lee County, Florida. In T. M. Missimer & T. M. Scott (Eds.), Geology and hydrogeology of Lee County, Florida. Florida Geological Special Publication 49 (pp. 67–90).

Mitchum, R. M., Jr., Vail, P. R., & Thompson, S., III, 1977. Seismic stratigraphy and global changes of sea-level, Part 2: the depositional sequence as a basic unit for stratigraphic analysis. In: C. E. Payton (Ed.), Seismic stratigraphy – Applications to hydrocarbon exploration. Memoir 26 (pp. 53–62). Tulsa: American Association of Petroleum Geologists.

Neton, M. J., Dorsch, J., Olson, C. D., & Young, S. C. (1994) Architecture and directional scales of heterogeneity in alluvial fan aquifers. Journal of Sedimentary Research, B64, 245–257.

Nishikawa, T., Siade, A. J., Reichard, E. G., Ponti, D. J., Canales, A. G., & Johnson, T. A. (2009). Stratigraphic controls on seawater intrusion and implications for groundwater management, Dominguez Gap area of Los Angeles, California, USA. Hydrogeology journal, 17, 1699–1725.

North, C. P. (1996) The prediction and modeling of subsurface fluvial stratigraphy. In P. A. Carling & M. R. Dawson (Eds.), Advances in fluvial dynamics and stratigraphy. Chichester, John Wiley & Sons.

Phillips, F.M., Wilson, J.L., and Davis, J.M., 1989, Statistical analysis of hydraulic conductivity distributions: A qualitative geological approach. In Proceedings Conference of New Field Techniques for Quantifying the Physical and Chemical Properties of Heterogeneous Aquifers (pp. 19–31). Dublin, Ohio: National Water Well Association.

Poeter, E., & Gaylord, D. R. (1990). Influence of aquifer heterogeneity on contaminant transport at the Hanford Site. Groundwater, 28(6), 900–909.

Ponti, D.J., Ehman, K. D., Edwards, B. D. Tinsley. J. C., III, Hildenbrand, T., Hillhouse, J. W., Hanson, R.T., McDougall, K., Powell, C. L., II, Wan, E., Land, M., Mahan, S., & Sarna-Wojcicki, A. M. (2007) A 3-dimensional model of water-bearing sequences in the Dominguez Gap Region, Long Beach, California. U.S. Geological Survey Open-File Report 2007-1013.

Posamentier, H. W., Summerhayes, C. P., Haq, B. U., & Allen, G. P. (1993) Sequence stratigraphy and facies associations. International Association of Sedimentologists Special Publication, 18. Oxford: Blackwell.

Posamentier, H. W., & Allen, G. P. (1999). Siliciclastic sequence stratigraphy: concepts and applications. Concepts in Sedimentology and Paleontology 7. Tulsa: SEPM.

Posamentier, H. W., & James, D. P. (1993). An overview of sequence-stratigraphic concepts: uses and abuses. Sequence stratigraphy and facies associations. In H. W. Posamentier, C. P. Summerhayes, B. U. Haq, & G. P. Allen (Eds.), Sequence stratigraphy and facies associations: International Association of Sedimentologists Special Publication 18 (pp. 3–18), Oxford: Wiley-Blackwell.

Reading, H. G. (Ed.) (1986a) Sedimentary environments and facies (2nd Ed): Oxford: Blackwell Scientific Publishing.

Reading, H. G. (1986b) Facies. In H. G. Reading (Ed.), Sedimentary environments and facies (2nd Ed) (pp. 4–19). Oxford: Blackwell Scientific Publishing.

Scharling, P. B., Rasmussen, E. S., Sonnenborg, T. O., Engesgaard, P., & Hinsby, K. (2009) Three-dimensional regional-scale hydrostratigraphic modeling based on sequence stratigraphic methods: a case study of the Miocene succession of Denmark: Hydrogeology Journal, 17, 1913–1933.

Schlager, W. (2005) Carbonate sedimentology and sequence stratigraphy. Concepts in Sedimentology and Paleontology 8. Tulsa: SEPM: Society for Sedimentary Geology.

Selley, R. C. (1985) Ancient sedimentary environments and their subsurface diagenesis (3rd Ed.). Ithaca: Cornell University Press.

Selley, R. C. (2000) Applied sedimentology. San Diego: Academic Press.

Sloss, L. L. (1963) Sequences in the cratonic interior of North America. Geological Society of America Bulletin, 74, 93–114.

Stalkup, F. I. (1986) Permeability variations observed at the faces of crossbedded sandstone outcrops. In L. W. Lake & H. B. Carroll Jr. (Eds.) Reservoir characterization (pp. 141–175). San Diego: Academic.

Sugarman, P. J., Miller, K. G., Browning, J. A., Kulpecz, A. A., McLaughlin, P. P., Jr., & Monteverde, D. H. (2005) Hydrostratigraphy of the New Jersey Coastal Plain: Sequences and facies predict continuity of aquifers and confining units. Stratigraphy, 2, 259–275.

Sugarman, P. J., & Miller, K. G. (1997) Correlation of Miocene sequences and hydrogeologic units, New Jersey Coastal Plain. Sedimentary Geology, 108, 3–18.

Vail, P.R., Mitchum, R.H., Jr., & Thompsom, S., III (1977a) Seismic stratigraphy and global changes in sea level, Part 3: Relative changes in sea level from coastal onlap. In C. E. Clayton (Ed.), Seismic stratigraphy – Application to hydrocarbon exploration. Memoir 26 (pp. 63–81). Tulsa: American Association of Petroleum Geologists.

Vail, P.R., Mitchum, R.H., Jr., & Thompsom, S., III (1977b) Seismic stratigraphy and global changes of sea level, Part 4: Global cycles of relative changes in sea level. In C. E. Clayton (Ed.), Seismic stratigraphy – Application to hydrocarbon exploration. Memoir 26 (pp. 83–97). Tulsa: American Association of Petroleum Geologists.

Van Wagoner, J. C., Mitchum, R. M., Campion, K. M., & Rahmanian, V. D. (1990), Siliciclastic sequence stratigraphy in well logs, cores, and outcrops: concepts for high-resolution correlation of time and facies. Methods in Exploration Series 7. Tulsa: American Association of Petroleum Geologists.

Van Wagoner, J. C., Posamentier, H. W., Mitchum, R. M. J., Vail, P. R., Sarg, J. F., Loutit, T. S., & Hardenbol, J. (1988). An overview of the fundamentals of sequence stratigraphy and key definitions. In C. K. Wilgus, B. S. Hastings, C. G. St. C. Kendall, H. W. Posamentier, C. A. Ross, & J. C. Van Wagoner (Eds.), Sea-level changes: An integrated approach. Special Publication 42 (pp. 39–45). Tulsa: SEPM.

Walker, R. G. (1984) General Introduction: Facies, facies sequences and facies models. In R. G. Walker (Ed.), Facies models (2nd Ed.). Geoscience Canada Reprint Series 1 (pp. 1–9). Toronto: Geological Association of Canada Publications.

Walker, R. G. (2006) Facies models revisited. In H. W. Posamentier & R. G. Walker (Eds.), Facies models revisited. Special Publication No. 84 (pp. 1–17): Tulsa: SEPM (Society for Sedimentary Geology).

Ward, W. C., Cunningham, K. J., Renken, R. A., Wacker, M. A., & Carlson, J. I. (2003) Sequence-stratigraphic analysis of the Regional Observation Monitoring Program (ROMP) 29A test corehole and its relation to carbonate porosity and regional transmissivity in the Floridan Aquifer System, Highlands County, Florida. U.S. Geological Survey Open-File Report 03-201.

Webb, E. K. (1994) Simulating three-dimensional distribution of sediment units in braided stream deposits. Journal of Sedimentary Research, B64, 219–231.

Webb, E. K. (1995). Simulation of braided channel topology and topography. Water Resources Research, 31, 2603–2611.

Webb, E. K., & Anderson, M. P. (1996) Simulation of preferential flow in three-dimensional, heterogeneous conductivity fields with realistic internal architecture. Water Resources Research, 32, 533–545.

Chapter 3
Siliciclastic Aquifers Facies Models

Siliciclastic aquifers are composed of sediment and rock that are dominated by silicate minerals, particularly quartz, feldspar, and clays. Siliciclastic aquifer properties are controlled by the grain size, sorting, and diagenesis of the sediments. Well-sorted sand and gravel facies deposited by flowing water and air tend to have the highest hydraulic conductivities and form aquifers, whereas low-energy clay-rich facies form confining and semiconfining strata. Facies models are provided for fluvial, alluvial fan, delta, eolian, glacial, and linear terrigenous shoreline (beach and barrier) depositional systems. Very large (multiple orders of magnitude) variations in hydraulic conductivity occur on multiple scales. A key issue for aquifer characterization is the connectivity and orientation of both clean sandy aquifer strata and clay-rich confining strata, which varies between depositional facies.

3.1 Introduction to Siliciclastic Aquifers

The hydraulic conductivity of siliciclastic deposits is largely a function of their depositional texture, which includes grain size, sorting, and matrix (clay and silt) content, and their mineralogical composition and subsequent diagenetic history. The composition of siliciclastic sediments depends upon the type of rock present in their source area, the extent of weathering and transport processes that remove the more chemically and physically unstable grains, and hydrodynamic conditions within the depositional environment, which control (in part) the grain size and sorting of the sediments. Siliciclastic sediments are classified primarily on the basis of their grain size and grain composition. The terms 'clay' and 'sand' technically refer to a specific size range of particles (Table 3.1). For example, terms such as 'medium sand' and 'medium-grained' have precise meanings, referring to a mean grain diameter of between 0.25 and 0.5 mm. Siliciclastic rocks have four main components: grains, matrix, cement, and porosity. The particle size boundary

Table 3.1 Grain size terminology of Folk (1974)

Terminology	Size (diameter) mm
Pebble	4–64
Granule	2–4
Very coarse sand	1.0–2.0
Coarse sand	(1/2) 0.5–1.0
Medium sand	(1/4) 0.25–0.5
Fine sand	(1/8) 0.125–0.25
Very fine sand	(1/16) 0.0625–0.125
Silt	(1/256) 0.0039–0.0625
Clay	<0.0039 ($\approx$4 l m)

between grains and matrix is usually placed at 30 µm (Dott 1964; Folk 1974), which is approximately the boundary between coarse and medium silt. Matrix thus consists of medium silt to clay-sized material in which individual grains are not visible to the naked eye. Cement is minerals that precipitated within pore spaces.

The main grain types in most sands and sandstones are quartz (Q), feldspar (F), and rock fragments (R). Rock fragments are also referred to as lithic (L) fragments. The composition of sandstones is commonly displayed using ternary QFR or QFL diagrams. The still widely used Dott (1964) classification scheme classifies sandstones based on their QFR ratio and percent matrix (Fig. 3.1). The similar sandstone classification of Folk (1974) is also widely used (Fig. 3.2). Dott (1964) used the term 'arenite' to describe sandstones that contain less than 15 % matrix in the intergranular pore spaces. Sandstones containing between 15 and 75 % matrix are referred to as 'wackes' and rocks with more than 75 % matrix are called 'mudstones'. For example, sandstones composed of greater than 95 % quartz grains with less than 15 % matrix are referred to as quartz arenites. Quartz is more resistant to chemical weathering and erosion than both feldspars and rock fragments. As sand is transported and weathered, its composition approaches the quartz pole of the QFR diagram and is said to increase in compositional maturity.

The porosity and permeability of siliciclastic aquifer systems are controlled by four main factors:

- primary depositional texture
- compaction
- cementation
- dissolution of unstable mineral phases.

The primary depositional texture is the grain size, sorting, and matrix content of the sediment. In general, the highest permeabilities occur in relatively coarse-grained, well-sorted sediments, with very little or no matrix. Fine-grained sediments with low matrix contents have intermediate permeabilities. The lowest permeabilities occur in rocks with high matrix contents, which include muds (and their lithified equivalents, mudstones and shales) and sands in which the intergranular space is filled with matrix (i.e., wackes) or cement.
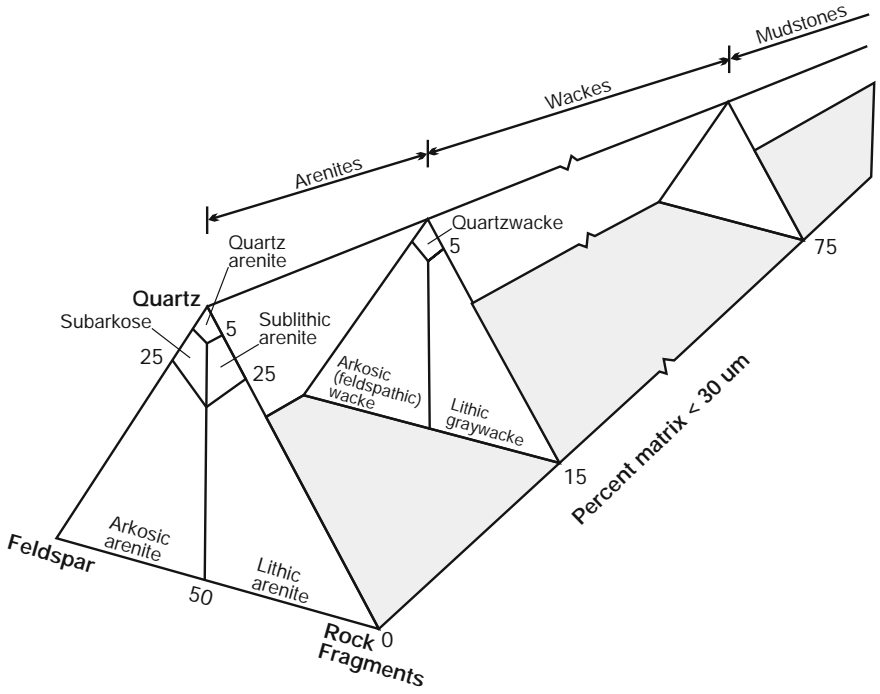
Fig. 3.1   Dott (1964) sandstone classification system

Fig. 3.2   Folk (1974) sandstone classification system
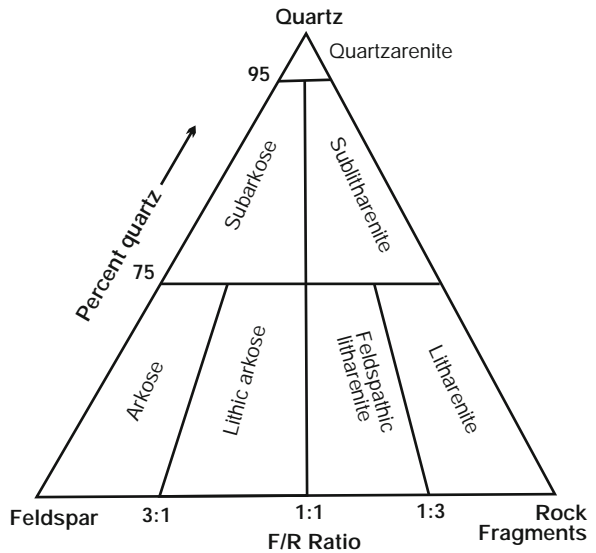
Compaction results in a tighter grain packing and associated reduction in porosity and permeability. Compaction can occur by the reorganization of grains into a tighter configuration, which is referred to as consolidation. Softer grains, such as rock fragments, may be plastically deformed and, in extreme cases, form what is referred to as pseudomatrix. The precipitation of cements results in the reduction in porosity and can have a disproportionate effect on reducing permeability if the initially precipitated cement fills pore throats.

The minerals that compose siliciclastic aquifers are generally poorly reactive in the sense that their rate of reaction is extremely slow under near-surface temperature, pressure, and chemical conditions. For example, groundwaters are commonly undersaturated with respect to quartz, but the rate of quartz dissolution is exceeding slow under near-surface water chemistry, temperature, and pressure conditions. Similarly, feldspars undergo alteration to form clay minerals, but the reaction is slow in most aquifers. Many of the accessory minerals found in siliciclastic sediments (e.g., zircon, tourmaline, rutile, ilmenite) are also poorly reactive. Hence, the enhancement of porosity and permeability by dissolution is generally not important under the chemical conditions typically occurring in aquifers. However, dissolution reactions can be important in deeply buried strata associated with oil and gas deposits.

Heterogeneity in siliciclastic aquifers is usually controlled primarily by depositional textural variations (i.e., differences in grain size and sorting). Primary variations in porosity and permeability may be either attenuated or amplified by diagenesis. Primary textures are related to the depositional environment, so understanding the depositional history of an aquifer and associated distribution of sediment types is a key element in the development of conceptual and numerical models of siliciclastic aquifers.

The principal values of facies analyses in siliciclastic aquifer systems lie in the insights it can provide on the distribution and continuity of transmissive clean (i.e., matrix poor) sand and gravel bodies that serve as aquifers or aquifer zones, and matrix-rich lithologies that act as semiconfining and confining units. The main siliciclastic depositional types that serve as aquifers are summarized in this chapter, and references are provided to more detailed discussions. It is worth noting that many of the key papers in the field date from the middle 1970s through the 1980s, which was arguably the golden age of sedimentological research that was driven by the needs of the oil and gas industry during that boom period. Some siliciclastic depositional environments, such as deep marine and lake (lacustrine), are either not addressed or only briefly mentioned because they uncommonly form significant aquifers.

3.2   Fluvial Systems

The term 'fluvial' refers to the actions of rivers or streams, whereas the related, more general term 'alluvial' refers to the action of flowing water. Alluvium refers to sediment deposited by flowing water, as in a river or stream bed, floodplain, or delta. In practice, more precise terms are preferred. For example, if a sediment or sedimentary rock was deposited by a river, then the preference is to refer to the deposits as 'fluvial' rather than 'alluvial'.

Fluvial aquifer systems can be broadly characterized based upon the dominant channel types (bed load, mixed load, or suspended load) and the erosional or aggradational nature of the main-stem (trunk) stream (Schumm 1977; Galloway and Hobday 1996). Three main channel types are recognized, which should be considered end members: anastomosing, meandering, and braided (Table 3.2). The two most common types of rivers are meandering (high sinuosity) and braided (low sinuosity).

River type depends upon a number of variables including channel slope, water flow (average and flood), bank stability, and sediment load (supply and grain size). A number of generalizations have been proposed in the sedimentology literature on the controls of channel type. However, Bridge (2001, 2003, 2006) cautioned that the correlation between channel pattern, type of sediment load, and bank stability is not generally supported by the data. Instead, the key control over whether a river is meandering or braided is the amount of water and sediment supplied during seasonal floods (Bridge 2001).

Alluvial aquifers may consist of either ancient river deposits or may be related to modern rivers. Sharp (1988) discussed the characteristics of large-scale floodplain alluvial systems associated with modern rivers in North America. The river systems were profoundly influenced by Pleistocene glacial events, with associated changes in sea level, discharge, and sediment supply. During times of lowered sea level, large rivers became entrenched in their present alluvial valleys. The shape and size of deposits depend upon the erosional relief and the nature of the eroded substrate

Table 3.2   Summary of fluvial channel types (after Galloway and Sharp 1998)

Channel type	Channel fill sediment	Channel geometry	Main deposits	Aquifer geometry
Bed load	Mostly (50–90 %) sand	Commonly braided	Channel and channel flank	Sheets or broad tabular belts of permeable sand
Mixed load	Sand (30–60 %), silt and clay	Meandering	Channel fill and varied floodplain	Irregular or beaded belts of permeable sediments
Suspended load	Very fine grained, low sand content	Highly sinuous to anastomosing	Swamp, lacustrine, muddy levee, crevasse splay and channel	Isolated permeable ribbons

(Collinson 1986a). Sharp (1988) divided the alluvial deposits into top stratum and substratum. The top stratum consists of the active channel, meander belt, and floodplain or basin and includes a variety of levee, point bar, crevasse splay, lacustrine, and overbank deposits. The substratum consists of coarse-grained sediments deposited atop the bedrock base of the valley and tends to have an overall upward decrease in grain size.

Fluvial deposits have a great degree of variability. A general pattern is that fluvial systems tend to be the setting of the deposition of relative-high hydraulic conductivity, often continuous, sand bodies that are elongate down-dip (i.e., roughly parallel to the river trend). The channel sands are surrounded, to varying degrees, by lower hydraulic conductivity floodplain muds. The basic element of facies analysis of fluvial aquifers is mapping the location of channel sands. Hall (1976), in an early example of a hydrofacies investigation of a fluvial system, mapped net sandstone thickness in Lower Cretaceous sandstone aquifers (Hosston and Hensel sandstones) in north-central Texas using electric and gamma ray logs, driller logs, borehole cuttings, and outcrop studies. Paleotopography influenced the location of channels and, thus, the accumulation of medium- to coarse-grained channel sands. Flow net analysis indicates that preferred groundwater flow paths coincide with the trends of maximum sandstone thickness. A wave-dominated delta sand facies was also identified, which is oriented parallel to strike (i.e., roughly normal to the channel sand orientation).

An important goal of facies analysis is developing the capability to predict the geometry of channel sands and sandstone from limited well data. One method is to estimate channel belt width from mean bank-full channel depth, which, in turn, is estimated from channel bar or dune height (Bridge and Mackey 1993; Bridge 2001, 2006). The application of facies analysis toward determination of the hydrogeology of fluvial deposits is far from an exact science. Bridge (2001) cautioned that it may not be possible to interpret specific fluvial depositional environments from logs alone and that there may not be an unambiguous relationship between depositional environment and the three-dimensional geometry of deposits formed in the environment. Nevertheless, it is important to appreciate that ambiguity and uncertainty are inherent in subsurface analyses, which can be reduced, but not completely eliminated, through methods such as facies analysis.

Miall (1985) introduced the architectural element analysis method, which is based on the thesis that at the scale of smaller macroform elements (up to about a few hundred meters in length and width), there are about eight basic architectural elements defined by grain size, bedform composition, internal sequences, bounding surfaces, and external geometry, which are:

- channel
- lateral accretion
- sediment gravity flow
- gravel bar and bedform
- foreset macroform
- sand bedform

- laminated sand sheets
- overbank fines

An attraction of the architectural element analysis is that the diversity of sediment types present in fluvial aquifer systems is reduced to just eight elements. A three-dimensional model of a fluvial aquifer would consist of a mosaic of the different architectural elements. The architectural element analysis approach has been adopted in some groundwater modeling studies of fluvial aquifer systems with the eight elements corresponding to hydrofacies and, in turn, model cell blocks. The major limitation of the architectural element analysis approach in groundwater investigations is that satisfactory definition of architectural elements requires outcrops at least several tens of meters in width in order to reveal cross-sectional geometry (Miall 1985). Vertical profiles, such as generated from well data, are of little use for the purpose of studying architectural elements (Miall 1985). A more general (fewer categories) architectural element approach is typically appropriate for groundwater investigations based on the more limited information available from well data.

3.2.1 Meandering River Facies

The meandering river is a classic facies model that well illustrates the potential applications of the facies model concept to groundwater resources investigations. Meandering river facies models and river facies models, in general, were reviewed by Reineck and Singh (1980), Cant (1982), Walker and Cant (1984), Collinson (1986a), Jordan and Pryor (1992), Miall (1996), and Bridge (2003), and are presented in sedimentology textbooks. Meandering rivers are characterized by wave-like channel loops or bends in which erosion occurs at the outer (concave) side (cutbank), and deposition occurs at the inner (convex) side, which is called the point bar (Figs. 3.3 and 3.4). The channels of meandering rivers tend to be relatively narrow and deep. Meandering rivers tend to occur in settings with relatively low-hydraulic gradients and discharges, high suspended load/bed load ratios, and cohesive bank materials.

Deposition occurs within both channel and overbank environments. Point bars grow laterally (lateral accretion deposits) and in the downstream direction. During flood events, fine sediments (clays, silts, and fine sands) are deposited on the adjacent floodplains (vertical-accretion deposits, overbank sediments). The floodplain is the strip of land that borders a stream channel and is normally inundated during seasonal floods. Floodplains consist of a variety of deposits (both fine- and coarse-grained) that have evidence for changes in flow velocity and desiccation. Depending upon the local environment, floodplain sediments may include plant debris, soil layers, plant and animal trace fossils, and non-marine fossils, such as bivalves, gastropods, vertebrates, and arthropods.

Fig. 3.3 Aerial photographs of meanders in the West Fork of the White River, north of Petersburg, Indiana, USA. The overall flow direction (arrow) is toward the south. Sand deposition occurs at convex point bars (which appear light colored) and erosion occurs on opposing concave cut banks (source U.S. Department of Agriculture)

As the river sediments accumulate within and adjacent to the channel (i.e., aggradation occurs), the river channel system builds up above the level of the surrounding floodplain. Eventually, a levee break occurs and the river abandons its current channel and establishes a new one. Crevasse splays are alluvial fan-like deposits that are laid down at the site of levee breaks. Channel abandonment, referred to as 'avulsion,' leads to the deposition of a series of channel deposits that roughly parallel the depositional slope. The abandoned channel loops are called 'oxbow' lakes (Fig. 3.4b) and tend to be filled with very fine-grained overbank sediments (silts and clays). Clay plugs deposited in oxbow lakes are important in that they provide resistance to lateral channel migration. Abandoned channels may contain either fining-upwards or coarsening-upwards facies sequences. Coarsening-upwards sequences may occur due to the progradation of crevasse splays into floodplain basins and lakes. Shales in abandoned channels tend to have

Fig. 3.4   Colorado River near
its headwaters in Rocky
Mountain National Park,
Colorado, USA. a Gravel and
cobble point bar (right) and
cut bank (left) on the
meandering channel.
b Oxbow lake isolated from
active channel

shoestring morphology and do not form regional confining units (Selley 1985).
Channel sandstones and adjoining floodplain mudstone or shale deposits are
commonly red-colored due to an oxic diagenetic environment (Fig. 3.5).

   Meandering rivers, through the avulsion process, results in the deposition of
relatively narrow or tabular bodies of sand (i.e., shoestring or ribbon sands) that are
elongated roughly in the direction of river flow. The sands deposited by lateral
accretion are surrounded by low-hydraulic conductivity overbank sediments
deposited on the floodplain (Fig. 3.6). Connectivity of sand deposits is a key issue
in water resources development as it controls large-scale aquifer properties. The
degree of interconnection of the channel sand deposits depends upon the rate of
aggradation, frequency of avulsion, and channel depth. Where the rate of aggra-
dation is low, meandering channels may completely or partially rework earlier
deposited channel sands. A key attribute of meandering river deposits is that the
lateral accretion can result in the deposition of continuous sheets of sand within a
river channel whose margins are no longer visible (Reading 1986).

Fig. 3.5 Fluvial red beds (Triassic) exposed near Breckenridge, Colorado, USA (bar scale is approximately 1 m)
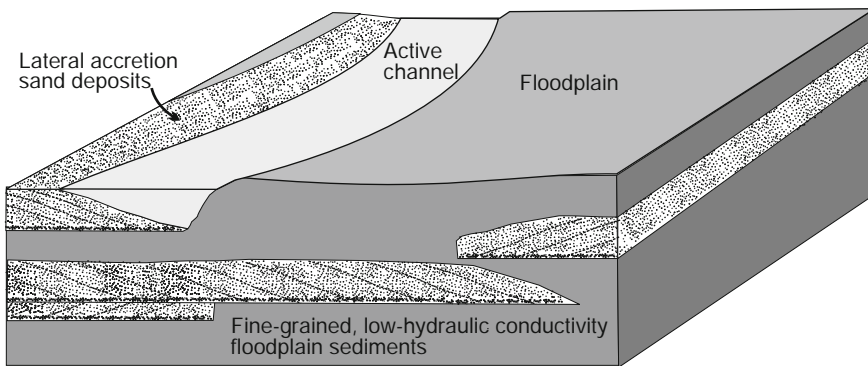
Fig. 3.6 Conceptual diagram of meandering stream deposits (not to scale). Elongate bodies of relatively coarse-grained lateral accretion deposits that constitute aquifers are juxtaposed with finer-grained grained vertical-accretion deposits

The general facies model diagram for a meandering stream is the classic fining-upwards lateral accretion sequence, which consists of five main facies, from the base upwards (Fig. 3.7):

- basal lag deposits consisting of coarse material that can be transported only during floods
- trough cross-stratified sands
- ripple cross-stratified sands
- parallel laminated sands

Fig. 3.7 Meandering river lateral accretion (point bar) facies model. The upwards decrease in grain size corresponds to a decrease in hydraulic conductivity

Plant root traces

Flood plain mud deposits

Ripple cross-bedded sands

Trough cross-bedded sands

Parallel-laminated sands

Basal lag deposit

Erosional contact

5 to 10 m

Hydraulic conductivity
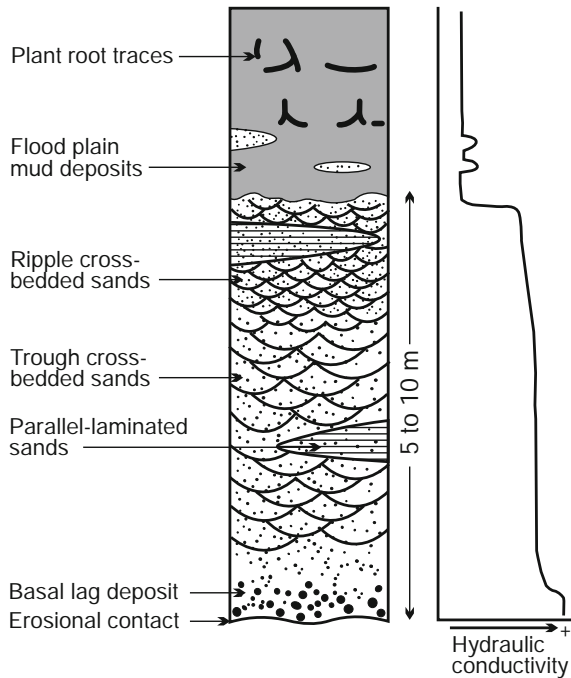
- muds that may contain plant fossils, desiccation cracks, carbonate nodules (caliche), and lenses and layers of sands.

Coal seams may form where plant material is abundant on floodplains. The meandering river facies model is characterized by an upwards fining of grain size, which will normally result in a concomitant upwards decrease in hydraulic conductivity. The lateral accretion deposits constitute the aquifer, whereas the muddy vertical-accretion deposits may form confining or semiconfining units. A characteristic feature of meandering river depositional systems is the high degree of textural variability, ranging from extremely high-permeability, clast-supported sands and gravels and extremely low-permeability silts and clays (Cant 1982).

From a study of reach of the Mississippi River, Jordan and Pryor (1992) recognized six hierarchal levels of heterogeneity, which were related to the hierarchal elements of petroleum reservoirs. The six levels are, in order of decreasing scale,

(1) entire meander belt system
(2) meander scroll, which consists of bodies of sand isolated from the laterally contiguous sand bodies by low-permeability abandoned clay plugs
(3) individual channel point bar and crevasse-splay deposits, which are separated by mud sheets associated with ponding at high river stages
(4) lobe sheets, which are sand bodies in point bars separated by thick sheets of mud and silt

(5) bedding units
(6) laminae.

The main reservoir or aquifer units are high-hydraulic conductivity point bar deposits and crevasse-splay sands. Low-permeability heterogeneities (i.e., mud and silt layers) at all levels within a fluvial meander system are the principal control on horizontal and vertical hydraulic conductivity and thus fluid flow (Jordan and Pryor 1992).

Aquifer characteristics depend upon the properties of the sediments deposited within an individual channel and the stacking and degree of amalgamation of channel deposits, which are determined by a combination of channel types and regional aggradation rate (Galloway and Sharp 1998). As a river laterally migrates across a floodplain, early deposited fluvial sediments are reworked to varying degrees. Preservation of channel deposits depends upon the elevation of superimposed erosion surfaces. The likelihood of the preservation of the lower parts of channel bar deposits increases with the vertical depositional rate relative to the channel lateral migration rate and the variability of channel scour depth and bar thickness (Bridge 2006). If the proportion of channel bar deposits to total deposits exceeds about 0.75, then all channel belts are connected and act as a single hydraulically connected sandstone body that has a width equal to the floodplain width (Bridge 2006).

3.2.2 Braided-Stream Facies

Braided streams, compared to meandering streams, are relatively straight, wide, and shallow. They are characterized by the presence of numerous dunes and bars in the channel, which during low flow periods, dissect (divides) the flow in a braided pattern (Fig. 3.8). The channel divides and rejoins around sand and gravel bars. The entire channel may be submerged during high-flow (flood) periods. Braided-stream facies were reviewed by Miall (1977, 1996), Cant (1977, 1982), Cant and Walker (1978), Rust (1978), Best and Bristow (1993), Walker and Cant (1984), Collinson (1986a), and many later published textbooks. Braided streams and their associated deposits are diverse and there are multiple facies models.

A characteristic feature of braided streams is that sand and gravel are transported mainly as bed load, while finer-grained sediments remain in suspension. Deposition of suspended sediments on inter-channel areas is minor. Braided streams are relatively unstable because the floodplain banks are thinner and more erodible than other channel types. Lateral channel migration coupled with aggradation leads to the deposition of sheet sands and gravels. Fine-grained overbank or floodplain deposits are relatively thin and uncommon.

Systems with low aggradation rates and high degrees of channel mobility experience a high degree of reworking of earlier deposited sediments. Scour pools form where the flow velocity is sufficiently high to locally mobilize sediments. The

Fig. 3.8 a Aerial photograph
of the braided Platte River
near Omaha, Nebraska, USA.
Flow direction (arrow) is to
the south (source U.S.
Geological Survey).
b Shallow braided stream at
Great Sand Dunes National
Monument, Colorado, USA
(note people on far bank for
scale)
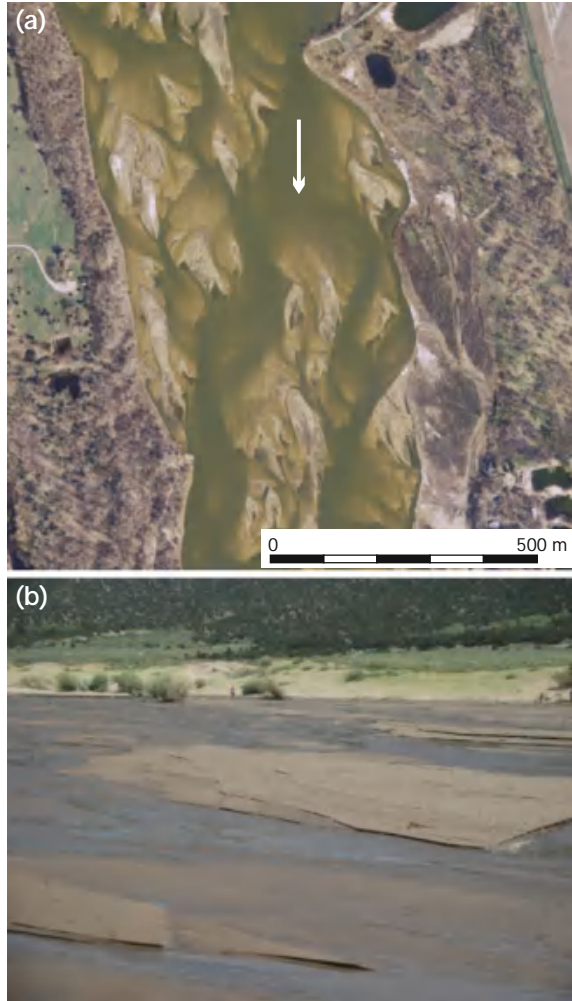
pools are later filled with cross-bedded sands. Scour fill deposits have the greatest
chance of being preserved in the geologic record because they are the deepest
deposits (Beres et al. 1999). A combined outcrop and GRP study of coarse-grained
braided-stream deposits in Switzerland indicated that most of analyzed architectural
elements were trough-shaped scour pool deposits (Beres et al. 1999). The basic
feature of braided-stream deposits is that they are composed predominantly of
planar or cross-bedded sands and gravels. Variations in grain size occur between
beds, which results in heterogeneity with respect to hydraulic conductivity.

3.2.3   Hydrogeology of Alluvial Aquifers

The key technical issue for alluvial aquifers is the pattern and organization of sandy and gravelly alluvium, particularly the distribution of coarse-grain (aquifer) and fine-grained (confining and semiconfining) strata. Galloway and Sharp (1998) described six types of aquifer heterogeneity in alluvial sediments

(1) external boundaries of sand bodies with less permeable strata
(2) variable degrees of interconnection (compartmentalization) of individual permeable units
(3) internal stratification within permeable units
(4) lateral and vertical trends or spatial variation of porosity and permeability within permeable units
(5) variable continuous low-permeability layers within permeable units
(6) permeability anisotropy.

Heterogeneity increases with decreasing scale of facies units and increasing mud or shale in the system (Galloway and Sharp 1998). Strong permeability contrasts occur between channel fill and floodplain deposits. Channel connectivity increases with percent sand. Steams may also exhibit a strong skin effect with river beds being lined with material with a much lower hydraulic conductivity than the underlying alluvial aquifer. Braided-stream deposits tend to be sheet-like, thick, laterally extensive, and composed predominantly conglomerates and coarse sands.

As fluvial deposits inherently have a high degree of fine-scale heterogeneity, the effective properties of much larger scale model blocks will be upscaled average values of the various component lithologies. Bierkins and Werts (1994) presented an up-scaling method for determining the effective hydraulic conductivity of cross-bedded point bar deposits from geometric parameters (spacing and orientation of lateral accretion surfaces) and permeability data from sands and bounding layers. The geometric data in shallow aquifers may be obtained from surface geophysics (e.g., GPR; Lesmes et al. 2002).

There has been considerable interest in the development of models that can be used to predict the architecture of subsurface fluvial deposits, which has been driven by their importance as hydrocarbon reservoirs. The basic modeling procedures consists of (Bridge 2006)

(1) determination of the geometry, proportional and location of different sediment body types (e.g., sandstones and shales) using well and geophysical data
(2) interpretation of the origin of the sedimentary bodies through a facies analysis
(3) prediction of sedimentary bodies characteristics using data from outcrop analogs
(4) stochastic modeling to simulate the alluvial architecture and properties of the sediment or rock between wells.

Some geostatistical methods that have been developed and employed to predict facies distributions between wells are discussed in Chap. 20. A key attribute of

fluvial systems that needs to be captured in geostatistical analyses is the continuity of sand bodies in the downslope direction, which can result in a significant anisotropy in transmissivity. Where local solute transport is of concern, it is important to have a sufficiently detailed field program to locate and map channel deposits and other features that may impact local groundwater flow.

3.3 Alluvial-Fan Deposits

3.3.1 Alluvial-Fan Facies

Alluvial conglomerates are minor components of the overall stratigraphic record, but are locally important aquifers, especially in mountainous arid lands. Alluvial fans are wedge-shaped sediment bodies that form where a river course passes from an area of high slope to one of low slope (Fig. 3.9). Alluvial-fan deposits were

Fig. 3.9 Alluvial fans. a Sangre De Christo Mountains, north of Alamosa, Colorado, USA. b Death Valley National Park, California, USA. The Death Valley fans extend into a playa with evaporite deposits
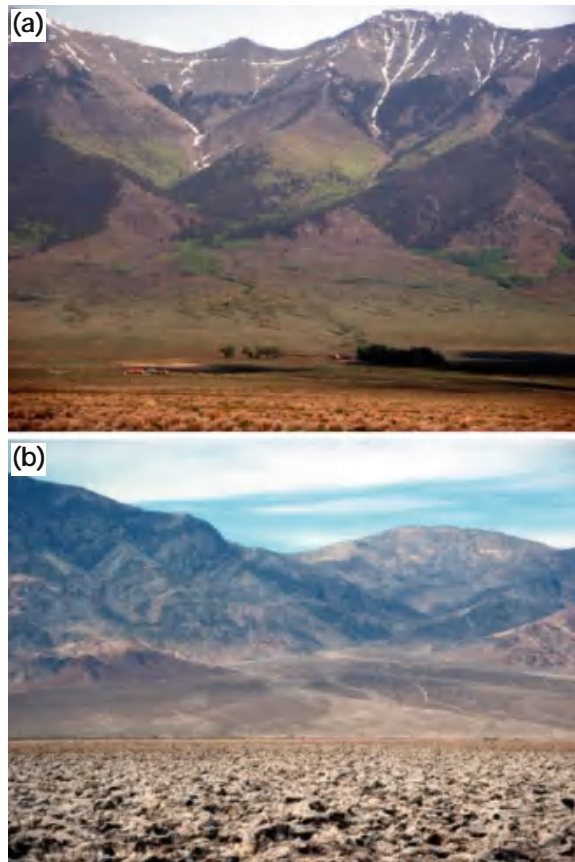
summarized by Bull (1972, 1977), Heward (1978), Cehrs (1979), Nielsen (1982), Rust and Koster (1984), Collinson (1986a), Blair and McPherson (1994), Neton et al. (1994), and McCloskey and Finnemore (1996) and are addressed in general sedimentology textbooks. Although alluvial fans are common in desert mountain regions, and fans in these regions have received a disproportionate amount of research interest, alluvial fans may occur in any climatic environment (Harvey et al. 2005).

Alluvial fans are best developed where streams or mass flows emerge from a confined valley or gorge into a lower-lying basin. The abrupt change in slope results in a rapid decrease in flow energy and bed shear stress, which leads to localized sediment deposition. Lack of confinement allows for horizontal expansion and deceleration of flow, and the deposition of some or all of the suspended sediment load. The deposited sediments are angular, poorly sorted, and coarse-grained because of their origin from fractured bedrock, a short transport distance to the fan, and the rapid and catastrophic nature of the active sediment-transport mechanism (Blair and McPherson 1994). Alluvial fans usually have their greatest thickness where a stream or streams enter a basin. Fans laterally merge into bajadas, and complex facies relationships may developed between coalescing fans (Nielsen 1982). The characteristic morphological features of alluvial fans are (Blair and McPherson 1994) a semiconical shape, restricted radial length, plano-convex cross-profile, and comparatively high radial slope.

The morphology, location, and composition of alluvial fans reflect to a large degree the interaction of climate and tectonism. Climate strongly influences flood power and sediment supply. Tectonism controls sediment production in the source area and the location and morphology of alluvial fans through its influence on topography and accommodation. The high relief of catchments is well suited for creating flash floods (Blair and McPherson 1994). Tectonism and climate interact to control sediment supply and whether a fan is prograding or retrograding, which in turn, determines whether the sediment deposits coarsen or fine upwards. Progradation of alluvial fans in a tectonically stable or gradually faulted setting, results in deposits with an upward increase in grain size and sorting. Periodic or episodic uplift can result in the stacking of coarsening- or fining-upwards sequences, depending upon local tectonic, climatic, and sedimentological dynamics. The stacking pattern and bedding characteristics of alluvial fan sequences is controlled by highly variable external factors, and there is usually no recognizable, repetitive vertical succession for alluvial-fan deposits (Neton et al. 1994).

The geomorphology and successions of deposited sediments of alluvial fans reflect the interaction between factors that influence (Harvey 2005, and reference therein) including

- fan context (tectonics, gross topography, accommodate space)
- water and sediment delivery to the fan (basin geology and relief and climate)
- the relationship between the fan and adjacent environments (base level).

The characteristics of alluvial-fan deposits that can be used for their identification in the geologic records include (Nielsen 1982)

- proximity to a structural high
- overall textural immaturity
- sparse fossil content (typically limited to plants and vertebrate bones),
- very poorly sorted coarse-grain deposits with large variations in grain size (clay to boulders)
- presence of both poorly sorted stream-flow deposits and unsorted debris-flow and mudflow deposits.

Early deposits in incipient fans include rock falls, rock slides, rock avalanches, and colluvial slides, which create a tallus slope characterized by a high slope and short radial length (Blair and McPherson 1994). Alluvial fans can be divided into a proximal, mid-fan, and distal facies (Fig. 3.10). The proximal facies consists of sediments deposited near the area of stream emergence from upland areas and contains the coarsest sediments (Fig. 3.11a). The proximal facies commonly contains an entrenched inner valley extending outwards onto the fan from the feeding mountain stream (Nielsen 1982). The proximal facies contains coarse-grained stream sediments, finer-grained inter-channel deposits and coarse debris-flow and landslide deposits.

The mid-fan and distal fan contains numerous distributary channels that radiate outwards from the inner-fan valley. The distributary channels are shallow and most commonly braided. The mid-fan facies contains more abundant better-sorted sands and gravels (Fig. 3.11b). The distal facies was deposited in the lower and outer parts of fan and contain finer-grained sediments. The distal alluvial-fan facies commonly grades into fluvial sediments deposited in alluvial plains. Large debris and mudflow deposits may extend a great distance down fan, and these mud-rich units can act as confining units amidst more transmissive sorted sands and gravels (Neton et al. 1994).
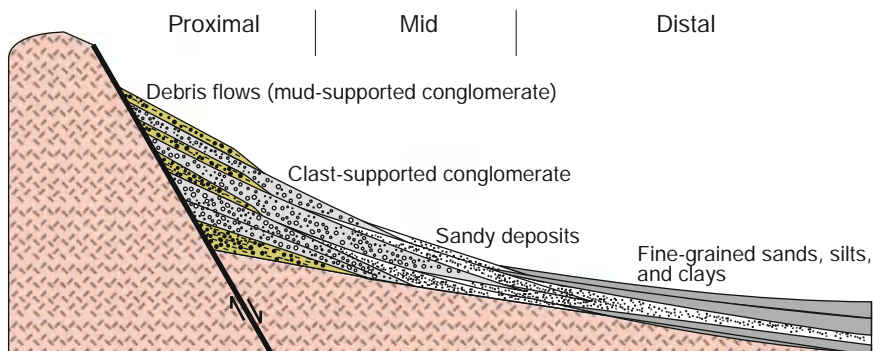
Fig. 3.10 Alluvial-fan cross-sectional diagram (after Rust and Koster 1984)

Fig. 3.11 Alluvial-fan
sediments. a Proximal fan
coarse debris-flow deposit,
White Tank Mountain Park,
near Phoenix, Arizona (scale
is approximately 1 m).
b Sandy alluvial-fan deposits,
Death Valley National Park,
California (lens cap for scale)
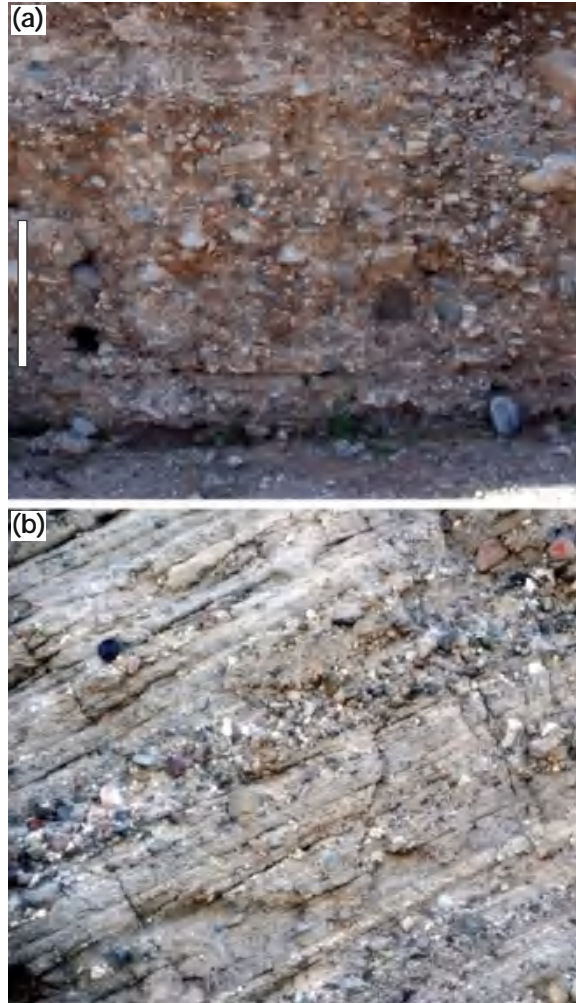
Three main fan coarse conglomerate facies types occur in alluvial fans (each of which contain variations) (Nielsen 1982; Rust and Koster 1984; Collinsion 1986b):

- framework-grain supported facies, which are deposited by aqueous flows (e.g., stream flows) that are energetic enough to keep sand in suspension
- stratified matrix (sand) supported facies, which are indicate of lower energy aqueous deposits
- unstratified matrix (sand and mud) supported facies, which indicate debris-flow (or mudflow) deposition.

Volumetrically, the two main sediment types in well-developed alluvial fans are debris-flow and sheet-flood deposits. Debris flows have a dense, viscous, clayey

matrix. The high viscosity of debris flows results in very poorly sorted deposits with large clasts 'floating" in the fine-grained matrix. Debris flows are relatively impermeable and occur in areas where the sediment source provides abundant muddy material, where slopes are steep and vegetation scarce, and rainfall is irregular. Sheet-flood deposits are a couplet with a lower coarse gravel and over-lying laminated finer-grained sandy member (Blair and McPherson 1994). Sheet-flow deposits are typically sand with little clay, fairly well sorted, and stratified (Nielsen 1982). A less common deposit is sieve-flow gravels through which flood waters completely infiltrate before reaching the fan fringe (Nielsen 1982).

3.3.2   Alluvial-Fan Hydrogeology

Alluvial fans are a critical source of freshwater in arid and semiarid lands. They are a major site of recharge and form excellent aquifers (Nielsen 1982). Alluvial fans have a high degree of variability in textural maturity and thus hydraulic conduc-tivity. Hydraulic conductivity can vary abruptly by over 12 orders of magnitude. Gravelly mud units have hydraulic conductivities in the range of 10^{-10}–10^{-5} cm/s. Sand and gravels without a mud matrix have hydraulic conductivities in the range of 10^{-5}–10^{2} cm/s (Neton et al. 1994). Transmissivity of alluvial-fan aquifers depend upon both the hydraulic conductivity of the sediments and the degree of connection of the more conductive matrix-poor sand and gravel units.

   The down-fan decrease in energy results in a corresponding decrease in grain size and bed thickness, which is manifested by an increase in abundance of sands and finer-grained beds at the expense of conglomerates. The down-fan decrease in grain size would be expected to result in a corresponding decrease in transmissivity. However, the proximal fan deposits (mud flows and debris flows) actually tend to have the lowest hydraulic conductivity and transmissivity (Cehrs 1979; Neton et al. 1994; McCloskey and Finnemore 1996). Down-fan sediments may be better sorted than upper-fan mudflow and debris deposits and may thus have greater hydraulic conductivities (Cehrs 1979; Neton et al. 1994). Alluvial-fan deposits contain interbedded stream-flow and debris-flow deposits, which is a source of a higher degree of heterogeneity. Stream-channel deposits consisting of sand and gravel occur where the flow is channelized. The channel deposits tend to be lenticular and may have a higher hydraulic conductivity than adjoining deposits due to a lower fine-grained matrix content.

   Middle-fan areas may retain the highest transmissivity due to better sorting and greater connectivity of the more conductive sand and gravel beds. Characterization of alluvial-fan aquifers thus requires consideration of both scale-dependent and directional heterogeneity in hydraulic conductivity. Directional heterogeneity occurs within fans, between fans (parallel to depositional strike), and cross-fan (perpendicular to strike; Neton et al. 1994).

Alluvial-fan systems are also characterized by fining and/or coarsening-upwards sequences of multiple scales, which reflect climatic variation, tectonics (periodic uplift), and sedimentological processes. Weissmann et al. (2005) proposed that erosion-bounded sequences of sediments in alluvial (fluvial) fans in the San Joaquin Basin of California are similar to sequences that develop in marine environments. Climatic variability appears to have been an important control in the development of sequences through its influence on the ratio of sediment supply to stream discharge. The sequence concept is proposed to result in a predictable distribution of facies that could aid in hydrogeological studies of alluvial-fan deposits (Weissmann et al. 2005).

3.4   Deltas

Deltas form where rivers enter a sea, lake, or other standing-water body and lose their competence to carry sediments. The rate of deposition of clastic sediments must also be greater than the rate at which the sediments can be dispersed by marine processes. Three main types of deltas are recognized based on the type of energy conditions at the river mouth: river- , wave- , and tide-dominated (or influenced). However, the delta types are actually end members and most deltas have mixed influences. In most deltas, the delta plain receives dissimilar rates of sediment supply, and it is not unusual for one part of a deltaic shoreline to be rapidly prograding seaward, while other parts are subject to reworking by marine processes (Coleman and Prior 1982). Deltaic rocks are important hydrocarbon reservoirs and have a received a great deal of study. Delta facies are summarized by Coleman and Prior (1982), Miall (1984), and Bhattacharya (2006).

Ancient deltas do not contain distinctive, diagnostic lithofacies, but rather consist of assemblages of lithofacies, each of which can occur in other depositional environments (Miall 1984). For example, distributary channel deposits are analogous to fluvial deposits. The identification of distributary channel sands as such is typically based on the sedimentological context of the sediments, particularly adjoining facies. Identification of deltaic sediments may not be possible based on a limited number of borehole data points.

The best known deltas are the river-dominated Mississippi (Fig. 3.12) and Nile deltas, which have the archetypical triangular shape. The main channel subdivides at the coast into multiple distributary channels. The characteristic environmental condition of river-dominated deltas are that tidal and longshore currents are weak, and the deltas tend to rapidly prograde seawards as sediment is deposited at the river mouth. Sediment deposition reflects a seawards decrease in energy. Fine-grained sediments are deposited as river energy decreases.

Deltas have three main geomorphic environments of deposition (Fig. 3.13):

- subaerial delta plain (topset)
- delta front (foreset)
- prodelta (bottomset)
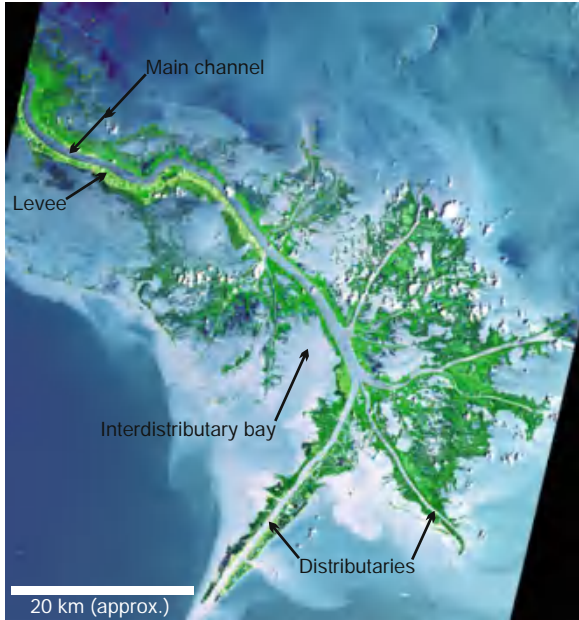
Fig. 3.12 Satellite image of the Mississippi River delta showing its dendritic distributary system (source NASA)
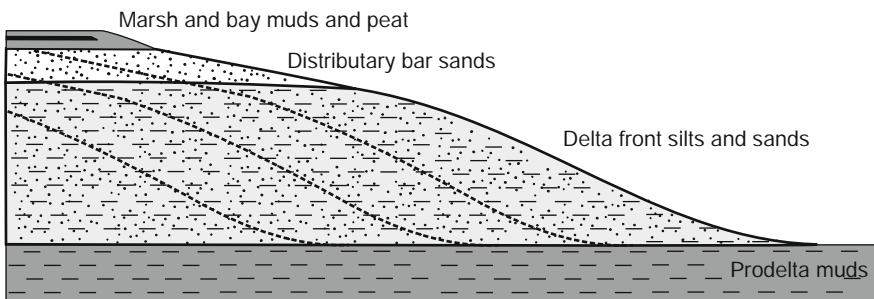
Fig. 3.13 Facies diagram of a river-dominated delta

The delta plain contains a wide variety of non-marine to brackish subenvironments such as distributary channels and levees, swamps, marshes, tidal flats, lagoons, and interdistributary bays. Interdistributary areas are less sandy than channels and commonly contain a series of relatively thin, stacked coarsening-upwards and fining-upwards successions, which can contain either freshwater, brackish, or marine biofacies.

The main site of sand deposition is the distributary-mouth bars at the delta front. Flow expansion and associated deceleration occurs resulting in the deposition of the bedload. Silts and clays remain largely in suspension and may be transported much greater distances than the bedload. Silts and clays are deposited out of suspension seawards of the distributary mouth in the prodelta environment and also on levees and in adjoining bays and marshes. Prodelta sediments typically have a lesser degree of bioturbation than nearby marine sediments, with the degree of bioturbation depending upon the sedimentation rate.

The characteristic facies sequence of river-dominated deltas is the progradational coarsening-upwards sequence (Fig. 3.13), whose thickness ranges from several to tens of meters (to greater than 100 m) depending upon the sediment load of the river and the depth of water of the receiving basin. The main depositional facies are the prodelta muds, which are overlain by delta-front silts and sands, and then distributary-mouth bar sands. The sequence is topped by delta-marsh deposits, which may include muds, peats, and eolian dune deposits.

Delta deposition involves the progradation, avulsion, and abandonment of distributary lobes and compaction and subsidence of earlier deposited sediments. The delta facies sequences may be overlain by another progradation sequence, a thick sequence of fine-grained marsh and bay deposits, or marine deposits.

Both wave- and tide-dominated deltaic systems are characterized by the reworking of earlier deposited sediments. Waves rework shoreline sediments and transport them along the direction of longshore drift currents. The resulting deposits are sandy beach ridges oriented parallel to the shore. Tide-dominated deltas experience reversing currents, which tend to rework sediments into a series of parallel linear or digitate ridges that are oriented parallel to the direction of tidal currents (Miall 1984). Ridges are separated by linear tidal channels. Tide-dominated deltaic deposits may be identified by evidence of reversed flow direction, such as herringbone cross-stratification. In the case of both wave- and tide-dominated deltas, fine sediments (silts and clays) are deposited offshore and in deltaic marshes.

The geometry of sand deposits varies depending upon the delta types and the degree of reworking of sediments. River-dominated sediments tend to result in the deposition of elongated sand bodies (e.g., shoestring sands) that are oriented perpendicular to the shore, whereas sand bodies in wave-dominated deltas tend to be orientated parallel to the shore. Deltaic environments have a high degree of heterogeneity with respect to permeability due to the juxtaposition of subenvironments with very different energy levels and thus, grain sizes, and the avulsion of distributary channels and thus, the main loci of sand deposition. Attempts to correlate delta facies must be carried out with care because of the numerous lateral facies changes.

3.5   Eolian Sand Deposits

Eolian (also spelled aeolian) sediments are deposited by the wind rather than water. Modern eolian sands are deposited in two main environments, sandy deserts and coastal dunes. The most prominent feature in eolian environments is sand dunes. Other important deposits are interdune sediments and sheet sands, which are deposited marginal to the dune complex. There are a wide variety of different eolian dune deposits ranging from small ripples, to dunes, and large compound dunes (mega-dunes or draas; Fig. 3.14). Dunes also vary in their size, shape, and orientation with respect to the predominant wind direction (either parallel or transverse). The size and geometry of dunes are controlled by both the wind regime and availability of sand (Brookfield 1984). Eolian sand deposition are also controlled by topography. The sand seas (ergs) of the Sahara tend to form in topographic depressions where the sand becomes trapped.

Most modern deserts are equilibrium surfaces in that sediments are being reworked with no net deposition (Selley 1985). Only about 25 % of deserts are covered with sand dunes. Sand dunes are dynamic environments and dunes are rarely preserved in the geological record intact. Many (if not most) recent large desert dune deposits are not in equilibrium with the present wind pattern due to Quaternary glacial climate change. Typically, only the lowest part of eolian bedforms are preserved (Brookfield 1984). Long-term preservation requires that the body of eolian strata be placed below some regional baseline of erosion, beneath which erosion does not occur (Mountney 2006). The rates of generation of accommodation and sediment accumulation are fundamental for the preservation of eolian deposits (Mountney 2006).

The sedimentary textures and structure of eolian deposits were reviewed by Ahlbrandt and Fryberger (1982), Selley (1985), and Mountney (2006). A characteristic feature of dune deposits is good sorting as wind energy is typically too low to transport granule-sized material and fines are blown away (Selley 1985).

Fig. 3.14 Very large compound dunes (draas), Great Sand Dunes National Park, Colorado, USA (note people for scale)

Fig. 3.15 Deflation surface
(desert pavement), Aruba

Wind is an efficient sorter of sediment on account of the low density and viscosity
of air. The normal size range for wind-driven sand bedload is 0.1–1 mm with a
modal size of about 0.3 mm (Collinson 1986a).

Eolian sediments are characterized by the absence of pebbles and clays and no
signs of aqueous biota (marine or non-marine). Sand is often well-rounded and may
have large-scale cross-bedding. Smaller-scale ripple-cross lamination may be
superimposed on the larger scale cross-bedding. Sedimentary structures may also be
preserved related to the avalanching of sand down the slip face of the dune
(Ahlbrandt and Fryberger 1982). Interdune areas may contain desert pavement (lag
deposits or deflation surfaces; Fig. 3.15), coarse-sand sheets, and small isolated
dunes and ripples.

Interdune environments may be either dry, damp, or wet. In the case of the latter
two, sedimentation is influenced by or controlled by moisture (Selley 1985;
Mountney 2006). In damp interdune environments, the depositional surface is in
contact with the capillary fringe and is characterized by a range of adhesion
structures and traces of plants and animals. In wet or flooded interdune environ-
ments, the water table occurs above the depositional surface for protracted periods
of time. Wet interdune deposits may include lacustrine deposits, desiccation fea-
tures, and plant and animal trace fossils. Interdune areas may form permeability
barriers where cemented by calcite, ferrocrete, or silcrete (Selley 1985). Sheet sands
often do not have a distinct dune form and are characterized by low- to
moderate-angle cross-stratification (Ahlbrandt and Fryberger 1982).

Eolian sands can generally be classified into three main sediment types
(Ahlbrandt 1979; Brookfield 1984):

- Well sorted to very well-sorted fine coastal dune sands
- moderately well to well-sorted fine to medium-grained land dune sands
- poorly sorted interdune and desert pavement (serir).

A hierarchy of bounding surface occurs within eolian deposits, which include (Brookfield, 1977; Mountney 2006)

- reactivation surfaces, which result from periodic lee-slope erosion followed by renewed sedimentation associated with a change in bedform migration direction, speed, asymmetry, or steepness,
- superimposition surfaces, which result from either the migration of superimposed dunes over a larger parent bedform or the migration of scour troughs on the lee slope of a bed form
- interdune migration surfaces, which result from the migration of bedforms separated by interdunes
- supersurfaces, which are laterally extensive surfaces formed by bypass or deflation.

A general facies model for eolian sand is moderately to well-sorted fine to medium-grained sands that contain multiple generations of bounding surfaces and laminations (Fig. 3.16). Internal structures include large-scale cross-bedding, planar laminations, ripple-cross laminations and grain-fall laminations. Marine fossils typically are absent. Inland dune deposits (analogous to model Saharan ergs) may have great geographic extent.

Fig. 3.16 General eolian facies diagram
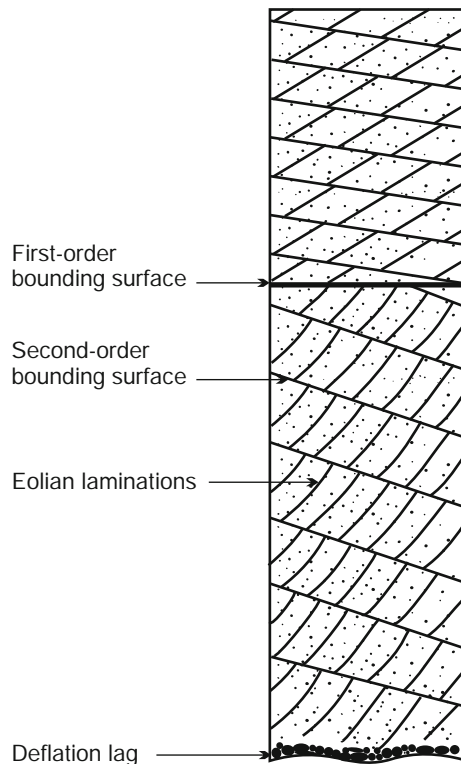
In general, eolian facies are more homogeneous than most other facies. However, Ahlbrandt and Fryberger (1982) cautioned that eolian deposits can be more complex than often considered. Permeability contrasts occur on a bed-by-bed basis, which creates an anisotropy that favors flow along rather than perpendicular to bedding. The permeability anisotropy may also be increased by preferential cementation of some laminae. Interdune and extradune deposits may also form impermeable or less permeable units interspersed with cross-bedded units, which could result in a vertical compartmentalization.

Eolian sands occur as either lenticular sand bodies or, more commonly, as sheet-like sand bodies. Sheet-like sand bodies in the Permian and Triassic of northwestern Europe and the Permian and Mesozoic of the southwestern USA are many hundreds of square kilometers in area and have thicknesses of hundreds of meters (Collinson 1986b). Extensive, thick sheets of eolian sands belonging to the Jurassic Aztec Formation are very well exposed near Las Vegas, Nevada, USA (Fig. 3.17a), and the Permian Schnebly Hill Sandstone and Coconino Sandstones are very well exposed in the Sedona area of Arizona, USA (Fig. 3.17b).

Fig. 3.17 a Massive eolian sandstones (Jurassic), Red Rock Canyon, near Las Vegas, Nevada, USA. Boundary between large cross-bedding sets is evident (dashed line). b Massive eolian sandstones (Permian), Sedona, Arizona, USA (note people for scale)
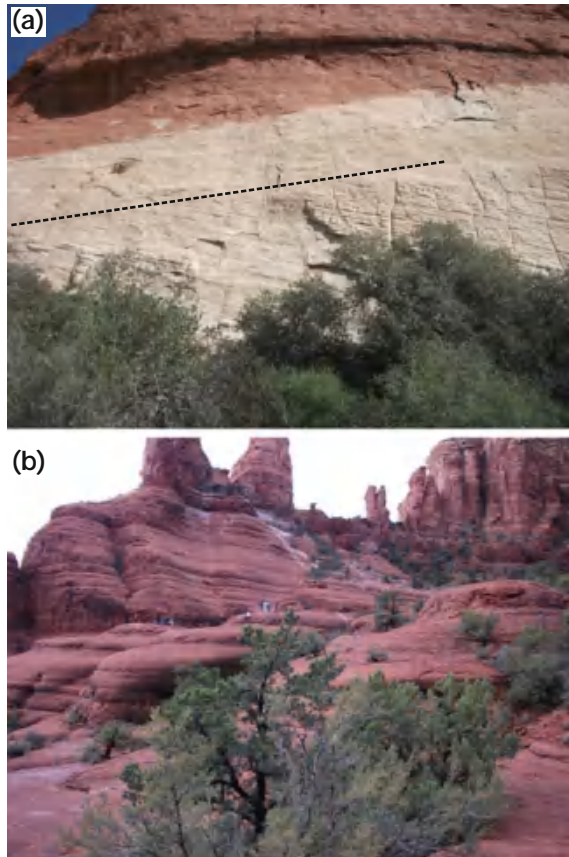
A minipermeameter study of Middle Jurassic eolian deposits from the Page Sandstone of Arizona, revealed a five orders of magnitude range in permeability (Chandler et al. 1989). The greatest contrast in permeability occurred between dune and interdune facies. Grain-flow sands had a greater mean permeability (7,829 md) than wind-ripple sands (2,289 md) and extra-erg and interdune deposits (665 md). A key observation is that bounding surfaces, especially the more extensive ones, form permeability barriers and tend to compartmentalize reservoirs and aquifers.

Four scales of heterogeneity with respect to permeability were recognized (Goggin et al. 1988; Chandler et al. 1989):

1st order: between eolian and non-eolian depositional facies
2nd order: geometric interrelationships and rock properties of dune, interdune, and sand sheet deposits
3rd order: internal arrangement of stratification types within individual dune cross-sets
4th order: microscope scale associated with the unique fabrics of eolian stratification types

The higher order scales of heterogeneity would be incorporated into groundwater models as anisotropy.

3.6 Lake (Lacustrine) Deposits

Lacustrine deposits tend to be fine grained and thus form confining units rather than aquifers. The deposits consist of sediments that settled out of suspension and traction deposits. Deltas form where rivers enter lakes, and turbidity currents may originate at deltas. Lakes may also be the site of carbonate mineral precipitation (limestone deposition). The key factors that control lake deposition are the degree of aridity and amount of sediment input.

A characteristic feature of lacustrine deposition is annual cyclicity that consists of a fine-scale alternation of sediment-rich and organic matter-rich layers, which is referred to as 'varves'. Siliciclastic sediments are brought into lakes during rainy periods and organic matter settles out with little dilution by siliciclastic sediments during dry periods (Selley 1985). In arid environments, evaporite minerals may also be present. Lacustrine deposits may be distinguished from deep-water marine deposits by an absence of marine fauna, presence of varves, and association with non-marine deposits. The Eocene Green River Formation in the western United Sates contains varved lacustrine deposits, which are very well known for their local extraordinary preservation of non-marine fish, plant, insect, and animal fossils (Fig. 3.18a).

Lacustrine deposits can have great thickness depending on local geological conditions. For example, the Late Miocene to early Pliocene Verde Formation (Fig. 3.18b) in north-central Arizona has a maximum thickness of over 600 m

Fig. 3.18 a Fish fossils in
the Eocene Green River
Formation, Wyoming, USA
(source U.S. National Park
Service. b Ancient American
Indian (Sinaguan) cliff
dwelling constructed in the
lacustrine Verde Formation,
which contains both
fined-grain limestone and
siliciclastsic deposits,
Montezuma′s Castle National
Monument, Arizona, USA.
Secondary porosity is well
developed in the limestone
strata
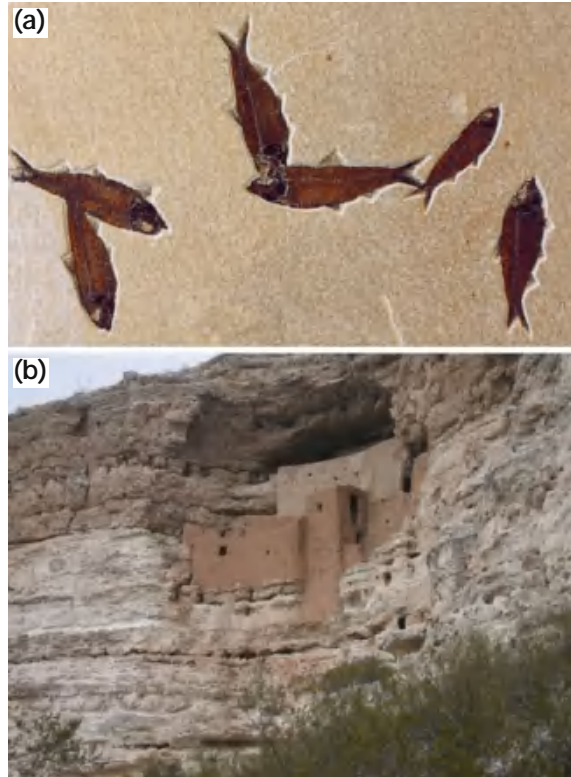
(Twenter and Metzger 1963). The Verde Formation is lithologically diverse, con-
taining fine-grained carbonate and siliciclastic deposits and, locally, evaporites. The
fine-grained lithologies are nearly impermeable, but groundwater is produced from
joints and solution cavities in limestones (Twenter and Metzger 1963). Dissolution
of evaporites can locally result in high groundwater salinities.

3.7   Glacial Sediments

Glacial sedimentary environments are described by Easterbook (1982), Eyles and
Miall (1984), Ashley et al. (1985), Edwards (1986), and Stephenson et al. (1988).
The surficial sediments in many high-latitude areas were deposited in glacial
environments. Glacial aquifer systems are characterized by complex boundary
conditions and often extreme internal heterogeneities on various scales, which
control groundwater flow and solute (contaminant) migration (Edwards 1986;
Stanford and Ashley 1998; Flemming 1998a, 1998b). Abrupt permeability contrasts
often occur.

Glaciers are unique sedimentary agents because (Stanford and Ashley, 1998)

• they deposit sediments on an entire subaerial landscape of irregular topography, not just base-level-controlled sedimentary basins
• they entrain, transport, and ultimately deposit sediments of all grain sizes
• they generate large volumes of meltwater that vary in discharge and location, both in time and space,
• they continuously encounter and create new topography as the move
• ice is the substrate and supporting material for sediments, which can create high-standing inverted sediment deposits upon melting.

A characteristic deposit of glaciers is diamicton, or diamict (sediment) and diamictite (rock), which is a generic term for poorly sorted gravel, sand, and mud deposits. Diamictons are the most common glacial sediment, but not all diamictons have a glacial origin. Debris-flow deposits are an example of a non-glacial diamicton. Glacial sediments occur in both continental and marine environments and encompass a diversity of deposits. Continental glacial sedimentary deposits include ground-ice, glaciofluvial, glaciolacustrine, and periglacial facies (Fig. 3.19). As a generalization, sediments deposited directly from ice are poorly sorted and unstratified diamictons, whereas sediments indirectly deposited by ice, such as deposits of meltwater streams and lakes, are better sorted and stratified.

Glacial tills, which are diamicton that deposited in direct contact with ice, is the most distinctive continental glacial facies (Fig. 3.20). Glacial tills include (Easterbrook 1982)
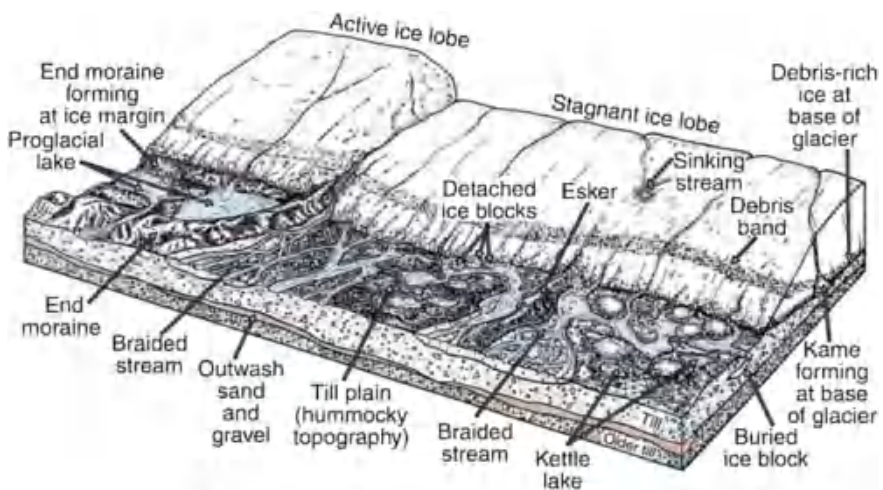
Fig. 3.19 Diagram of continental glacial sedimentary environments (from Illinois State Geological Survey 2008 and Lyle 2009)

Fig. 3.20 Glacial till near
Alma, Colorado USA. Note
the coarse size of clasts and
very poor sorting

- lodgement tills, which are deposited subglacially from basal debris-laden ice
- ablation tills, which are debris dumped on the land surface as ice melts away
- flow tills, which consists of debris that flowed off the glacial ice as mud flows.

Lodgement tills have characteristics of deposition under high-basal sheer stress such as a strong preferred direction of the long axis of clasts parallel to the ice flow vector (Easterbrook 1982; Eyles and Miall 1984). Ground-ice deposits include eskers, which are diamicton deposits in meltwater tunnels within and under the ice mass. Subglacial (lodgement) tills are characterized by (Easterbrook 1982; Edwards 1986)

- diamictons with often bimodal particle size distributions
- volumetrically almost entirely massive (not stratified)
- can be traced for at least several kilometers
- several meters to tens of meters thick
- contain a variety of clast types, some which may be faceted or striated

- may contains lenses of stratified sorted sediments and horizons of color or textural banding
- preferred orientation of long axes of elongated particles
- relatively high degree of compaction from weight of overlying ice
- erratic lithologies of stones and heavy minerals.

Glacial sediments consist of materials eroded by the glacier and materials that dropped onto the glacier from an adjoining valley. The composition of tills depends upon the composition and erodibility of intrabasinal and extrabasinal sources (Edwards 1986). Quaternary glacial environments often experienced several advances and retreats of glaciers. Glacial deposits thus reflect a complex record of multiple advances and spatial and temporal heterogeneity of depositional conditions during each advance (Stephenson et al. 1988). Advance and retreat of glaciers resulted in the horizontal and vertical juxtaposition of different glacial environments and associated sediment types and hydrogeological units (Stanford and Ashley 1998). Adjacent till deposits may have contrasting textures and composition, which can be used for correlation.

Glaciofluvial facies consists of glacial debris reworked by flowing water in broad outwash plains located beyond the terminus of the main ice mass. Glaciofluvial sediments are typically braided-stream deposits that are similar to other braided-stream sediments deposited in non-glacial environments (Eyles and Miall 1984; Edwards 1986; Heinz et al. 2003). The deposited strata consist of sands, sandstones, and conglomerates of varying stratification and sorting ranging from poor to excellent (Edwards 1986). Some general trends are a downgradient decrease in grain size, increase in sorting, and an overall reduction in hydraulic conductivity (Anderson 1989). The scale of the deposits is also highly variable. Regional accumulations attain thickness of 10 s of meters, widths of 10 s of km, and lengths of 100 s of km (Edwards 1986). Glaciofluvial deposits resemble humid alluvial-fan deposits in which braided streams are dominant and grade downstream into normal fluvial deposits. A glaciofluvial origin may be indicated that the proximity to till deposits and the presence of deformation structures related to the melting of buried ice.

Glaciolacustrine facies consists of sediments deposited in lakes either in direct contact with a glacier (proglacial) or downgradient within the outwash plain (periglacial). A characteristic feature of periglacial lakes is varves, which are seasonally formed horizontal couplets of clay and silt (Eyles and Miall 1984). In addition to fine-grained sediments that settled out of suspension, glacial lakes may also contain current-deposited (deltaic) sediments and, in proglacial lakes, ice-rafted debris. Glaciolacustrine depositional environments may be identified by intercalated diamicton beds and the presence of dropstones (i.e., clasts released by melting ice).

Periglacial facies include a diversity of deposits including eolian deposits (windblown silt, termed loess), mass-wasting products, and structures diagnostics of permafrozen ground (e.g., ice-wedge features; Eyles and Miall 1984). Marine glacial deposits are characterized by a greatly enhanced sediment supply and ice-rafted deposits. Downslope resedimentation is an important process. Proximal

marine glacial deposits consist of a wide range of diamicton facies including coarse-grained subaqueous fan deposits, ice-rafted sediments, and suspended deposits (Eyles and Miall 1984; Edwards 1986). There is a general seaward increase in marine deposition, which is manifested by marine fossils.

Sedimentary bed geometry varies with position with respect to the glacial and basin geometry (Stanford and Ashley 1998). For example, horizontally extensive tabular glaciofluvial deposits may form downgradient from glacial margins. Beaded or ridged deposits, such as moraines, eskers, and lacustrine deltas, may form at the glacial margin or in subglacial environments. Fine grained, basin-filling sediments may be deposited in glacial lakes and form confining units. Major groundwater sources commonly occur in valleys in which thick deposits of glaciofluvial sediments (outwash) and till accumulated (Stephenson et al. 1988).

Sedimentary characteristics and their hydraulic properties (mean grain size and sorting) depend upon the transporting agent (ice, water, or wind) and conditions with the depositional environments. The diversity of deposits results in numerous lithological discontinuities, which is perhaps the single most important factor affecting the overall hydrogeology of glacial terrains (Stephenson et al. 1988). The main aquifers in glacial deposits are often glaciofluvial outwash deposits (sands and gravels) and sandy diamictons that have a high-hydraulic conductivity (Stephenson et al. 1988). Clay-rich diamictons and lacustrine deposits, on the contrary, tend to have low-hydraulic conductivities and may act as semiconfining units. Basal tills may also have relatively low-hydraulic conductivities due to a high degree of compaction (over-consolidation) from the weight of the previously overlying ice. Fracture and weathering (pedoegeneis) can increase the hydraulic conductivity of low-hydraulic conductivity units (Stephenson et al. 1988). Geographically restricted bodies of high-hydraulic conductivity sediments often occur amidst low-hydraulic conductivity sediments (Stephenson et al. 1988).

Stanford and Ashley (1998) recommended that characterization of glacier aquifers should start with a geomorphic analysis (Stanford and Ashley 1998). The next step is identification and mapping of sediment bodies that have major hydraulic conductivity contrasts and their bounding surfaces. Investigation of internal hydraulic conductivity variability within mapped units is then performed. Variability in hydraulic conductivity within sedimentary packages is much less than within aquifers as a whole. Statistical and probabilistic methods, if used, are applied on the component pieces of the aquifer system, rather than on the much more variable bulk sediment packages of the aquifers.

Flemming (1998a, b) described glacial terrains as including both (1) sequences or groups of genetically related sequences that reflect deposition in a particular suite of sedimentary environments and (2) the overlying landscape, whose configuration is typically an indicator of the nature of the underlying sedimentary deposits. In glacial terrain analysis, individual lithostratigraphic units (e.g., individual sand and clay beds) are less significant than the overall depositional sequences or depositional setting. Landforms provide insights into the underlying geology and are important in their being responsible for hydraulic gradients and the location of recharge and discharge areas.

3.8 Linear Terrigenous Shorelines

Linear terrigenous shorelines occur where marine currents are strong enough to redistribute land-derived sediments. The depositional facies, such as bar and beach deposits, are oriented parallel to the shore. The type of shoreline locally present depends upon numerous factors with the following being most important (Selley 1985; Elliott 1986; Clifton 2006)

- physical regime (waves, tidal currents, and longshore currents)
- sediment supply
- climate
- tectonic setting
- sea level (whether locally rising, falling, or stable).

Depending upon the above factors, a beach may be in either a state of dynamic equilibrium, growing seawards (prograding), or experiencing net erosion (retreating). Beaches may be locally both prograding and retreating at a given geographic location (e.g., different parts of a barrier island). Beach sands tend to accumulate in settings in which headlands and other natural and anthropogenic features disrupt the longshore transport of sands (Fig. 3.21).

Linear terrigenous shorelines have four main environments (Table 3.3; Clifton 2006; Selley 1985):

- fluviatile coastal plain
- lagoon and tidal flat
- barrier islands and strand plains
- offshore marine shelf

Fluviatile coastal plains contain meandering or braided rivers with typical facies (Sect. 3.2). Fluvial sediments are characterized by a continental biota.

Fig. 3.21 Beach deposition between headlands, Western Australia near Albany
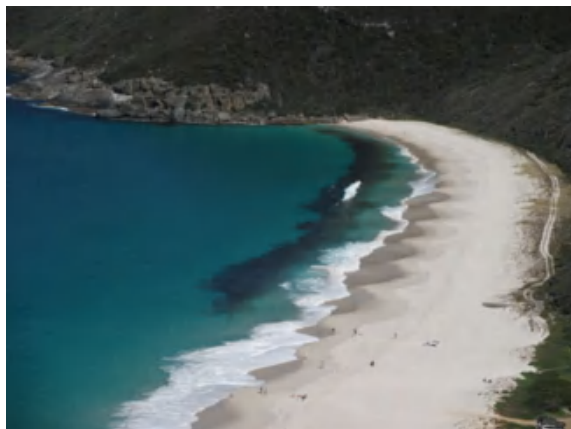
Table 3.3 Barrier island and strand plain facies progradational succession (after Selly 1985 and Clifton 2006)

Depth	Environment	Facies
Supratidal—non-marine	Fluviatile coastal plain	Meandering or braided river; continental biota
Supratidal—subtidal	Backshore	Freshwater to hypersaline facies such as tidal flat, lagoon, eolian
Intertidal	Foreshore	Flat-bedded sands
Subtidal	Shoreface	Mixed mud and storm-deposited sands; transitional to sandy foreshore
Deep subtidal	Shelf	Bioturbated marine muddy sediments
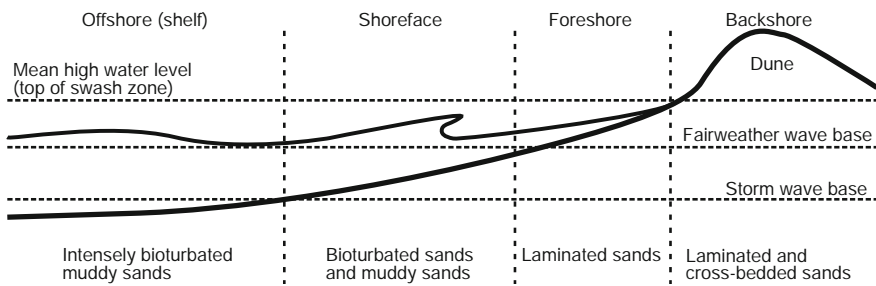
Fig. 3.22 General beach profile

The basic facies model is a shallowing- and coarsening-upwards progradational succession from shelf, to shoreface and foreshore, and then to backshore deposits (Figs. 3.22 and 3.23). The beach and shoreface have a concave upwards profile with a break in slope marking the shoreface-shelf transition. However, Clifton (2006) cautioned that the boundary between the shoreface and shelf is often considered to mark the fair-weather wave base, but this relationship is not always correct. The typical progradational (regressional) facies sequence consists of offshore deposits overlain by shoreface and then beach deposits. Progradation sequences have an overall upwards increase in grain size (decrease in silt and clay content), which results in a corresponding increase in hydraulic conductivity. Transgressive facies sequences have lagoonal, tidal channel, and washover deposits overlain by backshore (eolian dune) and beach deposits.

The classic shallowing-upwards sequence is most likely to be preserved in subsiding basins. Barrier island and strandplain sedimentation, by definition, occurs in shallow-marine environments and thus is especially sensitive to eustatic sea level changes and changes in sediment supply. In the absence of accommodation, barrier islands and strandplain deposits will likely undergo erosion (with the formation of unconformities) and redeposition.

Fig. 3.23 Prograding
(shallowing-upward) beach
facies model

Cross-bedded
eolian sands

Seaward-dipping
planar-laminated
sands

Mostly bioturbated
sands

Bioturbated
muddy sands

Backshore

Foreshore

Shoreface

Shelf

5 to 20 m

Hydraulic
conductivity
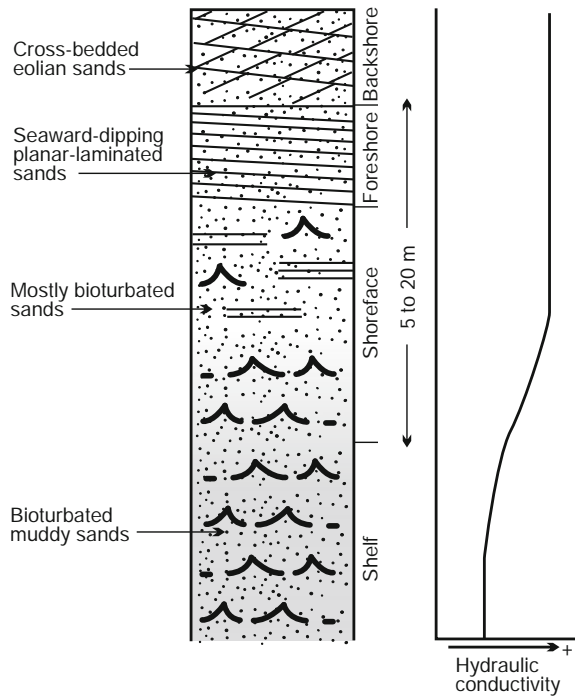
3.8.1 Beach and Strand Plain Facies

Barrier islands are sandy islands or peninsulas elongated parallel to the shore and
separated from the mainland by marshes, lagoon, or a shallow bay. Strand plains are
wider and lack well-developed lagoons and inlets (McCubbin 1982). Barrier islands
and strand plains were summarized by McCubbin (1982) and Reinson (1984).
Major environments include (1) beach and shoreface, (2) inlet channels and tidal
deltas, (3) washover fans on the landward or lagoonal side of barrier, and
(4) back-barrier region (lagoon). Sequences formed by the seawards progradation of
the beach and shoreface (nearshore) deposits account for a major part of the volume
of many Holocene barrier islands and strand plains (McCubbin 1982). A key aspect
of beach and shoreface deposits is the occurrence of seasonal or storm-related
cycles of erosion and deposition.

Beach and shoreface include four main subenvironments (McCubbin 1982;
Reinson 1984). The beach (foreshore) (Fig. 3.24) is dominated by swash-backwash
processes with the main sediments being planar-laminated sands. Bioturbation is
incomplete and sedimentary structures are preserved. The shoreface is the subtidal
zone than extends from the mean low tide line to the fair-weather wavebase (10
−20 m). Deposition in the shoreface is dominated by wave energy. The upper

Fig. 3.24 Foreshore (swash zone) and backshore dunes with vegetation. a Western Australia near Albany. b Fort Desoto State Park, St. Petersburg, Florida, USA

shoreface is dominated by wave surge and wave-generated currents. The main sediment types are planar-laminated sands and high-angle cross-bedded sands deposited by migration of ridge and runnels (sand bars). Biogenic structure are common, but the sediments are rarely completely bioturbated.

The lower shoreface is a lower energy environment dominated by slow deposition with pulses of rapid deposition during storms. The sediments tend to be finer grained (siltier) than the upper shoreface sediments. The main sediments tend to be fine and very fine sand with intercalated layers of silt and sandy mud. Bioturbation is also more intense due to lower energy level and slower deposition. The offshore subenvironment is usually not impacted by wave action and is characterized by slow deposition and intense bioturbation. Offshore sediments are finer grained and include sediments deposited out of suspension.

3.8.2 Lagoonal and Tidal Flat Facies

The lagoon and tidal flat setting contains a great diversity of depositional environments with salinities ranging from freshwater to hypersaline. Lagoonal and other back-barrier sediments include interbedded and interfingering sands, silts, clays, and organic material (peat). Tidal-inlet and washover sands are less commonly preserved. Tidal-inlet (Fig. 3.25) deposits are dominated by cross-bedded sands. Washovers form when storm tides overtop and erode channels through beach dune-ridges and transport sand landwards of the channels. The characteristic deposits are planar stratified sands.

Tidal flats and associated tidal channels, as the names imply, are coastal environments in which sediment deposition is under the influence of tidal cycles. Tidal flat environments were reviewed by Ginsburg (1975) and Weimer et al. (1982). Tidal flats (Fig. 3.26) may occur where there are measurable tidal changes and the absence of strong wave action. The lower energy regime of tidal flats allow for the deposition of finer-grained sediments than are deposited in nearby beach environments.

Tidal flats include three main zones: subtidal, intertidal, and supratidal. The subtidal zone is located below the mean low tide level. The intertidal zone is located between the mean low and high tide levels. The supratidal zone is located above the mean high tidal level. The term 'supratidal' is widely used in the literature and is retained herein. Weimer et al. (1982) recommended that 'supratidal' be dropped in favor of 'upper intertidal' to signify that it is subject to occasional tidal influences, but not on a daily basis.

Fig. 3.25 Tidal inlet through barrier island, Barefoot Beach, Collier County, Florida, USA. Islands are covered with mangroves and other salt tolerant vegetation

Tidal flats contain a diversity of subenvironments that are subject to a variety of sedimentological and biological processes. Sediment deposition is influenced by daily variations in water levels, reversals in flow direction, and wave action. Biological activity is also highly variable. Subtidal environments can have normal marine flora and faunas that are often similar to those in non-tidal shallow subtidal environments. The intertidal and supratidal zones contain a lower diversity of organisms, but often at very high numbers (Weimer et al. 1982). Reworking of sediments by benthic organisms (i.e., bioturbation) is also widespread. No sedimentary structures are restricted to the tidal facies. Recognition of tidal flats, therefore, requires examination of individual sedimentary and biogenic features and consideration of vertical and horizontal facies associations (Weimer et al. 1982).

A key point to understanding tidal flat environments is that present environments are not necessarily representative of the deposits that are preserved in the geological record (Weimer et al. 1982). The deposits most likely to be preserved are channel fill deposits, which constitute a relatively small part of tidal flat environments. Channels migrate across the tidal flat, eroding and redepositing sediment. Channel fills are the deepest and thickest features in the tidal flat environment, extending to the bottom of the channels. The greater depth of channels than other features in the tidal flat environment results in a much greater preservation potential (Weimer et al. 1982).

A basic facies sequence for tidal flats consists of cross-stratified and ripple-stratified sands overlain by fine-grained sands and muds deposited in a shallower-water environment. The sands and muds may be separated, as is the case for lenticular and flaser bedding, or may be mixed by bioturbation into a sandy marl. Evidence for flow reversal would be strongly suggestive of tidal conditions. Both ebb and flood cross-bedding may be preserved, but usually one direction dominates (Weimer et al. 1982).

3.8.3 Hydrogeology

Linear terrigenous shorelines are both sedimentologically and hydrogeologically complex. Modern beach and tidal flat deposits are not significant from a water resources perspective in that they contain commonly brackish, saline or hypersaline water. Backshore environments, such as well-developed dune or beach ridge complexes, may have a freshwater lens that is a usable water supply. Freshwater lenses on barrier islands are highly vulnerable to depletion and saline-water intrusion from over exploitation. Because of the erosion and redeposition, typical shallowing-upward progradation sequences may not be preserved. The sand bodies may be linear or sheet-like and are generally oriented with their strike parallel to the shore. Shoreline sand bodies may thus be oriented roughly perpendicular to fluvial sand bodies, which tend to be oriented normal to the shore. Beach sands may be differentiated from fluvial sands by the presence of marine fossils and, in deeper-water facies, by extensive bioturbation. Ancient beach deposits may have good aquifer properties because of their good sorting, with their hydraulic conductivity dependent on grain size and matrix (clay content).

References

Ahlbrandt, T. S. (1979) Textural parameters of eolian deposits. In E. D. McKee (Ed.), A study of global sand seas (pp. 21–51). U.S. Geological Survey Professional Paper 1052.

Ahlbrandt, T. S., & Fryberger, S .G. (1982) Introduction to eolian deposits. P. A. Scholle & D. Spearing (Eds.) Sandstone depositional environments. Memoir 31 (pp. 11–14). Tulsa: American Association Petroleum Geologists.

Anderson, M. P. (1989) Hydrogeologic facies models to delineate large-scale spatial trends in glacial and glaciofluvial sediments. Geological Society of America Bulletin, 101, 501–511.

Ashley, G. M., Shaw, J., & Smith, N. D. (1985) Glacial sedimentary environments. Short Course 16. Tulsa: SEPM (Society for Sedimentary Geology).

Beres, M., Huggenberger, P., Green, A. G., & Horstmeyer, H. (1999) Using two- and three-dimensional methods to characterize glaciofluvial architecture. Sedimentary Geology, 129, 1–24.

Best, J. L., & Bristow, C. S. (1993) Braided rivers. Special Publication 75. London: Geological Society.

Bhattacharya, J. P. (2006) Deltas. In H. W. Posamentier & R. G. Walker (Eds.), Facies models revisited. Special Publication 84 (pp. 237–292). Tulsa: SEPM (Society for Sedimentary Geology).

Bierkins, M. F. P., & Weerts, H. J. T. (1994) Block hydraulic conductivity of cross-bedded fluvial sediments. Water Resources Research, 30, 2665–2678.

Blair, T. C., & McPherson, J .G. (1994) Alluvial fans and their natural distinction from rivers based on morphology, hydraulic processes, sedimentary processes, and facies assemblages. Journal of Sedimentary Research, A64, 450–489.

Bridge, J. S. (2001) Characterization of fluvial hydrocarbon reservoirs and aquifers: problems and solutions: AAS [Asociación Argentina de Sedimentología] 8(2): 87–114.

Bridge, J. S. (2003) Rivers and floodplains. Blackwell Publishing, Oxford, 491 pp.

Bridge, J. S. (2006) Fluvial facies models: Recent developments. In H. W. Posamentier & R. G. Walker (Eds.) Facies models revisited. Special Publication No. 84 (pp. 85–170). Tulsa: SEPM (Society for Sedimentary Geology).

Bridge, J. S., & Mackey, S. D. (1993) A theoretical study of fluvial sandstone body dimensions. In S. S. Flint & I. D. Bryant (Eds.), Geological modeling of hydrocarbon reservoirs. Special Publication 15 (pp. 213–236). International Association of Sedimentologists.

Brookfield, M. E. (1977) The origin of bounding surfaces in ancient aeolian sandstones. Sedimentology, 24, 303–332.

Brookfield, M .E. (1984) Eolian facies. In R. G. Walker (Ed.), Facies models (2nd ed.). Geoscience Canada Reprint Series 1 (pp. 91–103). Toronto: Geological Association of Canada Publications.

Bull, W. B. (1972) Recognition of alluvial-fan deposits in the stratigraphic record. In J. K. Rigby & W. K. Hamblin (Eds.) Recognition of ancient sedimentary environments. Special Publication 16 (pp. 63–83). Tulsa: SEPM (Society for Sedimentary Geology).

Bull, W. B. (1977). The alluvial-fan environment. Progress in Physical Geography, 1, 222–270.

Cant, D. J. (1977) Development of a facies model for sandy braided river sedimentation: comparison of the South Saskatchewan River and the Battery Point Formation. In A.D. Miall (Ed.), Fluvial sedimentology. Memoir 5 (pp. 627–639). Calgary: Canadian Society for Petroleum Geologists.

Cant, D. J. (1982) Alluvial facies models and their application. In P. A. Scolle, P.A. & D Spearing (Eds.), Sandstone depositional environments. Memoir 31 (pp. 115–138). Tulsa: American Association of Petroleum.

Cant, D. J., & Walker, R. J. (1978) Fluvial processes and facies sequences in the sandy braided South Saskatchewan River, Canada. Sedimentology, 25, 625–648.

Cehrs, D. (1979) Depositional control of aquifer characteristics in alluvial fans, Fresno County, California. Geological Society of America Bulletin, 90, 1282–1309.

Chandler, M. A., Kocurek, G., Goggin, D. J., & Lake, L.W. (1989) Effects of stratigraphic heterogeneity on permeability in eolian sandstone sequence, Page Sandstone, northern Arizona. American Association of Petroleum Geologists Bulletin, 73, 658–668.

Clifton, H. E. (2006) Reexamination of facies models for clastic shorelines. In H. W. Posamentier & R. G. Walker (Eds.) Facies models revisited. Special Publication 84 (pp. 293–337). Tulsa: SEPM (Society for Sedimentary Geology).

Coleman, J. M., & Prior, D. B. (1982) Deltaic environment. In P.A. Scholle & D. Spearing (Eds.), Sandstone depositional environments. Memoir 31 (pp.139–178). Tulsa: American Association Petroleum Geologists.

Collinson, J. D. (1986a) Alluvial sediments. In H. C. Reading (Ed.), Sedimentary environments and facies (2nd ed.) (pp. 20–62). Oxford: Blackwell Scientific.

Collinson, J. D., 1986b, Deserts. In H. C. Reading (Ed.), Sedimentary environments and facies (2nd ed.) (pp. 95–112). Oxford: Blackwell Scientific.

Dott, R. H. (1964) Wacke, graywacke and matrix; what approach to immature sandstone classification? Journal of Sedimentary Petrology, 34, 625–632.

Easterbrook, D. J. (1982) Characteristic features of glacial sediments. In P. A. Scholle & D. Spearing (Eds.) Sandstone depositional environments. Memoir 31 (pp. 1–10). Tulsa: American Association Petroleum Geologists.

Edwards, M. (1986) Glacial environments. In H. C. Reading (Ed.) Sedimentary environments and facies (2nd ed.) (pp. 445–470). Oxford: Blackwell Scientific.

Elliott, T. (1986), Siliciclastic shorelines. In H. G. Reading (Ed.) Sedimentary environments and facies (2nd Ed.) (pp. 155–188). Oxford: Blackwell Scientific.

Eyles, N., & Miall, A. D. (1984). Glacial facies. In R. G. Walker (Ed.), Facies models (2nd Ed.). Geoscience Canada Reprint Series 1 (pp 15–38). Toronto: Geological Association of Canada Publications.

Flemming, A. H. (1998a) Using glacial terrain models to define hydrogeologic settings in heterogeneous depositional settings. In G. S. Fraser & J. M. Davis (Eds.), Hydrogeologic

models of sedimentary aquifers. Concepts in Hydrogeology and Environmental Geology 1 (pp. 26 –46). Tulsa: SEPM (Society for Sedimentary Geology).

Flemming, A. H. (1998a) Using glacial terrain models to characterize aquifer system structure, heterogeneity, and boundaries in an interlobate basin, Northeastern Indiana. In G. S. Fraser & J. M. Davis (Eds.), Hydrogeologic models of sedimentary aquifers. Concepts in Hydrogeology and Environmental Geology 1 (pp. 47–68). Tulsa: SEPM (Society for Sedimentary Geology).

Folk, R .L (1974) Petrology of sedimentary rocks. Austin, TX: Hemphill Publishing Co.

Galloway, W. E., & Hobday, D. K. (1996) Terrigenous clastic depositional systems (2nd Ed). Berlin: Springer.

Galloway, W. E., & Sharp, J. M., Jr. (1998) Hydrogeology and characterization of fluvial aquifer systems. In G. S. Fraser & J. M. Davis (Eds.), Hydrogeologic models of sedimentary aquifers. Concepts in Hydrogeology and Environmental Geology 1 (pp. 91–106). Tulsa: SEPM (Society for Sedimentary Geology).

Ginsburg, R. N. (1975) Tidal deposits. New York: Springer-Verlag.

Goggin, D. J., Chandler, M. A., Kocurek, G., & Lake, L.W. (1988) Patterns of permeability in eolian deposits: Page Sandstone (Jurassic), northeastern Arizona. SPE Formation Evaluation, June 1988, 297–306.

Hall, D. S. (1976) Hydrogeologic significance of depositional systems and facies in the Lower Cretaceous sandstones, north-central Texas: Texas Bureau of Economic Geology, Geological Circular 76-1.

Harvey, A. M., Mather, A .E., & Stokes, M. (2005) Alluvial fans: geomorphology, sedimentology, dynamics – introduction. A review of alluvial fan research. In A. M. Harvey, A. E. Mather, & M. Stokes (Eds.) Alluvial fans: Geomorphology, sedimentology, dynamics. Special Publication 251 (pp. 1–7). London: Geological Society.

Heinz, J., Kleineidam, S., Teutsch, G., & Aigner, T. (2003) Heterogeneity patterns of Quaternary glaciofluvial gravel bodies (SW-Germany): application to hydrogeology. Sedimentary Geology, 158, 1–23.

Heward, A .P. (1978) Alluvial fan sequence and megasequence models: with examples from Westphalian D-Stephanian B coalfields, Northern Spain. In A. D. Miall (Ed.), Fluvial sedimentology. Memoir 5 (pp. 669–702). Canadian Society of Petroleum Geologists.

Illinois State Geological Survey (2008) Quaternary glaciations in Illinois. Illinois State Geological Survey GeoNote 3.

Jordan, D. W., & Pryor, W. A. (1992) Hierarchial levels of heterogeneity in a Mississippi River meander belt and application to reservoir systems. American Association Petroleum Geologist Bulletin, 76, 1601–1624.

Lesmes, D. P., Decker, S. M., & Roy, D. C. (2002) A multiscale radar-stratigraphic analysis of fluvial aquifer heterogeneity, Geophysics, 67, 1452–1464.

Lyle, S. A. (2009) Glaciers in Kansas: Kansas Geological Survey Publication Information Circular 28.

McCloskey, T. F., & Finnemore, E. J. (1996) Estimating hydraulic conductivities in an alluvial basin from sediment facies model. Ground Water, 34, 1024–1032.

McCubbin, D.G., 1982, Barrier islands and strand-plain facies. In P. A. Scolle, P.A. & D Spearing (Eds.), Sandstone depositional environments. Memoir 31 (pp. 247–279). Tulsa: American Association of Petroleum.

Miall, A. D. (1977) A review of the braided river depositional environment. Earth-Science Reviews, 13, 1–62.

Miall, A. D. (1984) Deltas. In R.G. Walker (Ed.), Facies models (2nd ed.). Geoscience Canada Reprint Series 1 (pp. 105–118). Toronto: Geological Association of Canada Publications.

Miall, A. D. (1985) Architectural-element analysis: A new method of facies analysis applied to fluvial deposits. Earth Science Reviews, 22, 261–308.

Miall, A. D. (1996) Geology of fluvial deposits : sedimentary facies, basin analysis & petroleum geology. Berlin: Springer.

Mountney, N. P. (2006) Eolian facies models. In H. W. Posamentier & R. G. Walker (Eds.) Facies models revisited. Special Publication 84 (pp. 19–83): Tulsa: SEPM (Society for Sedimentary Geology.

Neton, M. J., Dorsch, J., Olson, C. D., & Young, S. C. (1994) Architecture and directional scales of heterogeneity in alluvial fan aquifers. Journal of Sedimentary Research, B64, 245–257.

Nielsen, T. H. (1982) Alluvial fan deposits. In P. A. Scholle & D. Spearing (Ed.) Sandstone depositional environments. Memoir 31 (pp. 49–86) Tulsa. American Association Petroleum Geologists.

Reading, H. G. (1986) Sedimentary environments and facies (2nd Ed). Oxford: Blackwell Scientific Publishing.

Reineck, H. E. & Singh, I. B. (1980) Depositional sedimentary environments. New York: Springer-Verlag.

Reinson, G.E. (1984) Barrier island and associated strand-plain systems. In R. G. Walker (Ed.), Facies models (2nd ed.). Geoscience Canada Reprint Series 1 (pp. 119–140). Toronto: Geological Association of Canada Publications.

Rust, B. R. (1978) Depositional models for braided alluvium. In A. D. Miall (Ed.) Fluvial Sedimentology. Memoir 5 (pp. 627–639). Canadian Society for Petroleum Geologists.

Rust, B. R., & Koster, E. H. (1984) Coarse alluvial deposits. In R.G. Walker (Ed.), Facies models (pp. 53–69). Toronto: Geological Society of Canada.

Schumm, S. A. (1977) The fluvial system. New York: John Wiley & Sons.

Selley, R. C. (1985) Ancient sedimentary environments and their subsurface diagenesis (3rd ed.). Ithaca: Cornell University Press.

Sharp, J. M., Jr. (1988) Alluvial aquifers along major rivers. In W. Back, J. S. Rosenshein, & P. R. (Eds.) Hydrogeology, The geology of North America (Vol. O-2, pp. 273–282). Boulder: Geological Society of America.

Stanford, S. D., & Ashley, G.M. (1998) Using three-dimensional geologic models to map glacial aquifer systems: An example from New Jersey. In G. S. Fraser & J. M. Davis (Eds.), Hydrogeologic models of sedimentary aquifers. Concepts in Hydrogeology and Environmental Geology 1 (pp. 69–84). Tulsa: SEPM (Society for Sedimentary Geology).

Stephenson, P. A., Fleming, A. H., & Mickelson, D. M. (1988), Glacial deposits. In W. Back, J. S. Rosenshein, J. S. Seaber (Eds.), Hydrogeology, The geology of North America (Vol. O-2, pp. 301–314). Boulder: Geological Society of America.

Twenter, F. R., & Metzger, D. G. (1963). Geology and ground water in Verde Valley–the Mogollon Rim Region, Arizona. U.S. Geological Survey Bulletin 1177.

Walker, R. G. & Cant, D. J. (1984) Sandy fluvial systems. In R. G. Walker (Ed.), Facies models (2nd ed.). Geoscience Canada Reprint Series 1 (pp. 71–89). Toronto: Geological Association of Canada Publications.

Weimer, R.J., Howard, J.D., and Lindsay, D.R., 1982, Tidal flats and associated tidal channels. In P. A. Scolle, P.A. & D Spearing (Eds.), Sandstone depositional environments. Memoir 31 (pp. 139–178). Tulsa: American Association of Petroleum.

Weissmann, G. S., Bennett, G. L., & Lansdale, A. L. (2005) Factors controlling sequence development of Quaternary fluvial fans, San Joaquin Basin, California, USA. In A. M. Harvey, A. E Mather, & M. Stokes (Eds.), Alluvial fans: Geomorphology, sedimentology, dynamics. Special Publication 251 (pp. 169–186). London: Geological Society.

Chapter 4
Carbonate Facies Models and Diagenesis

Carbonate aquifers consist of rocks composed mainly of the minerals calcite and dolomite. Carbonate minerals are generally much more chemically reactive under near surface geochemical conditions and thus undergo a much greater degree of chemical and physical alteration (diagenesis) than siliciclastic deposits. The textures and fabrics of carbonate sediments are strongly controlled by physical, chemical, and biological conditions in their depositional environment. The petrophysical properties of relatively young (Cenozoic) carbonates often still reflect depositional heterogeneities. In most older (Mesozoic and Paleozoic) carbonates, much of the depositional porosity and permeability has been lost or profoundly modified by physical and chemical diagenesis. Groundwater flow in older carbonates is largely controlled by secondary porosity, particularly fractures and solution conduits.

4.1 Introduction

Geological and petrophysical heterogeneity in carbonate reservoirs has received a great deal of study because these reservoirs contain a disproportionate amount of global oil reservoirs. The heterogeneity impacts secondary recovery with associated huge economic implications. It is the extreme heterogeneity of carbonate hydrocarbon reservoirs that distinguishes them from siliciclastic reservoirs (Lucia et al. 2003). Carbonate aquifers predominantly consist of rock that was deposited as sediments and biological precipitates composed of calcium carbonate in the form of the minerals calcite (both low and high magnesium) and its polymorph aragonite.

Carbonate sediments and rock are categorized according to the types of grains present and their texture, particularly the amount of carbonate mud. Carbonate sediments and rocks texturally vary depending upon whether they are mud-supported or grain-supported, and in the latter case, whether the intergranular space is either open (or filled with cement) or contains carbonate mud. In a grain-supported rock, the grains are in contact and form a self-supporting

Table 4.1   Dunham (1962) limestone classification

Original components not bound together				Original components bound together during deposition
Contains carbonate mud (micrite)			Lacks mud	
Mud-supported		Grain-supported		
Less than 10 % grains	Greater than 10 % grains			
Mudstone	Wackestone	Packstone	Grain stone	Boundstone

framework. With reference to the limestone classification scheme of Dunham (1962; Table 4.1), grain-supported rocks without intergranular mud are referred to as grainstones. Matrix-supported limestones are referred to as mudstones and wackestones. A packstone is a grain-supported rock that contains intergranular mud. A boundstone is a carbonate rock in which carbonate components are bound together at deposition, which includes some reefal rocks. For example, a grain-supported rock composed of mollusk shells in which the intergranular space contains mud is called a mollusk packstone. Reworked, rounded fossils fragments are referred to as 'bioclasts.' Carbonate sand beaches with no mud are thus typically composed of bioclast grainstone.

Calcium carbonate mud consists of micron-sized crystals and thus tends to have very low permeabilities despite high porosities. Grainstones, on the contrary, tend to have high permeabilities where the intergranular porosity is open (not filled with cement). Enos and Sawatsky (1981) reported the permeability of studied modern carbonate sediments has a range of 5 orders of magnitude (0.6–57,000 millidarcies). The muddiest sediments had the highest porosities and lowest permeabilities. Carbonate sediments thus tend to have very high degrees of heterogeneity with respect to hydraulic conductivity.

Calcium carbonate minerals are chemically reactive in near surface environments and, after deposition, undergo a variety of dissolution, precipitation, replacement, and alteration reactions. A characteristic feature of carbonate aquifers is that their chemical reactivity (i.e., susceptibility to dissolution) can result in the development of larger secondary pores. Secondary porosity (Fig. 4.1) may have orders of magnitude greater permeability than primary (matrix) porosity and very often dominates groundwater flow. The extreme manifestation of secondary porosity-dominated flow is karstic systems, in which groundwater flow occurs predominantly in large solution cavities or caverns (Chap. 18). Secondary porosity, in general, is much less well-developed in siliciclastic aquifers, which are composed of chemically stable silicate minerals.

Limestones can be roughly divided into two general types based on age: (1) Cenozoic and (2) Mesozoic and Paleozoic (Budd and Vacher 2004). Cenozoic carbonates that have never been deeply buried commonly retain relatively high porosities and hydraulic conductivities. Older limestones tend to be harder and have low matrix porosities, because of a longer diagenetic history and the effects of burial-related diagenetic processes, such as mechanical and chemical compaction.

Fig. 4.1 Large secondary pores (arrows) developed in Pleistocene limestone on Aruba

Groundwater flow in low-porosity Mesozoic and Paleozoic limestones is often essentially totally dominated by secondary porosity (fractures and karst features), often largely irrespective of depositional facies.

Whereas aquifer heterogeneity in siliciclastic aquifers is often related primarily to variations in depositional textures, heterogeneity in carbonate rocks typically has more complex controls, reflecting the interaction of primary textural and mineralogical variations and diagenesis. A key element of studies of carbonate aquifers is identification and characterization of secondary porosity features. Investigations of carbonate aquifers need to focus on techniques that have relatively large volumes of investigation. The hydraulic properties of matrix rock (i.e., rock adjoining fractures and solutions conduits) often has little relevance to groundwater flow in aquifers in which flow is dominated by solution conduit and fracture systems. However, matrix may still provide most of the storage in carbonate aquifers, which is important in solute transport.

An approach used to characterize carbonate hydrocarbon reservoirs is the use of rock fabrics as the basic elements. Rock fabrics, which are analogous to hydrofacies, are geological descriptors that characterize carbonate rocks according to particle size and sorting, interparticle porosity, and various types of secondary porosity. Depending upon the degree of diagenetic alteration, rock fabrics can or cannot be linked directly to depositional facies (Lucia et al. 2003). Each rock fabric has a specific porosity-permeability transform (Lucia et al. 2003).

4.2 Carbonate Diagenesis and Porosity and Permeability

Carbonate diagenesis is an important discipline that has received much investigation because of its control on the petrophysical properties of hydrocarbon reservoirs. Detailed reviews of carbonate diagenesis were prepared by Bathurst (1972),

McIlreath and Morrow (1990), Tucker and Bathurst (1990), and Moore (1989, 2001). Any discussion of the carbonate diagenesis in the context of aquifer characterization will be unavoidably cursory. However, there are a number of basic concepts that are important for understanding aquifer properties and heterogeneity in carbonate aquifers.

Diagenesis can overwrite primary differences in the porosity and hydraulic conductivity of carbonate rock. However, compositional variations often influence subsequent diagenesis. Carbonate sediments with high concentrations of metastable minerals (aragonite and high-magnesiun calcite) are more prone to diagenetic alteration (i.e., have a greater diagenetic potential) than sediments composed predominantly of the more stable low-magnesium calcite. Depositional textural variations also impact diagenesis and associated changes in the porosity and permeability of carbonate rocks.

Diagenesis has been divided into three main environments or stages, which are referred to as eogenetic, mesogenetic, and telogenetic (Choquette and Pray 1970). Early or eogenetic diagenesis occurs before deep burial, while the sediments are still under the significant influence of near-surface processes such as the influx of meteoric waters. Although the time of eogenesis may be geologically brief, eogenetic processes can be of extreme importance in diagenesis and porosity evolution (Choquette and Pray 1970). Mesogenesis refers to the time period after eogensis and before a final phase of imminent erosion and unconformity-related processes. Mesogenesis includes the burial-related diagenetic process of compaction. Telogenesis refers to processes that occur upon the uplift and erosion of older rock. There are four main processes by which the porosity and permeability of carbonate sediments and rocks are changed during diagenesis that are relevant to the hydrogeology of carbonate aquifers:

(1) eogenetic dissolution and precipitation
(2) physical and chemical compaction
(3) dolomitization
(4) karst dissolution processes.

The hydrogeology of karst systems and investigative methods are discussed in Chap. 18.

4.2.1   Eogenetic Dissolution and Precipitation

The bulk of carbonate sediments in the geological record were deposited in marine environments. Although diagenesis occurs within marine groundwater environments, much more intensive early diagenetic alteration occurs in meteoric groundwater environments associated with sea level change or uplift. When considered on a large (formation) scale, early diagenesis appears to have, at most, a modest effect on total porosity (Halley and Schmoker 1983; Scholle and Halley 1985; Saller et al. 1994). Limestones commonly leave the early diagenesis with

porosities close to depositional values. In the carbonate succession of South Florida, significant porosity reduction does not occur until the carbonate strata are buried several hundred meters below land surface (Halley and Schmoker 1983).

Early diagenesis can result in a profound reorganization of pore networks with concomitant changes in permeability and hydraulic conductivity. The dissolution of metastable carbonate grains, matrix, and cement can create or enhance secondary porosity with associated increases in hydraulic conductivity. The re-precipitation of the dissolved calcium carbonate as calcite cement can occlude porosity and reduce hydraulic conductivity either locally, near the site of dissolution, or elsewhere in the formation. Carbonate dissolution may occur in the soil zone or recharge area and precipitate further down the groundwater flow path. Positive feedback may also occur when the more permeable strata experience greater groundwater flow, which can, in turn, result in increased local dissolution and permeability.

Changes in the petrophysical properties of carbonate rocks due to eogenetic processes can have a profound impact on groundwater flow. Carbonate islands often exhibit a step-wise downward increase in hydraulic conductivity in the meteoric eogenetic zone with the development of karst-related secondary porosity. On dual-aquifer islands, Holocene carbonate sediments and rock with a relatively low hydraulic conductivity overlie Pleistocene reef deposits with a relatively high hydraulic conductivity (both primary and diagenesis enhanced; Vacher 1997). The high transmissivity reefal units allow for the passage of saline water and tidal fluctuations into the interior of islands. The base of the upper low hydraulic conductivity unit may mark the base of the freshwater lens. An example of a dual-aquifer island is Big Pine Island in the lower Florida Keys in which the oolitic limestones of the Miami Limestone overlie the much more transmissive reefal deposits of the Key Largo Limestone (Halley et al. 1997).

4.2.2 Physical and Chemical Compaction

Mesogenesis is dominated by burial-related processes, particularly compaction and cementation, which tend to progressively reduce porosity and permeability. Compaction can occur by physical and chemical processes. Physical compaction includes the rearrangement of grains into more tightly packed configurations (consolidation), grain breakage, and plastic deformation of unlithified or poorly lithified grains. Chemical compaction consists mainly of pressure solution phenomena. The solubility of calcite and other minerals increases with increasing pressure, which can result in local dissolution. Dissolution can occur at grain-to-grain contacts (i.e., intergranular pressure solution) or along discrete surfaces (i.e., stylolites; Fig. 4.2) and clay-rich solution seams in the rock. The calcite that dissolves along stylolites or solution seams is re-precipitated in the inter-stylolite areas as calcite cement, resulting in a reduction in porosity. Some beds may act as calcium carbonate 'donors' for calcite cementation in nearby 'recipient' beds (Scholle and Halley 1985).

Fig. 4.2 Stylolites (crenulate
dissolution surfaces) in the
Ulster White Limestone,
Northern Ireland. Belemnite
(arrow) is about 1 cm in
diameter
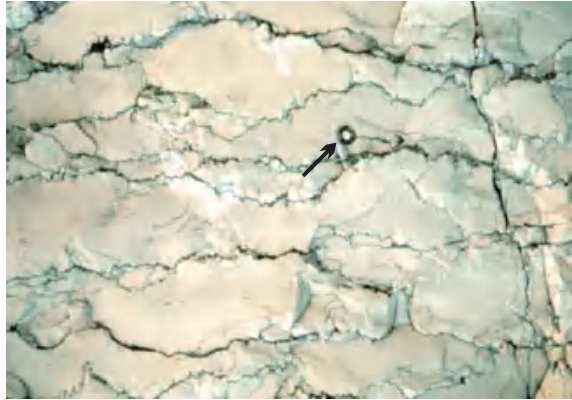
A key point as far as the cementation of limestones into low-porosity Mesozoic
and Paleozoic-type limestones is that an external source of calcium would require
an excessively large amount of fluid flow due to the low solubility of calcite and
thus concentrations of calcium and bicarbonate in pore waters. A pressure solution
origin for most of the porosity loss during burial diagenesis is a much more likely
explanation that is well supported by geological data (Scholle and Halley 1985).

Porosity within the shallow-water carbonate rocks of South Florida show a
gradual trend of decreasing porosity with depth, declining from values of 45 % near
surface to 25–30 % at a depth of 800 m (2,600 ft) (Halley and Schmoker 1983).
Considering also more deeply buried limestones, the decrease in average porosity
($\varnothing$, %) with depth (z) can be expressed as follows (Schmoker and Halley 1982)

$$\varnothing = 41.73 \mathrm{e}^{\left(\frac{-z}{2498}\right)} (z \text{ in meters}) \tag{4.1}$$

$$\varnothing = 41.73 \mathrm{e}^{\left(\frac{-z}{8197}\right)} (z \text{ in feet}) \tag{4.2}$$

Dolomites in South Florida have lower porosities near surface, but porosity does
not decrease as rapidly with increasing depth (Schmoker and Halley 1982).
Sandstones tend to have a higher median and maximum porosity at a given depth
than carbonate aquifers due to their lesser chemical reactivity (Ehrenberg and
Nadeau 2005).

Depositional and early diagenetic textures, porosity, and permeability are sub-
sequently modified during burial diagenesis. Budd (2001) and Budd and Vacher
(2004) investigated matrix permeability relationships in the Floridan Aquifer
System in west-central Florida by performing approximately 12,000 miniperme-
ameter measurements. The studied carbonate succession had a relatively simple
diagenetic history in which the strata experienced only gradual subsidence and are
currently at their maximum burial depths, which ranges up to 470 m. Although
permeability values have changed as a result of diagenesis, the relative relationship
of permeability with depositional textures has been retained. Permeability was

reported to have ranged over three orders of magnitude. Grainstones and sucrosic (loosely crystalline) dolomites have the greatest permeabilities, with mud-rich lithologies having the lowest values. Low hydraulic conductivity limestones exhibited low permeabilities at all depths, while high-permeability grainstones exhibited a systematic reduction in permeability with depth. Dolomites did not show a permeability versus depth trend. A key observation is that the reduction in permeability with depth is more rapid than the reduction in porosity (Budd 2001).

Budd (2001) and Ehrenberg et al. (2006) documented that limestones leave the near surface diagenetic environment with highly variable permeabilities that reflect primary textural differences and the effects of early diagenesis. The low hydraulic conductivity of mud-rich lithologies (mudstones and wackestones) is likely due to early pre-burial (near surface) cementation in addition to their fine pore size. Chemical compaction may also preferentially occur in fine-grained strata, particularly if they are clay-rich, which can result in the formation of tight limestone barriers that can compartmentalize hydrocarbon reservoirs (Ehrenberg et al. 2006) and act as confining or semiconfining units in aquifer systems.

4.2.3   Dolomitization

One of the enigmas of sedimentary geology is the abundance of dolomite in ancient limestones, despite its paucity in modern carbonate sediments and recent limestones. Dolomite is an ordered magnesium calcium carbonate that forms primarily by the replacement of a limestone (calcium carbonate) precursor. The term 'dolomite' is used for both the mineral dolomite and rocks composed predominantly of dolomite. The term 'dolostone' is also used for the rocks composed of dolomite.

Dolomitization is commonly expressed using the replacement reaction:

$$Mg^{+2} + 2(CaCO_3) \rightarrow MgCa(CO_3)_2 + Ca^{+2} \qquad (4:3)$$
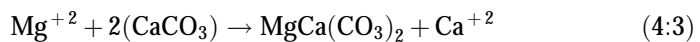
Dolomite has a smaller molar volume than calcite, so it has long been noted that dolomitization should result in an approximately 12 % reduction in porosity. However, with the addition of external calcium and carbonate, dolomite can also precipitate out of solution as a cement with a concomitant reduction in porosity. Hence, dolomitization does not inherently result in a change in porosity. However, dolomitization does change the texture of the rock and thus its permeability. Dolomite tends to precipitate as euhedral (i.e., well-formed with planar external faces) rhombohedral crystals (rhombs), which can form a high-porosity and permeability framework (Fig. 4.3a) or a dense interlocking mosaic with a very low porosity and permeability (Fig. 4.3b). Dolomitization can also form a more rigid framework that makes a rock unit less susceptible to subsequent compaction.

From a hydrogeological perspective, dolomitic strata should be treated as any other hydrofacies in terms of their hydraulic parameters. It is important to recognize that dolomitization, as a diagenetic process, may or may not bear a direct

Fig. 4.3 Thin section of
photomicrographs of
dolomites from the Floridan
Aquifer System, Daytona
Beach, Florida, USA.
Porosity is filled with
blue-stained epoxy. a Highly
porous incompletely
dolomitized limestone with
loosely packed rhombohedral
dolomite crystals. b Dolomite
consisting of densely packed
crystals and secondary pores
formed by the dissolution of
fossils
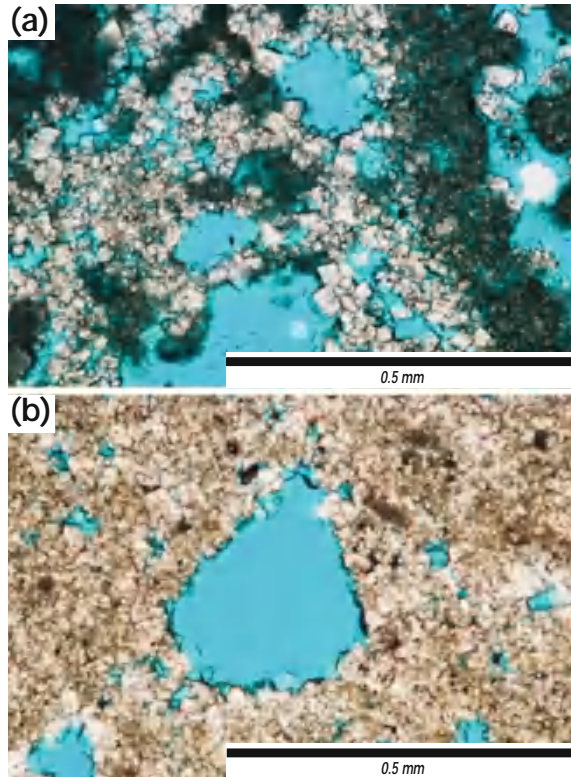
relationship with depositional facies. A relationship between dolomitization and
facies or sequence stratigraphy might occur when the geochemical processes
responsible for dolomitization are related in some manner to depositional envi-
ronment. In older (e.g., Mesozoic and Paleozoic) dolomites, entire formations are
largely dolomitized on a regional scale, and the cause of the dolomitization and
relationship to depositional facies is usually not relevant from a hydrogeological
perspective.

   The hydraulic properties of dolomite are also strongly influenced by the
occurrence of fracturing. Dolomitic units tend to be deformed in a more brittle
manner and thus have a greater tendency to have preserved fracturing than lime-
stones. Within the Floridan Aquifer System of South Florida (USA), hard, dense
dolomites have very low porosities and matrix permeabilities, but are often high
transmissivity flow zones because they are prone to fracturing, and the fractures
tend not to subsequently heal (Safko and Hickey 1992; Duerr 1995; Maliva et al.
2002; Gaswirth et al. 2006; Reese and Richardson 2008). Some fractured intervals
are regional features such as the so-called "boulder zone" of the Lower Floridan
Aquifer and Avon Park high transmissivity zone of west-central Florida. Elsewhere,
geographically localized dolomitic intervals that are fractured may be local,

bounded flow zones (Maliva et al. 2002). On the contrary, low-porosity dolomitic intervals in the Floridan Aquifer System that are not fractured have very low hydraulic conductivities and form effective confining units (Maliva and Walker 1998; Maliva et al. 2007). Hence, an important first step in investigations of carbonate aquifers is determining the primary controls over hydraulic conductivity and transmissivity.

4.3   Carbonate Facies and Sequence Stratigraphy

Shallow carbonate platforms, particularly in tropical settings, are the site of the rapid generation and accumulation of carbonate sediments and, as a result, are referred to as 'carbonate factories.' The substantial production of autochthonous sediments differs from siliciclastic depositional environments in which sediments have an external source, commonly being derived from the erosion of distant rock and transportation to the site of deposition. However, carbonate sediments are often reworked within the general environment in which they were formed and can be transported into nearby depositional environments. As biogenic sediments, carbonate sedimentation is controlled by local physical and chemical conditions within the environment of deposition. Carbonate sediment formation is restricted by ecological constraints on the occurrence of carbonate-secreting organisms. Carbonate sediments commonly accumulate in environments in which there is a low siliciclastic sediment input, which both affects carbonate sediment production and dilution of the carbonate content of the sediment. Carbonate depositional environments and facies were reviewed by Wilson (1975), Scholle et al. (1983), James (1984a, b), Read (1985), and Tucker (1985).

On a large-scale, carbonate sediment production and accumulation is sensitive to relative sea level changes. Relative sea level changes can occur due to actual eustatic rises in sea levels (such as occurs, for example, during interglacial periods) or local subsidence. Carbonate-secreting organisms have depth restrictions, which are typically related to other physical chemical characteristics of the environment. For example, photosynthetic organisms are restricted by the depth of sufficient light penetration. Wave energy decreases with depth in beach and nearshore environments.

Where carbonate sedimentation takes place without significant sea level change, carbonate sedimentation is affected by five major depositional mechanisms, giving predictive facies sequences (Tucker 1985):

(1) tidal flat progradation
(2) shelf-margin reef progradation
(3) vertical accretion of subtidal carbonates
(4) migration of carbonate sand bodies
(5) resedimentation processes, especially shoreface sands to deep environments.

A common theme in the depositional mechanisms is that due to the high productivity of tropical 'carbonate factories,' carbonate sedimentation rates exceed subsidence rates resulting in a net build up of carbonate deposits with associated vertical accretion (shallowing upwards), lateral accretion (progradation), and gravity flows to deeper-water environments.

The sequence stratigraphy of the carbonate sediments was reviewed by Handford and Loucks (1993), Kerans and Tinker (1997), Sarg (1988), and Schlager (2005). Sediment accumulation across carbonate platforms largely depends upon the local productivity of the marine-subtidal carbonate factory. A key factor, as far as carbonate sequence stratigraphy, is that carbonate accumulation rates can match or exceed the rise of sea level and that carbonate platforms often produce more sediment than can be accommodated by their tops, which build up close to sea level (Handford and Loucks 1993). Excess sediments are shed to adjacent slopes.

Changes in sea level impact sediment facies in a generally predictable manner, although there is considerable variation between sites. The response of carbonate sediments to sea level change were reviewed by Kendall and Schalger (1981) and Handford and Loucks (1993). During lowstands, the top of carbonate platforms are exposed, and sediment production is largely terminated. Exposure surfaces become widespread unconformities. The top of the exposed carbonate platforms are subject to karst-associated processes including the formation of sinkholes and caves. Along the platform or slope margins, erosion and down-slope resedimentation will occur to varying extents. The center of platforms may become cut-off from the sea and evaporite mineral deposition may occur.

The pattern of sediment deposition during transgressions depends upon the rates of relative sea level rise and carbonate sediment production. Very rapid sea level rise can result in platform drowning and sediment starvation, which results in the formation of hardgrounds and deposition being largely restricted to hemipelagic and pelagic sediments. More commonly, especially in tropical settings with minimal siliciclastic input, the rate of carbonate sediment accumulation over the long-term keeps pace with the rate of sea level rise. The balances between accumulation and sea level rise or subsidence can result in the deposition of thick successions of shallow-water carbonates. The response of carbonate sediment accumulation to sea level rise often has three phases (Kendall and Schlager 1981; Handford and Loucks 1993):

(1) start-up phase in which carbonate sediment accumulation lags the relative rise
(2) catch-up phase in which accumulation exceeds that sea level rise rate and the carbonate platform builds up to sea level.
(3) keeping-up phase in which accumulation at the platform tops is approximately equal to the sea level rise rate and the platform top remains at or very close to sea level.

Sedimentation accumulation may be more rapid along the rim of platforms or shelves and at isolated patch reefs, which can keep up with sea level rise. The remainder of the platform may remain drowned creating a deep central lagoon.

The high-stand systems track may be either aggradational or progradation. In the case of a prograding shelf, topographic features, such as beach-dune complexes, may form effective barriers to marine circulation and disconnect the self or platform from the open-marine environment, creating conditions favorable for evaporite deposition.

Changes in relative sea level affect the hydrology of shallowly buried carbonate sediments and thus their diagenesis, and, in turn, their porosity and hydraulic conductivity. The relationship between sequence stratigraphy and diagenesis was reviewed in detail by Moore (2001). Drops in relative sea level are particularly important from a diagenetic perspective in that they can result in exposure of carbonate sediments and, as a result, vadose zone and meteoric phreatic diagenetic conditions occur. Exposure can result in the development of karst and vadose zone cementation and alteration. The shallow freshwater phreatic environment is the main site of the dissolution of metastable (e.g., aragonite and high magnesium calcite) components and the re-precipitation of low-magnesium calcite cement with concomitant changes in porosity and hydraulic conductivity.

4.3.1   Shallowing-Upwards Sequences

Shallow-water carbonate sediments characteristically accumulate at rates much greater than the rate of subsidence (or sea level rise) because of the high rates of biological productivity. Carbonate sediments, therefore, tend to repeatedly build up to and above sea level. The resulting shallowing-upwards facies sequences are very common in the geological record (James 1984a; Tucker 1985). Shallowing-upwards facies models varies depending upon the energy of the environment and whether the subtidal facies is open-marine or lagoonal. The basic facies sequence includes five basic elements (James 1984a; Fig. 4.4). Deepening upwards sequences, which form when relative sea rise is greater than the accumulation rate, are much less common.

The bottom contact of the facies sequence is an unconformity, which is overlain by a high-energy transgressive (surf-zone) deposit. The surf-zone deposit may not be preserved or cannot be differentiated from the overlying subtidal open-marine or lagoonal zone. Subtidal marine facies are lithologically diverse ranging from carbonate muds to well-sorted carbonate sands. Characteristic features are the presence of marine fossils and high degrees of bioturbation, which tend to obliterate sedimentary structures. Intertidal deposits may consist of algal laminate mud deposits (i.e., stromatolites) or, in higher-energy environments, laminated carbonates sands. Supratidal environments may show evidence of desiccation and the reworking of sediments. Laminated sediments may become disrupted and reworked to form flat pebble conglomerates.
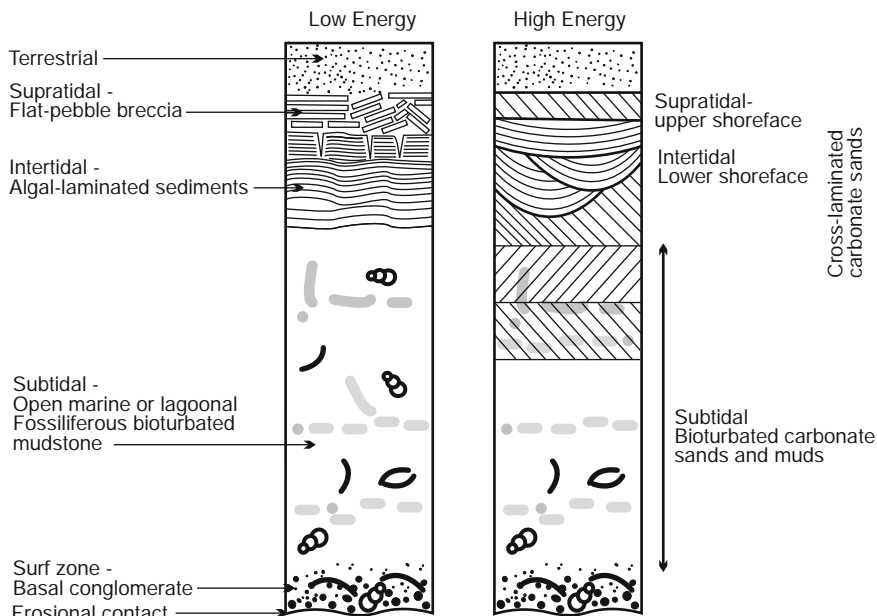
Fig. 4.4 Carbonate shallowing upward sequence facies models for low-energy (left) and high-energy (right) intertidal environments

4.3.2   Reefs

A reef is defined as "a carbonate build-up of skeletal organisms which at the time of formation was a wave resistant topographic feature which rose above the general level of the sea floor" (Selley 1985). Reefs differ from banks, which are syn-depositional topographic highs of non-wave resistant materials (Selley 1985). Fossil reefs contain a disproportionately large amount of the global oil and gas reserves and have, therefore, received a great amount of attention in the fields of carbonate sedimentology, paleontology, and petroleum geology (James 1983; 1984b). Reefs are very complex in terms of the growth stage and environmental controls over their morphology and biological composition and diversity. Reef facies also reflect the balance between growth of reef skeletons and their destruction by a variety of rasping, boring, and grazing organisms and storm activities. Reef-building fauna and flora have also changed over time with scleractinian corals dominating Cenozoic reefs.

Coral reefs often shelter a shallow-water lagoon from the open sea. Reefs may be divided into four main types based on whether or not a lagoon is present and, if so, the relationship of the reef to the lagoon (Fig. 4.5):

(1) fringing reefs—linear along coast with no intervening lagoon
(2) barrier reefs—linear with lagoon

Fig. 4.5 Diagram illustrating
classic evolution of reefs
around a volcanic core from a
fringing reef to a barrier reef
and an atoll (from Field et al.
2002)

Volcanic Island

Fringing reef

Barrier reef
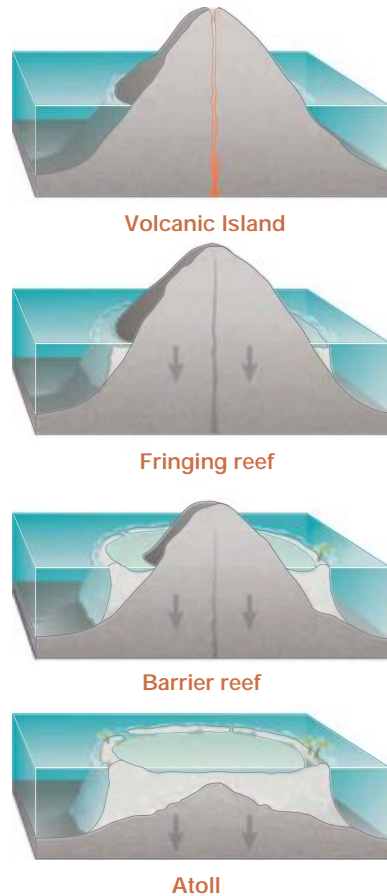
Atoll

(3) atolls—subscircular reefs enclosing lagoon from open water
(4) patch reefs—isolated reefs in lagoon behind barrier reefs and in atolls.

Cenozoic reef deposits vary depending on the relationship to current sea level
(Vacher 1997):

(1) modern sediments associated with modern reefs (e.g., Great Barrier reef
     islands)
(2) emergent islands—currently above sea level because they record one or more
     Quaternary sea level high stands (e.g., Key Largo Limestone, Florida Keys)
(3) emergent reefs that are above sea level due to uplift.

Reef deposits consist of three main facies: reef core, reef flank, and inner-reef
(Fig. 4.6). Reef core facies consists of the skeletons of reef-building organisms and
associated encrusting organisms and a matrix of carbonate mud and sand.
Reef-flank facies consist of bedded conglomerates and carbonate sands of
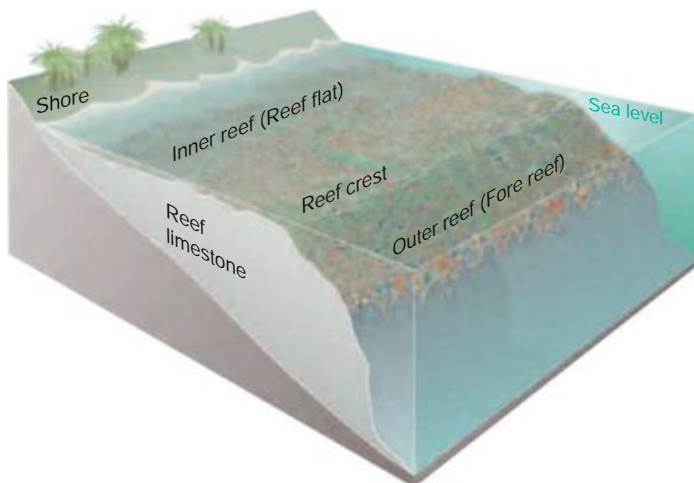
Fig. 4.6   Main reef facies (from Field et al. 2002)

reef-derived material that thin and dip away from the reef core. Inter-reef facies consist of normal, shallow-water, subtidal limestones, and siliciclastic sediments that are unrelated to reef formation.

Reef facies are too complex and diverse to adequately address in a text on aquifer characterization. Four main stages of reef growth are recognized: the pioneer, colonization, diversification, and domination stages (James 1983, 1984b). The composition and textures of reefs vary with environmental conditions and with the evolution of reef-forming organisms. The thickness and location of reefs depend upon the rate of basin subsidence and sea level change, with high rates of subsidence favoring thick reef deposits as the reefs grow up to sea level.

Modern reefs have high primary porosities and permeabilities due to the presence of open cavities that may be either filled with sediments or remain open. Secondary pores may form as the result of the dissolution or alteration of aragonitic skeletal materials. The porosity and permeability of ancient reefs may be drastically altered as a result of diagenesis. Reefal deposits are often high transmissivity units that may form one large continuous reservoir or aquifer or be broken into a series of layers with poor vertical connection because of permeability barriers such as hardgrounds and paleosols (James 1984b).

Although reefal carbonates can retain high transmissivities, they tend not to form major (regional) aquifers because of their limited areal extent. They are of greatest importance in reefal islands. However, the high-transmissivites of reefal limestone, which are favorable for high production rates, also allow the limestones to serve as conduits for horizontal and vertical flow of poorer-quality (saline) waters.

Reefal deposits may serve high-transmissivity flow zones within carbonate and mixed carbonate and siliciclastic aquifers. The Key Largo Limestone in Miami-Dade County, southeastern Florida, consists of Pleistocene reef deposits and

Fig. 4.7 Fossil (Pleistocene) coral reef, Key Largo limestone, Windley Key Fossil Reef Geological State Park, Florida Keys. Large *Diploria* sp. coral is evident (red dashed line). Vertical bar scale is approximately 1 m

constitutes part of the Biscayne Aquifer, which is the primary potable water source in the Miami-Fort Lauderdale metropolitan area (Parker et al. 1955; Hoffmeister 1974; Fish and Stewart 1991). The Key Largo Limestone interfingers with non-reefal limestones and has very high hydraulic conductivities, usually greater than 1000 ft/day (300 m/d; Fish and Stewart 1991). Where the Key Largo Limestone is exposed at land surface in the upper Florida Keys (Fig. 4.7), it produces only extremely limited quantities of freshwater because freshwater from precipitation readily flows to the sea and ocean water readily intrudes into the aquifer (Parker et al. 1955).

Examples of a pre-Cenozoic reef aquifers is the Permian Guadalupian Capitan Aquifer in west Texas and southeastern New Mexico (Motts 1968; Hiss 1980; Uliana 2001; George et al. 2011). The reefal carbonates have high transmissivities, but have limited use because of their marginal water quality.

The seaward of the reef are slope deposits that receive reef-derived sediments. The slope environment is transitional between the active and rapid production of calcium carbonate in the shallow-water platform and the slow gentle rain of fine-grained sediments in the basin (McIlreath and James 1984). The slope deposits consist of blocks and breccias of reef material (i.e., peri-platform tallus) that grades seawards into carbonate sands and then interbedded allochthonous sands and pelagic sediments.

Two types of carbonate margins are recognized: bypass and depositional environment (Enos and Moore 1983; McIlreath and James 1984). Bypass margins are characterized by steep slopes with submarine escarpments in which reef-derived sediments are transported from shallow to deep water without significant deposition on parts of the slope. The sediment transport may be channelized. Depositional margins have shallower slopes upon which carbonates sands are deposited. The fore-reef depositions thus consists of the interdigitation of allochthonous shallow-water carbonates sands and fine-grained pelagic and hemipelagic carbonates.

4.3.3 Carbonate Sands

Carbonate sand bodies may have greater hydraulic conductivities than adjoining carbonate mud-rich limestones and may, therefore, act as aquifers and aquifer zones. Most carbonate sands are composed of fragments of shells rounded to varying degrees (bioclasts), reworked lithified carbonate materials (intraclasts), and concentrically laminated grains (ooids) that form by calcite or aragonite precipitation, usually around a shell or rock fragments.

Carbonate sands are most commonly deposited in high-energy shallow-water environments, such as high-energy beaches (Fig. 4.8) and nonrestricted platforms in which current energy is sufficiently high to prevent deposition of carbonate muds. They represent the high-energy facies of shallowing-upwards sequences (Sect. 4.3.1). Carbonate sands may also be transported by gravity flows into deeper-water environments and by storms into sheltered lower-energy environments such as lagoons. Carbonate sand can form thick, relatively homogenous limestone units that are prized for building stone such as the Jurassic Portland Limestone of southern England (Fig. 4.9) and the Carboniferous Salem Limestone of Indiana (USA).

Carbonate sand may have greater primary (depositional) hydraulic conductivities than siliciclastic sands (for a given grain size) due to the occurrence of intragranular porosity and a looser grain packing caused by irregular grain shapes. As is the case for carbonate sediments in general, the petrophysical properties of carbonate sand units are largely dependent on their diagenetic history. Poorly cemented carbonate sands may retain high porosities and permeabilities. Conversely, well-cemented carbonate sands often have very low porosities and permeabilities and may act as confining units rather than aquifers, unless they have fracture or conduit secondary porosity.

Fig. 4.8 High-energy carbonate sand beach formed of comminuted coral and other skeletal grains. Dos Playas, Aruba

Fig. 4.9 Portland limestone, Tilly Whim Caves, Dorset, England. The caves are abandoned mines formerly used to produce the limestone building stone, which consists of cemented carbonate sand (bioclast grainstone)

4.3.4   Pelagic Carbonates

Pelagic carbonates are composed mostly of the fossils of planktonic organisms that were deposited out of suspension. Texturally, pelagic carbonates consists mostly of fossil mudstones and wackestones. Larger fossils may include both pelagic and benthic organisms, with the latter often having adaptations for living on a soft substrate. Pelagic carbonates may be reworked and redeposited by bottom currents. The purity of pelagic carbonates (i.e., calcium carbonate concentration) varies depending upon the amount of siliciclastic input, which usually consists mostly of clay-sized material. Pelagic carbonates may have a cyclic alternation of relatively clay-rich and clay-poor strata. Depending upon their composition, pelagic carbonates may have a very low diagenetic potential. For example, the Cretaceous/Tertiary chalks of northwestern Europe (Fig. 4.10) were deposited predominantly of low–magnesium calcite (as opposed to more reactive aragonite) and are thus still poorly lithified unless deeply buried. Diagenetic features include marine hardgrounds and chert (flint) formation. Pelagic carbonates may also have a high degree of heterogeneity where relative pure beds are interbedded with

Fig. 4.10 Upper Cretaceous chalk at Dover, southeastern England. World War II gun emplacements excavated into the soft chalk are shown for scale

Fig. 4.11 Lower chalk
(Dorset, England) with a
well-developed alternation of
relatively pure white chalk
beds and grayish clay-rich
marl beds (arrows)

clay-rich units. For example, the lower Chalk of southern England contains interbedded relatively pure chalk and clay-rich marl beds (Fig. 4.11).

Due to their very fine grain size, pelagic carbonates have very low matrix hydraulic conductivities. However, the aquifers may have well-developed secondary porosity and permeability. For example, the Cretaceous Chalk of southern England is used for water supply where it has enhanced transmissivity from fracturing.

References

Bathurst, R. G. C. (1972). Carbonate sediments and their diagenesis: Amsterdam: Elsevier.

Budd, D. A. (2001). Permeability loss with depth in the Cenozoic carbonate platform of west-central Florida. American Association Petroleum Geologists Bulletin, 85, 1253–1272.

Budd, D. A., & Vacher, H. L. (2004) Matrix permeability of the confined Floridan aquifer, Florida, USA. Hydrogeology Journal, 12, 531–549.

Choquette, P. W., & Pray, L. C. (1970) Geologic nomenclature and classification of porosity in sedimentary carbonates. American Association of Petroleum Geologists Bulletin, 54, 207–250.

Duerr, A. D. (1995). Types of secondary porosity of carbonate rocks in injection and test wells in southern peninsular Florida. U.S. Geological Survey Water-Resources Investigations Report 94–4013.

Dunham, R. J. (1962) Classification of carbonate rocks according to depositional texture. In W. E. Ham (Ed.), Classification of carbonate rocks. Memoir 1 (pp. 108–121); Tulsa: American Association of Petroleum Geologists.

Ehrenberg, S. N., & Nadeau, P. H. (2005) Sandstone vs. carbonate petroleum reservoirs: A global perspective on porosity-depth and porosity-permeability relationship. American Association of Petroleum Geologists Bulletin, 89, 435–445.

Ehrenberg, S. N., Eberli, G .P., Keramati, M., & Moallemi, S. A. (2006) Porosity-permeability relationships in interlayered limestone-dolostone reservoirs. American Association of Petroleum Geologists Bulletin, 90, 91–114.

Enos, P., & Moore, C. H. (1983) Fore-reef slope environment. In P. A. Scholle, D. G. Bebout & C. H. Moore (Eds.) Carbonate depositional environments. Memoir 31 (pp. 508–537). Tulsa: American Association of Petroleum Geologists.

Enos, P., & Sawatsky, L. H. (1981) Pore networks in Holocene carbonate sediments. Journal of Sedimentary Petrology, 51, 961–985.

Field, M. E., Cochran, S. A., & Evans, K. R. (2002) U.S. reefs – imperiled national treasures. U.S. Geological Survey Fact Sheet 025-02.

Fish, J. E., & Stewart, M. (1991) Hydrogeology of the Surficial Aquifer System, Dade County, Florida. U.S. Geological Survey Water-Resources Investigations Report 90-4108.

Gaswirth, S. B., Budd, D. A., & Crawford, B. R. (2006) Textural and stratigraphic controls on fractured dolomite in a carbonate aquifer system, Ocala Limestone, west-central Florida. Sedimentary Geology, 184, 241–254.

George, P. G., Mace, R. E., & Petrossian, R. (2011) Aquifers of Texas. Texas Water Development Board Report 380.

Halley, R. B., & Schmoker, J. W. (1983) High-porosity Cenozoic carbonate rocks of South Florida: Progressive loss of porosity with depth. American Association of Petroleum Geologists Bulletin, 67, 191–200.

Halley, R. B., Vacher, H. L., & Shinn, E. A., (1997) Geology and hydro-geology of the Florida Keys. In H. L. Vacher & H. L. Quinn (Eds.), Geology and hydrogeology of carbonate islands. Developments in Sedimentology 54 (pp. 217–248). Amsterdam: Elsevier.

Handford, C .R., & Loucks, R. G. (1993) Carbonate depositional sequences and system tracts – Responses of carbonate platforms to relative sea-level changes. In R. G. Loucks & J. F. Sarg (Eds.), Carbonate sequence stratigraphy. Recent developments and applications. Memoir 5 (pp 3–41). Tulsa: American Association of Petroleum Geologists.

Hiss, W.L. (1980) Movement of ground water in Permian Guadalupian aquifer systems, southeastern New Mexico and western Texas. In Guidebook, 31st Field Conference, Trans-Pecos Region (pp. 289–294). Socorro: New Mexico Geological Society.

Hoffmeister, J. E. (1974) Land from the sea. Coral Gables: University of Miami Press.

James, N. P. (1983) Reef Environment. In P. A. Scholle, D. G. Bebout & C. H. Moore (Eds.) Carbonate depositional environments. Memoir No. 31 (pp. 346–440). Tulsa: American Association of Petroleum Geologists.

James, N. P. (1984a) Shallowing – upwards sequences in carbonates. In R. G. Walker (Ed.) Facies models (2nd ed.) (pp. 213–228). Toronto: Geological Association of Canada Publications.

James, N. P. (1984b) Reefs. In R. G. Walker (Ed.) Facies models (2nd Ed.) (pp. 229–244). Toronto: Geological Association of Canada Publications.

Kendall, C. G. S. C., & Schlager, W. (1981) Carbonates and relative changes in sea level. Marine Geology, 44, 181–212.

Kerans, C., & Tinker, S. W. (1997) Sequence stratigraphy and characterization of carbonate reservoirs. Short course 40. Tulsa: SEPM (Society for Sedimentary Geology).

Lucia, J. F., Kerans, C., & Jennings, J. W., Jr. (2003) Carbonate reservoir characterization. Journal of Petroleum Technology, June 2003, 70–72.

Maliva, R. G., Guo, W., & Missimer, T. (2007) Vertical migration of municipal wastewater in deep injection well systems, South Florida, USA. Hydrogeology Journal, 15, 1387–1396.

Maliva, R. G., Kennedy, G. P., Martin, W. K., Missimer, T. M., Owosina, E. S., & Dickson, J. A. D. (2002), Dolomitization-induced aquifer heterogeneity: Evidence from the Upper Floridan Aquifer, Southwest Florida. Geological Society of America Bulletin, 114, 419–427.

Maliva, R. G., & Walker, C. W. (1998) Hydrogeology of Deep-Well Disposal of Liquid Wastes in Southwestern Florida, U.S.A. Hydrogeology Journal, 6, 538–548.

McIlreath, I. A., & James, N. P. (1984) Carbonate slopes. In R. G. Walker (Ed.) Facies models (2nd Ed.) (pp. 245–257). Toronto: Geological Association of Canada Publications.

McIlreath, I. A., & Morrow, D. W., (Eds.) (1990) Diagenesis, Geoscience Canada reprint series 4. St Johns Newfoundland: Geological Association of Canada Publications.

Moore, C. H. (1989) Carbonate diagenesis and porosity. Developments in Sedimentology 46. Amsterdam: Elsevier.

Moore, C. H. (2001) Carbonate reservoirs: porosity evolution and diagenesis in a sequence stratigraphic framework. Developments in Sedimentology 55. Amsterdam: Elsevier.

Motts, W. S. (1968) The control of ground-water occurrence by lithofacies in the Guadalupian reef complex near Carlsbad, New Mexico. Geological Society of America Bulletin, 79, 283–298.

Parker, G. G., Ferguson, G. E., Love, S. K., and others (1955) Water resources of southeastern Florida. U.S. Geological Survey Water-Supply Paper 1244.

Read, J. F. (1985) Carbonate platform facies models. American Association of Petroleum Geologists Bulletin, 69, 1–21.

Reese, R. S., & Richardson, E. (2008) Synthesis of the hydrogeologic framework of the Floridan Aquifer System and delineation of a major Avon Park permeable zone in Central and Southern Florida. U.S. Geological Survey Scientific Investigations Report 2007-5207.

Safko, P. S., & Hickey, J. J. (1992) A preliminary approach to the use of borehole data, including television surveys, for characterizing secondary porosity of carbonate rocks in the Floridan Aquifer System. U.S. Geological Survey Water-Resources Investigations Report 91-4168.

Saller, A. H., Budd, D. A., & Harris, P. M. (1994) Unconformities and porosity development in carbonate strata: Ideas from a Hedberg Conference. American Association of Petroleum Geologists Bulletin, 78, 857–872.

Sarg, J. F. (1988) Carbonate sequence stratigraphy. In C. K. Wilgus, C. A. Ross & H. Posamentier (Eds.), Sea-level changes - an integrated approach. Special Publication 42 (pp. 155–181). Tulsa: SEPM (Society for Sedimentary Geology).

Schlager, W. (2005). Carbonate sedimentology and sequence stratigraphy. Concepts in sedimentology and paleontology 8. Tulsa: SEPM (Society for Sedimentary Geology).

Schmoker, J. W., & Halley, R. B. (1982) Carbonate porosity versus depth: a predictable relation for South Florida. American Association of Petroleum Geologists Bulletin, 66, 2561–2570.

Scholle, P. A., Bebout, D. G., & Moore, C. H. (1983) Carbonate depositional environments. Memoir 31. Tulsa: American Association of Petroleum Geologists.

Scholle, P. A., & Halley, R. B. (1985) Burial diagenesis: Out of sight, out of mind. In N. Schineidermann & P. M. Harris, (Eds.) Carbonate cements. Special Publication 36 (pp. 309–334). Tulsa: Society of Economic Paleontologists and Mineralogists.

Selley, R. C. (1985) Ancient sedimentary environments and their subsurface diagenesis (3rd ed.). Ithaca: Cornell University Press.

Tucker, M. E. (1985) Shallow marine carbonate facies and facies models. In P. J. Brenchley & B. P. J. (Eds.). Sedimentology, recent development and applied aspects. Special Publication 18 (pp. 147–169). London: Geological Society.

Tucker, M. E., & Bathurst, R. G. C. (Eds.) (1990) Carbonate diagenesis: International Association Sedimentologists Reprint Series 1. Oxford: Blackwell Scientific Publications.

Uliana, N. M. (2001) The geology and hydrogeology of the Capital Aquifer – A brief overview. In R. E. Mace, W. F. Mullican, III & E. D. Angle (Eds.) Aquifers of West Texas. Report 356 (pp. 207–225). Austin: Texas Water Development Board.

Vacher, H. L. (1997) Introduction; Varieties of carbonate islands and a historical perspective. In H. L. Vacher & T. and Quinn (Eds.) Geology and hydrogeology of carbonate islands, Developments in sedimentology 54 (pp. 1–33): Amsterdam: Elsevier.

Wilson, J. L. (1975) Carbonate facies in geological history. New York: Springer-Verlag.

Chapter 5
Aquifer Characterization Program Development

Aquifer characterization programs need to be designed to provide the specific data required for groundwater resources projects, which commonly involves the development of conceptual and numerical groundwater models. Available characterization techniques are compiled in terms of the type of information provided and scale (investigated volume or radius of influence). Important considerations in the selection and implementation of characterization techniques are the investigated volumes and resolution of the technique, scale of aquifer heterogeneity, scale at which data will be used (e.g., model grid cell size), and whether or not solute transport is of concern. Selection of techniques should also consider the scale dependence of hydraulic conductivity values. Aquifer characterization techniques have underlying assumptions and limitations, and field conditions requirements that constrain their successful implementation.

5.1 Introduction

Numerous techniques are available to obtain and process data on the hydraulic, physical, and chemical properties of aquifers. The development of aquifer characterization programs involves the selection of a suite of techniques that can meet project-specific data requirements, are technically feasible at a project site, and can be accommodated by project budgetary and scheduling constraints. A key consideration is how the data are to be used. Data collected in aquifer characterization programs are commonly used to develop numerical groundwater models. Hence, the elements of an aquifer characterization program should be designed to meet the data requirements of the project-specific groundwater model. Projects concerned with aquifer water quality may require the use of techniques that allow the collection of representative water samples and perhaps also formation samples to allow for mineralogical analyses and modeling of fluid–rock interaction.

Technical feasibility addresses project logistical and hydrogeological constraints and also the local availability of required equipment and professional resources. For example, surface geophysical techniques (both land based and airborne) can cost-effectively provide information on local and regional hydrogeology and water quality, but may not be feasible in suburban and urban areas due to interference from anthropogenic features. The feasibility of borehole-based techniques depends on borehole conditions such as whether a formation is lithified, unconsolidated, or permanently cased off or screened. Groundwater investigations have budgetary limits that constrain the number and specific types of characterization techniques employed and the extent of their implementation (e.g., number of test wells and pumping tests performed).

An aquifer characterization program should always start with a rigorous review of available data on the aquifer or aquifer system of interest, which is referred to as a 'desktop' investigation. In most areas of the world, there is now at least some information available on local geology and hydrogeology, which can be used to develop an initial conceptual model. The conceptual model may include identification of basic hydrostratigraphy, sediment and rock types, and predominant porosity and permeability types. For example, it is clearly important to know at the start of the development of an aquifer characterization program if one is dealing with a karst or fractured system in which flow is dominated by secondary porosity. Local knowledge and experience can also be invaluable. Competent local hydrogeologists should, over the course of their work, develop a strong conceptual understanding of the areas in which they work. Local well drillers can also provide valuable information on local aquifers and drilling conditions.

5.2 Groundwater Model Scale

Groundwater models vary in their geographic and vertical extent and discretization, which refers to the division of the model domain into grid cells (finite-difference approach) or elements (finite-element discretization). The size of the project domain and discretization scale (e.g., grid cell dimensions) is project and thus model specific. Regional groundwater flow models often have geographic boundaries of 100 s of km and grid cells on the order of 1–10 km in length. On the contrary, models to evaluate solute transport at contamination sites, may have domain lengths of 1 km or less and local grid size in the core model area on the order 1 to 5 m (or even less). Models of solute transport, in general, require a smaller grid size in order to better capture flow-controlling aquifer heterogeneity.

A useful intellectual activity to understand the effects of volume of investigation and model scale is to superimpose a model grid cell on outcrop photos (Fig. 5.1) to visualize the type of aquifer heterogeneity that is incorporated as an average value (i.e., upscaled) into a model cell. Irrespective of modeling, the degree and scale of

aquifer heterogeneity are often not appreciated in studies relying solely on limited borehole or well data. Even for the relatively low heterogeneity strata illustrated in Fig. 5.1, a high degree of heterogeneity is evident as thin clay-rich beds separating thicker sandstone units. Clearly, permeability or hydraulic conductivity data from one or a limited number of core samples would not be expected to be representative of the average hydraulic conductivity (and thus transmissivity) of a 10 m by 100 m model grid cell. The layered heterogeneity would result in a high vertical to horizontal anisotropy.

The strata illustrated in Fig. 5.1 happen to have a high degree of horizontal continuity. A vertical series of fine-scale measurements, if strategically collected, could provide data on the vertical variation of hydraulic conductivity, which could be used to estimate the values of effective vertical hydraulic conductivity needed to evaluate vertical fluid flow and solute transport. Borehole geophysical data combined with pumping test data would likely be sufficient to deterministically characterize the layered heterogeneity within individual grid cells and perhaps across the model domain depending upon the degree of lateral heterogeneity and density (coverage) of logs. If horizontal heterogeneity is on a finer scale than data points (e.g., well spacing), and thus accurate deterministic mapping of heterogeneity is not possible, then geostatistical techniques may be employed to better capture the heterogeneity (Chap. 20).

Fig. 5.1 Photo of outcrop (Mesa Verde National Park, Colorado, USA) with superimposed, approximately 10 m by 100 m and 20 m by 200 m, grid cells

As a generalization, the volume of investigation of aquifer characterization techniques should be comparable with the scale of interest (e.g., model grid cell size). For a large-scale model, it is preferable to measure the transmissivity of the local aquifer through pumping tests rather than estimating a transmissivity from numerous small-scale hydraulic conductivity measurements. However, upscaling techniques are available to obtain equivalent parameter values (particularly hydraulic conductivity) for model grid cells from small-scale measurements (Chap. 16). Aquifer characterization programs need to be based on a firm understanding of the type of information provided by the various available techniques, the scale and limitations of each technique, and how the data will eventually be processed and used to achieve project goals.

5.3   Aquifer Characterization Techniques

A wide variety of techniques are available for evaluating the hydraulics and transport properties, water quality, and mineralogy of aquifers. Aquifer characterization techniques are addressed to varying degrees in most hydrogeology text books. Hydrogeology field techniques were reviewed in dedicated texts by Assad et al. (2004) and Weight (2008). Maliva and Missimer (2010, 2012) provided an overview of aquifer characterization techniques applicable to manage aquifer recharge and arid lands investigations. The U.S. Geological Survey published a series of Techniques of Water-Resources Investigations Reports, which are available online (http://pubs.usgs.gov/twri/) (Tables 5.1 and 5.2).

Lists of common aquifer characterization techniques are provided in Tables 5.1 through 5.3, which are sorted based on the type of information they provide and their volume of investigation, which is expressed in terms of radial distance from the sample point (e.g., well). Tables 5.1 through 5.3 are not exhaustive, and less commonly used techniques and applications of the listed techniques are available (and discussed in subsequent chapters). Assigned volumes of investigation are rough approximations that are intended to allow relative comparison of techniques. The actual volume of investigation for any given test will depend upon both site-specific hydrogeological conditions and test procedures, which are variable.

5.3.1   Aquifer Hydraulic Properties Evaluation Techniques

Fine-scale techniques include measurements that involve direct or indirect measurements of the porosity and permeability of sediments or sedimentary rock samples. The measurements may be performed either in the laboratory or field. Depending upon the technique and data processing methods used, either permeability or hydraulic conductivity values may be obtained. Direct measurements

Table 5.1 Techniques to determine aquifer hydraulic properties

Technique	Approximate scale (m)	Primary type of information
Fine-scale techniques		
Core permeameter	0.025–0.1	Porosity and permeability of core plugs and whole-core samples
Sand grain size analysis	0.05–0.1	Permeability estimated from grain size distribution
Minipermeameter	0.01–0.1	Permeability of slabbed cores or outcrop surfaces
Small-scale techniques		
Slug test	0.5–10	Hydraulic conductivity
Direct-push testing techniques	0.01–2	Hydraulic conductivity and lithology
Borehole geophysical techniques	0.01–2	Porosity, hydraulic conductivity profile, groundwater resistivity, lithology
Push-pull tracer tests and tracer dilution tests	0.1–10	Transport parameters (dispersivity)
Medium-scale techniques		
Packer pumping tests	5–100	Hydraulic conductivity and transmissivity
Single-well pumping tests	10–500	Hydraulic conductivity and transmissivity
Multiple-well tracer tests	5–100	Flow direction, location of flow zones, transport parameters (dispersivity and effective porosity)
Cross-well tomography	10–500	Identification of high and low porosity and permeability zones
Large-scale techniques		
Multiple-well aquifer pumping tests	10–5,000	Transmissivity, storativity, leakance
Karst system tracer tests	10–10,000	Flow paths and flow velocity
Very large-scale techniques		
Regional groundwater model calibration	1,000–20,000	Transmissivity, storativity, leakance
Tidal fluctuation analysis	500–50,000	Transmissivity, storativity

include core plug and whole-core porosity and permeability measurements and minipermeameter measurements performed on either slabbed core samples or outcrop surfaces. Indirect measurements techniques include estimation of permeability and hydraulic conductivity from sand grain-size data. Porosity may also be estimated from thin section petrography. Fine-scale measurements also include borehole-imaging techniques, which are of particular value for identifying secondary porosity features (e.g., fractures).

Small-scale aquifer characterization techniques include hydraulic testing techniques that involve the pumping or injection of small volumes of water. The volumes of investigation are on the decimeter to 10 m scale. Slug tests (Chap. 8) and

Table 5.2 Techniques to determine aquifer lithology and mineralogy

Technique	Approximate scale (m)	Primary type of information
Cutting and core description	0.01–0.1	Rock types, mineralogy, rock textures and fabrics
Thin section petrography	0.01	Rock types, mineralogy, rock textures and fabrics
X-ray diffractometry	0.01	Mineralogy
X-ray fluorescence	0.01	Elemental composition
Scanning electron microscopy and electron microprobe	0.01	Rock textures, mineralogy, and mineral elemental composition
Borehole geophysical logs	0.01–2	Primary lithology and mineralogy
Surface geophysics	1–200 (depth)	Large-scale lithology changes

Table 5.3 Techniques to determine water chemistry

Technique	Approximate scale (m)	Primary type of information
Thief sampler	0.05	Sample of water in a well presumably in equilibrium with formation water
Direct-push water samples	0.1–1.0	Sample of water in the immediate vicinity of probe
Borehole geophysical techniques	0.01–2	Data on fluid resistivity or conductivity in borehole and formation water resistivity
Packer testing	1–50	Sample of water from the vicinity of test interval
Surface geophysics	1–200+ (depth)	Data on formation resistivity that can be processed to obtain fluid resistivity and salinity
Monitoring and production wells	1–100+	Sample of water from the vicinity of a well or averaged sampled from capture area of production well

direct-push permeameter and injection logger (Chap. 12) are small-scale techniques. Small-scale techniques also include borehole geophysical logging techniques whose depth of investigation varies with tool type and configuration (Chap. 10). Push-pull tracer tests usually have volume of investigation in the 1 m to 10 s m ranges, with the actual value depending upon interval thickness, heterogeneity, effective porosity, and injected volume. Tracer dilution tests can measure local flow into and out of the borehole and thus reflect near-hole conditions and groundwater flow rates.

Medium-scale aquifer characterization techniques involve pumping of or injection into a single well. Packer tests and single-well pumping tests with durations of hours to days fall into the medium-scale range, which have volumes of investigations on the order of 10–100 s of meters. Tracer tests also commonly fall into the medium-scale category, although tests may be performed on closer-spaced wells, and some tests performed in karst terrains have lengths of a kilometer or

greater. Cross-well tomographic techniques also usually fall in the medium-scale category with the volume of investigation being the actual well spacing. Surface nuclear magnetic resonance soundings can, in theory, provide coarse-scale data on aquifer pore size distribution and, in turn, hydraulic conductivity, down to depths of 100 m or greater, but at the present time its operational accuracy appears restricted to locating relative transmissive strata rather than accurate values of hydraulic parameters.

Large-scale aquifer characterization techniques have a distance of investigation in the 100 m–10 km range. The main large-scale aquifer characterization technique is multiple-well aquifer pumping tests. Very large-scale techniques have scales of investigation of 10 s of km or greater and include calibration of regional models and tidal fluctuation analyses.

5.3.2   Aquifer Lithology and Mineralogy Evaluation Techniques

Data on aquifer mineralogy is important where fluid–rock interaction is of concern. Managed aquifer recharge (MAR) and injection well projects are sensitive to fluid–rock interactions because water that is introduced into a formation is usually not in chemical equilibrium with formation minerals and varies in composition and properties from native groundwater. Mineralogical investigations for MAR projects were reviewed by Maliva and Missimer (2010). Mineralogical characterization of aquifers most commonly requires collection of formation samples either in the form of well cuttings or cores. Techniques used to determine mineralogy of grab samples include visual examination (assisted with a hand lens or stereomicroscope), thin section petrography, and x-ray diffractometry (XRD; Sect. 9.6). Formation samples are essentially point samples that inherently have a very small volume of investigation. A common procedure for evaluating the mineralogy of an aquifer is to analyze a suite of samples selected as being representative of the various lithofacies present in the aquifer.

Mineral phases that are present in trace quantities can have a greatly disproportionate geochemical impact. For example, arsenic-bearing pyrite, present in aquifers at concentrations of much less than one mass percent, is the apparent source of arsenic that leached into water stored in some aquifer storage and recovery (ASR) systems. The leaching caused arsenic concentrations in the stored freshwater to exceed drinking water standards. If fluid–rock interactions involving trace minerals are a potential concern, then great care is required to insure that all rock types are sampled and that the sample analytical techniques used are capable of detecting the minerals of concern. Very fine resolution techniques, such as thin section petrography, scanning electron microscope, and the electron microprobe, are needed to identify trace minerals (especially if they are very finely crystalline) and determine their elemental composition.

Borehole geophysical logging techniques are available to identify and determine the approximate abundance of the primary minerals present in a formation. Natural gamma ray and resistivity logs are often used to differentiate between clay-rich strata and clay poor sands, sandstones, and limestones. Gamma ray spectroscopy logs provide information of elemental abundance, which data are further processed to determine mineralogy. The predominant minerals present in a rock may also be estimated using combinations of logs such a natural gamma ray, density and neutron, and photoelectric effect. Geophysical logging techniques have the advantage of providing a continuous profile (numerous high-frequency readings). Their main disadvantages are that they have a relatively low accuracy and can only identify a limited suite of minerals, albeit those most commonly found in sedimentary rocks. Geophysical logs used to determine mineralogy have a small volume of investigation, with depths of investigation into the formation usually ranging from the borehole wall to about 1–2 m.

Land-based and airborne surface geophysical techniques (Chap. 11) also fall into the large-scale category, as they can provide coarse-scale hydrogeological information down to depths of 100 s of meters below land surface. Surface geophysical techniques can provide information on the locations of some thick aquifer and confining units and their salinity. Surface geophysical survey techniques have the great advantage of the capability of cost-effectively providing extensive spatial coverage, which for airborne surveys can be in the range of 10 s of km (or more).

5.3.3   Water Chemistry Evaluation Techniques

Data on groundwater chemistry are typically obtained from grab samples collected from wells. Data on groundwater salinity can also be obtained from geophysical techniques. Where a well is continuously pumped (e.g., an on-line production well), samples may be collected directly from a sampling tap or port. In the case of a well in which water has been standing in the well for a prolonged period of time, the water at a given depth in the completion zone (i.e., screened or open-hole interval) may have a similar concentration as water in the adjacent formation, provided that there is not significant vertical flow within the well and gas exchange with the atmosphere. Discrete water samples may be obtained from specific depth intervals in wells using downhole sampling devices (e.g., thief samplers).

The most commonly used water sampling technique in non-continuously pumped wells is to purge a number of well volumes (usually three or more). The purging removes the stagnant water within the well, which is subject to physicochemical changes, so that a water sample 'representative' of in situ groundwater is obtained. A standard procedure is to also monitor the purge water for field parameters (e.g., pH, electrical conductivity, temperature, dissolved oxygen, oxidation reduction potential), which should stabilize (within 5 %) prior to sample collection. The entire completion zone is sampled by pumping a well. The composition of the water sample collected from a well is the transmissivity-weighted

average of the composition of water produced from the different zones intercepted by the well screen or open hole. The most transmissive zones will produce a proportionately greater amount of amount of water and thus have a larger contribution to the chemical composition of the sample.

Where entire-well, depth-averaged water samples are insufficient for a project, then a variety of techniques are available to collect water samples from specific depth intervals of aquifers. Water samples may be obtained by isolating intervals of an aquifer in wells or boreholes using inflatable packers. In shallow unlithified aquifers, direct-push sampling techniques are used to collect a series of water samples with depth as the tool string is advanced. Long-term, discrete-depth monitoring can be performed using multiple-well or multi-level sampling techniques.

The depth of investigation of samples of water obtained from a well or packer test zone depends upon the volume of water purged prior to sample collection and the effective porosity of the formation. Assuming water is produced from the zone of interest by horizontal displacement with minimal dispersive mixing (i.e., 'piston' flow), the radius of investigation can be calculated from the pumped volume (V_p), interval thickness (b), and effective porosity (n_e):

$$\frac{V_p}{n_e} = \pi r^2 b \qquad (5.1)$$

$$r = \sqrt{\frac{V_p}{n_e \pi b}} \qquad (5.2)$$

Water samples collected from monitoring wells that are pumped only during infrequent sampling events are derived from the immediate vicinity of the well. On the contrary, water samples collected from continuously pumped production wells are more representative of the average aquifer water composition in the capture zone, provided that groundwater pumping has not induced significant vertical leakage, recharge, or other flows into the aquifer. In the case of leaky aquifers, an equilibrium is reached between the rates of abstraction and rates of leakage into the aquifer. The composition of water samples from wells that have been pumped at high rates for prolonged periods of time prior to sample collection may not be representative of the 'normal' aquifer groundwater composition near the well. In the case of a contamination assessment, the water that leaks into the aquifer and contributes to the abstracted water could have contaminant concentrations either greater or less than the concentrations of ambient groundwater in the aquifer. The effects of vertical fluid migration on the chemistry of collected water samples are even a greater concern in the case of partially penetrating wells.

The salinity of groundwater can be estimated using resistivity-based borehole (Sect. 10.5) and surface (Sects. 11.2 to 11.4) geophysical techniques. The concentrations of total dissolved solids (TDS) and other salinity parameters (e.g., chloride) are calculated from fluid resistivity and conductivity values using empirical relationships. For wells that have been shut-in for an extended period of time and reached chemical equilibrium with adjoining groundwater, salinity versus

depth profiles may be obtained from fluid resistivity (or conductivity) logs. Salinity versus depth profiles can also be obtained from formation resistivity data obtained from standard resistivity or induction logs and porosity data. Pore water (groundwater) resistivity can be calculated from formation resistivity and porosity using the Archie (1942) equation (Sect. 10.7). Borehole geophysical logging techniques typically provide information on salinity within about 2 m of the borehole, with the actual value depending upon tool type and configuration and local geology. A deep-reading tool is needed to obtain formation resistivity values, beyond the drilling fluid invasion and transition zones.

Surface geophysical techniques performed on land and using airborne platforms have been successfully used to map vertical and geographical variations in formation resistivity, which can also be processed to obtain data on salinity using information on rock types and porosity. Depending upon the technique and equipment used, the depth of investigation may extend into the 100 s of m. Surface geophysical techniques have relatively low resolution and are most suitable for mapping pronounced variations in salinity such as the coastal interface between fresh and saline water.

5.4 Scale Dependence of Aquifer Properties

An important issue when developing an aquifer characterization program is first determining the scale of aquifer heterogeneity present in the studied area and the scales relevant to the project. The significance of aquifer heterogeneity varies depending upon whether the project is concerned solely with groundwater levels or if the simulation of solute transport is an objective. The approximate scales of techniques used to evaluate hydraulic conductivity are plotted on Fig. 5.2. A fundamental issue is the relationship between (Ptak et al. 2004):

- investigation scale (size of the domain of concern)
- scale of heterogeneity
- detection scale of investigation technique.

It has long been observed that the hydraulic conductivity measured in aquifers increases with scale of measurement (radius of influence). As reviewed by Neuman (1994) and Rovey and Cherkauer (1995), measured hydraulic conductivity values typically increase from the laboratory scale (grain size and permeameter measurements) to values obtained from slug tests, pumping tests, pressure injection tests, aquifer pumping tests, and then from regional model calibration. Dispersivity also shows a strong scale dependence (Sect. 1.4.5).

The increase in hydraulic conductivity with scale tends to have an upper limit, beyond which hydraulic conductivity becomes independent of the scale of measurement (Rovey and Cherkauer 1995; Schulze-Makuch et al. 1999). The upper limit depends upon the aquifer material. For example, within the carbonates studied
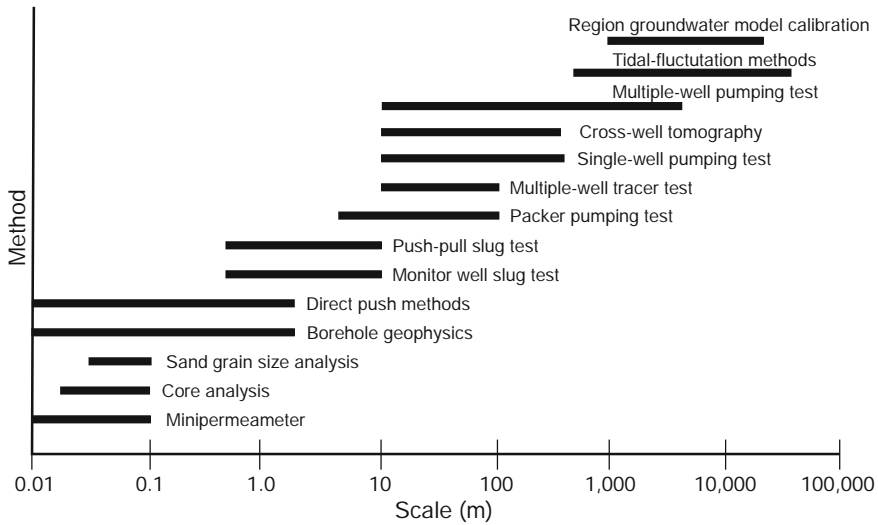
Fig. 5.2 Approximate scale (radius of investigated volume) of techniques used to measure hydraulic conductivity

by Rovey and Cherkauer (1995), the range of the scale increase in hydraulic conductivity correlated with the degree, and possibly type, of secondary porosity. Karstic limestones have a range of scale increase in hydraulic conductivity in kilometers or may not have an upper bound. Rovey and Cherkauer (1995) suggested that the scale dependency of hydraulic conductivity for a given formation might be used to evaluate the type and degree of development of secondary porosity.

Scale dependency of hydraulic conductivity is a function of the type of fluid flow in the medium (e.g., matrix, fracture, or conduit) and the degree of heterogeneity (Schulze-Makuch et al. 1999). Schulze-Makuch et al. (1999) proposed a scaling equation

$$K = cV^m \qquad (5.3)$$

where c is a parameter characteristic of the medium, V is the volume of medium being tested (m^3), and m is a scaling exponent. The value of m is about 0.5 for porous (intergranular) media and close to 1.0 for media with fracture and conduit flow. The definition of the volume of tested material used by Schulze-Makuch et al. (1999) is the volume of water used in the test. Equation 5.1 applies only below the upper boundary above which K is independent of V.

The increase in hydraulic conductivity with scale has been attributed to an increased likelihood that rare high-hydraulic conductivity flow zones or features will be encountered with increasing scale of measurement (e.g., Carerra 1993; Rovey and Cherkauer 1995; Schulze-Makuch et al. 1999; Schulze-Makuch and

Cherkauer 1998). The scale-dependent increase in hydraulic conductivity with test technique is related to the variance in hydraulic conductivity. As media approaches a homogenous character, no relationship between K and scale of measurement should occur.

Although fine-scale, high-resolution data appear attractive from a scientific perspective, they may not actually provide real benefits if the data have to be averaged (upscaled) to populate large-scale model grid cells or nodes. Upscaling of multiple finer scale measurements may be much less accurate than data collected at the project-appropriate scale in heterogeneous aquifers. For example, estimates the of aquifer transmissivity for an interval from multiple core measurements will tend to give much lower values than obtained from a full-well or packer pumping test, because the core analyses may miss the most permeable intervals that make the greatest contribution to the transmissivity. Frequently, the most permeable strata in cored intervals are either not recovered or are recovered as rubble zones. For example, at the Bolivar ASR site in South Australia, it was observed that hydraulic conductivity values obtained from core samples resulted in an underestimation of the transmissivity by a factor of almost 50. The bias toward low values was attributed to the preferential recovery of well-cemented sections of the aquifer (Pavelic et al. 2006). In general, there is a poor agreement between grain size- based hydraulic conductivity measurements and in situ field measurements of permeability, especially for fine-grained materials, because of the difference between bulk and matrix K due to macropores (Campbell et al. 1990).

The scale effect of increasing hydraulic conductivity values with a greater volume of investigation does not always occur. Desbarats and Bachu (1994) observed the opposite relationship in a comparison of transmissivity estimates from core plug analyses and drill stem (packer) tests (DSTs) in a Late Cretaceous sandstone from northeastern Alberta, Canada (Wabiskaw Member of the Manville Group). The median transmissivity from the DSTs was two orders of magnitude less than the values obtain from core data. The lower transmissivity values from the DSTs was suggested as possibly being due to the DST flow pattern being more spherical and thus possibly depressed by a lower vertical than horizontal hydraulic conductivity.

5.5   Constraints on Implementation of Characterization Techniques

Aquifer characterization techniques have underlying assumptions and limitations and field condition requirements that constrain their successful implementation. These constraints are addressed in the discussions of each technique. In addition, there are constraints associated project budgets and schedules and local availability of equipment and technical expertise.

Most aquifer characterization techniques require one or more wells or borings to either stress aquifers, record aquifer responses to stress (e.g., changes in pressure or water levels), or to provide access to the formation for measurement techniques (e.g., borehole geophysical logging) and sample collection. Borehole-based aquifer characterization techniques vary in their required borehole conditions, which may limit which techniques could be employed in a given investigation. Three main borehole conditions are

- lithified strata
- cased wells
- unconsolidated strata.

Formations that are lithified, or at least cohesive enough so that an open hole is stable, have a relatively high degree of flexibility in the types of characterization techniques that can be employed because they allow direct access to the formation. Open-hole conditions are suitable for hydraulic testing and borehole geophysical logging techniques. Lithified strata can also be cored with undisturbed samples obtained. Cased wells are the least flexible, particularly where previously constructed wells are used whose completion may not coincide with project data needs. For example, partially penetrating wells or wells with multiple-zone completions, present challenges for obtaining accurate data on aquifer hydraulic properties. Many geophysical logging techniques can either not be run on cased wells or provide lesser quality data due to attenuation of the formation signal by the casing. Some aquifer characterization techniques also have borehole diameter limitations. Logging tools have minimum borehole diameter requirements and often also lose accuracy or resolution above a tool or technique-specific maximum value. Borehole packers also have minimum and maximum borehole diameter limits.

Aquifer hydraulic testing in unconsolidated strata requires the installation of a permanent or temporary screen to keep the borehole open. Shallow unconsolidated strata can be investigated using direct-push technologies (Chap. 12), which allow for more rapid and less expensive collection of water samples and aquifer testing than is possible using conventional drilling techniques. Geophysical logs can be run in unconsolidated strata if the borehole is stabilized using drilling mud.

Aquifer characterization programs need to be designed so that they can be performed under project-specific well and borehole conditions. An equally important principle is that well and borehole drilling conditions should be specified so that they can accommodate the planned aquifer testing program. For example, a test well program should be designed backwards starting with the diameter and borehole requirements for a planned geophysical logging and other testing programs. The required borehole diameter for logging would dictate the minimum diameter of some casing strings. If the formation is unconsolidated, then the planned logging program may require the use of the mud-rotary drilling technique to provide a stable borehole.

Surface geophysical techniques can be valuable tools in aquifer characterization programs because of their typically lower cost and greater speed than borehole-based techniques, which allow for a greater spatial coverage (Sect. 11.1). However, it has not been uncommon for the results of surface geophysical investigations to fail to meet expectations. A fundamental limitation of surface geophysical techniques is that the data are processed using inverse modeling techniques, which do not provide unique solutions. Borehole drilling and testing are typically required to confirm (ground truth) or calibrate data obtained using surface geophysical methods. Geophysical techniques are also subject to interference and have basic constraints on their resolution, depth of investigation, and ability to provide usable data in various geological settings. Forward modeling, based on prior knowledge of local geology and the likely properties of the strata expected to be encountered, is strongly recommended to determine whether the target data are likely obtainable.

The adage, "failing to plan is planning to fail", apparently paraphrased from Benjamin Franklin, is apropos to aquifer characterization. Fundamental elements for planning an aquifer characterization program are

- determination of data requirements
- identification of techniques that can provide the required data at a project-appropriate scale
- evaluation of project-appropriate techniques for economic, technical, and scheduling feasibility
- development of an integrated program that accommodates the selected feasible characterization techniques.

5.6 Use of Aquifer Characterization Data

Values of aquifer properties obtained from well- or borehole-based techniques are point measurements that are representative of only a very small fraction of the total aquifer volume. The accuracy of each measurement is dependent on the assumptions and limitations of each technique used and data quality, which may be affected by inaccuracies in measurements and well and borehole conditions. Hence, any measurement of aquifer properties should always be considered an estimate. The professionals involved in a project, therefore, need to objectively evaluate the accuracy and representativeness of the data. Data quality is an especially important concern where external data (i.e., data collected and interpreted by others) are used, such as published transmissivity values from aquifer pumping tests, and where independent review and evaluation of the data is not possible.

The question arises as to how the data are to be used, which influences the aquifer characterization program. Individual data points, such as a transmissivity value from a pumping test, can be assumed to be correct and locally representative and, therefore, incorporated into a groundwater model as a fixed constant value. The value of other cells may then be estimated using geostatistical techniques such

as kriging (Sect. 20.2). Another option is to use field data as fixed pilot points in inverse modeling (Sect. 19.2.6).

An alternative approach is to use field data as initial estimates, subject to adjustment during model calibration. The extent to which a field data point may be adjusted during model calibration can be constrained. If a substantial change in the value of a field point (e.g., transmissivity value from a pumping test) is required to calibrate a model, then the reason for the need for the change needs to be investigated. The inconsistency between field data and model calibration results could indicate that the underlying conceptual model may be incorrect. Another possibility is that the field data could be incorrect due to poor field practices or mistakes in data processing.

Use of the data should be concordant with its quality. Data with relatively large inherent inaccuracies or inappropriate scales are not appropriate for applications where their accuracy is implicitly or explicitly assumed. For example, transmissivity values obtained from specific capacity data have relatively large uncertainties compared to values obtained from multiple-well pumping tests. The specific capacity-based transmissivity data are, therefore, suitable for initial estimates of transmissivities, but caution is advised before they are used as firm (fixed) values. Similarly, properly performed slug tests can provide accurate data on local aquifer hydraulic conductivity if performed correctly on properly developed boreholes. However, slug test-based transmissivity values should be viewed as rough estimates of large-scale aquifer transmissivity because they are based on a small volume of investigation and can be greatly impacted by borehole conditions.

References

Archie, G. E. (1942) The electrical resistivity log as an aid in determining some reservoir characteristics. Transactions American Institute of Mining Metallurgical and Petroleum Engineers, 146, 54–67.

Assaad, F. A., LaMoreaux, J. E., & Huges, T. (Eds.) (2004) Field techniques for geologists and hydrogeologists. Berlin: Springer.

Campbell, M. D., Starrett, M. S., Fowler, J. D., & Klein, J. J. (1990) Slug tests and hydraulic conductivity. In Proceedings 4th Petroleum and Organic chemicals in Groundwater. Prevention, Detection and Restoration (pp. 85–99). Dublin, Ohio: National Water Well Association.

Carrera, J. (1993) An overview of uncertainties in modelling groundwater solute transport. Journal of Contaminant Hydrology, 13, 23–48.

Desbarats, A. J. & Bachu, S. (1994) Geostatistical analysis of aquifer heterogeneity from the core scale to the basin scale: A case study. Water Resources Research, 30, 673–684.

Maliva, R. G., & Missimer, T. M. (2010) Aquifer storage and recovery and managed aquifer recharge using wells: Planning, hydrogeology, design, and operation: Houston: Schlumberger Corporation.

Maliva, R. G., & Missimer, T. M. (2012) Arid lands water evaluation and management: Berlin: Springer.

Neuman, S. P. (1994) Generalized scaling of permeabilities: Validation and effect of support scale. Geophysical Research Letters, 21, 349–352.

Pavelic, P., Dillon, P. J., & Simmons, C. T. (2006), Multiscale characterization of a heterogeneous aquifer using an ASR operation. Ground Water, 44, 155–164.

Ptak, T., Peipenbrink, M., & Martac, E. (2004) Tracer tests for the investigation of heterogeneous porous media and stochastic modelling of flow and transport – a review of some recent developments. Journal of Hydrology, 294, 122–163.

Rovey, C. W., III, & Cherkauer, D. S. (1995) Scale dependence of hydraulic conductivity measurements, Ground Water, 33, 769–780.

Schulze-Makuch, D., Carlson, D. A., Cherkauer, D. S., & Malik, P. (1999) Scale dependency of hydraulic conductivity in heterogeneous media. Ground Water, 37, 904–919.

Schulze-Makuch, D., & Cherkauer, D. S. (1998) Variations in hydraulic conductivity with scale of measurement during aquifer tests in homogenous porous carbonate rocks. Hydrogeology Journal, 6, 204–215.

Weight, W. D. (2008) Hydrogeology field manual (2nd Ed.). New York: McGraw Hill Professional.

Chapter 6
Borehole Drilling and Well Construction

Well construction and drilling techniques are reviewed focusing on the appropriateness of different methods for various aquifer characterization scenarios. The drilling method and well construction selected for an aquifer characterization program should be based on consideration of the type of testing to be performed, borehole conditions required for testing, formation conditions (borehole stability), formation sample requirements, well depth, water quality, planned use of the well after the completion of the program, local driller capabilities and expertise, drilling fluid disposal, local regulations, and cost. A key factor dictating drilling and formation sampling methods is whether or not a borehole is stable (i.e., penetrated strata are lithified or sufficiently cohesive). Wells should be designed, constructed, and developed to maximize well efficiency, particularly if they are to be used as production wells or for single-well hydraulic testing (e.g., slug testing).

6.1 Introduction

Boreholes and wells are fundamental to aquifer characterization because they are required for most hydraulic, water chemistry, and formation testing and sampling methods. The main exceptions are direct push technologies (DPT) and surface geophysical methods. However, the latter require some data from wells or boreholes for calibration and validation. There are three main types of wells used in aquifer characterization programs; exploratory, production, and monitoring. Exploratory or test wells, as the names imply, are primarily used for the collection of hydraulic, petrophysical, and lithological data, and formation and water samples. Production (or injection) wells are designed to produce (or accept) water, and are used in aquifer characterization programs to stress aquifers for hydraulic testing and to evaluate well yields. Monitoring wells (also referred to as monitor wells, observation wells, and piezometers) are usually constructed for the collection of water level data and samples for water chemistry analysis. Wells can be constructed

to serve multiple purposes. For example, exploratory wells are often completed for subsequent use as monitoring wells. Similarly, large-diameter test production wells installed as part of an exploratory well program may be brought into service as operational production wells.

6.1.1 Well Drilling Program Considerations

Water well design and drilling methods were reviewed by Driscoll (1986), Roscoe Moss Company (1990), Misstear et al. (2006), and Sterrett (2007). The design and construction of aquifer recharge wells were reviewed by Maliva and Missimer (2010). Well construction issues with respect to contamination assessment and monitoring were reviewed by Keely and Boateng (1987a), Aller et al. (1991), and Nielsen and Schalla (1991). Borehole and well drilling and construction methods for a given project are dictated by

- The planned use of the borehole or well in the aquifer characterization program (types of testing and sample collection to be performed)
- borehole conditions required for testing (e.g., minimum diameter for borehole geophysical logging)
- formation conditions within the strata to be tested and overlying strata, particularly whether or not strata are lithified and a borehole will be stable
- condition and water quality of overlying strata
- the planned use(s) of the well after the characterization program, including whether the well is temporary or permanent
- target depth
- number of zones to be tested
- depth to the water table
- capabilities of local drillers
- project budgetary constraints
- local regulatory requirements.

One of the most important considerations in determining a drilling program is whether or not the encountered strata will be lithified or sufficiently consolidated so that the borehole is stable (i.e., will remain open). Stable boreholes facilitate drilling and allow for open-hole completions and testing procedures. Where the formation is not stable, screened completions are usually required and the borehole must be drilled using either drilling muds, dual-tube methods, or other techniques in which the borehole is progressively cased off as drilling proceeds. Temporary screens can be used for testing of unconsolidated intervals.

Government well drilling and construction regulations may also have specific well construction and permitting requirements, which may include casing (e.g., type, wall thickness, and method of coupling) and grouting standards. The latter may specify the type of cement allowed (e.g., maximum percent bentonite gel allowed in Portland cement) and minimum grout thickness.

Fig. 6.1 Large-diameter, hand-dug water well, Wadi Qidayd, Saudi Arabia

The drilling plan for an aquifer characterization program should meet all of the above requirements. Well drilling specifications should allow for all of the planned elements of the testing program. Additionally, the well should be constructed with the desired completion and be suitable for its intended use.

A wide variety of well construction and drilling methods have been historically used. Inasmuch as the subject of this book is on aquifer characterization, the focus is on methods that are commonly used to obtain data on aquifer properties. For example, hand-dug, large-diameter wells (Fig. 6.1) are still used in parts of the world, but typically are not constructed for just aquifer testing purposes. Well construction techniques used to construct deep oil and gas wells are usually inappropriate for groundwater investigations. Perforated completions, which are widely used for oil and gas wells, are seldom used for shallow water wells. However, perforated completions are used for some deep injection wells.

Well construction usually comprises four or five distinct operations, some of which may be performed simultaneously (Driscoll 1986):

- borehole drilling
- installation of casing (one or more strings)
- installation of the screen and filter pack (if used)
- cementing (grouting) of the casing
- development of the well to remove drilling fluids, repair formation damage, and enhance well efficiency.

6.1.2   Exploratory and Monitoring Wells Versus Production Well Design

Permanent production and injection wells should have robust designs to provide for long-term mechanical integrity and performance. Casings should be constructed of materials that are not subject to excessive corrosion in the borehole geochemical environment. The well and wellhead design should also readily allow for future well rehabilitation activities.

An important issue for the construction of production and injection wells is to maximize well efficiency. Well efficiency (E, %) is defined in terms of the ratio of the theoretical and actual measured drawdowns (s) or specific capacities (flow rate divided by drawdown; Q/s):

$$E = \frac{s_{theoretical}}{s_{measured}} \cdot 100 \tag{6:1}$$

$$E = \frac{\left(\frac{Q}{s}\right)_{measured}}{\left(\frac{Q}{s}\right)_{theoretical}} \cdot 100 \tag{6:2}$$

The theoretical drawdown and specific capacity of a production well are the values that would be obtained in a 100 % efficient well. If the transmissivity of an aquifer can be estimated from either single or multiple-well pumping test (time-drawdown) data, then a theoretical specific capacity can be estimated for comparison with measured values. The theoretical drawdown can also be estimated from a semi-logarithmic plot of the distance-drawdown data from a constant-rate aquifer performance test by extrapolating the drawdown measured in observation wells to the radius of the production well (Fig. 6.2). The theoretical drawdown is compared to the measured drawdown in the production well at the same time as distance-drawdown data are collected. An efficiency of 70 to 80 % or better is usually obtained in a well in which good design, construction, and development practices have been followed.

Fig. 6.2 Well efficiency can be determined from the ratio of measured drawdown in a well (S_{meas}) to the theoretical drawdown (S_{theo}) obtained by extrapolating the distance-drawdown data to the well radius
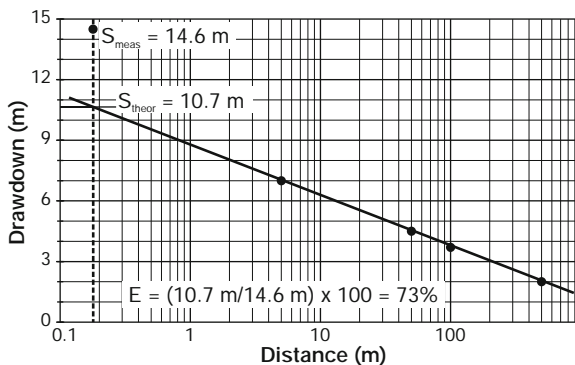
Well inefficiency is the result of head losses within a well. The main types of head loss are (1) frictional losses within the well casing, (2) head losses across the well screen and filter pack, and (3) formation damage (clogging) in the vicinity of the borehole (skin effect). Well construction, drilling, and testing methods should all be chosen so as to minimize all three of the main head losses to the extent practicable. Head losses within a well may be reduced by increasing the diameter of the well, which decreases the flow velocity and associated frictional head losses. The frictional head losses within casings of different material (roughness), diameters, and lengths, can be estimated for different flow velocities using the Hazen and Williams equation (Sect. 6.4.2).

Selecting the proper filter pack and screen slot size is also critical for maximizing well efficiency. It should be recognized that some head losses are either unavoidable or are deemed acceptable based on economic considerations. For example, the slot size of the screen, and, thus, open area, will be dictated to a large degree by the grain-size distribution of the aquifer. The additional costs to construct a larger diameter, more efficient, well may or may not be justified in terms of improved well performance.

Optimization of well efficiency is not a primary concern for the design and construction of monitoring wells. Instead monitoring wells should be constructed and developed in order to be a "transparent window" in which water level data and water samples can be collected that are representative of the water moving through the formation (Aller et al. 1991). Where monitoring wells are to be used for the assessment, remediation, and monitoring of contaminated sites, it is critical that the wells be constructed, developed, and sampled, in a manner that does not result in biased samples. For example, neither leaching from nor sorption onto casings should occur to the degree to which it could impact the concentrations of parameters of concern in collected water samples.

A monitoring well system should be designed to most efficiently meet project data needs. For one-time sampling of unconsolidated strata, direct push techniques (Chap. 12) may be the most cost-effective option. For some sites, more than one depth interval may need to be sampled. Options for monitoring multiple zones include (Aller et al. 1991).

- multiple single-zone wells
- flow through wells with long screens (dynamic sampling)
- nested wells in a single borehole
- multilevel samplers (e.g., Westbay® systems) in a single borehole

Individual well completions will usually be more economical at depths of less than 24 m or 80 ft (Aller et al. 1991). Individual, single-zone wells also have the benefit of technical simplicity and a much greater likelihood of zonal isolation. Nested wells and multilevel samplers may offer significant cost savings for monitoring of multiple zones at greater depths (Sect. 15.2).

6.2   Borehole Drilling Methods

6.2.1   Direct-Rotary Method

The direct-rotary method is the standard method used in the oil and gas industry and is widely used for the construction of groundwater wells in both consolidated and unconsolidated strata. The borehole is drilled using a rotating bit that is attached to the bottom of a string of drill pipe. The most commonly used drill bit is the tri-cone roller cone-type bit, which consists of three conically shaped rollers mounted with hardened steel or tungsten carbide teeth (Fig. 6.3a, b). The rotating cones result in a chipping and crushing action that allows penetration through hard rock. Other bit designs, including angle and wing (drag) configurations (Fig. 6.3c), are available, for drilling through specific rock and sediment types. Drilling fluid is circulated down the drill pipe, out the bit, and up to land surface in the annulus between the borehole wall and drill pipe (Fig. 6.4).

A variety of drilling fluids are used, including bentonite mud, organic polymers, straight water and air, air-polymer (foam) and air-water mixtures. The drilling fluid cools, lubricates, and cleans the drill bit and carries the cuttings to the surface. The main mud properties of concern are its viscosity and density, both of which need to be monitored during drilling. Drilling fluid should have a high enough viscosity to allow cuttings to be transported to the surface, but not so high as to impede pumping. When mud is used, the weight of the drilling fluid (determined by its density and the drilling depth) results in a hydrostatic pressure that prevents the borehole from collapsing and prevents fluid flow into the borehole. Greater hydrostatic pressure in the borehole than in the adjoining formation results in the flow (invasion) of drilling fluid into the formation (Fig. 6.5). Invasion will preferentially occur in the more permeable strata. Suspended material within the drilling fluid (mud and fine cuttings) are filtered out to varying degrees at the borehole wall resulting the formation of 'mudcake,' which tends to be thickest opposite the more permeable strata. The mud filtrate that enters the formation is often chemically dissimilar (e.g., has a different salinity and resistivity) to the native groundwater and may be detected by resistivity borehole geophysical logs. Development is critical for wells drilled using the mud-rotary method as the mudcake and any residual drilling fluids in the well must be removed.

The drill cuttings are removed from the circulating drilling fluid either by allowing them to settle out in mud pits or using desanders and a shale shaker (Fig. 6.6). The cleaned drilling fluid is then usually recirculated back down the well. Casing is installed by removing (tripping out) the drill pipe and bit, lowering the casing down the borehole, and then cementing the annulus between the casing and borehole wall.

The direct-rotary method can be used when drilling through almost all types of formation. The main advantages of the direct-rotary method are that it is rapid, widely available, and can be used in unconsolidated formations. Direct-rotary drilling also allows for the running of many borehole geophysical logs (except

Fig. 6.3 Photos bits of used
in water well drilling.
a Tri-cone bit. b Tiered
reamer bit with lead tri-cone
bit. c Wing or drag bit
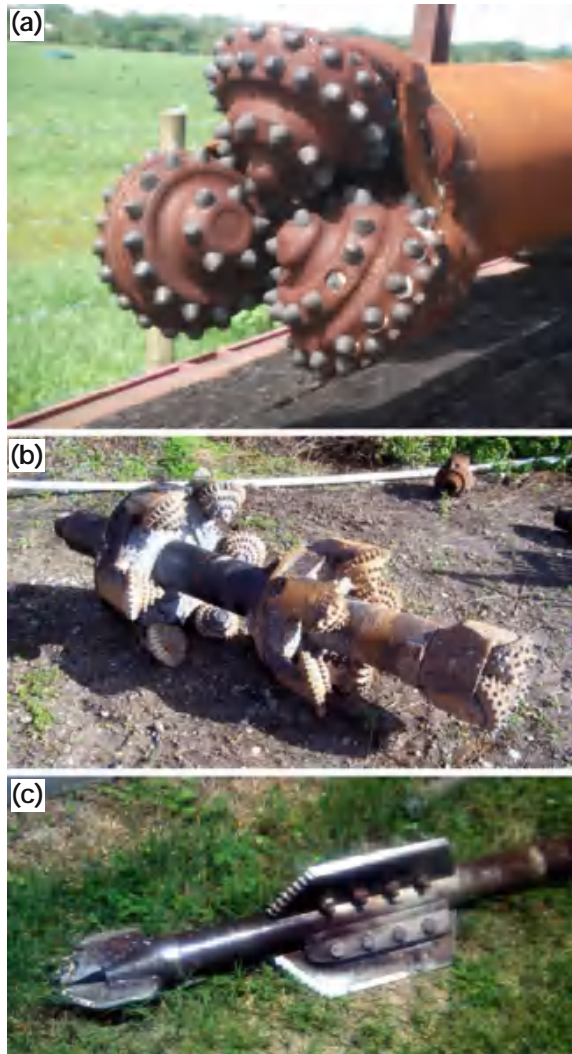
flowmeter), which were originally developed for the oil and gas industry in which
mud-rotary drilling is the norm. Disadvantages of the mud-rotary method are the
need to properly develop the wells to remove residual drilling fluids and generally
poor quality of recovered samples. In contaminated sites, proper disposal of drilling
fluids that were in contact with contaminated soil and water may be a significant
additional cost.

   Collection of water quality samples and aquifer hydraulic testing are also more
time consuming, and thus expensive, when drilling with mud. In consolidated
formations, water quality sampling and hydraulic testing may be performed using
straddle packers or single (off-bottom) packers. Water sampling and hydraulic

Fig. 6.4 Mud-rotary drilling
diagram. Mud is pumped
down the drill pipe and
returns to the surface with
entrained cuttings in the
annulus between the drill pipe
and the formation
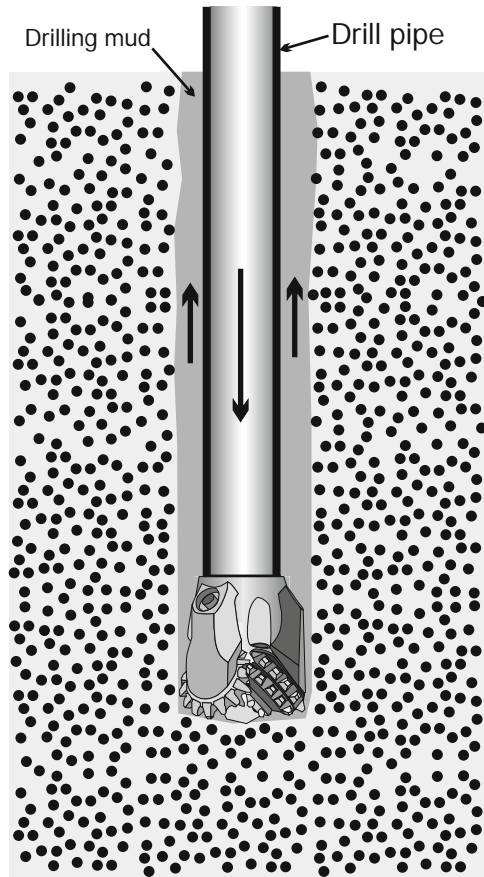
testing can be performed in unconsolidated formations by the installation of a
temporary well screen. An artificial filter pack may be required, the top of which
needs to be sealed with bentonite (or another means) to prevent the downward flow
of drilling mud. The tested interval needs to be thoroughly developed to remove the
drilling mud and mudcake. Profiles of transmissivity and water quality versus depth
can be obtained by the installation of a series of temporary screens during drilling,
although this process is time consuming.

    The air rotary method uses compressed air and commonly small quantities of
water or foam as the drilling fluid. It is typically used in consolidated formations
because drilling fluid is not required to stabilize the borehole. The advantages of the
air rotary drilling is the rapid transport of cuttings to land surface and thus minimal
contamination of cutting samples. The borehole is also cleaner and requires less
development. Well yield and water quality can also be estimated while drilling
using this method.

Fig. 6.5   Drilling fluid
invasion diagram. Drilling
mud preferential enters more
permeable beds resulting in a
thicker mudcake development
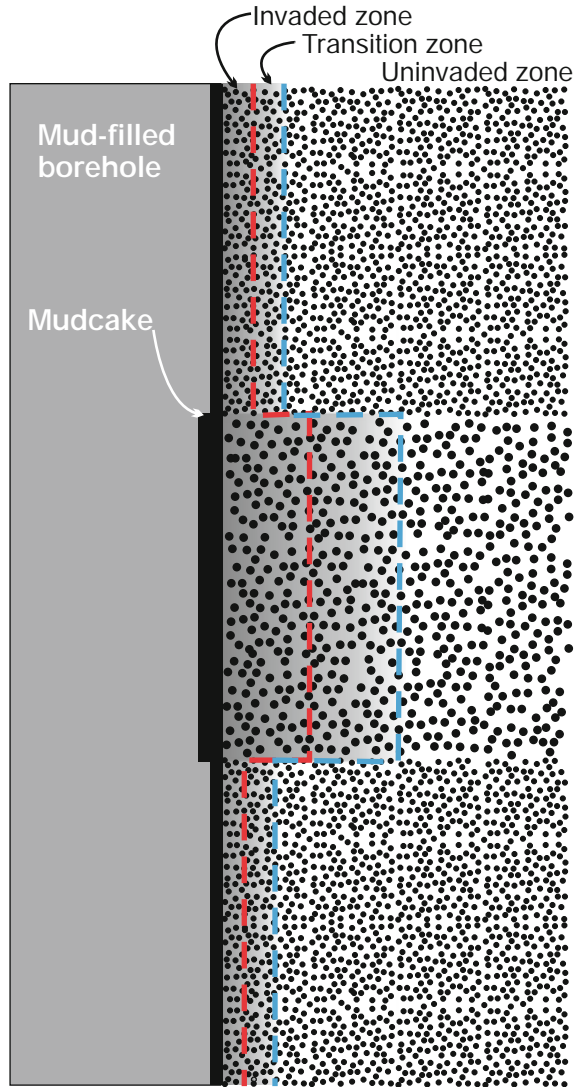
Biodegradable organic polymers are an alternative to bentonite-based drilling fluids. They have the advantage of being easier to flush from the borehole, potentially resulting in less development time and formation damage and a greater well efficiency. The main disadvantage of organic polymers is that if not completely removed from a well, they can be a food source for bacteria growth with associated well clogging or bacterial clearance issues. Hence, if organic polymers are used, an oxidizing agent (e.g., chlorine) should be used to ensure their complete removal.

Fig. 6.6 Desanders and shale
shaker used to separate
cuttings from the drilling mud

Limitations on pump capacity and thus effectiveness of cutting removal usually
limits the diameter of boreholes than can be drilled using the direct-rotary method to
a maximum of about 56 to 61 cm (22 to 24 in; Driscoll 1986).

6.2.2   Reverse-Circulation Rotary Method

The reverse-circulation rotary method differs from the direct-rotary method in that
the direction of drilling fluid circulation is reversed. Drilling fluids and entrained
cuttings are transported to the surface inside the drill pipe rather that in the annulus.
The reverse circulation is achieved by connecting the suction end of a large cen-
trifugal pump to a swivel that is connected to the drill pipe or through the use of an
air line installed inside the drill pipe. The reverse-circulation rotary drilling is the
least expensive method for drilling large diameter holes in unconsolidated (un-
lithified) formations (Driscoll 1986).

An important advantage of reverse-circulation drilling is that the up-hole velocity required to bring cuttings to land surface is controlled by the diameter of the drill pipe, rather than the usually much larger borehole diameter (Davis et al. 1991). The erosion of the borehole from the upwards movement of cuttings is also avoided.

6.2.3   Reverse-Air Rotary Method

The reverse-air rotary method creates the reverse-circulation by the use of an air line within the drill pipe. The discharge of air into the drill pipe creates an upward movement of air and water, which causes a suction to occur at the drill bit that induces the movement of water and cuttings from the formation upward to the surface through the drill pipe (Fig. 6.7). The produced water may be either

Fig. 6.7   Reverse-air rotary drilling diagram. Water is pumped up drill pipe using an air line
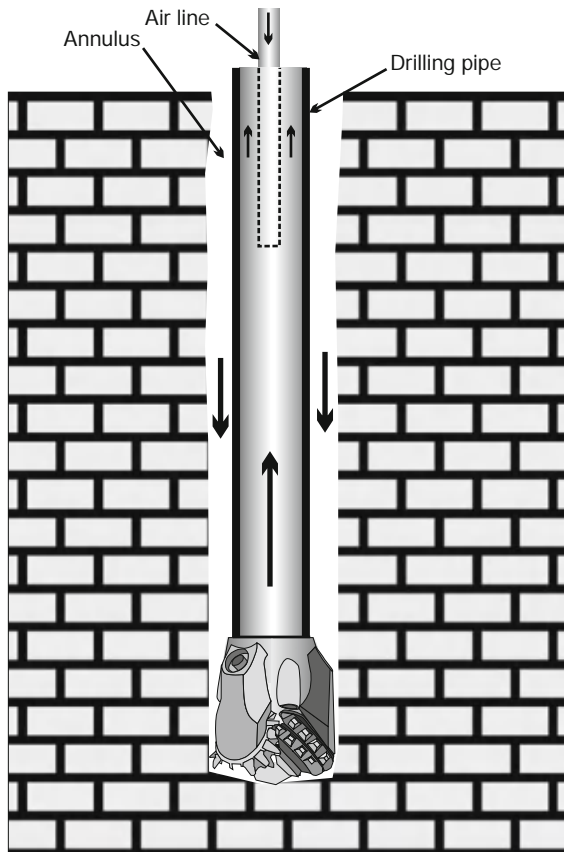
discharged to waste (open-circulation method), or after the cuttings are removed using desanders and shale shakers, the water is returned to the well through the annulus between the drill pipe and borehole wall (closed-circulation method).

The reverse-air rotary method is the preferred method for drilling through consolidated, water-producing strata. It has several great advantages. By not using drilling muds, it greatly reduces the potential for drilling fluid-induced clogging of the formation. The flow of water from the formation into the drill pipe actually acts to develop the well. The reverse-air rotary method also facilitates the collection of cuttings samples. The cuttings are clean (not covered with drilling mud) and are transported rapidly up the drill pipe to the drilling rig, which minimizes the potential for depth errors and the mixing of materials. Well yield and water quality can also be estimated while drilling using this method.

The reverse-air rotary method also allows for monitoring of changes in water quality (e.g., salinity and electrical conductivity) with depth. Changes in the chemistry of the produced water monitored at land surface usually reflect changes in the chemistry of the groundwater at the bottom of the hole. The produced water will come largely from the drill bit depth, although significant mixing may occur with water produced higher in the well when drilling through less conductive strata with a closed-circulation system. Thus, where water chemistry monitoring is important for a project, an open-circulation system should be used, if possible. Use of a closed-circulation system may be necessary where water disposal is a problem, such as, for example, when drilling through brackish or saline aquifers and the produced water cannot be discharged to the ground or a surface water body because of environmental concerns. The produced water is often very turbid which also causes disposal problems. Closed-circulation systems may introduce fine clay and silt-sized drilling cuttings back into the formation, which will later need to be removed during development. Wells drilled with a closed-circulation system, therefore, may require longer and more intense development to clean out the well, negating water management benefits.

The reverse-air rotary method cannot be used in unconsolidated formations because there is no drilling mud to stabilize the borehole. The method also requires that the formation produce sufficient water to allow for an upward flow in the drill pipe to land surface. The reverse-air rotary method thus cannot be used to drill through the unsaturated zone or in very poorly productive strata. It may be necessary to first drill using the direct-rotary method until enough transmissive strata are penetrated to allow for sufficient water flow for reverse-air rotary drilling. Alternatively, water can be added to the annulus at land surface until the well produces enough water.

6.2.4   Dual-Tube Reverse-Circulation Rotary and Percussion Methods

The direct-rotary and reverse-circulation rotary methods use a single drill pipe. Dual-tube methods utilize a second concentric tube or pipe. The fluid flow has a reverse-circulation pattern of downwards flow between the two drill pipes and upward through the inner pipe (Fig. 6.8). The outer pipe stabilizes the borehole and allows for drilling in unconsolidated strata without the use of drilling mud. Dual-tube (or dual-wall) drilling is performed using either the rotary method or percussion method. The use of the dual-tube rotary and percussion methods for groundwater exploration and monitoring was reviewed by Strauss et al. (1989). In the rotary method, a roller bit is attached to the inner drill pipe. The drill bit is usually only one nominal size larger than the diameter of the outer casing, which results in a thin annulus between the outer pipe and formation. For percussion

Fig. 6.8 Schematic diagram of the dual-tube reverse-circulation rotary drilling method. The very small annulus between the outer tube and the formation minimizes production of formation water during drilling
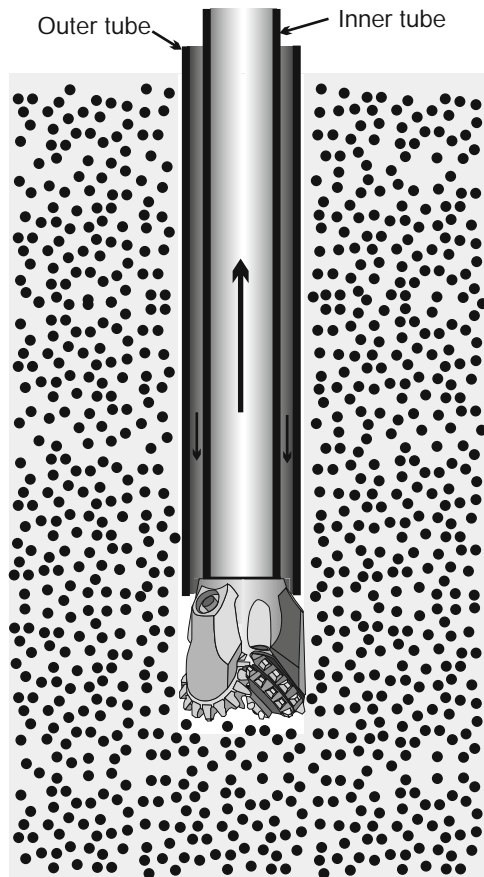
drilling, an open-face bit is used, which is attached to the outer pipe and driven by an above-ground pile hammer.

Dual-tube methods are attractive where there is a need to perform groundwater sampling while drilling, because they do not require the use of drilling muds and the small annulus between the outer drill pipe and formation minimizes fluid flow in the annulus. The tight borehole promotes the flow of fluids and entrained cuttings along the path of least resistance, which is the inner pipe (Strauss et al. 1989). Most of the produced water will, therefore, be derived from the drill bit depth. A representative water sample can be obtained by pumping (air lifting) through the drill string without a downward return flow.

Dual-tube methods also allow for the collection of superior quality cuttings samples. If a cone-type bit is used, then typical cuttings will be obtained. Large core pieces may be recovered if a hollow bit is used. The quality of the core samples is usually less than that obtained using conventional (e.g., wireline) coring techniques, but pieces large enough to obtain core plugs are commonly obtained.

A disadvantage of using the dual-tube method in unconsolidated strata is that the borehole will likely cave in, as the drill string is removed, which would prevent geophysical logging and the installation of casing and screen. Limited logs (e.g., natural gamma ray) may be run while the drill pipe is still in the borehole. Depending upon the type of drill bit used, small diameter (1 to 2 in; 2.5 to 5.1 cm) screens may be installed through the drill stem (Driscoll 1986). Another option is to introduce drilling mud into the borehole before and during the removal of the drill string to stabilize the borehole, perform geophysical logging, and then install a screen in the well. In aquifer characterization programs, dual-tube methods can be first used to obtain higher quality lithologic samples and water quality data (e.g., salinity versus depth profile). The borehole may subsequently be reamed to obtain a sufficient diameter for well completion.

6.2.5   Dual-Rotary Drilling

The dual-rotary drilling method was developed for efficient drilling through unconsolidated formations. Dual-rotary drilling rigs are commonly referred to as 'Barber' drilling rigs as the drilling technology was developed in 1979 by Barber Industries (now Foremost Industries) (Herrick 1994; Henahan 1999; Foremost Industries 2003). Dual-rotary drilling utilizes a drilling rig with two independent drive units. The lower drive unit advances a casing to which a carbide-studded shoe has been welded to the bottom casing joint. A top-drive rotary head handles a drill string equipped with either a down-the-hole hammer, drag bit or rolling cone bit, to drill inside or ahead of the casing. Inasmuch as the top and lower drive units are operated independently, the drill bit can be positioned either ahead of or behind the casing shoe. Depth-specific water and formation samples can be obtained because the outer casing largely seals off the overlying strata, minimizing the potential for cross-contamination.

The major advantages of the dual-rotary method for drilling production wells is that the outer casing keeps the borehole open and no drilling fluids are used to stabilize the hole. Once total depth is reached, the inner drill string is removed and the casing and screen are installed. The outer casing is simultaneously pulled out as the filter pack and sealing material (grout) are added. A limitation of dual-rotary drilling is that it requires specialized drilling rigs, which may not be locally available.

Dual-rotary drilling can also be used for the drilling of slant wells. Williams (2008) discussed the applications of slant wells drilled using the dual-rotary method for seawater supply for desalination facilities. Slant wells drilled under the seafloor may reduce the impacts to onshore freshwater resources and provide better hydraulic connectivity with the overlying seawater recharge source. Slant wells have greater screen lengths and thus can have greater well yields than vertical wells. The intake systems using slant wells may require fewer wells and pumps and have a smaller surface footprint. Williams (2008) also addressed some of the challenges associated with slant wells, such as maintaining borehole stability, and difficulties in well development and filter pack installation. The economic case for slant wells is uncertain. Although they may have greater well yields than vertical wells, their construction cost may be greater. Slant wells will likely also be more difficult to maintain (periodically rehabilitate) and in some areas there may not be drillers with the equipment to construct and rehabilitate the wells. Slant wells may be the preferred solution where surface impacts (footprint) are of concern, as multiple wells could be drilled radiating outwards from a single drilling pad.

6.2.6   Cable-Tool Drilling

Cable-tool drilling is by far the oldest drilling method, having been used for about 4,000 years. The basic method consists of repeatedly raising and dropping a heavy string of drilling tools with a chisel-shaped bit into the borehole, which breaks, crushes or loosens the formation. The crushed or loosened material forms a slurry, which is removed from the well by either bailing or using a sand pump. The cable-tool drilling system is designed so that the bit is slightly rotated each stroke in order to form a circular borehole. A steel casing is lowered down the well during drilling (especially when drilling through unconsolidated formations), which may be either the permanent casing or a temporary casing, to keep the well open during drilling. Where a temporary casing is used, the permanent casing and well screen are lowered inside the temporary casing and the filter pack is added and well grouted as the temporary casing is lifted out of the well.

Driscoll (1986) and Keely and Boateng (1987a, b) discuss some of the main advantages and disadvantages of the cable-tool method. The cable-tool method may be the best, and in some cases the only method available, for drilling in coarse glacial till, boulder deposits, and aquifers that are highly fractured, disturbed, or cavernous. Loss of circulation of drilling fluids is not a problem because the

cable-tool system does not require circulation of drilling fluids to remove cuttings and the drilled interval is quickly cased off. For aquifer characterization, cable-tool drilling also allows for accurate water and lithologic sampling during drilling and does not require the introduction of drilling fluids or other external liquids into the well (other than perhaps some water to create a slurry). Inasmuch as the upper strata are cased off during drilling, mixing of waters from different zones is largely avoided. The impacts from the drill bit may also induce fracturing that enhances permeability near the borehole.

Cable-tool rigs are also relatively reliable and inexpensive. The major disadvantages of the cable-tool method include that penetration rates are relatively slow and that heavier walled steel casings may be required (Driscoll 1986). Cable-tool-drilled wells are thus often slower to construct and, as a result, more expensive. Cable-tool drillers may not be locally available, because the method is not cost competitive with other drilling methods. In uncemented wells, the lack of a grout seal may allow migration of fluids through the annulus between the casing and formation. Also, the rate of casing corrosion may be much greater in cable-tool constructed wells because the formation fluids are in direct contact with the casing exterior. Differences in oxidation potential between the formation fluids and the injected or withdrawn fluids can cause rapid electrolytic corrosion.

6.2.7   Sonic or Rotary-Sonic Drilling

The sonic-drilling method, also referred to as the rotary-sonic and rotasonic method, is an attractive technique for obtaining shallow cores and installing monitoring wells in both unconsolidated sediment and rock. ASTM (2004) published proposed standards for sonic coring and provides a description of the technology. The sonic-drilling method utilizes high-frequency vibrational energy with downward pressure and rotation to advance the drilling tool. Typically the method is restricted to depths of 150 m or less, although greater depths are possible by drilling in stages. The depth limitation is due to dampening of vibrational energy, which is transmitted to the borehole wall (Stephan 1995). Sonic drilling is a dual-tube technique in which an inner drilling string and core barrel are vibrated into the formation. An outer casing is also advanced by vibrational action to seal off the upper strata and prevent collapse of the borehole. A one-piece core barrel is commonly used, but split barrels are also available, which allows for the recovery of less disturbed cores. The recovered core is extruded either into plastic sleeves or on visqueen for examination (Fig. 6.9). The core samples may then be boxed and archived. Upon removal of the inner drill string, a small-diameter monitoring well screen and casing can be installed.

The principal advantages of rotary-sonic drilling are that it is rapid, good-quality continuous core samples can be recovered, and there is a minimal generation of solid waste (well cuttings), which is an important economic consideration for contaminated sites. Proper disposal of contaminated cuttings and drilling fluids may

Fig. 6.9 Sonic drilling rig. Collected cores were laid out on visqueen for description and then boxed and archived

be a substantial cost at these sites. In addition, the sealing of upper strata by the outer drilling string facilitates the collection of representative water samples.

The quality of the core samples obtained by sonic coring can be impacted by core growth, rind formation, and compression or consolidation of samples. Core growth is the recovery of a length of core greater than the length of the actually drilled interval. The primary cause of core growth is extrusion stretch during the removal of the core material from the barrel (Ault et al. 1994). Core growth can be corrected for by applying a linear correction factor to the recovered core. The thickness of each interval is multiplied by the ratio of the cored depth interval to the length of the recovered core. Alternatively, if it is determined that the core growth has occurred in only one interval of core, then the correction can be applied only to that interval (Ault et al. 1994).

Rind formation occurs when the vibratory drilling action causes fine-grained material to migrate towards the outside of the core (Ault et al. 1994). The impacts of rind formation can be avoided by sampling from the center of the core. Soft (poorly indurated) rock may be compressed during coring, which can result in the collapse of large secondary pores. The quality of recovered core can also be influenced by drilling procedures. Key variables during drilling are the vibrational energy and downward pressure imparted to the drill bit (Stephan 1995). An optimal combination of both vibration pressure and downward pressure allows for efficient, rapid drilling, and sampling.

Drillers may prefer to take longer cores (e.g., 6 m or 20 ft), because it is quicker as there are fewer trips out of the hole. However, long cores can result in greater errors due to core growth and shift. Sonic-drilling method can be modified to perform in situ groundwater testing. The inner drill string can be fitted with a screen for formation water sampling and hydraulic testing (ASTM 2004).

6.2.8   Hollow-Stem Augers

The installation of environmental monitoring wells using hollow-stem augers (Fig. 6.10) was reviewed by Driscoll (1986), Keely and Boateng (1987a), Hackett (1987, 1988), Aller et al. (1991) and Davis et al. (1991). Hollow-stem augers are widely used for the installation of shallow (<50 m) monitoring wells because the method is relatively fast and inexpensive, and for most applications does not involve the use of drilling fluids. The augers act as a temporary casing to stabilize the borehole during drilling. The basic method is to drill to the target well depth with the bottom of augers sealed using either a pilot assembly consisting of a bottom plug, center bit, and central rod assembly or a disposable (commonly wooden) knockout plate. The pilot assembly and auger string are connected to the spindle of the drill rig using a double-adapter drive cap that ensures that the center rod and pilot assembly rotate along with the auger column. The ability to withdraw the center plug and bit for sampling, while the augers are still in place, is a principal advantage of the hollow-stem auger method (Davis et al. 1991).

Fig. 6.10 Hollow-stem auger drilling diagram. Screwing action brings cuttings to surface
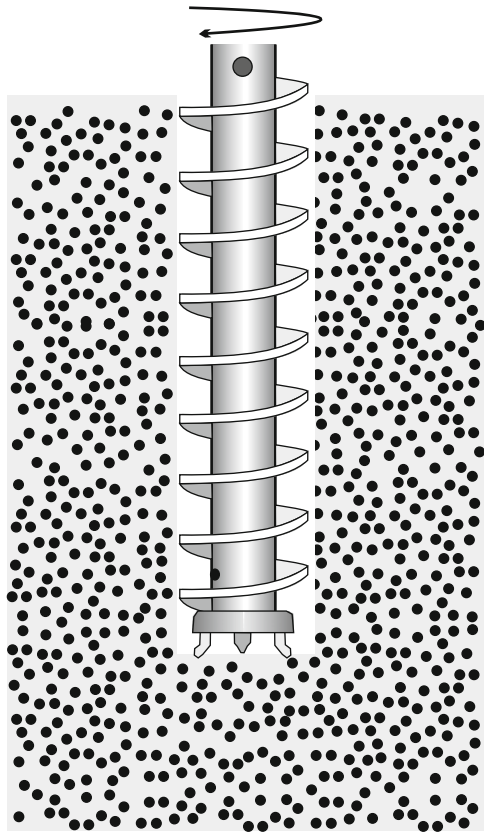
After reaching total depth, the pilot assembly is then removed or knockout plate dislodged and the well casing and screen are installed. In relative shallow wells in which the sediment is cohesive, the augers can be completely removed from the borehole prior to the installation of the casing and screen. Otherwise the casing and screen are installed within the augers. The filter pack and well sealant (bentonite pellets or chips, and then Portland cement or bentonite slurry) are added as the augers are withdrawn from the well.

Sediment samples can be collected during drilling using split spoons, Shelby (thin-walled) tubes, or core barrels. Commonly, the pilot assembly is removed and sediments samples collected using split spoons or a Shelby tube driven into the underlying, undisturbed sediments. Continuous core samples may also be collected using a core barrel sampler instead of the pilot assembly.

A main disadvantage of the hollow-stem augers is the disturbance of the formation, particularly the smearing of clays and silts on more permeable sand and gravel intervals (Keely and Boateng 1987a, b). Hollow-stem augers can also result in cross-contamination due to the mixing of sediments. Mixing of sediments can be managed by augering within a temporary steel casing with a drive shoe that is advanced during augering. The augers can be advanced in 0.3 to 0.6 m (1 to 2 ft) intervals followed by the driving of the casing (Keely and Boateng 1987a, b; Hackett 1988).

A problem that is sometimes encountered when drilling using hollow-stem augers is sand heaving, in which sand enters the bottom of the augers when the bottom plug is removed due to the greater hydrostatic pressure in the formation as compared to within the auger, which may not be full of fluid. The lifting of the bottom plug can create suction (negative pressure) that draws sediment into the well. Sand heaving can be managed by maintaining a positive pressure in the augers using drilling fluids or allowing the augers to fill with formation water by using, for example, screened augers (Hackett 1987; Aller et al. 1991).

Hollow-stem augering is most effective in unconsolidated muds, silts, and sands. Drilling and well installation can be difficult in hard consolidated rock (in which penetration can be very slow) and in glacial deposits with coarse cobbles and boulders. The later can be dealt with by breaking up the large clasts by drilling through the augers using a small tri-cone bit.

6.3 Formation Sampling

A fundamental part of well drilling for aquifer characterization programs is to obtain samples of subsurface strata for evaluation of site-specific hydrogeology (e.g., location and characteristics of aquifer and confining strata), and petrophysical and geochemical analysis. The sampling program depends upon the type of samples required and formation characteristics, particularly whether the strata are lithified, unlithified and cohesive, or unlithified and not cohesive. The main types of formation samples are cuttings, cores, and samples collected using split-spoon and

thin-walled samplers. Sampling methods for unconsolidated sediments were reviewed by Aller et al. (1991). Key objectives are to obtain representative samples, in which all constituents for a depth interval are recovered, and undisturbed samples, in which the pre-sampling relationship between the constituents in a sample are not altered (Davis et al. 1991).

6.3.1 Well Cuttings

Well cuttings are small fragments of rock and sediment produced during well drilling. In the different types of rotary drilling, the cuttings are typically screened out of the drilling fluid upon its returns to land surface. Sediment samples may also be collected off auger flights, with the most representative samples likely located near the inner part of the flights pulled from the bottom of the well. Inasmuch as cuttings are a normal byproduct of drilling, their collection involves minimal additional effort and cost, and they are thus the least expensive source of lithological data. However cuttings have significant limitations:

- The depth control of cuttings may be poor in deep wells.
- The small size of cuttings (often less than 1 cm) precludes observation of large-scale features in the formation, such as sedimentary structures, bedding, and large secondary pores.
- Drill cutting samples represent a mixture of the rock or sediment present in the sample interval. It is typically not possible to determine from the cuttings alone how the different rock types are distributed in the sampled interval.
- Drill cutting samples may be contaminated with material that fell into the borehole from above the sample interval.
- Cuttings may be biased towards harder lithologies. Softer material and very fine-grained material (finer than the collection screen size) may be underrepresented.

Care must be taken, particularly during mud-rotary drilling, to account for the time lag for cuttings to reach each land surface. The time lag becomes greater with increasing depth. The cuttings arriving at land surface may thus not be representative of the strata at the current drill bit depth. It is critical for the field geologist to pay attention and record the drilling action and penetration rate. The change from a soft to hard lithology is often marked by a downhole decrease in penetration rate and increase in vibration (chatter) of the drill string. The depth of the change in drilling behavior must be recorded and cuttings monitored to identify the harder rock when it arrives at land surface, which could be several minutes or more later. Geophysical logs can provide an in situ record of rock types, which can be used as a control to verify cutting depths. For example, the depths from which clay or shale cuttings were derived may be identified by a relatively high natural gamma-ray activity.

Fig. 6.11 Plastic sample trays are a convenient means for storing a set of well cuttings

Depending upon the project, cutting samples should be collected at 1.5 (5 ft) or 3 m (10 ft) intervals and at major lithological changes, and retained. Cutting samples are commonly collected in cloth drawstring bags, which have the advantage of being breathable, and thus allow samples to dry. Multi-compartment plastic trays are increasingly being used to archive samples, because they have the advantage of allowing 10 samples to be observed side by side (Fig. 6.11). The plastic trays are stackable and take up relatively little space, but must be handled with care to avoid spillage between compartments.

6.3.2   Coring

Coring is performed where high-quality, intact, formation samples are needed for petrophysical, mineralogical, and geochemical analyses. The basic coring techniques employed in the oil and gas industry and groundwater investigations are single-wall, wireline, sidewall, and sonic. Samples of unconsolidated formations can also be obtained using split-spoon samplers and Shelby tubes. The choice of coring method depends on the characteristics of the formation to be sampled, the amount (length) and diameter of core required, and project budget. Typically coring is considerably slower than other well drilling methods and is thus more expensive. Petrophysical testing is performed on either core plugs drilled from the core, which typically have diameters of 1.0 (2.5 cm) or 1.5 inch (3.8 cm), or on whole core samples. Petrophysical analyses performed on core samples include porosity,

permeability, bulk density, acoustic (sonic) velocity, and compressibility (e.g., bulk and Young′s modulus).

6.3.2.1   Single-Wall Coring

The single-wall coring system consists of a single cylindrical tube (core barrel) which is attached to a hollow cylindrical coring bit. The core barrel is attached to the drill string (drilling pipe). Bits used for drilling through lithified strata are usually set with industrial diamonds or tungsten carbide chips. The single-wall coring system is an old technology in the oil and gas industry, but is still used in groundwater investigations because it is rugged and relatively inexpensive. It is most suitable for homogenous hard rock. The major disadvantage of single-wall coring is that the entire drill string must be tripped out and back into the hole twice to take each core (once to install the core barrel and a second time to recover the core). Core barrels are commonly available in 0.6 m (2 ft) to 3.0 m (10 ft) lengths.

Double- and triple-wall coring systems are more widely used in the oil and gas industry. In these systems, a swivel prevents the inner tube from rotating, which allows for better core recovery in fractured and softer rock. However, the core barrel still needs to be tripped in and out for each core.

6.3.2.2   Wireline Coring

Wireline coring is a simple and economical method for obtaining long continuous cores of lithified materials (Fig. 6.12). The wireline coring system is a dual-wall system in which the bit is attached to the outer core barrel, which is attached to the

Fig. 6.12 HQ wireline core in a temporary core box for field descriptions

Table 6.1 Commonly used wire core bits

Type	Metric units (cm)		English units (in)	
	Hole diameter	Core diameter	Hole diameter	Core diameter
NQ	7.57	4.78	2.98	1.88
HQ	9.60	6.35	3.78	2.50
PQ	12.27	8.51	4.83	3.35

drill string. A short-length inner core barrel is positioned at the base of the drill pipe. As drilling proceeds, the core is pushed into the inner core barrel. To remove the core, an overshot is lowered on the end of a wireline, which attaches to the top of the inner core barrel. When the wireline is pulled back, the inner core barrel disengages itself and is retrieved to land surface. After the core is removed, the inner core barrel is lowered back to the bottom of the drill pipe, where it re-engages to the base of the outer core barrel. The major advantage of the wireline coring system is that the outer core barrel and drill string do not have to be tripped out of the hole to recover the core, which allows for rapid coring.

A variety of drill bit types are available for drilling through different types of rock. Three standard wireline core sizes are used in groundwater investigations, which are designated NQ, HQ, and PQ (trademarks of the Boart Longyear Corporation). The dimensions of commonly used cores bits are presented in Table 6.1.

Large-diameter cores provide more material for testing, but are more expensive to obtain and create logistical difficulties if the core is to be retained and archived. Consideration also needs to be given to additional planned testing and uses of the borehole. The hole diameters of NQ through PQ cores are usually too small for both the installation of a casing to convert the core hole into a monitoring well and for many geophysical logging tools to pass downhole during logging. Smaller diameter core holes may require reaming if they are to be geophysically logged or converted to a well. A pilot reaming bit is recommended, which has a protruding rod in front of the primary reaming bit. This allows the enlargement of the well without risk of deviation and creation of a double-hole condition.

6.3.2.3 Sidewall Coring

Sidewall cores are taken with a wireline tool after a borehole has been drilled. They have the great advantage that they can be taken after geophysical logging has been completed and the logs interpreted. Cores can be targeted at specific depth intervals of interest. The major disadvantage of sidewall coring is that smaller-sized cores are recovered and the cores are often of poor quality. Sidewall coring techniques, which were reviewed by Agarwal et al. (2014), are divided into percussion and rotary cores.

Percussion coring tools (referred to as 'core guns') are the older and still most commonly used technology. Samples are taken by firing hollow, barrel-shaped bullets into the formation using explosive charges. The limitation of percussion sidewall coring is that the impact of the bullet with the formation often damages the core, distorting porosity measurements.

Rotary sidewall coring tools use a small coring bit to drill out core plugs from the side of the borehole. Rotary coring avoids distortion that occurs during percussion coring. Advanced coring tools, such as the XL-Rock tool (mark of Schlumberger), can take large volume 1½-inch (3.8 cm) diameter plugs with lengths of 2.5, 3.0 or 3.5 inch (6.3, 7.6, and 8.9 cm).

Sidewall coring is commonly used in the oil and gas industry due to the high cost of drilling rig time. It is much quicker to take a series of sidewall cores using a wireline than to have to trip in and out of the hole to take conventional cores. However, wireline coring is usually a much less expensive option for shallow aquifers because of lower drilling costs. Sidewall coring systems are specialized equipment that may not be locally available outside of areas of oil and gas exploration and development activity.

6.3.2.4 Split-Spoon Samplers

Split-spoon sampling is a widely used technique for collecting samples of shallow unconsolidated sediments. The standard split-spoon sampler consists of a 18-inch (46 cm) long, 2-inch (5-cm) outer diameter tube that is longitudinally split into two fitted pieces. The barrel is completed with an open drive shoe (bit) that is often fitted with a sediment retainer. The barrel is driven into the sediment and then recovered and split open to reveal the recovered sediment. The top of the barrel is normally attached to a connector head that has a valve to allow air, water, and drilling fluids to escape. Samples can be collected either with or without a liner.

Split-spoon sampling is commonly performed in conjunction with hollow-stem augering. A borehole is drilled to the top of the strata to be sampled and then the split-spoon core barrel is driven through the sample interval. It is important that the hollow-stem augers be largely free of sediment before the split-spoon sample is taken in order to avoid sample contamination. Contamination with sediment from above would impact the first collected sediment in the samplers.

Split-spoon samplers are used in the Standard Penetration Test (SPT), which is a geotechnical method used to determine the density or compaction of a formation. The SPT uses standard split-spoon samplers, which are driven using a slide-hammer with a weight of 140 lbs (63.5 kg) and stroke distance of 30 inch (760 mm). The test is performed by counting the number of blows required to advance the sampler its 1.5-ft length in 0.5-ft intervals. The sum of the number of blows required for the second and third 0.5 ft of penetration is termed the "standard penetration resistance" or the "N-value". The SPT method is described in detail in ASTM Standard D1586-11 (ASTM, 2011). Split-spoon samples are considered disturbed and are not suitable for certain laboratory analyses, such as permeability testing.

6.3.2.5   Thin-Walled Samplers

Thin-walled samplers, which are commonly referred to as Shelby tubes, are used to obtain undisturbed samples of poorly to moderately compacted sediments. The thin-walled tube is pressed (as opposed to driven or hammered) into the formation. Disturbance of the samples is minimized by the thin wall of the tubes. The ratio of the area of the wall to the outer area of the tube should be 0.1 or less (Aller et al. 1991). Thin-walled samplers are not suitable for well-compacted sediments because of the low structural strength of the tubes.

Shelby tube samplers consist of a one-piece, thin-walled, hollow-steel tube with an open-end that has been honed to a cutting edge. A sampler head attaches the tube to the drill rod, and contains a check valve and pressure vents. Shelby tubes are generally used in cohesive soils. The sampler is advanced into the soil layer, generally 15 cm (6 in) less than the length of the tube. The vacuum created by the check valve and cohesion of the sample in the tube cause the sample to be retained when the tube is withdrawn. Use of thin-walled samplers for geotechnical purposes are presented in ASTM Standard D1587 (ASTM, 2012). Standard ASTM dimensions are 2 in (5 cm) outer diameter (OD), 36 in (94 cm) long, 18 gauge thickness; 3 in (7.6 cm) OD, 36 in (91.4 cm) long, 16 gauge thickness; and 5 in (12.7 cm) OD, 54 in (137 cm) long, 11 gauge thickness.

6.3.2.6   Piston Samplers

Commonly employed coring methods (e.g., split spoon) are usually unsuitable for unconsolidated sands and gravel because of poor retention and disturbance of the cored materials. Zapico et al. (1987) documented the "Waterloo cohesionless aquifer core barrel" system, which was designed to obtain high-retention cores from cohesionless sand and gravel below the water table. The Waterloo cohesionless aquifer core barrel system is a modification of an earlier piston coring device documented by Munch and Killey (1985). Drilling mud of a suitable density and viscosity is used to stabilize the borehole and minimize sand flow into the augers. Before coring, the center bit and drill string are carefully removed and the core barrel installed. The coring assembly consists of a steel outer core barrel, an aluminum or plastic liner, and a piston located atop the drive shoe. The piston is connected to land surface with a wireline. As the core barrel is driven into the sediment to be sampled, the piston remains stationary creating a vacuum (suction) during recovery that retains most of the formation water and sediment. Relatively undisturbed samples of the formation, including pore water, are retained in the inner liner. Zapico et al. (1987) documented average recoveries of 86 and 88 % from the Woolrich and North Bay sites, respectively, in Ontario, Canada.

Formation water samples can be obtained from cores collected using piston samplers by either compaction (squeezing of the sediment), centrifugation, displacement with immiscible fluids, or by suction using a needle inserted in the sample (Munch and Killey 1985; Zapico et al. 1987). Water samples from the cores

had similar specific conductance values as water samples collected from the same interval in nearby wells with multiple-level samplers (Hess and Wolf 1991).

6.3.2.7 Core Preservation

Inasmuch as coring entails a significant cost, it behooves professionals to preserve and store the recovered core. Cores can be a very difficult (i.e., expensive) to replace geological record. Ideally, long continuous cores taken in areas with a minimal geological record should be permanently archived. Some geological surveys have core storage facilities and welcome cores obtained by private parties. For example, on several projects the author worked on, the Florida Geological Survey archived project cores and arranged for their delivery to their storage facility.

At a minimum, cores should be retained through the duration of a project.

Cores are commonly stored in either cardboard or wooden boxes. Core samples should be carefully boxed and pieces marked with a felt tip marker or paint as to their orientation (up-direction). Orientation can be marked with either up arrows or red and black stripes, in which, by convention, the red stripe is on the right when the core is held so that its orientation is the same as in the hole. Depth intervals in which core was not recovered or core recovered as rubble should also be marked on the box. Intervals in which core pieces have been taken for analysis should also be noted with some type of spacer.

Cores are subject to a variety of chemical and physical processes after recovery. For groundwater investigations, drying and oxidation are of particular concern. Dissolved solids in the pore waters of the core will precipitate upon drying, which can affect the permeability of the core. Precipitation of dissolved solids is of greater concern with increasing groundwater salinity. Oxidation can impact the mineralogical composition of cores. For example, iron sulfide minerals may oxidize to iron oxyhydroxide minerals (i.e., rust). Volatilization and biological processes may also be a concern if samples are to be analyzed for organic compounds (e.g., petroleum constituents).

Plans for coring programs should consider how the core samples are going to be used. If core samples are to be used for geochemical investigations, then special core preservation techniques may be required. Special core preservation techniques were reviewed by Bajsarowicz (1992) and the American Petroleum Institute (1998). A common method is to select samples for special core analysis quickly upon recovery of the core and then rapidly wrap the pieces with multiple layers of plastic wrap and/or aluminum foil, followed by dipping the wrapped samples in paraffin wax or a plastic sealant.

6.4   Well Casing

The main design issues concerning well casings are (1) casing diameter, (2) construction material, (3) wall thickness, and (4) method of connecting casing joints (pipe segments). The ultimate use of the well is also an important consideration. A well that is to be used as a long-term production well should be designed to maximize longevity and efficiency. These considerations are less important for wells that are to be used only as part of an aquifer characterization program and will later be abandoned or retained for use only as monitoring wells. Cost is also an important consideration. For example, PVC is often the least expensive material and is thus preferentially used unless there is a compelling reason to use another more expensive material.

6.4.1   Collapse Strength

An important physical parameter for well casings is its collapse strength, or "resistance of hydraulic collapse pressure" (RHCP), which is the response to horizontal stress. Casing must be selected so that its collapse strength exceeds the net horizontal pressure it will experience with an appropriate safety factor. The horizontal pressure includes the hydrostatic pressure of the fluid column in the annulus between the formation and casing. In unconsolidated formations, the shifting of unconsolidated strata and the swelling of clays may also contribute to the horizontal pressure on the casing.

   The key issue concerning collapse pressure is the net pressure differential across the casing during cementing (grouting). Short-term collapse pressure is a major concern during cementing operations, when the weight of the cement grout column may exert a large hydrostatic pressure against the bottom part of the casing string. Collapse pressure is much less of a concern after the grout has properly cured and, in effect, reinforces the casing. When a casing is grouted using the pressure grouting method, from the bottom of the casing upwards, the annulus and internal pressure are approximately equal.

   The differential hydrostatic pressure during grouting can be calculated from the density of the cement slurry, the height of the cement column, and the density and height of water or mud inside the casing. Collapse strength is a function of the casing material, diameter, and wall thickness. Temperature is also a critical factor for plastic and to a lesser degree fiberglass reinforced plastic (FRP) casing. For a given casing material and wall thickness, collapse strength decreases with increasing diameter. Casing collapse strengths (or pressures) can be obtained from performance ratings provided by the manufacturer or some standard references (e.g., Driscoll 1986). Casing collapse strengths can also be calculated from casing diameters and wall thicknesses using standard equations for material types, which are summarized by Roscoe Moss Company (1990). For a given casing grade, (e.g.,

Schedule 40) wall thickness increases with casing diameter to compensate in part for the decreased collapse strength. Standard dimension ratio (SDR) casings of a given grade have the same collapse pressure regardless of diameter.

6.4.2   Casing Diameter

Casing diameters are selected primarily based on flow velocity considerations and the need for adequate space to accommodate pumps and other in-well equipment. The flow velocity should not be so high as to result in an excessive frictional head loss within the casing or at the point of entry into the casing. Casing diameters should also be sufficiently large to accommodate and provide sufficient clearance for the well pump and any other downhole equipment. Larger diameters wells have greater construction costs, so there is thus a tradeoff between well efficiency and cost. If a larger diameter casing is needed to accommodate the well pump, then the upper part of the well (in which the pump will be installed) can be constructed with a larger diameter than the lower part of the well using a reducer bushing or transition joints. The casing transition can also be accomplished by telescoping the lower, smaller diameter casings inside the upper, larger diameter casing and cementing the annulus.

   As a general rule, flow velocity within a well should be 5 ft/s (1.5 m/s) or less (Driscoll 1986). However, the head losses within well casings can be estimated using the Hazen-Williams Friction Loss Equation (Reeder 1975), as follows (using consistent units):

$$V = k \cdot C \cdot R_h^{0.63} \cdot S^{0.54} \tag{6.3}$$

$$Q = V \cdot A \tag{6.4}$$

$$S = H_f / L \tag{6.5}$$

where,

V   flow velocity
Q   discharge rate
A   cross-sectional area
K   a constant, 1.318 for English units (feet and seconds), 0.849 for SI units (meters and seconds)
C   Hazen-Williams coefficient or roughness value, which is a function of construction material
R_h hydraulic radius
S   energy slope (head loss divided by pipe length)
H_f head loss
L   pipe length

The hydraulic radius of a circular pipe is its cross-sectional area divided by its wetter perimeter (inner circumference for a full pipe). The hydraulic radius of a well casing is equal to its inner diameter divided by 4 (radius/2). For metric units, head loss (h, meters of water) per unit length of pipe (m), can be calculated as

$$h = 10.67 \cdot Q^{1.85} = (C^{1.85} D_h^{4.8655}):$$ (6.6)

where D_h is the inside hydraulic diameter (m). The value of the Hazen-Williams roughnesss coefficient varies with material. New polyvinyl chloride (PVC) and FRP has a value of 150, whereas new seamless welded steel has a value of 100 to 110. The coefficient value decreases with increasing roughness (e.g., from corrosion or scaling). These equations can also be solved using spreadsheets. In practice, a variety of engineering software packages exists, both free-ware and proprietary, that perform the Hazen-Williams calculations.

6.4.3 Casing Materials

The choice of casing materials and thickness is a basic design consideration for water wells. Common casing materials used for water wells are mild steel, stainless steel, PVC, FRP, and, less commonly, coated steel. The selection of materials depends upon the borehole depth (and thus required collapse strength) and potential for corrosion.

6.4.3.1 Mild Steel

Mild steel has historically been the most commonly used casing material for construction of water wells. Driscoll (1986) discussed in detail the use of the steel casing for water wells. The mild steel casing most commonly used for water wells conforms to either ASTM Standard A53/A53 M, American Petroleum Institute (API) standard specification 5L, or International Organization for Standardization standard ISO-3183. The major advantages of steel pipe are its low cost, wide availability over a broad range of diameters and wall thicknesses, and high collapse strength. Steel casing is commonly joined by butt welding, or less commonly, in the water wells, using threaded couplings. Joining casing by butt welding has the advantage of not having a larger diameter at casing couplings, which may necessitate a greater borehole diameter. In the oil and gas industry, casing ('tubing') joints are typically joined using threaded couplings. Threaded couplings are also used in deep injection wells constructed using oilfield methods.

The principal disadvantage of mild steel is that it is subject to corrosion, particularly in hydrogen sulfide-rich, brackish, and saline water aquifers. Steel casings

have remained intact for over 50 years in water wells completed in freshwater aquifers. Galvanic corrosion may occur where dissimilar metals are used in a well. Galvanic corrosion is of particular concern in attaching stainless steel screens to a mild steel casing, which is a common practice in water well construction. Dielectric couplings or isolation flanges can be used to isolate dissimilar metals, such as between a pump and the well drop pipe and casing.

6.4.3.2   PVC

PVC casing has the advantages of being corrosion resistant, widely available, relatively inexpensive and light weight, and easy to install. Its principle disadvantage is that it has a relatively low collapse strength, which may be reduced further by increases in temperature during cementing operations. PVC casing may not be suitable for some monitoring well applications because of the potential for sorption and leaching of trace amounts of some organic chemicals. PVC casing is joined using either threaded couplings, solvent-welded bell couplings, double female-type couplings, or a spline-lock mechanical joining system. Solvent-welded, bell joints are the traditional means used for joining plastic well casings. The joints are commonly reinforced using screws, which should be stainless steel and not penetrate through to the casing interior. Certa-Lok PVC casing, manufactured by the CertainTeed Corporation, uses a spline-locking design, which in the United States is becoming more widely used for production wells. The major advantage of the spline-lock system is that allows for rapid installation of the casing under all weather conditions and the casing can be dissembled if needed. Threaded couplings are widely used for small-diameter monitoring wells.

Coupling diameter is also a design consideration for PVC. The couplings of large diameter PVC pipes, whether it is a bell end or spline-lock mechanism, have a greater outer diameter than the rest of the casing joint. The borehole and outer casings of multiple-casing wells, therefore, must have a diameter sufficient to accommodate both the PVC casing and coupling, and leave room for an adequate cement grout thickness around the coupling and to lower a tremie pipe during cementing.

PVC casing performance ratings are in accordance with ASTM International Standard F-480-02 (Standard Specification for Thermoplastic Well Casing Pipe and Couplings Made in Standard Dimension Ratios (SDR), SCH 40 and SCH 80). Hydraulic collapse issues applicable to PVC casing are discussed by CertainTeed (2007), a major manufacturer of PVC well casing. CertainTeed recommends that a safety factor of two be applied for casing selection. The strength of PVC casing decreases with increasing temperature to a greater degree than other types of commonly used casings, such as FRP or steel. Increases in temperature caused by the hydration reaction during the curing of Portland cement grout can be transferred to the casing. The decrease in collapse strength is related to temperature by the following relationships 0.6 psi per °F, 1.1 psi per °C, and 7.4 kPa per °C (CertainTeed 2007).

The temperature increase due to heat of hydration is directly related to the thickness of the cement in the annulus. Driscoll (1986) recommended a maximum thickness of 2-in (5 cm) of cement, however greater grout thicknesses have been successfully emplaced. Centralization of the casing is also important in that an off-centered casing may have a greater cement thickness on one side, and thus greater heating (CertainTeed 2007). Zones of increased borehole diameter will also have increased cement thickness and thus, greater temperature increases. If a zone of borehole enlargement is detected on a caliper log, then consideration should be given to having a shorter cement stage over the zone, to reduce the differential hydrostatic pressure.

CertainTeed (2007) stated that there is no one recommendation for the maximum depth at which a typical size and class of PVC casing can be used. The author has successfully set 16-inch (41-cm) diameter SDR-17 casings in Palm Beach County, Florida, to a depth of 1,150 ft (351 m). The cement was installed in several stages so as to not exceed the collapse strength of the casing.

6.4.3.3 Fiberglass

Fiberglass reinforced plastic casing (FRP) is a commonly used alternative to PVC, particularly for deeper wells (>500 ft or 150 m). FRP casing is corrosion resistant and has greater collapse strength than PVC. Manufacturers of NSF certified FRP pipe include Burgess Well Company and GP Fiberglass, Ltd. Other manufacturers may also produce an equivalent casing type. High performance FRP pipe has been developed for the oil and gas industry, such as the product lines manufactured by Tubular Fiberglass Corporation and Fiberglass Systems. FRP casings are typically joined using threaded couplings. A critical issue for the installation of FRP casings (and other casings with mechanical couplings) is that the manufacturer's recommended installation procedures should be strictly followed to ensure successful installation of the casing and to comply with pressure rating requirements. Threaded couplings are vulnerable to damage and loss of integrity from improper installation.

6.4.3.4 Stainless Steel

Field testing of corrosion in wells clearly indicates that stainless steel has a substantially greater corrosion resistance than mild steel, with type 316L stainless steel having the greatest resistance (Geoscience Support Services 1999) of the commonly used alloys. Stainless steel alloys can provide a combination of corrosion resistance and strength, but at a higher cost than PVC, fiberglass, or mild steel casings. Stainless steel casings are thus used for deep permanent production or injection wells in which casing strength and corrosion resistance are major constraints. Stainless steel is more widely used for well screens. A great variety of stainless steel grades are available, which differ in their composition and properties such as hardness, strength, and corrosion resistance in various environments. The most

common types of stainless used in water wells are Types 304 and 316L. Type 304 stainless steel is often used in wells producing freshwater, but is subject to chloride corrosion. Type 316L is the preferred grade of stainless steel for wells completed in brackish and saline waters. Even more corrosion resistant alloys are available, such as the Duplex and Super Duplex stainless steel series, but they are very expensive and would not be necessary for the vast majority of aquifer characterization projects. The availability of stainless steel casings with acceptable wall thicknesses required for deep well construction is limited, especially based on the large increase in cost associated with even a small increase in the pipe wall thickness.

6.4.3.5   Coated Mild Steel

Coated mild steel pipe offers the advantage of steel strength and resistance to corrosion. Usually the inner surface is coated because it is in contact with water. The outer surface of the casing need not be coated if the casing is to be fully grouted. The coating can be applied in a liquid form or in a powder form. Fusion bonded epoxy (FBE) is widely used to coat pipe and steel fittings. The FBE coating consists of a powdered mixture of resin and hardener, which are unreacted at normal storage conditions. The powder mixture is electrostatically applied to the steel. At the elevated temperatures during application, the constituents of the powder melt and inter-react, and irreversibly fusion bond with the steel. Standard thicknesses of stand alone FBE coatings range between 250 and 500 l m.

The main point of weakness for coated steel is the connection between casing joints and any place where the coating is damaged and uncoated steel exposed. Accelerated corrosion may occur at breaks or damaged epoxy coating locations. Localized corrosion could impact the mechanical integrity of the casing as far as its ability to hold pressure.

6.5   Well Completions

Wells constructed in unconsolidated aquifers require a screened completion. Well screens and associated filter packs act to allow water to flow into a well while not allowing sediment to pass. The primary design objective for production wells is to minimize head losses (and thus maximize water production and well efficiency) while avoiding significant sediment production. There is much greater flexibility in the design of monitoring wells installed to only measure water levels or occasionally sample for water chemistry. Wells constructed in well-lithified rock or consolidated sediment may be completed with either an open hole (referred to a barefoot completion in the oil and gas industry) or a liner.

6.5.1   Well Screen Type

The selection of screen type and screen design for water wells requires consideration of entrance velocity, collapse strength, and sand retention, and the need for occasional rehabilitation. Most commonly used screen types are slotted or perforated screens, wire-wrapped or continuous slot screens, casing-based screens, and louvered (shuttered) screens (Fig. 6.13).

   The main design parameters for well screens are the slot size, slot open area, and entrance velocity. Average entrance velocity is calculated by dividing the flow rate through the screen by the total open area of the screen. It is desirable to maximize the slot size, and thus, open area of the screen in order to minimize entrance velocities and head losses across the screen. The slot size and filter pack sand and gravel size must also be small enough to prevent most sediment grains from passing through the screen. Driscoll (1986) provides an excellent discussion of the screen and filter pack selection, which is summarized herein.
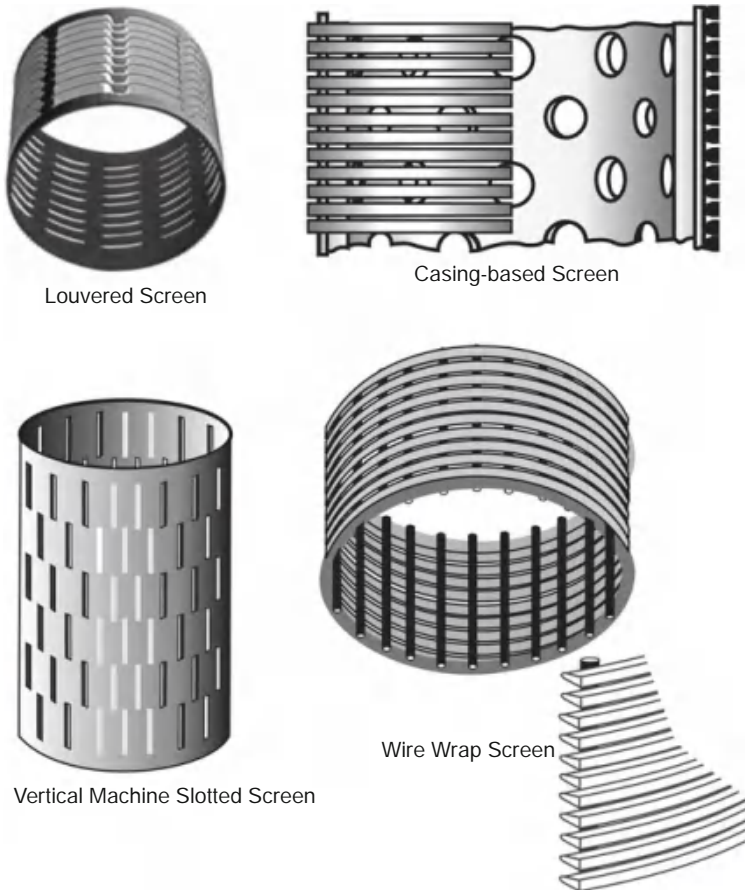
Fig. 6.13   Water well screen types (from Roscoe Moss 1990)

Historically, a maximum entrance velocity through a screen of 0.1 ft/s (0.03 m/s) has been used as the design standard for screened wells. The 0.1 ft/s (0.03 m/s) limit has also been incorporated into well construction regulations in many jurisdictions. The technical basis for the 0.1 ft/s (0.03 m/s) upper limit is open to question as being overly conservative, particularly because the science behind the value is scant and many wells successfully operate at higher entrance velocities (Roscoe Moss Company 1990, 2006). The 0.1 ft/s (0.03 m/s) maximum velocity may have significant trade impacts as it can necessitate the use of continuous wire-wrapped screens (with its large percentage of open area) versus other screen types, such as louvered screens. The slot open area per unit length of screen increases with diameter of the screen. However, larger diameter screens typically have a lesser collapse strength. Therefore, the selection of the screen diameter should be based on both maintaining a low entrance velocity into the well and on the strength necessary to avoid collapse pressure thresholds.

Each of the different screen types have their advantages and disadvantages and there is no universal optimal choice. Wire-wrapped screens have greater open areas, and thus lower entrance velocities, than louvered (or shutter) screens, but are generally more expensive. Wire-wrapped screens also allow for easier development because there is less deflection of the energy (such as from high pressure jetting) through the screen (Mansuy 1999). Wire-wrapped screens have lower collapse strengths than louvered screens and are more difficult or impossible to repair or restore to their original shape and structural integrity if damaged (Roscoe Moss Company 1990).

Slotted or perforated screens are the least expensive option, but have relatively low open areas compared to other screen designs, resulting in greater head losses and lower well efficiencies. Slotted and perforated screen wells are also more difficult to develop and rehabilitate. However, depending on pumping rate and aquifer thickness (screen length), the additional head losses may not be an overriding concern. Slotted screens are acceptable for monitoring wells. Machine-slotted PVC screens are very widely used for shallow monitoring wells.

The added strength in louvered versus wire-wound screens is advantageous for relatively deep wells. Louvered screens can also be more easily rehabilitated using a tight-fitting swab, but require a special upwards directed water jetting tool to clean the screen. The strength of louvered screens allows for more aggressive physical rehabilitation, which might permanently damage wire-wrapped screens. Casing-based screens are an attractive option for deep wells because their combined strength and large open area. The screen consists of a segment of steel casing through which holes have been cut. The casing is surrounded on the outside by a wire-wrapped screen. The internal casing provides strength and the screen allows for relatively large open areas.

An additional design option for sand control is prepacked screens, which are constructed of dual screens with an intervening permanent filter pack. The filter pack material is usually either a resin-coated gravel or sand or a silicate\ceramic proppant. Different filter pack size options are available. Prepacked screen are used in wells in which installation of a conventional filter pack is not technically possible or economical. Prepacked screens may be used, for example, in direct push wells, whose annulus is too small for the installation of a conventional filter pack.

Prepacked screens are often used in some non-vertical wells, which are subject to gravity settling of filter pack material. Prepacked screens also have the advantages of quicker installation, large open areas, and strength. The principle disadvantages of prepacked screens are that they are prone to plugging and difficult to clean.

As a general principle, a well screen should be chosen so as to maximize open area and thus well efficiency, while maintaining acceptable collapse strength. Screen manufacturers (e.g., Johnson Screens, Roscoe Moss, and Schlumberger) provide information about the dimensions, slot size, open area (percent and area per foot or meter), and tensile and collapse strengths of their various screens, which are now accessible on their internet sites. Well screens, even more so than casings, should be constructed of corrosion resistant materials. Stainless steel (316L) is the preferred material in many cases. Cost should be a secondary consideration for production wells, because the incremental cost difference between the various screen options is a small fraction of the total well construction cost. It is ill advised to sacrifice well performance for modest cost savings on the screen selection.

6.5.2   Filter Pack

Filter packs act to reduce the production of sand and increase well efficiency by increasing the effective hydraulic radius of the well. Screened wells may be completed with either a natural or artificial filter (gravel) pack. A natural filter pack is formed during the well development process by the removal of fine-grained material from the formation in the vicinity of the screen. An artificial filter pack consists of sand or gravel that is emplaced in the annulus between the screen and formation. The filter pack material should consist of graded, rounded sand or gravel that is composed predominantly of quartz.

The choice between natural and artificial filter packs should be based on the geological character of the aquifer and the type of screen selected for use (Driscoll 1986). In general, natural filter packs are effective for moderate to poorly sorted aquifers composed mostly of sand and granule-sized material with minimal fine-grained materials. Artificial filter packs are necessary for wells completed in more homogeneous formations composed mostly of fine-grained material with minimal coarser sand that could be concentrated into a graded filter pack. Artificial filter packs are also the preferred choice for stratified aquifers containing beds with greatly different grain sizes.

The procedures for selecting artificial filter back material and screen size are discussed in detail by Driscoll (1986), Roscoe Moss Company (1990), and Sterrett (2007). The selection of screen slot size and the filter pack material depends upon the grain size distribution of the aquifer strata. It is, therefore, important to obtain representative samples of the aquifer materials and have grain-size analyses performed. Most geotechnical laboratories can perform grain-size analyses, which basically involve recording the fraction of a sample that passes through a stack of sieves of progressively decreasing opening size.

A commonly used practice for selecting a slot size for screens in wells with a natural filter pack is to use a slot with that will retain 40 % of the aquifer material (Driscoll 1986). The 40 % retention value is based on a non-homogenous aquifer and a high reliability of the grain size analysis. A smaller slot size that will retain 50 % of aquifer material is recommended when there is doubt over the reliability of the grain size analysis.

For artificial filter packs, one method for selecting the filter pack grain size is to multiply the (d_{70}) size (70 % retained screen size) of the aquifer material by a factor of 4 to 10 (depending on aquifer grain size properties; Driscoll, 1986). The d_{10} size of the filter pack is obtained by multiplying the calculated d_{70} value by 2. A filter pack material should be identified and selected whose grain size distribution approximately matches the target sieve analysis. Providers of filter pack sands and gravels typically can provide a grain size distribution for their various material grades. A screen slot size should then be selected that will retain 90 % of the filter pack material.

6.5.3   Perforated Completions

Perforated completions involve the punching of holes in casing (usually cemented) using a string of shaped charges. Perforation procedures were reviewed by Bellarby (2009). The perforation ′gun′ may carry many dozens of charges, which are positioned at the desired depths. Shaped charges are used, which deform the casing and crush cement and formation material. Entrance holes are typically 0.2 to 0.4 inch in diameter and can penetrate 1 ft (30 cm) or more.

Perforations need to be cleaned of perforation and rock debris before they produce, such as by

- allowing the well to flow
- underbalance—pressure inside the casing is less than the formation pressure
- surging after perforation guns have been removed
- extreme overbalance—high pressures inside the casing forces debris deeper into the formation.

The advantages of perforated completions are an upfront selection of production and injection intervals, drilling-related formation damage can usually be bypassed, and the ability to add perforations at a later time. The main disadvantages are increased costs and relatively small open areas. Existing wells may be perforated at a later time to open a new production or monitoring zone.

6.5.4   Open-Hole Completions and Liners

The simplest and typically least expensive well completion option is an open hole, which is possible in lithified strata that does not produce much sand and is not prone to collapse. Open-hole completions also have the advantage of avoiding head losses associated with screens and allowing more direct access to the formation for well stimulation and rehabilitation activities. There are two main methods for construction of wells with an open-hole completion. The final casing may be set and cemented in place and then the open-hole is drilled to total depth. Alternatively, the borehole may be drilled to total depth, and then the casing seated and cemented in place at the top of the completion zone. A cement packer, basket, or similar device is commonly used to support the cement in the annulus and prevent it from entering the completion zone.

Non-cemented liners are used to provide protection of open holes from collapse and provide some sand control. They are essentially robust screens installed without a filter pack. Liners are usually either slotted or pre-holed. In deep wells, liners are usually suspended using a liner hanger. In shallow wells, the liner may be seated on the bottom of the hole and either extend upwards to the top of the completion zone or to land surface.

6.6   Well Development

6.6.1   Introduction

The two basic objectives of well development are repairing formation damage that occurred during well drilling and to alter the physical properties of the aquifer near the borehole so that water will flow more freely to a well (Driscoll 1986). A fully-developed well will have close to the maximum well efficiency with minimal production of sand, silt, and finer suspended solids. Well development techniques were reviewed by Driscoll (1986), Roscoe Moss Company (1990), and Sterrett (2007). Well rehabilitation techniques, which are also applicable to the initial well development, were reviewed by Mansuy (1999) and Houben and Treskatis (2007). The development strategies adopted for a given well should be tailored to the well construction type, drilling method, and aquifer lithology. Depending on planned uses of a well, disinfection (typically with a chlorine solution) should also be performed. Wells should be disinfected after development, in particular, if they are to be used for potable water supply or used for microbiological monitoring. The cited well development and rehabilitation references provide disinfection procedures.

Well development is a part of construction activities usually performed by a well driller. The project hydrogeologist or engineer should specify required methods and set performance standards for well development in the contract documents for the

driller. It is also important to address ancillary issues, such as the method for disposal of discharge water and chemicals used during development. Development standards vary depending upon the planned use of a well. Production wells are normally required to be clear and free of sediment. The water produced from the well pumped at its design capacity may be required to meet a specified turbidity standard (e.g., local drinking water standard) and sand content, such as not more than 1 mg/L as measured using a Rossum Sand Tester. Wells that are to be used to supply a membrane treatment facility are usually required to have a silt density index (SDI) of less than 3.

Proper development is also important if a well is to be pumped or otherwise stressed for an aquifer hydraulic test, especially for slug tests and single-well pumping tests. Incomplete development can result in excessive head losses within a well and thus affect the rate of flow into and out of the well. Development is a critical issue for slug tests because formation damage and screen and filter pack clogging will affect drawdown and recovery rates (Chap. 8). Well development is less of a concern for wells that will be used only for the monitoring of water levels.

The minimum well efficiency should be 70 % or 80 % at the well design capacity. If a well is less efficient, it is important to ascertain the cause of the inefficiency. Well efficiency is dependent upon well design and construction in addition to well development. If the inefficiency is due to head losses in the casing caused by too small of a diameter and/or a screen with too small of an open area, then well development will not be a remedy.

Two options exist for the contracting of well development. Well development can be contracted on a ʹlump sumʹ basis with the requirement that development continue until the performance standards are met. Alternatively, development can be contracted on a ʹtime-and-materialsʹ basis, in which the well driller is compensated for his actual effort. A lump sum cost eliminates financial uncertainty for the owner, but may result in a greater overall cost, especially if the development is completed quickly. A time and materials costing reduces risk for the driller, but adds an element of uncertainty to the owner costs. Commonly, a number of hours for development are placed in the schedule of contractual tasks. If additional hours are required, then those hours could be billed at a time and materials rate included in the contract.

6.6.2   Well Development Methods

The basic methods that are used for the initial development of wells differ primarily in their physical action (Table 6.2). Each of the basic methods has variations based on the equipment used and operational procedures. The optimal well development program for a given project depends upon both well construction and drilling method and the lithology of the aquifer. In general, wells drilled using the mud-rotary method and completed with screens require a high degree of development to remove the mudcake and drilling fluids present in the filter pack and that

Table 6.2 Summary of well development methods

Method	Action	Variations
Overpumping	Well is pumped at a greater than operational rate.	Well pump
		Air lift
Surging	Repeated reversals in flow	Air lift
		Well pump
		Surge block or swab
		Isolation/interval development
Mechanical	Direct contact methods used to dislodge material on inner surface of casing and screen	Brushing
		Scraping
Jetting	High pressure water flow clears screens, disrupts mudcake, and agitates and rearranges particles	Water jetting
		Water jetting combined with air lift.
Acidification	Dissolution of carbonate minerals	Hydrochloric acid
		Sulfamic acid
		Carbonic acid
Dispersants	Chemicals are added to disperse clays, which facilitates their removal by over pumping and surging	Sodium acid pyrophosphate
		Tetrasodium pyrophosphate
		Sodium tripolyphosphate
		Sodium hexametaphosphate

have invaded the formation. On the contrary, wells completed with open holes and drilled using the reverse-air rotary method usually requires less rigorous development.

The performance of wells completed in limestones can often be significantly improved by acidification at the time of construction and, at later times, as part of a rehabilitation program. The acid acts to increase the size of secondary pores and to strip away the borehole surface and associated clogging materials. Acidification is ineffective in siliciclastic aquifers that lack minerals that are soluble in the commonly used acids (e.g., hydrochloric, sulfamic, and carbonic). Acidification may also be effective in calcite-cemented sandstones.

6.6.2.1 Over Pumping

Over pumping is the pumping of a well at a higher rate than the well will be pumped when placed into service. The concept is quite simple; higher pumping

rates increase flow velocities in the filter pack and formation near the well, which entrain and remove fine particles. Particles that are not removed at the higher flow rates should not be produced at the lower operational pumping rates. The over pumping can be performed using a pump or by air lifting. The production of sand can damage a pump, so it is recommended that the permanent well pump not be used for over pumping (Driscoll 1986).

A limitation of pumping an entire well for development or rehabilitation is that water will be produced from the most transmissive intervals. The entire screen or open hole may not be adequately developed. The differential pressure (head) in the well from pumping is dissipated by flow into the well from transmissive intervals. Sufficient differential pressure may not occur across the least transmissive clogged intervals.

6.6.2.2   Surging

Surging or backwashing is a commonly used technique for development. Surging involves inducing frequent reversals of water flow through the screen and filter pack (if present in the well) and adjoining formation. The reversing direction of flow breaks down the bridges between grains and across screen openings, thereby allowing the removal of the finer particles, and rearranging the remaining grains in the filter pack and formation.

A commonly used method of surging is by air lifting. The surging system consists of an air line supplied by a compressor. The air line is used to both pump the well and create a reverse flow when the air supply is suddenly turned off. Water that has risen in the casing during pumping rapidly flows back down the well under gravity. Air lifting allows for frequent rapid reversals in flow direction as the air supply can be near instantaneously turned on and off or be significantly varied using a valve. The air-flow rate may be adjusted in the field to maximize the efficiency of the process.

Surging may also be performed by installing a temporary pump in the well. Flow reversals can be accomplished by turning the pump on and off or by varying the pumping rate in the same manner as surging with an air line. Mechanical surging is performed using tools that are moved up and down in the well, creating reversals in flow in the same manner as a piston. The tools used include surge blocks, plungers, and swabs (Driscoll 1986; Roscoe Moss Company 1990). Isolation tools, such as packers, may be used to develop the well in stages. The development energy is successively concentrated on short sections of the aquifer, which reduces the potential for sections of aquifer to escape being properly developed.

Swabbing also allows for isolation development and is an effective technique for developing screened wells. The double swab tool usually consists of two rubber belted steel plates attached to a segment of perforated drill pipe. The plates are close to the diameter of well screen. The lowering and raising of the swab creates pressure differentials that alternately forces water into and out of the filter pack and formation. The swabbing process can be combined with air lifting and chemical

injection (Driscoll 1986; Roscoe Moss Company 1990; Mansuy 1999). The main advantage of the double swab tool is that it focuses the development energy on short segments of the screen. Swabbing should be performed from the top of the screen downwards to avoid sand-locking.

6.6.2.3 Jetting

Jetting uses a high-velocity water stream to clear the screen, disrupt mudcake on the borehole wall, and agitate and rearrange particles in the filter pack and adjacent formation. The jetting tool contains two or more nozzles that direct a high-velocity jet of water horizontally (or at an angle for louvered screens) into the screen and filter pack. The tool is lowered down the well on a pipe and slowly raised or lowered and rotated to treat the entire screen. Jetting combined with air lifting is one of the most effective methods of the development of screened wells (Driscoll 1986). Jetting can be combined with the addition of a disaggregating agent to facilitate the rapid removal of clays.

6.6.2.4 Dispersants and Other Additives

Dispersants, such as polyphosphates, are used during well development to disperse and assist in the removal of clays. The use of polyphosphates in well development is addressed by Driscoll (1986). Commonly used dispersants include sodium acid pyrophosphate (SAPP), tetrasodium pyrophosphate (TSPP), sodium tripolyphosphate (STP), and sodium hexametaphosphate (SHMP). The addition of wetting agents, such as Pluronic F-68, to polyphosphates will increase their effectiveness in disaggregating clays. It is important that all polyphosphates be pre-mixed and be completely dissolved before they are introduced into the wells. Driscoll (1986) also recommends adding sodium hypochlorite (a disinfectant) to the solution to control the bacterial growth promoted by the presence of polyphosphates. Dispersants are used in conjunction with surging and jetting.

6.6.2.5 Acidification

Acidification is a very effective means for developing (stimulating) and rehabilitating wells completed in carbonate aquifers. Acidification can improve well performance by dissolving fine-grained carbonate minerals adhering to the borehole wall and filling pores, and by detaching adhering fine material through dissolution of the carbonate substrate and the effervescence of carbon dioxide bubbles. The effectiveness of acidification for improving the performance of newly constructed wells varies greatly between wells. Some wells completed within limestone aquifers experience a dramatic (>50 %) increase in specific capacity, whereas the benefits in other wells may be negligible. A short-term constant-rate pumping test or

step-drawdown test should be performed before and after acidification to determine baseline well performance and to evaluate the effectiveness of the acidification.

Commonly used acids for treating wells include hydrochloric acid (HCl), sulfamic acid (H_3NO_3S), and carbonic acid. Hydrochloric acid is relatively inexpensive, widely available, and highly effective. It comes in a concentrated liquid form, and thus, presents some hazard during transport and mixing. Sulfamic acid has the advantage of coming in a powdered or pelletized form, and is therefore safer to transport and handle. Sulfamic acid does not produce harmful fumes and is less corrosive than hydrochloric acid. NuWell 100, produced by Johnson Screens, is a sulfamic acid product that contains corrosion inhibitors. Sulfamic acid is slower acting than hydrochloric acid and should, therefore, be retained in the well for a longer period (at least 8 to 12 h). Carbonic acid forms by the dissolution of carbon dioxide in water. The carbon dioxide is commonly transported to the site in liquid form. Carbonic acid is a gentle, slow-reacting acid that has been used mainly for rehabilitation of wells, rather than initial development. The main advantage of carbonic acid compared to other common acids is that it is much safer and easier to handle, has a lesser potential for formation damage, and it does not add chloride or sulfate to the water. It is also non-corrosive and thus removal of the pumps or other equipment may not be required when carbonic acid is used for well stimulation and rehabilitation.

Acidification entails risks to personnel and for damage to the wells. Personnel handling acids and performing well acidification activities should be properly trained and use appropriate safety equipment, especially protective clothing. Danger may also arise from the build-up of great pressures within the well from released carbon dioxide gas. All work should be performed in strict accordance with applicable occupational health and safety regulations. Excessive acidification can damage formations by releasing insoluble residues that may accumulate on the borehole wall or clog pore throats. The disposal of spent acid recovered from wells should be performed in accordance with applicable environmental regulations.

References

Agarwal, A., Laronga, R., & Walker, L. (2014) Rotary sidewall coring - size matters. Oilfield Review, 25(4), 39–39.

Aller, L., Bennett, T. W., Hackett, G., Petty, R. J., Lehr, J. H., Sedoris, H., & Nielsen, D. M. (Eds.) (1991) Handbook of suggested practices for the design and installation of ground-water monitoring wells (Vol. 1). Environmental Monitoring Systems Laboratory, Office of Research and Development, US Environmental Protection Agency.

American Petroleum Institute (1998) Recommended practices for core analysis (2nd Ed.). Recommended Practice 40. Washington D.C.: American Petroleum Institute.

ASTM (2004) Standard practice for sonic drilling for site characterization and the installation of subsurface monitoring devices. D6914-04. West Conshohocken: ASTM International.

ASTM (2011) Standard test method for standard penetration test (SPT) and split-barrel sampling of soils. D1586-11. West Conshohocken: ASTM International.

ASTM (2012) Standard practice for thin-walled tube sampling of soils for geotechnical purposes (D1587 - 08(2012)e1). Conshohocken: ASTM International.

Ault, T. D., Logan, S., & Madaj, A.J. (1994) Rotary sonic drilling for environmental investigations – applications to stratigraphic characterization and correlation. In Proceedings Seventh Annual Outdoor Action Conference (pp. 821–636), Las Vegas, Nevada.

Bajsarowicz, C. J. (1992) Core alteration and preservation. In D. Morton-Thompson & A. M. Woods, A.M., eds., Development geology reference manual. Methods in Exploration Series 10 (pp. 127–130). Tulsa: American Association of Petroleum Geologists.

CertainTeed (2007) Selection of PVC well casing based on hydraulic collapse considerations. Valley Forge, Pa: Certainteed Corporation.

Davis, H. E., Jehn, J., & Smith, S. (1991) Monitoring well drilling, soil sampling, rock coring, and borehole logging. In D. M. Nielsen (Ed.), Practical handbook of ground-water monitoring (pp. 195–237). Chelsea. Michigan: Lewis Publishing.

Driscoll, F. G. (1986) Groundwater and wells (2nd ed.). St. Paul, Mn: Johnson Filtration Systems.

Foremost Industries (2003) Benefits of dual rotary drilling in unstable overburden formations. Calgary: Foremost Industries.

Geoscience Support Services (1999) Corrosion field test of steel commonly used in well casing and screen, Report to City of Fountain Valley.

Hackett, G. (1987) Drilling and constructing monitoring wells with hollow stem augers. Part 1: Drilling considerations. Ground Water Monitoring and Remediation, Fall 1987, 51–62.

Hackett, G. (1988) Drilling and constructing monitoring wells with hollow stem augers. Part 2: Monitoring well installation. Ground Water Monitoring and Remediation, Winter 1988, 60–68.

Henahan, M. (1999) Dual rotary drilling in unconsolidated overburden. Water Well Journal, July 1999, 66–68.

Herrick, D. (1994) Dual-rotary drilling – is it for you. Water Well Journal, Oct. 1994, 50–54.

Hess, K. M., & Wolf, S. H. (1991) Techniques to determine spatial variations in hydraulic conductivity of sand and gravel. Ada, Oklahoma: U.S. Environmental Protection Agency, Office of Research and Development.

Houben, G., & Treskatis, C. (2007) Water well rehabilitation and reconstruction. New York: McGraw-Hill.

Keely, J. F., & Boateng, K. (1987a) Monitoring well installation, purging, and sampling techniques - Part 1: Conceptualizations. Ground Water, 25, 300–313.

Keely, J.F., & Boateng, K. (1987b) Monitoring well installation, purging, and sampling techniques - Part 2: Case histories. Ground Water, 25, 427–439.

Maliva, R. G., & Missimer, T. M. (2010) Aquifer storage and recovery and managed aquifer recharge using wells: Planning, hydrogeology, design, and operation. Houston, Schlumberger Corporation.

Mansuy, N. (1999) Water well rehabilitation, a practical guide to understanding well problems and solutions. Boca Raton: Lewis Publishers.

Misstear, B., Banks, D., & Clark, L. (2006) Water wells and boreholes. Chichester: John Wiley & Sons.

Munch, J. H., & Killey, R. W. D. (1985) Equipment and methodology for sampling and testing cohesionless sediments. Ground Water Monitoring and Remediation, 5(4), 38–42.

Nielsen, D. M., & Schalla, R. (1991) Design and installation of ground-water monitoring wells. In D. M. Nielsen (Ed.), Practical handbook of ground-water monitoring (pp. 239–331). Chelsea, Michigan: Lewis Publishing.

Reeder, H. O. (1975) Injection-pipe system for artificial recharge: U.S. Geological Survey Journal of Research, 3, 501–503.

Roscoe Moss Company (1990) Handbook of ground water development. New York: John Wiley & Sons.

Roscoe Moss Company (2006) Entrance velocity: its importance to well design. Roscoe Moss Company Technical Memorandum 006-6.

Stephan, R. (1995) Rotasonic drilling: an alternative to conventional technology in environmental characterization studies. In Proceedings or the National Outdoor Action Conference and

Exposition, Aquifer Remediation/Ground Water Monitoring/Geophysical Methods, v. 9, pp. 325–337.

Sterrett, R. J. (2007) Groundwater and wells (3rd ed.). St. Paul, Minnesota, Johnson Screens.

Strauss, M. F., Story, S. L., & Mehlhorn, N. E. (1989) Application of dual-wall reverse-circulation drilling in ground water exploration and monitoring. Ground Water Monitoring and Remediation, 9(2), 63–71.

Williams, D. E. (2008) Research and development for horizontal/angle well technology. Denver: U.S. Department of the Interior, Bureau of Reclamation, Desalination and Water purification Research and Development Program Report No. 151.

Zapico, M. M., Vales, S., & Cherry, J. A. (1987) A wireline piston core barrel for sampling cohesionless sand and gravel below the water table. Ground Water Monitoring and Remediation, 7(3), 74–82.

Chapter 7
Aquifer Pumping Tests

Aquifer pumping tests are an integral component of aquifer characterization because they provide quantitative data on large-scale aquifer hydraulic properties such as aquifer transmissivity, storativity, and the vertical hydraulic conductivity (leakance) of confining strata. Aquifer performance tests (APTs), also referred to as aquifer pumping tests, involve the pumping of an aquifer at a known rate and the measurement of the corresponding changes in water levels in the pumped and observation wells. Aquifer hydraulic testing may also be performed by injecting water into a well. APTs can provide important information on well yields, well efficiency, and the stability of water quality. Successful aquifer hydraulic testing requires attention to detail and careful consideration of the underlying assumptions of the various methods used to interpret the data.

7.1 Aquifer Performance Test Design

Conceptually, the performance of APTs is simple; one or more wells are pumped and water levels are recorded in the pumped and, ideally, a number of observation wells. References that address APT design include Stallman (1969), Driscoll (1986), Kruseman and de Ridder (1991), Dawson and Istok (1991), and Walton (1991), in addition to basic discussions in most groundwater textbooks. The basic technical and operational challenges lie in obtaining data that are readily interpretable and representative of local aquifer conditions. For most tests, the pumping (or injection) rate should be constant and accurately measured. Changes in water levels in the pumped and observation wells should be accurately measured and recorded, and need to be only due to the pumping or injection performed as part of the test. If external factors (i.e., other than test pumping or injection) affect local water levels during a test, then the data should be corrected as part of the data analysis. External factors include, but are not restricted to, pumping by other aquifer users, local discharge and recharge, precipitation, and tidal effects. APTs can be

performed by recording water levels changes in a single pumped well (single-well test) or by pumping one (or more) wells and monitoring water levels in one or more observation wells (piezometers). Multiple-well tests are preferred because

- more accurate measurement of storativity values can be obtained
- time-drawdown data obtained from observation wells are less sensitive to well construction, well and formation clogging (skin damage), well-bore storage, and well development than data from pumped wells
- data from multiple observation wells can be interpreted using distance-drawdown methods
- observation well time-drawdown data are less sensitive to variations in pumping rate
- data from multiple observation wells can potentially detect directional aquifer anisotropy.

Single-well tests have the advantage of lower costs, especially if existing wells can be used and dedicated observation wells would have to be installed for a multiple-well test.

7.1.1 Observation Wells

As many observation wells as practically possible should be utilized in APTs, but it is certainly recognized that projects have financial constraints that limit the number of observation wells that may be installed for an APT. Where dedicated wells are to be installed for an APT, consideration needs to be given as to how to obtain the maximum value from the number of available wells. The observation wells should be installed at varying distances from the pumped well to allow data analysis using distance-drawdown methods. Distance-drawdown data are analyzed graphically using a logarithmic distance scale. Hence, the spacing of observation wells from the pumped well should be approximately logarithmic rather than linear, as data points with a linear spacing may plot very close together on a logarithmic scale. For example, a spacing of 5, 50, and 500 m, is preferred over a spacing of 100, 200, and 300 m. Ideally, observation wells should fully penetrate the aquifer of interest and also be installed at different directions from the pumped wells to evaluate aquifer anisotropy.

The preferred well spacing for a given test should be evaluated by a preliminary modeling analysis using best estimates of aquifer hydraulic parameters. The likely drawdowns can be estimated for different distances and pumping rates, which would serve as a guide to well spacing. For example, observation wells should not be installed so far from the pumped well that very little or no drawdown will occur, unless the purpose of the well is to monitor background water levels. Observation wells should also be installed in overlying and/or underlying aquifers if inter-aquifer leakage is an important project concern.

7.1.2   Test Duration and Pumping Rates

The pumping period for APTs should be as long and at as high a sustainable pumping rate as possible. Longer tests increase the likelihood that boundary conditions and inter-aquifer leakage can be detected and quantified, and, in unconfined aquifers, that delayed-yield and late Theis response phenomena can be observed. Longer test durations are also important where solute transport is a concern. An important consideration is that the hydraulic response of confined aquifers to pumping or injection is rapid (as a pressure wave), whereas solute transport occurs at the much slower rate of the flow of groundwater. Hence, an APT performed over the duration of a normal work day (8–10 h) is usually sufficient to determine the transmissivity and storativity of a confined aquifer. Test duration of several days or much longer may be needed to detected leakage, boundary effects, and the delayed-yield phenomenon.

Very long-duration (multiple week) tests may be needed to evaluate the effects of groundwater pumping on water quality, such as whether or not it induces horizontal or vertical saline-water intrusion. Indeed, such a determination is usually not definitively possible in a pumping test. For example, a 30-day pumping test may not directly indicate whether the saline-water interface may reach a wellfield several years into the future. However, if salinity significantly increases (or other water quality changes of concern occur) during an APT, then it should be taken as a red flag that the water quality at the test site is not stable and that further investigation is warranted.

The commonly used analytical methods to interpret pumping test data plot time on a logarithmic scale. Hence, the extension of a time-drawdown plot for an increase in test duration, for example, from 400 to 800 min, is small relative to the actual increase in duration (Fig. 7.1). The added value from the increase in the
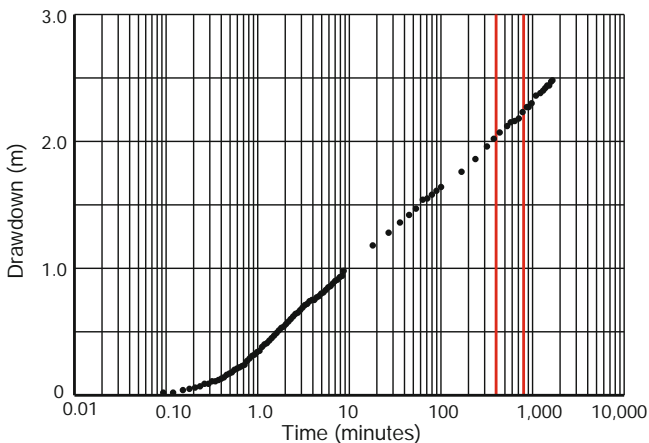
Fig. 7.1   Semilog time-drawdown plot. A doubling of the test duration from 400 to 800 min (red lines) results is a comparatively much shorter increase in the plot length

duration of a test may be minor, if the primary concern is obtaining a transmissivity and storativity value. An informed decision needs to be made as to whether the cost of obtaining the additional data is commensurate with its informational value.

Water disposal can be an important issue constraining the duration and pumping rate of APTs. Water produced during a test needs to be disposed of (or stored) in a manner such that it does not impact the test itself (e.g., by recharging the tested aquifer) or adversely impact the local environment. Water disposal is a particular concern in tests performed on aquifers that contain brackish or saline, or otherwise contaminated water, and there are prohibitions or restrictions on where the produced water can be discharged. For example, APTs performed as part of several investigations for brackish groundwater supply for desalination facilities in South Florida had to be performed for shorter durations than optimal because of limitations on how much brackish water could be discharged to fresh surface water bodies or to the ground.

7.1.3   Pumping Rate and Water Level Data Collection

The primary data collected during an APT are the pumping (or injection) rate and a time-series of water level measurements. It is imperative that these data are accurately measured and recorded. APTs are time-consuming and thus expensive to perform. It is thus critical that measures be taken to avoid having to repeat a test because of a data collection failure. Hence, redundancy in the data collection is strongly recommended.

Full-pipe flow rates are commonly measured using a totalizing flow meter. The flow meter should be recently (within the past 6 month) calibrated to ±5 % accuracy. The flow meter should also be installed along a straight-run section of pipe 5 to 10 pipe diameters away from pumps, valves, or bends in the pipe. A second means of measuring flow rate should also be available to confirm the flow meter readings, such as an orifice/manometer tube assembly or a second flow meter. For tests performed at low flow rates, pumping rates can be confirmed by recording the time required to fill a container of known volume (e.g., 55-gallon drum).

Drawdowns are now usually measured using electronic pressure transducers and data loggers. The older-style units have down-hole pressure transducers that are connected by a cable to a data logger at land surface. The older-style systems are being supplanted by down-hole water level probes that contain a pressure sensor and internal data logger. Some probes also have sensors that can measure temperature, conductivity, and other parameters. The normal mode of operation is to install the probes down a well (e.g., by suspending on a non-stretchable line or cable) and periodically retrieving the probes to download the data.

Data-logging systems have been known to not start properly, terminate during a test, or lose data, so there should be some redundancy in the data collection. Redundancy is particularly important if self-contained down-hole water-level probes are used that are not set-up for real-time readings at land surface during the

Table 7.1 Recommended minimum measuring frequency (modified from Kruseman and de Ridder 1991)

Time since start of pumping	Time intervals
0–2 min	5 s
2–5 min	20 s
5–15 min	1 min
15–50 min	5 min
50–100 min	10 min
100–8 h	20 min
8–48 h	60 min
48 h–6 days	3 times a day
6 days—shutdown of pump	1 time a day

test. Data collection should be confirmed during the test. Independent manual measurements of water levels using a water-level probe or tape is strongly recommended as a back-up and check on the data-logging system. It can be very costly to repeat a long-term APT, so attention must be paid to ensure that sufficient data are obtained for interpretation of the test results.

An automatic electric data-logging system should be used, preferably one that allows for measurements at a logarithmic time scale. Frequent readings (5 s maximum) are needed at the start of the test, whereas 20–30 min or longer-spaced readings are sufficient for the later part of the test (Table 7.1). The objective is to obtain a roughly equal frequency of readings for each log cycle of time. At least 12 h of background and recovery water-level data should be collected both before and after the APT. Twenty-four hours or greater is preferred, particularly for long-duration tests.

7.1.4 Practical Recommendations

As is generally the case for aquifer characterization methods, successful APTs require attention to detail, anticipation of potential problems, and having plans in place to deal with any problems that may arise. Some practical recommendations on the performance of APTs are (Maliva and Missimer 2010)

- On-site barometric pressures, rainfall, and water levels in background monitoring wells located outside of the estimated cone of depression should be recorded during the test to allow for detrending (correcting) the data for nonpumping-induced water level changes. Tide data should also be collected for sites located near the coast. In many areas, local tidal charts are available on line. Barometric pressure data is particularly important for the interpretation of data from unconfined (water table) aquifers.
- A short-duration step-drawdown test (e.g., at least three steps of 1-h duration at progressively increasing rates) should be initially performed to determine the optimal APT pumping rate. The pumping rate during an APT should be as high

a rate as possible to sufficiently stress the aquifer but must be maintainable at a constant rate during the full duration of the test. The short-duration step-drawdown test also fills the pump column and discharge line thus enabling a more rapid stabilization of pumping when the APT is started.

- The pumping rate should not vary by more than 10 % during the test, and preferably by less than 5 %. The pumping system should have a valve to allow for fine-scale adjustments of the flow rate. Frequent measurements of the pumping rate should be made and corresponding adjustments made to prevent trends of increasing or decreasing water levels over the course of the test. A short-duration excursion from the target pumping rate, or even the pump shutting off, is usually not a fatal problem in a long-term test if the problem is quickly corrected. Unidirectional drift in the pumping rate over the course of a test will complicate interpretation of the data.

- The pumping rate should be set below the maximum capacity of the pump to allow for upwards adjustments. Pumping rates may decrease over time due to aquifer (and thus well) drawdown. The performance of the pump may also fluctuate in response to daily fluctuations in ambient temperature. Upward adjustments are not possible if the pump is operating at its maximum rate at the start of the test. The type of pump to be used for an APT is an issue because centrifugal pumps have less flexibility than extended-shaft turbine and submersible pumps when significant drawdowns in the production well are anticipated.

- The exact time that the pump was turned on should coincide with the start ($t = 0$) of the data collection device. Ideally, all down-hole pressure transducer/data loggers should be programed using the same device to ensure synchronous data collection. In practice, it is difficult to get an instantaneous start of the pump and data collection. It is recommended that the data loggers be started a short time (5–15 s) before the start of pumping. The collected data could then be corrected in a spreadsheet by setting $t = 0$ at one (or one-half) time reading before the first drawdown response is evident in the data from the pumped well. It is more difficult to correct for a situation where the data collection started after the pump was turned on and some data were not recorded.

- Salinity measurements should be collected frequently (every 2–8 h) during APT tests on brackish-water aquifers or aquifer locations near the interface between fresh and saline waters. The measurements can be performed in the field using a conductivity meter or field chloride titration kit, or samples can be collected for laboratory analyses (or both).

- Recovery data should always be collected. Recovery data are often superior because they are much less impacted by fluctuations in pumping rate during startup and it is easier to obtain a near instantaneous shutdown of a pump.

- Water produced during an APT should be conveyed far enough away from the pumped and observation wells so as to not cause interference.

7.2   Aquifer Performance Test Interpretation

Aquifer performance test data are usually interpreted using analytical equations. Elementary interpretation of APT data is covered in virtually all introductory groundwater textbooks. Most notable specialized publications are Lohman (1972), Kruseman and de Ridder (1991), Walton (1997), and Kasenow (1997, 2006). A number of software packages are available for the interpretation of pumping test data including the commercial packages Aquifer Test Pro^{TM} and AQTESOLV^{TM}, and the U.S. Geological Survey AQTESSS series of spreadsheet programs (Halford and Kuniansky 2002). Excel-based programs for basic aquifer test analyses are available as freeware. Although aquifer test software facilitate the processing of APT test data, it is critical to understand each analytical method and the underlying assumptions. With respect to the use of computer codes for APT test interpretation (Kruseman and de Ridder 1991) cautioned that

> many of the codes are based on 'black box' methods which do not allow the quality of the field data to be checked. Interpreting a pumping test is not a matter of feeding a set of field data into a computer, tapping a few keys, and expecting the truth to appear.

7.2.1   Correction for Extraneous Impacts on Aquifer Water Levels (Detrending)

The raw hydraulic data from APTs are water level- (or pressure-) versus-time data from the pumped and observation wells. Water level and pressure data are then converted into pumping-induced changes, which are referred to as drawdown or recovery. It is necessary to correct the drawdown and recovery data for changes in water levels that were caused by activities or processes other than groundwater pumping performed as part of the APT. The externally caused changes in water levels may be either unidirectional, rhythmic fluctuations, or non-rhythmic fluctuations (Kruseman and de Ridder 1991). The externally caused changes in water levels include (but are not limited to) regional changes in water levels, barometric pressure changes, marine tidal cycles, earth tides, external (not test-related) groundwater pumping, recharge, loading, and rainfall. The external water level changes must be corrected for, or detrended from, the water-level data recorded during an APT in order to accurately interpret the impacts of pumping on the aquifer being assessed.

Failure to correct for external factors can result in grossly inaccurate interpretations. For example, the author was an expert witness in a lawsuit in which the opposing party misinterpreted the normal recession of the water table after a rainfall event from pumping-induced drawdown during an APT. All of the decline in the water table from the moment pumping of the underlying confined aquifer commenced was attributed to inter-aquifer leakage, even though it was obvious from

examination of the full dataset that the rate of decline of the water table was approximately the same before and after the start of pumping. Rather than pumping during the APT being responsible for a one foot (0.3 m) decline in water table elevation, in reality, there was essentially no impact from pumping. The incorrect interpretation of the response of the water table to pumping of the underlying aquifer was used to calibrate a groundwater model, which as a result, had no validity.

The effort involved in detrending is dependent upon the magnitude of extraneous impacts, which is in part a function of test length. For many tests of relatively short duration (≤ 8 h), extraneous effects may be insignificant, particularly in confined aquifers that are not located near coastal areas (and are thus not impacted by tides) and either do not have other users near the test site or the external pumping rates have a low variability. The rate of change in background water levels is often slow. During short-duration tests, not enough time may elapse for the external factors to materially impact the test data.

Some detrending is usually required for long-term, multiple-day tests. Data from unconfined aquifers especially requires detrending because measured water levels or well pressures are often significantly impacted by barometric pressure changes, local evapotranspiration, and recharge. If the ambient rate of change in water levels is fairly consistent over the duration of the test, based on data collected from background observation wells, then a simple linear correction factor can be applied to the data using a spreadsheet program. For example, the change in water levels in the background observation well could be added and subtracted (depending on the direction of change) from the water levels in the test observation wells. Software is available for more complex detrending. The USGS "DD estimate" software (Halford 2006) is used to correct for barometric pressure changes, earth tides, regional pumping, and recharge events.

7.2.2   Conceptual or Theoretical Model and Semilog Plots

The choice of a conceptual or theoretical aquifer model is a crucial step in the interpretation of pumping test data. If the wrong model is chosen, then the hydraulic characteristics calculated for the real aquifer will not be correct (Kruseman and de Ridder 1991). Key issues as far as conceptual models are the aquifer system structure and boundary conditions.

Semilogarithmic (semilog) time-drawdown plots, in which time is plotted on the x-axis using a logarithmic scale, are a valuable tool for detecting and characterizing boundary conditions. Interpretations of semilog plots are addressed by Walton (1970), Kruseman and de Ridder (1991) and Driscoll (1986). Time-drawdown data for parts of pumping tests that behave as ideal confined aquifers will plot on a straight line (Fig. 7.2), which corresponds to the Theis curve (Sect. 7.3.2). Departures from the straight line indicate that test conditions have departed from the Theis conditions. For example, a flattening of the time-drawdown curve (deflection
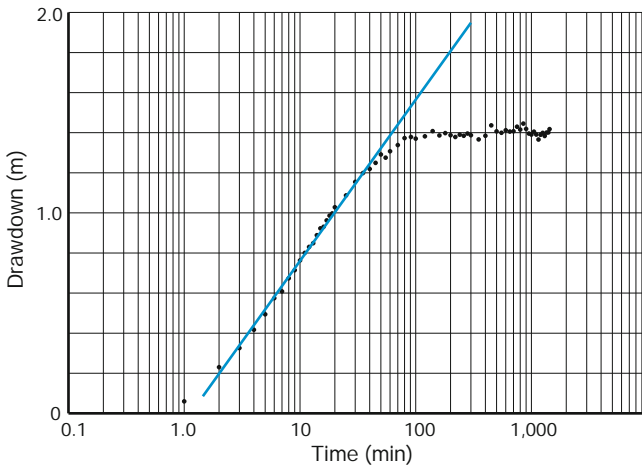
Fig. 7.2 Semilog plot of time-drawdown data from an APT observation well. Leaky aquifer conditions are evident by the sharp deflection of time-drawdown data to the right of the Theis curve (blue line), which plots as a straight-line

to the right), may be evidence that water is being added to the aquifer and, as a result, there is less drawdown at given times during the latter part of the test. Water may be added to the aquifer through leakage through adjoining aquitards (semi-confining units) or recharge (e.g., to an unconfined aquifer from a surface water body or precipitation). If the time-drawdown curve becomes horizontal (i.e., there is no change in water levels over time), groundwater pumping is being balanced by water added to the aquifer from leakage or recharge.

A steepening of the time-drawdown curve (deflection to the left of the Theis curve) may occur when the cone of depression from aquifer pumping reaches a boundary and can no longer expand in one (or more) directions. The presence of boundaries results in greater drawdowns at given times during the test. Time-drawdown curves with two separate linear segments may indicate the occurrence of two separate aquifer conditions. In the case of dual-porosity systems, the early segment reflects production from fractures or conduits, whereas the later segments reflect water production from the rock matrix. For unconfined aquifers, three curve segments reflect the delayed-yield phenomenon. The early segment reflects production of water from depressurization of the aquifer (confined aquifer behavior), whereas the latter segments reflects production of water from drainage.

Deviations of the early test data from the straight line may reflect a start-time error. The recorded time at the start of the test ($t = 0$) may not correspond to the exact start of pumping. A deviation to the right may be due to wellbore storage, in which case the initially produced water is water that is stored inside the well, as opposed to being produced from the aquifer.

The diagnosis of time-drawdown data from pumping tests can be significantly improved by also plotting the derivative of pressure (head) with respect to the

logarithm of time. The use of pressure derivatives to analyze oilfield testing data was presented by Bourdet et al. (1983, 1989) and has become a standard technique. Spane and Wusrtner (1993) and Renard et al. (2009) discussed the applications of the pressure derivatives to hydrogeological investigations and provided examples of log–log and semilog plot types that are diagnostic of conditions that might be encountered in groundwater investigations. The use of pressure derivatives is still uncommon in groundwater investigations. The method can potentially be a great value especially for interpreting data from tests conducted in complex hydrogeological settings in which the time-drawdown data indicate that the commonly used conceptual models may not apply.

7.2.3 Early Test Data

The first few minutes of the test should be given the least weight in the analysis of pumping test data. Several small errors can significantly impact the early data, which can have large impacts on analyses of the data when plotted on a logarithmic time scale (Maliva and Missimer 2010). The test start time ($t = 0$) for the pumping phase of an APT should be the moment that the pump was turned on to the constant rate to be used for the test and the aquifer potentiometric surface begins to react with a reduction in pressure. In practice, the pump start time often does not exactly coincide with the $t = 0$ time in the recorded data. A short time lag in the aquifer response may occur because of wellbore (casing) storage. A time lag may occur between the pressure decline in an aquifer due to pumping and the release of stored water. Instability in the pump discharge during start up is another source of pressure fluctuations. An additional factor that may impact time-drawdown data in a pumped well is head losses from formation damage, turbulent flow, and friction in the casing, well screen, and filter pack. The wellbore effects can result in a very rapid drawdown in the pumped well at the start of pumping.

The early test errors can have a large impact on how the data plots when a logarithmic time scale is used, which is the case for most analytic methods. A small time (e.g., 10 or 20 s) error makes a large difference on where the data for the first minute of a test plots on a logarithmic time-drawdown graph. After 2–3 min, the 10 or 20 s error becomes essentially imperceptible on a logarithmic scale and, therefore, does not impact calculated values of aquifer hydraulic parameters.

With regards to tests performed on unconfined aquifers, it is important to differentiate between time errors and wellbore effects in the early data and the delayed-yield phenomenon. In the case of delayed yield, the early data may give an accurate estimate of aquifer transmissivity, but a much too low estimate of specific yield (storativity). Late test data, on the contrary, are needed to accurately estimate specific yield. A good practice is to analyze data using both semilog and log–log time-drawdown plots, in order to identify data that plot on and off the Theis curve, and possible reasons for any departures from the Theis curve.

7.3   Analytical Methods

A variety of analytical methods have been developed to interpret aquifer pumping test data under different aquifer conditions. Some of the more basic and widely used methods are reviewed herein. A key issue is that all of the analytical methods have underlying assumptions. Departures from the assumed conditions can impact estimated values for aquifer hydraulic parameters. Actual aquifer conditions invariably depart from the assumed ideal conditions. Nevertheless, the analytical methods can still give useful estimates as their accuracy is often still satisfactory in the context of the uses of the data.

It is important to keep in mind that analytical methods do not provide unique result. Multiple sets of conditions can produce a given drawdown-versus-time plot. That an analytical or numerical method provides a good match to the field data is not proof that the interpretation is necessarily correct. Hence, it is important to start the aquifer pumping test interpretation process with a sound conceptual model of the hydrogeological system under consideration.

The two basic equations for interpreting pumping test data from confined aquifers are the Thiem method for state-steady flow and the Theis non-equilibrium equation for unsteady-state flow. Both methods are based on the assumptions that

- discharge from the pumping well(s) is constant
- the pumped well fully penetrates and receives water from the entire thickness of the aquifer
- flow into the well is radial, horizontal, and laminar
- the aquifer is homogenous and isotropic
- the aquifer is not leaky; there is no leakage of water into the aquifer from underlying and overlying strata
- the aquifer thickness is uniform
- the aquifer is confined and remains saturated throughout the entire test
- the aquifer is of infinite areal extent
- potentiometric surface is flat.

In addition for unsteady-state flow

- the radius of the well is very small and casing storage in negligible
- there is instantaneous removal of water from storage with a decline in head
- the coefficient of storage is constant.

Numerous variations of the Thiem and Theis methods were subsequently developed to address conditions that depart from the above assumptions, particularly leaky and unconfined aquifers. Several of the more commonly used modifications of the Thiem and Theis equations are discussed below.

7.3.1   Thiem Method

The Thiem (1906) method applies to steady-state flow conditions under which, by
definition, aquifer heads do not change over time. Inasmuch are heads are
unchanged, no water is being produced from storage. True steady-state conditions
are not possible in a confined aquifer. However, the Thiem method can be applied
to quasi-steady state conditions in which the hydraulic gradient does not change
over time, although the cone of depression is still growing (Kruseman and de
Ridder 1991). The Thiem method relates discharge to transmissivity and drawdown
in two piezometers

$$Q = 2p\, T\, \frac{(s_{m1} - s_{m2})}{\ln\left(\frac{r_2}{r_1}\right)} \tag{7:1}$$

where

T	transmissivity (m^2/d)
Q	discharge (m^3/d)
r_1, r_2	distances of piezometers '1' and '2' from the pumped well (m)
s_{m1}, s_{m2}	steady-state drawdown in piezometers '1' and '2' from the pumped well (m).

7.3.2   Theis Non-equilibrium Equation

The non-equilibrium equation developed by Theis (1935), a University of
Cincinnati geologist, revolutionized hydrogeology by enabling the connection
between well hydraulics and aquifer parameters to be understood. The most com-
mon methods used for the interpretation of APT test data are based on the Theis
(1935) non-equilibrium equation, where

$$s = \frac{Q}{4pT} \int_{u}^{\infty} \frac{e^{-1}\, du}{u} \tag{7:2}$$

where

$$u = \frac{r^2 S}{4Tt} \tag{7:3}$$

s	drawdown (m)
Q	pumping/discharge rate (m^3/d)
T	transmissivity (m^2/d)

u, du   empirically derived functions
r   distance from observation well (m)
t   time since pumping/discharge began (m)
S   storage coefficient (unitless)

The Theis equation can be rewritten as

$$s = \frac{Q}{4pT} W(u) \qquad (7:4)$$

where the integral $W(u)$ is referred to as the 'well function' or 'Theis well function'. Values of $W(u)$ versus $1/u$ are provided in most hydrogeology textbooks. The logarithmic plot of $W(u)$ versus $1/u$ is referred to as the Theis curve (Fig. 7.3a).

The Theis method for the interpretation of aquifer test data, which is also referred to as the 'log-log' or 'curve-matching' method, involves plotting a set of time-drawdown data for an APT on a square, logarithmic grid of the same grid size as a plot of $W(u)$ versus $1/u$. The graphs are shifted until the time-drawdown data are superimposed on the Theis curve with the axes of the two graphs parallel (Fig. 7.3b). A match point is selected, at which a set of values of s, t, $W(u)$, and u are obtained. To simplify the calculations, a match point of $W(u) = 1$, and $1/u = 1$ is commonly used and the s and t values are recorded for that match. Using the known values of Q and r and the match point values, the transmissivity and storage coefficient of the aquifer are calculated.

7.3.3 Cooper–Jacob Modification of the Theis Equation

The Cooper and Jacob (1946) modification of the Theis non-equilibrium equation, also known as the 'straight-line' method, is perhaps the most widely used method to analyze pumping test data because of its simplicity. A semilogarithmic plot of drawdown-versus-time is prepared, with drawdown on the linear scale. Data that meet the conditions of the Theis curve (i.e., fall on the Theis curve in a logarithmic plot) will plot on a straight-line (Fig. 7.4). Transmissivity and storativity are estimated from the slope of the line (Ds, change in drawdown over 1 log cycle) as follows:

$$T = \frac{2:3Q}{4pDs} \qquad (7:5)$$

$$S = \frac{2:25Tt_o}{r^2} \qquad (7:6)$$

where t_o = time at drawdown $s = 0$. The units of the parameters must be consistent (e.g., $T = m^2/d$, $Q = m^3/d$, $t = d$, $r = m$). The Cooper–Jacob method has all the assumptions of the Theis method, in addition to the requirement that the value of l be very small (less than about 0.05 or 0.01). The Cooper and Jacob method was
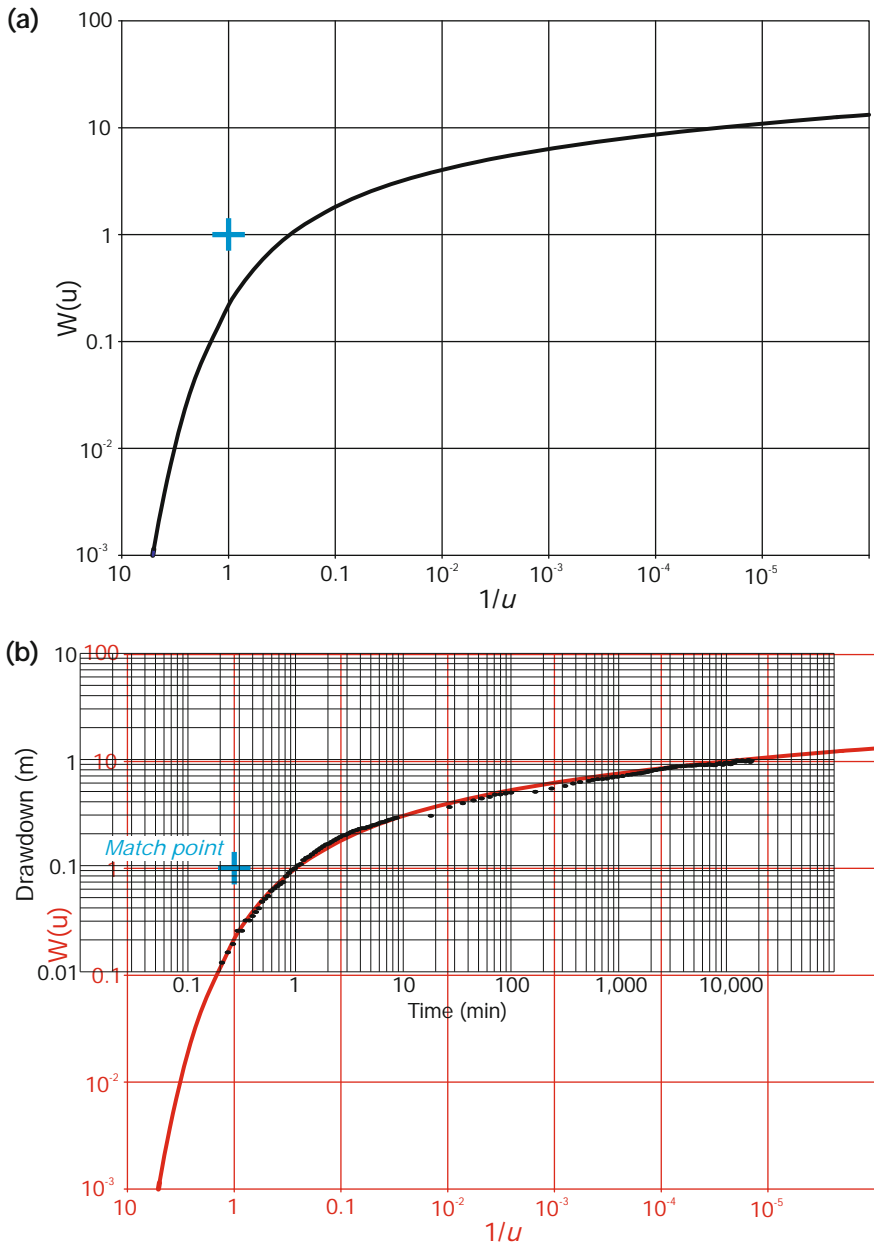
Fig. 7.3 a Theis curve. b Application of Theis method to observation well data from an APT in Lakeland Florida. The match points are $W(u) = 1$, $1/u = 1$, $s = 0.09$ m and $t = 0.27$ min, and calculated transmissivity is 13,700 m^2/d for a pumping rate of 16,400 m^3/d
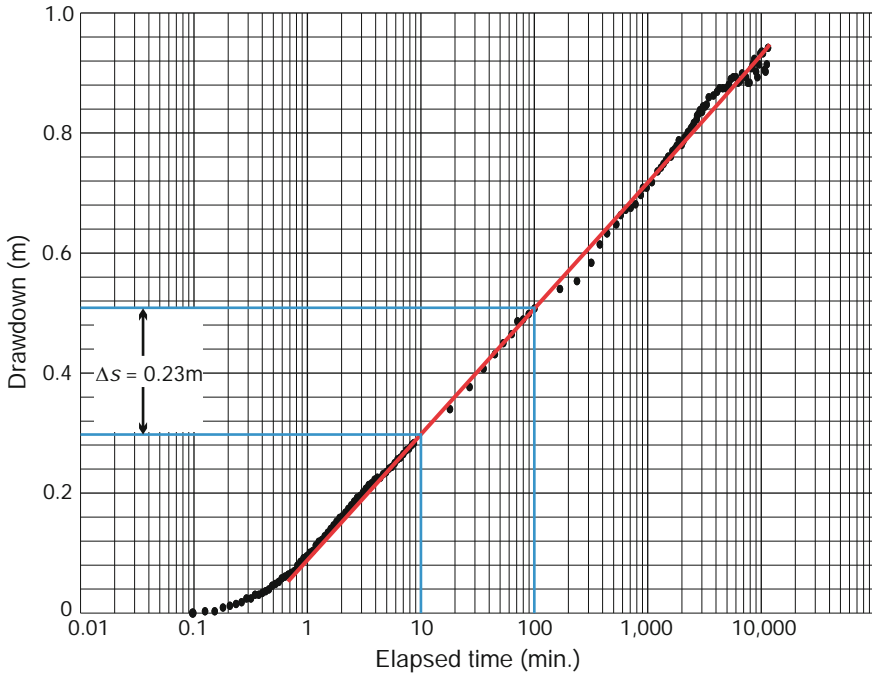
Fig. 7.4   Application of the Cooper and Jacob (straight-line) method to the Fig. 7.3 APT dataset. The Δs value of 0.23 m gives a calculated transmissivity of 13,100 m²/d

designed for confined aquifers but can be used with caution for unconfined aquifers (Walton 1962).

The Cooper and Jacob method is arguably the most often incorrectly applied aquifer test interpretation method because of the use of the wrong straight-line segment. The Cooper and Jacob method, as a simplification of the Theis non-equilibrium equation, is valid only for data that plot on the Theis curve on log-log plots (i.e., data that meet the assumptions of the Theis equation). Late data from pumping tests may plot on a straight-line (not uncommonly with a better fit than early data) but plot off the Theis curve and, therefore, should not be used with the Cooper and Jacob method. The late data may reflect recharge, leakage, aquifer boundaries, delayed yield, or aquifer heterogeneities.

For example, log–log and semilog log plots of data from a single-well pumping test are presented in Fig. 7.5. Both the very early and late data do not plot on the Theis curve and should, therefore, not be used with the Cooper and Jacob method. Where there is a question as to which straight line from a data set is appropriate for calculating hydraulic parameters, then Theis curve-matching analysis should be performed. The irony is that the Cooper and Jacob method was developed prior to the availability of personal computers as an alternative to more time-consuming curve-matching methods, but yet curve-matching may be needed to properly use the
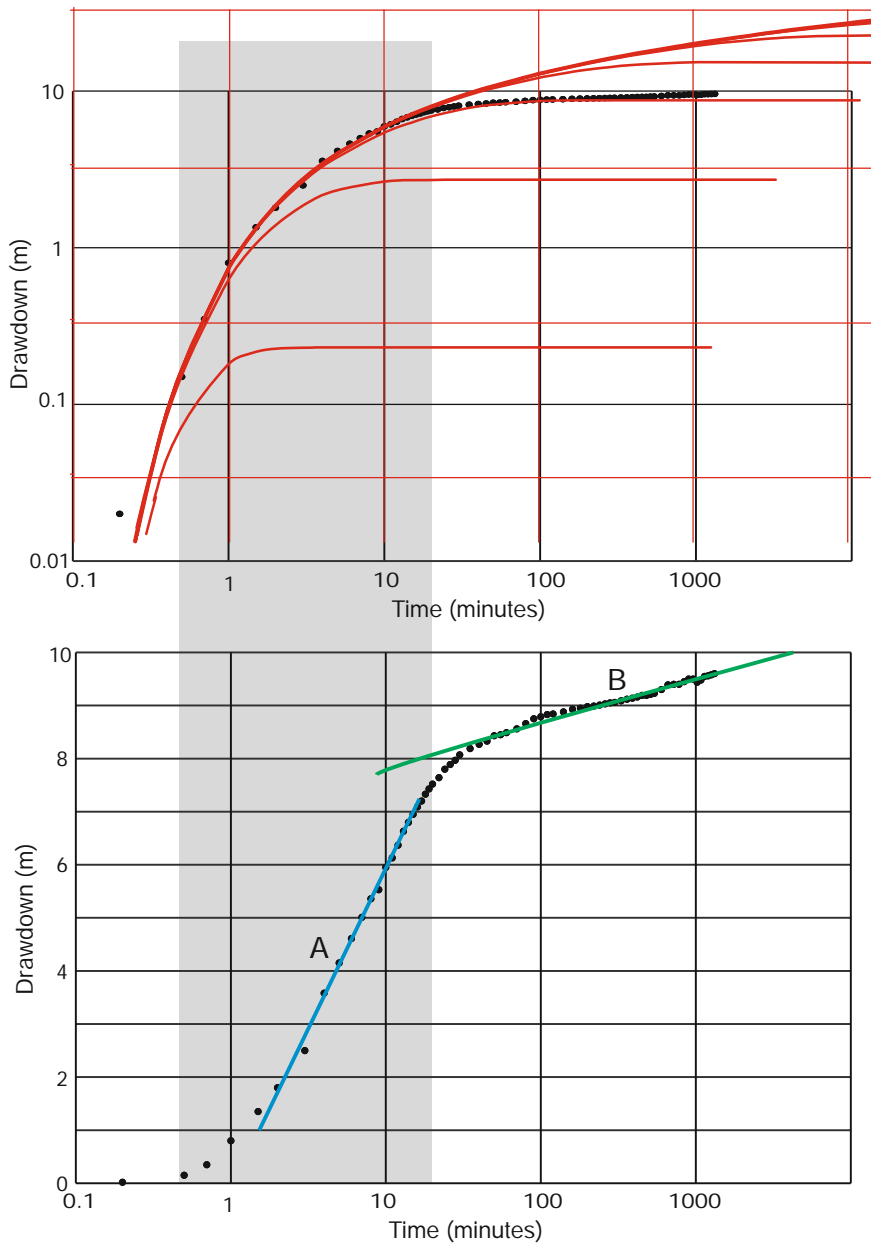
Fig. 7.5 APT data plotted for Hantush–Walton and Cooper and Jacob methods with the same logarithmic time scale. Only data from the time period in which data plot on the Theis curve should be used in the Cooper and Jacob method (curve A). Late data also plot on a straight line (B) but do not plot on the Theis curve and cannot be properly interpreted using the Cooper and Jacob method

Cooper and Jacob method. Pressure derivative plots may also be used to identify data influenced by boundaries and other non-deal conditions (Sect. 7.2.2).

7.3.4   Cooper and Jacob Distance-Drawdown Method

The Cooper and Jacob (1946) distance-drawdown method is used to estimate aquifer hydraulic properties from multiple-well APTs. The raw data are single drawdown measurement from each observation well that were recorded at the same time. The selected measurement time should be late enough into the test so that drawdown is detected in all wells, but not so late that the data no longer plot on the Theis curve. A semilogarithmic distance-drawdown plot in generated with distance on the logarithmic scale and a linear regression line drawn (Fig. 7.6). Transmissivity is calculated from the difference in drawdown over one log cycle of distance (Δs)

$$T = 2.303Q = 2\pi Ds \qquad (7.7)$$

$$S = 2.25Tt = r_0^2 \qquad (7.8)$$

where $r_0 =$ is the projected distance at a drawdown of zero. The theoretical drawdown at the pumped well (i.e., the drawdown that would occur in a 100 % efficient well) is determined by extrapolating the regression line to the radius of the well.

7.3.5   Cooper and Jacob Modification of the Theis Equation for Recovery Phase

Transmissivity is estimated from the recovery data in a similar manner to the Cooper–Jacob method with the exception that residual drawdown (s') is plotted

Fig. 7.6 Cooper and Jacob distance-drawn plot. Extrapolation of the regression line (red) to the well radius gives the drawdown in a 100 % efficient well. Transmissivity and storativity are calculated from the Δs and r_0 values
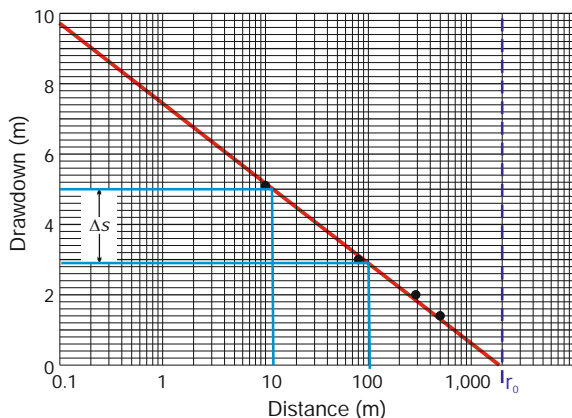
against equivalent time (t/t′), rather than drawdown-versus-time (Theis 1935). Transmissivity is calculated as follows

$$T = \frac{2.3Q}{4 \pi D s'}$$

(7.9)

where Ds' is the change in residual drawdown over one log cycle of equivalent time.

Residual drawdown is defined as the difference between observed water levels at time "t" after the pump was turned off and the static water level from before the start of pumping. Equivalent time (t/t′) is defined as the time since the aquifer test began (t) divided by the time since the pump was turned off (t′).

7.3.6   De Glee's Method—Steady-State Pumping of a Leaky Confined Aquifer

De Glee's method is the steady-state leaky aquifer equivalent to Thiem's method (Kruseman and de Ridder 1991). Leakage is considered to occur across a single aquitard.

$$s_m = \frac{Q}{2 \pi T} K_0 \left(\frac{r}{B} \right)$$

(7.10)

where

s_m steady-state drawdown in a piezometer distance "r" from the pumped well
$K_0(r/B)$ is a modified Bessel function that is determined through a curve-matching procedure
B   leakance factor (m)

$$B = \sqrt{KD \left(\frac{D'}{K'} \right)}$$

(7.11)

where
D′   saturated thickness of the aquitard (m)
K′   vertical hydraulic conductivity of the aquitard (m/d)

The curve-matching procedure involves a logarithmic type-curve of $K_0(x)$ versus X, where $X = r/B$, and a logarithmic plot of steady-state drawdown in each of piezometers (s_m) versus r.

7.3.7   Hantush–Walton Method

Hantush–Jacob (1955) and Walton (1960, 1962) modified the Theis non-equilibrium equation to provide a solution for leaky confined aquifers with no storage in the confining layers. The Hantush–Walton solution consists of a series of type-curves that branch off the Theis curve (Fig. 7.7). The Hantush–Walton method is a curve-matching procedure similar to the Theis method and involves the same equations. For a leaky aquifer, the curve-match will result in some of the later data plotting below the Theis curve, on one of the (r/B) curves. The leakance (L, 1/d) of the confining units is calculated as follows:

$$L = \frac{\left(\frac{r}{B}\right)^2}{r^2} T \qquad (7.12)$$

In order to calculate a leakance value, the APT must have a long enough duration so that the time-drawdown departs from the Theis curve and the (r/B) value can be determined. The late test data used to determine leakance values are most likely to be affected by extraneous influences on aquifer head (pressure) and thus need to be corrected (detrended). The calculated leakance values are non-directional, reflecting leakage from both the strata that overlie and underlie the pumped aquifer. Most of the leakage and, thus, the greatest part of leakance value, will be from the most conductive confining unit.

7.3.8   Boulton and Neuman Methods for Unconfined Aquifers

Unconfined aquifers differ from confined aquifers in that water is produced by the dewatering of the aquifer rather than only by expansion of water and compression of the aquifer. Analysis of APT data from unconfined aquifers requires a different methodology than is used for the analysis of a confined aquifer. Boulton (1954a, b, 1963) was the first to introduce the "delayed yield response" to unconfined aquifer test analysis. The major limitation of the Boulton method is that it requires the definition of an empirical constant, "Boulton's delay index", which is not related to any physical phenomenon (Kruseman and de Ridder 1991).

  Time-drawdown plots from unconfined aquifers typically have an "s" shape consisting of three segments (if the test is conducted for an adequate length of time) which are

- A steep early segment that covers a short time frame, commonly only several minutes in duration. The unconfined aquifer behaves in the same manner as a confined aquifer. Water is produced by expansion of water and compression of the aquifer. The early segment data follows the Theis curve.

(a)

(b)
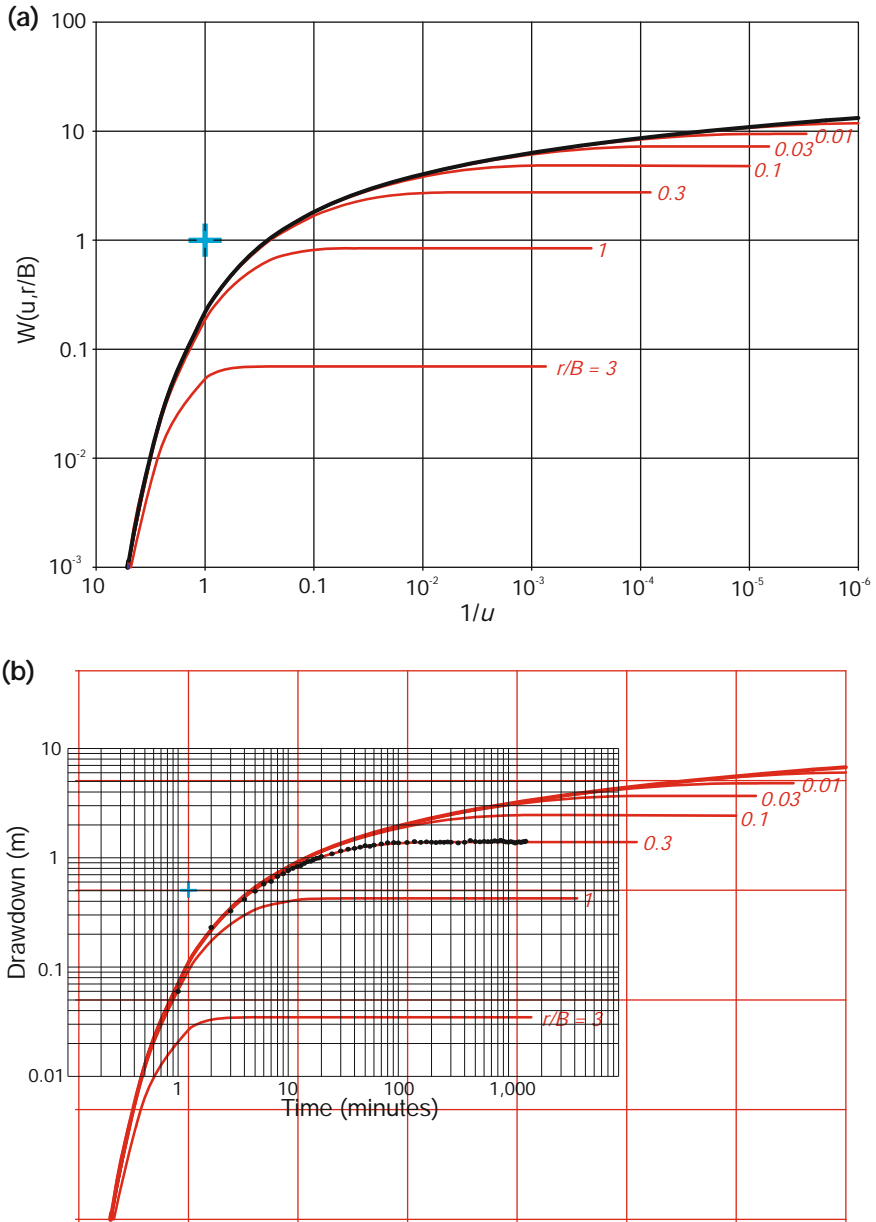
Fig. 7.7 a Hantush–Walton type curve. b Hantush–Walton curve match for pumping test data from Belle Glade, Florida

- A flat intermediate segment that is caused by gravity drainage into the pumped interval of the aquifer. This segment is similar to that found in leaky aquifers. This "delayed yield" segment can begin from a few minutes to over an hour after the test begins and last for periods up to weeks after pumping initiation.
- A relatively steep late segment that shows that the delayed-yield time period is over and an equilibrium has been reached between the rate of the decline of the water table and the rate of gravity drainage. The late segment data plots once more on the Theis curve.

An estimate of the aquifer transmissivity can be obtained using the early data. However, storativity values obtained from the early data will be too low since they are related to elastic storage. The storativity values obtained from the later segment (after the delayed yield has dissipated) are representative of the specific yield of the aquifer. The Neuman (1972) drawdown equations tend to provide reasonably accurate estimates for hydraulic conductivity and specific yield. The method has the same basic assumptions as the methods used for confined aquifers. The uniform aquifer thickness condition may not be met if the drawdown is large relative to the saturated thickness of the aquifer.

The Neuman method involves curve matching (Fig. 7.8) of both the early and late time-drawdown data in a similar manner as the Hantush–Walton method to obtain values of u_A, u_B, $W(u_A, b)$, and $W(u_B, b, b)$. The early-time data are interpreted using the equations (Neuman 1975)

$$s = \frac{Q}{4pK_h} W(u_A; b) \qquad (7{:}13)$$
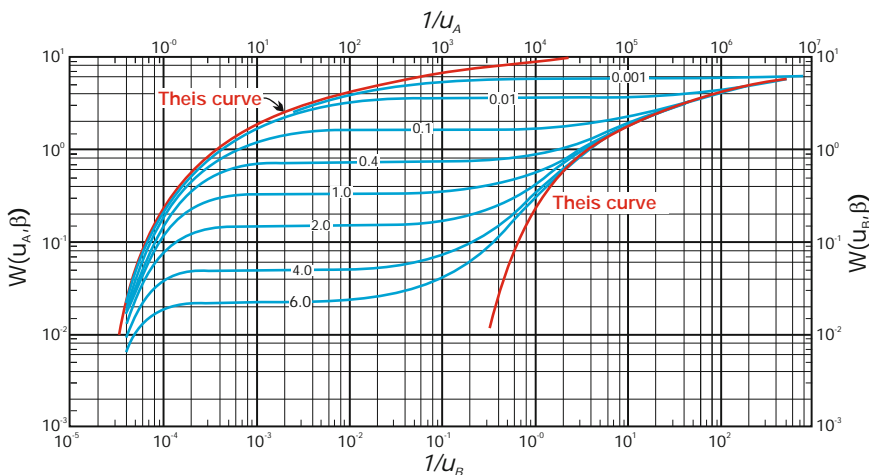
Fig. 7.8 Neuman (1975) delayed-yield type curves, which consists of early and late Theis curves (red) and a series of b curves (blue)

$$u_A = \frac{r^2 S_A}{4 K_h D t} \qquad (7{:}14)$$

where,

K_h horizontal hydraulic conductivity (m/d)
D original saturated aquifer thickness (m)
b Neuman's parameter
Q well discharge (m^3/d)
t time (at match point, d)
s drawdown (at match point, m)
r distance of well from pumped well (m)
S_A volume of water released from storage per unit surface area per unit decline of the water table (early-time storativity; dimensionless)

The late time (third segment) data are interpreted using similar equations

$$s = \frac{Q}{4 p K_h} W(u_B; b) \qquad (7{:}15)$$

$$u_B = \frac{r^2 S_Y}{4 K_h b t} \qquad (7{:}16)$$

$$b = \frac{r^2 K_v}{b^2 K_h} \qquad (7{:}17)$$

where,
Q well discharge (m^3/d)
b Neuman's parameter
S_Y volume of water release from storage per unit surface area per unit decline of the water table (specific yield)
K_v hydraulic conductivity for vertical flow
K_h hydraulic conductivity for horizontal flow

The methodology involves the following steps (Kruseman and de Ridder 1991):

(1)   Construct a family of type log-log curves of $W(u_A, u_B, b)$ versus $1/u_A$ and $1/u_B$ for a series of values of b.
(2)   Construct a log–log plot of drawdown (s) versus time (t) for the test data on the same scale as the type curves.
(3)   Match the early test data with one of the type 'A' curves and record the b value. Note the values of s, t, $1/u_A$ and $W(u_A, b)$ for an arbitrary point (commonly $1/u_A = 1$ and $W(u_A, b) = 1$).
(4)   Calculate values of $K_h b$ and S_A.

(5) Match the late test data with a type 'B' curve with the same b value as the selected type 'A' curve.
(6) Note the values of s, t, $1/u_B$, and $W(u_B, b)$ for an arbitrary point (commonly $1/u_B = 1$, and $W(u_B, b) = 1$).
(7) Calculate values of $K_h b$ and S_y using Eq. 7.16.
(8) Calculate value of kv from Eq 7.17.

7.3.9   Partially Penetrating Wells

A commonly encountered situation in pumping tests is that wells only partially penetrate the tested aquifer. Existing wells that were not constructed as part of the aquifer characterization program are sometimes used for pumping tests because of cost savings relative to constructing new fully penetrating wells. Production wells in thick aquifers or aquifers in which salinity increases with depth may be completed only in the upper freshwater-bearing part of the aquifer. Groundwater flow to a partially penetrating well has a vertical component, which violates the assumption of only horizontal flow to a well. Vertical hydraulic conductivity is typically less than horizontal hydraulic conductivity. The lower vertical hydraulic conductivity and longer flow paths results in a greater resistance to flow and thus greater head losses.

The effects of partial penetration on measured drawdowns is a function of the distance from the pumped well, the saturated thickness of the aquifer, the degree of penetration, and the anisotropy ratio of the aquifer (Walton 1962). Partial penetration effects become negligible at a distance of about two times the saturated thickness of the aquifer, depending upon the amount of penetration (Kruseman and de Ridder 1991). In the case of a heterogeneous aquifer in which the well is completed in the main flow zone, partial penetration effects may also be negligible. Todd (1980) noted that any well that is screened (or completed with an open hole) through 85 % or more of the aquifer's thickness may be considered to be a fully penetrating well.

Kruseman and de Ridder (1991) summarize the analytical methods for partially penetrating wells. Notable are the Hantush (1961a, b) methods for partially penetrating wells in confined aquifers, which are variations of the Theis and Hantush–Walton curve-matching methods. Kruseman and de Ridder (1991) provide step-by-step examples of the application of the Hantush (1961a, b) methods.

Aquifer tests completed in partially penetrating aquifers can also be interpreted using inverse numerical modeling techniques. The tested aquifer could be represented in the simulations by multiple zones in which one or more zones are pumped. This is essentially calibrating a model to a pumping test. Inverse modeling has the general limitation of non-uniqueness. Estimates of hydraulic parameter values may be constrained using values from analytical solutions.

7.3.10   Anisotropic Aquifers

The commonly used methods for interpreting pumping test data are based on the assumption of an isotropic aquifer. However, fractured-rock and karstic aquifers may have pronounced anisotropies. Perhaps the simplest method for estimating the degree and direction of anisotropy for two-dimensional flow is the Hantush and Thomas (1966) method. The drawdown contours of anisotropic aquifers tend to be elliptical rather than circular. The major and minor axes of anisotropy of the drawdown ellipse (a and b, respectively) are related to the corresponding principal transmissivities of the aquifer (T_x and T_y), by

$$\frac{T_x}{T_y} = \left(\frac{a}{b}\right)^2 \tag{7:18}$$

The orientation of the major axis of transmissivity (T_x) can be graphically estimated from the orientation of the drawdown ellipse. The Hantush and Thomas (1966) method is based on rays of observation wells radiating outwards from the pumped well. An effective transmissivity value 'T_e' is taken as the average value calculated for the well rays, which can be obtained using the distance-drawdown method. Transmissivity values in the principal direction are calculated using the relationship

$$\frac{a}{b} = \frac{T_e}{T_y} = \frac{T_x}{T_e} \tag{7:19}$$

The transmissivity in the direction of flow 'r' (T_r) is calculated as

$$T_r = \left(\frac{r^2}{ab}\right)T_e \tag{7:20}$$

and

$$T_r = T_x\left[\cos^2 h + \left(\frac{T_x}{T_y}\right)\sin^2 h\right] \tag{7:21}$$

where h is the angle between r and the x-axis, where the coordinate axes x and y are parallel to the principal direction of anisotropy.

Papadopoulos (1965) developed a method for analysis of pumping test data in anisotropic aquifers that is based on non-steady-state continuous pumping from a homogenous aquifer of infinite extent. A characteristic feature of anisotropic aquifers is that the velocity vector and hydraulic gradient vector are generally not parallel. The drawdown is in the form of an ellipse in which the short (minor) axis is in the direction of maximum transmissivity and the long (major) axis is along the minimum transmissivity axis. A minimum of three observation wells at different directions and distances from the pumping well are necessary. The Papadopoulos

(1965) method is a modification of the curve-matching and straight-line methods in which the time-drawdown data and orthogonal distances from the pumped wells are used to calculate the values of the principal (maximum and minimum) transmissivities and orientation of the direction of maximum transmissivity.

The Hantush (1966) method for analysis of pumping tests in leaky anisotropic aquifers requires data from three groups of observation wells located on radial lines. The data for each radial row of wells is interpreted using standard leaky isotropic aquifer methods. The values for a, b, and h, are calculated from the transmissivity, diffusivity (T/S) and "B" values from the three rows of well, where B is square root of transmissivity divided by leakance,

$$B = \sqrt{T = (k' = b')} \tag{7:22}$$

and k′ and b′ are the hydraulic conductivity and thickness of the semiconfining unit.

Motz (2009) evaluated the anisotropic properties at an Upper Floridan Aquifer wellfield in West-Central Florida, using data from a multiple-well pumping test. The data were evaluated using both the graphical estimation method (Hantush and Thomas 1966) and a weighted least squares-based type-curve analysis (Maslia and Randolph 1987). The results of the weighted least squares procedure are consistent with the results of the earlier studies at the wellfield. The ratio of anisotropy from the weighted least squares procedure was 3.26 compared to an average ratio of 1.63 from the graphic method. The estimated orientation of the major axes of transmissivity is similar.

A common denominator of analytical methods for evaluating aquifer anisotropy is that they are data intensive, requiring a considerable number of monitoring wells with a specified radial pattern. Such observation well data are commonly not available or are too expensive to install for the purpose of evaluating anisotropy. Where drawdown data from a more limited number of wells suggest aquifer anisotropy (e.g., based on an elliptical shape of iso-drawdown contours), then inverse numerical modeling techniques (Sect. 7.4) may be a practical data analysis technique. The model grid would be rotated to parallel the axes of the drawdown contour ellipse.

7.3.11   Dual-Porosity System

Dual-porosity systems contain two porosity domains: a matrix domain that constitutes the bulk of the rock and porosity, but has a relatively low permeability, and a secondary porosity domain that has a low porosity, but most of the permeability of the rock. Secondary porosity includes fractures and solution conduits. The situation becomes even more complex when there are more than two porosity domains such as the case where there is matrix, fracture, and conduit porosity. Time-drawdown data from pumping tests performed in fractured rock cannot necessarily be properly analyzed using methods based on homogeneous single-porosity conditions. Models appropriate for homogenous aquifers may be appropriate where fractures are
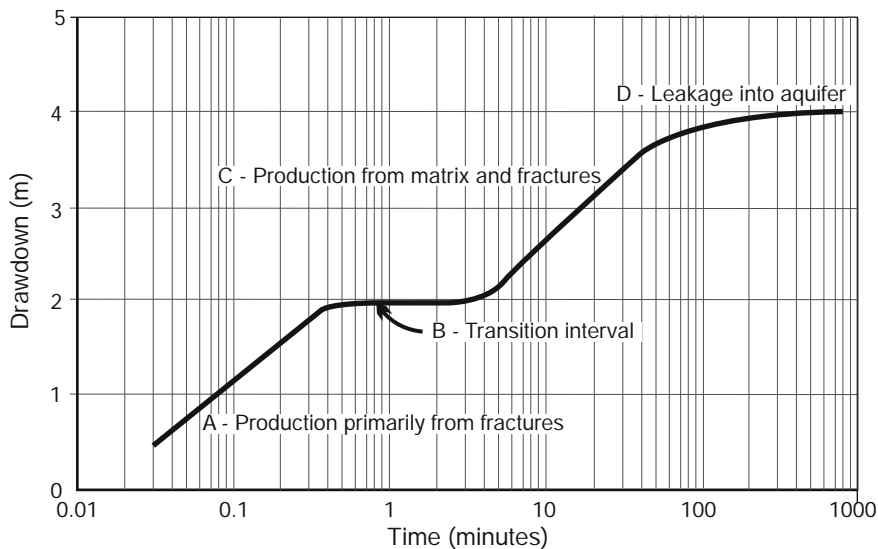
Fig. 7.9 Hypothetical time-drawdown plot for an observation well from a pumping test in a dual-porosity aquifer. The early data (a) reflects production from fractures, which constitutes a small percentage of the total porosity of the aquifer. Following a transitional interval (b), an interval is reached (c) where water is produced simultaneously from the fractures and matrix and the curve approximately matches the Theis curve. The time-drawdown curve may later flatten (d) due to leakage into the aquifer

numerous, well-connected, and evenly distributed throughout the rock and the matrix has a very low permeability (Kruseman and de Ridder 1991).

Methods for analyzing aquifer test data in dual-porosity systems were reviewed by Kruseman and de Ridder (1991). In dual (or multiple) porosity aquifers, groundwater is produced first solely from the fractures, which results in a pressure differential between the fractures and matrix. The pressure differential is equilibrated by the flow of water from the matrix blocks into the fractures. Dual-porosity conditions theoretically yield two parallel lines on a semilogarithmic plot of pressure versus time with an intervening transition zone that corresponds to the onset of interporosity flow (Gringarten 1987; Kruseman and de Ridder 1991; Anderson et al. 2006). Semilog time-drawdown plots may include four segments (Fig. 7.9):

(1) a short-duration, early steep segment, in which drawdown in fractures is occurring faster than water is released from the matrix blocks
(2) a relatively flat transitional segment between the first and third segments
(3) a steeper segment in which the matrix drawdown at each location becomes fully coupled to the fracture network drawdown and approximates the porous drawdown function of Theis (1935)
(4) a leaky or boundary response segment, in which the time-drawdown data departs from the Theis curve.

Gringarten (1987) noted that dual-porosity conditions are more readily observed on log–log plots of pressure change (derivative) versus time. Dual-porosity conditions are identified by an "s-shaped" curve characterized by a minimum on the pressure derivative curve that is indicative of heterogeneous flow conditions.

The early data (first segment) can be interpreted using the Cooper–Jacob straight-line method, in which the storativity is the value for the fractures or conduits (Warren and Root 1963; Kazemi et al. 1969; Kruseman and de Ridder 1991). The flow of fluids and solutes between the fractures and matrix blocks can be impeded by the presence of a fracture skin. A fracture skin was defined by Moench (1984) as a thin layer of impermeable material, deposited on the surfaces of matrix blocks, that serves to impede the free exchange of fluid between the blocks and fractures. Fracture skins are caused by mineral alteration or deposition, which result from the interconnected fissures serving as conduits for the flow of mineral-charged (or geochemically active) water (Moench 1984).

Since transfer between matrix and fractures or conduits is not significant in the early data, fracture skins are not yet an issue. The storativity values interpreted from the second straight-line segment is the sum of the storativity of the fractures and matrix blocks. Once flow between the matrix and fractures becomes significant and fracture skin effects and pressure differentials within matrix block may need to be considered. Transmissivity and storativity may be over-estimated if the wrong segment of the time-drawdown data set is used. Moench (1984) presented an analytical method that allows for simulation of the effects of fracture skins.

7.4   Numerical Aquifer Test Interpretation Techniques

The valid criticism has been raised that the analytical methods that have been traditionally used for the analysis of aquifer performance test data are becoming obsolete because they are based on simplified conceptual models that are not representative of actual aquifer hydrogeology, particularly with respect to heterogeneity (Yeh and Liu 2007; Walton 2008). As is discussed in Sect. 7.3, the various analytical methods have underlying assumptions, which typically involve ideal conditions that are seldom, if ever, completely met in real world pumping tests. Traditional analytical methods for interpreting pumping test data by treating the medium to be homogenous could lead to biased estimates of hydraulic conductivity (Wu et al. 2005; Yeh and Liu 2007). Time-drawdown data, and thus estimated transmissivity and storativity values, are impacted by local heterogeneity near pumping and observation wells.

The recommended alternatives include numerical inversion techniques, such as programs based on the MODFLOW code. For example, a small-scale model of the pumping test vicinity could be developed and the model calibrated to drawdowns observed in observation wells. The model could have multiple layers to simulate inter-aquifer leakage and partial penetration of wells. Suspected aquifer heterogeneity and anisotropy could be incorporated into the model. The calibration could

be performed either manually or using calibration software (e.g., PEST; Doherty and Hunt 2010).

Numerical modeling-based methods have the advantages of flexibility to simulate complex hydrogeological conditions and few underlying assumptions. However, inverse modeling suffers from the nonuniqueness of solutions. The traditional analytical methods still have great utility because they provide rapid solutions (particularly using aquifer test analysis software) and the data collected from many aquifer performance tests, which often only involve one or two observation wells, are inadequate for more complex treatments. Analytical solutions may instead be used to provide initial estimates of hydraulic parameters, which may be judiciously adjusted during groundwater flow model calibration. However, if the values of hydraulic parameters estimated from analytical solutions and model calibration are significantly different, then the cause of the discrepancy needs to be investigated.

7.5 Estimating Transmissivity from Specific Capacity Data

Specific capacity is defined as the pumping rate (Q) divided by drawdown (s). Very often, wells in which existing time-drawdown data from pumping tests are available are sparse. However, specific capacity data may be much more abundant. In the absence of time-drawdown data, transmissivity (T) values can be estimated from specific capacity data.

Theis (1963) presented a method for estimating the specific capacity of wells completed in unconfined aquifers, based on the equation

$$T' = \frac{Q}{s}(K - 264 \log 5S + 264 \log t) \qquad (7.23)$$

where
Q   pumping rate in gpm
s   drawdown (ft)
S   storativity (dimensionless)
t   time since the start of pumping (days)
T′ uncorrected transmissivity (gpd/ft)
K   coefficient that depends of the well radius and filter packer. Theis (963) proposed that a value of $1300 \cdot (1 \pm 0.3)$ is appropriate for small-diameter wells

The method assumes a 100 % efficient, fully penetrating well. For wells that have a significant inefficiency, specific capacity should be corrected (increased) to the value in a 100 % efficient well so as to be representative of the aquifer (not the inefficient well). True transmissivity is calculated using a graph provided by Theis

(1963) of T' versus Q/s for different transmissivity values. Brown (1963) presented a similar method for confined aquifers

$$T' = \frac{Q}{s}(K - 264 \log 5S \times 10^3 + 264 \log t) \qquad (7.24)$$

where K has values of 2,477 and 2,318 for 0.5 ft (15.2 cm) and 1.0 ft (30.5 cm) diameter wells, respectively. Both Eqs. 7.23 and 7.24 require an estimated storativity value.

Transmissivity can be estimated from specific capacity using a modification of the Jacob equation (Theis 1963)

$$T = \frac{Q}{4p\,s} \ln\left(\frac{2.25Tt}{r_w^2 S}\right) \qquad (7.25)$$

Q   pumping rate (m^3/d)
s   drawdown (m)
r_w well radius (m)
T   Transmissivity (m^2/d)
t   time since start of pumping (days)
S   storativity

Equation 7.25 is also valid for English units (feet instead of meters may be used so long as the units are consistent). Equation 7.25 was modified by Bradbury and Rothschild (1985) to include effects of wells losses and partial penetration

$$T = \left(\frac{Q}{s - s_w}\right)\left(\frac{1}{4p}\right)\left[\ln\left(\frac{2.25Tt}{r_w^2 S}\right) + 2S_p\right] \qquad (7.26)$$

where s_w is well losses and Sp is a partial penetration factor, which is a function of the ratio of the length of the open interval to the aquifer thickness.

The ASTM (2005) standard method uses the equation

$$T = \frac{Q}{s}\left(\frac{1}{4p}\right)\left(-0.5772 - \ln\left(\frac{r^2 S}{4T't}\right)\right) \qquad (7.27)$$

where

T' provisional transmissivity (ft^2/d)
Q   pumping rate (ft^3/d)
s   drawdown (ft)
r   well radius (ft)
T   estimated transmissivity (ft^2/d)
t   time since start of pumping (days)
S   storativity (dimensionless)

If the calculated transmissivity is not within 10 % of the provisional transmissivity, then transmissivity is recalculated using the calculated transmissivity as the new provisional transmissivity. ASTM (2005) recommends using a storativity of 0.2 for unconfined aquifers and $b \times 10^{-6}$ for confined aquifers, where b is the aquifer thickness.

Equations 7.25, 7.26, and 7.27 cannot be solved directly for transmissivity, as T is on both sides of the equation. Instead transmissivity is estimated using iterative numerical techniques. Values of T are estimated until the estimated value and calculated value are in acceptable agreement. Bradbury and Rothschild (1985) presented a computer program to perform the calculations and spreadsheets are also available or can be written that perform the calculations. Equations 7.25 through 7.27 require that the storage coefficient be known and have the same assumptions as the Theis non-equilibrium equation such as a non-leaky, homogenous, and isotropic aquifer of infinite areal extent.

An obvious limitation of methods that estimate transmissivity from specific capacity is that drawdown in pumped wells is also a function of well efficiency, which for small-diameter wells pumped at high rates, in particular, may be substantial. Frictional head losses within casings can be estimated using the Hazen–Williams equation (Sect. 6.4.2) and the drawdown values accordingly adjusted. Specific capacity data also need to be corrected for partial penetration and the presence of nearby hydrogeological boundaries.

Transmissivity values obtained from specific capacity value data are based on a smaller volume of investigation than values from multiple-well pumping tests. Bradbury and Rothschild (1985) indicated that they obtained a good agreement between transmissivity values obtained from specific capacity tests and pumping tests. Razack and Huntley (1991) on the contrary, reported that methods based on specific capacity tended to under-predict transmissivity. The under-prediction appears to be due to turbulent well losses (Razack and Huntley 1991). Huntley et al. (1992) reported that analytic solutions tend to overestimate transmissivity in fractured crystalline rocks.

An alternative to the analytic approach is an empirical approach using regression analyses of specific capacity and transmissivity values from pumping tests from the same aquifer (Razack and Huntley 1991; Huntley et al. 1992; Mace 1997). The best fit regression line for a fractured-rock aquifer near San Diego, California is (Huntley et al. 1992)

$$T = 0.29 \left(\frac{Q}{s} \right)^{1.18} \tag{7.28}$$

with T and Q/s in units of ft^2/min.

Mace (1997) evaluated transmissivity and uncorrected specific capacity data from the karstic Edwards Aquifer of central Texas and obtained the relationship

$$T = 0.76\left(\frac{Q}{s}\right)^{1.08} \qquad (7.29)$$

with T and Q/s in units of m^2/d. The 95 % prediction interval of Edwards Aquifer data spans 1.4 log cycles. Huntley et al. (1992) reported that the 90 % prediction interval for the fractured rock data includes about 1.1 log cycle. However, the error needs to be considered in the context of 4 or 5 order of magnitude range in transmissivity. Even though there is a significant error associated with the trans-missivity estimates, the data are still useful (Mace 1997). Mace (1997) reported that the empirical relationship obtained for the Edwards Aquifer may be appropriate for some other karstic aquifers such as the Floridan aquifer system of the southeastern United States.

The simplest method to estimate transmissivity from specific capacity is that of Driscoll (1986) which uses a constant coefficient for confined and unconfined aquifers

$$T = 2000(Q/s)(\text{confined aquifers}) \qquad (7.30)$$

$$T = 1500\,(Q/s)(\text{unconfined aquifers}) \qquad (7.31)$$

where the units for transmissivity, pumping rate, and drawdown, are gallons per day/ft, gallons/min, and feet, respectively.

The metric versions for the above equations are

$$T = 1.385(Q/s)(\text{confined aquifers}) \qquad (7.32)$$

$$T = 1.042(Q/s)(\text{unconfined aquifers}) \qquad (7.33)$$

where the units for transmissivity, pumping rate, and drawdown, are m^2/d, m^3/d, and m, respectively. Specific capacity data should be corrected for well losses to be more representative of the aquifer.

7.6   Tidal Fluctuation Methods

Aquifer hydraulic parameters can be estimated from the response of aquifers to tidal fluctuations in nearby surface water bodies. The tidal responses measured in wells will have a reduced amplitude and a phase shift, which are the basic data used to calculate hydraulic parameters. The tidal efficiency (T_e) at a well is the ratio of the change in water levels in a well to the tidal change in the surface water body. Other factors, such as earth tides, atmospheric pressure changes, and aquifer pumping, can also cause changes in water levels in well. Barometric efficiency (B_e) is the ratio of the change of water level in an open well to the atmospheric pressure change.

The advantages of using tidal data to estimate aquifer hydraulic parameters are

- significantly lower cost than testing that involves pumping and injection
- data can help validate the results of aquifer testing
- large volume of investigation.

The accuracy of analyses of tidally influenced data sets for the estimation of aquifer parameters depends upon being able to resolve the amplitude and phase of the various harmonic components of the data sets. The data need to be detrended to filter out the effects of earth tides, atmospheric pressure changes, and other impacts, using techniques such as regression analysis (Merritt 2004). Although the data acquisition costs are modest, analysis of tidal data may require considerable technical sophistication, especially where the water level data are materially impacted by non-tidal processes.

Various analytical methods have been developed to calculate hydraulic parameters from different aquifer and surface water body configurations. Ferris (1951) presented a methodology for analyzing tidal data in aquifers that subcrop out in the tidal surface water body. The stage-ratio method is based on a semilogarithmic plot of stage-ratio (logarithmic scale) versus the distance of wells from the edge of the surface water body. Stage ratio is the ratio of the amplitude of groundwater change to the corresponding surface water change. The time-lag method is based on the slope of a regression of time lag versus distance.

The stage-ratio method, using the original English units, is as follows (Ferris 1951):

$$T = 4.4 \frac{Dx^2 S}{t_o} \tag{7.34}$$

where
T   transmissivity (gpd/ft)
Dx   difference in distance over one log cycle stage-ratio (ft)
t_o tidal period (days)
S   storativity (dimensionless)

The time-lag method is as follows (Ferris 1951):

$$T = 6.0 \frac{x^2 S t_o}{t_1^2} \tag{7.35}$$

where
x   distance from subcrop body (ft), from graph
t_1 time lag (in days) at distance 'x', from graph

Both the stage-ratio method and time-lag method require an estimate of the aquifer storativity to calculate a transmissivity value. Published applications of the Ferris (1951) methods are provided by Halbert and Jensen (1996).

Van der Kamp ([1972](#)) provided an analytical solution to determine aquifer parameters for the case of a non-leaky confined aquifer that extends below the sea and does not subcrop out. Merritt ([2004](#)) provides a detailed discussion of the application of the Van der Kamp ([1972](#)) method to the Floridan aquifer system in southwestern Florida. Pressure loading of a confined aquifer behaves inland, at a distance from the oceanic loading, as if an oscillatory pumping and injection sequence were being performed in the aquifer at the coast line (Merritt [2004](#)). The equation for calculating transmissivity from amplitude ratio is

$$T = \frac{p\,x_o^2}{s\left[\ln\frac{2r}{L_e}\right]^2}S \qquad (7{:}36)$$

where

T transmissivity (m^2/d or ft^2/d)
S storage coefficient (dimensionless)
x_o distance from shore line (m or ft)
L_e loading efficiency (dimensionless)
r observed amplitude ratio (dimensionless)
s period of the harmonic oscillation (days)

Loading efficiency can be calculated from barometric efficiency, which can, in turn, be calculated using the method of Clark ([1967](#)), Merritt ([2004](#)).

The phase shift equation is

$$T = \frac{p\,x_o^2}{sU^2}S \qquad (7{:}37)$$

where U = phase difference (radians).

General and additional specific solutions for analyzing tidal fluctuations are provided by Jiao and Tang ([1999](#)), Li and Jiao ([2001a](#), [b](#), [2002a](#), [b](#)), and Rotzoll et al. ([2013](#)).

Tidal fluctuation data can be used to evaluate large-scale variations in transmissivity. For example, Rotzoll et al. ([2013](#)) observed a dampening of the tidal signal in the Northern Guam Lens Aquifer (Territory of Guam, USA), which was best explained by a lower permeability layer immediately inside the coastal boundary. The difference in hydraulic conductivity between the interior and peripheral areas of the aquifer was attributed to a diagenetic reduction in hydraulic conductivity along the coast and a dissolutional increase in hydraulic conductivity in the interior.

7.7   Hydraulic Tomography

Traditional pumping test analysis methods assume aquifer homogeneity and, at best, predict average drawdown over some volume of the aquifer (Yeh and Liu 2007). Inversion procedures, which involve calibration of spatially distributed parameters, are ill-posed problems that inherently lead to nonunique solutions. Yeh and Liu (2007) proposed that the hydraulic tomography technique is a better means for collecting and analyzing data for aquifer characterization. Hydraulic tomography involves sequentially pumping or injecting water at one interval in a monitoring well and monitoring the hydraulic response at a large number of other subsurface locations (Yeh and Liu 2000, 2007).

Many sets of head-versus-discharge (or recharge) data are obtained. The drawdown data from all the tests are then processed using inverse-modeling techniques to interpret the spatial distribution of hydraulic parameters (hydraulic conductivity and specific storage) of the aquifer (Yeh and Liu 2000, 2007; Zhu and Yeh 2005). Yeh and Liu (2000) developed a successive sequential linear estimator (SSLE) method for interpreting steady-state hydraulic tomography data and applied it to a hypothetical three-dimensional heterogeneous aquifer. Zhu and Yeh (2005) extended the SSLE method to transient hydraulic tomography and also demonstrated the approach on a hypothetical three-dimensional heterogeneous aquifer.

Ideally, multiple-zone monitoring wells are used to collect drawdown data at different depths. However, hydraulic tomography could be performed at lower resolutions using fully screened wells. Laboratory and field testing indicate that transient hydraulic tomography involving the inversion of multiple pumping tests can provide improved results compared to analyses of individual pumping tests. Berg and Illman (2011, 2013, 2015) applied transient hydraulic tomography (THT) to highly heterogeneous glaciofluvial sediments on the University of Waterloo campus, Waterloo, Ontario, Canada (Fig. 7.10). The study site contained nine wells (each with multiple observation points or screened intervals) located in a 15 m by 15 m square. Nine pumping tests were performed and the data interpreted by inverse modeling using the three-dimensional THT code developed by Zhu and Yeh (2005). The study area was previously investigated in detail using standard techniques (e.g., permeameter and grain size measurements and pumping tests). The THT results were evaluated against known stratigraphy and permeability data and by comparing predictive simulation results based on THT tomograms with pumping tests data from tests that were not used to generate the tomograms.

The University of Waterloo campus THT testing captured most of the salient features of the glaciofluvial aquifer and aquitard system. Significant discrepancies occurred in the lower part of the domain in which little or no drawdown was recorded during the duration of the pumping tests (Berg and Illman 2011). Berg and Illman (2013) subsequently compared steady-state hydraulic tomography analysis with data interpretations assuming a uniform aquifer with an effective hydraulic conductivity in three directions estimated through automatic model calibration and
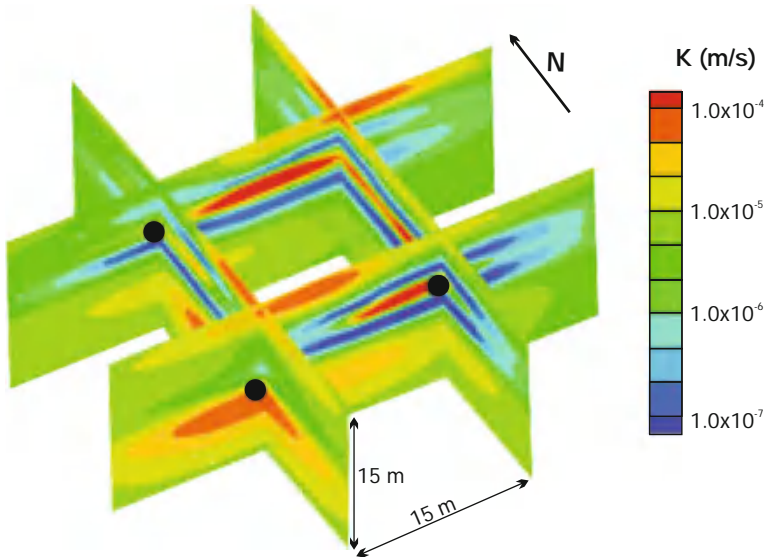
Fig. 7.10 Hydraulic conductivity tomogram of the University of Waterloo (Canada) Campus Research Site (from Berg and Illman 2013). Solid black circles indicate pump well location

stochastic inverse modeling of four individual pumping tests. Hydraulic tomography was better able to capture features known to be present at the site.

In a later study, Berg and Illman (2015) compared hydraulic tomography at the University of Waterloo site to a suite of 'traditional' techniques used to characterize aquifer heterogeneity including kriging using permeameter data, transitional probability/Markov chain geostatistics, geological modeling, and stochastic inverse models conditioned to local hydraulic conductivity data. The methods were assessed on their ability to predict drawdown data not used in the calibration effort. The results indicate that transient hydraulic tomography analysis performs considerably better than other traditional methods, which was attributed to hydraulic tomography integrating drawdown data from different pumping tests at different locations.

Illman et al. (2012) compared the costs and benefits of aquifer heterogeneity characterization using cores and hydraulic tomography. The hydraulic tomography was performed using data from four pumping tests in which a straddle-packer system was used to isolate a pumped section of the aquifer and water levels were measured using multiple-zone observation wells. The major advantage of hydraulic tomography is that it uses pumping test data and, therefore, directly considers hydraulic conductivity in the hydraulic parameter estimation process. It also avoids sample disturbance and representativeness issues of core samples and analyses (Illman et al. 2012).

A limitation of hydraulic tomography is the general non-uniqueness of the solutions of inverse methods. Bohling and Butler (2010) observed that "as with all

groundwater flow inverse problems, the hydraulic tomography analysis is inherently nonunique because of the underlying physics, in this case, the spatial averaging incorporated in the measurement of pumping-induced drawdown." Bohling and Butler (2010) demonstrated through forward modeling that multiple parameter fields can exactly reproduce the "true" drawdown simulated using the "true" parameter field. They further observed that the inherent physics-imposed non-uniqueness of the inverse problem faced in hydraulic tomography can only be addressed through recruiting information external to the test, that is, regularization of the data. Regularization is the process of encouraging estimated parameters to reflect a preferred state, which may be a model based on prior knowledge of the system.

Illman et al. (2012) indicate that cost analysis show that the hydraulic tomography method is more expensive than core analysis, and that there would be significant cost savings if equipment can be rented and/or reused. Bohling and Butler (2010) further noted that hydraulic tomography involves a level of expense and field effort that most practitioners will find difficult to justify.

7.8   Data Analysis: What Do the Data Mean

All of the commonly used analytical methods are based on a set of assumptions as to aquifer structure (e.g., homogeneity, anisotropy, leakiness of confining units, well penetration), some of which are not met to varying degrees in actual aquifers. The question arises as to the accuracy of values of aquifer properties obtained from the traditional methods when, for example, a method based on a homogenous aquifer assumption is applied to a heterogeneous aquifer (Wu et al. 2005). Or, more specifically, what do transmissivity and storativity values calculated using the Theis or Cooper and Jacob methods mean for heterogeneous aquifers (Wu et al. 2005)?

Wu et al. (2005) concluded that storativity values obtained from observation wells using the traditional Theis analysis are likely weighted averages of the storativity values of the part of the aquifer between the pumped and observation well, and cautioned that the value may not be representative of the aquifer as whole. Transmissivity values, on the contrary, are a weighted average of the transmissivity values in the entire domain, with values being potentially influenced by any large-scale or strong anomaly within the cone of depression. Early-time transmissivity and storativity values change with time (duration of pumping). Only after sufficiently long pumping is conducted does the estimated transmissivity values come close to, but still does not, equal, some mean of the aquifer (Wu et al. 2005).

It has been observed that during pumping tests on heterogeneous aquifers, drawdown data from different time periods collected at a single location may produce different estimates of aquifer properties (Butler 1990). The log-log and semilog methods may provide different estimates of flow properties in

non-uniform aquifers due to their measurement of properties in the different parts of the aquifer. The magnitude of the difference between the two methods has been suggested to be a function of the degree of aquifer heterogeneity (Butler 1990).

A key point is that during long-duration pumping tests, the aquifer near the pumped well approaches a steady-state condition and provides an insignificant contribution to the well discharge (Theis 1940; Butler 1990). The portion of the aquifer controlling drawdown is a concentric, outwardly migrating and expanding zone, referred to as the front of the cone of depression. In a uniform aquifer, the inner and outer radius of the portion of the aquifer contributing 95 % of the flow to the well can be calculated as (Streltsova 1988; Butler 1990):

$$r_{inner} = \sqrt{0.1 Tt = S} \tag{7.38}$$

$$r_{outer} = \sqrt{14.8 Tt = S} \tag{7.39}$$

where t is the time since the start of pumping.

The effect of near well material is greatest in the log-log (curve matching) method, because the method is based on total drawdown, rather than the rate of change of drawdown, and the early data is the area of greatest curvature, which tends to be emphasized during data analysis (Butler 1990). Drawdown in the pumping well is also impacted by skin damage. Use of medium to late data in the semilog method reduces the effects of skin effects and near well aquifer hetero-geneity. However, late data may be impacted by leakage and boundary effects. Multiple-well tests in which the observation wells are located far from the pumping well are least impacted by the property of materials in the immediate vicinity of the observation and pumping wells (Butler 1990). Drawdown at distant observation wells should be only weakly dependent on analytical methodology. Slug tests measure near well material and are most sensitive to skin effects.

Although, multiple-well aquifer pumping tests have a greater volume of inves-tigation than single borehole testing methods (e.g., packer tests, slug tests), the results may not be representative of the aquifer as whole. Time-drawdown and recovery-drawdown data from monitoring wells in aquifers with a pronounced seasonal water use pattern can be viewed as long-term pumping tests (Butler et al. 2013). The aquifer response to seasonal pumping can provide insights into aquifer boundary conditions and compartmentalization, which may not be evident in conventional, relatively short-term pumping tests (Butler et al. 2013). Values of aquifer hydraulic parameters obtained using standard analytical procedures, whose assumptions may not be met by the tested aquifers, may thus be considered as initial estimates subject to adjustment during the calibration of larger-scale models.

References

Anderson, M., Jones, M., Lewis, S., and Baxter, K. (2006) Obtaining reliable aquifer and well performance hydraulic parameter values in a double porosity aquifer: examples from artificial recharge trials in South London. In Recharge systems for protecting and enhancing groundwater resources, Proceedings of the 5th International Symposium on Management of Aquifer Recharge, Berlin, Germany, 11–16 June 2005 (pp 331–336). Paris: UNESCO.

ASTM (2005) Standard test method for determining specific capacity and estimating transmissivity at the control well: ASTM Standard 05472-93 (reapproved 2005). West Conshohocken: ASTM International.

Berg, S. J., & Illman, W. A. (2011), Three-dimension transient hydraulic tomography in a highly heterogeneous glaciofluvial aquifer-aquitard system. Water Resources Research, 47, W 10507.

Berg, S. J., & Illman, W. A. (2013) Characterization of hydraulic conductivity heterogeneity with steady state hydraulic tomography: Field study in a highly heterogeneous glaciofluvial deposit. Groundwater, 51, 29–40.

Berg, S. J., & Illman, W. A. (2015) Comparison of hydraulic tomography with traditional methods at a highly heterogeneous site. Groundwater, 53, 71–89.

Bohling, G. C., & Butler, J. J., Jr. (2010) Inherent limitations of hydraulic tomography. Ground Water, 48, 809–824.

Boulton, N. S. (1954a) Unsteady radial flow to a pumped well allowing for delayed yield from storage. International Association of Scientific Hydrology Publication, 37, 472–477.

Boulton, N. S. (1954b) The drawdown of the water table under nonsteady conditions near a pumped well in an unconfined formation: Institute of Civil Engineers Proceedings (London), Part 3, 564–579.

Boulton, N. S. (1963) Analysis of data from non-equilibrium pumping tests allowing for delayed yield from storage. Institute of Civil Engineers Proceedings (London), 26, 469–482.

Bourdet, D., Ayoub, J. A., & Pirard, Y. M. (1989). Use of pressure derivative in well-test interpretation. SPE Formation Evaluation, 4(2), 293–302.

Bourdet, D., Whittle, T. M., Douglas, A. A., & Pirard, Y. M. (1983). A new set of type curves simplifies well test analysis. World Oil, 196(6), 95–106.

Bradbury, K. R., & Rothschild, E. R. (1985) A computerized technique for estimating hydraulic conductivity of aquifers from specific capacity data. Ground Water, 23, 240–245.

Brown, R. H. (1963) Estimating the transmissibility of an artesian aquifer from the specific capacity of a well. In R. Benthall (Ed.), Methods of determining permeability and transmissibility and drawdown (pp. 336–338). U.S. Geological Survey Water-Supply Paper 1536-I.

Butler, J. J., Jr. (1990) The role of pumping tests in site characterization: some theoretical considerations. Ground Water, 28, 394–402.

Butler, J. J., Jr., Stotler, R. L., Whittemore, D. O., & Reboulet, E. C. (2013) Interpretation of water level changes in the High Plains Aquifer in western Kansas. Groundwater, 51, 180–190.

Clark, W. E. (1967) Computing the barometric efficiency of a well. Journal of the Hydraulic Division, American Society of Civil Engineers, 93(HY4), 93–98.

Cooper, H. H., Jr., & Jacob, C. E. (1946) A generalized graphical method for evaluating formation constants and summarizing well-field history. Transactions American Geophysical Union, 27, 526–534.

Dawson, K. J., & Isotak, J. D. (1991) Aquifer testing: Design and analysis of pumping and slug tests: Boca Raton, Florida: Lewis Publishers.

Doherty, J. E., & Hunt, R. J. (2010) Approaches to highly parameterized inversion: A guide to using PEST for groundwater-model calibration. US Department of the Interior, US Geological Survey.

Driscoll, F. G. (1986) Groundwater and wells (2nd Ed.). St. Paul, MN Johnson Filtration Systems.

Ferris, J. G. (1951) Cyclic fluctuations of water level as a basis for determining aquifer transmissibility. Proceedings of the Brussels Assembly of the International Union of Geodesy

and Geophysics (v. 2, pp. 148–155). Republished as U.S.G.S. Ground-Water Hydraulic Section Contribution No. 1.

Gringarten, A. C. (1987) Type-curve analysis: what it can and cannot do. Journal of Petroleum Technology, 39(1), 11–13.

Halbert, W. E., & Jensen, R. E. (1996) Influence of tidal fluctuations on coastal aquifers: General principles and case studies. In Proceedings 10th National Outdoor Action Conference and Exposition, May 13–15, Las Vegas, Nevada. National Ground Water Association, pp. 575–591.

Halford, K. J. (2006) Documentation of a spreadsheet for time-series analysis and drawdown estimation: U.S. Geological Survey Scientific Investigations Report 2006-5024.

Halford, K. J., & Kuniansky, E. L. (2002) Spreadsheets for the analysis of aquifer-test and slug-test data, version 1.2: U.S. Geological Survey Open-File Report 02-197.

Hantush, M. S. (1961a) Drawdown around a partially penetrating well. Journal of the Hydraulics Division, Proceedings of the American Society of Civil Engineers, 87(HY4), 83–98.

Hantush, M. S. (1961b) Aquifer tests on partially penetrating wells. Journal of the Hydraulics Division, Proceedings of the American Society of Civil Engineers, 87(HY4), 171–194.

Hantush, M. S. (1966) Analysis of data from pumping tests in anisotropic aquifers. Journal of Geophysical Research, 71, 421–426.

Hantush, M. S., & Jacob, C. E. (1955) Non-steady radial flow in an infinite leaky aquifer. American Geophysical Union Transactions, 36, 95–100.

Hantush, M. S., & Thomas, R. G. (1966) A method for analyzing a drawdown test in an anisotropic aquifer. Water Resources Research, 2, 281–285.

Huntley, D., Nommensen, R., & Steffey, D. (1992) The use of specific capacity to assess transmissivity in fractured rock aquifers. Ground Water, 30, 396–402.

Illman, W. A., Berg, S. J., & Alexander, M. (2012) Cost comparison of aquifer heterogeneity characterization methods: Ground Water Monitoring & Remediation, 32(2), 57–65.

Jiao, J. J., & Tang, Z. (1999) An analytical solution of groundwater response to tidal fluctuation in a leaky confined aquifer. Water Resources Research, 35, 747–751.

Kasenow, M. (1997) Applied groundwater hydrology and well hydraulics. Highlands Ranch, Colorado: Water Resources Publications.

Kasenow, M. (2006) Aquifer test data: evaluation and analysis. Highlands Ranch, Colorado: Water Resources Publications.

Kazemi, H., Seth, M. S., Thomas, G. W. (1969) The interpretation of interference tests in naturally fractured reservoirs with uniform fracture distribution. Society of Petroleum Engineers Journal, 246, 463–472.

Kruseman, G. P. & de Ridder, N. A. (1991) Analysis and evaluation of pumping test data. Wageningen, The Netherland: International Institute for Land Reclamation and Improvements Publications.

Li, H., & Jiao, J. J. (2001a) Tide-induced groundwater fluctuation in a coastal leaky confined aquifer system extending under the sea. Water Resources Research, 37, 1165–117.

Li, H., & Jiao, J. J. (2001b) Analytical studies of groundwater-head fluctuation in a coastal confined aquifer overlain by a semi-permeable layer with storage. Advances in Water Resources, 24, 565–573.

Li, H., & Jiao, J. J. (2002a) Analytical solutions of tidal groundwater flow in coastal two-aquifer system. Advances in Water Resources, 25, 417–426.

Li, H., & Jiao, J. J. (2002b) Tidal groundwater level fluctuations in L-shaped leaky coastal aquifer system. Journal of Hydrology, 268, 234–243.

Lohman, S. W. (1972) Ground-water hydraulics. U.S. Geological Survey Professional Paper 708.

Mace, R. E. (1997) Determination of transmissivity from specific capacity tests in a karst aquifer. Ground Water, 35, 738–742.

Maliva, R. G., & Missimer, T. M. (2010) Aquifer storage and recovery and managed aquifer recharge using wells: Planning, hydrogeology, design, and operation. Houston: Schlumberger Corporation.

Maslia, M. L., & Randolph, R. B. (1987), Methods and computer program documentation for determining anisotropic transmissivity tensor components of two-dimensional ground-water flow.U.S. Geological Survey Water Supply Paper 2308.

Merritt, M. L. (2004) Estimating hydraulic properties of the Floridan Aquifer System by analysis of earth-tide, ocean-tide, and barometric effects, Collier and Hendry Counties, Florida. U.S. Geological Survey Water-Resources Investigations Report 03-4267.

Moench, A. F. (1984) Double-porosity models for a fissured groundwater reservoir with fracture skin". Water Resources Research, 20, 831–846.

Motz, L. H. (2009) Multiple-pumped-well aquifer test to determine the anisotropic properties of a karst limestone aquifer in Pasco County, Florida, USA. Hydrogeology Journal, 17, 855–869.

Neuman, S. P. (1972) Theory of flow in unconfined aquifers considering delayed response of the water table. Water Resources Research, 8, 1031–1045.

Neuman, S. P. (1975) Analysis of pumping test data from anisotropic unconfined aquifers considering delayed gravity response. Water Resources Research, 11, 329–342.

Papadopoulos, I. S. (1965) Nonsteady flow to a well in an infinite anisotropic aquifer. In Proceedings Dubrovnik Symposium, International Association of Scientific Hydrology, Vol. 1 (73), pp. 21–32.

Razack, M., & Huntley, D. (1991) Assessing transmissivity from specific capacity in a large heterogeneous alluvial aquifer. Ground Water, 29, 856–861.

Renard, P., Glenz, D., & Mejias, M. (2009) Understanding diagnostic plots for well-test interpretation. Hydrogeology Journal, 17, 589–600.

Rotzoll, K., Gingerich, S. B., Jenson, J. W., & El-Kadi, A. I. (2013) Estimating hydraulic properties from tidal attenuation in the Northern Guam Lens Aquifer, Territory of Guam, USA. Hydrogeology Journal, 21, 643–654.

Spane, F. A., Jr., & Wurstner, S. K. (1993), DERIV: A computer program for calculating pressure derivatives for use in hydraulic test analysis. Ground Water, 31, 814–822.

Stallman, R. W. (1969) Aquifer testing design, observation, and data analysis. U. S. Geological Survey Techniques of Water Resources Investigations, Chapter B1, Book 3.

Streltsova, T. D. (1988) Well testing in heterogeneous formations. New York: Wiley.

Thiem, G. (1906) Hydrologische methoden. Leipzig: Gebhardt.

Theis, C. V. (1963) Estimating the transmissibility of a water-table aquifer from the specific capacity of a well. In R. Benthall (Ed.), Methods of determining permeability and transmissibility and drawdown (pp. 332–336). U.S. Geological Survey Water-Supply Paper 1536-I.

Theis, C. V., 1935, The relation between the lowering of the piezometric surface and the rate and duration of discharge of a well using groundwater storage: Transactions American Geophysical Union, 16, 519–524.

Theis, C. V. (1940) The source of water derived from wells. Civil Engineering, 10(5), 277–280.

Todd, D. K. (1980) Groundwater hydrology (2nd Ed.). New York: John Wiley.

Van der Kamp, G. (1972) Tidal fluctuations in a confined aquifer extending under the sea. Proceedings International Geological Congress, 24(11), 101–106.

Walton, W. C. (1960) Leaky artesian aquifer conditions in Illinois. Illinois State Water Survey Report of Investigations 39.

Walton, W. C. (1962) Selected analytical methods for well and aquifer evaluation. Illinois State Water Survey Bulletin 49.

Walton, W. C. (1970) Groundwater resource evaluation. New York: McGraw-Hill.

Walton, W. C. (1991) Principles of groundwater engineering. New York: CRC Press.

Walton, W. C. (1997) Practical aspects of ground water modeling (3rd Ed.). Westerville, Ohio: National Ground Water Association.

Walton, W. C. (2008) Upgrading aquifer test analysis. Ground Water, 46, 660–662.

Warren, J. E., & Root, P. J. (1963) The behavior of naturally fractured reservoirs". Society of Petroleum Engineers Journal, 3, 245–255.

Wu, C. M., Yeh, T. C. J., Zhu, J., Lee, T. H., Hsu, N. S., Chen, C. H., & Sancho, A. F. (2005).
    Traditional analysis of aquifer tests: Comparing apples to oranges? Water Resources Research,
    41(9). W09402.

Yeh, T.-C., & Liu, S. (2000) Hydraulic tomography: Development of a new aquifer test method.
    Water Resources Research, 36, 2095–2105.

Yeh, T.-C., & Liu, S. (2007) Time to change the way we collect and analyze data for aquifer
    characterization. Ground Water, 45, 116–118.

Zhu, J., & Yeh, T.-C. (2005) Characterization of aquifer heterogeneity using transient hydraulic
    tomography. Water Resources Research, 41(7), W07028.

Chapter 8
Slug, Packer, and Pressure Transient Testing

Slug tests are a commonly used method to determine the hydraulic conductivity of strata near a borehole. The tests involve recording the water level (pressure) response in a well to an instantaneous increase or lowering of water level. Slug tests have the advantage of being quick, inexpensive to perform, and do not generate water that requires disposal, which is an important consideration at contaminated sites. The quality of data obtained from slug tests is strongly dependent on well and borehole conditions, particularly skin effects. Multiple-level slug tests performed on a single well or borehole are used to obtain hydraulic conductivity-versus-depth profiles. Straddle-packer and single-packer tests allow for the evaluation of hydraulic properties and collection of water samples from discrete intervals. Pressure transient testing is an important tool in oil and gas industry that has applications in groundwater investigations for evaluation of aquifer properties and wellbore conditions.

8.1 Slug Tests

Slug tests are used to determine the hydraulic conductivity of an aquifer from the response to an instantaneous addition or withdrawal of a volume of water (slug). The slug could be the actual addition or extraction of water. More commonly, the tests are performed by either the insertion or withdrawal of a solid pipe or by changing water levels in a well using air pressure or a vacuum. Slug testing procedures were reviewed by Butler (1998), Cunningham and Schalk (2001), Weight (2008), and Chen et al. (2012).

Slug tests have the disadvantages of a small volume of investigation (compared to aquifer pumping tests) and susceptibility to well skins and formation damage affecting test results. Slug tests only provide information on the hydraulic conductivity of the strata close to the tested well. However, slug tests have the advantages that they can be performed quickly and inexpensively, and can utilize

small-diameter monitoring wells. For contaminated sites, slug tests also have the great advantage of not requiring either the pumping of water or addition of water into the aquifer. Proper disposal of produced water at contaminated sites can be a major logistical and cost issue for conventional pumping tests. Hence, slug tests remain an important tool for aquifer characterization.

8.2 Slug Testing Procedures

Simple, inexpensive tools for slug tests can be fabricated by filling lengths of PVC or steel pipe of various diameters and lengths with concrete. An eyelet anchored in the concrete is used to attach a rope or monofilament line to the slug. Slug tests are performed by quickly lowering and raising the tool in the well (Fig. 8.1). A falling-level (slug-in) test is performed by the lowering of the tool into the well. A rising level (slug-out) test is performed by lowering a tool into the well and allowing water levels to recover to static (background levels). The slug test is then performed by quickly removing the tool. Slug-out tests are also referred to as bail tests. In practice, falling- and rising-head tests are often performed sequentially in wells.
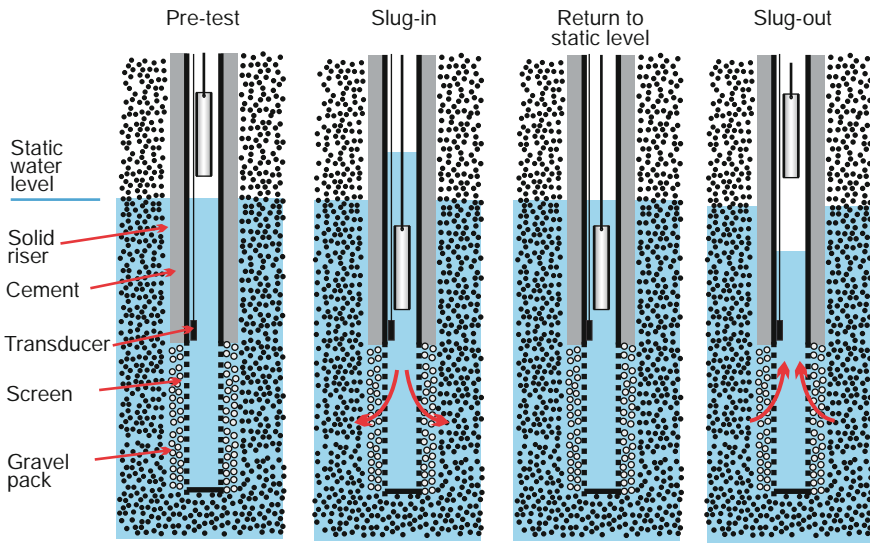
Fig. 8.1 Conventional slug test. Before the start of the test, the water is at static level. Lowering of the slug into the water causes water level in the well to rise (slug-in test), which then declines as water flows into the adjoining aquifer. After well level has returned to static level, the slug is quickly removed, which causes a temporary lowering of water level and flow into the well (slug-out test)

   Slug tests may also be performed by depressing water levels in a well by pressurizing the well casing using either air or another gas (nitrogen). These 'pneumatic' tests have the advantage of allowing for a near instantaneous change in water level, which is critical for tests performed in formations with very high hydraulic conductivities. Pneumatic slug-out tests are performed by increasing the pressure in the casing, which lowers the water level, and then quickly releasing the pressure, allowing water level to recover. A slug-in test uses a vacuum pump to increase the water level in a well. The tests are performed by quickly releasing the vacuum. A key requirement of pneumatic slug tests is that water levels cannot be dropped below the top of the well screen or open-hole interval. Apparatuses for performing pneumatic slug tests in direct-push installed and other types of wells are described by Prosser (1981), Leap (1984), McLane et al. (1990), Schmidley and Kirsch (1994), Bartlett et al. (2004), and ASTM (2006a).

   The raw data from slug tests is frequent measurements of water level versus time. Water level data are now usually recorded using pressure transducer and data logging systems, which allow for the accurate measurement and recording of water levels at small time intervals. In the past, water levels were measured either manually or using mechanical chart recorders. Self-contained water-level data logger units are now commonly used, but have the disadvantage that the units need to be recovered to read the data and reinstalled if a test is to be repeated (unless connected by a cable to land surface).

   With respect to slug tests performed using self-contained pressure-transducer systems that are not readable at land surface and standard pipe-type slugs, the following basic procedure is recommended:

(1) Pretest. Determine the well construction (total depth, screen depth, filter pack material, type, and depth) and depth to water.
(2) Select an appropriate slug size (diameter and length) and determine the depth to which it will be lowered. The slug cable should be marked for the planned depth.
(3) Install the transducer below the planned depth of the lowered slug. The transducer should have an appropriate depth rating for its installation depth and be set for high-frequency linear readings (0.5 or 1.0 s).
(4) Confirm that water levels have returned to static levels. This can be done using a water level meter. Alternatively, a sufficient minimum recovery time can be determined from experiences at previous tests in the study area.
(5) Quickly lower the slug into the well (slug-in test). Allow for sufficient time for water levels to recover to static level. The time should be based on experiences at other wells in the study area or by measuring water levels in the well. In a moderate- to high-transmissivity formations, water level will often recover within 5–10 min. The time of slug introduction should be accurately recorded. However, with high-frequency water level readings, the time of introduction of the slug may be satisfactorily determined from the initial recorded change from static water level.

(6) Once the water level in the well has returned to static level, perform a 'slug out' test by quickly removing the slug. Allow sufficient time for water level to recover to static level.

(7) The test can either be directly repeated or the water level probe can be recovered and data can be downloaded and reviewed before repeating the test.

(8) Data should be reviewed in the field (before moving on to the next well) to determine if the tests have been successfully performed. Potential problems include not allowing enough time for water levels to recover and movement of the transducer during the introduction and removal of the slug.

Butler et al (1996, 2003) recommended performing multiple tests for each interval using different displacements. Repeat tests allow the viability of the theory underlying the analysis model to be assessed and aid in the selection of the most appropriate model for test analysis (Butler 1998; Butler et al. 2003; Sellwood et al. 2005). A reproducible dependence on the direction of slug-induced water flow (i.e., different results are obtained for slug-in and slug-out test) can indicate that further well development is necessary (Butler 1998; Butler and Healey 1998; Sellwood et al. 2005).

Average hydraulic conductivity values obtained from pumping tests tend to be greater than values obtained from multiple slug tests, which has been attributed to the larger volume of investigation and incorporation of zones of high hydraulic conductivity in pumping tests. Butler and Healey (1998) proposed that the difference between average hydraulic conductivity obtained from pumping tests and slug tests may be due in some circumstances to incomplete well development, and uncertainty concerning aquifer thickness and vertical anisotropy.

Incomplete development can result in the hydraulic conductivity values calculated from slug tests reflecting the much lower hydraulic conductivity of altered, near-well material rather than the formation itself (Freeze and Cherry 1979; Butler and Healey 1998). Skin effects may be the result of residual drilling fluids, fine-grained material (e.g., clays) dragged down into the test zone of the borehole, and biofilms (biochemical layers or mats). The occurrence of skin effects may be indicated by changes in calculated hydraulic conductivity values between successive tests on the same well or between slug-in and slug-out tests (Butler and Healey 1998). Incomplete development of wells used for slug tests appear to be extremely common (Butler and Healey 1998). Development of a gravel pack next to the well by surging and backwashing may increase measured hydraulic conductivity values. The test data may thus reflect the high hydraulic conductivity of the gravel pack rather than the formation (Freeze and Cherry 1979).

Hydraulic conductivity estimates from pumping tests, in contrast to those from slug tests, are not heavily impacted by near-well conditions or vertical anisotropy (Butler and Healey 1998), especially in the case of estimates based on data from multiple-well tests. Skin effects have a far greater influence on the rate of flow into and out of wells, than on the degree to which water levels in an observation well reflect aquifer water levels or heads. Poorly developed observation wells may provide good-quality water-level data, but slug tests on such wells may provide

incorrectly low hydraulic conductivity values. The primary conclusion of Butler and Healey (1998) is that the importance of appropriate procedures to develop wells in which slug tests are to be performed cannot be overestimated. As a generalization, much less effort is typically made in developing small-diameter monitoring wells used for slug tests, than for larger diameter production wells.

Butler et al. (1996) proposed guidelines for improving the performance and analysis of slug tests include the following:

- Three or more tests should be performed on each well. Variations in results, particularly a progressive decrease in hydraulic conductivity may indicate an evolving skin effect caused by mobilization of fine materials.
- Two or more different displacements (H_0) should be used during testing of a given well. Test results should be independent of H_0.
- Slugs should be introduced in a near instantaneous manner and an estimate be obtained of the initial displacement. The normalized difference between the displacement volume and recorded displacement should be 10 % or less. Instantaneous displacement is particularly important in wells completed in strata with very high hydraulic conductivities because water levels very quickly recovery to static level.
- Appropriate data acquisition equipment should be used, which is now normally electronic pressure transducers and dataloggers. High data acquisition rates are especially needed for rapidly responding wells (i.e., wells complete in very high hydraulic conductivity strata).
- Methods chosen for data analysis should be appropriate for site conditions. Anisotropy can result in under estimation of hydraulic conductivity if it is not accounted for in the data analysis.
- Use of pre- and post-analysis plots should be an integral component of the data analysis. Deviations between fitted theoretical models and test data should be investigated and may indicate incorrect values were used for model parameters.
- Appropriate well construction parameters should be used. For example, the effective screen length and radius parameters in analyses should be the length and radius of the gravel pack.

Bartlett et al. (2004) compared the results of over 296 pneumatic slug tests performed at a test site (Naval Facility, Port Hueneme, California) on different well types, including standard hollow-stem auger wells and direct-push wells with different diameters and prepacked screen designs. The results of the investigation were that there were no statistical difference between the different prepacked screened well types and also between direct-push, no-pack wells, and drilled wells. A statistical difference in hydraulic conductivities was present between drilled wells and driven wells with prepacked screens. One explanation for the greater hydraulic conductivity of drilled wells is that there is a greater effective radius when a natural filter pack is developed. Bartlett et al (2004) suggested that the differences in hydraulic conductivity values observed amongst wells are largely due to spatial heterogeneity rather than differences in well construction and installation or test method.

8.3   Multilevel Slug Tests

Profiles of hydraulic conductivity with depth can be obtained by multilevel slug tests. The technique involves performing a series of slug tests on aquifer intervals that are isolated using single or straddle packers. General packer testing procedures are discussed in Sect. 8.6.1. The slug tests are performed in the same manner as tests performed on entire wells. Multilevel slug tests can be performed on wells with open-hole or screened completions. However, straddle-packer slug tests are not suitable in screened wells in which a high permeability backfill material is used or if the formation does not collapse against the screen (Meville et al. 1991). The main attractions of multilevel slug tests is that they can be performed rapidly and without generating water that requires disposal, which is an important consideration in some contaminated sites (Meville et al. 1991). Melville et al. (1991) documented multilevel slug testing performed in a siliciclastic aquifer near Mobile, Alabama. The test data were interpreted using the methods of Cooper et al. (1967) and Widdowson et al. (1990). The Widdowson et al. (1990) method, which considers both radial and vertical flow gave hydraulic conductivity values approximately 2/3 of the values obtained using the Cooper et al. (1967) method. The hydraulic conductivity profiles generated using multilevel slug tests were comparable to the values obtained from tracer tests.

   Multilevel slug testing was performed at the Geohydrologic Experimental and Monitoring (GEMS) site near Lawerence, Kansas, using a packer system that is suitable for small-diameter (5 cm) monitoring wells (McElwee and Zemansky 1999; McElwee and Ross 2001; Ross and McElwee 2007). The slug tests were able to characterized heterogeneity in hydraulic conductivity in the investigated alluvial aquifer. The data were used to create cross sections and three-dimensional fence diagrams of hydraulic conductivity.

8.4   Slug Test Data Interpretation

The interpretation of slug tests can be much more complex than performing the actual tests. A variety of different methods (and refinements thereof) have been developed to interpret the water level-versus-time data. The most commonly used methods are those of Hvolsev (1951), Bouwer and Rice (1976), and Cooper et al. (1967), which are summarized herein. Slug test data interpretation methods were developed as manual graphical techniques. Commercial and freeware packages are now available for more automated interpretation of slug test data. However, it behooves professionals involved in interpretation of slug test data to understand the underlying methods and associated assumptions. The critical issue is performing tests and interpreting the data is to obtain hydraulic conductivity values that actually reflect the properties of the aquifer material near the well.

Fig. 8.2 Hypothetical time-draw data for a slug test showing the triple-line effect. The first steep segment represents drainage from the filter packer. The second segment, which includes most of the change in normalized heads, is the formation response, which is used for the test analysis. The third segment is a tailing effect and represents a small fraction of the total recovery
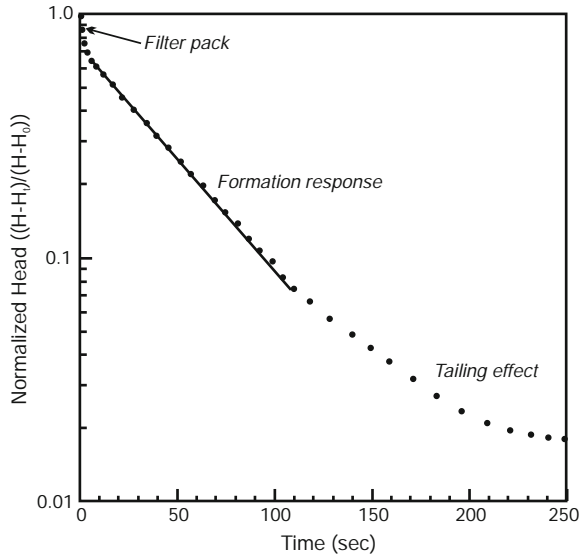
Data interpretation starts with a semi-logarithmic (semilog) time-recovery plot with recovery or normalized recovery on the logarithmic axis. The data should ideally be plot on a straight line. In practice, the data may show a double or triple-line effect (Fig. 8.2). In plots with two straight-line segments, the early, steeper segment may reflect drainage from the gravel pack. The later, less-steep segment should be used to estimate the hydraulic conductivity of the formation (Bouwer 1989). A third segment may also be present, which is a "tailing effect" (Weight 2008) in which water levels slowly asymptotically approach static level. The tailing effect represents only small fraction of the total recovery.

8.4.1 Hvorslev Method

The Hvorslev (1951) method is based on consideration of the hydrostatic time lag, which is the time required for a desired degree of hydrostatic pressure equalization to occur between soil (i.e., the tested formation) and a borehole. The underlying concept is that the rate of flow into a well is a proportional to hydraulic conductivity and the difference in water level from static level (Hvorslev 1951; Freeze and Cherry 1979);

$$Q(t) = pr^2 \frac{dh}{dt} = FK(z - y) \tag{8.1}$$

where

Q(t)   is the rate of flow into the well at time t (m^3/s)
F   shape factor
K   hydraulic conductivity (m/s)
x   difference in head from static head at t = 0 (m)
y   recovery in head at time t

The term $(z − y)$ is referred to as the active head, which is difference in head from static level (H) at time t.

The rate of flow into a well decreases over time as the pressure differential is progressively reduced. The basic time lag (T_0) is defined as the time required for equalization of the pressure difference when the original rate of flow is maintained. The basic time lag in practice is obtained from the head ratio (HR) or normalized head, which is the ratio of the difference in head from static level (H) at time 't' (H_t), to the difference in head from static level at the start of the test (H_0)

$$\text{Normalized head} = \text{HR} = \frac{(H − H_t)}{(H − H_0)} \tag{8.2}$$

With respect to a slug-out test, the head ratio is equal to the drawdown at time 't' divided by the maximum drawdown that occurred at the start of the test (i.e., at t = 0). The basic time lag is the time corresponding to a head ratio of 0.37, which in manual calculations is determined graphically (Fig. 8.3).

The basic equation for determining hydraulic conductivity from slug test data in the Hvorslev (1951) method is

$$K = \frac{A}{Ft_0} \tag{8.3}$$

Fig. 8.3 Semilog plot of slug test data from Daytona Beach, Florida, illustrating the graphical determination of the basic time lag (T_0) of Hvorslev (1951)
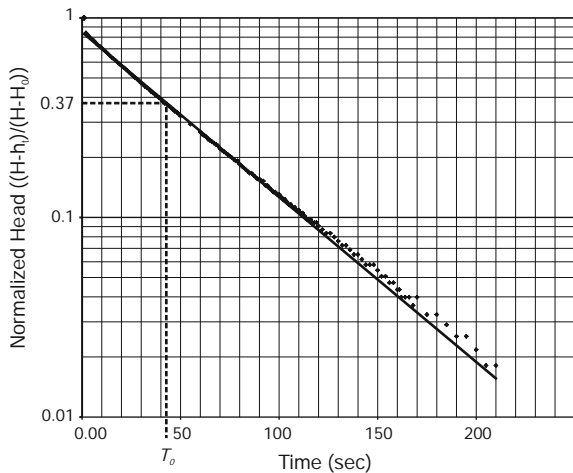
where
A   is the cross-sectional area of the well casing (solid riser) (m^2)
F   shape factor
t_0 basic time lag (s)

The shape factor varies with aquifer and well configuration. The commonly used equations for the horizontal (radial) hydraulic conductivity (K_h) of a partially penetrating screened well that does not abut an impermeable unit are

$$K_h = \frac{r_c^2 \ln\left(\frac{mL_e}{R_w}\right)}{2L_e t_0} \tag{8.4}$$

$$m = \sqrt{K_H = K_v} \tag{8.5}$$

where
r_c radius of the well casing (riser) (m)
L_e length of the screen (m)
R_w radius of the screen including the filter pack (m)
m square root of the horizontal to vertical hydraulic conductivity anisotropy ratio (unit less).

For isotropic aquifers, m = 1 and Eq. 8.4 reverts to the commonly used form of the Hvorslev equation. R_w can also be considered the distance between the center of the well and undisturbed formation. Equation 8.4 is applicable where L_e/R_w is greater than 8. Alternative equations for other well configuration are provided by Hvorslev (1951).

The Hvorslev method assumes that the soil and water are incompressible (specific storage of the formation is zero), the flow required for pressure equalization does not cause significant drawdown of groundwater levels, and friction losses in the casing are negligible for the small rates of flow that occur during pressure equalization. Other assumptions are that the aquifer has an infinite depth and directional anisotropy (k_v and k_h) are constant. The method can be used for both fully and partially penetrating wells. The test measures properties of the soils in the vicinity of the well, and calculated hydraulic conductivity values are sensitive to disturbance, segregation, and consolidation of the soil (Hvorslev 1951).

Muldoon and Bradbury (2005) presented a variation of the Horoslev method that accounts for the geometry of boreholes and packers assemblies used for small-interval packer tests

$$K_h = \frac{d^2 \ln\left[\left(\frac{mL_e}{D}\right) + \sqrt{1 + \left(\frac{mL_e}{D}\right)^2}\right]}{8L_e T_0} \tag{8.6}$$

where
D   diameter of borehole (m)
d   diameter of standpipe (riser) (m)

The Hvorslev method is based on a value of normalized head rather than the slope of the normalized head-versus-time plot and is, therefore, sensitive to errors in the head value at the start of the test (H_0). For example, an incorrectly large H_0 value can result in an incorrectly small T_0 value and a larger calculated hydraulic conductivity value. In the slug test dataset illustrated in Fig. 8.4, an anomalous initial head increase of 1.67 m was recorded at $t = 1$ s. Using 1.67 m as the H_0 value affects the calculated normalized head values of the subsequent measurements, resulting in an approximately 4.5 times greater calculated K value than if 0.84 m (head increase at $t = 2$ s) is used as the H_0 value. The 0.84 m increase in water level is close to the theoretical increase in water level calculated from the dimensions of the slug used in the test. The hydraulic conductivity value obtained using 0.84 m as H_0 is within 5 % of the value obtained using the Bouwer and Rice method. Anomalous initial readings may be the result of a 'splash' effect caused by the freefall of the slug into the water. Regrettably, slug test data are often interpreted by copying and pasting time and head data into processing software without a quality review, resulting in spurious interpretations.
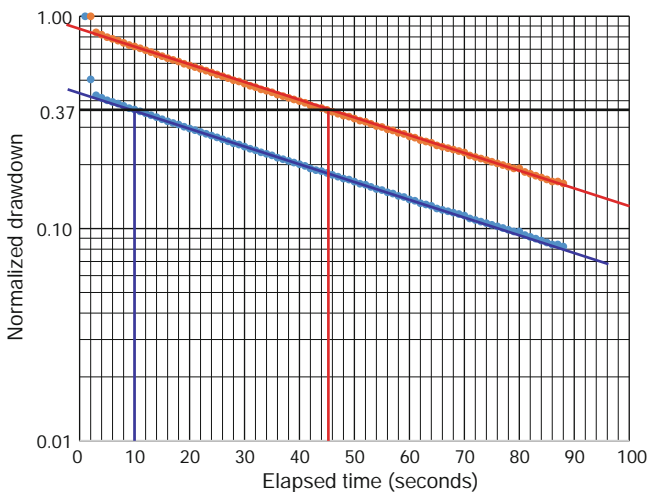
Fig. 8.4 Example of potential error in the application of Hvorslev method from the use of an incorrect initial head value (H_0) from 'splash' or other effects. Use of an anomalous initial head increase of 1.67 m at $t = 1$ s gives a basic time lag (T_0) of 10 s (blue values) compared to value of about 45 s obtained if the increase of 0.84 m at $t = 2$ s is used (red values). The 0.84 m rise in water level is consistent with the slug volume

8.4.2   Bouwer and Rice

The Bouwer and Rice (1976) method was developed for rising water levels in completely or partially penetrating wells in unconfined aquifers. The method is also appropriate for confined aquifers and for falling-level tests provided that the static water level is above the screened or open-hole section of the borehole (Bouwer 1989).

The Bouwer and Rice method is based on the Thiem equation

$$Q = 2pKL_e \frac{y}{\ln\left(\frac{Re}{r_w}\right)} \tag{8:7}$$

where

y   the vertical distance between water level in the well and static head (i.e., drawdown; m)

L_e the length of the screen (m)

R_e the effective radius over which the head difference (y) is dissipated

r_w distance between well center and undisturbed aquifer (gravel pack and developed zone)

The effective radius can also be considered the distance from the center of the well to the part of the aquifer not affected by the slug test.

Assuming homogenous, isotopic aquifer conditions in which the aquifer drawdown from the slug test is negligible, hydraulic conductivity is calculated as

$$K = \frac{r_c^2 \ln\left(\frac{R_e}{r_w}\right)}{2L_e} \frac{1}{t} \ln\frac{y_0}{y_t} \tag{8:8}$$

where y_0 = drawdown at time t = 0 and y_t = drawdown at time 't', and r_c = diameter of the casing in which water level changes are occurring, which is usually the solid riser. Where water level rises are occurring in the screen or open hole, then the thickness and porosity of the gravel pack needs to be considered and an equivalent radius must be calculated (Bouwer 1989).

The method involves a semi-logarithmic plot of y_t (drawdown at elapsed time 't', on log scale) versus time. From the part of the data that plots on a straight line, y at time t = 0 (y_0) and y_t at an arbitrarily selected time 't' are obtained (Fig. 8.5). The value of the parameter $\ln(R_e/r_w)$ is determined from the saturated thickness of the aquifer (b), L_e (screen length), and the distance from the water table to the bottom of the well (L_w). Bouwer and Rice (1976) presented two equations for calculating ln (R_e/r_w) for partially penetrating (Eq. 8.9) and fully penetrating (Eq. 8.10) wells.

Fig. 8.5 Semilog plot of slug
test data from Daytona Beach,
Florida, illustrating the
graphical determination of the
y_0, y_t, and t parameters for the
Bouwer and Rice (1976)
method
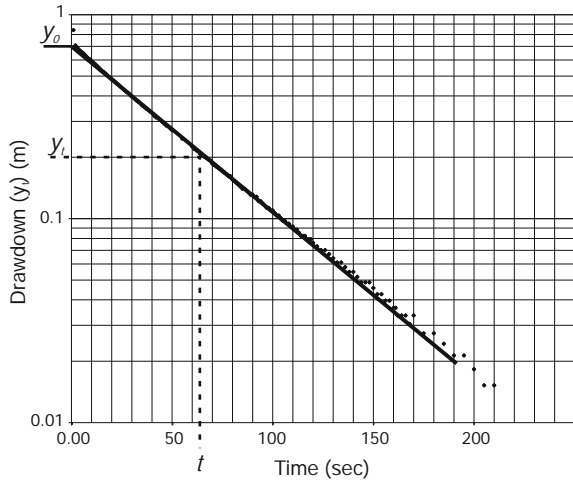
$$\ln \frac{R_e}{r_w} = \left[\frac{1{:}1}{\ln \left(\frac{L_w}{r_w} \right)} + \frac{A + B \ln[(b - L_w){=}r_w]}{L_e{=}r_w} \right]^{-1} \qquad (8{:}9)$$

$$\ln \frac{R_e}{r_w} = \left(\frac{1{:}1}{\ln(L_w{=}r_w)} + \frac{C}{L_e{=}r_w} \right)^{-1} \qquad (8{:}10)$$

where A, B, and C are dimensionless parameters. Bouwer and Rice (1976) provided
analog modeling curves that relate A, B, and C to L_e/r_w (Fig. 8.6). Yang and Yeh
(2004) published fourth-degree polynomials for calculating the A, B, and
C coefficients, where x is $\log(L_e/r_w)$

Fig. 8.6 Graphs used to
calculate Bouwer and Rice
(1976) A, B, and C parameters
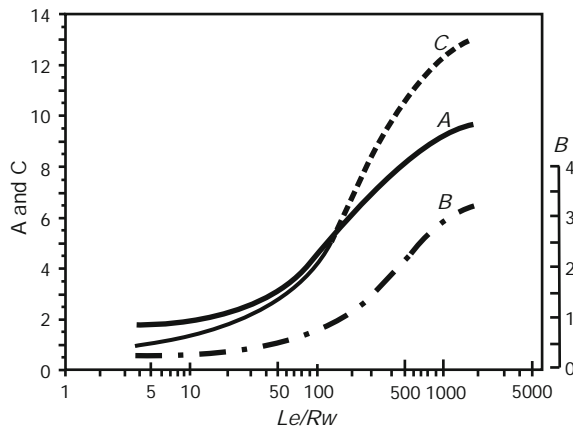
$$A(x) = 1.353 + 2.157x - 4.207x^2 + 2.777x^3 - 0.460x^4 \qquad (8.11)$$

$$B(x) = -0.401 + 2.619x - 3.267x^2 + 1.548x^3 - 0.210x^4 \qquad (8.12)$$

$$C(x) = -1.605 + 9.496x - 12.317x^2 + 6.528x^3 - 0.986x^4 \qquad (8.13)$$

8.4.3   Cooper et al. Method

The Cooper et al. (1967) method is a curving-matching technique, which starts with a semi-log plot of normalized head (y-axis) versus time (s) on the log scale (x-axis). The curve matching is performed using a series of semi-log type of curves, which are plots of normalized head (y-axis) versus Tt/r_c^2 for different values of a (Fig. 8.7), where

$$a = \frac{r_s^2}{r_c^2} S \qquad (8.11)$$
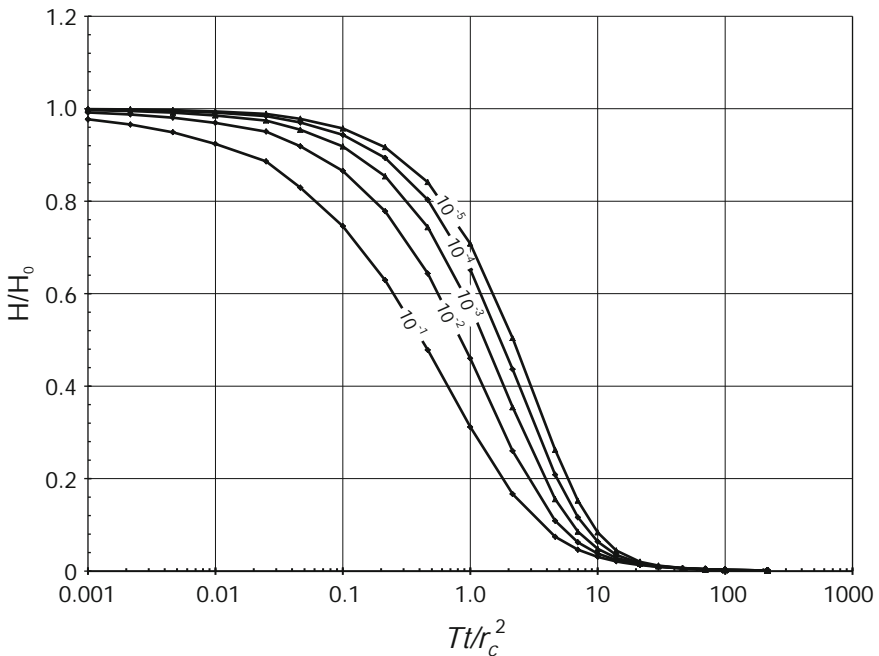
Fig. 8.7   Cooper et al. (1967) types curves for wells of finite diameter and a values of 10^{-1}, 10^{-2}, 10^{-3}, 10^{-4}, and 10^{-5}

T   transmissivity (cm^2/s)
t   time (s)
r_c radius of casing (riser) over which water level fluctuates (cm)
r_s radius of screen, open hole, or filter pack (cm)
S   storage coefficient

The curve matching is performed by overlaying the data plot on the type-curve so that the arithmetic axes are coincident. The data plot is then shifted horizontally until a best fit is achieved with an a curve. Transmissivity is calculated using the value of time (t) that overlies $Tt/r_c^2 = 1.0$ on the type curves,

$$T = 1.0 \frac{r_c^2}{t} \qquad (8.12)$$

Storage coefficient can also be calculated from the a value. However, Cooper et al. (1967) cautioned that the calculated values have a questionable reliability because of the similar shape of the curves. The Cooper et al. (1967) method is based on fully penetrating wells in confined aquifers. However, Cooper et al. (1967) noted that the technique would also be appropriate to partially penetrating wells completed in aquifers in which vertical permeabilities are only a small fraction of horizontal permeabilities.

8.4.4 Comparison of Hvorslev, Bouwer and Rice, and Cooper et al. Methods

A variety of methods are available to interpret slug test data. An obvious question is which method provides hydraulic conductivity values that most accurately reflect actual values. Clearly this depends upon the extent to which conditions at a tested well meet the underlying assumptions of the analytical methods. However, the values of hydraulic conditions (e.g., anisotropy ratios) at test sites are commonly not well constrained. Nevertheless, the commonly used data analysis methods may still provide reasonably accurate estimates of hydraulic conductivity for tests performed outside of the analytical method design conditions.

A study of slug test results at the Georgetown Site (South Carolina, USA) provides important insights on the variation in hydraulic conductivity values calculated using different methods (Mas-Pla et al. 1997). Data from 24 slug tests performed on a 5 m by 5 m area of a shallow stratified sand aquifer were analyzed using the Hovorslev, Bouwer and Rice, and Cooper et al. methods. The geometric means of the three methods ranged from 1.08×10^{-5} to 1.65×10^{-5} m/s. The Hvorslev and Bouwer and Rice methods gave similar mean hydraulic conductivity values and variances, while the Cooper et al method results had a much greater variance. The Cooper et al. method gave higher values for high hydraulic

conductivity zones and lower values for low hydraulic conductivity zones. Mas-Pla et al. (1997) concluded that the Hovorslev and Bouwer and Rice methods gave hydraulic conductivity values that were most representative of the sandy aquifer at the Georgetown site.

Campbell et al. (1990, p. 89) concluded that

> The Hvorslev method is widely used for reasons that are more related to historical precedence than to technical justification. The method has widespread acceptance and meets the perceived needs of the engineering profession because the method has produced results that seem to be reasonable approximations of in situ permeability.

Campbell et al. (1990) proposed that the Bouwer and Rice method is the method of choice because the method's results are consistent with other more cumbersome and time-consuming methods.

Hyder et al. (1994) evaluated the ramifications of using conventional interpretation techniques where the underlying assumptions are not met, and concluded that there are many commonly faced field conditions where the conventional methodologies for the analysis of response data from slug tests appear not to be viable. One source of large errors is associated with low hydraulic conductivity skins on the borehole walls. The response data may reflect the low hydraulic conductivity skin rather than adjacent formation. Hydraulic conductivity values obtained using the Horslev and Bouwer and Rice methods are particularly vulnerable to the effects of low hydraulic conductivity skins (Butler 1998). The actual effective screen length may be less than the nominal screen length used in the Horoslev method if part of the screen or gravel pack is clogged (Butler and Healey 1998). Failure to account for vertical anisotropy (Hyder et al. 1994) can lead to an under estimation of hydraulic conductivity by as large as a factor of three.

Software packages are available that will interpret slug test data using multiple methods and provide their corresponding hydraulic conductivity values, which allows for comparison. If the different methods give similar results, then the mean or median value might be utilized in an aquifer characterization program for at least an initial estimate of local aquifer hydraulic conductivity. However, agreement of values is not assurance that the calculated values are correct (i.e., representative of the formation) if the rate of flow into the well is strongly influenced by skin effects. If the methods give significantly different results, then the potential causes of the disagreement should be investigated.

8.4.5 Oscillatory Response

Slug tests performed in aquifers with high hydraulic conductivities may have oscillatory water level-versus-time plots (Fig. 8.8), which cannot be properly interpreted using the standard data interpretation methods. These tests are also referred to as underdamped tests. Oscillations in water levels occur when the recovery of water is so rapid that it overshoots the static water level due to inertia.

Fig. 8.8 Example of an
oscillatory slug test response
(Gems4S well; Butler and
Garnett 2000)
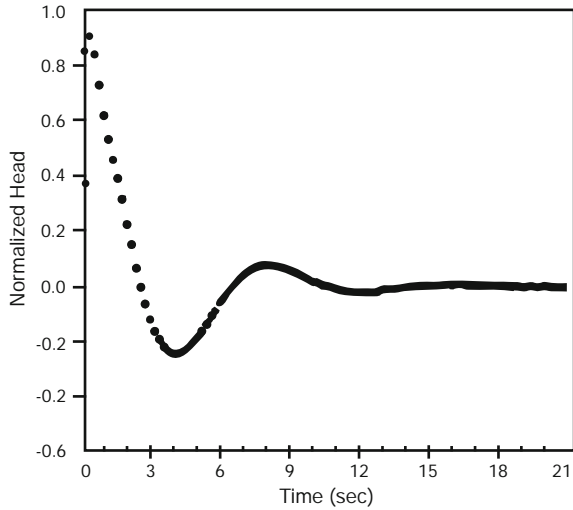
Springer and Gelhar (1991), Butler (1998), Butler and Garnett (2000), and Butler
et al. (2003) presented a curve-matching extension of the Bouwer and Rice and
Hvorslev methods to interpret oscillatory slug test data. Theoretical type curves
generated using a spreadsheet are graphically fit to normalized plots of slug test data.

8.4.6   Alternative Slug Test Interpretation Methods

Slug test data are usually analyzed using the Hvorslev and Bouwer and Rice
methods and, less commonly, the Cooper et al. methods. Other interpretative
methods have been developed in order to better simulate actual flow conditions, as
opposed to being based on simplifying assumptions. The most commonly used slug
test interpretation methods assume that flow into the well is radial and that vertical
flow is negligible. Widdowson et al. (1990) presented a method for interpreting
straddle-packer slug tests that incorporates aquifer anisotropy (and thus vertical
flow) and the position of the test interval with respect of aquifer boundaries, which
is based upon earlier work by Dagan (1978). The Widdowson et al. (1990) method
has three main elements

 (1) A dimensionless discharge parameter (P) is calculated from test conditions
      data using tables of (H/L) versus $\log_{10}(L/r_w)$, for different anisotropy rations
      (K_r/K_z), where
      H   distance from packer to nearest confining layer (distance from the
              furthest packer to the boundary used)
      L   packer test interval

r_w radius of well screen

K_r, K_z radial and vertical hydraulic conductivity respectively

(2) A second parameter "B" is calculated from the slope of a conventional semi-log plot of drawdown (y) versus time (log scale).

$$B = |\log_{10}(y_2 = y_1| = (t_2 - t_1) \qquad (8:13)$$

where y_1 and y_2 are the drawdowns at times t_1 and t_2.

(3) Hydraulic conductivity is then calculated as

$$K_r = \frac{(r_c^2 - r_w^2)}{2PL} 2{:}30B \qquad (8:14)$$

where

r_c radius of casing in which water level fluctuations occur and the slug applied

r_w radius of plunger (slug) used to perform the test

A limitation of the Widdowson et al. (1990) method is that it requires prior knowledge of aquifer anisotropy. However, the difference in value of P between anisotropy ratios of 5:1 and 10:1 is about 11 % or less. For higher degrees of anisotropy, flow will be predominantly radial and potential errors in conventional slug test interpretation methods due to non-radial flow will be small. Zlotnick (1994) presented an extension of the Bouwer and Rice (1976) method to include anisotropic conditions that also requires knowledge of the anisotropy ratio determined by other means. A corrected well radius is used, which is the well radius (r_w) divided by the square root of the anisotropy ratio (K_r/K_z).

8.5   Interference Tests

Slug tests are typically performed on one interval at a time in a single well. Interference tests involve the monitoring of two separate intervals during a single test. Single-well interference tests monitor water levels in two packed-off zones in the same well. Cross-well interference tests monitor water levels in a stressed well and one or more observation wells.

Single-well interference tests can be used to calculate the vertical hydraulic conductivity (K_v) of a confining or semiconfining unit. Paradis and Lefebvre (2013) presented the results of a proof-of-concept study performed on Quaternary-aged surficial sediments at Saint-Lambert-de-Lauzon, Quebec, Canada. The test equipment consisted of a three-packer assembly that isolates stressed and observation intervals. An instantaneous pressure pulse is induced using the pneumatic method

in the stressed interval and the resulting drawdowns are measured in both the stressed and observation interval. The method is essentially an extension of the multilevel slug test procedure except that it requires an additional observation interval at the bottom of the assembly (Paradis and Lefebvre 2013).

The single-well interference test provides data on K_h, K_v/K_h, and specific storage (Ss), which can be determined using either numerical inversion or a semi-analytical technique (Paradis and Lefebvre 2013). The calculated K_v values were in agreement with permeameter test results conducted from the same tested intervals. The test response may be effected by the skin effects in the same manner as occurs in single-interval tests. Hydraulic short circuiting can also adversely impact test results (Paradis and Lefebvre 2013).

Cross-well slug-interference tests are performed by applying an instantaneous rise or lowering of water in one well, in the same manner as a conventional slug test, and measuring the response in one or more observation wells (Novakowski 1989; Spane 1996; Spane et al. 1996). Spane et al. (1996) documented that under favorable conditions (e.g., observation well is located within 30 m of stressed well), the slug-interference method can give comparable results to a conventional constant-rate pumping test. In order to maximize the slug test response, it was recommended that the well bore storage be minimized by isolating the test interval with a downhole packer and that the size of the slug (volume of injected and recovered water) be maximized. The collected data are analyzed using a curve-matching technique. The slug-interference method requires considerable field effort if a packer is installed and is more computationally complex than the analysis of conventional pumping tests. However, the slug-interference test has the great advantage for contaminated sites in that it does not require the pumping of water that requires proper disposal (Spane et al. 1996).

8.6   Packer Tests

Packer testing involves the use of inflatable packers to isolate part of a borehole for hydraulic testing and/or water quality sampling. Packer testing is employed in aquifer characterization programs because it provides zonal isolation and thus greater vertical resolution of aquifer heterogeneity. The application of packer testing to hydrogeological investigation was reviewed by Brassington and Walthall (1985). Packer testing is used mainly to

- determine aquifer and confining unit hydraulic parameters
- measure piezometric heads
- collect water samples.

A basic limitation of packer testing is that it can only be performed on a stable borehole, which is needed to both seat the packers and to allow for pumping of (or injection into) the tested interval. Packer testing is most commonly performed in

groundwater investigation on open boreholes in lithified strata. The tests could also be performed on screened intervals, but the potential exists for leakage around the packers through between the annulus (gravel pack) between the well screen and formation. The tested interval must also be developed to remove drilling fluids and minimize or eliminate skin effects (e.g., mudcake and formation damage). The tests normally cannot be performed when drilling mud is required to maintain borehole stability.

8.6.1 Packer Testing Procedures

Packer tests conducted for groundwater investigations are performed using retrievable inflatable packers. An inflatable packer is essentially a cylindrical expandable plug that is used to isolate part of a well. The main components of the commonly used inflatable packers are a rubber element, which is reinforced with a high-strength material, such as Kevlar, and a pipe mandrel upon which the rubber element is attached. The pipe mandrel also provides a conduit for pumping or injection of water and room for instrumentation cables. Packer systems can be installed using either drill pipe or a wire line. Inflatable packer systems are available for a wide range of borehole sizes, including, at the low-end of the spectrum, systems that can be run in Boart Longyear NQ (75.7-mm, 3-in. borehole diameter) core barrels.

Two basic types of packer tests are commonly performed: straddle or dual-packer tests and single or off-bottom tests (Fig. 8.9). Straddle-packer tests employ two separate packers to isolate the intervening borehole interval. The length of the test interval can be adjusted by changing the spacing between the packers. Single-packer tests employ one packer to isolate the bottom of the borehole. The preferred straddle-packer testing system consists of two inflatable packers and three pressure transducers located below, between, and above the packers. The pressure transducers located above and below the tested interval are used to determine if there is short circuiting around the packer elements. Pressure changes within the packed-off interval should not be detected above and below the packers if the test interval is hydraulically isolated. A submersible pump may be installed between the packers. Where large diameter drill pipe is used to support the packer system, a submersible pump may alternatively be installed within the riser pipe.

Aquifer pumping tests performed using packers are performed in a similar manner as aquifer pumping tests performed on entire wells. The test interval should be first developed by pumping until water chemistry stabilizes. If pressure transducers readable at land surface are installed above and below the packer assembly, then an initial evaluation of the packer seal may be performed before the start of the test. After development, water levels are allowed to recover to background levels. Following the pumping phase, recovery data are normally recorded.

Both straddle and single-packer tests have their advantages and disadvantages. Straddle-packer tests can be run after drilling and geophysical logging of the entire

Fig. 8.9 Conceptual diagram
of a straddle-packer and
single-packer test
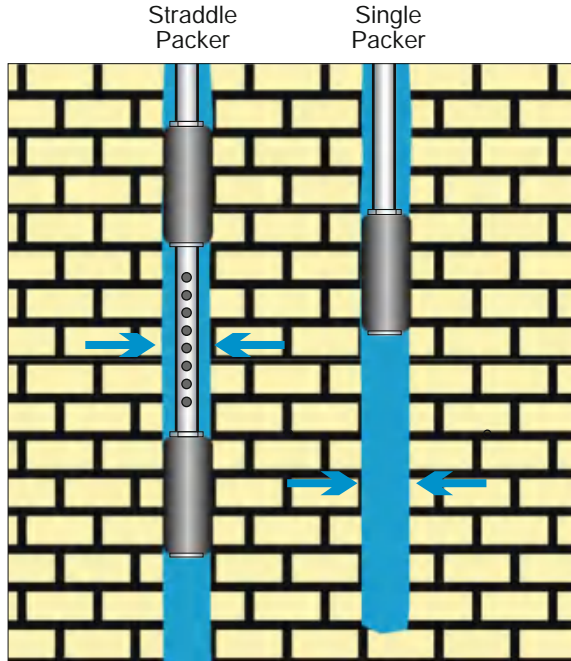
borehole. The depth intervals for tests can be determined upon review of the
lithological and geophysical logs. Multiple tests can also be efficiently performed
by lowering or raising the packer test assembly without having to trip out and back
in to the hole for each tests. Single-packer tests are less prone to leakage as only one
packer is set. Off-bottom testing can be performed immediately after drilling to a
target depth, which may reduce the development time.

Four types of packer tests that are commonly performed in groundwater
investigations (Quinn et al. 2012):

- constant-rate and step injection (Lugeon) tests
- rising and falling head slug tests
- constant-rate and step pumping tests
- recovery tests.

Packer testing equipment is usually very heavy and, therefore, a drilling rig or crane
is needed to install and support the equipment. Well drillers are commonly con-
tracted to perform the test under the supervision of the project hydrogeologist.
Where numerous packer tests are performed (either for a single or multiple pro-
jects), it can be cost effective to assemble a dedicated packer testing system.
Holloway and Waddel (2008) and Quinn et al. (2012) described a multiple-method
packer systems that are capable of efficiently performing all four types of tests. The
integrated systems include two packers, one or two pumps installed between
packers, and pressure transducers located above, between, and below the packers.

8.6.2 Potential Error Sources

The main source of error associated with packer testing is short circuiting of water around the packer elements. Short circuiting can result from a poor packer seal, which may be due to borehole roughness or irregularity, or the use of an improperly sized packer. Inflatable packers are designed to expand to a limited extent and over expansion can result in a poor seal and packer damage.

It is a normal and recommended practice to first run a caliper log or borehole video on the borehole in order to identify areas with borehole conditions that are suitable for the tight seating of packers. Short circuiting may also occur through the formation adjoining the packer, either through fractures (or other secondary porosity features) or the rock matrix. Tests results can also be impacted by skin effects, which may be due to inadequate well development, clogging after construction, and clogging due to suspended solids used in injection tests. Errors in the data analysis may occur as result on non-Darcy flow, which is a greater concern for fractured rock systems in which high flow velocities may occur (Quinn et al. 2012). Errors in the data analysis may also occur if test and aquifer conditions greatly depart from the assumptions of the analytical equation used to interpret the data.

Constant-rate pumping tests are equivalent to single-well aquifer pumping tests in that measured drawdowns are impacted by wellbore effects such as skin effects and frictional head losses. Head losses due to friction will be much greater in packer tests because water is being pumped through a small-diameter drill pipe or tubing. Hence, drawdown measured in the drill pipe near land surface may be much greater than the drawdown (pressure decrease) measured using a transducer set in the packer zone.

8.6.3 Packer Test Data Analysis

Packer test data are analyzed using the same methods as applied to well testing. Time-drawdown data from packer tests are commonly interpreted using a method based on the Theis non-equilibrium equation, either a curve matching or, more commonly, the Cooper and Jacob straight-line method (Sect. 7.3.3). An average hydraulic conductivity value of the tested interval is obtained by dividing the transmissivity value obtained for the tested interval by the thickness of the interval.

Packer tests usually do not follow the assumptions of the Theis non-equilibrium equation, particularly as only part of the aquifer or confining unit is being tested (i.e., partially penetrating conditions occur during the test) and, therefore, vertical flow occurs. The occurrence of vertical flow in packer tests tends to result in an over estimation of hydraulic conductivity (Johnson and Frederick 1997). Alternative methods that may be more appropriate include the Hantush–Walton method for leaky aquifers (Sect. 7.36), and, in the case of fractured aquifers, dual-porosity (e.g., Moench 1984) methods (Johnson and Frederick 1997). Transmissivity may also be

estimated from specific capacity using empirical nonlinear relationships previously established at the site (Johnson and Frederick 1997). As is the case for pumping tests in general, logarithmic and semi-logarithmic plots of the time-drawdown data can reveal departures from ideal (Theis curve) conditions, which can guide subsequent quantitative analysis of the data.

8.6.4   Injection and Lugeon Tests

Constant-pressure injection tests involve injecting water at a constant pressure and recording the change in flow rate over time. They are most often performed to assess low hydraulic conductivity rock. A key consideration is not injecting at such a high pressure as to induce fracture dilation and hydrofracturing, which would increase calculated hydraulic conductivity values. The tests are typically performed on discrete intervals isolated by packers. ASTM (2006b) provides a standard method for constant-head injection test in low permeability rocks. Hydraulic conductivity and storativity data are calculated from flow rate-versus-time plots using the Jacob and Lohman (1952) curve-matching method.

The Lugeon test method was initially developed to assess the need for foundation grouting at dam sites. The basic procedure consists of the performance of a series of steady-state, constant-rate injection tests at progressively increasing and then decreasing pressures. For example, Houlsby (1976) proposed a five-step cycle at low, medium, peak, medium, and then low pressure. Alternatively, a nine-step cycle may be used. The test units (Lugeon value) is the rate of water injected (L/min) per meter of test interval at an over (excess) pressure of 1 MPa.

$$\text{Lugeon} = \frac{q}{L}\frac{P_0}{P} \tag{8.15}$$

where,
q   injection rate (L/min),
L   length of test interval (m),
P   test pressure (MPa), and
P_0 reference pressure (1 MPa, 1145 psi).

A Lugeon unit is the conductivity required for a flow rate of 1 L/min per meter of test interval under a constant pressure of 1 MPa. Under ideal conditions, one Lugeon is equivalent to 1.3×10^{-5} cm/s (Fell et al. 2005).

Variations in the Lugeon value between steps can be indicative of flow conditions (laminar versus turbulent) and temporary or permanent development or dilation of fractures. In the case of laminar flow without the formation or dilation of fractures, the results (Lugeon values) for all steps should be similar. The high pressure used for standard Lugeon tests can cause hydrofracturing, which would result in a greater Lugeon value for the highest pressure step. It is, therefore,

recommended that tests for hydrogeological investigation be performed at low pressures (below fracture pressures; Houlsby 1976). A representative K value is selected based on data trends observed throughout the test (Houlsby 1976).

Interpretation of Lugeon tests was reviewed by Lancaster-Jones (1975), Houlsby (1976), Brassington and Walthall (1985), Fell et al. (2005), and Quiñones-Rozo (2010). Some aquifer test analysis software packages (e.g., AquiferTest Pro^{TM}) have programs for interpretation of Lugeon test data. Transmissivity and average hydraulic conductivity values are calculated using the Thiem equation,

$$T = Kb = \frac{Q}{2pDh} \ln\left(\frac{r_e}{r_b}\right) \qquad (8{:}16)$$

where,

T   transmissivity (m^2/d)
K   hydraulic conductivity (m/d)
B   tested interval thickness (m)
Dh   increase in bottom-hole pressure (net injection head; m of water)
Q   injection rate (m^3/d)
r_e effective radius (m)
r_b borehole radius (m)

The effective radius (radius of investigation) is the radius at which injection no longer causes a pressure change. Calculated transmissivity and hydraulic conductivity values are not sensitive to r_e values of 5 to 10 m, which are commonly used.

8.7   Dipole-Flow Tests

Dipole-flow test setup consists of three packers that isolate two chambers. Water is pumped from the upper chamber into the lower chamber with the flow rate and pressure changes in both chambers recorded (Kabala 1993; Zlotnick and Zurbuchen 1998, 2003). Pressure may also be monitored above and below the packer assembly in order to detect leakage around the packers. In a uniform infinite aquifer, radial hydraulic conductivity can be calculated from the equation for a steady-state test (Zlotnick and Ledder 1996; Zlotnick and Zurbuchen 1998, 2003)

$$K_r = \frac{Q}{2p(Dh)D} \ln\left(\frac{4aU(k)D}{er_w}\right) \qquad (8{:}17)$$

where (using consistent units)

K_r radial hydraulic conductivity (m/d)
Dh   difference in hydraulic head between the upper and low chambers (m)
Q   recirculation rate (m^3/d)

Δ   ½ chamber length (m)
a   anisotropy ratio, $(K_r/K_z)^{0.5}$,
e   2.7182,
r_w borehole radius (m)
U(k) dipole shape function, which ranges from 0.5 to 1.0, depending on k, the
      ratio of packer length (L_p, distance between midpoints of packer zones) to
      chamber length, k = $L_p/2\Delta$.

$$U(k) = \left(\frac{k^2}{k^2-1}\right)^{\frac{k}{2}}\left(\frac{k-1}{k+1}\right)^{\frac{1}{2}} \tag{8:18}$$

The three-packer DFT is effective for evaluation of horizontal hydraulic conductivity profiles, but lacks the sensitivity to accurately quantify vertical hydraulic conductivity (Halihan and Zlotnick 2002). Halihan and Zlotnick (2002) presented an alternative dipole-flow test (DFT), referred to as the asymmetric DFT, which utilizes only a single packer that subdivides the aquifer into an upper and low zone. An analytical (type-curve) method for interpreting asymmetric DFT data was provided. The advantage of the asymmetric DFT over a symmetric DFT is that it is less costly and simpler to install and perform tests. Halihan and Zlotnick (2002) reported that with shallow wells, the system could be raised and lowered by hand. Care must be taken to avoid excessive drawdown (drainage of the upper chamber) and excessive pressure build-up in the lower chamber, which could induce fracturing.

Major advantage of the dipole test is that it does not require water to be added or removed from the formation, which can be an important consideration for contaminated sites. However, it can result in the local redistribution of contaminants between tested zones. A limitation of the method is that it requires values for various parameters, which may not be well known (Butler 2005). Results are also dependent on well development and completion (gravel filter pack).

Zlotnick and Zurbuchen (2003) compared three borehole hydraulic test methods for estimating hydraulic conductivity in an unconfined heterogeneous alluvial in the Platte River watershed of Nebraska. The evaluated tests were

• multilevel slug tests (MLST)
• borehole flowmeter (electromagnetic) (BFT)
• steady-state dipole-flow test (DFT)

The test results demonstrated that there was a strong correlation between the three methods, with an especially strong correlation between the DFT and MSLT. The correlation between the BFT and other two methods was not quite as strong.

8.8 Pressure Transient Testing

8.8.1 Introduction

Pressure transient testing has been used in the oil and gas industry since the 1930s to evaluate wellbore condition and reservoir properties. Pressure transient testing is analogous to pump testing in water wells. However, oilfield pressure transient testing has some specialized applications for aquifer characterization, particularly with respect to deep injection systems. For example, pressure fall-off tests are a type of transient pressure test that are used to evaluate deep injection wells utilized for the disposal of liquid wastes (Johnson and Lopez 2003). Pressure transient testing is conceptually simple, but quite complex in practice, particularly with respect to the interpretation of the data. The history of pressure transient testing was reviewed by Ramey (1982).

Pressure transient testing essentially involves the monitoring of pressure in a well, or multiple wells, in response to a pressure transient, which can be generated by an abrupt change in pumping (flow) or injection. The transient may be the result of either the termination or initiation of production or injection (or reduction in their rates). The data from the tests are compared to modeled responses for various reservoir or aquifer conditions until a satisfactory match is obtained. One of the earliest types of pressure transient testing involved monitoring of bottom-hole pressure (BHP) after a well was shut in. The rate at which BHP increases to static pressure is used to determine the permeability of a formation.

Summaries of pressure transient testing are provided by Deruyck et al. (1992) and Schlumberger (2006). There are a number of dedicated books on pressure transient testing because of its great importance in the oil and gas industry (e.g., Lee 1993; Lee et al. 2003; Kamal 2009; Kuchuk et al. 2010). In the oil and gas industry, the design and interpretation of pressure transient test is a specialized discipline and typically proprietary software packages are used. Pressure transient tests can be designed to provide specific information, for example (Deruyck et al. 1992),

- very short-term impulse test are used to test the near wellbore region for formation damage
- long-term testing is used to investigate reservoir boundaries
- multiple-well interference test can yield data on the transmissivity and storativity of the strata between the wells.

Identification of formation damage is a critical issue because of the high costs of well stimulation. It is important to determine, for example, whether the low productivity of a well is caused by plugging of the well (or other skin damage), a low formation permeability, or small reservoir size. Similarly, pressure transient testing has been used for injection wells to determine whether low injectivity is due to formation damage (which could be addressed through development and stimulation activities) or a low injection zone transmissivity.

8.8.2 Data and Analysis Procedures

The basic data from pressure transient testing is the measured pressure (P) versus time since the transient was initiated (elapsed time; Dt). Data are usually plotted in cartesian, semilog, and log-log scales. In the widely used semilog Horner plot, P is plotted against dimensionless time $(t_p + Dt)/Dt$ (on log scale), where t_p is the duration of the flow period (Fig. 8.10). The Horner plot is appropriate when injection or production prior to shut in was performed at a constant rate. Other semilog plots used in pressure transient test analysis are the Miller Dyes Hutchinson (MDH) plot (log t), Agarwal time plot (equivalent t), and superposition time plot. Log–log plots are also typically used in which DP and its derivative are plotted against Dt (Fig. 8.11). The derivative of pressure is obtained from the slope of the semilog (e.g., Horner) plot.

The shape of the Horner and log–log plot reflects

- wellbore storage
- radial flow to the well, which plots on a straight line
- boundary effects (e.g., faults and other no-flow boundaries)

Radial flow data are the basis for pressure transient calculations. For example, the radial flow data plot on a straight line on a Horner plot, the slope of which (m) is used to calculate permeability and skin factor
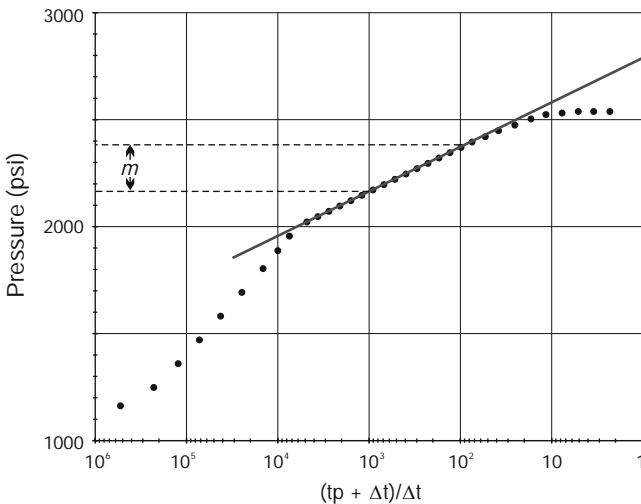
Fig. 8.10 Example of a Horner plot for a pressure build-up test. Permeability is calculated from the slope (m) of the straight-line segment
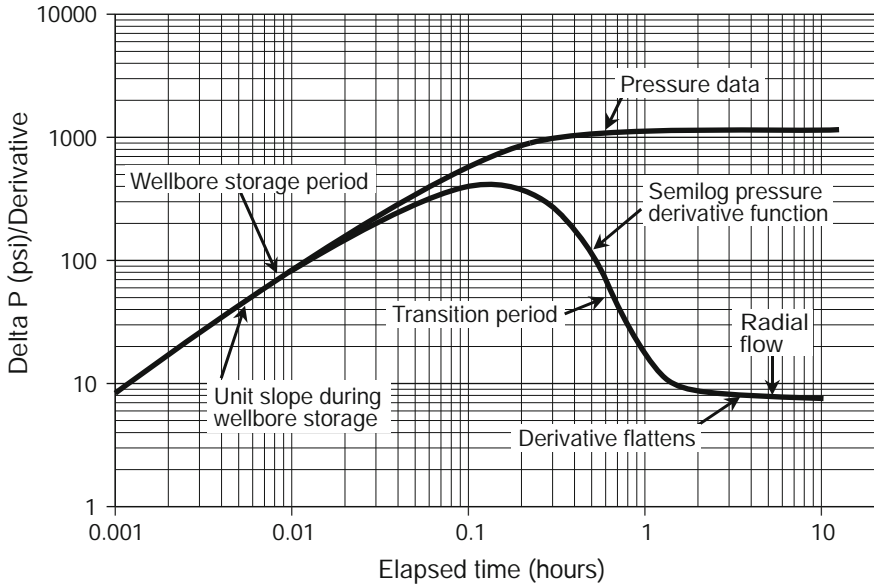
Fig. 8.11   Example of a log-log plot of a pressure transient (pressure fall-off) test (USEPA 2002)

$$k = \frac{162.6Q\mu}{mb} \tag{8.19}$$

$$SF = 1.153\left[\frac{\Delta P_{1h}}{m} - \log\left(\frac{k}{\mu\,C_t r_w^2}\right) + 3.23\right] \tag{8.20}$$

where

k   permeability (md)
Q   pumping or injection rate (bbl/day)
μ   viscosity (cP)
b   aquifer thickness
m   slope of semilog straight line (psi/log cycle)
ΔP_{1h} pressure change after the first hour of shut in (psi)
Ct   total compressibility of formation and fluids (psi^{-1})
R_w wellbore radius (ft)
SF   skin factor (dimensionless)

Skin factor is abbreviated as 'SF' herein as opposed to the conventionally used 'S'
in order to avoid confusion with storativity, which is also abbreviated as 'S'.
Formation damage is indicated by a SF of greater than zero. The pressure (head)
loss associated with the skin (ΔP_s) is calculated as

$$DP_s = 0.87SF \cdot m \tag{8.21}$$

The above equations are in standard oilfield units, which can be converted into equivalent English and SI units used for groundwater investigations. The recovery phase of aquifer pumping tests is essentially a shut-in test. Manahan (1998) provides as example where the Horner plot method was used to calculate wellbore head (skin) losses in water production wells in Tortola, British Virgin Islands.

In a log–log plot of the derivative of pressure (P′) versus Dt, P′ is a constant value in the radial flow part of tests. Permeability can be calculated for P′ values using Eq. 8.22 for a water reservoir (aquifer)

$$P' = 70.6 \frac{QI}{kh} \tag{8.22}$$

where
Q   flow rate (barrels/day; B/d)
k   permeability (mD)
h   thickness of the flowing unit (ft)
l   reservoir fluid viscosity (cp)

Design of pressure transient tests often involves forward modeling so as to evaluate the feasibility of detecting and characterizing the anticipated reservoir features (Deruyck et al. 1992). Tests should be designed so as to reach radial flow and provide a duration of data sufficient for the analysis of the radial flow period. Data interpretation involves first a model diagnosis to determine the reservoir model that provides the best possible fit to the data. The subsequent history matching involves the adjustment of model parameters in order the established a model that predicts the pressure response through all phases of the test and satisfactorily accounts for all of the data (Deruyck et al. 1992). The current state of the art is software that can generate pressure response curves under all conceivable conditions (Ramey 1982).

8.8.3   Step-Rate Injection Tests

Step-rate injection tests are used to evaluate the formation fracture pressure of injection wells (Singh et al. 1987). Multiple steps are performed at progressively greater injection rates and usually both bottom-hole and surface pressure are recorded. The selection of injection rates is based upon design injection rates and pressures and anticipated fracture pressure (formation parting pressure), which are obtained from an estimated fracture gradient derived from regional data. The
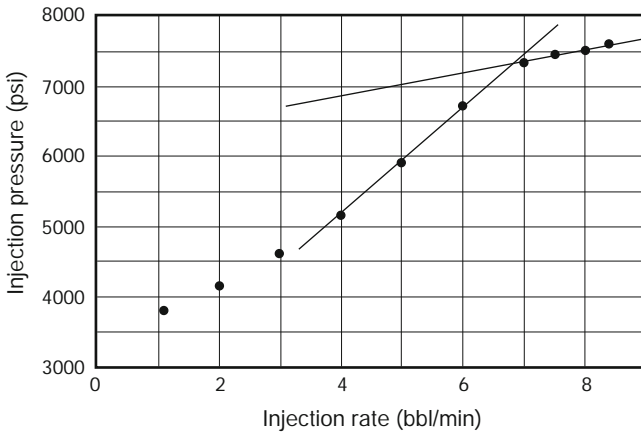
Fig. 8.12 Example of a step-rate injection test. The break in slope at about 7,300 psi marks the increase in transmissivity associated with reaching the formation parting pressure

initiation of fracturing is indicated by a break (decrease in slope) in the downhole pressure versus injection rate plot (Fig. 8.12). The break in slope is the result of an increase in transmissivity caused by the formation and propagation of fractures. In the case of injection well systems, the site-specific formation parting pressure is used to determine the maximum allowable injection pressure.

References

ASTM (2006a) Standard practice for field pneumatic slug (instantaneous change in head) tests for determining hydraulic properties of aquifers with direct push ground water samplers: ASTM International Standard D 7242-06. West Conshohocken: ASTM International.

ASTM (2006b) Standard test method for determining transmissivity and storage coefficient of low-permeability rocks by in situ measurements using the constant head injection test. ASTM Standard D4360-96 (Reapproved 2002). West Conshohocken: ASTM International.

Bartlett, S. A., Robbins, G. A., Mandrick, J. D., Barcelona, M., McCall, W., and Kram, M. (2004) Comparison of hydraulic conductivity determinations in direct push and conventional wells. Naval Facilities Engineering Command, Engineering Service Center Technical Report TR-2252-V.

Bouwer, H. (1989) The Bouwer and Rice slug test – an update. Ground Water, 27, 304–309.

Bouwer, H., & Rice, R.C. (1976) A slug test for determining hydraulic conductivity of unconfined aquifers with completely or partially penetrating wells. Water Resources Research, 12, 423–428.

Brassington, F. C., & Walthall, S. (1985) Field investigation using packers in hydrogeological investigations. Quarterly Journal of Engineering Geology and Hydrogeology, 18, 181–193.

Butler, J. J., Jr. (1998) The design, performance, and analysis of slug tests. Boca Raton: Lewis Publishers.

Butler, J. J., Jr. (2005) Hydrogeological methods for estimation of spatial variations in hydraulic conductivity. In Y. Rubin & S. S. Hubbard (Eds.), Hydrogeophysics (pp. 25–58). Dordrecht, Springer,

Butler, J. J., Jr., & Garnett, E. J. (2000) Simple procedure for analysis of slug tests in formations of high hydraulic conductivity using spread sheet and scientific graphics software. Kansas Geological Survey, Open-File Report 2000-40.

Butler, J. J., Jr., Garnett, E. J., & Healey, J. M. (2003) Analysis of slug tests in formations of high hydraulic conductivity. Ground Water, 41, 620–630.

Butler, J. J., Jr., & Healey, J. M. (1998) Relationship between pump-test and slug-test parameters: scale effect or artifact? Ground Water, 36, 305–313.

Butler, J. J., Jr., McElwee, C. D. & Liu, W. (1996) Improving the quality of parameter estimates obtained from slug tests. Ground Water, 34, 480–490.

Campbell, M. D., Starrett, M. S., Fowler, J. D., & Klein, J. J. (1990) Slug tests and hydraulic conductivity. In Proceedings 4th Petroleum and Organic Chemicals in Groundwater. Prevention, Detection and Restoration, pp. 85–99.

Chen, C.-S., Sie, Y.-C., & Lin, Y.-T. (2012) A review of the multilevel slug test for characterizing aquifer heterogeneity. Terrestrial Atmospheric and Oceanic Sciences, 23(2), 131–143.

Cooper, H. H., Jr., Bredehoeft, J. D., & Papadopulos, I. S. (1967) Response of a finite-diameter well to an instantaneous charge of water. Water Resources Research, 3, 263–269.

Cunningham, W. L., & Schalk, C. W. (Comps.) (2001) Groundwater technical procedures for the U.S. Geological Survey. U.S. Geological Survey Techniques and Methods 1-A1.

Dagan, G. (1978) A note on packer, slug, and recovery tests in unconfined aquifers. Water Resources Research, 14, 929–934.

Deruyck, B., Ehlig-Economides, C., & Joseph, J. (1992) Testing design and analysis. Oilfield Review, 4(2), 28–45.

Fell, R., MacGregor, P., Stapledon, D., & Bells, G. (2005) Geotechnical engineering of dams. London: Taylor & Francis.

Freeze, R. A., & Cherry, J. A. (1979) Groundwater. Englewood Cliffs, Prentice-Hall.

Halihan, T., & Zlotnick, V. A. (2002) Assymetric dipole-flow test in a fractured carbonate aquifer. Ground Water, 40, 491–499.

Holloway, O. G., & Waddel, J. P. (2008) Design and operation of borehole straddle packer for groundwater sampling and hydraulic testing of discrete intervals at U.S. Air Force Plant 6, Marietta, Georgia: U.S. Geological Survey Open-File Report 2008-1349.

Houlsby, A. C. (1976) Routine interpretation of the Lugeon water test. Quarterly Journal of Engineering and Hydrogeology, 9(4), 303–314.

Hvorslev, J. (1951) Time lag and soil permeability in ground-water observations. Vicksburg, Mississippi: Waterways Experimental Station, U.S. Army Corps of Engineers,

Hyder, Z., Butler, J. J., Jr., McElwee, C. D., & Liu, W. (1994) Slug tests in partially penetrating wells. Water Resources Research, 30, 2945–2957.

Jacob, C. E., & Lohman, S. W. (1952) Nonsteady flow to a well of constant drawdown in an extensive aquifer. Transactions of the American Geophysical Union, 33, 559–569.

Johnson, G. S., & Frederick, D. B. (1997) Straddle-packer aquifer test analyses of the Snake River Plain aquifer of the Idaho National Engineering Laboratory. Moscow, Idaho: Idaho Water Resources Institute.

Johnson, K., & Lopez, S. (2003) The nuts and bolts of falloff testing. U.S. Environmental Protection Agency Region 6 (March 5, 2003).

Kabala, Z. J. (1993) The dipole flow test: A new single-borehole test for aquifer characterization. Water Resources Research, 29, 99–107.

Kamal, M. M. (2009) Transient well testing. Richardson, Texas: Society of Petroleum Engineers Monograph Series Vol. 23.

Kuchuk, F. J., Onur, M., & Hollaender, F. (2010) Pressure transient formation and well testing: Convolution, deconvolution and nonlinear estimation. Amsterdam: Elsevier.

Lancaster-Jones, P. F. F. (1975) The interpretation of the Lugeon water-test. Quarterly Journal of Engineering Geology and Hydrogeology, 8, 151–154.

Leap, D. I. (1984) A simple pneumatic device and technique for performing rising water level slug tests. Ground Water Monitoring and Remediation, 4(4), 141–146.

Lee, W. J. (1993) Pressure transient testing. In D. Morton-Thompson & A. M. Woods (eds.), Development Geology Reference Manual, AAPG Methods in Exploration Series No. 10 (pp. 477–481). Tulsa: American Association of Petroleum Geologists..

Lee, J., Rollins, J. B., & Spivey, J. P. (2003) Pressure transient testing. Richardson, Texas: Society of Petroleum (SPE).

Manahan, W. S. (1998) Ocean conversion seawater desalination facility reverse osmosis wellfield expansion Tortola, B.V.I. In Third International Symposium on Water Resources. Fifth Caribbean Islands Water Resources Congress (Proceedings, pp. 207–212), American Water Resources Association.

Mas-Pla, J., Jim Yeh, T. C., Williams, T. M., & McCarthy, J. F. (1997) Analysis of slug tests and hydraulic conductivity variations in the near field of a two-well tracer experiment site. Ground Water, 35, 492–501.

McElwee, C. D., & Ross, H. C. (2001) Towards a 3-D picture of hydraulic conductivity with multilevel slug tests. Kansas Geological Survey Open-File Report 2001-51.

McElwee, C. D., & Zemansky, G. M. (1999) Improved definition of hydraulic conductivity structure using multilevel nonlinear slug tests. Kansas Geological Survey Open-File Report 1999-57.

McLane, G. A., Harrity, D. A., & Thomsen, K. O. (1990) A pneumatic method for conducting rising and falling head tests in highly permeable aquifers. In Proceedings of 4th Annual NWWA Outdoor Action Conference, pp. 1219–1231.

Melville, J. G., Molz, F. J., Güvem, O., & Widdowson, M. A. (1991) Multilevel slug tests with comparisons to tracer data. Ground Water, 29, 897–907.

Moench, A. F. (1984) Dual-porosity models for a fissured groundwater reservoir with fracture skin. Water Resources Research, 20, 831–846.

Muldoon, M., & Bradbury, K. R. (2005) Site characterization in densely fractured dolomite: Comparison of methods. Ground Water, 43, 863–876.

Novakowski, K. S. (1989) Analysis of pulse interference tests. Water Resources Research, 25, 2377–2387.

Paradis, D., & Lefebvre, R. (2013) Singe-well interference slug tests to assess vertical hydraulic conductivity of unconsolidated aquifers. Journal of Hydrology, 478, 102–118.

Prosser, D. (1981) A method of performing response tests on highly permeable aquifers. Ground Water, 10, 588–592.

Quiñones-Rozo, C. (2010) Lugeon test interpretation, revisited. In Collaborative Management of Integrated Watersheds, U.S. Society of Dams, 30th Annual Conference, pp. 405–414.

Quinn, P., Cherry, J. A., & Parker, B. L. (2012) Hydraulic testing using a versatile straddle packer systems for improved transmissivity estimation in fractured-rock boreholes: Hydrogeology Journal, 20, 1529–1547.

Ramey, H. J., 1982, Pressure transient testing. Journal of Petroleum Technology, 34(7), 1407–1413.

Ross, H. C., & McElwee, C. D. (2007) Multi-level slug tests to measure 3-D hydraulic conductivity distributions. Natural Resources Research, 16, 67–79.

Schlumberger (2006) Fundamentals of formation testing. Sugar Land, Texas: Schlumberger Marketing Communications.

Schmidley, E. B., & Kirsch, M. C. (1994) Application of a packer system pneumatic slug test method for estimating hydraulic conductivities of fractured rock aquifers. In Proceedings of the Focus Conference on Eastern Regional Ground Water Issues, National Ground Water Association, pp. 391–406.

Sellwood, S. M., Healey, J. M., Birk, S., & Butler, J. J., Jr. (2005) Direct-push hydrostratigraphic profiling: coupling electrical logging and slug tests. Ground Water, 43, 18–29.

Singh, P. K., Agarwal, R. G., & Krase, L. D. (1987, January). Systematic design and analysis of step-rate tests to determine formation parting pressure. In SPE Annual Technical Conference and Exhibition. Society of Petroleum Engineers. Society of Petroleum Engineers, SPE-16798.

Spane, F. A. (1996) Applicability of slug interference tests for hydraulic characterization of unconsolidated aquifers: (1) analytical assessment. Ground Water, 34, 66–74.

Spane, F. A., Thorne, P. D., & Swanson, L. C. (1996) Applicability of slug interference tests for hydraulic characterization of unconsolidated aquifers: (2) field test examples. Ground Water, 34, 925–933.

Springer, R. K. & Gelhar, L. W. (1991) Characterization of large-scale aquifer heterogeneity in glacial outwash by analysis of slug tests with oscillatory response, Cape Cod, Massachusetts. U.S. Geological Survey Water-Resources Investigations Report 91-4034 (pp. 36–40).

USEPA (2002) UIC pressure fall off testing guidelines (3rd Rev.). U.S. Environmental Protection Agency Region 6.

Weight, W. S. (2008) Hydrogeology field manual (2nd Ed.). New York: McGraw-Hill.

Widdowson, M. A., Molz, F. J., & Melville, J. G. (1990) An analysis of technique for multilevel and partially penetrating slug test data. Ground Water, 28, 937–945.

Yang, S.-Y., & Yeh, H.-D. (2004) A simple approach using Bouwer and Rice's method for slug test data analysis. Ground Water, 42, 781–784.

Zlotnick, V. (1994) Interpretation of slug and packer tests in anisotropic aquifers. Ground Water, 32, 761–766.

Zlotnick, V. A., & Ledder, G. (1996) Theory of dipole flow in uniform anisotropic aquifers. Water Resources Research, 32, 1119–1128.

Zlotnick, V. A., & Zurbuchen, B. R. (1998) Dipole probe: design and field application of a single-borehole device for measurement of vertical variations of hydraulic conductivity. Ground Water, 36, 884–893.

Zlotnick, V. A., & Zurbuchen, B. R. (2003) Field study of hydraulic conductivity in a heterogeneous aquifer: comparison of single-borehole measurements using different instruments. Water Resources Research, 39, 1101, WR001415.

Chapter 9
Small-Volume Petrophysical, Hydraulic, and Lithological Methods

Small-volume methods are, in essence, point measurements of the petrophysical and hydraulic properties and lithology of aquifer and confining strata. Small-volume methods have the advantage that they are often relatively simple and inexpensive to perform, but have the limitation that the results of individual analyses are usually not representative of the tested hydrogeological unit as a whole. They can provide valuable information on small-scale heterogeneity, which is important for understanding and predicting solute-transport. Hydraulic conductivity is determined by core analyses, minipermeameter testing, and using grain size data. Methods used to evaluate the lithology and mineralogy of aquifers include core and cutting descriptions, thin-section petrography, and x-ray diffractometry. Thin-section petrography, scanning electron microscopy, and mercury-injection porosimetry are used to evaluate pore type and size distribution.

9.1 Introduction

Small-volume methods refer herein to analyses that are usually performed on hand or smaller-sized samples, although some cores and sand samples may be somewhat larger. In relatively homogeneous formations, small-volume data may provide reasonable estimates of bulk aquifer properties, which would be of value if data from larger-scale tests are not available. Small-volume measurements are useful for evaluating aquifer heterogeneity. For example, hydraulic conductivity of small (core or core plug-sized) samples of the rock matrix can be compared to formation-scale values obtained from pumping tests to evaluate the contribution of secondary porosity (e.g., fractures and conduits) to the aquifer transmissivity. In carbonate rocks with well-developed secondary porosity, average hydraulic conductivity values obtained from pumping tests may be orders of magnitude greater than the hydraulic conductivity values obtained from core analyses. Data on the properties of the rock matrix are needed for dual-domain solute-transport models.

Most lithological analyses are performed on small-volume samples. Samples may be collected and analyzed either in a random pattern or at pre-determined regular intervals (e.g., every foot or meter), or selectively to include samples that are representative of the various lithologies present in the investigated strata. A combination of these sampling strategies may be optimal, with a random or interval sampling performed to obtain an unbiased sample population of average conditions and targeted samples collected of strata that might be of mineralogical or geochemical significance. Trace mineral phases may have a disproportionate geochemical impact. For example, the release of arsenic from the dissolution of pyrite present in trace quantities (much less than 1 % of the formation mass) is a major regulatory and operational issue for aquifer storage and recovery (ASR) systems in Florida and elsewhere. Sampling to evaluate the arsenic concentration of an aquifer might target lithologies that are potentially rich in pyrite.

9.2 Core Analyses

Core samples are collected as part of aquifer characterization programs to obtain high-quality samples for lithological, petrophysical, and chemical analyses. Coring procedures are discussed in Sect. 6.3.2. Analyses of core samples are commonly performed by commercial laboratories, the largest of which focus primarily on the needs of the oil and gas industry. Some geotechnical laboratories, as well as some universities and geological surveys, are also equipped to perform routine core analyses. Equipment for core analysis is commercially available. Core analysis procedures were reviewed by Monicard (1980), Ethridge (1992), API (1998), and Anderson et al. (2013).

Core analyses are usually performed on either core plugs drilled from whole core samples, whole core samples, or sidewall cores. Core plugs have standard diameters of 1 inch (2.5 cm) and 1.5 inches (3.8 cm). The plugs are taken in either the horizontal or vertical direction. Core plugs may be drilled out by members of a project team, if they have access to core storage and handling facility with the required equipment (water-cooled and lubricated drill press and bits). Most core laboratories will perform sample preparation, particularly the drilling of core plugs, which entails additional laboratory and shipping costs. If a modest number of core analyses are to be performed, then selected pieces of a core may be shipped to a core laboratory for processing and analysis.

Routine core analyses include porosity, permeability (hydraulic conductivity), and grain density. Cores samples are typically also described for lithology to various degrees of detail and may be slabbed and photographed. Core samples may also be analyzed for geomechanical properties (Young's modulus, Poisson's ratio, compressional and shear velocity). More advanced techniques include core computer tomography (CT), which is performed to detect and evaluate internal structures, such as bedding planes, vugs, fractures, and pore geometry. In the oil and gas industry, entire cores may be run through a core gamma ray logger, which measures the natural

gamma radiation emitted by the core. Comparison of a core gamma ray log with a borehole gamma ray log from the same depths allows for the correlation of core depth with log (borehole) depth (i.e., identification and correction of core shifts).

Porosity and hydraulic conductivity are the primary parameters of interest for groundwater investigations. Core analyses have the inherent limitation that only a minute fraction of the aquifer is being tested, which is the volume of the core sample. Another important limitation of core analyses is that permeability and hydraulic data from cores are often not representative of the average value or transmissivity of the formation because the most permeable strata tend to be under represented. It is not uncommon for the most permeable strata to either not be recovered or be recovered as rubble. Large secondary porosity features that dominate flow are often also not recovered or recorded in cores. Hence, a first step in core analysis is evaluation of the percent of core recovery from the depth interval under investigation and consideration of what strata may not have been recovered and how the absence of the unrecovered strata may impact data analysis and interpretation.

9.2.1   Porosity Measurement

The porosity (n) of a core sample is determined from the bulk volume (V_B) of the sample and either the volume of grains or rock (V_G) or pore volume (V_P), as follows

$$n = \frac{V_P}{V_B} = \frac{V_B - V_G}{V_B} = \frac{V_P}{V_P + V_G} \tag{9:1}$$

For core samples, bulk volume can be calculated from the dimensions of the sample. Inasmuch as core and core-plug samples are typically right circular cylinders, their volume can be calculated as the product of their cross-sectional area and length (l),

$$V_B = \frac{pd^2l}{4} \tag{9:2}$$

where d is the diameter.

Bulk volume can also be measured using Archimedes principle by weighing a saturated sample suspended in air (w_a) and then weighing the sample submerged under a liquid (w_l). The bulk volume is the weight difference divided by the liquid density (q_l).

$$V_B = \frac{(w_a - w_l)}{q_l} \tag{9:3}$$

The measurements may be performed using a non-wetting liquid (e.g., mercury) that does not enter the pore spaces. Alternatively, if a wetting liquid is used (e.g., water), w_a is the weight in air of the sample saturated with the liquid.

A third method used for determining the bulk volume of samples is by fluid displacement. The bulk volume of a sample is equal to the volume of liquid it displaces when submerged. The bulk volume will be underestimated if some of the fluid enters the pores before the displaced water volume in measured. Therefore, a non-wetting fluid (not water) should be used. Mercury is most often used as a non-wetting fluid.

Grain volume (V_g) can be determined from the mass of the core plug and the average density of the grains or rock. Grain density, in grams per cubic centimeters (milliliters), may be obtained from the specific gravity of the minerals, which are typically reported using freshwater as the reference substance. The density of water is approximately 1 g/cc, with the exact values depending upon temperature and pressure. The average grain or rock density may be estimated from the percentages of the main mineral phases present and their known (published) specific gravities. The specific gravities of the common sedimentary rock minerals quartz, feldspar (orthoclase), and calcite, are 2.65, 2.56, and 2.71, respectively. The difference in specific gravity between the minerals is modest and, thus, inaccuracies in the estimated mineral abundances will not have a great impact on calculated grain volumes.

Commercial core laboratories, particularly for oil and gas industry work, usually measure porosity by helium porosimetry. Helium gas is inert and is able to fill all connected pore spaces. A helium gas-expansion pycnometer is based on Boyle's law, which states that for a fixed amount of gas at a constant temperature, pressure and volume are inversely proportional. The basic principle is that if a given volume of gas is added to a chamber containing a solid, the lesser gas volume caused by the solid grains or rock results in a measurably greater pressure then would occur in an empty chamber. The helium (gas) pycnometer apparatus has two chambers of known volumes, a reference chamber and sample chamber with volumes V_r and V_c, respectively. At the start of a test, the two chambers are open to each other and the initial, ambient pressure is measured (P_a). The valve between the two chambers is closed and, for the common system design, the sample chamber is pressurized to pressure (P_i). The valve is then opened and a final pressure is measured (P_f). Sample volume (V_s) is calculated as follows (using consistent units)

$$V_s = V_c - \frac{V_r}{\left(\frac{P_i - P_a}{P_f - P_a}\right)} \tag{9:4}$$

If P_a is zeroed prior to pressuring, then the equation simplifies to

$$V_s = V_c - \frac{V_r}{\left(\frac{P_i}{P_f}\right)} \tag{9:5}$$

Helium pycnometers are calibrated against samples with known V_G values. Grain densities are calculated by dividing the sample mass by the measured V_G values.

9.2.2 Hydraulic Conductivity and Permeability Measurement

Hydraulic conductivity and permeability measurements are based on Darcy's Law. The rate of fluid (liquid or gas) flow through a sample is proportional to the head gradient and the permeability of the sample. The hydraulic conductivity of a core sample with respect to water (of a given temperature and density) can be measured directly by recording the rate of flow of water through the sample. Core analyses performed by laboratories that cater to the oil and gas industry usually measure the flow rate of air or another gas (e.g., nitrogen or helium) through a sample and process the data to provide intrinsic permeability values, which are usually expressed in millidarcies. For groundwater investigations, permeability values are converted to hydraulic conductivity values, which require information on the viscosity and density of water under aquifer temperature conditions.

A key aspect of hydraulic conductivity measurements is that the flow of fluid must actually be through the sample, and not along the boundary between the sample and the holder (i.e., there should not be significant bypass flow). Commercial laboratories usually use a Hassler type core holder (or comparable system) in which the sample is placed in a tight elastomer sleeve that prevents bypass flow. Hassler type core holders can place radial pressure on the core sample to duplicate deep formation conditions.

Hydraulic conductivity and permeability are measured using either the constant-head or falling-head method (Fig. 9.1). The constant-head permeameter is conceptually the simplest instrument as it is based directly on Darcy's law. A differential pressure (head, Dh) is applied across the sample and the rate of discharge is recorded once steady-state flow through the sample is established. In the simple type of system illustrated in Fig. 9.1, a constant head is maintained by connecting the sample holder to a reservoir whose water level is kept constant.

The hydraulic conductivity of the sample is calculated as follows:

$$K = \frac{QL}{ADh} \tag{9:6}$$

where,
K   the hydraulic conductivity (cm/s),
Q   the flow rate (cm^3/s),
L   the length of the sample, (cm)
A   the cross-sectional area of the sample (cm^2), and
Dh   head differemce (cm)

Constant Head   **Falling Head**
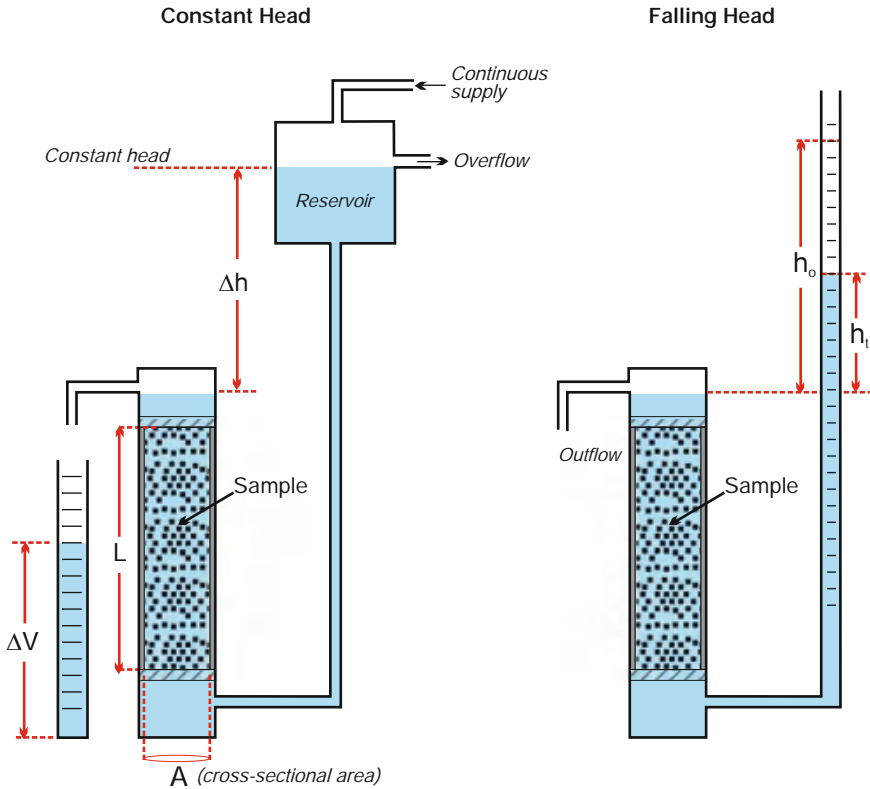
Fig. 9.1 Conceptual diagrams of basic falling-head and constant-head permeameters used to determine hydraulic conductivity

Gas (air) permeability measurements are performed using a constant-head methodology in which a gas of know viscosity and density (e.g., air, nitrogen, helium) is induced to flow through a sample at a constant rate and the pressure drop across the sample is measured. Air permeability (k_a, md) is a function of the dynamic viscosity of air (l, cP) and the pressure drop across the core plug (DP, atm) as follows:

$$k_a = \frac{l\,Q}{A}\frac{L}{DP}\,1000 \tag{9:7}$$

where,
Q   volumetric air flow rate (cm^3/s),
L   core length (cm)
A   cross-sectional area of the core (cm^2)

Air permeability measurements result in a significant overestimation of water permeability because of the 'Klinkenberg effect'. The Klinkenberg effect is caused by 'gas slippage' at pore walls. Liquids experience greater flow resistance (drag) at pore walls than gases. Gas slippage results in greater gas flow at a given differential pressure and thus greater calculated permeability values than obtained using water. The Klinkenberg effect has greater importance for fine pore sizes. The Klinkenberg effect can be corrected for and laboratory reports often include an air permeability value and a 'Klinkenberg permeability' or 'Klinkenberg-corrected permeability'.

The falling-head permeameter used to measure hydraulic conductivity of sediment and rock samples consists of water reservoir attached to one end of the sample. A burette or other graduated device is typically used for the reservoir (Fig. 9.1). A water flow is first established through the sample to ensure that it is fully saturated. The actual test is then performed by refilling the reservoir and recording the initial and final heads and the elapsed time (Dt). Hydraulic conductivity is calculated using the equation

$$K = 2.303 \left(\frac{A_r L}{A_c Dt} \right) \log \left(\frac{h_0}{h_t} \right) \tag{9.8}$$

where,

K   hydraulic conductivity (cm/s)
A_r cross-sectional area of the reservoir (graduated device; cm^2),
L   core length (cm)
A_c cross-sectional area of the core (cm^2),
h_0 and h_t initial and final head (cm)

Several repeat analyses should be performed for each test to ensure consistent results. Advantages of the falling-head test are that it is simple to perform and the equipment required for a basic apparatus is relatively inexpensive. A limitation of hydraulic conductivity measurements using water with heads generated by gravity is that an exceedingly long time may be required to achieve an adequate flow volume through very low-permeability samples because of the small heads applied. Constant-head permeameters using gases are more suitable for low-permeability samples because of the low viscosity of gases and greater heads can be applied. Use of gas for permeability measurements is also preferred where the flow of water through a sample could affect its petrophysical properties, such as where the formation contains evaporite or water sensitive minerals (e.g., swelling clays). Hydraulic conductivity measured under laboratory conditions should be corrected for temperature-dependent differences in viscosity if the laboratory temperature is significantly different from aquifer temperatures. Changes in reservoir water levels may need to be corrected for evaporation for long-duration falling-head tests.

9.2.3   Analyses of Unconsolidated Sediments

Core analyses of unconsolidated strata can be performed on artificial cores, which are packed cylinders of sediment samples, or actual cores collected using thin-walled samplers (e.g., Shelby tubes). Hydraulic conductivity measurements of soils were reviewed by Daniel (1994). Sediment samples may be analyzed using either a flexible-wall or rigid-wall permeameter. Flexible-wall permeameters allow for the application of a confining pressure and are considered to be less susceptible to sidewall leakage (Samingan et al. 2003). Rigid-wall permeameters have the advantages of being simpler and less expensive (Daniel 1994). ASTM (2010) developed a standard for hydraulic conductivity measurements using flexible-wall permeameters. Both rigid-wall and flexible-wall sample holders are commercially available.

A source of error in analyses of the unconsolidated sediments is that the original grain packing and heterogeneity (e.g., fine-scale layering) is disturbed to varying degrees during sample collection and preparation and, therefore, the measured hydraulic conductivity values may differ from in situ values. Use of relatively undisturbed core samples is preferred over repacked samples. However, the coring process can impact sample properties.

Cai et al. (2015) proposed an integrated laboratory method, called the modified constant-head permeameter test (MCHP), to determine directional hydraulic conductivity in fine- to medium-grained sandy sediments. Percussion drilling was used to obtain 10 cm diameter core samples. Vertical hydraulic conductivity was measured using 25 cm long whole core samples. Horizontal hydraulic conductivity was measured on 3.8 cm diameter samples taken horizontally from the 10 cm diameter cores. Quality control procedures are recommended. For example, whether or not the horizontal core samples were disturbed is evaluated by comparing bulk densities. The experimental procedures also include controls to ensure that samples are fully saturated when hydraulic conductivity is measured. As is always the case in aquifer characterization, meticulous attention to detail is critical for ensuring the collection of high-quality data.

9.2.4   Core-Flow Tests

The petrophysical properties of rock can be altered as the result of fluid-rock interactions, which is an important concern for recharge and injection well systems in which the water that is introduced into a formation is chemically dissimilar to the native groundwater. The potential for fluid-rock interaction can be evaluated by core-flow tests in which the water used in the test is chemically similar to (or an actual sample of) the water to be introduced into the formation. The preferred method is to first saturate the core sample with either actual native aquifer water or reconstituted aquifer water, and then obtain a baseline hydraulic conductivity value

with the native water. The core sample is next tested with the water(s) to be introduced into the formation (e.g., Mukhopadhyay et al. 2004). Changes in hydraulic conductivity would reflect either clogging processes, which decrease hydraulic conductivity, or dissolution processes, which increase hydraulic conductivity.

Core-flow tests are most easily performed using a constant-head permeameter, which allows for multiple pore volumes to pass through the sample. Core-flow tests have the same basic requirements as routine core analyses, such as accurate data measurements and avoidance of bypass flow. In addition, the tests should have a sufficient long duration and flow through volume so that the test could detect gradual changes in porosity and permeability. Core-flow tests have particular value for evaluating the water sensitivity of formations because hydraulic conductivity decreases from clay swelling and dispersion are usually rapid. Dissolution and precipitation process, on the contrary, may be quite slow. Chemical analysis of the influent and effluent can provide information of geochemical processes active during the test. Core-flow through tests can also be used to evaluate the effectiveness of a rock or sediment in filtering out suspended solids.

9.2.5   Mercury-Injection Porosimetry

Mercury-injection porosimetry is a widely used technique in the oil and gas industry to measure the capillary pressure and estimate the pore-size distribution of core samples. Mercury, which is a non-wetting liquid, is injected into samples at progressively increasing pressures, with both injection pressure and percent saturation (porosity filled) recorded (Fig. 9.2). The basic principle is that the hydraulic pressure applied for injection of mercury into the sample is inversely proportional to the pore radii in the sample. Greater pressures are required to push mercury into smaller pores. The pressure and percent saturation data are processed to determine pore throat radii, pore throat size distribution, and mean hydraulic radius (MHR). Mercury-injection porosimetry was reviewed by van Brakel (1981), Webb (2001) and Giesche (2006).

Mercury-injection porosimetry is a standard test in the oil and gas industry and there are many commercial laboratories that can perform the analyses. However, it is a specialized technique with respect to groundwater investigations as it has limited practical applications. One notable example of the use of the mercury-injection porosimetry in a groundwater project is in support of an investigation of an aquifer storage and recovery project in Kuwait, where it was used to investigate the susceptibility of a formation to physical clogging (Mukhopadhyay et al. 2004). The issue of concern is the relationship between the size of suspended particles and the MHR. If the particles are smaller than the MHR, then it was thought that they can pass through most pore throats and would have a lesser impact on hydraulic conductivity.
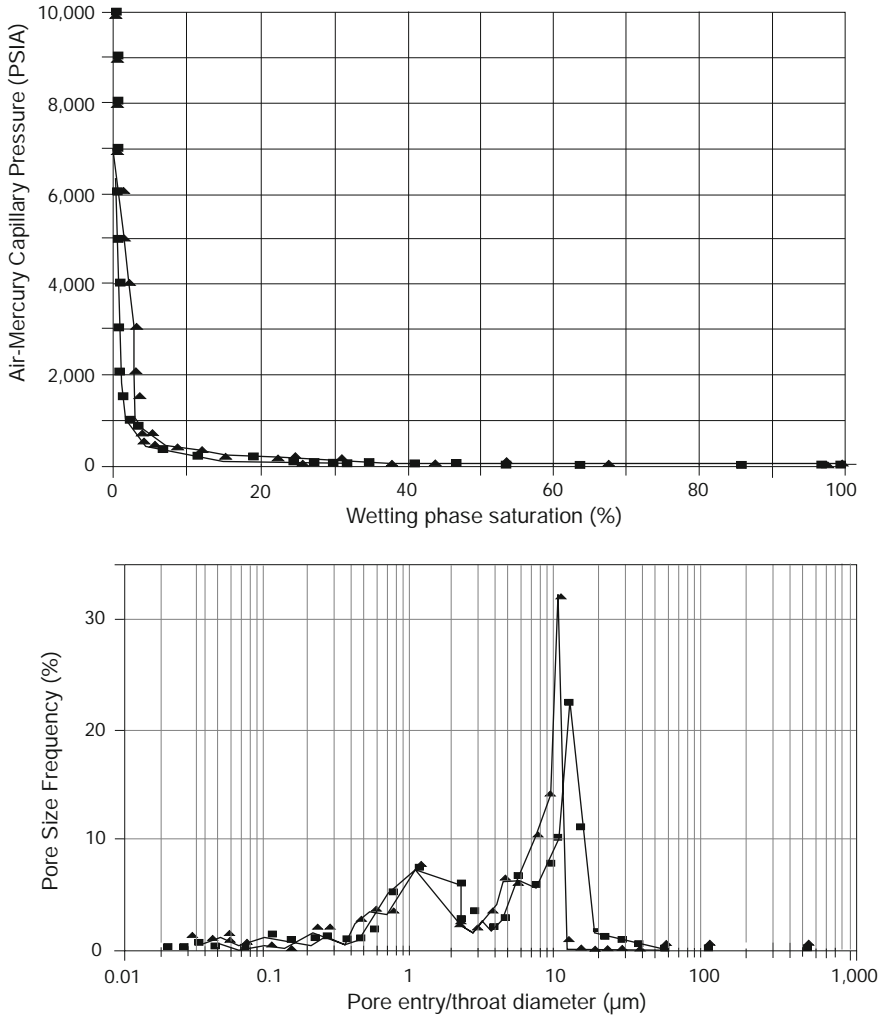
Fig. 9.2 Example of mercury-injection porosimetry data. Plots are of capillary pressure versus saturation (top) and pore throat diameter distribution (bottom) under ambient (squares) and in situ stress (triangles) conditions (from Keighin 1997)

9.3 Minipermeameter

The minipermeameter has emerged as a cost-effective tool for performing rapid and inexpensive permeability measurements on cores and outcrops. The design and operation of the minipermeameter was described by Goggin (1993), Sutherland et al. (1993), Sharp et al. (1994), and Hurst and Goggin (1995). The basic design of a minipermeameter consists of a hollow probe tip that is fitted with an O-ring to

allow for a tight pressure seal with a slabbed core or outcrop surface. Air (or nitrogen gas) is injected into the sample through the probe, the rate of flow of which is a function of the injection pressure and permeability of the sample. Readings are made once a steady-state, constant injection pressure and air flow are achieved. The air flow rate and injection pressure data are converted to permeability values using empirical relationships based on standard core analyses and minipermeameter readings of the same sample.

The conventional minipermeameter utilizes surface sealing between the probe and formation, which is susceptible to leakage. An alternative design is the small-drill-hole minipermeameter, in which permeability is measured in a hole drilled into the formation and then vacuum cleaned (Dinwiddie 2005). The main advantages of the small-drill-hole minipermeameter are (Dinwiddie 2005):

- minimization of the influence of outcrop weathering on permeability
- provision of an operator-independent sealing mechanism
- the potential for collection of samples at multiple depths behind the outcrop surface
- that the method can be performed on weakly cemented rock in which obtaining intact core plugs is often not possible.

The probe described by Dinwiddie (2005) is designed to be run on holes drilled with a 1.6 cm (5/8 inch) diameter masonry bit.

The major advantage of the minipermeameter is that the technique is rapid and inexpensive. As a result, a very large number of the analyses may be performed in a study, which would be cost prohibitive using routine core-plug analyses. Such large data sets are of clear value as input for geostatistical methods. The miniperme-ameter technique also has the advantage of being non-destructive as it does not require the drilling of holes into cores.

For example, over 12,000 minipermeameter measurements were performed in a study of matrix permeability in the Floridan Aquifer in west-central Florida (Budd and Vacher 2004). The limitation of the minipermeameter is that is has a very small volume of investigation, which is a function of the probe tip diameter. The probe tip used in the Budd and Vacher (2004) study was 0.3 mm in diameter. The quality of the data obtained depends upon the skill and diligence of the operator. Multiple analyses should be performed at each spot and standards run frequency to ensure the accuracy of the measurements and to obtain a satisfactory calibration. Another significant issue in the interpretation of the data is whether the measurement is a horizontal or vertical permeability value, or, more likely, a combination of both.

Several studies have been performed comparing the results of minipermeameter and core-plug permeability measurements. Sharp et al. (1994) observed that the minipermeameter tends to give greater permeability values than core-plug analyses with the discrepancy increasing with decreasing permeability. It was posited that the discrepancy was due to leakage at the probe tip and gas slippage (Klinkenberg effect). Probe leakage becomes a more significant issue for uneven surfaces and low-permeability media.

In other studies, the minipermeameter and core-plug permeability measurements gave similar values. For example, in a study of Lower Cretaceous sandstones from Wyoming, Schatzinger and Tomutsa (1999) reported that core-plug and minipermeameter analyses gave similar ranges of permeability for equivalent depositional facies. Chandler et al. (1989) similarly documented that minipermeameter and core-plug analyses from each depositional environment of the eolian Page Formation (Middle Jurassic) of Arizona gave comparable permeability values.

Taylor and Vinopal (1999) in a study of the Tensleep Formation of Wyoming performed minipermeameter measurements at a density of 8–10 measurement per foot (0.3 m) of core, whereas conventional core-plug analyses were performed every one foot. It was observed that in samples with relatively uniform matrix porosity and permeability, less expensive minipermeameter analyses provided equivalent data to that provided by more expensive conventional core-plug analyses. In samples containing fractures and vugs (i.e., more heterogeneous porosity and permeability), minipermeameter readings, when performed at a high sample resolution ($\approx$10/ft), provide more representative permeability values than a single core-plug analysis performed over the same interval.

A primary application of the minipermeameter in groundwater investigations is that it could be used to provide large quantities of data for geostatistical analyses. Analyses of core samples could be used to provide facies-specific data. If one or more exposures of an aquifer are available, then permeameter data could be used to obtain geospatial permeability data. The small volume of investigation of the minipermeameter allows for the evaluation of the skins (alteration zones) of fractures (Sharp et al. 1994). Disadvantages of the minipermeameter are that results may vary depending upon field conditions and between different operators, and field measurements can be affected by water saturation (Hornung and Aigner 1999).

9.4   Sand Grain Size Analysis

There has been considerable research on the use of grain (particle) size distribution to estimate permeability in unconsolidated sediments. The grain size distribution of unconsolidated sediments can be readily measured in materials in the sand and granule-size range by sieving. It is simpler, quicker, and less expensive to measure grain size distribution than to directly measure permeability.

A fundamental requirement for the use of grain size distribution to determine permeability is that representative sediment samples be collected and analyzed. The samples should undergo minimal mixing during collection (i.e., sample should be derived entirely from the depth interval to be tested) and there should be no size separation during collection. The preferred method for collection of samples at depth is through coring. In shallow strata, grab samples may be collected from the walls or bottom of excavations or using a post-hole digging tool or hand auger. Sediment samples collected from the discharge of rotary drilling should be avoided as size separation occurs during transport to land surface. Very fine-grained (silt and

clay-sized) material may pass through sample collection screens and not be recovered. Another basic requirement is that the sediment be completely uncon-solidated and non-cohesive. Partial cementation or cohesion from clay minerals can bind fine-grained particles into grain clusters that are incorrectly measured as coarse-grained particles. The grain size distribution of samples is processed using empirical relationships to obtain permeability values.

9.4.1 Grain Size Analysis Procedures

Measurements of the grain size distribution of sand and coarse-grained materials are normally performed by dry sieve analysis. The procedure for performing sieve analyses are included in most geotechnical and soil mechanics text books. Soil testing methods, in general, are presented in the U.S. Department of Agriculture laboratory methods manual (USDA 2014). ASTM (2007) developed a standard method for grain size analysis. The basic procedure for the dry sieve analysis of a sand sample consists of the following steps:

(1) Oven dry and very gently disaggregate the sample using a mortar and pestle if there is some adherence of grains.
(2) Gently clean each sieve with a brush and weigh each sieve and the bottom pan.
(3) Stack sieves in descending order with the sieve having the largest opening on top and a pan on the bottom.
(4) Weigh the sample to be tested. An approximately 100 g sample is sufficient for analysis of sand-sized sediment. A larger sample is appropriate for gravel-sized material.
(5) Place the sample on a mechanical shaker for 10–15 min.
(6) Starting with the coarsest sieve, weight the sieve or pan and calculate the mass of material retained.
(7) Calculate the percent retained and a cumulative mass retained and percent finer.
(8) Generate a semi logarithmic plot of percent finer (i.e., percent of material that passed through a sieve) versus grain size (taken as sieve size) in millimeters, with grain size on a logarithmic axis (Fig. 9.3).

The mesh sizes of the sieves used should be based upon the grain size of the material. The coarsest sieve in the stack should be the minimum size that allows all of the material to pass. The smallest sieve size used is a U.S. No. 200 mesh, which has an opening of 0.074 mm. Smaller particles cannot be accurately measured by dry sieving. Using a greater number of sieves increases the resolution of the size distribution curve. A reasonable approach is to use a fixed ratio between mesh sizes of the square root of two (1.414), which results in a doubling of the mesh opening area at each sieve size (Table 9.1). The mesh size of sieve stack increases in 1.414 times steps from the No. 200 sieve (Option A). Alternatively, the sieve stack could be ordered so that the mesh sizes correspond to the boundaries between grain size categories (Option B).
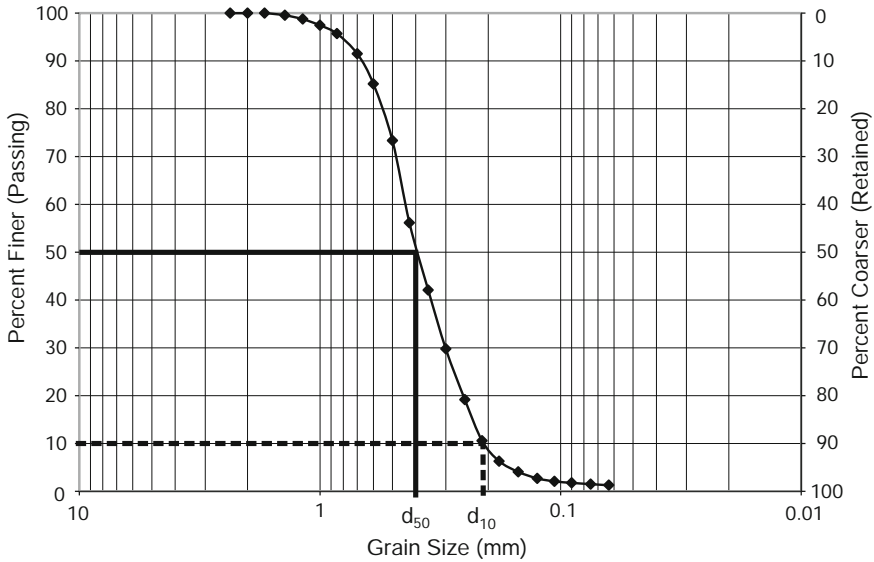
Fig. 9.3 Example of a sand grain size analysis chart for a sample from South Florida. The d_{10} and d_{50} diameters are the value for which 10 % and 50 %, respectively, of the mass of the sample is finer

Table 9.1 Recommended sieve sizes for grain size analysis

Option A		Option B	
U.S. standard mesh no.	Mesh size (mm)	U.S. standard mesh no.	Mesh size (mm)
6	3.36	5	4.0
8	2.38	7	2.83
12	1.68	10	2.0
16	1.19	14	1.41
20	0.84	18	1.00
30	0.59	25	0.71
40	0.42	35	0.50
50	0.30	45	0.35
70	0.21	60	0.25
100	0.149	80	1.77
140	0.105	120	0.125
200	0.074	170	0.088
		200	0.074

The main parameters used in the analysis of grain size data are 'd' values, which are the grain diameters at which a specified percentage of a sample's mass is composed of smaller particles. For example, the d_{10} diameter is the diameter at which 10 % of a sample's mass is comprised of smaller particles (i.e., passes

through the corresponding-sized sieve). The d_{50} diameter is the 'mass median diameter' as 50 % of the sample is comprised of smaller particles and 50 % of larger particles. For example, the d_{10} and d_{50} of the sample whose grain distribution is provided in Fig. 9.1 are approximately 0.21 and 0.36 mm, respectively.

Grain size analyses are performed by commercial geotechnical laboratories. However, standard commercial geotechnical sieve analyses usually utilize a lesser number of sieves than is optimal for grain size analyses for permeability determination.

9.4.2 Estimation of Permeability from Grain Size Data

Empirical relationships used to estimate permeability from grain size distribution were reviewed by Masch and Denny (1966), Bear (1972), Vukovic and Soro (1992), Nelson (1994), Detmer (1995), Batu (1998), Kasenov (2002), Odong (2007), and Rosas et al. (2014). The results of some of the more important investigations on the relationship between sand grain distribution and permeability are reviewed herein.

Nelson (1994) and Masch and Denny (1966) reviewed some of the early work on the relationship between the grain size distribution of unconsolidated sands and permeability. Permeability was related to grain size (median or mean diameter), sorting (standard deviation, uniformity coefficients), surface area, other size distribution variables (e.g., skewness and kurtosis), and diagenetic effects. Masch and Denny (1966) prepared artificial sand samples with different grain sizes, sorting, skewness and kurtosis, and measured their permeability using a constant-head permeameter. Their results confirmed the general observation that permeability increases with grain diameter, which, in turn, correlates with pore-size diameter. For a given median grain size, permeability increases with increasing sorting (i.e., decreasing standard deviation). With poorer sorting, there is a greater potential for interstitial clogging with finer sediments. The dependence of permeability on standard deviation was more pronounced for coarse-grain sands. Masch and Denny (1966) generated a series of predictive curves that relate permeability to median grain diameter for different standard deviation values. Nelson (1994) also observed that the presence of very fine silt and clay produced low permeabilities at high porosities. A disproportionately small amount of fines can dramatically reduce the permeability of unconsolidated sands.

Panda and Lake (1994) reported that permeability is sensitive to porosity, followed by grain size and sorting. Variations in mean grain size were found to contribute more to differences in permeability than variations in porosity and sorting. It was found that it is difficult to represent permeability as a single-value function of porosity. Panda and Lake (1994) observed that facies-differentiated samples tend to have better correlations between $\log_{10}$ permeability and porosity than undifferentiated samples.

There has been much effort in develop empirical equations that can be used to estimate hydraulic conductivity from grain size distribution. Few of the formula give generally reliable results because of the difficulty of including all the variables in porous sediments that may affect permeability and hydraulic conductivity (Todd 1980). Most of the empirical formula relates permeability to the square of effective or characteristic grain size with the general form (Todd 1980)

$$k = cd^2 \qquad (9:9)$$

where 'c' is a dimensionless coefficient and 'd' is grain size (diameter) is mm. Equation 9.9 can be modified to calculate hydraulic conductivity by using a coefficient with units of one divided by the product of length and time.

Historically, the most commonly used formula is the Hazen (1911) formula, which has the form

$$K = C_H d_{10}^2 \qquad (9:10)$$

where C_H is a coefficient that is a function of porosity. A similar equation uses the median grain size (d_m or d_{50}) instead of the d_{10} diameter. Shepard (1989) performed statistical power regression analyses of 19 sets of published grain size and laboratory analyses, and found that most values of the exponent are significantly less than 2.0. Shepard (1989) proposed the following alternative expression

$$K = Cd_m^{1:65 \text{ to } 1:85} \qquad (9:11)$$

The values of the coefficient 'C' and the exponent are higher for samples with greater textural maturity. Shepard (1989) generated linear relations between grain size and hydraulic conductivity for glass spheres, and texturally mature dune, beach, and channel sands.

The Kozeny-Carman equation is one of the more commonly used derivations of hydraulic conductivity from grain size distribution (Bear 1972)

$$K = \left(\frac{qg}{v}\right) d_m^2 \left(\frac{n^3}{180(1-n)^2}\right) \qquad (9:12)$$

where
K   hydraulic conductivity (cm/s)
n   porosity (fractional)
q   density (g/cm^3)
g   gravitational acceleration (981 cm/s^2)
m   dynamic viscosity (g/cm/s)
d_m is representative grain size (cm)

The choice of d_m value affects the calculated hydraulic conductivity value. Values of d_m used include median, geometric mean, and d_{10} grain sizes.

Alyamani and Şen (1993) proposed an alternative equation that also relates hydraulic conductivity to a squared function of grain size

$$K = 1300[I_o + 0.025(d_{50} - d_{10})]^2 \qquad (9.13)$$

where hydraulic conductivity is in units m/d, and I_o = x-intercept of line formed by the d_{50} and d_{10} sizes (mm) of grain size distribution curve.

Detmer (1995) examined grain size distribution, porosity, and permeability relationship in sands from the Albuquerque Basin, New Mexico, USA. Permeability was measured using a syringe-based minipermeameter that had a range of 0.6–270 D (0.5–165 m/d). The main results are

- there is a poor correlation between porosity and permeability
- there is an inverse relationship between permeability and degree of cementation (as qualitatively evaluated in the field).
- permeability is correlated with grain size, particularly the size of the finest materials (d_{10} and d_{20} diameters),
- a better correlation of grain size and permeability occurred for cut samples (material retained on the 2 mm sieve was excluded).

The poor correlation between porosity and permeability suggests that it may not be worth the effort to measure porosity (Detmer 1995).

Detmer (1995) compared the accuracy of several equations for predicting the hydraulic conductivity of the Albuquerque Basin sands. The best correlation was obtained using the Kruger and Zamarin equations, respectively (Detmer 1995; Kasenov 2002):

$$K = 240\left(\frac{n}{(1-n)^2}\right)d_e^2 \qquad (9.14)$$

$$K = 8.07\left(\frac{n^3}{(1-n)^2}\right)Ctd_e^2 \qquad (9.15)$$

K   hydraulic conductivity (m/d)
n   porosity (fraction)
d_e effective grain diameter, d_{10} (mm)
C $(1.275 - 1.5n)^2$
t   0.807 for a temperature of 10 °C

Berg ([1970](#)) proposed an equation relating permeability to grain size and sorting:

$$k = 80{:}8n^{5:1}d_{50}^{2}e^{-1:385P} \tag{9:16}$$

where

k   permeability (md),
d_{50} medium grain diameter (mm),
n   fractional porosity
P   sorting term, which is equal to $P_{90} - P_{10}$ (P is in phi units, $-\log_2 d$)

Other factors beyond grain size and porosity affect hydraulic conductivity. Sperry and Peirce ([1995](#)) evaluated the effects of grain shape on hydraulic conductivity. Grain shape was quantified through the slope of the 'angle of repose', which is greater for less spherical particles. The influence of particle shape on hydraulic conductivity increases with increasing size. Sperry and Peirce ([1995](#)) suggested that irregular packing at finer grain sizes (295–351 l m of less) does not result in significant differences in the size of pore throats. Grain shape can be accommodated in hydraulic conductivity estimates through adjustments in the value of Hazen coefficient and exponent (which are higher for samples with greater textural maturity).

Sediments are anisotropic to varying degrees in that vertical hydraulic conductivities are usually less than horizontal hydraulic conductivities. Comparison of hydraulic conductivity values obtained from directional permeameter measurements and grain size analyses indicates that values obtained from grain size analyses are intermediate between vertical and horizontal values obtained by permeameter measurements of core samples (Cai et al. [2015](#)).

The question arises as to the degree to which empirical equations relating hydraulic conductivity to grain size distribution and porosity are generally applicable beyond the samples set upon which they were derived. Pryor ([1973](#)) in a study of 992 sand samples from river bars, beaches, and dunes, concluded that the ideal relationships between permeability, porosity, and textural characteristics that have been observed by various authors for artificially packed particles are only weakly demonstrated by beach and dune sands and not demonstrated for river-bar sands. The different styles of natural grain packing between river bar and beach sands was suggested to be the cause of deviations from the ideal model.

Rosas et al. ([2014](#)) assessed the accuracy of 20 empirical methods for estimating hydraulic conductivity from grain size data by comparing the measured hydraulic conductivities of 431 samples with predicted values. The hydraulic conductivity of the sand samples was measured using a constant-head permeameter. Samples were classified as to depositional environments and subenvironments. It was observed that the 20 empirical methods resulted in a very wide range of predicted values. Specific-environment empirical equations were shown to predict hydraulic conductivity values more accurately than other equations for a given depositional environment or subenvironment. However, all of the equations still had a high degree of predictive error.

A simple regression analysis was used to assess the linear relationship between measured and estimated values. The results of the analysis are linear equations for the measured hydraulic conductivity as a function of the estimated value. The beta coefficients within the empirical equations were adjusted in order to obtain a linear equation with a unit slope. The measured hydraulic conductivity values are represented by an offset of the linear fit of the estimated hydraulic conductivity values. The modified empirical equations with adjusted beta values and offsets produced the most accurate predictions of hydraulic conductivity (Rosas et al. 2014).

A key conclusion of Rosas et al. (2014), and this review of previous studies, is that empirical grain size-permeability relationships are not necessarily transferable from one location to another. The different empirical formulas that relate hydraulic conductivity to grain size distribution can give greatly different values for a given sample. Some of the empirical formulae were developed for specific grain size ranges and should be strictly used only within their domain of applicability (Odong 2007). Some equations work better for sediments from specific depositional environments (Rosas et al. 2014). Grain size data can be a useful source of information on hydraulic conductivity but care should be taken in selecting the appropriate equation to process the data. Use of multiple equations (such as compiled by Rosas et al. 2014), screened based on applicability to project sample conditions allow for an evaluation of the uncertainty in hydraulic conductivity values. It is recommended that the equation(s) used in an investigation be validated against some direct hydraulic conductivity measurements run on the same samples as the grain size analyses.

9.5   Lithological Analysis

Lithological analysis is the evaluation of rock and sediment types, mineralogy, and texture, including porosity and permeability types. The lithology of aquifer and confining strata are determined from direct observations and analyses of rock samples and indirect methods, such as borehole geophysical logging. The importance of lithological analyses varies between projects. Identification of lithofacies is a fundamental part of facies analyses and, in turn, the development of conceptual models and ultimately numerical models. Lithological and mineralogical data are also important for projects in which fluid-rock interactions are a concern. Lithological analyses start with a description of the sediment and rock. More specialized techniques, such as thin-section petrography, x-ray diffractometry, and scanning electron microscopy are then employed, as needed, to provide more specific data on the studied strata.

9.5.1   Well Cutting and Core Descriptions

Well cuttings are small fragments of rock and sediment produced during well drilling. The cuttings are typically screened out of the drilling fluid upon its return

to land surface. Well cuttings are the normal byproduct of drilling and their collection involves minimal additional effort and costs. However, analysis of well cuttings has significant limitations, which are

- The small size of cuttings, often less than 1 cm, precludes observation of large-scale features in the formation, such as sedimentary structures, bedding, and large secondary pores. Large fossils cannot be recovered.
- Well cuttings samples represent a mixture of the rock or sediment present in the sample interval. It is typically not possible to determine from the cuttings alone how the different rock types are distributed in the sample interval.
- Well cuttings samples may be contaminated with material that fell into the borehole from above the sample interval.
- The recovered well cuttings may be biased, particularly towards harder lithologies. Softer material and very fine-grained material (finer than the collection screen size) may be under represented because they combine with the drilling mud or are dispersed in the drilling fluid or discharged water.

Nevertheless, well cuttings are often the only samples available from most wells and an experienced geologist can use them to perform an accurate evaluation of subsurface geology, particularly if the analysis of cuttings is performed in conjunction with geophysical log analysis. For example, a sample from a 10-foot (3 m) thick depth interval may consist of mixed sandstone and shale cuttings. The shale would likely appear on a natural gamma ray log as intervals with higher activity. The geophysical log, therefore, can provide the specific depths in the sample interval from which the shale cuttings were derived.

Description of well cuttings and cores samples is a basic part of exploratory well projects and well drilling, in general. However, the quality of sample descriptions that are performed nowadays in groundwater investigations is often appallingly bad. This stems in large degree to those entering the hydrogeology discipline having an inadequate background in sedimentary geology field and laboratory procedures. It is also due to inadequate on-the-job training of entry level staff. The poor quality of lithological descriptions is very unfortunate because an important source of information is not being obtained. Sample description procedures in the context of managed aquifer recharge projects were reviewed by Maliva and Missimer (2010) and are applicable to hydrogeological studies in general. The Shell Oil Company Sample Examination Manual (Swanson 1981), distributed by the American Association for Petroleum Geologists, is an excellent, widely used reference on sample description. Detailed and accurate lithological descriptions do not take more time (and thus money) than poor-quality work; they require instead trained and motivated field staff.

High-quality analysis of cuttings starts with the collection of a good set of cutting samples whose recorded depths actually coincide with the borehole depths from which they were obtained. Accurate depth control requires that the field geologist know both the current drill bit depth and the time required for cuttings to reach land surface. The time lag is greater for mud-rotary drilling than air and reverse-air drilling and increases with increasing depth.

Samples should be collected at a minimum of 1.5 m (5 ft) or 3 m (10 ft) intervals and at major lithologic changes. The occurrence of a change in lithology is often indicated by a change in drilling action and penetration rate. A change from a soft to hard lithology is often marked by a decrease in penetration rate and increase in vibration (chatter) of the drill string. The field geologist needs to pay attention and record the drilling action and penetration rate, and observe the cutting stream for the suspected change in lithology.

Cutting samples are commonly collected in cloth drawstring bags, which have the advantage of being breathable, and thus allow the samples to dry. A common method for saving sets of cutting samples for archiving is by using specially designed envelopes. Multi-compartment plastic trays are increasingly being used, which have the advantage of allowing 10 samples to be observed side by side.

Initial basic sample descriptions should be made in the field. Often when drilling is rapid, there may not be time in the field for complete description of each cutting sample. Sample descriptions may need to be completed later in the office or laboratory. For projects in which lithological data are particularly important, it is recommended that a thorough description of the samples be performed under less hectic conditions in the office or laboratory using a stereomicroscope.

Maliva and Missimer (2010) presented two examples of actual descriptions of limestone cuttings that were taken from different well completion reports for ASR projects:

(1) Limestone, soft, chalky, cream
(2) LIMESTONE, brownish yellow (10YR6/6), bioclast grainstone. The bioclasts are mostly fine to medium sand-sized. Mostly hard, moderate visible porosity, and apparent permeability. Minor small echinoids (1049–1056; *Neolaganum dali*) and trace dictyoconid foraminifera.

The first description provides minimal useful information, whereas the second description captures much of the essential features of the rock. Unfortunately the quality of the first description is becoming the norm, whereas the second description should be the standard for any competent field geologist.

It is recommended that samples be described in the following manner or order (Maliva and Missimer 2010):

• basic lithology (e.g., limestone, sandstone, shale, sand)
• color, described on wet (moist) samples using a color chart based on the Munsell system
• textural and compositional description, using Folk (1974), Dunham (1962) or Dott (1964) classification schemes
• grain size (particularly for siliciclastic sediments and rocks)
• hardness
• apparent porosity and permeability
• accessory minerals
• fossils
• additional comments.

Additional tools that are useful for sample description are a hand lens or magnifying glass, dilute hydrochloric acid (10 % v/v) and Alizarin red-S solutions, and either a small metric ruler or sand grain size chart. Calcite and aragonite react vigorous to dilute hydrochloric acid. Whereas, non-carbonate minerals do not. Dilute hydrochloric acid can be used, for example, to determine whether or not sandstone is cemented with calcite. Alizarin red-S solution preferentially stains calcium carbonate (calcite and aragonite) but not dolomite and quartz.

9.5.2   Thin-Section Petrography

Thin-section petrography is the most useful technique for characterizing the composition and textures of rock. The problem is that very few hydrogeologic and engineering firms have the equipment and trained staff to perform the analyses. A thin section is a thin (typically 30 l m thick) sliver of rock or sediment that is glued onto a glass slide. They are prepared by first grinding a flat surface on a sample, which is then glued onto a glass slide. Most of the sample in then cut off. The remainder of the sample in next carefully ground down to obtain the desired thickness. There are numerous commercial thin-section preparation services worldwide.

Thin sections are examined using a petrographic microscope, which is essentially a transmitted-light microscope equipped with two polarizing filters oriented at 90 degrees to each other. Some petrographic microscopes are also equipped to view samples under reflected light. Thin-section petrography is a specialized discipline onto itself, which requires both training and experience to master. The technique is used to identify minerals based on their form and optical characteristics. The various fossil types are identified based on their size, shape, and microstructures (Fig. 9.4). Thin-section petrography also allows for the identification of cement and porosity types. Often samples to be thin sectioned are vacuum impregnated with colored epoxy that facilitates identification of pores in the sample. Imaging processing software is available that can calculate the visible porosity by quantifying the area of the stained epoxy.

Thin-section petrography is particularly useful for identifying minerals that are present in trace quantities (<1 volume %), and may be below the detection limits of other techniques (e.g., x-ray diffractometry). Trace mineral may be identified using thin-section petrography if they are included in the thin section and have a crystal size sufficiently large to observe their optical properties. The American Association of Petroleum Geologists published two very useful memoirs on the thin-section petrography of sandstones and carbonates (Scholle 1979; Scholle and Ulmer-Scholle 2003). Flügel (2004) prepared an excellent guide to the carbonate rock types.

The preferred situation is to have an experienced geologist/petrographer on the project team to perform the thin-section analyses. In practice, thin-section analyses or descriptions are often performed by commercial laboratories, as most hydrogeological and engineering consulting firms do not have the capability of performing

Fig. 9.4 Thin-section
photomicrographs of
dolomitic limestone from the
Avon Park Formation (Middle
Eocene), Daytona Beach,
Florida. Porosity is filled with
blue-dyed epoxy. Large
foraminifera is evident in the
middle of top photograph and
top of the bottom photograph.
Moldic pores (m) and
dolomite crystals (clear
rhombohedra) are evident
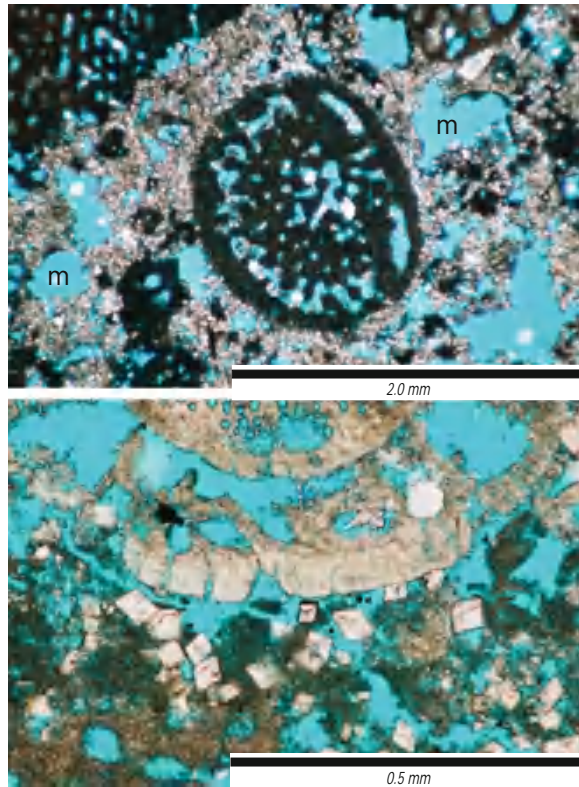
the work in house. Commercial laboratories will provide a sample description and
photographs. Inasmuch as the bulk of the work load for commercial petrographic
laboratories is now for the oil and gas industry, they may not focus on aspects of
rocks that are more important for groundwater projects, such as the presence of
volumetrically minor reactive mineral phases. It has been the author's observation
that the quality of commercial thin-section descriptions is mixed.

9.5.3 Scanning Electron Microscopy and Electron Microprobe Analyses

Scanning electron microscopy (SEM) uses an electron beam to provide a
high-magnification and high-resolution image of the surface of a material (Fig. 9.5).
The interaction of the electron beam with the material surface generates three
signals: secondary electrons, backscattered electrons, and X-rays. Secondary elec-
trons are emitted from the surface of the sample and are used primarily for imaging.
Backscattered electrons (BSE) are electrons from the primary beam that are

Fig. 9.5 SEM photograph of
a sample of the Avon Park
Formation (Middle Eocene),
Daytona Beach, Florida,
showing smooth-faced,
euhedral dolomite crystal
(d) and microporous matrix.
Microfossils (coccoliths; c)
are evident
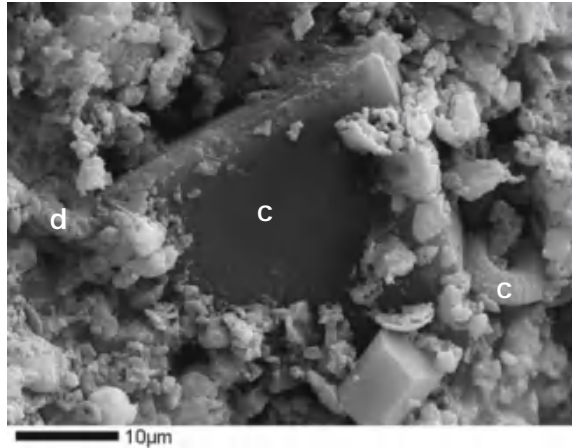
reflected back from the material surface. Backscattered imaging is commonly
performed on polished thin sections and is used to differentiate between minerals.
Minerals that contain high atomic number elements appear brighter. The interaction
of the electron beam with samples also causes the emission of X-rays, which have
energy levels characteristic of each element. SEMs, particularly newer models, are
commonly equipped with an Energy Dispersive X-ray Spectroscopy (EDS) unit,
which allows for the elemental analyses. The ratio of elements obtained from a
crystal is used to identify its mineralogy.

The electron microprobe (EM) is similar to the SEM in that it emits a beam of
electrons, which interacts with the tested material to generate x-rays that are charac-
teristic of each element. The electron microprobe has a very fine resolution and can
analyze the composition of a single sand grain or cement crystal (or commonly
multiple areas or zones within a grain or crystal). The EM is a sophisticated tool and
requires training to properly operate and obtain accurate data. Most major universities
have an EM and many allow outside use of the equipment under supervision for a fee.

Both the SEM and EM are not widely used in groundwater investigations. They
have specialized applications in projects where interaction of fluids with aquifer
minerals are concern. For example, the leaching of arsenic into water stored in ASR
systems has occurred in some ASR systems in Florida. Both SEM and EM were
used to confirm that arsenic-bearing pyrite was the likely source of the arsenic
(Price and Pichler 2006; Lazareva and Pichler 2007).

9.5.4   X-Ray Diffractometry

Powder x-ray diffraction analysis (XRD) is a standard technique for mineral
identification, which was reviewed by Jenkins and Snyder (1996) and Poppe et al.
(2001). XRD is based on the diffraction of an x-ray beam off of the planes of atoms

in crystal structures. The diffraction angles and intensity of the diffracted beams are a function of the crystal structure of the mineral phase. XRD provides the most definitive mineral identification. Diffraction patterns can be conceptualized as a unique fingerprint of a mineral.

The basis of XRD analysis is Bragg's Law as follows:

$$nk = 2d \sin h \qquad (9{:}17)$$

where,

n   the order of the diffracted beam,
k   the wavelength of the incident x-ray beam,
d   spacing between atomic planes, and
h   angle of the diffracted beam

Inasmuch as k is known and h is the measured parameter in XRD analysis, the 'd' spacings of the various atomic planes can be calculated. Analyses for whole (bulk) rock analyses are typically performed using a finely ground, powdered sample mounted on a glass slide. The analyses may also be performed on thin sections. The output is an X-ray diffractogram, which is a plot of X-ray beam intensity (counts) versus degrees 2h (Fig. 9.6). X-ray diffractograms appear as a
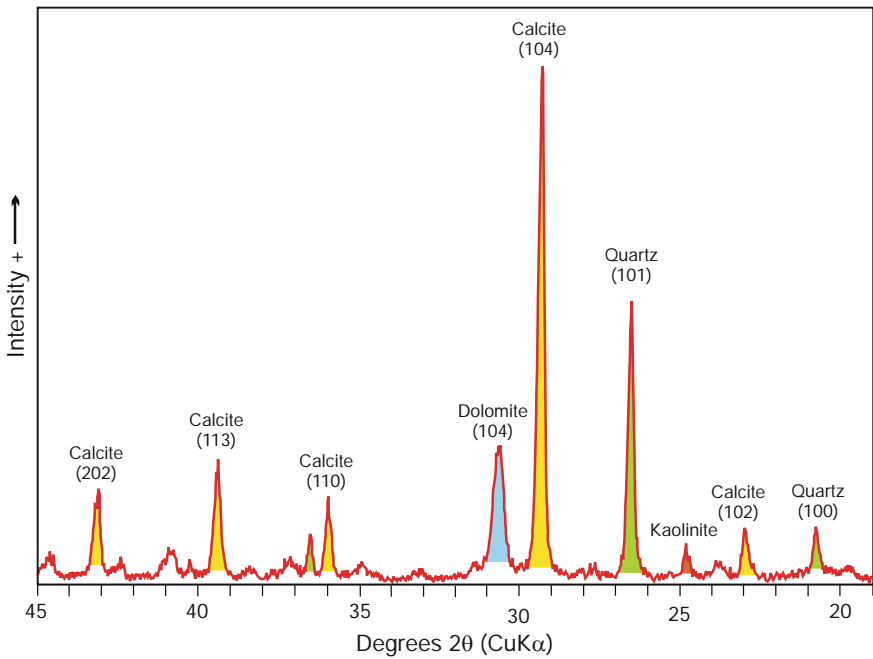
Fig. 9.6 Example of an X-ray diffractogram of a Cretaceous chalk sample composed mostly of calcite, with less abundant quartz, dolomite, and kaolinite

series of peaks separated by intervals of low-intensity (background) response. The X-ray diffractograms are interpreted by comparing the peak patterns (degrees 2h or d-spacings and relative intensity) against standard diffractograms for minerals. In order for a mineral to be detected, its characteristic XRD peaks must be clearly above the background noise level. The detection limit for XRD is approximately 2 %. XRD has the advantage that it can detect very fine-grained or crystalline materials that are too small to identify using thin-section petrography.

XRD is the primary method used to identify clay minerals. Special sample preparation techniques are required to separate the clay-sized fraction, prepare oriented slides, and treat the sample (e.g., heating and glycolation) to facilitate mineral identification. Standard whole rock analysis methods should not be used for clay mineral identification. The U.S. Geological Survey published a laboratory manual for XRD analysis of clay minerals (Poppe et al. 2001), which is a very good basic reference.

XRD analyses are typically run by either commercial laboratories and under contract by universities. XRD systems have become more automated and programs are commonly used that interpret the diffractograms with regard to mineral phases present and their estimated abundance. It is critical to discuss in advance with the laboratory the type of analyses (e.g., whole rock versus clay mineral) required and the laboratory sample requirements.

X-ray fluorescence is a related x-ray-based technology that is used determine the elemental composition of samples. A primary x-ray beam illuminates the same. The sample is excited and emits x-rays whose wavelengths are characteristic of the types of atoms present in the sample. Elemental data can be processed to obtain an estimate of mineralogy. XRF is not commonly used in aquifer characterization.

References

Alyamani, M. S., & Şen, Z. (1993) Determination of hydraulic conductivity from complete grain-size distribution curves. Ground Water, 31, 551–555.

ASTM (2007) Standard test method for particle-size analysis of soils (D422–63(2007)e2). West Conshohocken: ASTM International.

ASTM (2010) Standard test methods for measurement of hydraulic conductivity of saturated porous materials using a flexible wall permeameter (D5084–10). West Conshohocken: ASTM International.

Anderson, M. A., Duncan, B., & McLin, R. (2013) Core truth in formation evaluation. Oilfield Review, 25(2), 16–25.

API (1998) API Recommended practices for core analysis (API RP40). Washington, D.C.: American Petroleum Institute.

Batu, V. (1998) Aquifer hydraulics: A comprehensive guide to hydrogeologic data analysis. New York: John Wiley.

Bear, J. (1972) Dynamics of fluids in porous media. New York: Dover Publications.

Berg, R. R. (1970) Method for determining permeability from reservoir rock properties. Transactions Gulf Coast Association Geological Societies, 20, 303–317.

Budd, D. A., & Vacher, H.L. (2004) Matrix permeability of the confined Floridan Aquifer, Florida, U.S.A. Hydrogeology Journal, 12, 531–547.

Cai, J., Taute, T., Hamann, E., & Scheider, M., 2015, An integrated laboratory method to measure and verify directional hydraulic conductivity in fine- to medium sandy sediments. Groundwater, 53, 14–150.

Chandler, M. A., Kocurek, G., Goggin, D. J., & Lake, L.W. (1989) Effects of stratigraphic heterogeneity on permeability in eolian sandstone sequence, Page Sandstone, northern Arizona. American Association of Petroleum Geologists Bulletin, 73, 658–668.

Daniel, D. E. (1994) State-of-the art: Laboratory hydraulic conductivity tests in saturated soils. In D. E. Daniel & S. J. Trautwein. S. J. (Eds.), Hydraulic conductivity and waste contaminant transport in soil (pp. 30–78). Philadelphia: American Society for Testing and Materials.

Detmer, D. M. (1995) Permeability, porosity, and grain-size distribution of selected Pliocene and Quaternary sediments in the Albuquerque Basin. New Mexico Geology, 17(4), 79–87.

Dinwiddie, C. L. (2005) The small-drillhole minipermeameter probe for in-situ permeability measurement. SPE Reservoir Evaluation & Engineering, 8, 491–501 (SPE 84595-PA)

Dott, R. H. (1964) Wacke, graywacke and matrix; what approach to immature sandstone classification? Journal of Sedimentary Petrology, 34, 625–632.

Dunham, R. J. (1962) Classification of carbonate rocks according to depositional texture. In W. E. Ham (Ed.), Classification of carbonate rocks. Memoir 1 (pp. 108–121). Tulsa: American Association of Petroleum Geologists.

Ethridge, F. (1992) Part 5. Laboratory methods. In D. Morton-Thompson & A. M. Woods (Eds.), Development geology reference manual. Methods in Exploration Series 10. (pp. 195–258). Tulsa: American Association Petroleum Geology

Folk, R. L. (1974) Petrology of sedimentary rocks. Austin: Hemphill Publishing Co.

Flügel, E. (2004) Microfacies of carbonate rocks, analysis, interpretation and application. Berlin: Springer.

Giesche, H. (2006). Mercury porosimetry: a general (practical) overview. Particle & particle systems characterization, 23, 9–19.

Goggin, D. J. (1993). Probe permeametry: is it worth the effort? Marine and Petroleum Geology, 10, 299–308.

Hazen, A. (1911) Discussion: dams on sand foundations. Transactions, American Society of Civil Engineers, 73, 199.

Hornung, J., & Aigner, T. (1999) Reservoir and aquifer characterization of fluvial architectural elements: Stubensandstein, Upper Triassic, southwest Germany. Sedimentary Geology, 129, 215–280.

Hurst, A., & Goggin, D. J. (1995) Probe permeametry: an overview and bibliography. American Association of Petroleum Geologists Bulletin, 79, 463–473.

Jenkins, R., & Snyder, R. L. (1996) Introduction to x-ray powder diffractometry. New York: John Wiley & Sons.

Kasenov, M. (2002) Determination of hydraulic conductivity from grain size analysis. Highlands Ranch: Water Resources Publications.

Keighin, C. W. (1997). Physical properties of clastic reservoir rocks in the Uinta, Wind River, and Anadarko Basins, as determined by mercury-injection porosimetry. U.S Geological Survey Bulletin, 2146-G, 73–83.

Lazareva, O., & Pichler, T. (2007). Naturally occurring arsenic in the Miocene Hawthorn Group, southwestern Florida: Potential implication for phosphate mining. Applied geochemistry, 22, 953–973.

Maliva, R. G., & Missimer, T. M. (2010) Aquifer storage and recovery and managed aquifer recharge using wells: Planning, hydrogeology, design, and operation. Houston: Schlumberger Corporation.

Masch, F. D., & Denny, K. J. (1966) Grain size distribution and its effect on the permeability of unconsolidated sands. Water Resources Research, 2, 665–677.

Monicard, R. P., 1980, Properties of reservoir rocks – Core analysis. Paris: Editions Technip.

Mukhopadhyay, A., Al-Awadi, E., Oskui, R., Hadi, K., Al-Rywaih, F., Turner, M. & Akber, A. (2004) Laboratory investigations of compatibility of the Kuwait Group aquifer, Kuwait, with possible injection waters. Journal of Hydrology, 285, 158–176.

Nelson, P. H., (1994) Permeability-porosity relationships in sedimentary rocks. The Log Analyst, May-June 1994, 38–62.

Odong, J. (2007) Evaluation of empirical formulae for determination of hydraulic conductivity based on grain-size analysis. Journal of American Science, 3(3), 54–60.

Panda, M. N., & Lake, L.W. (1994) Estimation of single-phase permeability from parameters of particle-size distribution. American Association of Petroleum Geologists Bulletin, 78, 1028–1039.

Poppe, L. J., Paskevich, V. F., Hathaway, J. C., & Blackwood, D. S. (2001) A laboratory manual for X-ray diffraction. U.S. Geological Survey Open-File Report 2001–41.

Price, R. E., & Pichler, T. (2006). Abundance and mineralogical association of arsenic in the Suwannee Limestone (Florida): Implications for arsenic release during water–rock interaction. Chemical Geology, 228, 44–56.

Pryor, W. (1973) Permeability-porosity patterns and variations in some Holocene sand bodies. American Association of Petroleum Geologists Bulletin, 57, 162–189.

Rosas, J., Lopez, O., Missimer, T. M., Coulibaly, K.M., Dehwah, A.H.A., Sesler, K., Lujan, L. R., & Mantilla, D. (2014) Determinations of hydraulic conductivity from grain-size distribution for different depositional environments: Ground Water, 52, 399–413.

Samingan, A. S., Leong, E. C., & Rahardjo, H. (2003). A flexible wall permeameter for measurements of water and air coefficients of permeability of residual soils. Canadian Geotechnical journal, 40, 559–574.

Schatzinger, R. A., & Tomutsa, L. (1999) Multiscale heterogeneity characterization of tidal channel, tidal delta and foreshore facies, Almond Formation outcrops, Rock Springs uplift, Wyoming. In R Schatzinger & J. Jordan (Eds.) Reservoir characterization – recent advances. Memoir 71 (pp. 45–56). Tulsa: American Association of Petroleum Geologists.

Scholle, P. A. (1979) A color illustrated guide to constituents, textures, cements and porosities of sandstones and associated rocks. Memoir 28. Tulsa: American Association of Petroleum Geologists.

Scholle, P. A., & Ulmer-Scholle, D. S. (2003) Color guide to petrography of carbonate rocks. Memoir 77. Tulsa: American Association of Petroleum Geologists.

Sharp, J. M., Jr., Fu, L., Cortez, P., & Wheeler, E. (1994) An electronic minipermeameter for use in the field and laboratory. Ground Water, 32, 41–46.

Shepard, R. G. (1989) Correlation of permeability and grain size. Ground Water, 27, 633–638.

Sperry, J. M., & Peirce, J. J. (1995) A model of estimating the hydraulic conductivity of granular material based on grain shape, grain size, and porosity. Ground Water, 33, 892–898.

Sutherland, W. J., Halvorsen, C., Hurst, A., McPhee, C. A., Robertson, G., Whattler, P. R. & Worthington, P. F. (1993). Recommended practice for probe permeametry. Marine and Petroleum Geology, 10, 309–317.

Swanson, R. (1981) Sample examination manual. Methods in Exploration 1. Tulsa, American Association of Petroleum Geologist.

Taylor, L. H., & Vinopal, R. J. (1999) Conventional core vs. mini-permeameter measurements: Tensleep Formation. In Proceedings SPE Rocky Mountain Region Meeting, Gillette, Wyoming, 15–18 May, 1999 (SPE 55971).

Todd, D. K. (1980) Groundwater hydrology (2nd ed.). New York, John Wiley & Sons.

USDA (2014) Kellogg soil survey laboratory methods manual. Soil Survey Investigations Report No. 42, Version 5.0. Lincoln, Nebraska: U.S. Department of Agriculture, Natural Resources Conservation Service.

van Brakel, J. (1981) A Special Issue Devoted to Mercury Porosimetry. Powder Technology, 29, 1–209.

Vukovic, M., & Soro, A. (1992) Determination of hydraulic conductivity or porous media from grain-size composition. Highlands Ranch: Water Resources Publications.

Webb, P. A. (2001). An introduction to the physical characterization of materials by mercury intrusion porosimetry with emphasis on reduction and presentation of experimental data. Norcross, Georgia: Micrometrics Instrument Corp.

Chapter 10
Borehole Geophysical Techniques

Borehole geophysical logging is a fundamental element of aquifer characterization because it can provide essentially continuous in situ measurements of the petro-physical properties, lithology, location and types of secondary porosity, and pore-water quality (salinity) of the logged strata. Flowmeter logs and some advanced geophysical logs, such as nuclear magnetic resonance, can also provide information of aquifer heterogeneity with respect to hydraulic conductivity. The greatest value is obtained from borehole geophysical logging when it is performed in conjunction with other aquifer testing methods, such as aquifer performance (pumping) tests, packer tests, and core analyses. Geophysical logs are commonly only qualitatively interpreted in groundwater investigations. However, much quantitative information can be obtained from logs provided that adequate quality assurance and control practices are followed in the data collection, calibration, and processing.

10.1 Introduction

Borehole geophysical logging has long been a critical tool in the oil and gas industry because of the wealth of data that it can cost-effectively provide. Detailed reviews of geophysical logging principles and applications, with a focus on the oil and gas industry, were provided by Schlumberger (1989a, b), Asquith and Krygowski (2004), and Serra (2008). The applications of borehole geophysical logging to groundwater investigations were reviewed by Driscoll (1986). Keys (1989, 1990, 1997), Collier (1993), Wempe (2000), Kobr et al. (2005), Maliva et al. (2009a), and Maliva and Missimer (2010, 2012).

Borehole geophysical logs can provide valuable information for groundwater resources investigations on

- aquifer hydrogeology, particularly the locations of aquifers and confining strata
- groundwater salinity
- porosity and permeability
- location, size, and orientation of fractures and other secondary porosity features
- aquifer heterogeneity, including the location of preferential flow zones
- aquifer mineralogy.

The greatest value is obtained from borehole geophysical logging when it is performed in conjunction with other aquifer testing methods. For example, aquifer pumping tests can provide information on the transmissivity of the tested strata. The combination of pump testing and flowmeter logging can provide additional information on aquifer heterogeneity, particularly the presence and hydraulic properties of flow and nonproductive zones within an aquifer. Time series of logs can be used to evaluate changes in groundwater salinity over time, such as may occur at saline-water interfaces. Borehole geophysical logs run for formation or aquifer characterization are usually run on open holes during well construction, prior to the installation of casing and screens. However, some geophysical logs can be run on cased holes (Sect. 10.13).

An overview of basic and advanced borehole geophysical techniques, as applied to groundwater investigations, is provided in this chapter. The emphasis is on the types of information that can be obtained from the various types of logs and the limitations of the methods. The development of a logging program for a groundwater investigation should start with a consideration of the specific data required or desired, the capabilities, and limitations of the various logs in the anticipated formation and borehole conditions, and the costs to both run and process the logs. Borehole geophysical logs can be roughly divided into two suites, basic and advanced, based on their sophistication, information provided, availability, and cost to run. The basic geophysical log suite typically run for groundwater investigations includes some, or all, of the following logs: caliper, natural gamma ray, resistivity (long-short-normal and dual induction), spontaneous potential, temperature, fluid resistivity, flowmeter, and sonic (acoustic). Nuclear borehole logs (neutron and density logs) are less commonly run in groundwater investigations because of concerns (or local prohibitions) over the use of radioactive sources in freshwater aquifers.

Some of the basic geophysical logs that are still widely used for groundwater investigations have been supplanted by more advanced logs in the oil and gas industry. Nevertheless, they still provide useful information and are typically inexpensive to run. Local geophysical loggers, or well drillers with logging equipment, that can run at least some of the basic geophysical logs are present in most areas. Advanced borehole geophysical logs, such as nuclear magnetic

resonance, elementary capture spectroscopy, and imaging logs, can provide fine-scale information on aquifer composition and properties that may be of great value for hydrogeologically complex projects (e.g., managed aquifer recharge systems; Maliva et al. 2009a; Maliva and Missimer 2012).

Log interpretation is the process by which measured parameters are translated into the petrophysical properties of interest, such as porosity, permeability, lithology, and mechanical rock properties (Schlumberger 1989a, b). A primary variable of interest in groundwater investigations is hydraulic conductivity, which cannot be directly measured using borehole geophysical logs. Hydraulic conductivity can be estimated from other parameters, such as porosity, grain size, and pore-size distribution. Flowmeter logs can be used to apportion transmissivity calculated by other means (e.g., aquifer pumping tests) between aquifer zones and, in turn, to calculate the average hydraulic conductivity for each zone.

Qualitative interpretation of geophysical logs is not complicated and many groundwater professionals can perform an elementary analysis of borehole geophysical logs. However, if the investment is made to run geophysical logs, then it should follow that a commensurate effort be made to extract the maximum value from the logs through quantitative interpretation. Greater technical expertise is necessary for accurate quantitative analysis of borehole geophysical data. Commonly, geophysical logs are run and are given only a cursory examination before they are filed with the geological logs in the appendices of reports. There is a lost opportunity to more carefully analyze and assess aquifer properties.

10.2   Quality Assurance and Quality Control

The amount and accuracy of information that can be derived from geophysical logs depends upon the type and quality of the logs and the knowledge and effort-expended by scientists or engineers in processing and interpreting the logs. The accuracy of log data is a major area of weakness in the groundwater logging industry. Logging for water resources investigations can be greatly improved by running suites of logs that are compatible with both borehole conditions and the petrophysical properties of the aquifer (Collier 1993). Cursory examination of geophysical logs can provide qualitative information on lithologic and water quality variations within a borehole. More detailed analyses can provide quantitative data on the petrophysical properties of tested strata, provided that the logs are of high quality. The importance of quality control in borehole geophysical logging cannot be over-emphasized if the data are to be quantitatively interpreted.

The accuracy of quantitative analyses of geophysical log data depends upon the accuracy of the unprocessed raw data, and the 'correctness' of the algorithms used

to process the data. Calibration and standardization are important parts of quantitative geophysical log interpretation, which are discussed by Keys (1989). Calibration is the process of converting the measured units of log response into units that measure rock characteristics. Logging tools can be calibrated under laboratory conditions using specially prepared core holes. Oil field tools are often calibrated using University of Houston calibration pits. Standardization is the process of checking the response of the logging tools in the field against known portable standards. It is also standard correct practice to run a repeat section of a log to evaluate whether or not there is any drift or artifacts in the measurements. Repeat sections should be essentially identical.

The raw data recorded during geophysical logging requires processing in order to obtain the petrophysical data of interest. For example, transit time data from a sonic log is processed to obtain porosity values, which is often the primary parameter of interest. Processing involves applying algorithms to the raw data, which include empirical constants. Data processing also involves applying corrections for borehole and geological conditions, such as for borehole diameter, invasion, bed thickness, and adjacent beds (Collier 1993). The values of empirical constants may be determined using field data. For example, geophysical log-based interpretations of porosity and pore-water salinity can be checked against core porosity data and water quality data from packer tests. If site-specific data are not available for local ground truthing of geophysical log interpretations, then algorithms and associated empirical constants derived from historic logging experience in the investigated lithologies in the project site region (i.e., local default values) are often used. As a general principle, geophysical log interpretations should be viewed as best estimates, for which the confidence of its accuracy increases with the degree to which the data can be checked or calibrated against well-specific or local data.

The accuracy of the depths should also be checked against known depths, such as the base of casing strings. Many logging tools include a natural gamma ray detector, which is very useful for determining if the multiple logs run on a borehole are in sync as far as depth and for making any necessary depth corrections during processing.

A key part of quality control in geophysical logging is having the process observed by geoscientists who are knowledgeable of the project objectives, local hydrogeology, and logging procedures. The geoscientist needs to be in the logging truck during the entire operation and be prepared to request reruns (if problems occur) and documentation of field standardization. The field geoscientist should also ensure that proper logging procedures are followed (e.g., appropriate logging speeds).

10.3 Caliper Logs

Caliper logs measure the diameter of the logged borehole, which is needed for the interpretation of other logs and for well construction. Mechanical caliper log tools used in groundwater investigations have metal arms that are maintained in contact with the borehole wall by spring pressure. In a typical caliper log, the arms are

connected to a potentiometer, in which resistance is linearly proportional to the extent to which the arms are opened. Changes in resistance are converted to voltage changes, which are sent to the surface either directly or converted to a varying pulse rate (Keys 1989). Logging tools usually have either three arms that move together or two orthogonally oriented pairs of independently linked arms, which provide measurements of borehole diameter in two directions (X-Y probe). The three-armed probe provides an approximate average diameter of the borehole. The X-Y probe is preferred because it provides information on the asymmetry of the borehole. Less commonly available are tools with 4 or 6 independent arms, which can provide greater detail on borehole irregularities.

Acoustic or sonic caliper tools measure borehole diameter from the return time of high-frequency acoustic pulses. They are typically used in groundwater investigations for only special applications, such as logging very large diameter holes. Acoustic caliper logs may record four traces at 90° spacings or provide 360° profiles of the borehole.

Many other geophysical logs cannot be accurately interpreted without detailed data on borehole diameter. The logs produced by every geophysical tool that emits and receives any type of artificial pulse, whether radio waves, electric fields, or radiation, is dependent on the distance between the source, the wall of the borehole, and the collector. For example, the intensity of the measured gamma ray log response is dependent on the distance between the formation and the receiver. Therefore, a caliper log should be run as part of every borehole geophysical log suite, especially if the data are to be quantitatively interpreted.

Caliper logs also provide information on the lithology and hydrogeology (Fig. 10.1). Caliper logs are used to detect secondary porosity features, such as fractures and solution conduits, which are evidence by increases in borehole diameter. A spiky caliper log pattern may be indicative of fractured rock. Borehole diameter is often related to the hardness of the rock. Poorly indurated formations may be 'washed out' (i.e., experience greater erosion during drilling) and thus have a greater borehole diameter. Well-indurated rock, on the contrary, may have borehole diameters close to the bit size (i.e., close to gauge). In holes drilled using the mud-rotary method, permeable zones may be marked by a smaller borehole diameter due to the greater development of mudcake.

Information of borehole diameter is needed during well construction to confirm that the borehole has sufficient diameter to set casing and to calculate theoretical required filter pack and cement volumes. Borehole diameter may decrease after drilling by the swelling clay (montmorillonite) zones. It is clearly important to know if there any constrictions in a borehole that could impede casing installation and cementing before the start of casing installation.
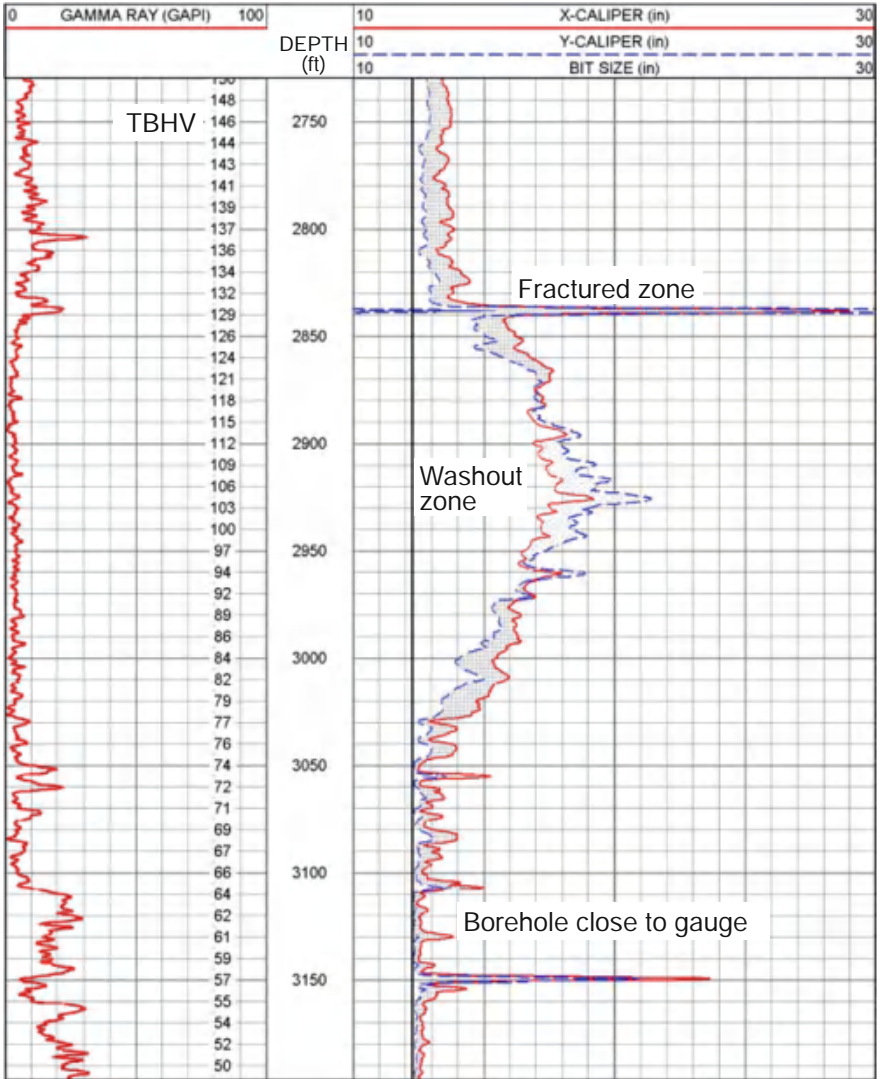
Fig. 10.1   Caliper log showing a washout interval, local enlargement due to fracturing, and an interval in which the borehole diameter is close to bit size (close to gauge). The total borehole volume (TBHV) is also calculated from the bottom of the hole upwards. A natural gamma ray log is provided

10.4   Natural Gamma Ray Log

The natural gamma ray log (or just gamma ray log) is one of the most widely run and useful logs for groundwater investigations. Natural gamma ray logs are used primarily for correlation between wells and for determination of shale or clay volumes.

The natural gamma ray log records the total gamma radiation detected within a selected energy range (Schlumberger 1989a; Keys 1989). Gamma ray activity is commonly expressed in terms of American Petroleum Institute (API) gamma ray units. The API unit is defined from an artificially radioactive formation constructed at the University of Houston to simulate about twice the radioactivity of shale. The artificial formation generates, by definition, 200 API units.

The detected gamma radiation is derived predominantly from the decay of potassium 40 and the uranium and thorium decay series. Rock and sediment types that have relatively high concentrations of potassium, uranium, and thorium tend to have relatively high gamma ray log responses.

The most commonly run natural gamma ray log (GR) measures the total radioactivity of the formation. The GR tool is compact and is commonly included on other tools to allow for depth correction between logs. For example, if a logged interval has a pronounced gamma ray peak (or other clear response signature) at a given depth, then the depths of all logs run on a well or borehole should be adjusted so that the peak occurs at the same depth in each log.

The natural gamma ray log response commonly reflects the shale or clay content of a formation, as clay minerals are often more radioactive than clean quartz sands and carbonates. However, some detrital and authigenic minerals (e.g., phosphates, some feldspars, micas, heavy minerals, glauconite), may have relatively high natural radioactivities (Keys 1989). Gamma ray spectroscopy logs measure both total radioactivity and the concentrations of potassium, thorium, and uranium that are producing the radioactivity. Gamma ray spectroscopy logs useful for detection, identification, and evaluation of radioactive minerals and determining the source of the total radioactivity detected by the GR log. Potassium radioactivity usually originates from micas, feldspars, micaceous clays (illite), and radioactive evaporites (Schlumberger 1989a). Thorium radioactivity is indicative of shales and heavy minerals. Uranium radioactivity is often indicative of phosphates and organic matter.

Gamma ray log response is sensitive to the borehole environment. Gamma ray activity is inversely related to borehole diameter. Gamma rays emitted by formation minerals are absorbed or scattered by processes, such as the photoelectric effect, Compton scattering, and pair production (Schlumberger 1989a). The rate of the absorption is dependent upon the density of the formation. Gamma ray response is also influenced by the composition of the borehole fluid, tool position within the borehole, presence of casing and cement, logging speed, and time constant (vertical smoothing; Schlumberger 1989b; Serra 2008).

Within a mixed siliciclastic aquifer, the gamma ray log can be used to differentiate between clay-rich beds, which tend to be confining units, and relatively clean sands, which tend to be productive units (Fig. 10.2). Bed boundaries are usually placed at a point midway between the maximum and minimum deflection of the anomaly (Schlumberger 1989a). The 'shaliness' of sand and sandstone formations may be estimated from the gamma ray index (I_{GR}; Asquith and Krygowski 2004):
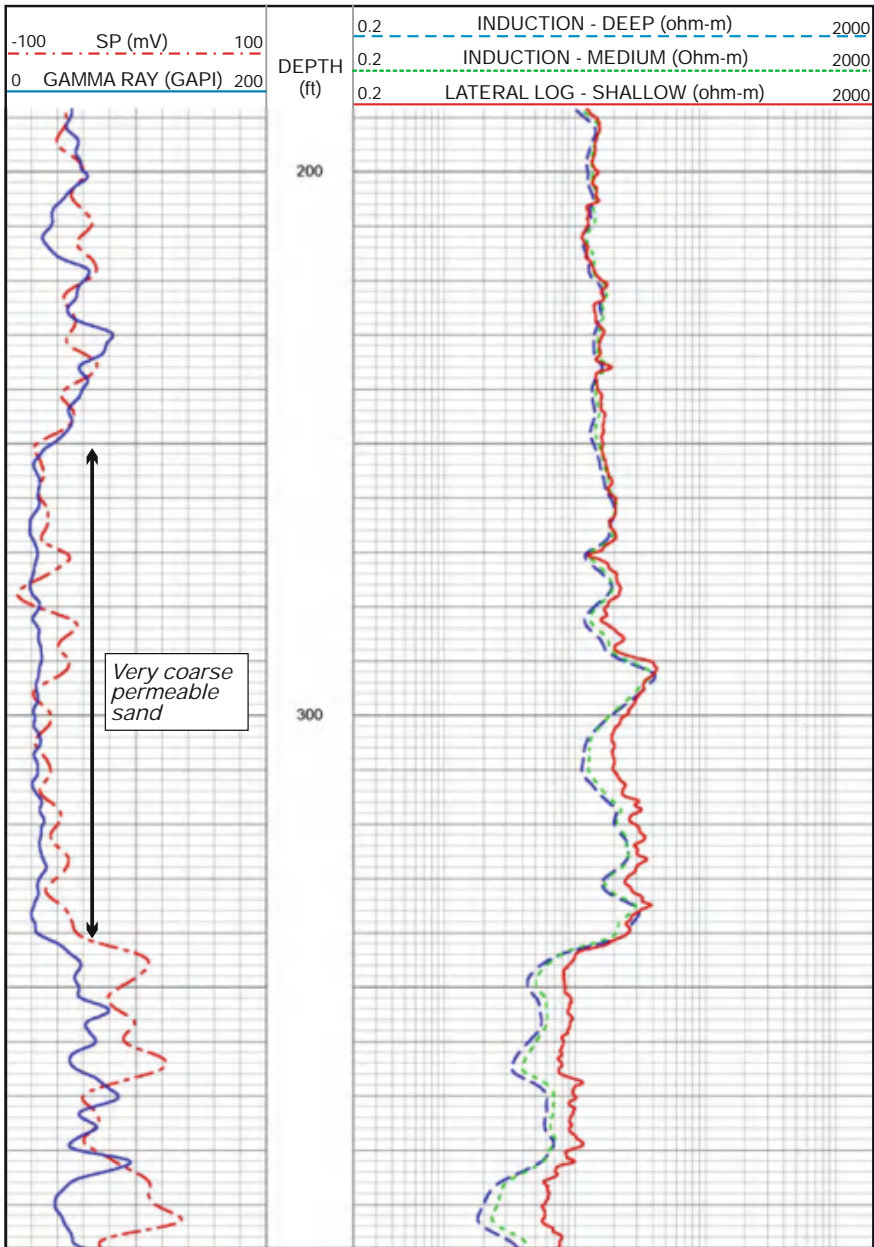
Fig. 10.2 SP, dual induction, and gamma ray logs of a very-coarse permeable sand interbedded between more clay-rich strata. The less clay-rich sand is marked by a deflection of the SP curve to the left (indicating a greater salinity than the drilling fluids) and lesser gamma response

$$I_{GR} = \frac{GR_{log} - GR_{min}}{GR_{max} - GR_{min}} \qquad (10.1)$$

where

GR$_{log}$ Gamma ray reading of the formation
GR$_{min}$ Minimum gamma ray response from a clean sand or limestone
GR$_{max}$ maximum gamma ray response for shale or clay bed

As a first-order estimation, the volume of shale can be assumed to be equal to I_{GR} (linear response; Asquith and Krygowksi 2004). Asquith and Krygowski (2004) provide several nonlinear response equations, which may be more accurate than the linear response relationship.

Gamma ray logs are particularly useful when combined with a high-quality analysis of well cuttings. As an in situ measurement, the gamma ray log can be used to provide a more refined depth control for the well cuttings samples, which may be important for well design. For example, accurate determination of the depth intervals of more productive sand units in an aquifer is critical for the installation of well screens at optimal depths. Gamma ray log patterns are also used for inter-well correlations, particularly where there is some lithological control.

Gamma ray logs have been prepared for outcrops and cores using a standard logging sonde or, more commonly, a hand-held gamma ray scintillometer, which provide insights into the interpretation of gamma ray logs (Slatt et al. 1992). Slatt et al. (1992) observed that correlations based solely on gamma ray logs from a studied quarry face were very different than correlations made in which geological data from the exposure were also considered. A key conclusion for log interpretation, in general, is that without some knowledge of depositional geometries and an understanding of lateral facies changes, proper correlation of stratigraphic intervals or depositional cycles at the scale of individual beds or groups of beds is difficult (Slatt et al. 1992). Therefore, care should be taken when attempting correlations based solely on gamma ray logs.

Local or regional stratigraphic correlations can be made where marker beds or intervals with distinct gamma ray geophysical signatures are present. For example, phosphate-rich and clay-rich strata have distinctive gamma ray patterns that can be correlated across southwestern Florida (Maliva et al. 2006). Gamma ray data were invaluable in this investigation because many of the wells do not have lithological logs. Gamma ray log data allowed for accurate correlation between wells in which there is lithological control.

Gamma ray logs have also been used for facies analyses of sandstones (Serro and Sulpice 1975; Rider 1990; Geel 2002). The basic theory is that gamma ray log response correlates with clay content, which, in turn, is related to grain size. For example, a bell-shaped curve with a persistent upwards increase in gamma ray activity may be indicative of a fining-upwards sequence. Gamma-ray log shape is not an infallible indicator of lithofacies because other factors can influence log response. Feldspathic sands may have high gamma-ray activities that are comparable to that of clays and shales. Some clays (e.g., kaolinite) have a low

radioactivity. Clay content may also not be correlated with grain size in deposits that had a long duration of winnowing (Rider 1990).

10.5   Electrical and Resistivity Logs

The electrical resistivity of a formation is largely a function of its porosity and the resistivity of the formation water. Resistivity is the inverse (reciprocal) of electrical conductivity. In the oil and gas industry, resistivity-based logs are widely used to evaluate hydrocarbon saturation, which is the fraction of the pore volume occupied by hydrocarbons. In groundwater investigations, formation water resistivity is largely a function of salinity.

Types of resistivity (X-m) that are important for log analysis are

R_w resistivity of the formation water
R_{mf} resistivity of the mud filtrate (drilling fluid after solids have been filtered out)
R_t resistivity of the uninvaded zones of a formation
R_{xo} resistivity of the flushed zone of a formation
R_o resistivity of a water-filled formation
R_a apparent resistivity (calculated, uncorrected R_t value)

Resistivity logs have the following applications for groundwater investigations

- lithology determination
- estimation of porosity
- estimation of groundwater resistivity and thus salinity
- identification of permeable zones from drilling-fluid invasion
- correlation between wells
- identification of fractures and bedding orientation (dipmeter logs).

10.5.1   Spontaneous Potential

The spontaneous potential (SP) log is the oldest borehole geophysical log. The SP log records the natural potential (i.e., DC voltage) that develops between an electrode in the borehole and a fixed electrode at land surface. The electrical potential is generated by the interactions between formation waters, conductive drilling fluids, and certain ion-selective rocks, such as shales (Schlumberger 1989a). The SP response includes an electrochemical component and, in some cases, a typically minor electrokinetic (streaming) component caused by the flow of electrolytes (ions) in a permeable medium. An electrokinetic potential may be produced by mud filtrate flowing through mudcake deposited on borehole walls and into adjoining permeable strata.

The primary applications of SP logs are to identify and map strata containing interbedded shale (or clay) beds and lithological correlations. SP logs can also be used as a qualitative indicator of permeability. However, there is no direct relationship between the value of permeability and porosity and the magnitude of SP log deflections. The shape of SP logs can provide information on lithology, bed thickness, and the clay content of permeable beds. For example, fractures that are flow zones might be evident by narrow and comparatively sharp negative anomalies mainly produced by electrokinetic potentials (Kobr et al. 2005).

The SP log requires that the drilling fluid be conductive and that a salinity difference occurs between the drilling fluid and native formation water. The SP log units are millivolts (mV). SP log data are not interpreted in absolute values, but rather in terms of the direction and magnitude of the deflection from a shale baseline (Fig. 10.3). Permeable units are identified by deflections of SP logs from the shale baseline. If the formation water in a permeable unit is more saline (less resistive) than the drilling fluid (e.g., mud filtrate) in the adjoining borehole ($R_{mf} > R_w$), then the reflection would be to the left of the shale baseline (i.e., the potential will be less). Conversely, if the formation water is fresher (more resistive) than the drilling fluid ($R_{mf} < R_w$), then the deflection at a permeable unit will be to the right (i.e., the potential will be greater). The boundaries between permeable zones and nonpermeable (shale) zones are placed at the point of inflection (Hilchie 1979; Asquith and Krygowski 2004).

The main potential applications of SP logs for groundwater investigations are

- location of permeable beds
- location of shale or clay beds (confining units)
- inter-well correlation
- determination of formation water resistivity.

For quantitative analyses, a key value is the static spontaneous potential (SSP), which is the maximum spontaneous potential that a thick, shale-free porous and permeable formation can have for a given value of R_{mf}/R_w. Formation water resistivity can be estimated from the SSP using the equation (Schlumberger 1989a)

$$SSP = -K \, \log\left(\frac{R_{mfe}}{R_{we}}\right) \tag{10:2}$$

where
K $61 + 0.133T_f$
K $65 + 0.24T_c$
SSP   log deflection in millivolts
T_f borehole temperature in degrees Fahrenheit
T_c borehole temperature in degrees Celsius
R_{mfe} equivalent resistivity of the mud filtrate (X-m)
R_{we} equivalent resistivity of the formation water (X-m)
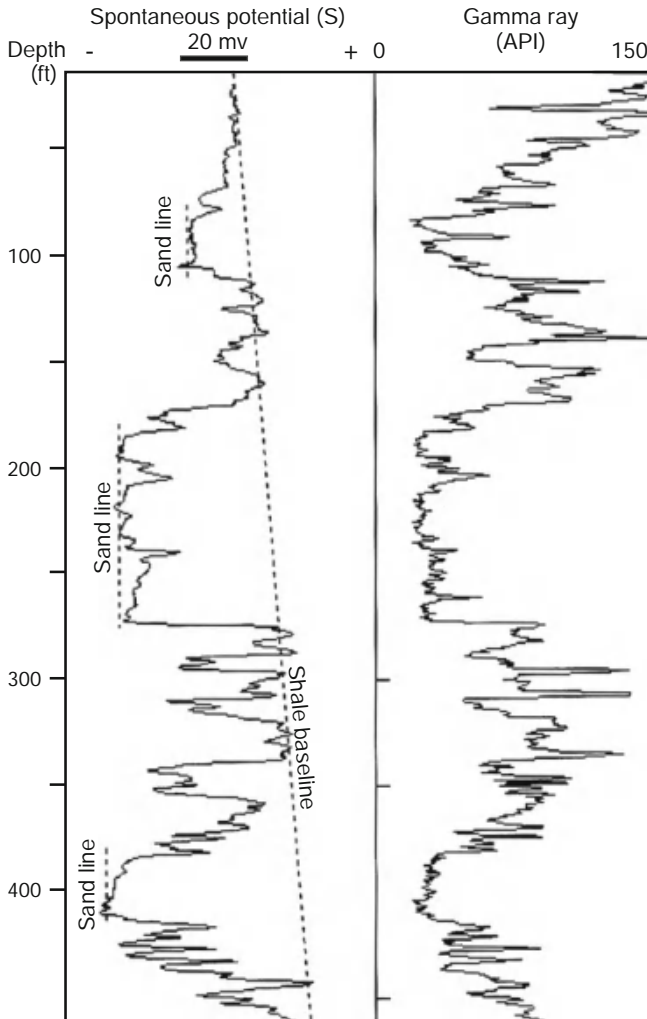
Fig. 10.3 SP and gamma log from the Dakota Aquifer of Kansas showing the responses of shale and sands (modified from Macfarlane et al. 1998)

The values of R_{mf} are measured during logging and need to be converted to R_{mfe} values, which has been traditionally performed using a correction chart. The calculated R_{we} values are similarly converted to R_w values, which are used to determine salinity. Keys (1989, 1990) cautioned that Eq. 10.2 is based on the assumptions that (1) the formation water is very saline, (2) NaCl is the predominant salt, and (3) the mud is relatively fresh and contains no unusual additives.

The SP log tends to be of limited value in most groundwater investigations because of small salinity differences between borehole fluids and native

groundwater. Also many aquifers do not have thick shale beds needed to establish a shale baseline. The SP log's greatest value may lie in evaluating brackish and saline groundwater in siliciclastic aquifer systems, where substantial salinity differences may occur between fresh drilling fluids and formation waters. The SP logs may also be used for qualitative analysis of salinity trends and the identification of permeable beds, particularly in conjunction with other logs. In practice, the SP log is very inexpensive to run and is routinely included with resistivity logs even if it is unlikely to provide useful information.

10.5.2   Resistivity Logs

Resistivity logs are very commonly used in groundwater investigations because they can provide information on

- the location of permeable zones
- porosity
- formation water salinity
- lithology

Resistivity logs are of great value in the oil and gas industry because they can differentiate between hydrocarbon-bearing zones and water-bearing zones. A great difference in resistivity occurs between hydrocarbons and the commonly saline formation waters. The rock matrix (grains and cements) of sedimentary rocks are mostly nonconductive. The ability of a formation to transmit electrical currents is, therefore, almost entirely a function of the water in the pores (both porosity and salinity). Resistivity logs are sensitive to all water in a formation, including clay and capillary-bound water, in additional to moveable water.

The most basic resistivity logs introduce a current to the formation and measure the resulting difference in potential (voltage). The relationship between electrical resistance, potential, and current is expressed by Ohm's law:

$$r = V/I \qquad\qquad (10:3)$$

where,
r   resistance (X)
V   potential (volt)
I   current (A)

Resistivity is an intrinsic property of a material, which is defined as follows:

$$R = rA/L \qquad\qquad (10:4)$$

where
R   resistivity (X-m)
r   resistance (X)
A   cross-sectional areas normal to the flow of current (m^2)
L   length (m)

Equation 10.4 requires that measured resistance values be processed for the geometry of the investigated aquifer volume (A and L parameters) in order to determine resistivity, the parameter of interest.

The resistivity of saturated geologic formations can be quantitatively analyzed using the Archie (1942) equation:

$$\frac{R_o}{R_w} = F = \frac{a}{\slash^m} \qquad (10{:}5)$$

where
m   constant (cementation factor or exponent), which is commonly between 1.8
    and 2.0
R$_o$ resistivity of a 100 % water-saturated formation (X-m) (true resistivity)
R$_w$ resistivity of pore waters (X-m)
F   formation factor (dimensionless)
$\slash$ porosity (m^3/m^3)
a   tortuosity factor, a constant that is usually equal to 1.0. Both R$_o$ and R$_w$ are at
    formation temperature.

Hingle (1959) and Pickett (1968, 1973) presented graphical methods for solving Archie′s equation. Kwader (1986) provides an example of the use of Archie′s equation and a Hingle plot to process resistivity and porosity data to obtain groundwater salinity in Tertiary carbonates of southeastern Coastal Plain of the United States.

Archie′s equation is applicable where the electrical conductivity through inter-connected pore space is much greater than all other forms of electrical conductivity in the formation (Kobr et al. 2005). The presence of intergranular clay or clay coatings on grains can invalidate Archie′s equation, particularly in fresh and brackish water (Kobr et al. 2005). A number of modifications of the Archie equation to shaly or clayey strata have been proposed. One modification for 100 % water saturation is Schlumberger (1989a)

$$\frac{1}{R_0} = \frac{(1 - V_x)}{FR_w} + \frac{CV_x}{R_x} \qquad (10{:}6)$$

V$_x$ bulk volume fraction of clay or shale (fractional)
C   empirical coefficient
R$_x$ term related to the resistivity of shale or clay (X-m)

When V_x is zero, Eq. 10.6 reduces to the Archie equation (Eq. 10.5) for 100 % water saturation.

The default cementation factor (m) of 2, is fairly accurate in rocks dominated by intergranular porosity. However, the cementation factor may be markedly different from (greater than) 2 in limestones in which the porosity is primarily secondary (e.g., moldic; Focke and Munn 1987; Wempe 2000). Fissured and fractured rock may have values less than 2. Quantitative analysis of resistivity logs in heterogeneous reservoirs and aquifers may require that they be interpreted by layers (intervals) on the basis of the predominant rock type (Focke and Munn 1987).

A number of different types of resistivity logs have been developed and used in the oil and gas industry and groundwater investigations. A voluminous literature exists on resistivity logging techniques and interpretative methods (e.g., Asquith and Krygowski 2004). In order to quantitatively analyze resistivity logs, calculated apparent resistivity (R_a) values must be converted to true resistivity (R_t) values by correcting for the various extraneous factors that affect resistivity measurements. The extraneous factors include the resistivity of the invaded zone (the zone in which drilling fluids entered the formation), the depth of invasion, resistivity of the drilling fluid (mud) and mud filtrate, borehole diameter, bed thickness, mudcake presence and thickness, and the thickness and resistivity of adjacent beds (Keys 1989; Collier 1993). Mud filtrate is the water that passes through the mudcake that develops on the borehole wall and thus enters (invades) the formation. Resistivity values are also a function of temperature, and thus, temperature corrections should be applied to R_w and R_{mf} values, if there are substantial differences in temperature between land surface (where resistivity measurements of fluids are made) and the formation (Asquith and Krygowski 2004). The methods for correcting for extraneous factors and obtaining true resistivity values are reviewed by Schlumberger (1989a) and Asquith and Krygowski (2004).

The normal resistivity and lateral logging tools consist of two current electrodes located near the top and bottom of the tool and intervening potential electrodes. The potential electrodes measure the voltage drop when a constant alternating current is applied to the current electrodes. The volume and depth of investigation increases with increasing potential electrode spacing. Commonly, potential electrodes with spacings of 16 and 64-inches (40.6 and 162.6 cm) are used, which are referred to as the short- and long-normal logs. The short-normal log is considered to investigate only the invaded zone, whereas the long-normal log is considered to investigate both the invaded zone and the zone where native formation water is present.

Induction logs have largely replaced resistivity logs in the oil industry and are now widely used for groundwater investigations. The dual-induction log is based on Faraday's law in which a changing electromagnetic field can generate an electric current. A high-frequency alternating current is passed through transmitter coils in the logging tool (sonde), which generates an alternating magnetic field in the formation. The alternating magnetic field, in turn, generates current loops in the formation, which flow in paths coaxial to the sonde. The current loops produce their own magnetic field, which induces a current when they cross the receiver coils of the sonde. The recorded signal is proportional to the conductivity of the formation.

Practical induction logging tools use several arrays of coils, which are designed to achieve a specific targeted focusing and depths of investigation. Induction logs are generally recommended for holes drilled with moderately conductive (i.e., fresh-water) to nonconductive muds, and in empty or air-filled holes (Schlumberger 1989a).

A typical dual-induction sonde consists of a deep-induction and a medium-induction array on the same sonde, in which the two arrays share the same transmitters but have different receivers. The dual-induction log is often combined with a shallow laterolog, which is referred to as either the dual-induction laterolog (DIL) or dual-induction focused log. DIL logs thus have three tracks, shallow lateral log, and medium and deep induction, which record resistivity at different depths of investigation (Fig. 10.4). The greater depth of investigation of the deep-induction log and focusing of the current allows for the determination of more accurate values of the true formation resistivity (R_t). Array resistivity tools have a greater number of receivers and thus investigate more depths into the formation.

Separation of the three DIL or normal resistivity tracks is a manifestation of the invasion of drilling fluids into the formation, with the shallow logs tending to reflect the composition of drilling fluids (mud filtrate) and deep logs tending to reflect the composition of the native formation waters. Deep-induction readings can be corrected using true resistivity values (R_t) and the depth of invasion calculated using 'tornado' charts (Asquith and Krygowski 2004). Drilling-fluid invasion is indicative of the presence of permeable strata. However, if the drilling fluids and formation waters have similar salinities (resistivities), then invasion may not be detectable. In the dual-induction log segment provided in Fig. 10.4, invasion is not evident in the upper part of the log where the brackish drilling fluid and formation water have similar salinities. Invasion becomes evident at depth once formation salinity increases to seawater values. It is, therefore, important to record the resistivity of drilling fluids during logging. The depth of invasion is inversely proportional to porosity, with greater depths occurring in low-porosity strata (Collier 1993). For a given volume of invasion water, the fluid will occupy a greater volume of sediment or rock with lower porosities.

Resistivity log data are quantitatively analyzed using Archie's equation to determine porosity or salinity. If the salinity (and thus resistivity) of the formation waters is known, then Archie's equation can be used to estimate formation porosity. Porosity measurements are normally based on measurements of the formation resistivity close to the borehole (i.e., invaded zone) using the equation (Asquith and Krygowski 2004).

$$\emptyset = \left(\frac{aR_{mf}}{R_{xo}}\right)^{\frac{1}{m}} \tag{10:7}$$

The value of R_{mf} can be obtained from measurements of the drilling fluid. Wempe (2000) calculated porosity from gamma ray and resistivity log data by first determining clay content using gamma ray logs. The formation factor (F) was next
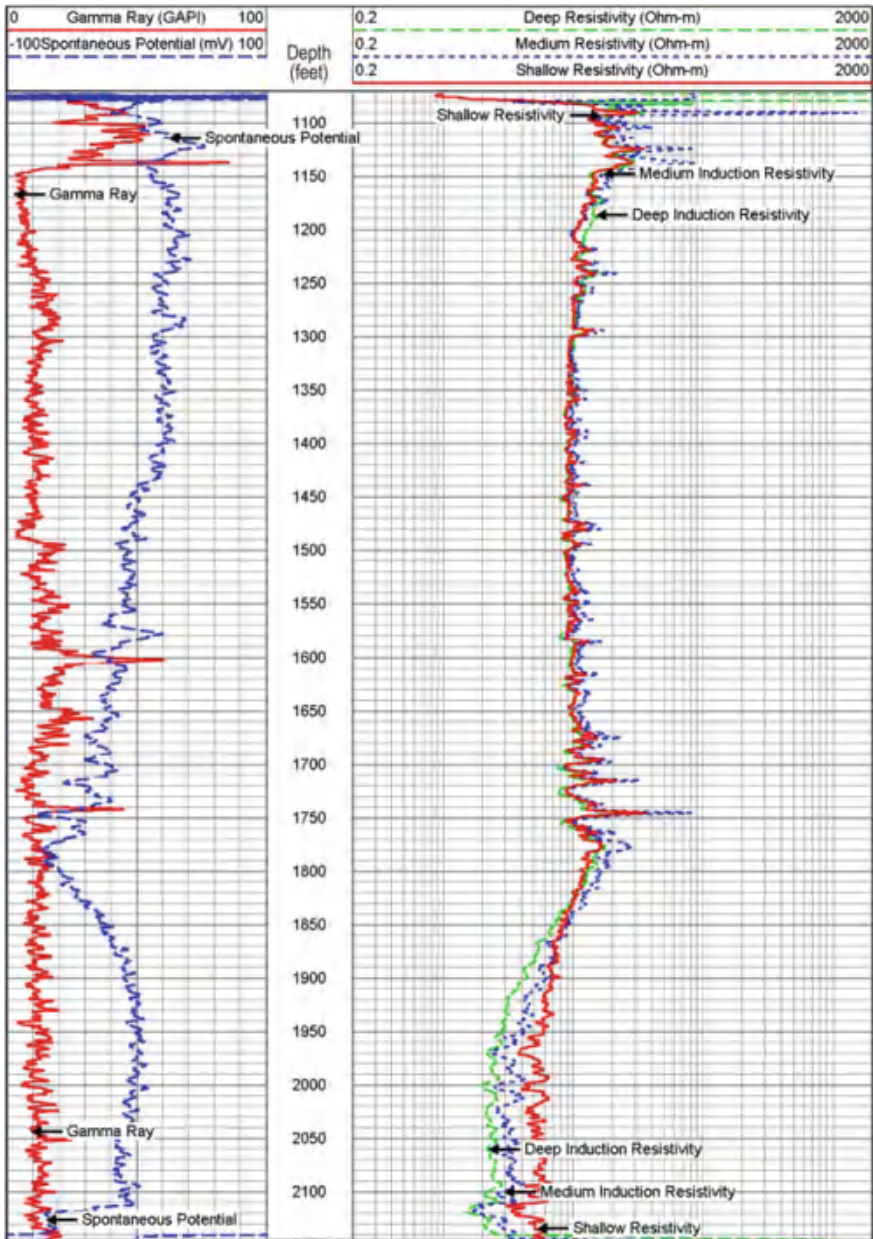
Fig. 10.4 Dual-induction log of a relatively homogenous limestone interval (Floridan Aquifer, Hialeah, Florida). A pronounced down-hole increase in salinity from mildly brackish to seawater values is evident by the sharp decrease in resistivity from 1780 to 1950 ft. The increase in the difference in salinity between the drilling fluids and pore waters below 1780 ft allows for invasion to be detected as evidenced by separation of the resistivity tracks

determined using a clay-corrected form of Archie's equation. Porosity was next calculated from F using lithology-specific cementation factors (m) determined by calibration of corresponding log-determined and laboratory-measured porosity data.

Similarly, if the porosity of the formation is known, then Archie's equation can be used to estimate the resistivity of the formation water. The resistivity of water varies with temperature according to Arp's formula:

for Fahrenheit

$$R_{T1} = R_{T2}\left(\frac{T_2 + 6.77}{T_1 + 6.77}\right) \tag{10.8}$$

for Celsius

$$R_{T1} = R_{T2}\left(\frac{T_2 + 21.5}{T_1 + 21.5}\right) \tag{10.9}$$

where R_{T1} and R_{T2} are resistivities at T_1 and T_2, respectively. After correcting log-derived formation water resistivity data for the values at 25 °C, specific conductance (SC, µhmos/cm or µS/m) can be calculated as

$$SC = \frac{10,000}{R_{w,25\,°C}} \tag{10.10}$$

where $R_{w,25\,°C}$ = temperature-corrected formation water resistivity. Specific conductance can, in turn, be converted to total dissolved solids (TDS) or chloride concentration using empirical relationships established from local water quality data (e.g., Reese 1994). Thus, a combination of resistivity, temperature, and porosity logs can be processed to provide a salinity-versus-depth profile (Fig. 10.5). In groundwater investigations, porosity data from a sonic log and formation resistivity from a deep-induction log are commonly used to generate log-derived TDS plots. Where quantitative data on formation porosity are not available, formation water salinity can still be roughly estimated by using porosity values estimated from core data, examination of cuttings, or by bracketing the likely porosity values.

Microresistivity logs utilize a sidewall pad tool that carries short-spaced electrode devices, which are pressed against the formation wall. The logs are used to measure the resistivity of the flushed zone (R_{xo}) and to determine the presence of permeable beds by detecting the presence of mudcake (Schlumberger 1989a). Mudcake is indicative of invasion and thus permeable formations. Porosity may also be determined from microresistivity logs, if the resistivity of the invaded fluid (i.e., mud filtrate or water used for drilling) is known.

Dipmeter logs (e.g., HDT high-resolution dipmeter tool and SHDT dual-dipmeter tool, marks of Schlumberger) are a variety of microresistivity logs, which contain four pads that record microresistivity at a 90° spacing. The data are processed using proprietary pattern-recognition techniques to pick out correlated features on the curves (Schlumberger 1989a). The dipmeter log can provide data on
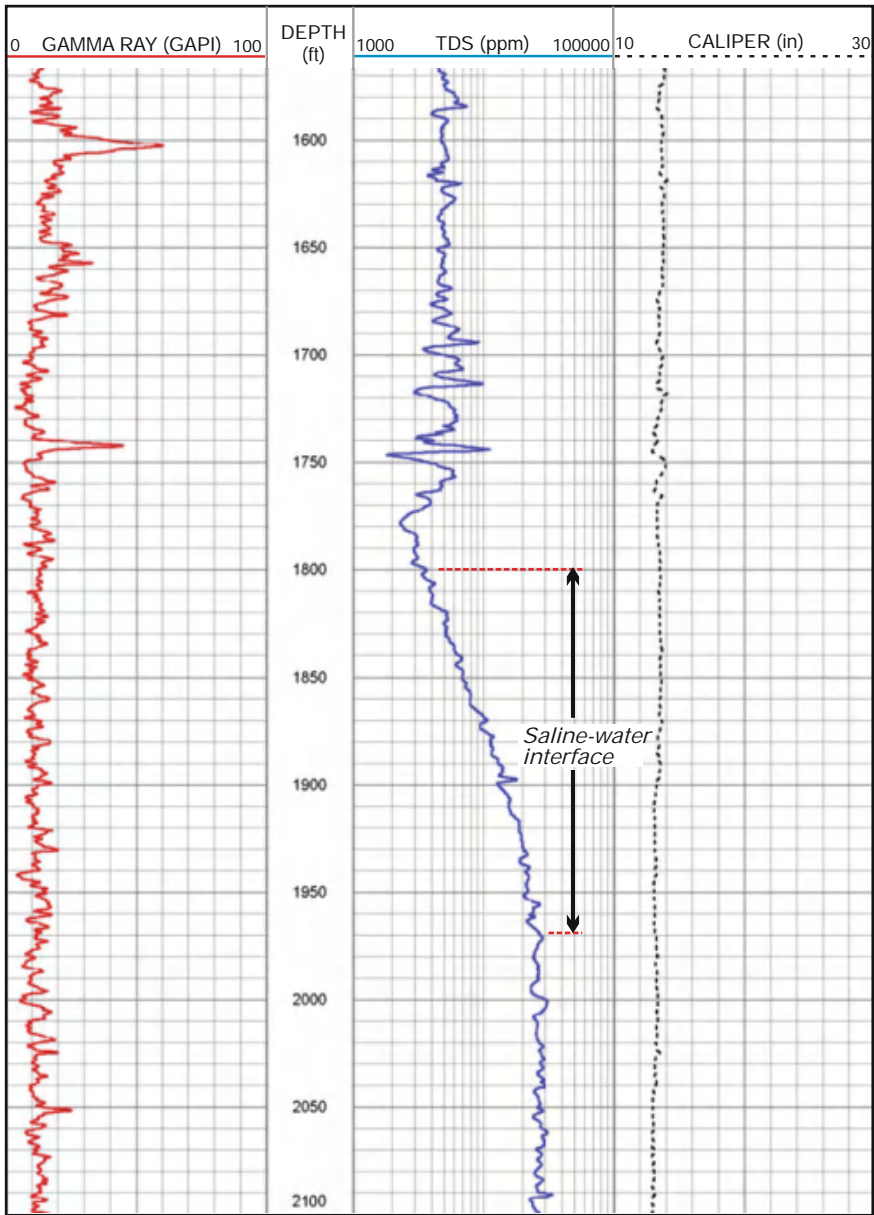
Fig. 10.5 Log-derived total dissolved solids (TDS) plot, which shows a pronounced downhole increase in salinity between about 1800 and 1970 ft, reaching near seawater values. The plot was generated to determine the depth of the 10,000 mg/L TDS isopleth at a deep injection well site

structural dip, the presence and orientation of faults, fractures, and sedimentary bedding. Fractures tend to have the greatest effect on shallow resistivity and may be indicated by spurious low resistivity reading that are not evident on medium- or deep-resistivity logs (Schlumberger 1989a). Fluid-filled fractures have reduced resistivity compared to adjoining unfractured rock.

10.6   Sonic (Acoustic) Logs

Sonic or acoustic logs use the velocity, amplitude, and phase relationships of transmitted sound waves to obtain information on the physical properties of the tested formation. The three main sonic waves of concern in geophysical logging are, in order of their time of arrival, compressional, shear, and Stoneley waves. The sonic logging tool has one or more transmitters and typically two or more receivers. The most basic sonic log is the velocity or transit log, which records the travel time of compressional sound wave pulses.

The travel time of a sound wave from the transmitter to a receiver includes three components: (1) travel time from the transmitter through the borehole fluid to the formation, (2) travel time within the formation, and (3) travel time from the formation through the borehole fluid to the receiver. The travel time within the borehole fluid depends upon the diameter of the borehole and the orientation and position of the sonde within the borehole. The velocity of sound waves in a formation is a function of both the rock or sediment type (matrix) and its porosity. Usually, the speed of sound in drilling fluids is less than that in the formation and, as a result, the formation signal arrives first.

The data desired is the travel time through the formation, which is the total travel time minus the travel times through the borehole fluid between the tool and formation. The formation travel time is determined by using logging tools having two or more receivers at different spacings. The travel time in the formation is calculated by subtracting the travel times between the receivers, which would result in the canceling out of (or compensation for) borehole travel time effects. Transit times within the formation are expressed as interval transit times using the units of either microseconds per meter (μs/m) or microseconds per foot (μs/ft). Borehole effects can be further compensated for by having transmitters above and below the receivers and averaging the calculated transit times. Borehole compensated sonic logs are essential for quantitative analysis of the sonic log data.

More modern acoustic logs allow for the digital recording of the entire received waveform, from which compression, shear, and fluid (Stoneley) arrivals can be separated and quantitatively analyzed (Serra 2008). The Array sonic log, which contains an array of eight widespread piezoelectric receivers, is used to find and analyze all propagating waves in the composite waveform (Schlumberger 1989a). The attenuation of Stoneley waves can be used to identify permeable zones in a formation (Sect. 15.1.1).

Porosity (ϕ) is estimated from interval sonic transit times using the Wyllie et al. (1958) formula

$$\phi = \frac{Dt_{log} - Dt_{ma}}{Dt_f - Dt_{ma}} \qquad (10:11)$$

where

Dt_{log} interval transit time of the formation (measured; µs/m)
Dt_{ma} interval transit time of the matrix (µs/m)
Dt_f interval transit time in the wellbore fluid (µs/m)

Interval transit times (Dt_{ma} and Dt_f) of some common sedimentary rock types and fluids are provided in Table 10.1.

Sonic logs commonly include tracks for sonic transit time and sonic porosities (Fig. 10.6), which are typically calculated using a constant matrix interval transit time based on the predominant lithology of the logged strata. This approach can result in significant errors in characterizing formations containing inter-bedded strata of different lithologies. Sonic logs often include a variable density log (VDL), which is an intensity modulated-time presentation of the sonic wave train from the transmitter pulse (Fig. 10.7). The amplitudes of the wave forms produce a variable density that is presented versus time, shown in color or, more commonly, as gray or black bands. The horizontal scale of the VDL log is in units of time (µs), in which the earliest arrivals are on the left. The frequency of waves is related to the width of the bands.

Sonic transit times are influenced by the type, size, and distribution of pores, borehole size, drilling mud, invasion, and fracturing. Sonic transit time and VDL logs are useful for the detection of fractures and cavities. Unfractured rock usually has a VDL log pattern of continuous parallel bands, whereas fractured intervals may have an offset or a disrupted (chaotic) pattern and exceedingly long sonic transit times.

Table 10.1   Interval transit times of different matrices and fluids

Matrix or fluid type	Interval transit time (µs/ft)	Interval transit time (µs/m)
Limestone	47.6–52.6	156.2–172.6
Dolomite	42.0–47.6	137.8–156.2
Sandstone (slightly consolidated)	58.8–66.7	192.9–218.8
Sandstone (consolidated)	52.6	172.6
Shale	62.5–167.0	205.1–5 47.9
Anhydrite	50	164
Freshwater	200	656
Brine	189	620
Fresh mud	189	620

Sources Keys (1989), Schlumberger (1989a), and Asquith and Krygowski (2004)
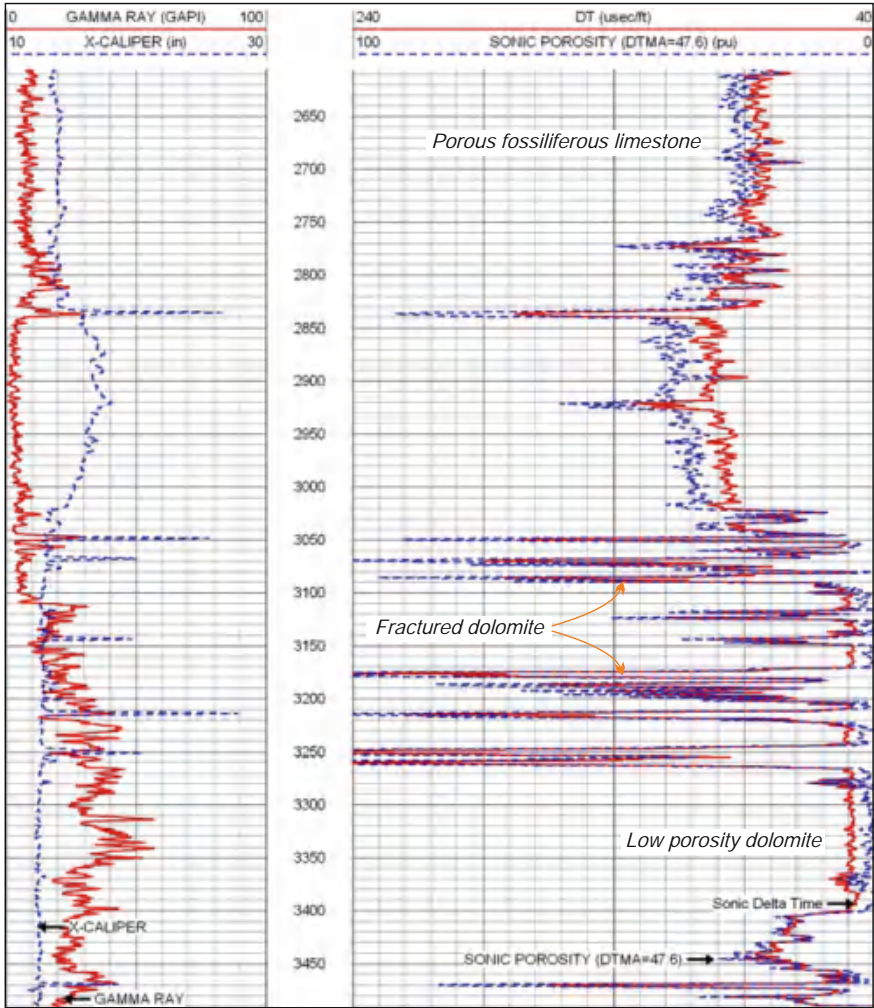
Fig. 10.6 Sonic log with tracks for transit time (DT) and sonic porosity. Log shows responses of porous limestone, hard low-porosity dolomite, and fractured dolomite, which has extremely long transit times

As a generalization, sonic logs 'see' the continuous phase. For example, isolated vugs that constitute a small percentage (<5–10 %) of a formation may not be detected by a sonic log (Serra 2008). Sonic logs respond to secondary porosity differently than neutron and density logs. Sound takes the quickest path, which is not through vugs and fractures (Asquith and Krygowski 2004). Porosity values calculated using the Wyllie et al. (1958) formula are primary or matrix
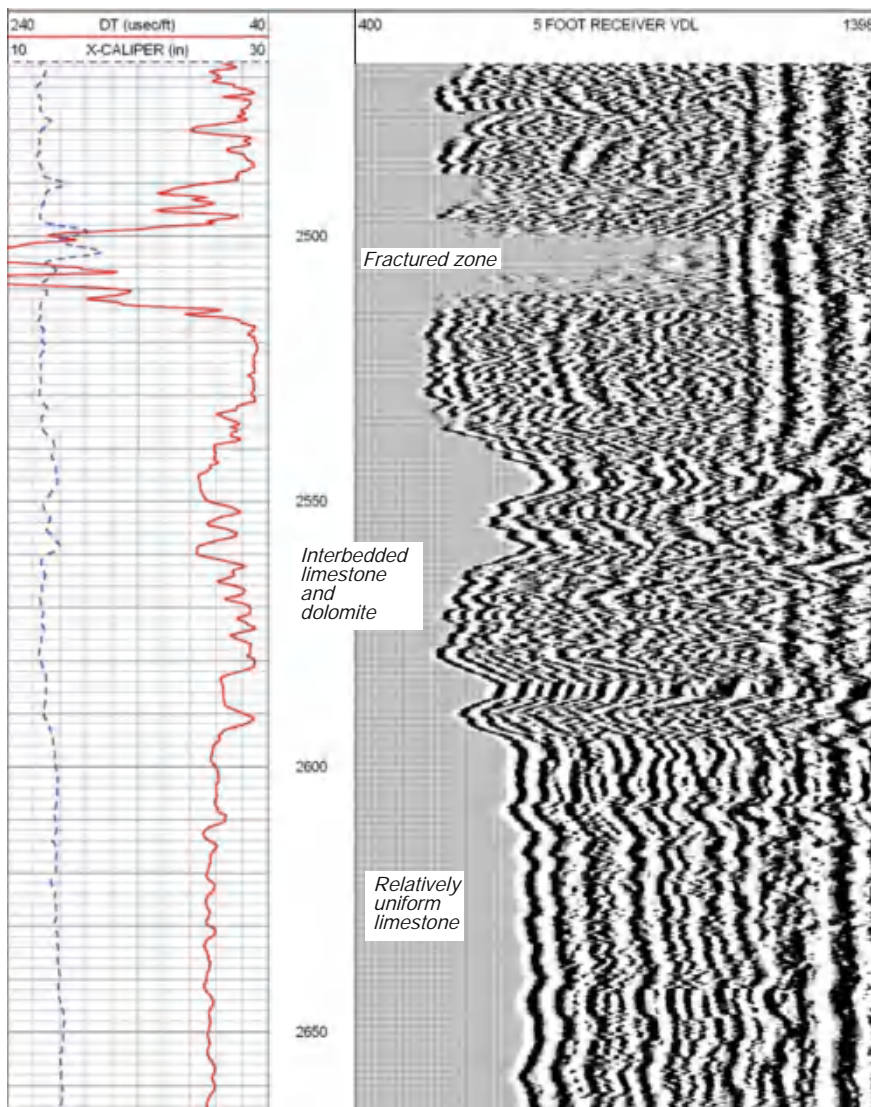
Fig. 10.7   Sonic log with VDL showing response of fractured rock, relatively uniform unfractured rock (limestone) and interbedded rock of different porosity (limestone and dolomite)

(intergranular or intercrystalline) porosity and will be underestimations of total porosity, if vuggy or fracture porosity is present. The percentage of vuggy or fracture porosity can be estimated by subtracting the sonic porosity from the total porosity obtained by other means, such as a neutron log (Schlumberger 1989a; Asquith and Krygowski 2004)

$$\emptyset_2 = \emptyset_{total} - \emptyset_{sonic} \qquad (10{:}12)$$

where $\emptyset_2$ = secondary porosity, $\emptyset_{total}$ = total porosity, $\emptyset_{sonic}$ = sonic porosity.

Kennedy (2002) cautioned that the assumption that sonic logs do not see vugs, fractures, and intraparticle porosity is simplistic and, depending upon circumstances, may be wrong. Hence, the importance of having some knowledge of rock types present during the interpretation of well logs.

In unconsolidated or insufficiently consolidated sands, the Wyllie equation gives porosity values that are too high. An additional empirical compaction factor is applied for the calculation of the porosity of unconsolidated sands using sonic log data:

$$\emptyset = \left(\frac{Dt_{log} - Dt_{ma}}{Dt_f - Dt_{ma}} \right) \frac{1}{C_p} \qquad (10{:}13)$$

$$C_p = \frac{Dt_{shale} C}{100} \qquad (10{:}14)$$

where
C_p compaction correction factor
C constant (normally between 1 and 1.3)
Dt_{shale} interval travel time for shale adjacent to the formation of interest

10.7   Nuclear Logging

Nuclear logs, which include density and neutron logs, are primarily used to determine the porosity of formations. Density and neutron logs are uncommonly run in groundwater investigations because they usually utilize radioactive sources. The use and transport of radioactive sources is controlled by various governmental jurisdictions, and prohibitions may be in place against the use of radioactive sources in aquifers containing freshwater that are (or may be) used as drinking water sources. The legal liabilities and obligations associated with the use of radioactive sources may result in an unacceptable risk to some loggers, consultants, and well owners. This liability stems from regulatory requirements that obligate the logger, well owner, or consultant to recover the source if it is lost in the borehole. Tools with accelerator-based sources have been developed, but are not widely used for groundwater investigations because of cost and availability.

10.7.1 Density Log

The density log (also referred to as the gamma–gamma log) measures the density of electrons in a formation, which is related to the bulk density of the formation. The logging tool consists of a gamma ray source, either Cobalt-60 or Cesium-137, which emits gamma rays into the formation, and two gamma ray detectors (in borehole compensated tools). The emitted gamma rays collide with electrons in the formation, and as a result, lose some of their energy to the electrons, which is known as Compton scattering. The scattered gamma rays that reach detectors at fixed distances from the source are counted. The density of higher energy electrons in a formation, and thus, the number of scattered electrons that reach the detectors, is related to the bulk density (q_b) of the formation, as quantified in g/cc. Formation density is a function of mineralogy and porosity. For water-filled sandstones, limestones, and dolostones, the bulk density measured by the density log is practically identical to the true bulk density of the rock. A small correction factor needs to be applied to obtain a true bulk density for a few substances, such as gypsum, anhydrite, and coal (Schlumberger 1989a).

Gamma ray interactions in the lower energy range are governed by the photoelectric effect, which is strongly dependent upon lithology and only slightly dependent on porosity. The photoelectric effect is a low-energy interaction in which a gamma ray collides with, and is absorbed by, an atom, with the resulting emission of a photoelectron. The mostly tightly bound electrons (i.e., those in the K shell) have the greatest ability to absorb gamma rays. Heavy (large atomic number) elements absorb low-energy gamma rays more strongly than lighter elements. The photoelectric effect will thus vary with elemental composition and thus mineralogy.

Photoelectric (PEF) logs record the photoelectric absorption index, whose units are barnes per electron (b/e). The photoelectric effect curve appeared in second-generation density tools, which are commonly referred to as "Litho" or "Spectral" tools (Schlumberger 1989a; Asquith and Krygowski 2004). The photoelectric effect of sandstones is less than 2 b/e and that of limestones and dolostones are about 5 and 3, respectively (Asquith and Krygowsski 2004). PEF logs can thus be used to differentiate between limestones, dolostones, and sandstones. The PEF log is inherently imprecise and is not particularly accurate for quantifying the percentage of minerals present (Kennedy 2002). The PEF log can differentiate between "pure" limestone and dolomite, but intermediate readings are not linearly related to the quantity of dolomite in the formation (Kennedy 2002). Variations in the calcium to magnesium ratio of both limestones and dolomites will affect their photoelectric absorption. Photoelectric effect logs are valuable for determination of mineralogy, especially, when used in conjunction with other logs. For example, a downhole transition from sandy phosphatic limestone to less porous clean limestone in the Upper Floridan Aquifer system of South Florida is marked by a decrease in gamma ray activity, increase in photoelectric absorption, and decrease in density and neutron porosity (Fig. 10.8). Cross-plots of photoelectric absorption index versus potassium concentration and thorium/potassium ratio obtained from
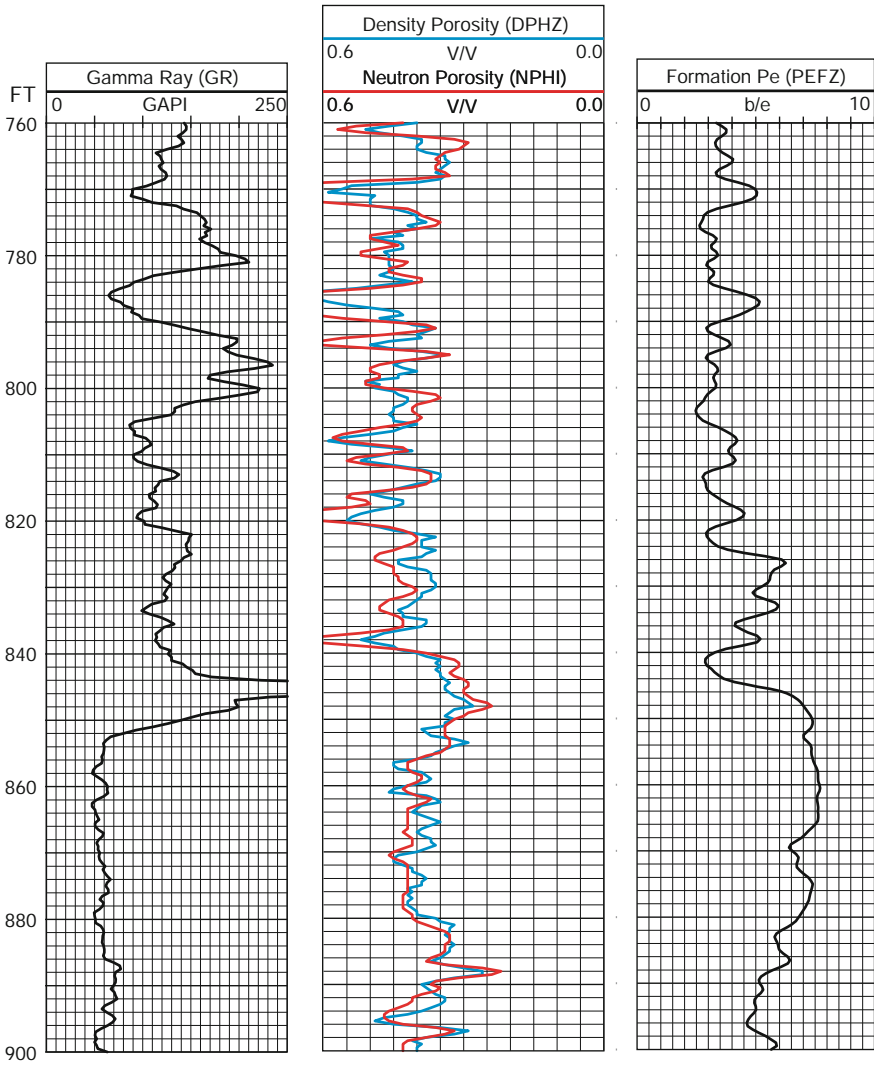
Fig. 10.8 Natural gamma ray, density and neutron porosity, and photoelectric adsorption logs for exploratory well GLF-6, located near Moore Haven, Glades County, Florida. A downhole transition to relatively pure limestone occurs at about 846 ft as indicated by a decrease in gamma ray activity and increase in photoelectric adsorption

natural gamma ray spectroscopy logs can be used to identify clay minerals (Schlumberger 1989a).

   The porosity of a formation (ϕ) is a function of the bulk density of the formation (q_b), matrix density (q_{ma}), and pore-fluid density (q_f), as follows

$$\slash = \frac{q_{ma} - q_b}{q_{ma} - q_f} \qquad (10{:}15)$$

where densities are expressed in units of g/cm^3. Calculated porosity values thus depend upon the value used for the matrix density. The matrix densities (q_{ma}) can be estimated from the specific gravity of the predominant mineral phase. For freshwater to moderately brackish water and fresh drilling muds, a q_f of 1 g/cc may be used.

10.7.2   Neutron Log

Neutron logs are used to determine the porosity of formations by measuring the amount of hydrogen present in a formation. For clean formations having minimal clay mineral contents, the bulk of the hydrogen in a formation is present in pore fluids, which is water in groundwater investigations. Therefore, neutron logs are used to measure the porosity of the saturated formation. Similar neutron probes are used to measure water content in unsaturated strata.

Neutrons are classified as a function of their energy, which ranges from thermal neutrons with an energy of 0.025 eV to high-energy neutrons with energies greater than 10 meV. Neutrons emitted from a source interact with atomic nuclei in the formation in a variety of manners. In inelastic scattering, fast neutrons collide with a nucleus and excite it to a higher energy state. The nucleus quickly returns to its ground state and usually emits one or more gamma rays at energies unique to the target nucleus. Measurements of the gamma rays are used to calculate the abundance of elements.

Elastic scattering occurs when neutrons are rapidly slowed down by elastic collisions with a nucleus. The neutron logging tool generates high-energy neutrons from either a chemical source, which commonly consists of a mixture of americium and beryllium, or a particle accelerator. The fast nuclei collide with the nuclei of the formation material, each time losing some of their energy. The greatest energy loss occurs when the neutron collides with a nucleus of similar mass (i.e., hydrogen nucleus). The neutrons that are slowed down to thermal velocities, corresponding to energies of about 0.025 eV, are captured by the nuclei of other atoms, which then emit high-energy gamma rays. The slowing down of neutrons, and thus formation of thermal neutrons and emission of gamma rays, depends largely on the amount of hydrogen in the formation, and thus fluid-filled porosity (Schlumberger 1989a; Serra 2008). The logging tool detects either the gamma rays or thermal neutrons.

Neutron logging tools are standardized using the API neutron unit. The 1000 API standard corresponds to the reading in a formation block at the University of Houston, which consists of freshwater-saturated Indiana limestone with a porosity of 19 %. Logs are typically scaled in apparent limestone porosity units by conversion from API units. Neutron logs are also affected by the lithology of the matrix rock, and are reported in limestone, dolomite, or sandstone porosity units. Neutron

porosity is equal to true porosity, if the lithology corresponds to neutron porosity units. Otherwise, the neutron porosity must be corrected to true porosity (Schlumberger 1989a; Asquith and Krygowski 2004). Neutron and density log measurements are affected by aquifer lithology in a different manner. Cross plots of density versus neutron porosity values allow for the determination of both aquifer lithology and true porosity (Fig. 10.9). The neutron tool measures all water in a
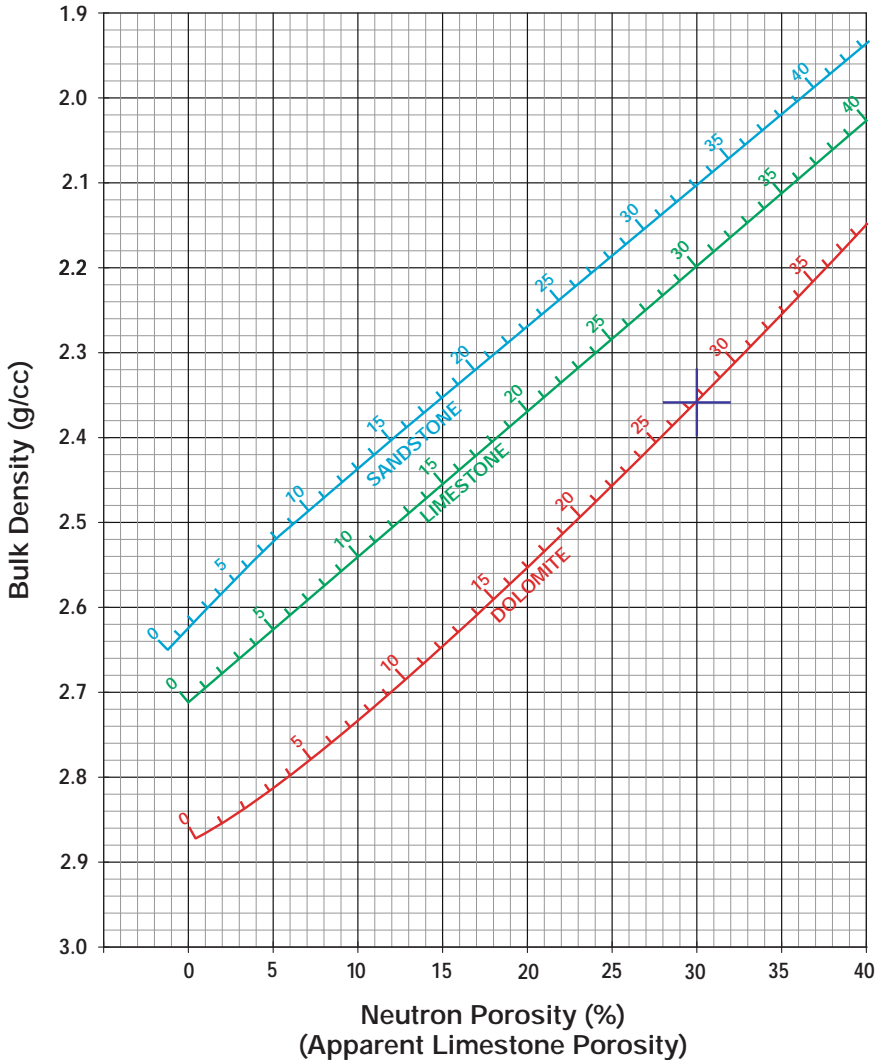
Fig. 10.9 Chart for interpreting neutron porosity and density log data for boreholes filled with freshwater (Schlumberger 1989a). For example, a neutron porosity of 30 % (in limestone porosity units) and a density of 2.36 g/cc, would indicate the presence of dolomite with a true porosity of 27.5 %

formation, including water bound in shales and hydrated minerals (e.g., clays, gypsum), and water present in the borehole. Bedded gypsum is often essentially nonporous and is identifiable by densities of close to 2.31 g/cc (and thus close to zero porosity density) and a very high neutron porosity, often greater than 50 %.

Neutron tool responses are dependent upon the tool types and, therefore, logs must be interpreted using charts or programs designed for the specific log (Asquith and Krygowski 2004). High salinities can affect calculated neutron porosities as the sodium chloride takes up space and reduces the hydrogen density. A correction needs to be applied if the groundwater is saline or hypersaline. Neutron logs are affected by borehole conditions including mud type (density and salinity), borehole diameter, tool position, and the presence of casing and cement. The most commonly used compensated neutron logs (CNL), contains one source and two detectors. Neutron porosity is calculated from the ratio of the counting rates of the two detectors, which greatly reduces the effects of wellbore parameters (Schlumberger 1989a, b).

10.8   Flowmeter Logs

10.8.1   Introduction

Flowmeter logs are commonly used in groundwater investigations to evaluate aquifer heterogeneity. Flowmeter logs measure the vertical velocity of water flow in a well relative to the tool at the depth at which the logging tool is positioned. Flowmeter logging and its applications to hydrogeologic investigations has been discussed by Javandel and Witherspoon (1969), Keys (1989), Molz et al. (1989, 1990, 1994), Kabala (1994), Paillet (1998), Paillet and Crowder (1996), Boman et al. (1997), Paillet and Reese (2000), and Maliva and Missimer (2010). A basic limitation of flowmeters logs is that they cannot be performed on mud-filled boreholes.

Flowmeter readings are performed either while the tool is being raised or lowered (trolling measurements) or at a number of depths in a well while the tool is not being moved (stationary readings). Trolling logs provide a continuous flow profile of the well, whereas the stationary mode provides measurements of the flow in the well at specific depths. Logs are typically run under static (no flow) and dynamic conditions, in which the well is either pumped at a constant rate or allowed to flow under artesian pressure. Trolling flowmeter log readings depend upon (1) the velocity of water flow in the well at the measuring point and (2) the rate and direction at which the logging tool is being moved. The line speed during trolling logs should be continuously recorded when running a trolling flowmeter log. It is imperative that the tool be retrieved at a constant rate and that the pumping rate or natural flow rate also be held constant during dynamic logs. Three main types of flowmeter logs are commonly run in groundwater investigations: (1) spinner,

(2) electromagnetic, and (3) heat-pulse. The impeller or spinner-type flowmeter logs are most commonly used, particularly in flowing wells and for dynamic tests. Each method has its strengths and weaknesses based on the borehole conditions and rate of flow.

The pattern of flowmeter logs can provide insights into hydraulic conductivity distribution. Patterns of gradual increase in flow into a well are often indicative of a flow system dominated by primary porosity, although a system with evenly distributed secondary porosity might also give this response. On the contrary, sharp steps in logs may be indicative of a thin flow zone, such as a hydraulically active fracture or karst conduit. Care must be taken in the interpretation of uncorrected flowmeter logs, because a sharp change in response could alternatively be related to a change in borehole diameter. Quantitative evaluation of flowmeter logs requires either correction for variations in borehole diameter, as measured using a caliper log (flowmeter interpretation log), or the by use of logging tools equipped to divert flow through an area of constant diameter.

Low-resolution trolling flowmeter logs that are commonly performed in groundwater investigations are sufficient to identify major flow zones and unproductive intervals. Data from the static and dynamic impeller flow meters logs may be sufficient to subdivide an aquifer into several zones and approximately apportion the total transmissivity between zones, but there may be significant noise in the data.

Flow velocity also varies within a borehole, with the greatest velocities occurring in the center of the borehole and lower velocities occurring near the borehole wall as the result of friction. It is therefore important for the flowmeter tool to be centralized within the borehole. Large variations in borehole diameter and borehole wall roughness (rugosity) can cause high degrees of turbulence, which can impact flowmeter log readings. Calculated flow rates may be overestimated in intervals of increased borehole diameter where flow is focused (and measured) in the center of the well. The effects of changes in borehole diameter are often much greater than the effects of local inflow (Paillet 2004). Syms (1982) proposed that the effects of changes in borehole diameter on flowmeter response can be removed by calculating flow rates at points in the well with the same diameter. Flowmeter logs may also give incorrect results in wells that are not fully developed and significant formation damage or skin effects occur (Young et al. 1998).

10.8.2   Spinner Flowmeter

The spinner or impeller flowmeter is the oldest flowmeter technique used in groundwater investigations. The spinner tool has an impeller whose rate of rotation is a function of the rate of fluid flow past the tool. The log output is the rotation rate, which is recorded as counts or rotations per second. The rotation rate is proportional to the fluid flow velocity. Trolling logs are run under both static and dynamic conditions. Dynamic logs are often run while the logging tool is being lowered

through the well and then again while the tool is being retrieved. Logging upwards tends to provide less useful information because the logging tool is being moved in the direction of water flow, and thus the flow velocity past the tool is low and the tool may stall. The main shortcoming of spinner-type flowmeters is the lack of sensitivity to low-velocity flow (Keys 1989).

The location of flow zones can be identified as depth intervals in which the borehole diameter-corrected flow velocity in a well increases (i.e., more water is entering a well). Flow into a borehole is indicated by increased separation of the static and dynamic tracks, provided that there is not a change in borehole diameter (Fig. 10.10). Spinner flowmeter logs provide information about flow velocity (v) within the tested borehole. The key variable of concern is discharge rate (Q), which is the product of flow velocity and borehole cross-sectional area (A)

$$Q = v \cdot A \qquad (10:16)$$

Unless the flowmeter log is run in a screened interval (in which the diameter is constant), a caliper log should be run to measure borehole cross-sectional area. The measured velocities should be normalized to the borehole cross-sectional area to assess flow at all intervals.

10.8.3 Electromagnetic Borehole Flowmeter (EBF)

The electromagnetic borehole flowmeter (EBF) is based on Faraday's law of induction. Flow rate is measured from the voltage induced by a conductor (such as water) moving at right angles through a magnetic field. The voltage is proportional to the velocity of the moving conductor. The EBF records flow in the same manner as the electromagnetic flowmeters that are widely used on horizontal pipes. Water flow in EBF tools is through a vertical tube in the center of the probe, which is surrounded by an electromagnet. An inflatable packer can be used to divert the entire well flow through the EBF tool. Inasmuch as the central tube of the EBF tool has a known constant diameter, the EBF provides a direct measure of flow rate. In large diameter wells, the EBF can be operated without a packer in the same general manner as a spinner flowmeter, with the measured flow through the tool being proportional to the total flow through the well. The EBF can be run in both trolling and stationary mode, although most of the reported applications used a stationary mode.

Some applications of the EBF are discussed by Young et al. (1998) and Dinwiddie et al. (1999). The main advantages of the EBF are that it can operate at lower flow velocities than the spinner log and, when used with a packer, it provides a direct measurement of flow rate without the need to correct for variations in borehole diameter. The sensitivity of the EBF to low flow rates enables it to better detect interzone flow within a well. A comparative study of impeller and electromagnetic flowmeters indicate that both logs provide comparable and interpretable
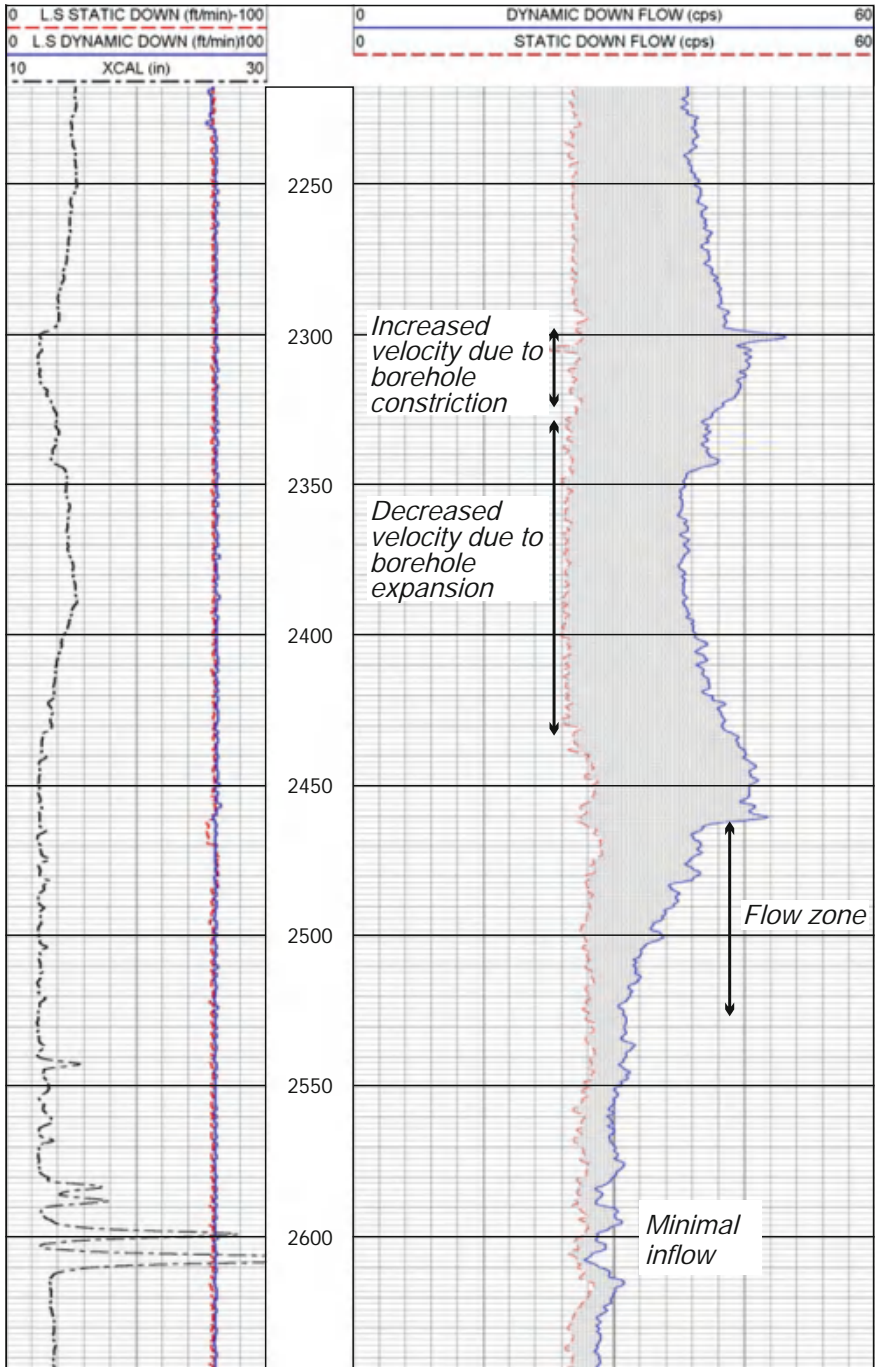
Fig. 10.10 Flowmeter log run of the pilot hole of an injection well in Hialeah, Florida. Logs shows intervals impacted by changes in borehole diameter and a major flow zone

results, with the EBF having the advantage of a greater flow range and the ability to simultaneously collect temperature and fluid resistivity data (Newhouse et al. 2005). EBF also has no moving part and is thus not hampered by mechanical problems (Boman et al. 1997).

A limitation of the EBF is that the head loss through the tool is a function of the flow velocity, which will vary depending on pumping rate and the position of the tool within a well (Dinwiddie et al. 1999). The head loss will be greatest at the top part of the tested interval, which has the greatest flow rate and velocity. Pumping rates should, therefore, be selected that are adequate to stress the zones of interest but not be too high as to cause excessive and variable head losses within the EBF tool during logging. Bypass flow around the packer may be significant in gravel packed wells (Dinwiddie et al. 1999). Bypass flow can result in an erroneous high permeability zone at the top of the well screens, where bypass flow can no longer occur and water flows back into the well (Butler 2005). Background electromagnetic currents may also affect EBF readings (Young et al. 1998). At the present time, EBF flowmeter logging equipment is not as widely available as spinner logging equipment.

Calibration of the EBF tool is important. Calibration of the EBF tool can be checked by running the tool in the upper cased part of the well while pumping at a known rate. Where a high degree of accuracy is required, multiple runs should be performed at different pumping rates.

10.8.4   Heat-Pulse Flowmeter

The heat-pulse flowmeter (HPFM) measures the velocity of water flow by recording the travel time of a heated packet of water (Hess 1982). The logging probe consists of a horizontal wire-grid heating element and heat sensors (thermistors) located above and below the grid. Pulses of electric current are applied to the heating grid, which produces a packet of heated water. The direction and rate of water flow is determined from the elapsed time between the application of the electric pulse and the detection of the warmed water by either the upper or lower thermistor. Flow rate is calculated from the elapsed time and the distance between the heating grid and thermistor. The HPFM is very sensitive and can measure very low flow rates. It is particularly useful for detecting interzone flow in wells in static tests. The HPFM is not suitable for measuring flow rates greater than about 8 L/min (2 gpm).

Paillet et al. (1987) and Paillet (1998) documented the use of high-resolution heat-pulse flowmeter log data to evaluate the transmissivity of fractures in essentially impervious crystalline bedrock. Fractures were identified using an acoustic-televiewer log. Inasmuch as the matrix is impermeable, the flow between two flowmeter readings reflects flow from the fractures. The transmissivity of the fractures is calculated from the transmissivity of the interval and the number of fractures. The aperture of equivalent fractures (smooth parallel wall fractures with

the same properties of observed fractures) was calculated using the cubic law
(Paillet et al. 1987)

$$T = (qgb^3) = 12l \qquad (10.17)$$

where l is the viscosity of water, q is the density of water, g is the acceleration of
gravity, and b is the aperture of the equivalent fracture. Paillet et al. (1987)
demonstrated how the HPFM could be used to determine whether fractures iden-
tified using borehole imaging logs are hydraulically active or inactive.

10.8.5   Interpretation of Flowmeter Log Data

For log runs in a screened well or a well in which the cross-sectional area is near
uniform, the discharge will be proportional to the measured flow velocity, provided
that significant vertical head (pressure) differentials do not occur in the tested
interval. Where significant variation in diameter and cross-sectional area occurs, the
flowmeter log data must be corrected using borehole dimensional data obtained
from a caliper log. A basic processing technique for evaluating the fraction of the
total well discharge (F_d) passing through the borehole at various depths (d) is to
normalize the product of flowmeter log velocity readings (v; unprocessed log
output) and cross-sectional area at the sample depth (v_d and A_d) with the product
within the casing ($v_c A_c$), where 100 % of the flow occurs:

$$F_d = \frac{(v_d A_d)}{(v_c A_c)} \qquad (10.18)$$

The conversion factor to change the raw flowmeter log readings in rotation rate
to velocity need not be considered as it would cancel out. The discharge at any
depth (Q_d) in the well can be calculated from the well pumping rate (Q_T) as:

$$Q_d = F_d \cdot Q_T \qquad (10.19)$$

The fraction or amount of the total flow entering a well from the aquifer at any
depth interval is the difference between the F_d and Q_d values calculated for the top
and the bottom of the interval. Plots of the percentage of well discharge versus
depth (flowmeter interpretation log) allows for the location and quantification of
flow zone contributions from tested intervals.

The transmissivity and average hydraulic conductivity of an aquifer layer can be
calculated from flowmeter log data as follows (Javandel and Witherspoon 1969;
Molz et al. 1989, 1990)

$$T_i = T \frac{DQ_i}{Q_t} \qquad (10.20)$$

$$K_i = \frac{T\left(\frac{DQ_i}{Q_t}\right)}{b_i} \qquad (10.21)$$

where,

T_i transmissivity of the tested interval (m^2/d)
T aquifer transmissivity (m^2/d) determined from a pumping test
K_i average hydraulic conductivity of aquifer interval "i" (m/d)
DQ_i change in flow rate over tested interval (m^2/d)
Q_t the total flow rate of well (m^2/d)
b_i the thickness of layer (m)

The above equation is based on the assumptions of (pseudo)steady-state conditions (DQ_i and Q_T do not change over time), horizontal flow, minimal screen, and head losses within the well, and no ambient flow in the well. Pseudo-steady conditions will occur when (Javandel and Witherspoon 1969; Molz et al. 1989, 1990)

$$\frac{r_w^2 * S}{4 * T * t} \setminus 0:01 \qquad (10.22)$$

where,

r_w well bore radius (m),
S aquifer storage coefficient (dimensionless), and
t time since the start of pumping (days)

The above condition is very quickly met after the start of pumping in confined aquifers, which have low storativity values.

    Hydraulic conductivity of the interval between two static readings can also be calculated using the Cooper and Jacob (1946) equation for partially penetrating wells, which requires information on the drawdown (DH$_i$) and storativity (S$_i$) of the interval, which are usually estimated (Young 1995; Boman et al. 1997):

$$K_i = \frac{(DQ_i - Dq_i)}{2pDH_ib_i} \ln\left[\frac{1:5}{r_e}\left(\frac{K_ib_it}{S_i}\right)^{1=2}\right] \qquad (10.23)$$

where

r_e effective well radius
Dq_i ambient flow in layer (i)
DQ_i induced flow in the "i"

K_i hydraulic conductivity calculated using iterative techniques
S_i Storativity of interval "i" estimated using average specific storage
b_i thickness of layer "i"

The effects of ambient interzone flow (i.e., vertical head gradients) can be compensated for by subtracting two steady-steady flow profiles according to the equation (Paillet 1998; Paillet and Reese 2000)

$$\frac{T_i}{\sum T_i} = \frac{Q_i^a - Q_i^b}{\sum \left(Q_i^a - Q_i^b \right)} \tag{10:24}$$

where, Q_i^a and Q_i^b are the outflows from zone "i" under two steady-state conditions. One of the steady-state runs could be performed under ambient (static) conditions.

The US Geological Survey developed the flow-log analysis of single holes (FLASH) program to interpret flow log data (Day-Lewis et al. 2011). The FLASH program is based on the Thiem equation and requires high-resolution flow logs run under ambient and stressed conditions. The underlying equations are

$$Q_i^a = -\frac{2pT_i^{\mathrm{factor}}T^{\mathrm{total}}\left(h_w^a - h_i^0\right)}{\ln\left(\frac{r_0}{r_w}\right)} \tag{10:25}$$

$$Q_i^s = -\frac{2pT_i^{\mathrm{factor}}T^{\mathrm{total}}\left(h_w^s - h_i^0\right)}{\ln\left(\frac{r_0}{r_w}\right)} \tag{10:26}$$

where
Q_i^a volumetric flow of zone "i" under ambient conditions
Q_i^s volumetric flow of zone "i" under stressed conditions
T_i^{factor} fraction of borehole's transmissivity contributed by flow zone "i"
T^{total} total transmissivity of the tested borehole
r_w borehole radius
r_0 radius beyond which heads do not change as result of pumping
h_w^a head in well under ambient conditions
h_w^s head in well under stressed condition
h_i^0 head in aquifer at a distance of r_0

There are thus two equations with four unknowns (T_i^{factor}, T^{total}, r_0, and h_i^0). If T^{total} is known, then the values of other variables can be estimated through a calibration process. The model calibration is performed by changing parameters until the modeled flow profile matches the interpreted (field) data. The principle calibration parameters are T_i^{factor} and Dh ($h_w - h_i$). The results are not sensitive to r_0 value.

Although the basic data collection and analyses involved in the flowmeter method are quite simple, care must be taken to come as close as possible to meeting all assumptions and measuring only the actual flow caused by pumping (Molz et al. 1990). More detailed and accurate data on aquifer heterogeneity may be obtained from flowmeter logging if more meticulous high-resolution procedures were used. A series of closely spaced stationary readings may be performed to more accurately measure the contribution from identified flow zones. Paillet (2004) discusses some of the corrections that may need to be applied to high-resolution heat and electromagnetic flowmeter logs run in irregular and large diameter boreholes. Attention to quality assurance, such as instrument calibration and test repeatability, is also important.

10.9 Temperature and Fluid Resistivity Logs

Temperature and fluid resistivity (or conductivity) logs measure the respective properties of the borehole fluids. The two logs are often run using a combined probe in a single pass and may be run under either static or dynamic (pumped or flowing) conditions. Temperature is usually measured using a high-resolution thermistor and fluid resistivity is usually measured with a pair of electrodes. Temperature logs often record both actual temperature and differential temperature, which is the rate of change of temperature with depth.

Static temperature logs are usually run after the well has been shut in for enough time to allow the water inside the well to reach thermal equilibrium with the adjoining formation. Water temperature is needed for quantitative interpretation of some other geophysical logs, such as the determination of salinity (TDS concentrations) from resistivity logs. Formation temperature data are also needed for geochemical modeling because equilibrium constants are a function of temperature. Information on borehole fluid resistivity is used for the interpretation of SP and resistivity logs.

Temperature logs are also performed to evaluate well cementing operations. The curing of cement is an exothermic reaction. The generated heat of hydration of cement emplaced in the annulus between the casing and formation can be detected and measured using a temperature probe run inside the casing. If curing proceeds too rapidly, the temperature will 'flash,' resulting in a spike in the temperature log. Conversely, a significant drop in temperature across a section of casing may indicate the absence of cement in part of the annulus.

Dynamic temperature and fluid resistivity logs are used in groundwater investigations to detect flow zones. The dynamic logs record the weighted average temperature and resistivity of the water that flowed into a well at or below the probe depth. Abrupt changes in borehole fluid temperature and fluid resistivity trends in dynamic logs are indicative of the presence of local flow zones (Fig. 10.11). For
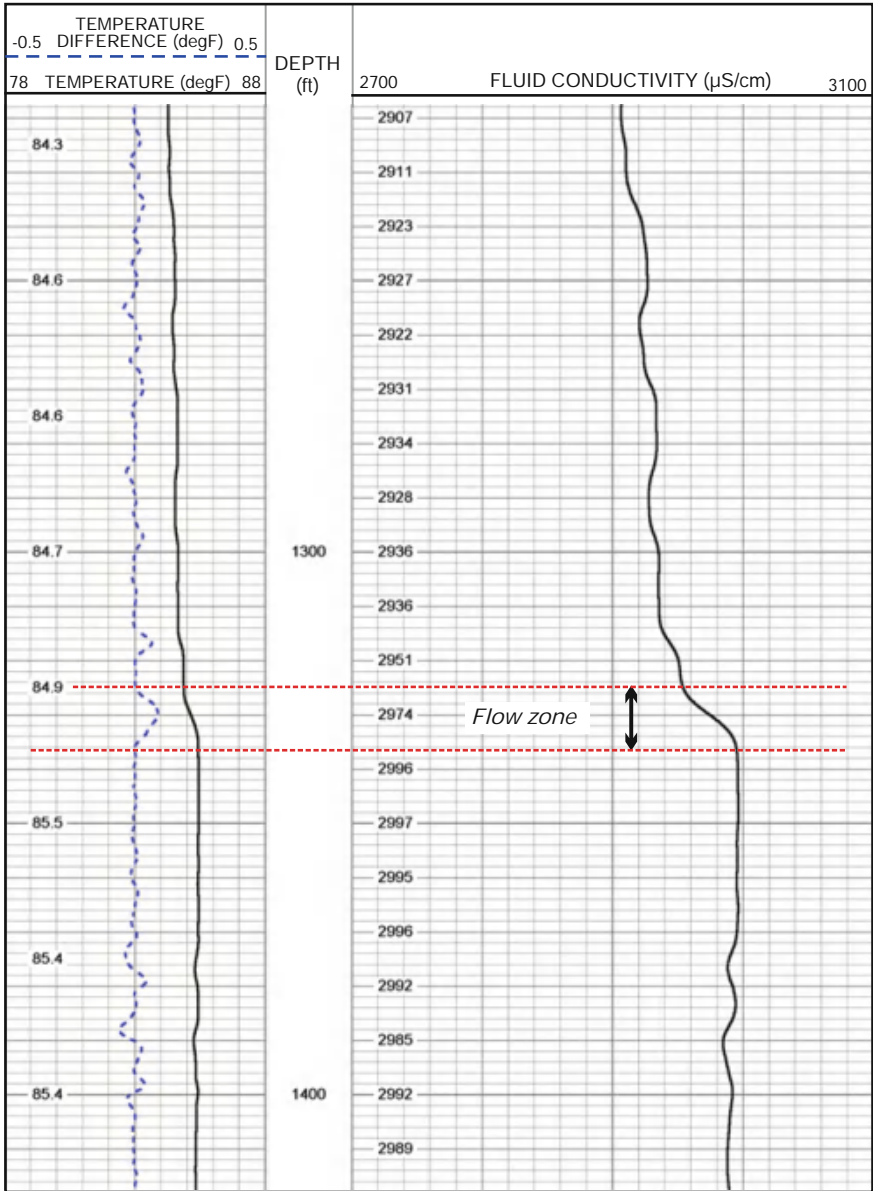
Fig. 10.11 Dynamic temperature and fluid conductivity log. Location of a flow zone is indicated by relatively abrupt changes in both temperature and fluid conductivity

example, if significant changes in dynamic fluid temperature and resistivity occur across a fractured zone, then it is usually evidence that the zone is producing water and is thus hydraulically active.

10.10   Borehole Imaging Logs

Borehole imaging logs provide images of the borehole wall that are used to identify sedimentary structures, fractures, and other hydrogeological features (e.g., voids), which may have significance for groundwater flow. Imaging techniques are often used for

- structural interpretation, such as the detection and orientation of faults, fractures, and structural dip
- differentiation between open and healed (closed) fractures
- measurement of fracture aperture, which is used to estimate fracture permeability
- identification and characterization of sedimentary structures, such as bedding (scale and orientation)
- stratigraphic and structural interpretations, including bedding (scale and orientation) and biogenic structures (e.g., bioturbation)
- detection and quantification of diagenetic structures, such as secondary porosity and nodules
- evaluation of the mechanical integrity of well casings.

The most important applications of borehole imaging logs in aquifer characterization is the identification of secondary porosity features, such as fractures and cavities, which may have high permeabilities and, as a result, act as preferential loci for groundwater flow. Borehole imaging logs vary in their image type, such as optical, acoustic, and resistivity. Lovell et al. (1999), Prensky (1999), Hurley (2004), Williams and Johnson (2004), Serra (2008), and Lagraba et al. (2010) provide overviews of the history and applications of borehole imaging technology, including references to key papers.

The choice of borehole imaging log should depend upon expected formation response, type of drilling fluid used (and current borehole fluid), and expected borehole conditions, such as size, shape, and rugosity. An in-gauge borehole with minimal amounts of rugosity is critical for acquiring high-quality borehole images (Lagraba et al. 2010). Microresistivity imaging logging may be preferred for formations in which there are strong contrasts in resistivity, such as between clean sands and shales. Optical imaging logs may be a cost-effective option where boreholes are filled with clear water and the formation has color contrasts. Microresistivity imaging logs may identify resistivity contrasts that represent features not apparent in visible light (Prosser et al. 1999).

10.10.1   Borehole Video Survey

Borehole video surveys are performed by slowly lowering a video camera down a well and recording the optical images. Borehole video surveys are, by far, the most

commonly run imaging log in hydrogeological and water-well investigations. Downhole video cameras have become relatively inexpensive and most local geophysical loggers and some well drillers can run a survey at a modest cost. The surveys are used to

- obtain data on local hydrogeology
- evaluate and document the mechanical integrity of wells
- evaluate the condition of wells and determine the cause of well problems, such as clogging
- evaluate the effectiveness of well rehabilitation activities (before and after surveys).

Borehole video surveys require that the wells be filled with clear (nonturbid) water. Newly constructed wells should be thoroughly developed to remove residual drilling fluids. In the case of injection wells, multiple casing volumes of clear water may need to be injected in order to obtain an acceptably low turbidity. It is strongly recommended that the tool used has both a downhole and a lateral view camera and records in color. The lateral camera allows for close-up images to be made of the well casing, screen, and borehole wall in open-hole intervals. Most downhole cameras with vertical and lateral image capabilities move on a swivel to change the field of view, which allows for very detailed observations to be made of critical well construction features, such as the base of the casing (casing seat). It also allows images to be made of the interior of cavities and close-up views of sedimentary structures and fossils.

10.10.2 Optical Televiewer

The optical televiewer (OPTV) tool generates a continuous, oriented, high-resolution 360° image of the borehole wall using an optical imaging system (Williams et al. 2002; Cunningham et al. 2004; Williams and Johnson 2004; Bechtel et al. 2007; Roberson and Hubbard 2010). The OPV uses a ring of lights to illuminate the borehole, a conical or hyperbolic reflector, and a camera to record the images. The rotating reflector focuses slices of the borehole wall in the camera lens. OTV images can be collected in boreholes that are filled with clear water or air. Turbidity of the borehole fluids and coatings on the borehole walls impact the quality of OTV images. The OTV will also not be able to detect features, if there is not an associated difference in color. The image can be presented unwrapped or as cyclinder resembling a core.

OPTV images can be readily and rapidly interpreted to identify sedimentological and diagenetic features that are significant for groundwater flow. The images can be processed to determine the orientation of fractures, faults, and bedding planes, as well as the size of fracture apertures. Lithological and associated porosity variations can be detected, which can be used for stratigraphic correlation (Fig. 10.12). The

digital images can also be processed to provide estimates of vuggy porosity based on grayscale contrasts between vugs and adjoining limestone matrix. OPTV logs may underestimate vuggy porosity if some pores are not darker than the adjoining matrix (Cunningham et al. 2004).
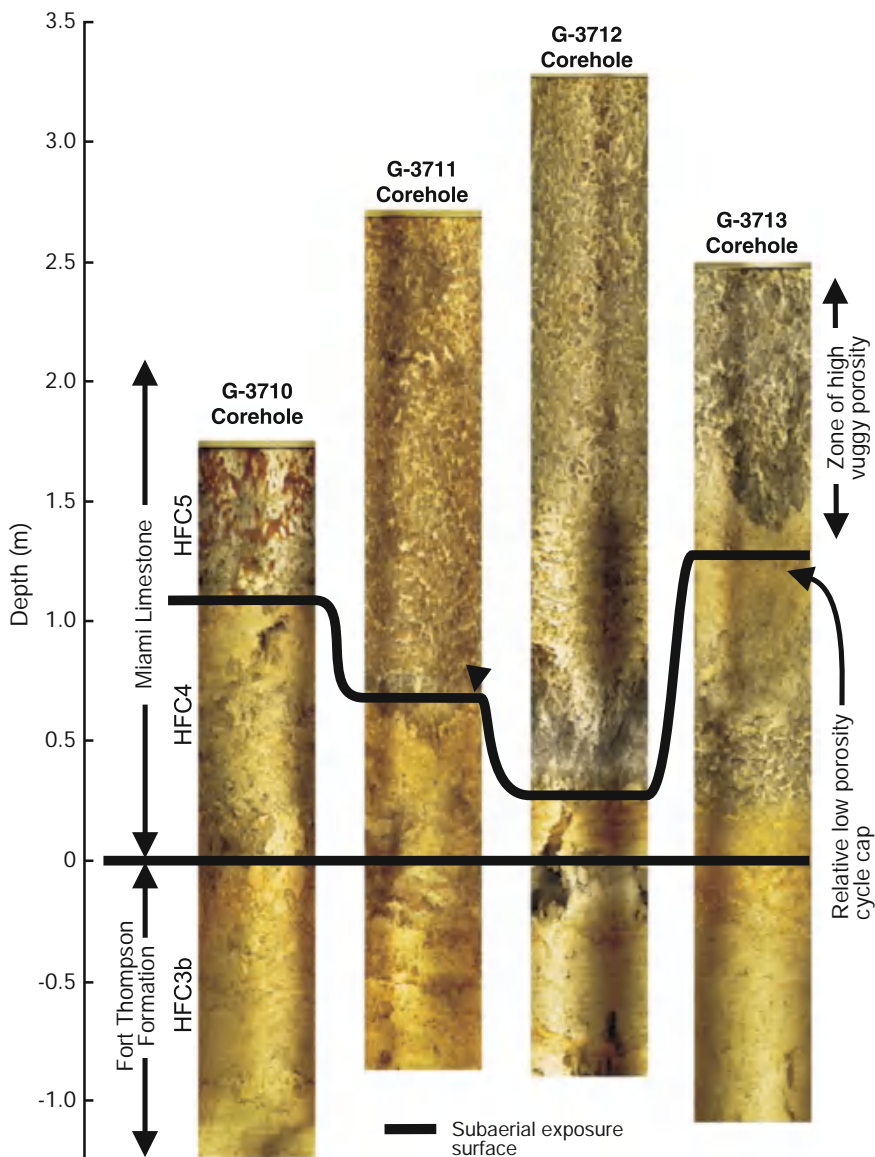
Fig. 10.12   Optical image logs used for stratigraphic correlation from the Biscayne Aquifer, Miami-Dade County, Florida (from Cunningham and Sukop 2011)

10.10.3   Acoustic-Televiewer Log

The acoustic-televiewer log (ATV), which is also referred to as the borehole tele-viewer log (BTV), is based on the emission of ultrasound pulses from a rotating sensor and the recording of the amplitude and travel time of the signals reflected back off of the borehole wall. A 360° image of the borehole wall is generated, which is typically presented as a flat "unwrapped" diagram. A magnetometer provides azimuthal information. Advantages of ATV logs is that they provide 100 % coverage of the borehole circumference for all borehole diameters and they can be run in mud-filled holes. The resolution of the logs depends upon the beam width, beam frequency, transducer rotation speed, and the logging speed (Lagraba et al. 2010). Image quality is strongly affected by borehole irregularity.

The travel time of the reflected signal is a function of the borehole diameter and fluid density. High-resolution caliper measurements can be obtained from the transit time measurements, provided that the density of the borehole fluid is known. The amplitude of the return signal is a function of the acoustic impedance (product of density and sonic velocity) of the formation. Low-amplitude or high transit time features by convention are shaded a dark color (Hurley 2004; Fig. 10.13). High-amplitude and low transit time features are shown as lighter colors (shades of brown, orange, yellow, or white). ATVs provide qualitative information on porosity, which is related to transit time.

The ATV log is very useful for revealing secondary porosity, structural, and sedimentological features, such as fractures, fault planes, and bedding. Resolution is on the millimeter scale. The ATV log is used to determine the orientation of fractures and other planar features (e.g., bedding planes). Vertical fractures appear as vertical lines and horizontal fractures appear as horizontal lines. Fractures or bedding that dip between vertical and horizontal appear as sinusoidal traces. Angles of dip can be calculated from the amplitude of the sinusoidal traces and borehole diameter. ATV logs work best where there are large contrasts in acoustic impedance in formation, with the extreme example being between solid rock and open factures or cavities.

The ATV is not commonly used in groundwater investigations because of the high cost of the equipment and the need for experienced operators. It has been applied in investigations where information is required on the abundance and extent of fractures and other secondary flow features. In Florida, for example, the ATV log has become a standard tool for confinement analyses of deep injection well systems, where the integrity of confining strata is an important technical and regulatory concern.
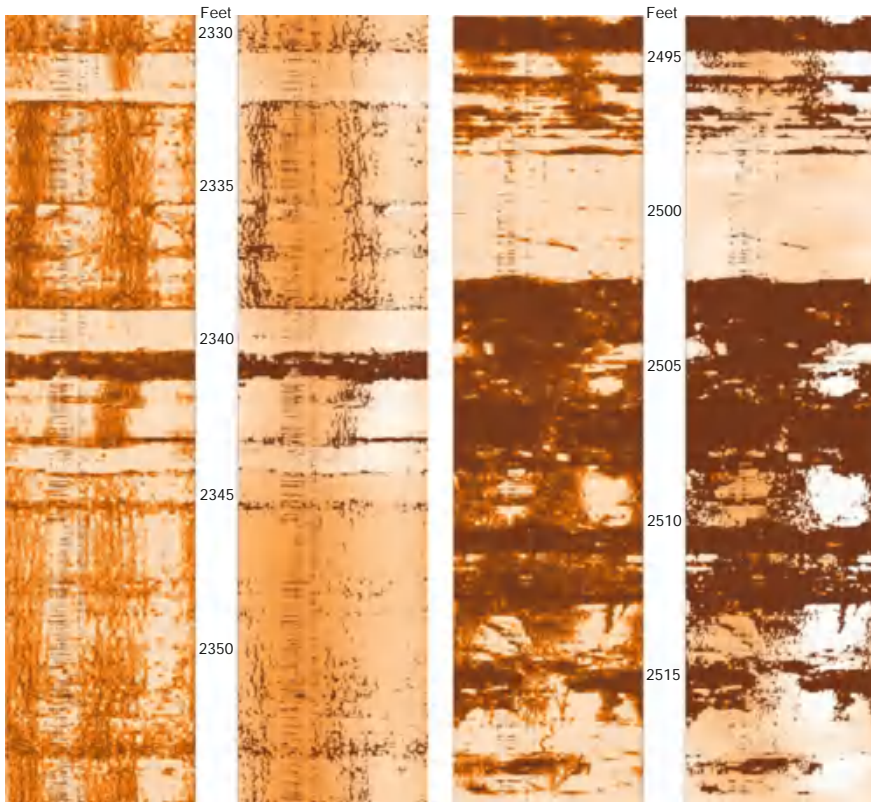
Fig. 10.13 Acoustic televiewer images of horizontally bedded limestone and dolomite (left) and fractured, vuggy dolomite (right), Eocene-aged Avon Park Formation, Hialeah, Florida. Low-porosity, hard dolomite is light colored, porous limestone appears orange-brown, and open pores are very dark colored

10.10.4   Microresistivity Imaging Logs

Microresistivity imaging is another technique that can be used to obtain high-resolution images of borehole walls in mudded boreholes. The FMI (mark of Schlumberger) Fullbore Formation MicroImager is an example of a microresistivity imaging tool. The Formation MicroScanner (FMS, mark of Schlumberger) is an earlier generation microresistivity imaging log. The basic concept of the FMI is that an applied voltage causes alternating current to flow from each of up to 192 electrode buttons on the sonde through the formation to a receiver electrode located higher on the sonde. As the current emerges from a button on a tool pad, its path is initially focused on a small volume of the formation directly facing the button. The current path then expands rapidly to cover a large volume of formation between the button and upper electrodes. The measured current consists of a high-resolution

component, modulated by resistivity variations in the formation directly facing the button, and a low-resolution component modulated by the resistivity of the zone between the button and the upper electrode. The high-resolution component dominates the generated image because its value varies between buttons. A 360° oriented image of the borehole wall is generated, which is typically presented as a flat "unwrapped" colored diagram (Fig. 10.14), similar to that of the ATV. The FMI log has a vertical and azimuthal resolution of 5 mm (0.2 in.). The dimensions of any feature that is 5 mm (0.2 in.) or larger can be readily estimated from the image if there is a sufficient resistivity contrast Finer-scale features, as small as 50 μm, that contain conductive fluids may be visible on the FMI logs. The resolution of the FMI log can be compromised by borehole irregularity (rugosity).

The resolution of microresistivity logs is better than that of ATV logs due to the fact that the range of resistivity values occurring in reservoir (aquifer) rocks is generally much greater than the range of acoustic impedance values (Lagraba et al. 2010). Microresistivity logs do not provide complete coverage of the borehole circumference. Due to the fixed number of pads and pad size, borehole coverage decreases with increased diameter. As pad devices, microresistivity tools are highly sensitive to mud cake content and thickness, borehole shape, and borehole rugosity (Lagraba et al. 2010). Measured microresistivity values are a function of the porosity, pore fluid resistivity (salinity), cementation, and clay content, through the Archie relationship, as is the case for conventional resistivity logs (Prensky 1999).

Macroporosity measurements from FMI logs are used to quantify the distribution of porosity in carbonate rocks. The matrix (intergranular and intercrystalline) porosity of a formation can be quantified by subtracting the FMI macroporosity from total porosity obtained from other logs (e.g., sonic, neutron, density, NMR). In a conductive drilling mud environment, open fractures will be much darker than the surrounding rock due to mud filling the fractures. The aperture, orientation, and density of fractures can be calculated from the image. FMI images allow for the visualization of sedimentary and structural features, such as bedding, lamination, brecciation, and slumping. Structural strike and dip can be determined from the orientation of bedding.

Microresistivity imaging can have great value for interpretation of deposition environment and evaluating aquifer heterogeneity. Experience is required to recognize and interpret different bedding surfaces and determine their orientation. Interpretations can be improved by comparison of logs with core or outcrops (Luthi 1990; Donselaar and Schmidt 2010). Luthi (1990) provides an example of how microresistivity imaging logs could be used to evaluate aquifer structure. In deltaic sands, cross-bed dips were used to determine paleoflow direction and, in turn, local channel axis trend. Channel axial trend can control larger-scale aquifer anisotropy.

Donsleaar and Schmidt (2010) performed an investigation in which microresistivity logs were recorded in two 200 m deep wells located behind cliff-face outcrops. The studied strata were Miocene fluvial deposits in the Elbro Basin of Spain. The depositional environment and characteristics of rock could be identified from bedding pattern and dips and resistivity trends. For example, fining-upwards sequences of meandering river deposits could be identified by an up-hole decrease
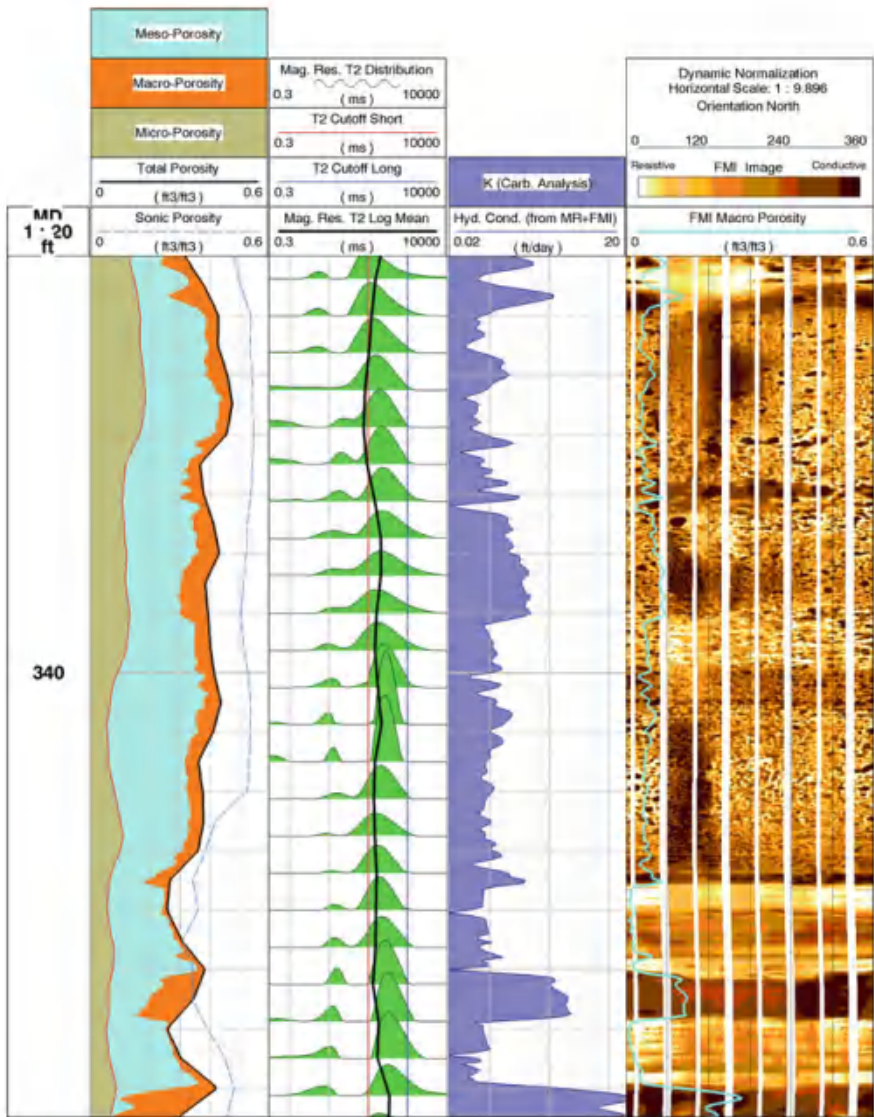
Fig. 10.14 NMR and FMI log from an ASR exploratory well in Florida. Bedding and small vugs caused by the dissolution of fossils are evident in the FMI log (right track). The T2 distributions (second track from left) and FMI macroporosity are used to determine the pore-size distribution (left) track and hydraulic conductivity (third track from left)

in resistivity, which was also manifested by an increase in gamma ray activity. Intervals with a unidirectional and gradually changing dip were interpreted to represent the lateral accretion surfaces of point bars. Intervals of seemingly randomly distributed dips were interpreted as trough cross-bedding intervals. Braided river facies were identified by their uniformly high resistivities (from low clay contents) and absence of a grain size trend.

10.11   Nuclear Magnetic Resonance Logs

Nuclear magnetic resonance (NMR) logging provides a measure of the total fluid-filled porosity and pore-size distribution of a formation from which the bound and moveable water distribution and permeability (and in turn hydraulic conductivity) are estimated. Current NMR logging techniques were discussed by Kenyon et al. (1995), Coates et al. (1999), Allen et al. (2000), Meuger and Prammer (2002); Henderson (2004), Freedman (2006), Serra (2008), and Klubac et al. (2013).

The NMR tool contains a large permanent magnet that aligns the non-lattice bound hydrogen atoms (i.e., protons) in the formation along the magnetic field vector, which is referred to as the longitudinal direction. The non-lattice bound hydrogen atoms in groundwater systems occur almost entirely in water molecules. A series of magnetic pulses from a radio frequency antenna on the tool causes the hydrogen nuclei (protons) to precess around the direction of the polarization field (transverse direction). The precessing protons create oscillating magnetic fields that generate weak radio signals, which are measured by the NMR tool. After each radio frequency (RF) pulse, the protons start to relax toward the original direction of polarization. The signal decays exponentially with a characteristic time constant (T_2), which is called the transverse relaxation or decay time.

Ideally, the protons will continue to precess around the direction of the external magnetic field until they have an interaction that causes their spin orientation to become out of phase with the other protons. The important relationship for the NMR log is that the rate of relaxation is primarily related to interaction of protons with a pore wall (grain-surface interaction). The rate of proton interaction with pore walls is inversely related to the pore size. In smaller diameter pores, the protons will reach a pore wall faster, and have shorter relaxation times, than would occur in larger-diameter pores. The rate of relaxation is also a function of the grain-surface relaxivity (i.e., ability of grain surfaces to relax protons), which varies with rock type and grain surface roughness. The distribution of relaxation (T_2) times provides a measure of the distribution of pore sizes.

NMR relaxation data are displayed as plots of T_2 times in milliseconds versus incremental porosity. The total area under the T_2 distribution curve reflects the relaxation of all the precessing protons and is proportional to the total water-filled porosity (Fig. 10.14). Empirical algorithms and relaxation time cutoffs based on NMR measurements of thousands of core samples from around the world are used to interpret the T_2 distribution. Relaxation time cutoffs divide the T_2 distribution

into different pore-size bins (e.g., clay-bound water, capillary-bound water, microporosity, and mesoporosity).

The principal value of NMR logging for water resources investigations is that it provides estimates of permeability and hydraulic conductivity. Permeability can be estimated from the NMR total porosity and T_2 distributions using empirically established relationships. However, permeability is controlled by the pore-throat size distribution rather the pore size. NMR pore-size data can be used to estimate permeability because a general relationship often exists between pore size and pore-throat size, particularly in granular sediments and rocks (e.g., sands and sandstones). Permeability can be calculated from the NMR total porosity and T_2 distributions using empirically established relationships. The Timur-Coates (T-C) and SDR equations (Sect. 16.2.2) are commonly used to calculate permeability values from NMR data. Both of these equations are based on the Kozeny–Carman relationship, which relates permeability to the porosity and the total surface area of the material.

The transmissivity values of an interval of an aquifer can be estimated by integrating the NMR hydraulic conductivity over the depth interval. However, the NMR log may under estimate the contribution of discrete fractures to transmissivity in dual-porosity systems. Comparison of transmissivity values obtained from aquifer performance (pumping) tests and NMR logs may provide an estimation of the contribution of fractures and conduits to the transmissivity of the tested interval. The accuracy of NMR applied in water resources investigations has not yet received much study. Maliva et al. (2009b) reported that a transmissivity value (44.1 m^2/d) obtained from Eocene limestones in South Florida by integrating NMR hydraulic conductivity values was in the range of values (22.7–59.5 m^2/d) obtained from aquifer flow test and specific-capacity data.

NMR data can be effected by factors others than pore size. Agut et al. (2000) discussed the effects of mineralogy on the T2 cutoff between free (continuous permeability) and bound (irreducible) water. Paramagnetic elements, such as iron, manganese, and nickel, present in the formation rock lead to a faster proton relaxation because they have strong local magnetic fields. The presence of small amounts of dolomite also has a great impact on the T2 cutoff for irreducible water saturation. For strata containing complex lithologies, accurate mineralogical analysis is necessary to understand and correctly analyze NMR data (Agut et al. 2000).

Klubac et al. (2013) documented the application of NMR logs to unconsolidated sediments of the High Plains aquifer (U.S.A). NMR hydraulic conductivity values were compared to values obtained from conventional means, such as borehole flowmeter logs and sidewall cores. Hydraulic conductivity values were calculated using the SDR and T-C equations using standard values for the empirical coefficients. The high-resolution NMR data were up-scaled to the same scale as the flowmeter hydraulic conductivity values. The best fit was obtained using the T-C equation, with NMR hydraulic conductivity values being within an order of magnitude of flowmeter log values. A better fit (low residual error) was obtained when the T-C constants were determined by calibration with the flowmeter log data. Thus acceptable accuracy data on hydraulic conductivity can be obtained using standard

constant values, but greater accuracies may be obtained by adjusting the constants through calibration with other hydraulic conductivity data. Over time, a database of the best default values for a given aquifer or lithologies may become available (Klubac et al. 2013).

Interpretation of NMR data is more difficult in carbonate rocks because of the complex heterogeneous nature of the pore networks (Henderson 2004). The correlation between pore size and pore-throat size may be weak in some carbonate rocks, and permeability may be over estimated in carbonates with isolated vuggy porosity. Carbonates commonly have multiple pore-size distributions. Diffusion from micropores decreases their T2 contribution and diffusion into macropores increases their T2 contribution. The end result is the merging of the two peaks to produce a unimodal T2 distribution that bears little resemblance to the bimodal distribution one would expect from a dual-porosity system (Allen et al. 2000).

Parra et al. (2001, 2003) used image processing techniques to determine pore-size distributions from x-ray computed tomography (CT), thin-section optical microscopy, and scanning-electron microscopy data. Theoretical T2 distributions were then calculated from the pore-size distributions and compared to measured NMR T2 distributions. The NMR logs were found to give lower permeabilities in vuggy carbonate, particularly in the highest permeability zones. Acoustic log data (full waveform sonic) can image vuggy carbonate rocks. Parra et al. (2001, 2003) recommended the vuggy carbonate aquifers be analyzed using a combination of NMR and acoustic logging.

From a practical perspective, NMR and microresistivity imaging logs can be an alternative to coring for evaluation of fine-scale aquifer heterogeneity. A major advantage of the advanced logs is that they provide a continuous record, whereas core recovery may be significantly less than 100 % and recovery may be biased toward better lithified and thus less permeable strata. The log-based approach will also typically be less expensive than obtaining a core and performing numerous finely spaced core-plug or minipermeameter analyses. The main disadvantages of using advanced logs to evaluate aquifer heterogeneity are that borehole conditions may not be ideal and hydraulic conductivity is indirectly quantified with associated inaccuracy.

10.12   Geochemical Logs

Geochemical logs provide data on the elemental composition and mineralogy of a formation. The logs use a neutron source and determine mineralogy from the emitted gamma rays. From log-derived mineralogy, it is possible to derive or infer a number of other formation properties including matrix density and porosity, cation exchange capacity, intrinsic permeability and grain size (Herron and Herron 1990). Elemental spectroscopy logs are reviewed by Barson et al. (2005). The application of the earlier Geochemical Logging Tool (GLT; mark of Schlumberger) was reviewed by Herron and Herron (1990). The Elemental Capture Spectroscopy (ECS; mark of Schlumberger) tool uses a standard americium beryllium (AmBe)

neutron source (similar to that used for neutron logs) and a bismuth germanate (BGO) detector to measure gamma rays released as the result of the collision and interaction of the emitted neutrons with atomic nuclei in the formation. The reservoir saturation tool (RST; mark of Schlumberger) is similar to the ECS tool except that it employs a pulsed electronic neutron generator and thus does not have a radioactive source. The released gamma rays have characteristic energies that depend upon the specific element and type of interaction. The ECS differs from the neutron log in that the sonde measures the full spectrum of gamma rays generated from neutron-element interactions.

The measured gamma ray energy spectrums are processed using an algorithm to determine the contributions from specific elements based on the known detector responses. The relative elemental spectral yields are then converted to dry-weight elemental concentrations using an oxide closure method. The elemental concentration data are next processed to quantify the minerals present using empirical relationships derived from core chemistry and mineralogical databases. The ECS and RST logs can provide measurements of the abundance of common sedimentary rock types and constituents, including calcite, dolomite, total clay (and some clay mineral types), QFM (quartz, feldspar, and mica), siderite, and pyrite. The ECS log measurements have sensitivities of 1 % dry-weight concentration or less.

A general source of error for geochemical logging tools is that elemental data are transformed into abundances of a limited number of chemical mineral equivalents, which may not reflect true formation mineralogy (Herron and Herron 1990). Minerals vary in composition and, uncommonly, formations may contain minerals that contribute to the suite of elements, but are not part of the model (i.e., library of minerals considered). Over 3,000 minerals have been identified, but the vast majority of sediments contain only ten minerals: quartz, four clay minerals, three feldspar minerals, and two carbonate minerals (Pettijohn 1975; Blatt et al. 1980; Herron and Herron 1990). Even when some minerals are misidentified, the calculated total amounts of framework grains, clay minerals, and carbonate minerals remain fairly accurate (Herron and Herron 1990).

10.13 Cased-Hole Logs

Most borehole geophysical logs are designed to be run on open (uncased) boreholes. Cased-hole geophysical logs were originally developed in the oil and gas industry, in part, to provide depth control for well perforation. Cased-hole geophysical logs can be of value for aquifer characterization by providing lithological and petrophysical data on existing wells. Not uncommonly, little or no geological and hydrogeological data were either collected or retained during the installation of water wells. The later logging of these wells can provide data (often inexpensively) that are useful for groundwater investigations. Although the quality of data from logging existing cased wells may be modest, logging of cased wells can be a cost-effective alternative to drilling and logging new boreholes.

10.13.1   Cased-Hole Logging Techniques

Cased-hole geophysical logging has some inherent limitations. The presence of a cemented in-place steel or PVC casing can isolate the formation from the signal transmitted by the logging probe (sonde). Logs that require direct formation contact are thus usually not suitable for cased boreholes. Standard electrical logs that involve the direct transmission of electrical currents to the formation can also not be run on cased wells. Measurements using electrical properties can normally not be run inside a steel casing. The volume of the investigation of a log includes the casing and cement grout, which need to be considered in the data analysis. Some common geophysical logs used in groundwater investigations and the borehole conditions under which they can be successfully run are summarized in Table 10.2. Gamma ray and neutron-based logs can be used to log formations through steel casing. However, neutron log response is affected by hydrogen in PVC casing.

Table 10.2   Borehole geophysical logs and borehole requires

Log	Type of information	Open hole	PVC-cased hole	Steel cased hole
Electric (single point, long- and short-normal resistivity, spontaneous potential)	Lithology, formation water resistivity	Yes	No	No
Resistivity (dual induction)	Lithology, formation water resistivity	Yes	Yes	No
Natural gamma ray and spectral gamma ray	Lithology, particularly clay content	Yes	Yes	Yes
Gamma–gamma (density) porosity	Porosity, lithology	Yes	No	No
Neutron porosity	Porosity	Yes	Limited[a]	Yes
Sonic	Porosity	Yes	Limited	Limited
Caliper	Borehole diameter	Yes	No	No
Fluid temperature and conductivity	Fluid temperature and conductivity	Yes	No	No
Flow meter	Flow distribution in well	Yes	No	No
Borehole video	Formation structures and features	Yes	No[b]	No[b]
Casing collar locator	Base of steel casing	No	No	Yes

[a]Neutron logging is problematical due to hydrogen and chlorine in PVC
[b]Can be run as part of casing inspection/integrity test

Thermal decay time (TDT; mark of Schlumberger) logs, such as the TDT-K and Dual-Burst TDT tools, are types of neutron logs that are specifically designed for cased wells (Schlumberger 1989b). The TDT logs use a neutron generator in the sonde to repeatedly emit pulses of high-energy neutrons. As is the case for the standard neutron logs, the high-energy neutrons are quickly slowed down to the thermal energy range. The thermal neutrons are captured by nuclei with the resulting emission of gamma radiation. The TDT logs record the thermal neutron cross section of the formation from the rate of decay of the thermal neutrons, which is caused by neutron capture or neutron migration (diffusion). Inasmuch as chlorine is by far the strongest neutron absorber of the common earth elements, the TDT log response is determined primarily by the chlorine present in the formation as sodium chloride in the pore waters. The neutron decay rate is thus primarily a function of the porosity, salinity, and shaliness (clay content) of the formation, similar to the response of resistivity logs (Schlumberger 1989b). The decay rate curves for each fast-neutron pulse contains distinct segments reflecting borehole and casing decay, formation decay, and background gamma radiation.

Natural gamma ray and gamma ray spectroscopy logs (Sect. 10.12) can be run on cased holes. Gamma ray spectroscopy logs use a neutron source and a spectrometer system that can analyze gamma ray spectral intensities attributed to common elements found in sedimentary formations. The data are processed to calculate basic petrophysical properties, such as lithology, shale volume, porosity, and pore fluid types (Schlumberger 1989a, b). However, elements present in cement grout will also contribute gamma rays.

Sonic logs, such as the array sonic and long-spaced sonic (LSS, mark of Schlumberger) tools can provide information on formation properties where the casing is well cemented to the formation (i.e., acoustically coupled) and, therefore, the casing signal is attenuated and the formation signal dominates (Schlumberger 1989b). Induction-based resistivity logs can be successfully run on PVC-cased wells. However, the quality of the petrophysical data obtained by standard borehole geophysical logs run on cased holes is often considerably less than that obtainable from the same logs run on open holes because the casing and grout attenuates the formation signal or response. Accurate quantitative interpretation of the logs may not be possible, but valuable qualitative data may still be obtained, such as the locations of zone of high porosity.

Cased-hole logs may also provide (or be modified to provide) specific information related to casing and grout. Cement and sector bond logs are used to evaluate cement bonding in cased wells. Advanced varieties of logs have been developed for the oil and gas industry specifically for cased holes. These logs include the Schlumberger cased hole dynamics tester, cased hole formation resistivity, sonic scanner, dipole shear sonic imager, and RST Pro reservoir saturation tool. These advanced logs may not be cost-effective for shallow groundwater wells, particularly where there is a limited saturated thickness.

10.13.2   Hydrogeological Applications of Cased Hole Geophysical Logs

Electromagnetic induction logs run on PVC-cased wells can provide information on groundwater salinity. Induction logs can provide a higher vertical-resolution profile of changes in resistivity (conductivity) with depth that is typically not possible using grab samples from a limited number of monitoring points. Time series of analyses can be used to detect changes in salinity over time.

Electromagnetic induction logs were run at five sites in the northeastern United States to detect electrically conductive (high dissolved solids) contaminants, such as landfill leachate and salt used for road deicing (Williams et al. 1993). The logs were run on 2-inch (5-cm) diameter PVC wells in sand and gravel aquifers. A gamma ray log was also run to detect clay-rich intervals, which also have elevated electrical conductivities. Contaminated waters were detected by a high electromagnetic (EM) conductivity and low gamma ray response. The data were processed by first adjusting the log EM conductivity to values at a standard temperature of 25 °C. Regression methods were then used to establish a relationship between log EM conductivity and specific conductance (from well data) in clean sand and gravel. The method could not be used in clay-rich zones. Mack (1993) similarly documented the use of EM and gamma ray logging to detect electrically conductive landfill leachate contamination in a glacial aquifer in Vermont (USA).

Electromagnetic induction logs run on PVC-cased wells were used to obtain data on changes in chloride concentration with depth in the Coastal Aquifer System of Los Angeles County, California (Land et al. 2004). The relationship between chloride concentration and conductivity was obtained from a regression of a plot of chloride concentration, obtained from bulk sampling, against the average induction log conductivity observed within the screened interval of the well. There was considerable scatter in the data as constituents other than chloride affected the measured conductivity (Land et al. 2004). Gamma ray logs were useful to evaluate lithology. For example, depth intervals with high electromagnetic conductivity and low gamma ray activity likely contain saline water, whereas intervals with a high conductivity and high gamma ray activity likely include clay-rich, fine-grained strata.

Sequential electromagnetic induction logs were run on PVC-cased monitoring wells in the San Jaoquin Groundwater Subbasin of Northern California to monitor changes in chloride concentration over time (Metzger and Izbicki 2013). The study area is an inland site with lower salinities than occur in coastal sites that experience saline-water intrusion. Aquifer lithology is constant during sequential or time-series analyses, so the changes in bulk EM resistivity can only be caused by changes in groundwater quality. Chloride concentration was estimated using an empirical relationship between electromagnetic resistivity and chloride concentration, which was obtained from log runs on screened intervals from which chloride

concentration data was obtained by conventional water quality sampling and from water samples extracted from core samples. Calculated pore-fluid concentrations were judged to be best interpreted in the relative sense rather than in terms of absolute numbers (Metzger and Izbicki 2013).

10.14   Development of Borehole Geophysical Logging Programs

The fundamental issues for the development of a borehole geophysical logging program for a water resources project are

- determination of the specific data needs that could potentially be met by geophysical logging
- identification of the types of logs that could meet the data requirements
- evaluation of whether the logs can be run and provide interpretable data under the site-specific borehole conditions
- how the data are to be subsequently used.

The developed logging program should cost-effectively provide the required data for the project. Mobilization and site time are major costs for logging programs. There is usually only one practical opportunity to run some logs (e.g., before the casing is set) and that a valuable opportunity might be lost to obtain site-specific hydrogeological data, which could be useful in the future. Often the costs to run some additional logs are very modest (relative to project total budgets), particularly, if they can be combined on a logging tool (i.e., simultaneously run). Depending upon location, mobilization of the logging truck can be a large part of total logging costs.

Logging programs should be project and site-specific. Conventional logging suites usually include some or all of the following basic logs

- natural gamma ray
- caliper
- resistivity (short and long normal) or dual induction (DIL)
- spontaneous potential (usually routinely run with resistivity logs)
- sonic.

For non-mudded, stable boreholes, the following logs may be run to evaluate aquifer heterogeneity, particularly the location of flow zones:

- Flowmeter (static and dynamic)
- Temperature (static and dynamic)
- Fluid resistivity (static and dynamic)

Depending upon borehole conditions and project data requirements, a borehole imaging log might also be run. Advanced borehole geophysical logs, such as NMR

and geochemical, may additionally be run for projects in which detailed information on aquifer petrophysical properties and mineralogy are needed. The cost of advanced logs depends on logging truck mobilization distance. Hence, total costs for advanced logs may be considerably greater outside of 'oil patch' areas where the advanced logging equipment is based.

References

Agut, R., Levallois, B., & Klopf, W. (2000) Integrating core measurements and NMR logs in complex lithology. Presented at the SPE Annual Technical Conference and Exhibition, Dallas, 1–4 October. SPE-63211-MS.

Allen, D., Flaum, C., Ramakrishnan, T. S., Bedford, J., Castelijns, K., Fairhurst, D., Gubelin, G., Heaton, N., Minh, C. C., Norville, M. A., Seim, M. R., Pritchard, T., & Ramamoorthy, R. (2000) Trends in NMR logging. Oilfield Review, 12(3), 2–19.

Archie, G. E. (1942) The electrical resistivity log as an aid in determining some reservoir characteristics: Transactions American Institute of Mining Metallurgical and Petroleum Engineers, 146, 54–67.

Asquith, C., & Krygowski, S. (2004). Basic well log analysis (2 Ed.). Methods in Exploration No. 16: Tulsa: American Association of Petroleum Geologists.

Barson, D., Christensen, R., Decoster, E., Grau, J., Herron, M., Herron, S., Guru, U.K., Jordán, M., Maher, T. M., Rylander, E., & White J. (2005) Spectroscopy: The key to rapid, reliable petrophysical answers. Oilfield Review, 17(2), 14–33.

Bechtel, T. D., Bosch, F. P., & Gurk, M. (2007), Geophysical methods. In N. Goldscheider & D. Drew (Eds,), Methods in karst hydrogeology, IAH: International Contributions to Hydrogeology 26 (pp. 171–200). Lieden: Taylor and Francis.

Blatt, H., Middleton, G., 7 Murray, R. (1980) Origin of sedimentary rocks. Englewood Cliffs, New Jersey: Prentice-Hall.

Boman, G. K., Mole, F. J., & Boone, K. D. (1997) Borehole flowmeter application in fluvial sediments: methodology, results, and assessment. Ground Water, 53, 443–450.

Butler, J. J., Jr. (2005) Hydrogeological methods for estimation of spatial variations in hydraulic conductivity. In Y. Rubin & S. S. Hubbard (Eds.), Hydrogeophysics (pp. 25–58): Dordrecht: Springer.

Coates, G. R., Xiao, L., & Prammer, M. G. (1999) NMR logging, principles and applications. Houston: Halliburton Energy Services.

Collier, H. A. (1993) Borehole geophysical techniques for determining the water quality and reservoir parameters of fresh and saline water aquifers in Texas. Report 343. Austin: Texas Water Development Board.

Cooper, H. H., Jr., & Jacob, C. E. (1946) A generalized graphical method for evaluating formation constants and summarizing well-field history. Transactions American Geophysical Union, 27 (4), 526–534.

Cunningham, K. J., Carlson, J. I., & Hurley, N. F. (2004) New method for quantification of vuggy porosity from digital optical borehole images as applied to the karstic Pleistocene limestone of the Biscayne aquifer, southeastern Florida. Journal of Applied Geophysics, 55, 77–90.

Cunningham, K. J., & Sukop, M. C. (2011) Multiple technologies applied to characterization of the porosity and permeability of the Biscayne Aquifer, Florida. U.S. Geological Survey Open-File Report 2011–1037.

Day-Lewis, F. D., Johnson, C. D., Paillet, F., & Halford, K. J. (2011) A computer program for flow-log analysis of single holes (FLASH). Ground Water, 49, 926–931.

Dinwiddie, C. L., Foley, N. A., & Molz, F. J. (1999) In-well hydraulics of the electromagnetic flowmeter. Ground Water, 37, 305–315.

Donselaar, M. E., & Schmidt, J. M. (2010) The application of borehole image logs to fluvial facies interpretation. In M. Pöppelreiter, C. Garciá-Carballido, & M. Kraaijveld (Eds.), Dipmeter and borehole image log technology, Memoir 92 (pp. 145–166). Tulsa: American Associations of Petroleum Geologists.

Driscoll, F. G. (1986) Groundwater and wells (2nd Ed.). St Paul: Johnson Filtration Systems.

Focke, J. W., & Munn, D. (1987) Cementation exponents in Middle Eastern carbonate reservoirs. SPE Formation Evaluation, June 1987, 155–167.

Freedman, R. (2006) Advances in NMR logging. Journal of Petroleum Technology, 58(1), 60–66.

Geel, C. R. (2002) Enhancing the gamma-ray log through geological input: evaluating thin-bedded turbidite sequences. In M. Lovell & N. Parkinson (Eds.) Geological application of well logs, Methods in Exploration 13 (pp. 15–26). Tulsa: American Associations of Petroleum Geologists.

Henderson, S. (2004) Nuclear magnetic resonance logging. In C. Asquith & S. Krygowski (Eds.) Basic well log analysis (2nd Ed.) Methods in Exploration 16 (pp. 103–113). Tulsa: American Association of Petroleum Geologists.

Herron, M. M., & Herron, S. L. (1990) Geological applications of geochemical well logging. In A. Hurst, M. A. Lovell & A. C. Morton (Eds.), Geological applications of wireline logs. Special Publication No. 48 (pp. 165–175). Lomdon: Geological Society.

Hess, A. E. (1982) A heat-pulse flowmeter for measuring low velocities in boreholes. U.S. Geological Survey Open File Report 82-699.

Hilchie, D. W. (1979). Old (pre-1958) electrical log interpretation: Golden: D. W. Hilchie Inc.

Hingle, A. T., 1959, The use of logs in exploration problems. Paper presented at SEG 29th Annual Meeting.

Hurley, N. F., 2004, Borehole images. In C. Asquith & S. Krygowski (eds.), Basic well log analysis (2nd Ed) Methods in Exploration 16 (pp. 151–163). Tulsa: American Association of Petroleum Geologists.

Javandel, I.,& Witherspoon, P. A. (1969) A method of analyzing transient fluid flow in multi-layered aquifers. Water Resources Research, 5, 856–869.

Kabala, Z. J. (1994) Measuring distribution of hydraulic conductivity and specific storage by the double flowmeter test. Water Resources Research, 30, 685–690.

Kennedy, M. C. (2002) Solutions to some problems in the analyses of wells in carbonate rocks. In M. Lovell & N. Parkinson (Eds.), Geological application of well logs, AAPG Memoirs in Exploration 13 (pp. 61–73). Tulsa: American Association of Petroleum Geologists.

Kenyon, B., Kleinberg, R., Straley, C., Gubelin, G., & Morriss, C. (1995) Nuclear magnetic resonance imaging – technology for the 21st century. Oilfield Review, 7(3), 19–33.

Keys, W. S. (1989) Borehole geophysics applied to ground water investigations. Dublin, Ohio: National Water Well Association.

Keys, W. S. (1990) Borehole geophysics applied to ground-water investigations. Techniques of Water-Resources Investigations of the United States Geological Survey, Book 2, Chapter E2.

Keys, W. S. (1997) A practical guide to borehole geophysics in environmental investigations. Boca Raton: Lewis Publishers.

Klubac, K., Knight, R., Song, Y.-Q., Bachman, N., Grau, B., Canna, J., & Williams, J. (2013) Use of NMR logging to obtain estimates of hydraulic conductivity in the High Plains aquifer, Nebraska, USA. Water Resources Research, 49, 1871–1886.

Kobr, M., Mareš, S, & Paillet, F. (2005) Borehole geophysics for hydrogeological studies: principles and applications. In Y. Rubin & S. S. Hubbard (Eds.) Hydrogeophysics (pp. 291–331). Dordrecht, Springer.

Kwader, T. (1986) The use of geophysical logs for determining formation water quality. Ground Water, 24, 11–15.

Lagraba P., J. O., Hansen, S. M., Spalburg, M., & Helmy, M. (2010) Borehole image tool design, value of information, and tool selection. In M. Pöppelreiter, C. Garciá-Cballido & M. Kraaijveld (Eds.) Dipmeter and borehole image technology, Memoir 92 (pp. 15–38). Tulsa: American Association of Petroleum Geologists.

Land, M., Reichard, E. G., Crawford, S. M., Everett, R. R., Newhouse, M. W., & Williams, C. F. (2004) Ground-water quality of coastal aquifer system in the West Coast Basin, Los Angeles County, California, 1999–2002. U.S. Geological Survey Scientific Investigations Report 2004-5067.

Lovell, M. A., Williamson, G.,& Harvey, P. K. (1999) Borehole imaging: applications and case studies. Special Publication 159. London: Geological Society.

Luthi, S. M. (1990) Sedimentary structures of clastic rocks identified from electrical borehole images. In A. Hurst, M. A. Lovell & A. C. Morton (Eds.), Geological applications of wireline logs, Special Publications 48 (pp. 3–10). London: Geological Society.

Mack, T. J. (1993) Detection of contaminant plumes by borehole geophysical logging. Ground Water Monitoring and Remediation, 13(1), 107–114.

Maliva, R. G., & Missimer, T. M. (2010) Aquifer storage and recovery and managed aquifer recharge: Planning, hydrogeology, design, and operation. Houston: Schlumberger Corporation.

Maliva, R. G., & Missimer, T. M. (2012) Arid lands water evaluation and management. Berlin: Springer.

Maliva, R. G., Clayton, E. A., & Missimer, T. M. (2009a) Application of advanced borehole geophysical logging to managed aquifer recharge investigations. Hydrogeology Journal, 17, 1547–1556.

Maliva, R. G., Missimer, T. M., Clayton, E. A., & Dickson, J. A. D. (2009b) Diagenesis and porosity preservation in Eocene microporous limestones, South Florida, USA. Sedimentary Geology, 217, 85–94.

Maliva, R. G., Missimer, T. M., & Guo, W. (2006) Structural deformation of the Southern Florida Peninsula during the Late Miocene to Early Pliocene: Geophysical log evidence: Gulf Coast Association of Geological Societies Transactions, 56, 527–538.

Macfarlane, P. A., Doveton, J. H., & Whittemore, D. O. (1998) User's guide to the Dakota Aquifer in Kansas. Kansas Geological Survey Technical Series 2.

Meuger, S., & Prammer, M. (2002) Developments in NMR logging, In. Lovell, M., and Parkinson, N., (eds.) Geological application of well logs. Methods in Exploration 13 (pp. 55–59). Tulsa: American Association of Petroleum Geologists.

Metzger, L. F., & Izbicki, J. A. (2013) Electromagnetic induction logging to monitor changing chloride concentrations. Groundwater, 51, 108–121.

Molz, F. J., Boman, G. K., Young, S. C., & Waldrop, W. R. (1994) Borehole flowmeters: field applications and data analysis. Journal of Hydrology, 163, 347–371.

Molz, F. J., Morin, R. H., Hess, A. E., Melville, J. G., & Güven, O. (1989) The impeller meter for measuring aquifer permeability variations: evaluation and comparison with other tests. Water Resources Research, 25, 1677–1683.

Molz, F. J., Güven, O, & Melville, J. G. (1990) A new approach and methodologies for characterizing the hydrogeologic properties of aquifers: U.S. Environmental Protection Agency, Robert S. Kerr Environmental Research Laboratory, Ada, Oklahoma Report EPA/600/2-90/002.

Newhouse, M. W., Izbicki, J. A., & Smith, G. A. (2005) Comparison of velocity-log data collected using impeller and electromagnetic flowmeters. Ground Water, 43, 434–438.

Paillet, F. L. (1998) Flow modeling and permeability estimation using borehole flow logs in heterogeneous fractured formations. Water Resources Research, 34, 997–1010.

Paillet, F. L. (2004) Borehole flowmeter applications in irregular and large diameter boreholes: Journal of Applied Geophysics, 55, 39–60.

Paillet, F. L., & Crowder, R. E. (1996) A generalized approach for the interpretation of geophysical well logs in ground-water studies. Ground Water, 34, 663–898.

Paillet, F. L., Hess, A. E., Cheng, C. H., & Hardin, E. (1987) Characterization of fracture permeability with high-resolution vertical flow measurements during borehole pumping. Ground Water, 25, 28–40.

Paillet, F. L., & Reese, R. S. (2000) Integrating boreholes logs and aquifer tests in aquifer characterization. Ground Water, 38, 713–725.

Parra, J. O., Hackert, C. L., Collier, H. A., & Bennett, M., (2001) NMR and acoustic signatures in vuggy carbonate aquifers. Transactions of the Society of Petroleum and Well Log Analysts (SPWLA) 42nd Annual Logging Symposium, Houston, Texas.

Parra, J. O., Hackert, C., Bennett, M. & Collier J. A. (2003), Permeability and porosity images based on NMR, sonic, and seismic reflectivity: Application to a carbonate aquifer. Leading Edge, 22, 1102–1108.

Pettijohn, F. J. (1975) Sedimentary rocks (3rd ed). New York: Harper & Row.

Pickett, G. R. (1968) A review of current techniques for determination of water saturation from logs. Journal Petroleum Technology, 18, 1425–1433.

Pickett, G. R. (1973), Pattern recognition as a means of formation evaluation. The Log Analyst, 14 (4), 3–11.

Prensky, S. E. (1999) Advances in borehole imaging technology and applications. In M. A. Lovell, G. Williamson, & P. K. Harvey (Eds.) Borehole imaging: Applications and case histories, Special Publication 259 (pp. 1–43). London: Geological Society.

Prosser, J., Buck, S., Saddler, S., & Hilton, V. (1999) Methodologies for multi-well sequence analysis using borehole image and dipmeter data. In M. A. Lovell, G. Williamson, & P. K. Harvey (Eds.) Borehole imaging: Applications and case histories, Special Publication 259 (pp. 91–121). London: Geological Society.

Reese, R. S. (1994) Hydrogeology and the distribution and origin of salinity in the Floridam Aquifer System, southeastern, Florida. U.S. Geological Survey Water-Resources Investigations Report 94–4010.

Rider, M. H. (1990) Gamma-ray log shape used as a facies indicator: critical analysis of an oversimplified methodology. In A. Hurst, M. A. Lovell & A. C. Morton (Eds.), Geological applications of wireline logs, Special Publication 48, (pp. 113–120). London: Geological Society.

Roberson, S., & Hubbard, B. (2010) Application of borehole optical televiewing to investigation the 3-D structure of glaciers: implications for the formation of longitudinal debris ridges, midre Lovénbreen, Svalbard. Journal of Glaciology, 56, 143–156,

Schlumberger (1989a) Log interpretation principles/applications. Sugarland, Texas: Schlumberger.

Schlumberger (1989b) Cased hole log interpretation principles/applications. Houston: Schlumberger.

Serra, O. (2008) Well logging handbook. Paris: Éditions Technip.

Serro, O., & Sulpice, L. (1975) Sedimentological analysis of shale-sand series from well logs. Society of Petrophysicists & Well Log Analysts 16th Annual logging Symposium. SPWLA Document 1975-W.

Slatt, R. M., Jordan, D. W., D'Agostino, A. E., & Gillespie, R. H. (1992) Outcrop gamma-ray logging to improve understanding of subsurface log correlations. In A. Hurst, C. M. Griffiths, and P. F. Worthington (Eds.), Geological applications of wireline logs II, Special Publication 65 (pp. 3–19). London: Geological Society.

Syms, M. C. (1982) Down hole flow meter analysis using an associated caliper log. Ground Water, 20, 606–610.

Wempe, W. L. (2000) Predicting flow properties using geophysical data: Improving aquifer characterization. Dissertation, Stanford University.

Williams, J. H., Lane, J. W., Singha, K., & Haeni, F .P. (2002) Application of advanced geophysical logging methods in the characterization of a fractured-sedimentary bedrock aquifer, Ventura County, California. U.S. Geological Survey Water-Resources Investigations Report 00-4038.

Williams, J. H.,& Johnson, C. D. (2004) Acoustic and optical borehole-wall imaging for fractured-rock aquifer studies. Journal of Applied Geophysics, 55, 151–159.

Williams, J J., Lapham, W. W., & Barringen, T. H. (1993) Application of electromagnetic logging to contamination investigations in glacial sand-and-gravel aquifers. Ground Water Monitoring and Remediation, 13(3); 129–138.

Wyllie, M. R. J., Gregory, A R., & Gardner, G. H. F. (1958) An experimental investigation of factors affecting elastic wave velocities in porous media. Geophysics, 23, 459–493.

Young, S. C. (1995) Characterization of high-K pathways by borehole flowmeter and tracer tests. Ground Water, 33(2), 311–381.

Young, S. C., Julian, H. E., Pearson, H. S., Molz, F. J., & Boman, G. K. (1998) Application of the electromagnetic borehole flowmeter. U.S. Environmental Protection Agency, Office of Research and Development, Report EPA/600/R-98/058.

Chapter 11
Surface and Airborne Geophysics

Surface and airborne geophysical methods can be a valuable element of aquifer characterization programs because they typically are less expensive and can be performed quicker than methods that require the drilling of boreholes, which allow a larger number of measurements and thus greater spatial coverage. The greater spatial coverage comes at the expense of lesser vertical resolution. Surface and airborne geophysical methods are used for initial site reconnaissance and for interpolation of data between boreholes. These methods detect contrasts in subsurface geological and hydrogeological properties. Resistivity-based methods have great demonstrated value for hydrogeological investigations because of the wide range of resistivity values in naturally occurring rocks and soils. DC resistivity and electromagnetic methods (FEM and TDEM) have been successfully used to obtain one-, two-, and three-dimensional data on the lithology and salinity of subsurface strata. Seismic reflection and refraction surveys provide information on subsurface stratigraphy and structure. Newer techniques, such as surface nuclear magnetic resonance, can provide data on aquifer transmissivity. Surface geophysical data are interpreted using inversion methods, which do lead to unique solutions. Borehole geological, geophysical, hydraulic, and water quality data are needed to calibrate, validate, and constrain the interpretations of surface geophysical data. Forward modeling of the geophysical response to the anticipated hydrogeological conditions is a valuable means to determine, in advance, if a target is detectable using a given technique and to select and design the appropriate testing procedures for an investigation.

11.1 Introduction

Surface geophysical methods can provide information on local hydrogeology, which compliments, but not replaces, borehole-based field measurements. There is a wide variety of specific applications of surface geophysical methods for aquifer characterization, including determination of the (ASTM 1999)

- depth, thickness, and areal extent of soil and unconsolidated sediments
- depth to bedrock
- depth, thickness, and lateral continuity of rock layers
- depth to the water table
- salinity and salinity changes, such as vertical and horizontal saline-water intrusion and soil salinity
- location of fractures and fault zones
- location of voids (caverns) and sinkholes
- soil and rock properties.

Basic references on surface geophysics and applied geophysics, in general, include Zohdy et al. (1974), Telford et al. (1990), Eastern Research Group (1993), USACOE (1995), Reynolds (1997), Sharma (1997), American Society of Civil Engineers (1998), Milson (2003), Burger et al. (2006), Kirsch (2008), and Dentith and Mudge (2014). The Eastern Research Group (1993), in a study performed for the U.S. Environmental Protection Agency, provided an extensive bibliography of papers on the application of geophysical methods for the characterization of contaminated sites.

Surface geophysical methods are particularly valuable for detecting contrasts in subsurface geological and hydrogeological properties, which include changes in lithology, the contact between aquifer and confining strata, and the boundaries between waters with pronounced differences in salinity (e.g., interface between fresh and saline groundwater). A key issue is selecting a method in which the signal is sensitive to the contrast between the target and surroundings. Some of the specific advantages of surface geophysical techniques in groundwater investigations are

- a reduction in need for intrusive sampling
- a lower cost than monitoring well installation and test borings, which allows for a much greater sampling densities
- some methods measure parameters directly related to hydrogeological parameters of interest
- more accurate interpolation between sparse borehole data
- less time may be required than methods involving the drilling of new boreholes
- surface geophysics are often a less expensive means to collect areally-extensive data sets.

The principal disadvantages of surface geophysical methods are a lesser vertical resolution, the requirement of a high degree of technical sophistication to process and interpret the data, and uncertainties in interpretations. Surface geophysical methods rarely measurement groundwater properties per se, but rather provide information on groundwater from other measured properties (e.g., bulk resistivity). Surface geophysical data are interpreted using inversion solutions in which cause is inferred from effects. Forward solutions, on the contrary, proceed from cause to effect. Inversion solutions essentially involve finding a best-fit solution between theoretical geophysical responses generated for various earth models (e.g., configurations of layers and their properties) and the actual field (measured) data. Inversion

solutions are not unique and ambiguity applies to the interpretations from all geophysical methods, which can be reduced by an understanding of the geological reality (American Society of Civil Engineers 1998). Surface geophysical interpretations are more accurate if the data processing is based on a sound conceptual knowledge of the strata being evaluated. Borehole geological, geophysical, hydraulic, and water quality data are thus needed to calibrate, validate, and constrain the interpretations of surface geophysical data. It is also advisable to use several complementary geophysical methods in an integrated exploration program rather than relying upon a single method (American Society of Civil Engineers 1998).

It has not been uncommon for the results of surface geophysical investigations to fail to meet expectations. One the most important factors for the success of geophysical surveys are the competence of the person or team responsible for planning, carrying out the survey, and interpreting the data. A thorough understanding of the method's theory, field procedures, and interpretation, along with an understanding of local geology, are necessary to successfully complete a survey (ASTM 1999). Perhaps the most important question for surface geophysical investigations is whether or not the required data can be obtained using methods under consideration. Key requirements for successful geophysical investigations include

- a conceptual understanding of the problem (target) and the physical contrast that is likely to exist
- selection of a method that is appropriate to the target
- using available control to reduce non-uniqueness and equivalence.

Forward modeling of the geophysical response to the anticipated hydrogeological conditions is a valuable tool to determine in advance if a target is detectable using a given technique and to select and design the appropriate testing procedures for an investigation (Fitterman and Stewart 1986; Mills et al. 1988; Minsley et al. 2011). Based on prior knowledge of local geology and the likely properties (e.g., resistivities) of the strata that will be encountered, it is possible to model the expected geophysical response and then determine whether or not it would be detectable. Failure to adequately evaluate in advance whether or not the target data for a project site is obtainable using the proposed surface geophysical techniques can result in costly and embarrassing failed surveys that had no prospect for success.

11.2 Electrical Resistivity and Electromagnetic Techniques

Electrical resistivity and electromagnetic methods are collectively referred to as geoelectric techniques. Both methods are based on the resistance to the passage of an electrical current offered by soil and rock. The magnitude of the resistance depends largely upon the rock and sediment type, porosity (value and degree of interconnection), and the salinity of the pore waters. No other physical property of naturally occurring rocks and soils displays such a wide range of values as

resistivity. Hence resistivity-based methods have great demonstrated value for obtaining data on subsurface hydrogeology (Zohdy 1974).

Electrical resistivity methods provide information on underlying geoelectric layers, which do not necessarily coincide with geological layers (Zohdy 1974). Geoelectric layers are defined by resistivity and thicknesses. The boundaries of geoelectric layers are commonly differences in salinity, degree of saturation, and rock or sediment type. The relationship between electrical resistance, potential, and current is expressed by Ohm's law

$$r = V/I \tag{11.1}$$

where, r is resistance (ohms), V is potential (volts), and I is current (amperes). Resistivity (R) is an intrinsic property of a material, which is defined as follows

$$R = r\,A/L \tag{11.2}$$

where, A is the cross-sectional areas normal to the flow of current (m^2) and L is length (m). The unit of resistivity is the ohm-m. Equation 11.2 indicates that the measured resistance values must be processed for the geometry of the investigated aquifer volume (A and L parameters) in order to determine resistivity, the parameter of interest.

The resistivity of rock or sediment is related to formation water resistivity and porosity through the Archie (1942) equation (Sect. 10.5.2). Archie's equation is applicable when the electrical conductivity through interconnected pore space is much greater than all other forms of electrical conductivity in the formation. Archie's equation can fail (i.e., provide incorrect results) in freshwater environments and in the presence of intergranular clay or clay coatings on grains, which can allow for surface conductance (Purvance and Andricevic 2000). Measured resistivity values are a function of both groundwater resistivity and the aquifer or formation porosity. A given formation resistivity value can thus be produced by a range of combinations of formation water resistivity (i.e., groundwater salinity) and porosity values. Hence, the importance of having some independent information on local geology, such as approximate aquifer porosity, which can constrain the interpretation of resistivity data. Where geology (porosity) does not spatially vary rapidly, resistivity-based methods can be very effective in detecting the presence of groundwater and changes in salinity.

Resistivity methods are particularly useful for the location of interfaces between materials with sharply different lithologies and resistivities, such as the

- interface between saline and fresh groundwater
- contact between porous rock and impermeable (very high-resistivity) bedrock
- location of relatively high-resistivity freshwater-bearing coarse sediments (e.g., channel deposits) amidst less resistive clayey deposits
- top of the water table
- groundwater quality variations (e.g., leachate from landfills).

A critical consideration is that the target should have a significant resistivity contrast in order for it to be detected. Resistivity-based methods may not be able to detect the water table, if it is not associated with a significant change in resistivity. Resistivity methods are well suited for detecting changes in salinity, and have been demonstrated to be particularly useful for determining the location and shape of coastal saline-water interfaces.

11.3   DC Resistivity Method

The direct current (or low frequency AC) resistivity method is one the oldest and still mostly widely used surface geophysical technique because the instrumentation is inexpensive, data processing tools are widely available, and the relationship between resistivity and hydrogeological properties, such as porosity, moisture content, and salinity, are reasonably well established (Binley and Kemna 2005). The applications of the DC resistivity method to groundwater investigations are discussed in detail by Zohdy (1974). The basic data collection method is that an electrical current is applied to the ground using two current electrodes. Either a direct current (DC) or usually now a very low frequency (<20 Hz) AC current is used. The difference in potential (voltage) is measured between two additional (potential) electrodes that do not carry current.

A number of different electrode arrays are used in the DC resistivity method, which vary in the configuration and the relative spacing of the current and potential electrodes. The oldest and conceptually simplest configuration is the Wenner electrode array, in which there is equal distance spacing between the four electrodes (Fig. 11.1). The Schlumberger electrode array also has a symmetric collinear configuration, but differs from the Wenner array in that the distance between the two potential electrodes is much less than the distance between the current and potential electrodes. The dipole-dipole array consists of two closely spaced pairs of current and potential electrodes. The professional planning a surface geophysical surveys needs to be aware of the various electrode configurations and their appropriateness for a given survey type and setting.

The raw data for electrical resistivity testing are the electrical current (I), potential difference between the two potential electrodes (DV), and the electrode spacing. Geoelectrical data are usually expressed in terms of apparent resistivities (R_a ohm-m, X-m)

$$R_a = K \frac{DV}{I} \tag{11:3}$$

where K is a dimensionless geometrical factor and DV = potential difference (volts)

The equation for the geometrical factor depends upon the type or array and the electrode spacing (Zohdy 1974). In the conceptually simplest array, the Wenner

Wenner Array

Schlumberger Array

Dipole-Dipole Array
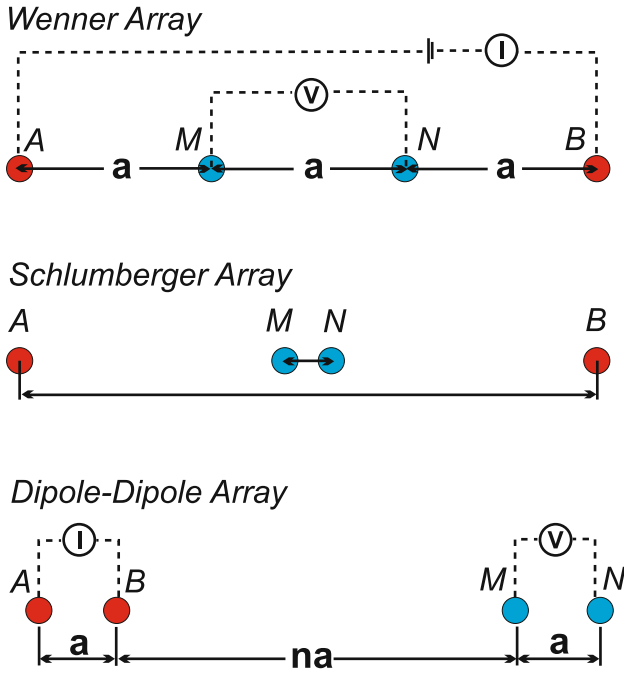
Fig. 11.1 Schematic diagram of the Wenner, schlumberger, and dipole-diploe electrical resistivity arrays. An electrical current (I) is applied to the current electrodes (A, B) and the potential difference (V) is measured between two potential electrodes (M, N)

array, the spacing (a) between the collinear electrodes are equal and the apparent resistivity is calculated as

$$R_a = 2p \, a \, V = I \tag{11:4}$$

Soundings are performed by increasing the spacings of the current (AB) and potential (NM) electrodes. With the Schlumberger array, soundings are performed by increasing the spacing of the current electrodes. The Schlumberger array allows for quicker analyses because the inner (potential) electrodes are only occasionally moved during a vertical sounding, whereas with the Wenner array, all four electrodes are moved for each reading.

Apparent resistivity is calculated using the Schlumberger array as (Zohdy 1974)

$$R_a = p \frac{\left(\frac{\overline{AB}}{2}\right)^2 - \left(\frac{\overline{MN}}{2}\right)^2}{\overline{MN}} \left(\frac{DV}{I}\right) \tag{11:5}$$

Apparent resistivity (R_a) values do not directly relate to any property of the underlying sediment and rock. The depth of investigation increases with electrode

spacing, which is often expressed as one-half the distance between the current electrodes (AB/2). However, there is no universal quantitative relationship between electrode spacing and depth of investigation. Ground-based resistivity methods are affected by decreasing vertical resolution with increasing depth due to the averaging effect of electrical properties with depth.

DC resistivity surveys are performed in either surface profiling or vertical electrical sounding (VES) mode. Surface profiling involves measurements taken at different positions while keeping the electrode spacing constant. Surface profiling is used, for example, to map differences in salinity at a given approximate depth interval. VES is performed at a single site by progressively increasing the electrode spacing to determine variations of electrical properties at depth at a given location in space. Surface profiling and VES are combined to produce 2-D or 3-D images of subsurface resistivity.

In practice, individual VES soundings are now seldom performed. The current state of the art is multielectrode, continuous vertical electrical sounding (CVES) and electrical resistivity tomography (ERT) systems and the interpretation of the data in the form of electrical resistivity tomograms. A prototype CVES system was described by Van Overmeeren and Ritsena (1988). Multicore cables are used with electrode take-outs at evenly spaced intervals, commonly 5 m (16.4 ft). The electrodes are individually addressable, so it is possible through the selection of electrodes to vary the location and depth of investigation of each reading, as well as the type of electrode array. The Wenner array or a combination of Wenner and Schlumberger arrays are typically used because of their collinear electrode spacing. If dedicated electrodes are used, time-lapse resistivity profiles could be performed to monitor temporal changes in salinity (e.g., De Franco et al. 2009).

CVES/ERT systems are controlled by a portable computer, which is programmed to control which electrodes are energized as current electrodes and which electrodes collect voltage data. Rapid readings can be performed to collect data at different locations and depths along the electrode cable transect. The collected data for each reading include, at a minimum, the electrode geometry, and measured current, voltages and spontaneous potentials. The data are preprocessed to obtain apparent resistivity values. Profiles (i.e., cross sections) of apparent resistivity versus electrode spacing (AB/2) are processed using inversion techniques to obtain an electrical resistivity tomogram or pseudo-section of bulk resistivity versus depth. Three-dimensional surveys are possible if the electrodes are arranged in a grid. Binley and Kemna (2005) emphasized that pseudo sections do not necessarily provide an accurate image of surface resistivity; they merely serve as a means of plotting measured data. The data require further processing to obtain profiles of, for example, salinity versus depth.

The raw data for resistivity soundings is presented as a plot of apparent resistivity versus current electrode spacing (AB/2), which are normally plotted on logarithmic scales (Fig. 11.2). Quantitative analysis of surface resistivity data is performed using inverse modeling techniques, which involves the comparison of measured sounding curves to calculated theoretical sounding curves. The theoretical sounding curves are generated based on conceptual earth models that can
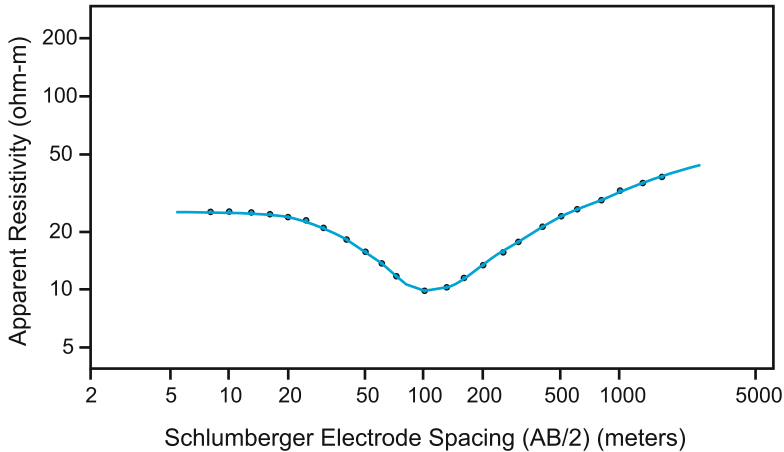
Fig. 11.2 Example of schlumberger sounding curve (from Zohdy 1974)

incorporate different numbers of layers, layer thicknesses, and layer resistivities. Curve matching is now performed using inversion software (which is commercially available), which involves iterative schemes in which the model is continuously updated until an acceptable match (specified error level) is reached between the field data and model.

Inversion methods, in general, do not provide unique solutions. Information on local geology and hydrogeology and the geoelectric properties of the local sediment and rock, allows for better constrained and thus more accurate inversion solutions. Borehole resistivity logs in the survey area, in particular, can provide useful information on the resistivity values of the underlying strata and the general geoelectric stratigraphy.

Once bulk resistivity has been interpreted using inversion techniques, ground-water resistivity and salinities can be determined using Archie's (1942) law if some data are available on porosity or groundwater salinity from boreholes or laboratory measurements. Borehole resistivity, salinity, and porosity data from points along resistivity soundings and profiles are used to calculate formation factors, which can be used to interpret bulk resistivity data, provided that the geology is relatively homogenous or well constrained (e.g., Wilson et al. 2005).

DC resistivity readings are weighted averages of effects produced over a large volume of material with near surface materials contributing most heavily. The method produces smooth curves that do not lead themselves to high-resolution interpretations (USACOE 1995). DC resistivity has a shallow to moderate depth of investigation. Vertical electrical soundings have been performed to depths of 500 m (1,640 ft) or greater (e.g., Worthington 1977). In order to achieve great sounding depths, very large ($\geq 1,000$ m; $\geq 3,280$ ft) electrode spacings and increased current are required. Electromagnetic methods (Sect. 11.4) are usually used instead for deep soundings.

Electrical resistivity analyses can be impacted by a variety of extraneous factors, which are discussed by Zohdy (1974). Some of the more important extraneous

factors are buried metal objects in investigation areas, discontinuous layers, and equipment problems such as current leakage from poorly insulated cables. Interpretation of vertical sounding data (either DC resistivity or TDEM) is also complicated if significant lateral heterogeneity in resistivity occurs near the sounding site and if the strata are not flat-lying.

11.4   Electromagnetic Surveys

Electromagnetic (EM) methods induce currents within the Earth without the requirement of direct contact with the ground. EM methods are performed either on the ground or using an airborne platform. EM methods are based on Faraday's Law, in which a changing magnetic field can generate an electrical current, and Ampere's Law, in which a changing electric field can generate a magnetic field. The basic theory of electromagnetic induction is discussed in most geophysics texts (e.g., Telford et al. 1990; Milson 2003; Burger et al. 2006). Conceptually, an alternating current loop on or above land surface induces a primary magnetic field that spreads out above and below the transmitter. The primary magnetic field induces an alternating current in subsurface conductors, which are referred to as 'eddy currents'. The eddy currents, in turn, induce a secondary magnetic field that differs from the primary magnetic field in both amplitude and phase. An EM receiver loop detects both the primary and secondary magnetic fields.

Electromagnetic methods can be divided into time-domain (TDEM) and frequency domain (FEM) or continuous wave (CW) systems. The TDEM soundings are also referred to transient electromagnetic (TEM) soundings. Frequency domain techniques are often referred to as just electromagnetic (EM) methods. Frequency domain techniques induce a primary magnetic field using the flow of sinusoidal alternating current at either one or more frequencies in a wire or coil (transmitter coil). The receiver coil intercepts the primary and secondary electromagnetic fields created by the induced eddy currents. Transient systems, on the contrary, induce electromagnetic fields through transient pulses of electric current. TEM methods tend to have greater depths of investigation and are more widely used in groundwater investigations to obtain data on subsurface lithological and salinity changes. TEM systems have the practical advantage that the large primary field is not present during measurements, which allows for the better detection of small signals above background noise (Telford et al. 1990). FEM systems are more portable and more commonly used for investigations of shallow geology and hydrogeology.

The choice between EM and electrical (resistivity) methods largely depends on the target. Electrical methods are better at resolving resistive targets, whereas EM methods are better at resolving conductive (low resistivity) targets. For example, ERT may be the best option for mapping the base of an aquifer where it is underlain by a high-resistivity confining unit or bedrock. TDEM is commonly used to map the downward transition from fresh to more conductive saline groundwater. EM methods also tend have a greater depth of investigation and lower costs.

11.4.1   Frequency Domain Electromagnetic Surveys

A simple, widely used type of FEM system consists of two horizontal coplanar coils (transmitter and receiver), connected by a shielded cable, that are a fixed distance apart. For small portable systems, the coils are attached to the ends of a rigid pole, and the entire apparatus can be carried by a single person. The depth of penetration is related to frequency and the coil separation, with a greater separation resulting in a greater effective depth of investigation. A generalization is that the maximum depth of penetration is roughly equal to twice the coil separation, but in practice the depth is often less (Milson 2003). As frequency decreases, the influence of deeper parts of the section becomes more pronounced (Goldman and Neubauer 1994).

The basic underlying principle of FEM is that the magnitude and phase of induced electromagnetic currents are related to subsurface electrical conductivity. Subsurface electrical conductivity is, in turn, related to soil and rock lithology, degree of saturation, and water salinity. The primary advantages of FEM methods are that they do not require ground contact and the measurements can be performed quickly, which allows for the economical coverage of large areas. FEM is commonly performed in the profiling mode using a constant coil separation to detect and map lateral changes in shallow subsurface geological and hydrogeological conditions. For example, FEM surveys can be used to map the location of subsurface channels, if they are less conductive (more resistive) than surrounding clay-rich strata. FEM may also detect changes in salinity.

As is the case with DC resistivity data, measured conductivity values are integrated over a volume of soil or rock. Inversion techniques are, therefore, necessary in order to quantitatively evaluate subsurface hydrogeology. FEM surveys are susceptible to interference from power lines and metallic features, such as metal pipes and fences. However, FEM surveys are commonly performed specifically to locate subsurface metallic objects, such as underground storage tanks and buried drums (Fig. 11.3). Readings are apparent resistivity rather than true resistivity. However, usually spatial variations in conductivity are of primary interest, rather than the actual conductivity values. FEM surveys are commonly performed in an 'anomaly finding' mode (USACOE 1995).

11.4.2   Time-Domain Electromagnetic (TDEM) Soundings

The major technical challenge of electromagnetic methods is to separate the secondary magnetic field signal from the stronger primary field. TDEM achieves separation of the primary and secondary field signals by using a pulsed electrical signal and measuring the decay of the secondary field after the primary field is turned off. The decay rate of the secondary field is inversely proportional to conductivity with highly conductive beds having slower decay rates. Either spatially separate transmitter and receiver coils are used, or more commonly, field soundings
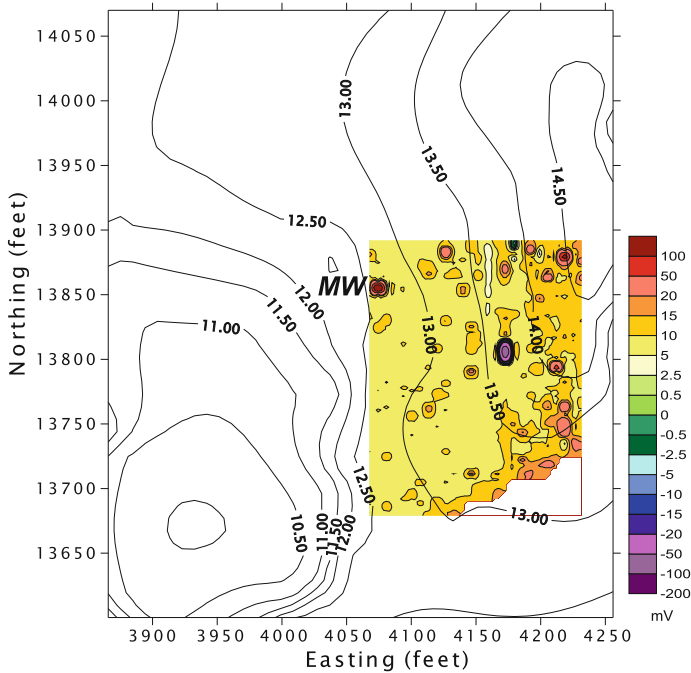
Fig. 11.3   EM survey data from the USEPA characterization test cell (CTC) site at the Naval Base Ventura County, Port Hueneme, California. Detected anomalies were ferrous and nonferrous metallic objects within the depth range of the instrument, including a monitoring well (MW). Ground elevation contours are in feet (from Werkema 2004)

are performed using a smaller receiver coil that is placed in the center of a larger transmitter coil.

The optimal size of the transmitter loop and applied current can be determined by forward modeling using layered-earth computer programs, which allow for the evaluation of whether the physics of TDEM soundings will allow for detection to the target depth (American Society of Civil Engineers 1998). TDEM surveys with 100 m (328 ft) transmitter loops have been used to obtain estimates of resistivity down to depths of several hundred meters (or ft), which would require electrode arrays several kilometers (miles) in length if conventional DC resistivity methods were to be used (Milson 2003). That small transmitter loops can be used for much larger exploration depths simplifies field procedures and allows for improved lateral resolution (Goldman and Neubauer 1994).

As is the case for the DC resistivity method, the raw data are processed using inversion techniques involving fitting theoretical responses from hypothetical earth models to the measured response (Fig. 11.4). The model is refined until the theoretical response matches the observed or measured field response. TDEM data processing method does not yield a unique solution and the results should be ground-truthed against resistivity (salinity) data from one or more wells located in
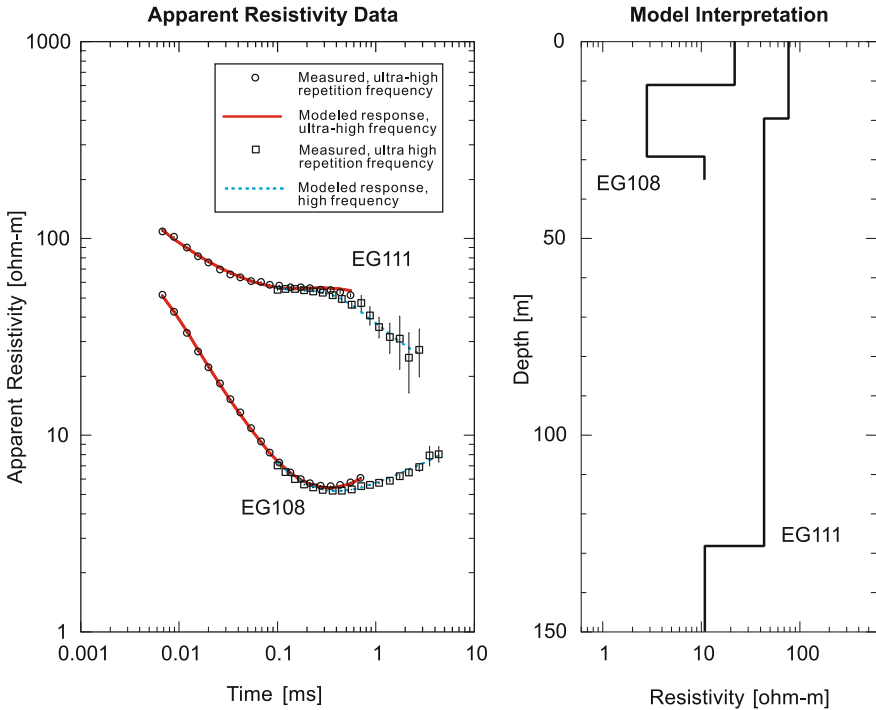
Fig. 11.4 Example of TDEM data interpretation from a survey performed in the Everglades National Park, Florida, USA (from Fitterman et al. 1999). Inversion techniques are used which involve matching modeled theoretical responses for hypothetical earth models to the measured data

the study area. TDEM is also a relatively coarse technique. The minimum thickness zone that can be resolved by TDEM is several orders of magnitude greater than what can be resolved by borehole electric logs.

TDEM works best for identifying and locating sharp contrasts in resistivity, such as those occurring at major lithological changes or significant changes in salinity at the freshwater–saltwater interface. TDEM is better suited for detecting highly conductive targets (e.g., saline water) than poorly conductive targets (Fitterman and Stewart 1986). Care must be taken to avoid interference from conductive items (metal) in the sounding vicinity. Localized good conductors, such as buried metallic objects or sulfide ore bodies, generate eddy currents that can dominate decay curves and prevent valid depth soundings (Milson 2003). TDEM soundings give reasonably accurate average depths to sloping interfaces and are less sensitive to variable surface topography compared to other surface geophysical methods (American Society of Civil Engineers 1998).

11.5   Self Potential

Self-potential is an instrumentally simple method that involves measurement of natural current potentials. The basic equipment is a pair of electrodes, wire, and a precise millivoltmeter. One electrode is located at a base position and a second roving electrode is moved around the study area. Self potentials are generated in four main manners (Telford et al. 1990; USACOE 1995):

- electrokinetic or streaming potential resulting from the movement of fluid containing ions
- liquid junction or diffusion potential caused by the displacement of ionic solutions of different concentrations
- mineralization, or electrolytic contact, potential produced at the surface of a conductor with another medium
- Nernst or shale potential, which occurs when similar conductors have a solution of differential concentrations about them.

Application of self-potential include (1) locating areas of groundwater flow in fractured rock and sinkholes, (2) locating leaks in canals and reservoirs, (3) detecting and monitoring the movement of contaminant plumes (Telford et al. 1990; Eastern Research Group 1993; USACOE 1995). Despite having its simplicity, the self-potential is uncommonly used in groundwater investigations because of its limited applications.

11.6   Induced Polarization

Induced polarization (IP) involves similar electrode configurations as DC resistivity. IP methods are based on the ability of some materials to become electrically polarized and 'store' electrical energy. When the electrical current is turned off, the potential difference (measured by the potential electrodes) often does not instantaneously drop to zero. Instead there is a rapid initial drop in voltage, followed by a gradual decay as the stored electrical energy is discharged. The IP method utilizes the measured decaying potential versus time.

Induced potential can be quantified in terms of chargeability (M), which is ratio of induced, secondary potential (V_s) to the maximum potential (V_m);

$$M = V_s = V_m \tag{11:6}$$

Chargeability is also quantified as the integrated area under the voltage versus time curve between two times (t_1 and t_2) with the unit of milliseconds.

$$M = \frac{1}{V_m} \int_{t_2}^{t_1} V_t \, dt \tag{11:7}$$

Induced polarization is strongly affected by processes at the fluid-grain interface. Grain-surface chemistry is a function of lithology, particularly clay content (Sumner 1984; Brinley and Kemna 2005). The polarized materials, in essence, behave as electrical capacitors. Time-domain IP measures the voltage decay with time after current injection is terminated. Frequency domain measures phase-shifted voltage relative to an injected alternating current.

IP is rarely used as a stand-alone method in groundwater investigations. Inasmuch as IP and DC resistivity can use the same electrode arrays, they are often performed together. The value of the IP method is that it can reveal structural layering that is not evident by DC resistivity. For example, sands containing saline or brackish water may have a similar resistivity as some freshwater-containing shales. These units may be differentiated based on their different chargeability. It is emphasized again the importance of having, at the start of surface geophysical investigation, an understanding of the composition and properties of the strata present in the study area and their general response to different geophysical methods. This understanding should serve as the basis for determining which methods should be employed.

11.7 Applications of Resistivity and EM Surface Geophysics to Groundwater Investigations

Resistivity-based surface geophysical techniques continue to have a wide range of applications for groundwater resources evaluation. Their greatest value is realized in projects in which there is sharp resistivity contrast of interest. Applications of DC resistivity and electromagnetic methods to groundwater investigations were reviewed by Maliva and Missimer (2012) with respect to arid lands and are summarized below.

Electrical and EM methods differ in their sensitivities to near surface conditions and the type of geoelectric layeing. ERT can be effective at mapping the top of a resistive layer (e.g., contact between an aquifer and underlying bedrock), but has poor penetration through resistive layers (i.e., detecting the base of a high-resistivity layer and underlying layers). TDEM has poor resolution of shallow features and a poor sensitivity to high-resistivity layers. However, shallow resistive layers do not prevent the electromagnetic field from penetrating to deeper layers. Hence, TDEM has a greater ability to detect deep conductive layers.

11.7.1 Mapping of Saline-Water Interface

Both DC resistivity and TDEM have been successfully used in numerous studies to map the vertical and horizontal location of saline-water/freshwater interfaces. EM methods are particularly well suited for mapping the interface because of the large

contrast in resistivity (conductivity) between freshwater and saline water. An important observation, in many of the studies, is that mapping of the saline-water interface is best performed in conjunction with monitoring well water quality data and borehole geophysical data. Borehole geophysical data, for example, provides information on the resistivity of subsurface strata and allows for selection of the appropriate geoelectrical model among multiple potential options.

Zohdy (1974) provides references to some early (1950s and 1960s) case histories, including documentation of a U.S. Geological Survey investigation at the White Sands Missile Range in New Mexico, where electrical soundings were successfully used to map the base of the freshwater aquifer. The saline-water interface was mapped in a karstic limestone aquifer in coastal west-central Florida using the DC resistivity method (Fretwell and Stewart 1981). The Fretwell and Stewart (1981) study illustrates that multiple interpretations of resistivity data may be plausible. An intermediate-depth low-resistivity zone could be either (1) a more permeable zone sandwiched between less permeable zones, (2), a tongue of saline water sandwiched between freshwater water zones, or (3) a low resistivity clay lying between more resistive limestones.

VES and TDEM were successfully used the map variations in salinity related to the saline-water interface in northeastern Spain (Seara & Granda 1987), coastal Monterey County, California (Mills et al. 1988), western Yemen (Van Overmeeren 1989), east-central Florida (Blackhawk Geosciences 1992; Subsurface Detection Investigations 1995), northwestern Malaysia (Samsudin et al. 2008), Morocco (Benkabbour et al. 2004), the North Island of New Zealand (Wilson et al. 2005), Malaysia (Abdul Nassir et al. 2000), the Fujairah and Kalbha coast of the United Arab Emirates (Sherif et al. 2006), and the Batinal coast of northern Oman (Abdalla et al. 2010; Fig. 11.5). The latter study involved two surveys performed 5 years apart, which were able to detect an approximately 600 m recession (seaward migration) of the interface. The recession was attributed to increased recharge induced by a wadi dam and regulation of groundwater pumping.

Time-lapse resistivity tomography was performed in the Venice Lagoon area of Italy (De Franco et al. 2009). The ERT program was set up to perform 10 resistivity tomographic measurements per day over a nine month period starting in November 2005. The time-lapse ERT program was able to detect spatial (horizontal and vertical) and temporal variations in saline-water intrusion. Seasonal variations in water quality are evident on the tomograms.

Resistivity methods can be used to locate freshwater lenses, particularly where there is a sharp resistivity contrast between the freshwater-saturated strata, overlying desiccated strata, and underlying strata that contain saline waters. Young et al. (2004) documented the use of TDEM soundings to detect and map freshwater lenses in karstic limestones in Central Oman. Freshwater lenses form atop the regional saline aquifers as a result of episodic focused recharge. The TDEM data could detect the base of the freshwater lenses (i.e., contact with underlying saline waters). However, the top of the lenses and their thickness could not be resolved (Young et al. 2004). The results of this investigation demonstrate the value of the
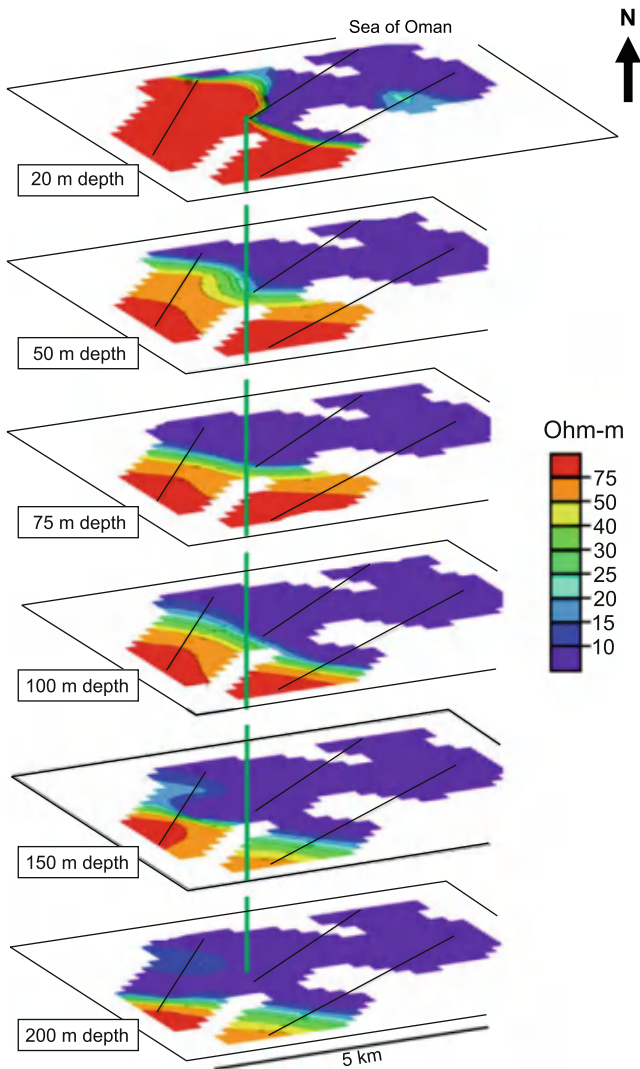
Fig. 11.5 TDEM-derived planar maps of formation resistivity at various depths at Wadi Al Hawasinah, Northern Oman. Low resistivities (blue shades) represent the presence of saline water, which progressively extend a greater distance landwards with depth (from Abdalla et al. 2010)

TDEM survey data as a relatively low-cost reconnaissance tool to locate potential freshwater resources, which would be further assessed using test wells.

CVES was used by Goes et al. (2009) to map the location and thicknesses of fresh to slightly brackish groundwater lenses in the province of Zealand in the coastal zone of the Netherlands (Fig. 11.6).
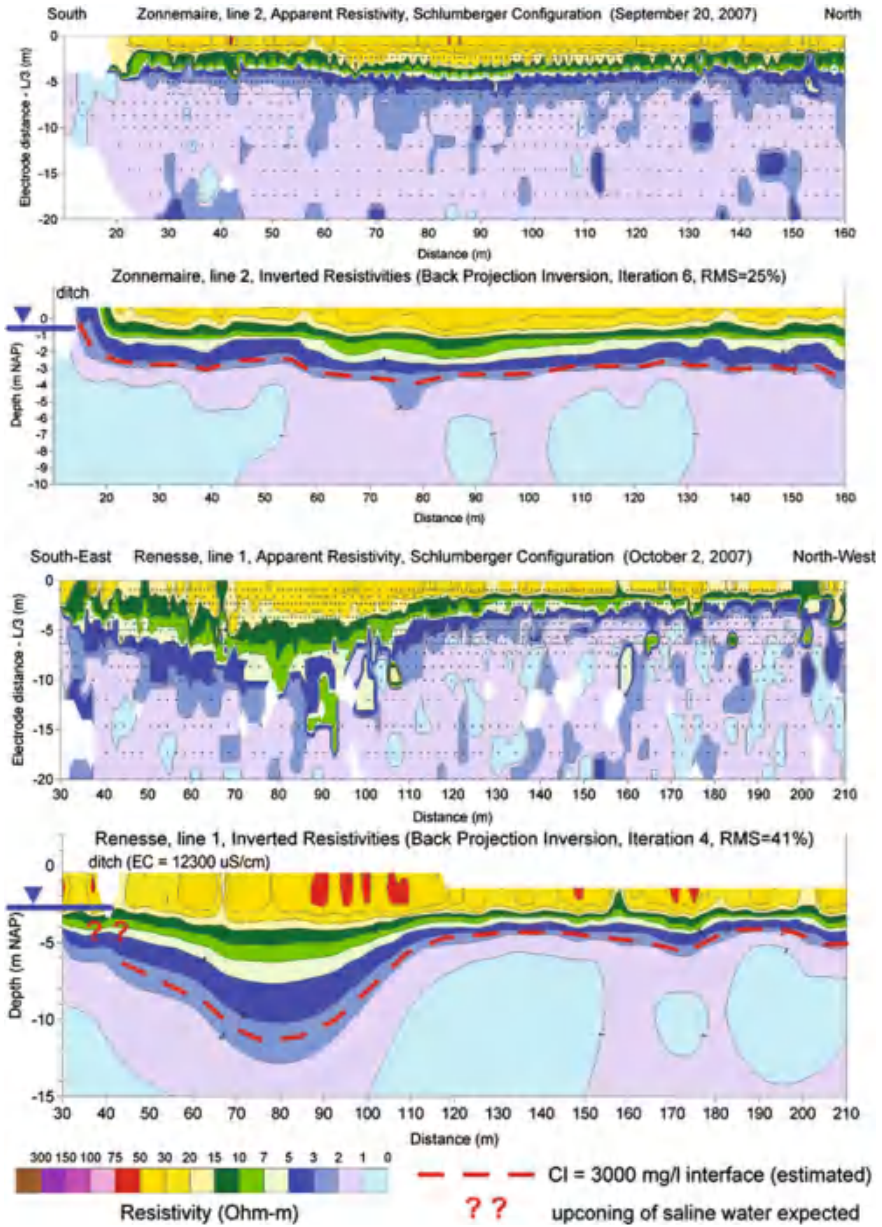
Fig. 11.6 Examples of CVES profiles from Zealand, The Netherlands, showing fresh to slightly saline groundwater lenses indicated by relatively high resistivities (from Goes et al. 2009, copyright: European Association of Geoscientists & Engineers)

11.7.2 Depth to the Water Table

DC resistivity and electromagnetic methods can be used to locate the approximate position of the water table, where it is marked by a relatively sharp downward decrease in resistivity from highly resistive dry sediment or rock to less resistive saturated strata. However, the decrease in water content (and thus resistivity) above the water table may be gradual and there may not be a distinct, detectable geo-electrical boundary. Borehole testing and forward modeling is thus recommended to determine whether mapping of the water table is feasible and whether a given instrument or array is appropriate for the project.

11.7.3 Formation and Aquifer Mapping

Changes in lithology and water saturation are often associated with substantial changes in formation resistivity, which can be detected using DC resistivity and EM surveys and soundings. Surface resistivity has been used to differentiate between coarse-grained aquifers (e.g., channel deposits) within or between finer-grained semi-confining strata, the contact between dry and moist deposits, and the tops and bottoms of aquifers. Information on subsurface geology obtained from DC resistivity and electromagnetic surveys can be used to make more informed decisions as to the best location for either test wells or production wells. A common application of surface geophysics is to map the location of shallowly buried alluvial aquifers. Relatively clean (clay poor) sands and gravels and can be differentiated from adjoining low hydraulic conductivity finer-grained (clay-rich) sediments by a greater resistivity (e.g., Driscoll 1986).

The contact between aquifer strata and underlying bedrock is often a sharp geoelectric boundary, which can be either a downward increase in resistivity, where the bedrock is crystalline or nonporous sedimentary rock, or a downward decrease in resistivity, where a freshwater aquifer is underlain by clay-rich strata. The U.S. Geological survey demonstrated how surface geophysical methods can be used to map and characterize surficial and a gravel deposits (Lucius et al. 2007). A TDEM survey was used to the map contact between alluvial sand and gravel deposits and underlying bedrock (Fig. 11.7).

Worthington (1977) documented the use of DC resistivity surveys to delineate the most promising sites for future groundwater development in the Kalahari Desert of what is now Namibia. The base of the sedimentary basin could be identified by the high-resistivity of the basement rock. Correlations were observed between the geoelectrically derived thickness, resistivity, and transverse resistance of the main aquifer (Middle Kalahari) and the yield of boreholes. The main value of the resistivity survey method is that it could allow for the optimization of the initial stages of groundwater exploration in arid and semiarid regions, in general, by increasing the probability of successful wells.
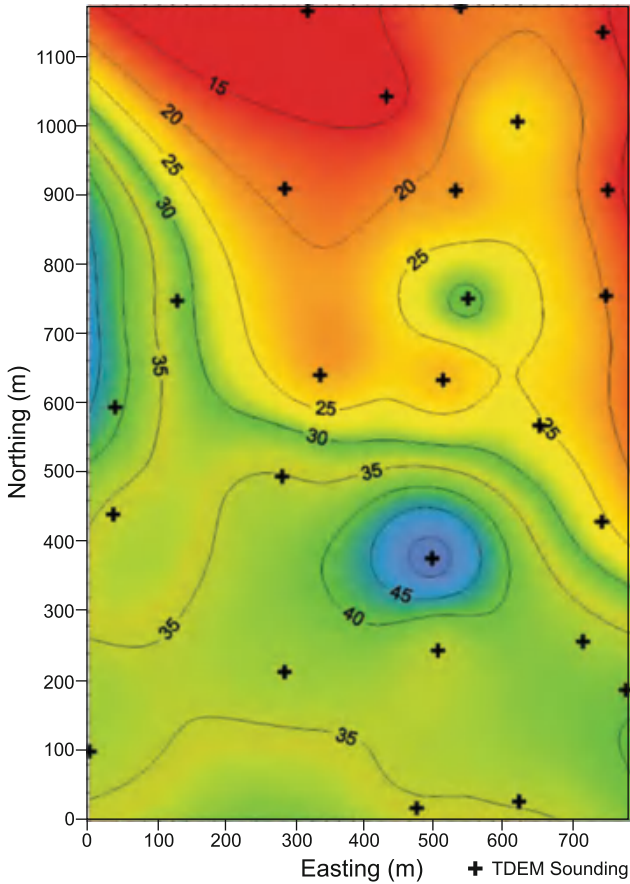
Fig. 11.7 Contour map (interval = 5 m) of the contact between alluvial sand and gravel deposits and underlying bedrock generated from TDEM survey data (from Lucius et al. 2007)

Taylor et al. (1992) documented the detection of faults in an alluvial piedmont aquifer north of Reno, Nevada, using closely spacing TDEM soundings. Faults could be detected by contrasts in resistivity, but not by the actual values. The TDEM survey data provided guidance concerning the extent of areas that likely have significant groundwater resources and thus reduced the number of wells required to characterize the resources.

TDEM sounding have been successfully utilized for the characterization of alluvial aquifers in the Middle East, where it has been used to map buried pale-ochannels that are important aquifer zones (Fitterman et al. 1991) and to broadly define aquifer zones (Young et al. 1998). Fitterman et al. (1991) also demonstrated the importance of using auxiliary data, such as well logs, to a construct a geophysical model used for the interpretation of the data. Initial geophysical interpretations made without the benefit of well information failed to identify the

resistive gravels that form the main body of the aquifers. The gravels were detectable using a refined model based on well data.

11.7.4   Mapping of Recharge Areas

In some arid settings, saturated shallow sediments may be distinguished from dry sediments by differences in resistivity. Resistivity profiles and soundings were used to map the location of deep percolation and recharge in the Amargosa Desert Basin of Nevada, USA (Abraham and Lucius 2004; Stonestrom et al. 2007). Three main categories of alluvium were detected based on their resistivities:

(1) low water content coarse gravels and highly desiccated surface material (R > 200 X-m)
(2) moist alluvium (R < 20 X-m)
(3) other low to low-medium water content alluvium in areas without active recharge (intermediate values of R).

The DC resistivity data revealed areas of low resistivity, and thus high water content, beneath the ephemeral stream channels (Fig. 11.8). The geophysical data suggest that recent recharge is negligible in the interchannel areas.

11.7.5   Mapping Contaminant Plumes

Plumes of contaminated water may be mapped, if the water has a marked difference in electrical conductivity than native groundwater. Landfill leachate, in particular,
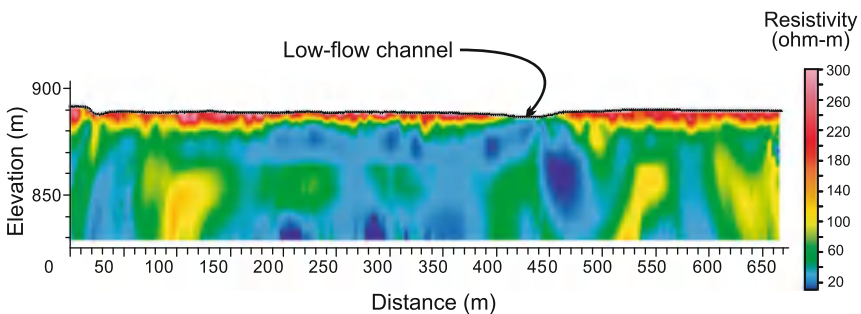
Fig. 11.8 DC resistivity cross section from the Amargosa Desert, Nevada, in which focused recharge is evident under an ephemeral channel by lower resistivitiies, which reflect a greater moisture content (from Stonestrom et al. 2007)

often has elevated concentrations of dissolved solids. Mapping of landfill leachate and other industrial plumes in shallow aquifers using resistivity surveys was documented by Urish (1983), Russell and Higer (1988), de Lima et al. (1995), Acworth and Jorstad (2006), and Reyes-López et al. (2008). As is the case of surface geophysical investigations in general, data on groundwater salinity and site hydrogeology should be first evaluated to determine whether or not there is a sufficient contrast in the electric conductivity to be detected and to assist in data processing.

11.7.6   Mapping of Regional Aquifer Flow Orientation (Fractured Rock Aquifers)

Preferred orientation of fractures can result in hydraulic and electrical anisotropies in aquifers. Surface azimuthal resistivity (DC resistivity and EM) methods have been used to determine the orientation of fractures in aquifers and thus the preferred direction of groundwater flow (e.g., Eastern Research Group 1993; Zoldny 1970; Skinner and Heinson 2004). Variations in anisotropy with depth are investigated by changing the electrode spacing. Processing of the apparent resistivity versus geographic orientation data requires use of two or three-dimensional models to calculate real-earth resistivities and actual anisotropy direction. Skinner and Heinson (2004) demonstrated the utility of both DC and EM resistivity in providing a noninvasive determination of the orientation of the maximum hydraulic connection in a fractured rock aquifer in the Clare Valley, South Australia.

11.8   Ground-Penetrating Radar

Ground-penetrating radar (GPR) uses pulses of electromagnetic radiation in the radio and microwave bands (10–3,000 MHz) to detect subsurface structures. GPR is a widely used technique to investigate shallow strata, which is employed in many disciplines, in addition, to hydrogeology. GPR, for example, is used in archeology to locate buried structures, and for site investigations to locate buried objects, such as pipes, tanks, and drums. The physics of GPR is discussed in detail in most surface geophysics textbooks (e.g., Telford et al. 1990; Reynolds 1997; Milson 2003; Burger et al. 2006), and is reviewed by Baker et al. (2007) and Jol (2009). A GPR system consists of one or two antennae, a digital control unit, and a power supply. Either separate antennae are used for transmission and reception of signals or a single antenna is used for both. GPR units can be operated using a battery and many models are small enough so that they can be mounted on wheels, and towed and operated by one person.
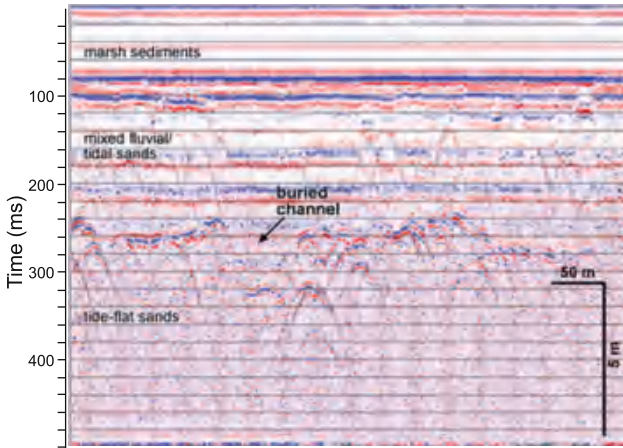
Fig. 11.9 Ground-penetrating radar imagery from mouth of the South Fork of the Skagit River (Washington, USA) showing buried marsh and tidal channels and associated facies (from Grossman 2005)

The basic principle is that a pulse of electromagnetic waves generated by a transmitting antenna travels through the tested soil or rock at a velocity that is primarily a function of the permittivity (dielectric constant) of the material. When the wave hits an object or layer with a different permittivity, part of the signal is reflected to the surface and is detected by a receiving antenna. Part of the wave energy also continues to travel downward, and may be reflected back by deeper reflectors. The digital control unit of the GPR systems records the reflections as two-way travel times (usually in nanoseconds). The data are processed and plotted as two-way vertical travel time (y-axis) versus horizontal distance (x-axis) profiles (Fig. 11.9).

The electrical conductivity of a material influences penetration depth. Low-conductivity materials, such as unsaturated and coarse-grained sediments and solid rock, cause little signal attenuation and have relatively great penetration depths. Saturated sediments, on the contrary, have relatively high electrical conductivities and permittivities. The water table may thus be a strong GPR reflector due to the difference in electrical properties. The principal limitation of GPR for aquifer characterization is its shallow depth of investigation in saturated sediments, typically 10–30 m or less. Hence, GPR is not an applicable method for most groundwater investigations. As is the case with surface geophysics in general, GPR investigations should start with a careful evaluation of site conditions to determine if the targets are discernible and within the depth of investigation (USACOE 1995).

The great advantage of GPR is that it can be performed rapidly, is relatively inexpensive to run, has high vertical and horizontal resolution, and usually close to

real-time initial interpretation. In shallow aquifers, GPR can be used to map the depth to bedrock, depth to the water table, and the thickness of soil. It can be used to map buried channels, if there is a significant difference in resistivity between channel and adjoining sediments or rock (Fig. 11.9). Inasmuch as the dielectric permittivity of unsaturated sediment is a function moisture, GPR is also used to measure soil moisture (e.g., Huisman et al. 2003; Lunt et al. 2005). GPR has the advantages of being a noninvasive method that can cost-effectively provide a greater spatial density of soil moisture measurements than is practically possible using conventional point measurement methods (e.g., gravimetric, neutron probe, and time-domain reflectometry techniques).

11.9   Surface Nuclear Magnetic Resonance

Surface nuclear magnetic resonance (SNMR) methods, which are also referred to as magnetic resonance soundings (MRS), are based on the same principles as borehole NMR (Sect. 10.11). There is growing interest in SNMR because it is the only method that can directly detect freshwater in the subsurface and it provides information on pore-size distribution, which can be used to estimate hydraulic conductivity. MRS theory is discussed by Schirov et al. (1991); Goldman et al. (1994), Sushakov (1996), Yaramanci (2000); Legchenko et al. (2002, 2004), Roy and Lubczynski (2003), Yaramanci and Müller-Petke (2009), and Knight et al. (2012). MRS has already passed the experimental stage and is evolving into a useful tool for applied hydrogeophysics (Yaramanci and Müller-Petke 2009).

The basic concept of MRS is that a current loop at land surface is used to generate an excitation pulse that causes hydrogen protons to precess around the local magnetic field of the Earth. The depth of investigation is a function of the excitation intensity (q), which is the product of the current intensity (I_o) and duration (s):

$$q = I_o s \qquad (11:8)$$

The units of q are ampere-milliseconds. The data recorded for each excitation pulse are the dead time delay, initial amplitude (E_o), relaxation or decay time (T), and phase.

Pore wall interaction is the key relaxation process, which is correlated with pore size. Precessing protons will interact with a pore wall more rapidly in sediments or rock with small pores. The relaxation times that are used in SNMR analyses are the observed longitudinal relaxation time $\left(T_1^*\right)$ and transverse relaxation time $\left(T_2^*\right)$. SNMR data are interpreted using inversion techniques. One equation used to estimate transmissivity from SMMR data is (Legchenko et al. 2002; Vouillamoz et al. 2007a; Boucher et al. 2009)

$$T_{SNMR} = C_{p/SNMR}\left(T_1^*\right)^2 z \qquad\qquad (11.9)$$

where,

T_{SNMR} transmissivity (m^2/s)
C_p parametric factor (m/s/ms^2)
T_1^* observed longitudinal relaxation time (ms)
z saturated thickness of aquifer (m)
$/_{SNMR}$ water content estimated from SNMR (dimensionless, m^3/m^3)

SNMR inversion solutions are not unique, so it is critical to have field data for calibration (Legchenko et al. 2002; Roy and Lubczynski 2003; Boucher et al. 2009). It is not possible for a particular layer to determine from SNMR data alone both the layer thickness and water content (Legchenko et al. 2004). There is an equivalence in the $/_{SNMR}\cdot z$ term in Eq. 11.9 in that, for example, a saturated layer 10 m thick with a 10 % saturated porosity cannot be accurately differentiated from a saturated layer 5 m thick with a 20 % saturated porosity (Vouillamoz et al. 2007b).

Accurate interpretation of SNMR data requires some data on aquifer transmissivity in the study area in order to obtain the value of C_p. SNMR data has a large volume of investigation, so the data represents a volumetric average value rather than a point measurement. In dual-porosity systems, the data will tend to represent the bulk matrix porosity (which contains most of the water) rather than volumetrically minor secondary porosity, which may provide most of the hydraulic conductivity.

Both the amplitude and phase of the SNMR signal are affected by electrical conductivity. SNMR data cannot be accurately interpreted in isolation. SNMR and electrical or electromagnetic (resistivity) methods should always be performed together, especially at sites where no existing information on local hydrogeology is available (Yaramanci 2000). Performance of both MRS and TDEM at each station allows for a combined interpretation that may be more accurate than the separate results from each method alone (Goldman et al. 1994; Goldman and Neubauer 1994; Yaramanci 2000; Legchenko et al. 2004). SNMR and TDEM have been proven to be effective in detecting the presence and amount of groundwater and evaluating its salinity (Goldman et al. 1994). The same transmitter loop could be used for both methods, reducing the survey time as laying out the transmitter loop is the most time consuming operation in both methods (Goldman and Neubauer 1994).

SNMR signals are susceptible to distortion by ambient electromagnetic noise of different origins, such as nearby power lines and lightening, and the presence of geological conductors (certain rock types, coatings on grains). SNMR may have an insufficient depth of investigation where shallow electrically conductive (e.g., clayey) layers screen a deeper aquifer (Roy and Lubczynski 2003; Vouillamoz et al. 2007a).

SNMR is a promising, noninvasive method for obtaining a large data set of transmissivity and specific yields for shallow aquifers, which can aid in aquifer model parameterization (Boucher et al. 2009). SNMR may provide specific yield and transmissivity data in remote areas where pumping and observation wells needed for a suitable aquifer pumping test are rare. Intensive research is still needed to determine all the parameters that influence the SNMR measured decay times and to develop techniques to improve the signal-to-noise ratio (Yaramanci and Müller-Petke 2009).

The results of some earlier published studies demonstrated the value of SNMR as a screening tool, in combination with other surface geophysical methods, for identifying areas that are more likely to have higher transmissivities and greater well yields (e.g., Vouillamoz et al. 2007a, 2008; Shah et al. 2007; Boucher et al. 2009). The key issue is whether the SNMR surveys will save money, which depends upon the costs of the surveys and well construction, and the improvement in the well success rate (Vouillamoz et al. 2007a). SNMR would be expected to give more accurate results in nonconsolidated sediments because their free water content is high enough to achieve an acceptable signal-to-noise ratio (Vouillamoz et al. 2007b). The maximum current depth for aquifer characterization is about 100 m. Single layer aquifers are more favorable for SNMR because of a loss of resolution with depth in multilayered aquifers and the non-uniqueness of geophysical interpretations (Vouillamoz et al. 2007b). SNMR also has applications for detecting water-filled cavities in karst systems (Chalikakis et al. 2011). Given the current interest in this geophysical method in government, academic, and private sectors, the SNMR method has great potential to significantly advance the way we evaluate and manage groundwater aquifers (Knight et al. 2012).

11.10   Magnetotellurics

Magnetotelluric methods are a passive means for obtaining information on the conductivity of subsurface strata by measuring naturally occurring, time-varying electric and magnetic fields at the Earth's surface. Lightning strikes and the interaction of the solar wind and the ionosphere generate natural electromagnetic fields in the Earth's atmosphere, which induce electric currents in the subsurface whose flow can be detected at land surface. Magnetotelluric methods were reviewed by Simspon and Bahr (2005) and Berdichevsky and Dmitriev (2008).

At each sampling location, measurements are typically made over a range of frequencies (typically from 10^{-3} Hz–100 kHz) of the Earth's magnetic field in two horizontal and the vertical directions, and the electric field is measured in two horizontal directions. Phase differences between the electric and magnetic components are also recorded. The data are processed using inversion methods to determine variations in the resistivity of subsurface strata. The Earth's electromagnetic

field has skin effects, which result in higher frequency ranges providing information on shallow depths, and lower frequency ranges providing information from greater depths.

The controlled source audio-frequency magnetotelluric (CSAMT) method involves transmitting a controlled signal over a suite of frequencies into the ground from a transmitter site at one location, and measuring the electric and magnetic fields at receiver sites in the area of interest. The CSAMT method was discussed in detail by Zonge and Hughes (1991). The CSAMT method was developed to improve the low signal strength to noise ratio problem of the magnetotelluric method.

Magnetotelluric methods are used obtain information on deep structure and stratigraphy, and may also differentiate between aquifers containing fresh and saline waters. They have the advantages of being a relatively rapid, cost-effective means to investigate a large area and having a greater depth of investigation (up to about 1,000 m; 3,000 ft) compared to electrical resistivity methods. The main limitations of magnetotelluric techniques are the potential for interference from buried conductors, non-uniqueness of data processing, and modest resolution. Magnetotelluric methods have the greatest value as an initial reconnaissance tool in frontier areas where there are limited geological and hydrogeological data. For example, CSMAT was used by Lluria (1990) to locate a fractured bedrock aquifer associated with a deep buried attachment fault in Arizona.

11.11   Seismic Reflection and Refraction

Seismic reflection and refraction techniques are used to obtain information on subsurface structure. Seismic reflection surveys are a fundamental data source in the oil and gas industry and are addressed in virtually all introductory geophysics textbooks. The most commonly used methods in groundwater investigations are based on the reflection or refraction of seismic compressional waves (p-waves), which are the fastest moving waves. The equipment consists of a source, one or more receivers called geophones (hydrophones in waterborne surveys), and seismographs, which are equipment that record the geophone signals.

Sound or seismic waves traveling through the earth may be reflected or refracted off the boundary between materials that have a different acoustic impedance, which is the product of the seismic wave velocity and density of the rock. Acoustic impedance changes often correspond to formation boundaries or the contact between major lithologic changes within a formation. The recorded data in the seismic reflection method is the two-way travel time for waves to reach reflectors and return to a receiver or multiple receivers at the surface. The depths to each reflector are calculated based on the known seismic velocities of the materials penetrated by the waves and the two-way travel time. The seismic velocities can be

obtained from sonic velocity logs run in a nearby borehole or calculated from known depths to reflectors in a nearby well.

Seismic refraction methods are similar to reflection methods in that they utilize a source and multiple receivers (geophones). Rather than being reflected from a surface or boundary, the seismic waves travel along the boundary before being refracted upwards or downwards. An important assumption of the refraction methods is that velocity of seismic waves increases with depth, otherwise waves would be refracted downwards rather than upwards towards the receivers. Hence, if there is a velocity inversion situation, there will be blind zones and all depths estimated below the inversion become erroneous. Properly interpreted, the refraction data provide estimates of the thickness and depth of geologic layers (including the water table).

Seismic reflection has a greater depth of penetration and better lateral resolution than the refraction method, but data processing is more complex than for seismic refraction and, as a result, the method is more expensive to run. Seismic reflection is well suited for marine settings (e.g., oceans, lakes, rivers, canals) where the inability of water to transmit shear waves makes collection of high-quality reflection data possible even at very shallow depths. Marine surveys are also less expensive because continuous surveys can be performed by towing the equipment using a boat, but have that limitation that suitable surface water bodies are often not located at the sites of hydrogeological investigations.

The effort involved in performing seismic reflection surveys greatly varies. The methods used to generate the sound waves include boomers, electrical discharge (sparkers), air guns, water guns, and, for land-based operations, explosive charges and seismic vibration trucks. In simple shallow surveys, only several receivers are used, whereas, hundreds or thousands of receivers may be employed in three-dimensional seismic surveys conducted for the oil and gas industry. The recorded data require substantial signal and image processing before it can be interpreted.

Although seismic reflection and refraction surveys can provide high-quality information on subsurface geology, they are not a routine tool in groundwater investigations. The high costs of seismic surveys restrict their employment to projects where there is a specific need for information on subsurface geological structure. Seismic surveys may provide information on the geology of shallow aquifers including the location of the aquifer-bedrock contact and other structural features that may impact groundwater flow. Seismic surveys may also be of value in investigations where data are required on the continuity of aquifer or confining strata.

Marine seismic reflection surveys have been run by the U.S. Geological Survey (USGS) in South Florida, for example, to map shallow aquifers (e.g., Missimer and Gardner 1976; Cunningham et al. 2001; Kindinger 2003). The surveys in southwestern Florida detected pronounced subsurface folding for which there is no suggestion at the essentially flat-flying land surface (Fig. 11.10). The USGS performed seismic reflection surveys in lakes in the central and northeastern part of
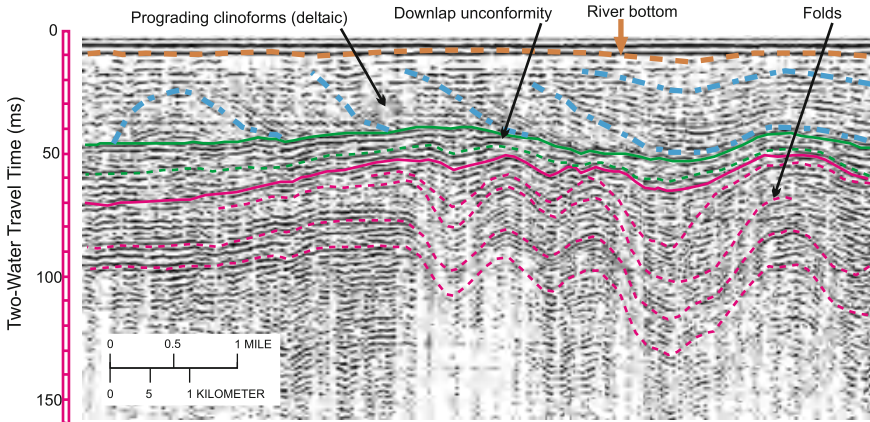
Fig. 11.10 Segment of a seismic reflection profile run on the Caloosahatchee River in southwestern Florida, USA). The profile reveals subsurface depositional and structural features (e.g., prograding clinoforms, folds) for which there is no suggestion at land surface (from Cunningham et al. 2001)

Florida to identify zones of buried karstic collapse (e.g., Kindinger et al. 1994, 2000; Spechler 2001), which are suspected as possibly resulting in enhanced vertical flow to the underlying aquifer. The USGS survey also performed marine seismic reflection survey in Biscayne Bay, off of Miami-Dade County, Florida, in which faults and suspected karstic collapse structures where identified that intersect a confining zone important for on-shore deep injection well systems (Fig. 11.11; Cunningham et al. 2012; Cunningham 2015). However, seismic surveys can identify subsurface structures, but do not provide information on whether or not identified features are hydraulically active. For example, the faults identified in the Cunningham et al. (2012) and Cunningham (2015) study could be either vertical flow conduits or could be impermeable features that have no impact on vertical groundwater flow.

There have been a number of studies in which seismic reflection surveys were used to map the boundary between unconfined aquifer strata and underlying bedrock or a clay aquitard, and thus the thickness of aquifer strata, and structures within an aquifer (e.g., Hunter et al. 1984; Haeni 1986; Miller et al. 1989; Cardimona et al. 1998). Information of the depth to bedrock may also be obtained using DC resistivity and EM methods. The question arises as to which method (or combination of methods) can most cost-effectively provide the required information.

Seismic refraction surveys have been used to determine the depth of shallow fracturing and weathering in Paleozoic siliciclastic bedrock aquifers (Gburek et al. 1999). The refraction surveys showed that the aquifer could be characterized by four distinct layers (overburden, highly fractured, moderately fractured, and poorly fractured) with a downward increase in seismic velocity. Core observations and
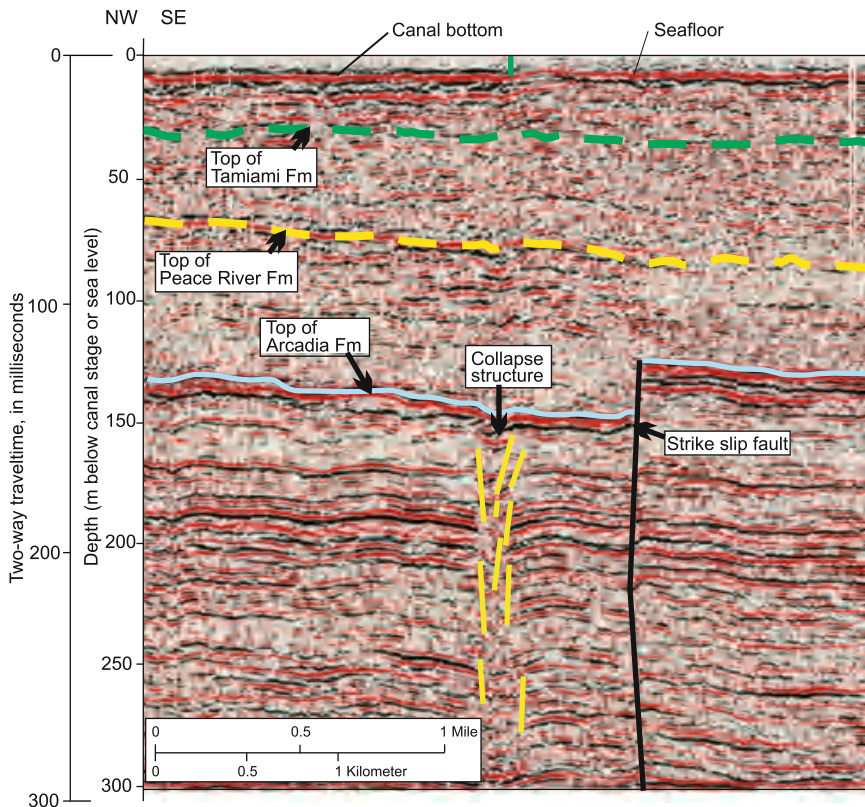
Fig. 11.11 Seismic reflection profile from Miami-Dade County, Florida, USA, showing a near-vertical strike-slip fault and a narrow karst-collapse structure west of the fault (modified from Cunningham 2015)

packer testing results demonstrate that the increase in seismic velocity corresponds to a decrease in the extent of fracturing and, in turn, a decrease in hydraulic conductivity and effective porosity.

11.12 Gravity

11.12.1 Introduction

In accordance with Newton's second law, the gravitational acceleration (g) at a point on the surface of the Earth is a function of the underlying mass of the earth and radius of the earth

$$g = G\frac{m}{r^2} \tag{11:10}$$

where

G gravitational constant (6.673×10^{-11} N m^2 kg^{-2}; m^3 kg^{-1} s^{-2})
m mass of the earth (kg)
r radius of the earth (m)

The SI unit for gravitational acceleration is the Gal, which is equal to 1 cm/s^2. The milligal (mG) is equal to 1×10^{-3} Gal and the microgal (lG) is equal to 1×10^{-6} Gal. Changes in the mass of water underlying a survey point will result in a change in the gravitation acceleration at the point, which, depending upon the magnitude of the change, may be detectable with a sensitive gravimeter. Microgravity surveys are used in groundwater investigations is as a monitoring tool for the mass of water in unconfined aquifers and in the unsaturated zone. Changes in water levels in unconfined aquifers caused by pumping or recharge (natural or artificial) are the result of a change in the total volume, and thus mass, of water in storage. Changes in water levels in wells completed in confined aquifer are due mainly to changes in pressure and there is thus not a corresponding change in the mass of water. Microgravity surveys are also used to identify karst features and for geological (bedrock/basement) mapping.

Gravitational methods are discussed in most geophysics textbooks (e.g., Telford et al. 1990; Milson 2003; Burger et al. 2006). The measured (observed) gravitational accelerations (g_{obs}) are affected by several factors or processes, which require corrections including

- Latitudinal variation (g_n). Gravitational acceleration is greater near the equator than at the poles and a correction needs to be applied for the station latitude.
- Free air correction (FA_{cor}). A decrease in gravitational acceleration occurs with increasing altitude (i.e., distance from the center of the earth). The altitude of the stations must therefore be accurately measured using GPS or other techniques.
- Bouguer correction (B_{cor}). An excess of material between sea level and the station, which results in an increase in gravitational acceleration.
- Terrain correction (T_{cor}). Nearby variations in altitudes above and below the station altitude can effect measured gravitation acceleration.

Gravitational acceleration data are often expressed in terms of Bouguer anomaly (Dg_b) defined as:

$$Dg_b = g_{obs} - g_n + FA_{cor} - B_{cor} \tag{11:11}$$

Gravitational acceleration measurements are also effected by instrument drift and Earth tides, for which corrections must be applied. Earth tides are an elastic deformation of the Earth caused by the gravitational fields of Sun and Moon. The normal procedure is to establish one or more base stations at which measurements

are periodically made during a gravitational survey. Earth tidal effects can be corrected by frequent measurement of the base station or determined using widely available computer programs.

Relative gravity surveys are typically performed for groundwater investigations, in which readings record the gravity difference between two points, one which is normally a base station. The base station is typically located in a stable area not affected by aquifer water level changes (e.g., bedrock area adjacent to the groundwater basin). Microgravity surveys in groundwater investigations can also be performed relative to absolute gravity by establishing absolute gravity base stations (e.g., Jacob et al. 2010; Koth and Long 2012). Gravimeters used for absolute gravity measurements are less portable and the measurements are more involved than relative gravity measurements. Absolute gravity measurements are rarely performed for groundwater investigations.

11.12.2   Relative Gravity Surveys

The primary use of microgravity surveys in groundwater investigations is to determine changes in the mass of water at a survey point, which are evaluated through changes in gravitational acceleration rather than the actual values of gravitational acceleration. Changes in aquifer water storage are evaluated through time series of relative gravity measurements performed at the same points. Performing time series of measurements at the same locations eliminate the need for some corrections, such as for terrain and latitude, provided that there are no regional changes in non-aquifer mass or altitude. If a microgravimeter is placed at the same position for each measurement at a location, then any site effects should cancel out. Relative gravity data still need to be corrected for instrument drift, Earth tides, and environmental effects (Davis et al. 2008). The monitoring stations should be marked so that subsequent readings can be performed at the exact same spot. Concrete pads are the preferred option (e.g., Pool and Schmidt 1997). Davis et al. (2005, 2008) used metal spikes to mark sites, which have the advantage of being locatable using a metal detector if they became covered.

Pool and Schmidt (1997) documented procedures used for a relative gravity survey employed in a groundwater investigation in the Tucson, Arizona area, which are generally applicable to surveys performed to evaluate change in stored water mass. Differences in gravity were measured relative to a base station located in a bedrock area that is far enough away from the study area so as to not be impacted by changes in the mass of water in the aquifer. Instrument drift was evaluated by performing closed-loop gravitation surveys that started and ended at the bedrock base station. Linear drifts between the initial and final readings at the base station can be readily corrected. Nonlinear survey drifts caused by inaccurate approximations of Earth tides, changes in the temperature of the instrument housing, atmospheric effects, and jarring of the instrument are more difficult to correct. Pool

and Schmidt (1997) used algorithms to correct for Earth tides and conducted surveys at times corresponding to linear portions of the Earth tide curves whenever possible.

Changes in gravitational acceleration (Dg) associated with changes in the density of an unconfined aquifer strata, such as caused by dewatering, can be calculated using the Bouguer slab equation as follows:

$$Dg = 0.04193hDq \qquad (11.12)$$

where,

Dg   change in acceleration in mGal
h   thickness of buried slab (i.e., aquifer that was dewatered) (m)
Dq   density change (g/cm^3)

The density change is the product of the specific yield (S_y) and density of water (≈ 1 g/cm^3)

$$Dq = S_y q_w \qquad (11.13)$$

The magnitude of the change in the measured gravitational acceleration depends only on the change in density and thickness, but not on burial depth (Turcotte and Schubert 1982). Gravitational surveys provide data on changes in the mass of water, which have to be corrected for water density and porosity (storage coefficient) to estimate corresponding changes in aquifer water level (and moisture content within the vadose zone). The change in gravitational acceleration (l Gals) can be expressed as a function of specific yield (S_y) and the interval of water table fluctuation (b) by the equations (Pool and Eychaner 1995: Pool 2008)

$$Dg = 41.9 S_y b(m) \qquad (11.14)$$

$$Dg = 12.77 S_y b(ft) \qquad (11.15)$$

where,

b(m)   interval of water table fluctuation in meters
b(ft)   interval of water table fluctuation in feet

Equations 11.14 and 11.15 are based on the assumption of a planar water table. Three-dimensional inverse modeling can be used to assess aquifer properties and changes in groundwater storage between two gravity surveys. For example, Gehman et al. (2009) utilized a modeling procedure that started with a planar assumption and progressively added topographic complexity until the model calibration met specific criterion (target root mean square error). Koth and Long (2012) reported that changes in groundwater storage could be quantified with an accuracy of about ±0.5 ft (0.15 m) of water per unit area of aquifer.

The basic limitation of microgravity measurements is that they provide information only on total mass change and not where the change occurs. Complex relations between aquifer water levels and gravity may occur in areas with multiple compressible aquifers. Gravity change at land surface may result from aquifer compaction and changes in the amount of water stored in pore spaces. Changes in water storage may occur in the vadose zone, a perched aquifer, or the phreatic zone (or a combination thereof). Although conceptually simple, microgravity measurements require meticulous field procedures and accurate corrections for extraneous factors in order to obtain accurate data on changes in water storage. Microgravity measurements are point measurement and require remobilization to a site for each measurement. Microgravity surveys are thus typically performed to evaluate long-term changes in water storage.

11.12.3 Applications of Microgravity Surveys to Groundwater Investigations

Microgravity data has particular value for measurement of natural and managed aquifer recharge in unconfined aquifers. It has been used to increase the density of monitored points as a less expensive alternative to the installation of additional monitoring wells. Microgravity-determined water levels are less accurate than standard well measurements and continuous monitoring is not practical. Microgravity monitoring data augments, but does not replace, water level data from monitoring wells. Microgravity also can be used to measure changes in the mass of the water in the unsaturated zone. A combination of data on changes in the mass of water and aquifer water levels (obtained from monitoring wells at microgravity monitoring locations) has been used to determine the specific yield of aquifers.

Microgravity data were used by Pool and Schmidt (1997) for quantification of the increase in the volume of water in storage due to recharge, and subsequent decreases caused by groundwater withdrawals, at an artificial recharge project at Rillito Creek, Arizona (Fig. 11.12). A good correlation occurred between water level and gravity data in wells located in the recharge area. Moderate to poor correlation occurred elsewhere, which Pool and Schmidt (1997) interpreted as being caused by storage changes in perched aquifers and the unsaturated zone. Microgravity data were also used to map the mounding of the water table at the Lancaster, California, ASR site (Howle et al. 2002).

High-precision relative microgravity surveys were conducted before, during, and after infiltration in order to track groundwater movement, in lieu of installing more expensive multiple groundwater monitoring wells, at the Weber River Basin Aquifer Storage and Recovery Pilot Project in Utah (Chapman et al. 2008). The microgravity survey detected changes in the mass of infiltrated water including the development of a perched aquifer above a clay layer. The Weber River ASR study results indicate the microgravity time series and water level monitoring data are
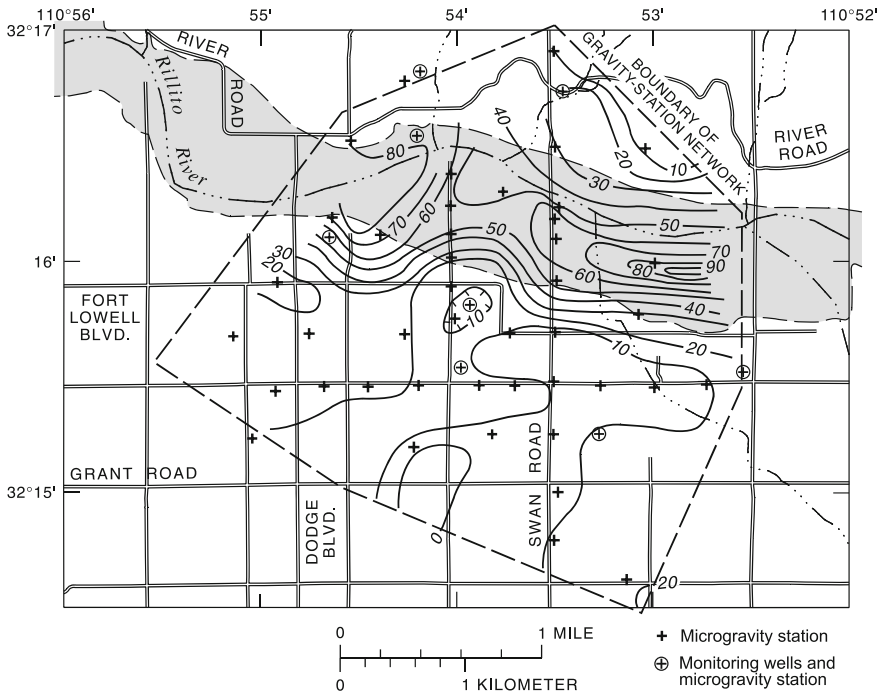
Fig. 11.12 Change in microgravity (uGals) as a result of aquifer recharge in the vicinity of an ephemeral river channel (Rillito Creek, Arizona) between early December 1992 to early March 1993 (from Pool and Schmidt 1997)

complimentary to each other and that microgravity surveys are not a substitute for a groundwater monitoring wells (Chapman et al. 2008).

Microgravity was successfully used to map the location of stored water at the City of Arvada ASR project in Colorado (Davis et al. 2005, 2008), which stores water in an abandoned underground coal mine (Leyden Mine). Rubble zones from collapsed shafts and any remaining open mine shafts provide water storage. Time-lapse microgravity measurements were successfully used to identify the locations of water-filled rubble zones (Davis et al. 2005, 2008).

Microgravity surveys were used to map seasonal changes in water storage in karst aquifers, which were found to be heterogeneous with respect to water storage (Jacob et al. 2010; Koth and Long 2012). In the Durzan karst basin of the French Massif Central, the greatest seasonal changes in gravity were found to occur in topographically low areas with thick accumulations of sediment that have high water retention capacities (Jacob et al. 2010).

11.12.4 Gravity Recovery and Climate Experiment (GRACE)

The Gravity Recovery and Climate Experiment (GRACE) space mission was launched to study processes involving changes in the Earth's mass distribution. The remarkably successful GRACE mission demonstrated the utility of satellite gravity measurements for measuring basin-wide changes in water storage (Wahr et al. 2004). There has been a plethora of studies that utilize GRACE data to document changes in regional water supplies. The GRACE mission was launched by NASA on March 17, 2002, and consists of two identical satellites orbiting in the same plane and acting in unison (NASA 2003; Fig. 11.13). Global coverage is roughly every 30 days, so the data are locally available on roughly monthly time steps. The mission had a planned duration of 5 years, but was subsequently extended and is expected to continue until 2016, based on the actual mission status (Günter et al. 2007). The follow-up system 'GRACE-FO' (GRACE Follow On) is scheduled to launch in August 2017.

The basic principle behind the GRACE mission is that changes in the speed and distance between the twin satellites are induced by local changes in the gravitational field of the Earth. As the satellites pass over a gravity anomaly, the associated change in the speed of the lead satellite causes a change in the distance between the two satellites, which is measured using an extremely precise (within 10 | m) microwave ranging system. The distance between the satellites closes as the trailing satellite passes over the anomaly. Satellite global positioning systems (GPS) are used to determine the exact position of the satellites over the Earth to within a centimeter or less. The raw data require considerable processing to obtain changes in water total volume (e.g., Swenson and Wahr 2002) before the hydrologic parameters of interest, such as soil moisture, groundwater recharge, and evapotranspiration, can be determined.

Satellite gravity measurements have the clear limitation of a very coarse spatial resolution (Becker 2006) and are thus not suitable for local studies. The spatial

Fig. 11.13 Artist rendition of the GRACE system (from NASA Jet Propulsion Laboratory)
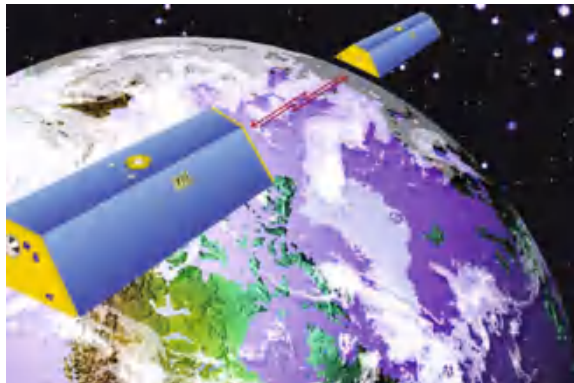
resolution for water mass variability was initially estimated to be 200,000 km^2 and could be closer to 500,000 km^2 (Rodell et al. 2007). GRACE FO is planned to have a finer spatial resolution. The GRACE data are processed to provide information on changes in terrestrial water storage (DTWS). Changes in TWS (DTWS) are equivalent to the change in soil moisture (DSM) and groundwater storage (DGWS),

$$DTWS = DSM + DGWS \qquad (11:16)$$

A main application of GRACE to groundwater investigations is to map changes in groundwater storage, which requires data on changes in soil moisture that are obtained by other means. Rodell et al. (2009), for example, evaluated changes in soil–water storage using data from another satellite-based program, the Global Data Assimilation Systems (GLDAS). Other factors that can contribute to DTWS are changes in surface water, ice and snow, and biomass (Strassberg et al. 2009). The accuracy of calculations of DGWS depends on the accuracy of the measurement of DSM and other changes in the TWS. The change in DGWS may be small relative to the change in DSM (e.g., Rodell et al. 2007). Areas with conditions favorable for deriving groundwater storage changes from GRACE data may be those where the DGWS changes are large in absolute terms and also relative to variation in other storage components (Günter et al. 2007).

An rapidly increasing number of papers have been published using GRACE data to quantify groundwater storage changes, including studies on the High Plains Aquifer of the United States Great Plains (Strassberg et al. 2007, 2009), northern India (Tiwari et al. 2009; Rodell et al. 2009; Fig. 11.14), the Salado Basin of Argentina
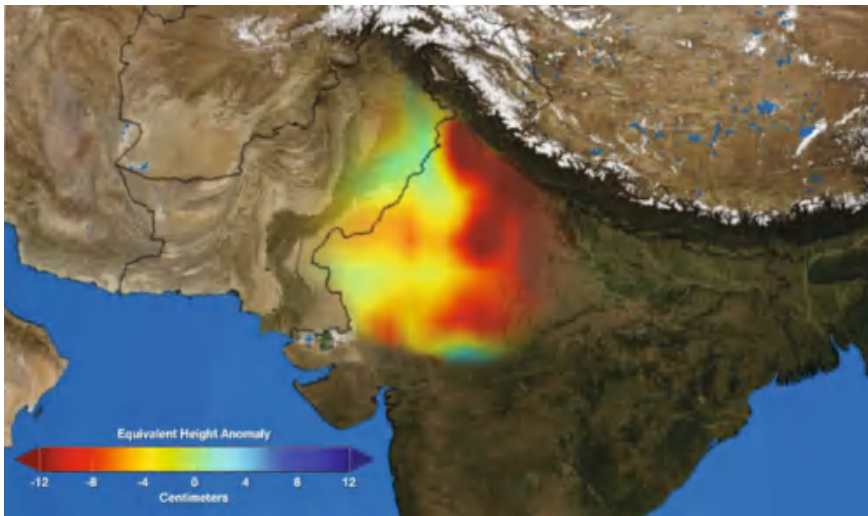
Fig. 11.14   GRACE groundwater depletion map for northern India between November 2002 and November 2008. Changes in groundwater mass are expressed as equivalent height anomalies in centimeters (from NASA Goddard Space Flight Center)
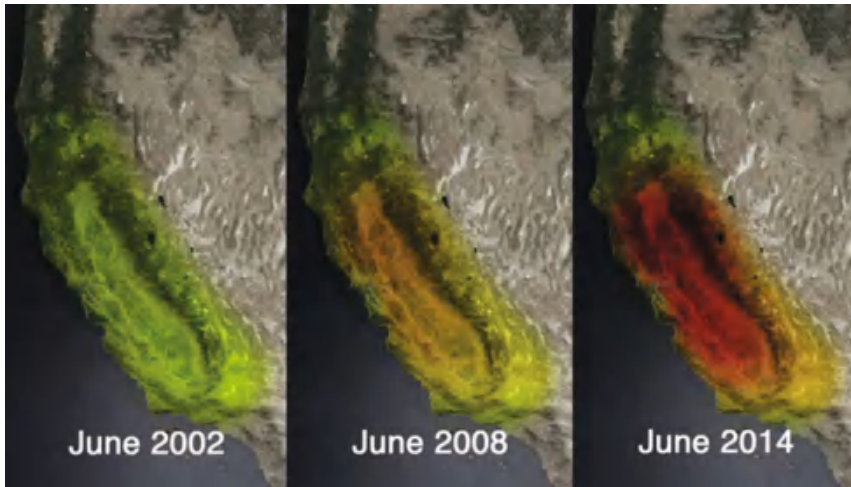
Fig. 11.15   GRACE images of declining water storage in California in June 2002 (left), June 2008 (center) and June 2014 (right). Colors progressing from green to orange to red represent greater accumulated water loss between April 2002 and June 2014 (from NASA/JPL-Caltech/University of California, Irvine)

(Cesanelli and Guarracino 2011), Europe (Anderson et al. 2005), Australia (García-García et al. 2011), North China (Feng et al. 2013), and the Central Valley of California (Famiglietti et al. 2011; Scanlon et al. 2012; Fig. 11.15). Global rates of nonrenewable groundwater depletion were reviewed by Richey et al. (2015). These studies have received considerable mass-media attention as they vividly illustrate aquifer depletion.

Satellite-based gravity data, such as from the GRACE mission, will play an expanding role in water resources evaluation and management on a global basis. Future gravity satellite missions are expected to offer greater spatial resolution and more precise determination of water storage changes (Günter et al. 2007). However, satellite-based data will have a much more limited role for local-scale water resource evaluation because of their low spatial resolution and relevance to mainly unconfined aquifers. Gravity-based estimates of groundwater storage may have great value in data-poor regions of the world (i.e., large parts of developing areas) and in regions were data are not centralized or are unobtainable due to political boundaries (Rodell et al. 2007). The greatest value is obtained from surface geophysical techniques when they are used in conjunction with well data. GRACE and GRACE-FO can provide low-resolution data on large-scale water storage trends, which is needed for evaluation of water budgets. Local data on aquifer water levels from wells will be still be needed for local groundwater management.

11.13   Airborne Geophysics

Airborne geophysical methods allow for the efficient coverage of large geographic areas and can be performed in areas poorly accessible to ground travel. Both ground and airborne geophysical methods have the advantage of allowing for a high density of measurements and greater areal coverage than is practicably possible using borehole-based techniques. Very large areas can be covered in a short time at a lower cost compared to ground-based investigations, but at the expense of lesser lateral and vertical resolution and greater uncertainty. There is an economy of scale associated with airborne geophysics in terms of costs per unit area. There is a minimum survey area below which it is not economically reasonable (Viezzoli et al. 2012).

As is the case for surface geophysical methods in general, there needs to be contrasts in the properties of the subsurface strata that can be measured by the geophysical method. Measured differences in subsurface properties should also be interpretable in terms of obtaining the desired data For resistivity (conductivity) based methods, the measured differences in resistivity may be due to porosity, mineralogy, and/or formation water salinity. Forward modeling is recommended to make a proper method selection (Abraham et al. 2012). Airborne geophysical data, as is the case for surface geophysical techniques in general, are processed using inversion techniques, which do not provide unique solutions. An important issue with interpretations of surface and airborne geophysical data obtained using inversion methods is that the uncertainty inherent in the interpretations is often not reflected in the output.

Airborne electromagnetic (AEM) methods are the most widely used techniques for groundwater investigations because they provide data on resistivity, which in some circumstances is related to groundwater salinity and presence of clean (clay free) sands and gravels that may serve as aquifers. AEM data are collected and processed to obtain maps of formation resistivity at different depth levels and resistivity versus depth profiles. Other airborne geophysical methods, such as magnetic, radiometric, and gravity surveys have much more limited applications to groundwater investigations. Airborne magnetics are used in mining investigations to locate mineral deposits and may provide some information of basin geometry, such as the location and depth of crystalline bedrock.

11.13.1   Airborne Electromagnetic Methods

AEM methods can provide data on the salinity and lithology. Some specific uses of AEM are (Paterson and Bosschart 1987; Paine and Minty 2005; Viezzoli et al. 2012)

- mapping of groundwater contamination with saline water (e.g., from a tsunami)
- mapping of saline-water intrusion in coastal aquifers

- location of freshwater areas amidst poorer quality water that could be potential potable water sources
- mapping inland salinization (mobilization of salts by rising groundwater levels)
- mapping of hydrogeological units (aquifers and confining units), including karstic conduits.

Where local groundwater is fresh, changes in resistivity may be related to porosity and clay mineral concentration. Clean sands and gravels may have greater resistivities than adjoining clay-rich confining strata. Sand and gravel aquifers may be either more or less resistive than the underlying bedrock depending upon the bedrock lithology.

AEM surveys are performed using either FEM or TDEM. FEM methods are commonly used because of they are rapid, less expensive, and have a higher spatial resolution and stronger response or discrimination capability within shallow strata (Steur et al. 2009; Oldenborger et al. 2010, 2013; Abraham et al. 2012). The depth of resolution of airborne FEM methods is about 80 m. FEM is thus more suitable for shallow investigations. FEM is particularly appropriate where an electrically resistive target overlies an electrically conductive lithology, which, for example, often occurs at the water table.

Time-domain electromagnetic methods (TDEM, TEM) have the advantage of higher power and increased depth of penetration and vertical resolution, but are more expensive. Deep targets with more conductive lithologies are best mapped with TDEM (Abraham et al. 2012; Viezzoli et al. 2012). Several studies compared the results of airborne and ground-based surface geophysical methods. Helicopter-based FEM and TDEM and land-based TDEM and DC resistivity were compared by Steur et al. (2009) at the Cuxhaven Valley in northern Germany. Sørensen and Auken (2004) documented the SkyTEM helicopter-borne TDEM system. Airborne EM systems, such as SkyTEM, continuously record raw data from soundings, laser altitude readings, GPS position, and instrument pitch and role.

AEM studies require sophisticated processing to obtain accurate results. AEM readings are very sensitive to anthropogenic interference, such as from power lines and metallic structures. They are thus unsuitable for developed (e.g., urban and suburban) areas. Accurate hydrogeological data from AEM surveys require (Viezzoli et al. 2013)

- good calibration of the data acquisition system
- monitoring of the system at all times during acquisition
- appropriate processing of the derived raw data
- accurate inversion of the electrical resistivity-depth model.

A key point concerning quality control is that (Viezzoli et al. 2012)

> quantitative results demanded from AEM for hydrogeological applications can only be achieved by means of good data quality, proper and transparent data processing, accurate full data inversion, and proper integration with ancillary information.

Processing inaccuracies or even just different approaches can lead to incorrect geophysical results, which can lead, in turn, to inaccurate and misleading interpretations (Viezzoli et al. 2013). Users of AEM data (e.g., hydrogeologists) are typically not experts in data acquisition and processing, but need to become aware of the different processing techniques and their consequences for interpretation (Viezzoli et al. 2013). As is the case for surface geophysical techniques in general, ground truthing using well data is critical for evaluating the accuracy of AEM data.

11.13.2   Mapping of Bottom and Top of Aquifers

The bottom of shallow aquifers is often the boundary with either high-resistivity bedrock or low-resistivity clay-rich strata. In both cases, a sufficient resistivity contrast may occur that is detectable by surface and airborne geophysical methods. AEM was used, for example, to map the base of aquifer in the North and South Platte and Lodgepole Creek valleys of western Nebraska (Abraham et al. 2012). The primary aquifers consist of Quaternary to Oligocene siliciclastic sediments with relatively high resistivities (40–500 ohm-m). The aquifers are underlain by silts and shales with resistivities in the range of 3–20 ohm-m. Frequency domain AEM using a helicopter platform was employed, which had a depth of investigation of approximately 80 m. Land-based TDEM soundings, which had a much greater depth of investigation (50–500 m), were also performed at 16 sites. Base of aquifer picks made by AEM were compared to the local stratigraphy and lithology known from test-hole lithological and borehole geophysical data. The thickness of aquifer material was calculated by subtracting the base of aquifer elevations from surface elevations obtained from a digital elevation model (DEM). A map of the saturated thickness of the aquifer was obtained by subtracting the base of aquifer elevations from the corresponding water table elevations (Abraham et al. 2012; Fig. 11.16).

AEM and magnetometer data were used to map the presence of groundwater resources in the San Pedro Valley of southern Arizona (Wynn 2002). The magnetometer data provided information on the depth to the crystalline basement and thus the potential storage capacity of basin sediments. AEM maps were used to identify more conductive groundwater-bearing sediments that are potential targets for groundwater development.

Airborne TDEM was applied in the Lower Rio Grande Valley (Cameron, Hidalgo and Willacy Counties) of southern Texas (Paine 2000) to assess groundwater resources, particularly depths to the water table and the quality of potential water sources. Sinuous features, suggesting the presence of channel or channel complex deposits, were found in the conductivity images. The sinuous features were less conductive than adjacent areas, which suggested that they are coarse deposits that contain relatively freshwater. The AEM data allowed for the identification of favorable targets for groundwater exploration by providing information on depths, lithology, and water quality of aquifers, but there is still considerable uncertainty concerning the actual values of hydrogeological properties of the target zones or aquifers.

11.13.3 Mapping Incised Pleistocene Valleys

An important and successful application of airborne electromagnetic (AEM) is the mapping of Pleistocene alluvial aquifers in Europe and North America. Valleys incised into older sediments and rock are filled with alluvial sediment, which serve as important local aquifers. The valley-fill deposits are commonly overlain by flat-lying glacial sediments, so that there is no surface manifestation of the aquifers. AEM (TDEM) is an appropriate method for the mapping of valley-fill aquifers because of their relatively shallow depths (up to several hundred meters) and common electrical resistivity contrasts between the alluvial sediments and adjoining sediments or rocks. The aquifers are commonly either relatively high-resistivity sands deposited in valleys that were incised into low-resistivity clays or moderate-resistivity sands deposited in valleys incised into high-resistivity bedrock or cleaner sands. Geophysical methods have been used to map the course, lateral extent, and internal structures of valley aquifers (Steur et al. 2009).

While AEM may reveal the presence of valley-fill aquifers, the best definition and characterization of aquifers is obtained when multiple data sources are used, including well data and other surface geophysical techniques (e.g., seismic reflection and gravity) (Gabriel et al. 2003; Steur et al. 2009). Identification of valleys is difficult with AEM alone where the valley-fill and adjacent sediments have similar electrical resistivities (Gabriel et al. 2003).

AEM is being implemented country-wide in Denmark for groundwater resources evaluation. Several studied have documented the detection of buried incised valleys using AEM. Auken et al. (2008) documented the use of helicopter TEM (SkyTEM) data to identify valleys incised in Paleogene clays in the Stjaer field area. SkyTEM was also used map buried valleys in Ringkøbing Fiord, Denmark (Kirkegaard et al. 2011) and an area of central Denmark (Høyer et al. 2015; Fig. 11.17). The valleys are overlain by glacial till with varying clay contents and glacial sands with mixed resistivity. Helicopter-borne TDEM was also successfully used to map valley-fill aquifers in the northern Germany (Gabriel et al. 2003) and the Spiritwood Valley of southern Manitoba, Canada (Oldenborger et al. 2010, 2013).

11.13.4 Groundwater Salinity Mapping

AEM is well suited to mapping changes in salinity, such as fresh-saline water interface, because salinity changes tend to correspond with large changes in resistivity. Smith et al. (2004) documented the use of fixed-wing aircraft TEM measurements near Nyborg, Denmark, to map the thickness of the freshwater
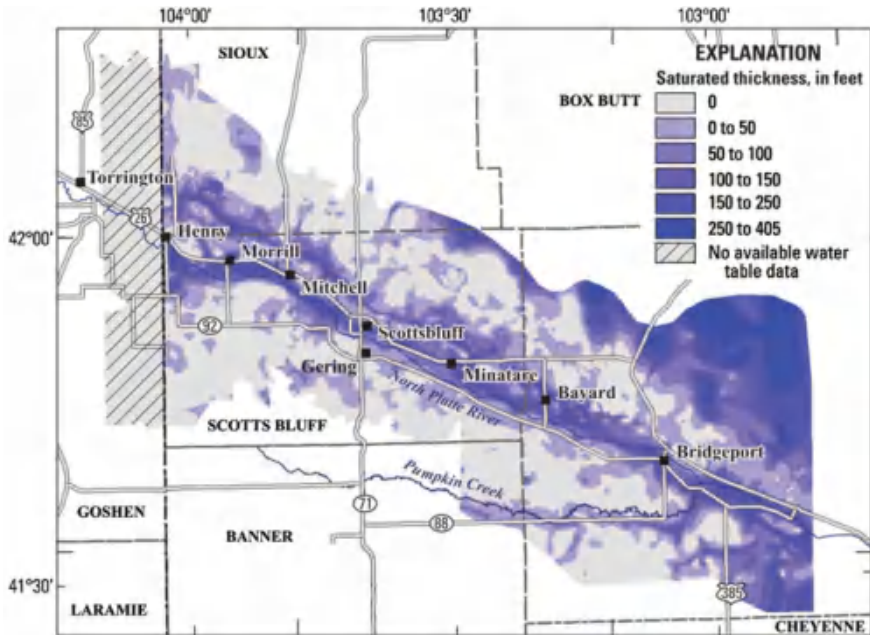
Fig. 11.16 Saturated thickness of the unconfined aquifer in the North Platte River valley of western Nebraska calculated from base of aquifer data obtained using AEM and ground-based TDEM soundings and water table elevation data (from Abraham et al. 2012)

aquifer above saline groundwater. The depth of the fresh-saline water interface agreed well with estimates from ground TEM soundings. The AEM could not resolve changes in resistivity close to land surface that were mapped with CVES.

Integrated ground conductivity, helicopter-borne FEM, ground-based TDEM, and borehole (induction logs and water quality) data were used to map areas of groundwater salinization near the Red River, Montague County, Texas (Paine 2003). The AEM data was used to map the lateral extent and intensity of salinization, and to guide TDEM sounding and borehole locations. The TDEM data was used to determine the tops and bottoms of the saline-water plumes. Borehole induction logs allowed for greater resolution of the vertical extent of salinization. Chloride concentration was estimated using site-specific empirical data on the relationship between chloride concentration and conductivity. Many of the high conductivity anomalies detected with the AEM coincide with known brine pits from oil drilling operations.

Helicopter electromagnetic (HEM) survey was successfully used to map saline-water intrusion in the Everglades National Park of South Florida (Fitterman and Deszcz-Pan 2001, 2002; Stewart et al. 2002). The Everglades National Park is
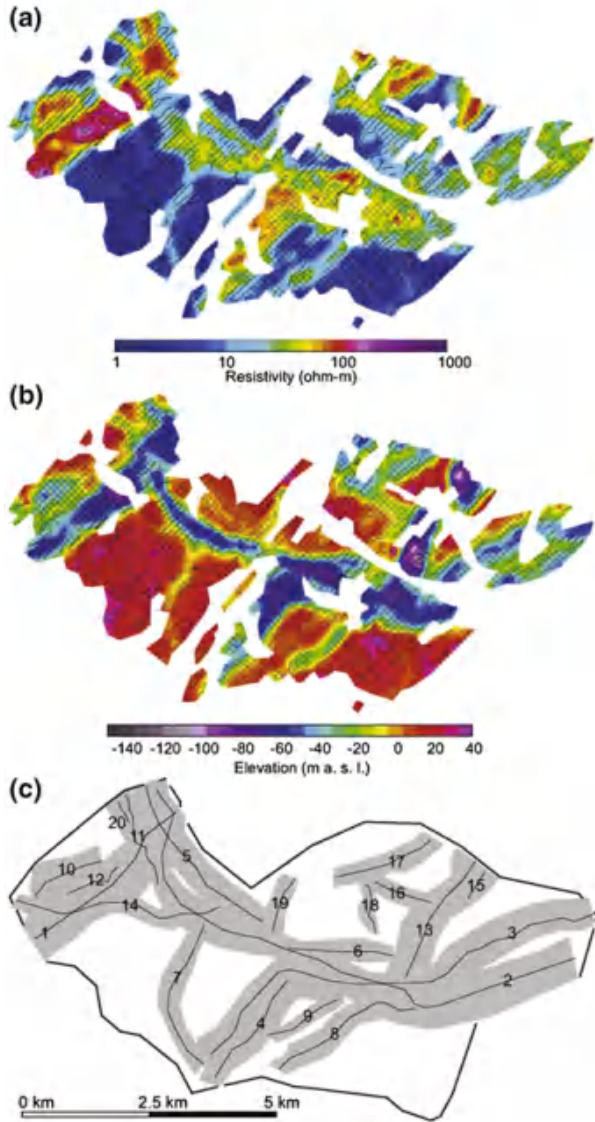
Fig. 11.17 SkyTEM interpretation of buried valleys from central Denmark. a Horizontal slice through the 3-D resistivity volume at an elevation of 5 m above sea level. b Depth to the top of the deepest conductive layer (Paleogene clay). c Map of interpreted buried valleys (gray) (from Høyer et al. 2015, copyright: Elsevier)

an ideal area for a helicopter electromagnetic (HEM) investigation of saline-water intrusion because the interface occurs at shallow depths, strata are flat-lying to subhorizontal and do not contain significant amounts of clay, and there is minimal
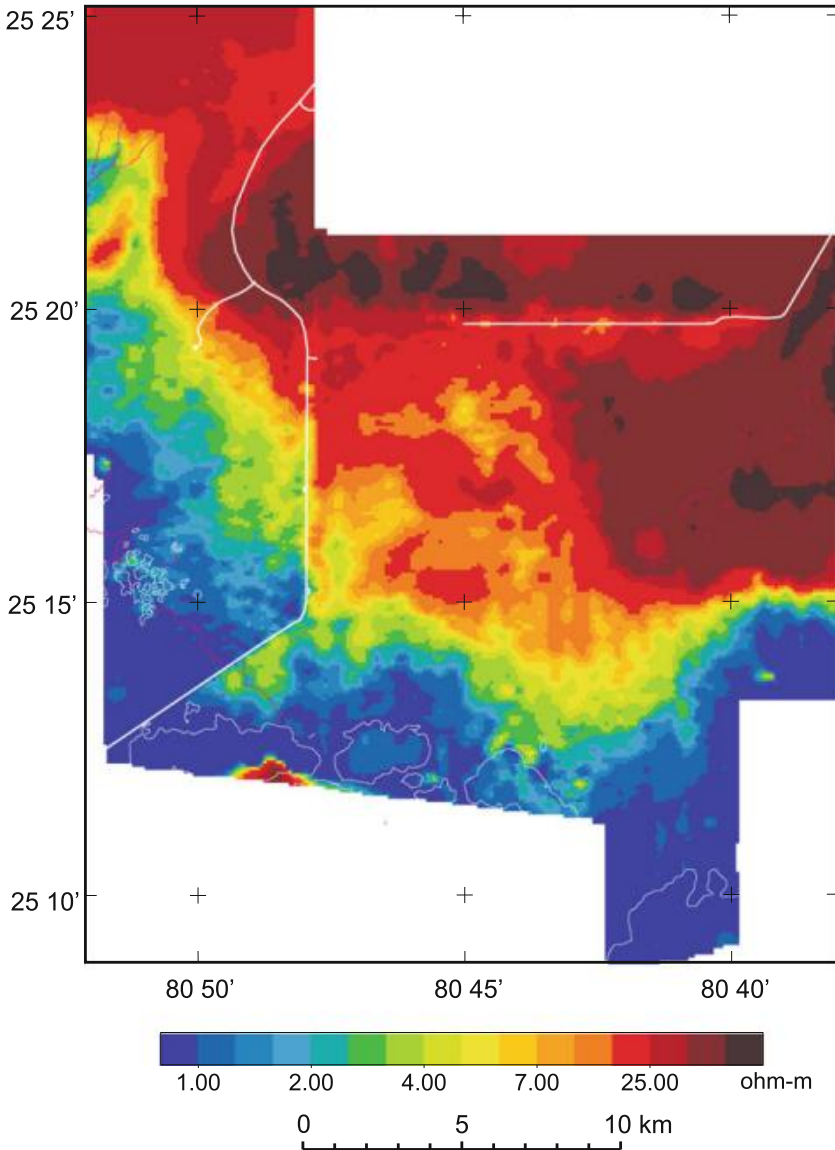
Fig. 11.18 HEM apparent resistivity map for approximately 5–10 m depth range in the Everglades National Park, Florida, which illustrates a southward increase in salinity towards Florida Bay (from Stewart et al. 2002)

anthropogenic interference (Fitterman and Deszcz-Pan 2001, 2002). The HEM survey results clearly distinguish variations in the resistivity, and thus salinity, in the water table aquifer (Fig. 11.18).

A combination of magnetometer and AEM surveys using a fixed-wing aircraft platform were performed in West Texas to detect oil and gas exploration and production wells and local groundwater salinization that was associated with the drilling and operation of the wells (Paine and Collins 2003). The magnetometer could detect isolated individual wells or clusters of closely spaced wells.

11.13.5 Managed Aquifer Recharge Screening

AEM data was used as screening tool to identify potential wellfield locations for the Broken Hill Managed Aquifer Recharge (MAR) Project, in western New South Wales, Australia (Lawrie et al. 2012; Brodie et al. 2013). Over 31,000 km of airborne TDEM data were collected at a line spacing of between 200 and 300 m. The AEM data is an element of an integrated investigation to develop a conceptual hydrogeological model of the study area and for mapping and assessment of MAR potential targets (Brodie et al. 2013). AEM data were used to identify areas that are likely most favorable for managed aquifer recharge, which are targets for subsequent more detailed aquifer characterization.

AEM was feasible for Broken Hill Managed Aquifer Recharge project because it is a rural area with thus a low degree of anthropogenic interference. AEM is typically not feasible in urban and suburban areas, which have an abundance of electrical lines, metal pipes, and other conductors that are sources of interference. Inasmuch as managed aquifer recharge projects are commonly implemented near areas of relatively intense water use, and thus development activity, AEM has limited applications. Decisions as to whether to employ AEM need to be based on evaluation of the potential for the considered methods to provide usable data. There should be a sufficient contrast in the resistivity of subsurface materials (e.g., between aquifer and non-aquifer strata) and minimal likely interference from anthropogenic features.

References

Abdalla, O. A. E., Ali, M., Al-Higgi, K., Al-Zidi, H., El-Hussain, I., & Al-Hinai, S. (2010) Rate of seawater intrusion estimated by geophysical methods in an arid region: Al Khabourah, Oman. Hydrogeology Journal, 18, 1437–1445.

Abraham, J. D., Cannia, J. C., Bedrosian, P. A., Johnson, M. R., Ball, L. B., & Sibray, S.S. (2012) Airborne electromagnetic mapping of the base of aquifer in areas of western Nebraska. U.S. Geological Survey Scientific Investigations Report 2012–5219.

Abraham, J. D., & Lucius, J. E. (2004) Direct current resistivity profiling to study distribution of water in the unsaturated zone near Amargosa Desert Research Site, Nevada. U.S. Geological Survey Open-File report, 2004–1319.

Abdul Nassir, S. S., Loke, M. H., Lee, C.-Y., & Nawawi M. N. M. (2000) Salt-water intrusion mapping by geoelectrical imaging surveys. Geophysical Prospecting, 48, 647–661.

Acworth, R. I., & Jorstad, L. B. (2006). Integration of multi-channel piezometry and electrical tomography to better define chemical heterogeneity in a landfill leachate plume within a sand aquifer. Journal of Contaminant Hydrology, 83(3), 200–220.

American Society of Civil Engineers (1998) Geophysical exploration for engineering and environmental investigations. Reston, Virginia: ASCE Press.

Anderson, O. B., Seneviratne, S. I., Hinderer, J., & Viterbo, P. (2005) GRACE-derived terrestrial water storage depletion associated with the 2003 European heat wave: Geophysical Research Letters, 32, L18405.

Archie, G. E. (1942) The electrical resistivity log as an aid in determining some reservoir characteristics: Transactions American Institute of Mining Metallurgical and Petroleum Engineers, 146, 54–67.

ASTM, 1999, Standard guide for selecting surface geophysical methods. D6429–99 (reapproved 2011). West Conshohocken: ASTM International.

Auken, E., Christiansen, A. V., Jacobsen, L. H., & Sørensen, K. I. (2008) A resolution study of buried valleys using laterally constrained inversion of TEM data. Journal of Applied Geophysics, 65, 10–20.

Baker, G. S., Jordan, T. E., & Pardy, J. (2007) An introduction to ground penetrating radar (GPR). In G. S. Baker & H. M. Jol (Eds.), Stratigraphic analyses using GRP. Special Paper 439 (pp. 1–18). Boulder: Geological Society of America.

Becker, M. W. (2006) Potential for satellite remote sensing of ground water. Ground Water, 44, 306–318.

Benkabbour, B., Toto, E. A., & Fakir, Y. (2004) Using DC resistivity method to characterize the geometry and the salinity of Plioquaternary consolidated coastal aquifer of the Mamora plain, Morocco. Environmental Geology, 45, 518–526.

Berdichevsky, M. N., & Dmitriev, V. I. (2008) Models and methods of magnetotellurics. Berlin, Springer.

Binley, A., & Kemna, A. (2005) DC resistivity and induced polarization methods. In Y. Rubin & S. S. Hubbard (Eds.), Hydrogeophysics (pp. 129–156). Dordrecht, Springer.

Blackhawk Geosciences, 1992, Time-domain electromagnetic measurements east-central Florida. St. Johns River Water Management District Special Publication SJ92–SP5.

Boucher, M., Faureau, G., Vouillamos, J. M., Nazoumou, Y., & Legchencko, A. (2009) Estimating specific yield and transmissivity with magnetic resonance sounding in an unconfined sandstone aquifer (Niger). Hydrogeology Journal, 17, 1805–1815.

Burger, H. R., Sheehan, A. F., & Jones, G. H. (2006) Introduction to applied geophysics: Exploring the shallow subsurface. New York: W.W. Norton.

Brodie, R. S., Lawrie, K., Dillon, P., Tan, K., Gibson, D., Clarke, J., Magee, J., Christensen, N. B., Halas, L., Somerville, P., Gow, L., Apps, H., Vanderzalm, J., Page, D., Brodie, R. C., Hostetler, S., Abraham, J., & Miotlinski, K. (2013) An integrated approach to developing hydrogeological conceptual models to underpin assessment of managed aquifer recharge options, darling floodplain, N.S.W., Australia. In Procceedings 8th International Symposium on Managed Aquifer Recharge, Beijing, China.

Cardimona, S. J., Clement, W. P., & Kadinsky-Cade, K. (1998). Seismic reflection and ground-penetrating radar imaging of a shallow aquifer. Geophysics, 63, 1310–1317.

Cesanelli, A., & Guarracino, L. (2011) Estimation of regional evapotranspiration in the extended Salado Basin (Argentina) from satellite gravity measurements. Hydrogeology Journal, 19, 629–639.

Chalikakis, K., Plagnes, V., Guerin, R., Valois, R., & Bosch, F. P. (2011) Contribution of geophysical methods to karst-system exploration: an overview. Hydrogeology Journal, 19, 1169–1180.

Chapman, D. S., Sahm, E., & Gettings, P. (2008) Monitoring aquifer recharge using repeated high-precision gravity measurements: a pilot study in South Weber, Utah. Geophysics, 73(6), WA83–WA93.

Cunningham, K. J. (2015) Seismic-sequence stratigraphy and geologic structure of the Floridan aquifer system near "Boulder Zone" deep wells in Miami-Dade County, Florida: U.S. Geological Survey Scientific Investigations Report 2015–5013

Cunningham, K. J., Locker, S. D., Hine, A. C., Bukry, D., Barron, J. A., & Guertin, L. A. (2001) Surface-geophysical characterization of ground-water systems of the Caloosahatchee River Basin, Southern Florida. U.S. Geological Survey Water-Resources Investigations Report 01-4084.

Cunningham, K. J., Walker, C., & Westcott, R. L. (2012) Near-surface, marine seismic-reflection data define potential hydrogeologic confinement bypass in the carbonate Floridan aquifer system, southeastern Florida. Society of Economic Geophysicists Annual Meeting, Las Vegas, Nevada.

Davis, K., Li, Y., Batzle, M., & Raynolds, B. (2005) Time-lapse gravity monitoring of an aquifer storage recovery project in Leyden, Colorado. Colorado School of Mines, Center for Gravity, Electrical & Magnetic Studies,

Davis, K., Li, Y., & Batzle, M. (2008) Time-lapse gravity monitoring: a systematic 4D approach with application to aquifer storage and recovery. Geophysics, 73(6), WA61–WA-69.

De Franco, R., Biella, G., Tosi, I., Teatini, P., Lozej, A., Chiozzotto, B., Giada, M., Rizzetto, F., Claude, C., Mayer, A., Bassan, V., & Gasparetto-Stori, G. (2009) Monitoring the saltwater intrusion by time lapse electrical resistivity tomography: The Chioggia test site (Venice Lagoon, Italy). Journal of Applied Geophysics, 69, 117–130

De Lima, O. A. L., Sato, H. K., & Porsani, M. J. (1995) Imaging industrial contaminant plums with resistivity techniques. Journal of Applied Geophysics, 34, 93–108.

Dentith, M., & Mudge, S. T. (2014) Geophysics for the mineral exploration geoscientist. Cambridge U.K.: Cambridge University Press.

Driscoll, F. G. (1986) Groundwater and wells (2nd Ed.). St. Paul: Johnson Filtration Systems.

Eastern Research Group (1993) Use of airborne, surface, and borehole geophysical techniques at contaminated sites. A reference guide. U.S. Environmental Protection Agency, Office of Research and Development, Document EPA/625/R-92–007.

Famiglietti, J. S., Lo, M., Ho, S. L., Bethune, J., Anderson, K. J., Syed, T. H., Swenson, S. C., de Linage C. R., & Rodell, M. (2011). Satellites measure recent rates of groundwater depletion in California's Central Valley. Geophysical Research Letters, 38(3).L03403

Feng, W., Zhong, M., Lemoine, J. M., Biancale, R., Hsu, H. T., & Xia, J. (2013). Evaluation of groundwater depletion in North China using the Gravity Recovery and Climate Experiment (GRACE) data and ground-based measurements. Water Resources Research, 49(4), 2110–2118.

Fitterman, D. V., & Deszcz-Pan, M. (2001) Saltwater intrusion in Everglades National Park, Florida measured by airborne electromagnetic surveys. In First International Conference on Saltwater Intrusion and Coastal Aquifers, Monitoring, Modeling, and Management, Essaouria, Morocco, April 23–25, 2001.

Fitterman, D. V., & Deszcz-Pan, M. (2002) Helicopter electromagnetic data from Everglades National Park and surrounding areas, Florida: Collected 9–14 December 1994. U.S. Geological Survey Open-File Report 02-101.

Fitterman, D. V., Menges, C. M., Al Kamali, A. M., & Essa Jamma, F. (1991) Electromagnetic mapping of buried paleochannels in eastern Abu Dhabi Emirate, U.A.E. Geoexploration, 27, 111–133.

Fitterman, D. V., & Stewart, M. T. (1986) Transient electromagnetic soundings for groundwater: Geophysics, 51, 995–1006.

Fitterman, D. V., Deszcz-Pan, M., & Stoddard, C. E. (1999) Results of time-domain electromagnetic soundings in Everglades National Park, Florida. U.S. Geological Survey Open-File Report 99–426.

Fretwell, J. D., & Stewart, M. T. (1981) Resistivity study of a coastal karst terrain, Florida. Ground Water, 19, 156–162.

Gabriel, G., Kirsch, R., Siemon, B., & Wiederhold, H. (2003) Geophysical investigation of buried Pleistocene subglacial valleys in northern Germany. Journal of Applied Geophysics, 53, 159–180.

García-García, D., Ummenhofer, C. C., & Zlotnick, V. (2011) Australian water mass variations from GRACE data linked to Indo-Pacific climate variability. Remote Sensing of Environment, 115, 2175–2183.

Gburek, W. J., Folmar, G. J, & Urban, J. B. (1999) Field data and groundwater modeling in a layered fractured aquifer, Ground Water, 37, 175–184.

Gehman, C. L. Harry, D. L., Sanford, W. E., Stednick, J. D. & Beackman, N. A. (2009) Estimating specific yield and storage change in an unconfined aquifer using temporal gravity surveys. Water Resources Research, 45, W00D1.

Goes, B. J. M., Oude Essink, G. H. P., Vernes, R. W., & Sergi, F. (2009). Estimating the depth of fresh and brackish groundwater in a predominantly saline region using geophysical and hydrological methods, Zeeland, the Netherlands. Near Surface Geophysics, 7, 401–412.

Grossman, E. (2005). Deltaic Habitats in Puget Sound—Natural Versus Human-Related Change. Soundwaves, Dec. 2004/Jan. 2005, http://soundwaves.usgs.gov/2005/01/fieldwork3.html

Günter, A., Schmidt, R., & Döll, P. (2007) Supporting large-scale hydrogeological monitoring and modeling by time-variable gravity data. Hydrogeology Journal, 15, 167–170.

Goldman, M., & Neubauer, F. M. (1994) Groundwater exploration using integrated geophysical techniques. Surveys in Geophysics, 15, 331–361.

Goldman, M., Rabinovich, B., Rabinovich, M., Gilad, D., Gev, I., & Schirov, M. (1994) Application of the integrated NMR-TDEM method in groundwater exploration in Israel. Journal of Applied Geophysics, 31, p. 27–52.

Haeni, F. P. (1986). Application of continuous seismic reflection methods to hydrologic studies. Groundwater, 24(1), 23–31.

Howle, J. F., Phillips, S. P., & Ikehara, M. E. (2002) Estimating water-table change using microgravity surveys during an ASR program in Lancaster, California. In P. Dillon (Ed.), Management of aquifer recharge for sustainability (pp. 269–272). Lisse: Swets & Zeitlinger,

Høyer, A.-S., Jørgensen, F., Sandersen, P. B. E., Viezzoli, A., & Møller, I. (2015) 3D geological modelling of a complex buried-valley network delineated from borehole and AEM data. Journal of Applied Geophysics, 122, 94–102.

Huisman, J. A., Hubbard, S. S., Redman, J. D., & Annan, A. P. (2003) Measuring soil water content with ground-penetrating radar: a review. Vadose Zone Journal, 2, 476–491.

Hunter, J. A., Pullan, S. E., Burns, R. A., Gagne, R. M., & Good, R. L. (1984). Shallow seismic reflection mapping of the overburden-bedrock interface with the engineering seismograph-some simple techniques. Geophysics, 49, 1381–1385.

Jacob, T., Bayer, R., Chery, J., & LeMoigne, N. (2010) Time-lapse microgravity surveys reveal water storage heterogeneity of a karst aquifer. Journal of Geophysical Research – Solid Earth, 115, B06402.

Jol, H.M. (Ed.) (2009) Ground penetrating radar theory and applications. Amsterdam: Elsevier.

Kindinger, J. (2003) Lake Belt study area: high-resolution seismic reflection survey, Miami-Dade County Florida. U.S. Geological Survey Open-File Report 02–325.

Kindinger, J. L., Davis, J. B., & Flocks, J. G. (1994) High-resolution single-channel seismic reflection surveys of Orange Lake and other selected sites of North Central Florida. U.S. Geological Survey Open-File Report 94–616.

Kindinger, J. L., Davis, J. B., & Flocks, J.G. (2000) Subsurface characterization of selected water bodies in the St Johns River Water Management District, Northeast Florida. U.S. Geological Survey Open-File Report 00-180.

Kirkegaard, C,. Sonnenberg, T. O., Auken, E., & Jørgensen, F. (2011) Salinity distribution in heterogeneous coastal aquifers mapped by airborne electromagnetic. Vadose Zone Journal, 10, 125–135.

Kirsch, R. (Ed.) (2008) Groundwater geophysics: A tool for hydrogeology. Berlin: Springer

Knight, R., Grubewald, E., Irons, T., Dlubac, K., Song, Y., Bachman, H. N., Grau, B., Walsh, D., Abraham, J. D., & Cannia, J. (2012) Field experiment provides ground truth for surface magnetic resonance measurements. Geophysical Research Letters, 39, L03304.

Koth, K. R., & Long, A. J. (2012) Microgravity methods for characterization of groundwater storage changes and aquifer properties in the karstic Madison aquifer in the Black Hills of South Dakota, 2009–2012. U.S. Geological Survey Scientific Investigations Report 2012-5158.

Lawrie, K. C., Brodie, R. S., Tan, K. P., Gibson, D., Magee, J., Clarke, J. D. A., Halas, L., Gow, L., Somerville, P., Apps, H. E., Christensen, N. B., Brodie, R. C., Abraham, J., Smith, M., Page, D., Dillon, P., Vanderzalm, J., Miotlinski, K., Hostetler, S., Davis, A., Ley-Cooper, A. Y., Schoning, G., Barry, K. & Levett, K. (2012) Broken Hill Managed Aquifer Recharge (BHMAR) Project: Securing Broken Hill's Water Supply: Assessment of conjunctive water supply options involving managed aquifer recharge and/or groundwater extraction at Menindee Lakes: Data acquisition, processing, analysis and interpretation method. Record 2012/011. Canberra: Geoscience Australia

Legchenko, A., Baltassat, J.-M., Beauce, A., & Bernard, J. (2002) Nuclear magnetic resonance as a geophysical tool for hydrogeologists. Journal of Applied Geophysics, 50, 21–46.

Legchenko, A., Baltassat, J.-M., Bobachev, A., Martin, C., Robain, H., & Vouillamoz, J. M. (2004) Magnetic resonance sounding applied to aquifer characterization. Ground Water, 42, 363–373.

Lluria, M. R. (1990) Controlled source audio-frequency magnetotellurics; an effective surface geophysical tool in the exploration for groundwater hosted in fractured bedrock aquifers. In Proceedings of the National Outdoor Action Conference on Aquifer Restoration, Ground Water Monitoring and Geophysical Methods 4, pp. 1143–1157.

Lucius, J. E., Langer, W. H., & Ellefsen, K. J. (2007) An introduction to using surface geophysics to characterize sand and gravel deposits. U.S. Geological Survey Circular 1310.

Lunt, I. A., Hubbard, S. S., & Rubin, Y. (2005) Soil moisture content estimation using ground-penetrating radar reflection data. Journal of Hydrology, 307, 254–269.

Maliva, R. G., & Missimer, T. M. (2012) Arid lands water evaluation and management. Berlin: Springer.

Miller, R. D., Steeples, D. W., & Brannan, M. (1989). Mapping a bedrock surface under dry alluvium with shallow seismic reflections. Geophysics, 54(12), 1528–1534.

Mills, T., Hoekstra, P., Blohm, M., & Evans, L. (1988) Time domain electromagnetic soundings for mapping seawater intrusion in Monterey County, California. Ground Water, 26, 771–782.

Milson, J. (2003) Field geophysics (3rd Ed.). Chichester: John Wiley & Sons.

Minsley, B. J., Ajo-Franklin, J., Mukhopadhyay, A., and Morgan, F. D. (2011) Hydrogeophysical methods for analyzing aquifer storage and recovery systems. Ground Water, 49, 250–269.

Missimer, T. M., & Gardner, R. A. (1976) High-resolution seismic reflection profiling for mapping shallow aquifers in Lee County, Florida. U.S. Geological Survey Water-Resources Investigations report 76–45.

NASA, 2003, Studying the Earth's gravity from space: The Gravity Recovery and Climate Experiment (GRACE). NASA Facts. The Earth System Sciences Pathfinder Series, FS-2002-1-029-GSFC (rev. December 2003).

Oldenborger, G. A., Pugin, A. J.-M., Hinton, M. J., Pullan, S. E., Russell, H. A. J., & Sharpe, D. R. (2010) Airborne time-domain electromagnetic data for mapping and characterization of the Spiritwood Valley aquifer, Manitoba, Canada. Geological Survey of Canada, Current Research 2010–2011.

Oldenborger, G. A., Pugin, A.J.-M., & Pullen, S. E. (2013) Airborne time-domain electromagnetic, resistivity and seismic reflection for regional three dimensional mapping and characterization of the Spiritwood Valley aquifer, Manitoba, Canada. Near Surface Geophysics, 11, 63–74.

Paine, J. G. (2000) Identifying and assessing ground water in the Lower Rio Grande Valley, Texas, using airborne electromagnetic induction. Report prepared for the Texas Water Development Board by the Texas Bureau of Economic Geology.

Paine, J. G. (2003) Determining salinization extent, identifying salinity sources, and estimating chloride mass using surface, borehole, and airborne electromagnetic induction methods. Water Resources Research, 39(3), 1059.

Paine, J. G., & Minty, B. R. S. (2005) Airborne hydrogeophysics. In Y. Rubin & S. S. Hubbard (Eds.) Hydrogeophysics (pp. 333–357). Dordercht: Springer.

Paine, J. G., & Collins, E. W. (2003) Applying airborne electromagnetic induction in groundwater salinization and resources studies, West Texas. In Proceedings, Symposium of the Application of Geophysics to Engineering and Environmental Problems: Environmental and Engineering Geophysical Society (pp. 722–738).

Paterson, N. R., & Bosschart, R. A. (1987) Airborne geophysical exploration for ground water. Ground Water, 25, 41–50.

Pool, D. R. & Eychaner, J. H. (1995) Measurement of aquifer-storage change and specific yield using gravity surveys. Ground Water, 33, 425–432.

Pool, D. R. (2008) The utility of gravity and water-level monitoring at alluvial aquifer wells in southern Arizona: Geophysics, 73(6), WA49–WA59.

Pool, D. R., & Schmidt, W. (1997) Measurement of ground-water storage change and specific yields using the temporal-gravity method near Rillito Creek, Tucson, Arizona. U.S. Geological Survey Water Resources Investigations Report 97–4125.

Purvance, D.T., & Andricevic, R. (2000) On the electric-hydraulic conductivity correlationin aquifers. Water Resources Research, 36, 2905–2913.

Reyes-López, J. A., Ramírez-Hernández, J., Lázaro-Mancilla, O., Carreón-Diazconti, C., & Garrido, M. M. L. (2008). Assessment of groundwater contamination by landfill leachate: a case in México. Waste Management, 28, S33–S39.

Reynolds, J. M. (1997) An Introduction to applied and environmental geophysics. Chichester: Wiley.

Richey, A. S., Thomas, B. F., Lo, M. H., Reager, J. T., Famiglietti, J. S., Voss, K., Sawnson, S., & Rodell, M. (2015). Quantifying renewable groundwater stress with GRACE. Water Resources Research, 51, 5217–5238.

Rodell, M., Chen, J., Kato, H., Famiglietti, J.-S., Nigro, J., & Wilson, C. R. (2007) Estimating groundwater storage changes in the Mississippi River Basin (USA) using GRACE: Hydrogeology Journal, 15, 159–166.

Rodell, M., Velicogna, I., & Framigletti, J. S. (2009) Satellite-based estimates of groundwater depletion in India. Nature, 460, 999–1002.

Roy, J., & Lubczynski, M. (2003) The magnetic resonance sounding technique and its use for groundwater investigations. Hydrogeology Journal, 11, 455–465.

Russell, G. M., & Higer, A. L. (1988) Assessment of ground-water contaminations near Latana landfill, Southeast Florida. Ground Water, 26, 156–164.

Samsudin, A. R., Haryono, A., Hamzah, U., and Rafek, A. G. (2008) Salinity mapping of coastal groundwater aquifers using hydrogeochemical and geophysical methods: a case study from North Kelantan, Malaysia. Environmental Geology, 55, 1737–1743.

Scanlon, B. R., Longuevergne, L., & Long, D. (2012). Ground referencing GRACE satellite estimates of groundwater storage changes in the California Central Valley, USA. Water Resources Research, 48(4). W04520.

Schirov, M., Legchenko, A., & Creer, G. (1991) A new direct -invasive groundwater detection technology for Australia. Exploration Geophysics, 22, 333–338.

Seara, J. L., & Granda, A. (1987) Interpretation of IP time domain/resistivity soundings for delineating sea-water intrusions in some coastal areas of the Northeast of Spain. Geoexploration, 24, 153–167.

Shah, S. D., Kress, W. G., & Legchenko, A. (2007) Application of surface geophysical methods, with emphasis on magnetic resonance soundings, to characterize the hydrostratigraphy of the Brazos River Alluvium Aquifer, College Station, Texas, July 2006 – A pilot study. U.S. Geological Survey Scientific Investigations Report 2007–5203.

Sharma, P. V. (1997) Environmental and engineering geophysics. Cambridge: Cambridge University Press.

Sherif, M., El Mahmoudi, A., Garamoon, H., Kacimov, A., Akram, S., Ebraheem, A., and Shetty, A. (2006) Geoelectrical and hydrochemical studies for delineating seawater intrusion in the outlet of Wadi Ham, UAE. Environmental Geology, 49, 536–551.

Simpson, F., & Bahr, K. (2005) Practical magnetotellurics. Cambridge: Cambridge University Press.

Skinner, D., & Heinson, G. (2004) A comparison of electrical and electromagnetic methods for the detection of hydraulic pathways in a fractured rock aquifer, Clare Valley, South Australia. Hydrogeology Journal, 12, 576–590.

Smith, R. S., O'Connell, M.D., & Paulson, L.E. (2004) Using airborne electromagnetic surveys to investigate the hydrogeology of an area near Nyborg, Denmark. Near Surface Geophysics, 2, 123–130.

Sørensen, K. I., and Auken, E. (2004) SkyTEM: A new high-resolution helicopter transient electromagnetic system. Exploration Geophysics, 35, 191–199.

Spechler, R. M. (2001) The Relation between structure and saltwater intrusion in the Floridan Aquifer System, Northeastern Florida. In E. L. Kuniansky (Ed.), U.S. Geological Survey Karst Interest Group Proceedings (pp. 25–29). U.S. Geological Survey Water-Resources Investigations Report 01-4011.

Steur, A., Siemon, B., & Auken, E. (2009) A comparison of helicopter-borne electromagnetic in frequency- and time-domain at the Cuxhaven valley in northern Germany. Journal of Applied Geophysics, 67, 194–205.

Stewart, M. A., Bhatt, T. N., Fennema, R. J., & Fitterman, D. V. (2002) The road to Flamingo: An evaluation of flow pattern alterations and salinity intrusion in the Lower Glades, Everglades National Park. U.S. Geological Survey Open-File Report 02–59.

Stonestrom, D.A., Prudic, D.E., Walvoord, M.A., Abraham, J.D., Stewart-Deaker, A.E., Glancy, P.A., Constantz, J., Lacniak, R.J., and Andrasji, B.J., 2007, Focused ground-water recharge in the Amargosa Desert Basin. In D. A. Stonestrom, J. Constantz, T. P. A. Ferré & S. A. Leake (Eds.), Ground-water recharge in the arid and semiarid southwestern United States (pp. 107–136). U.S. Geological Survey Professional Paper 1703.

Strassberg, G., Scanlon, B. R., & Rodell, M. (2007) Comparison of seasonal terrestrial water storage variations from GRACE with ground-water level measurements from the High Plains Aquifer (USA). Geophysical Research Letters, 34, L14402.

Strassberg, G., Scanlon, B. R., & Chambers, D. (2009) Evaluation of groundwater storage monitoring with the GRACE satellite: Case study of the High Plains aquifer, central United States. Water Resources Research, 45, W05410.

Subsurface Detection Investigations (1995) Time domain electromagnetic mapping of salt water in the Floridan Aquifer in Northeast and East-Central Florida, St. Johns River Water Management District, October 1995. St. Johns River Water Management District Special Publication SJ95–SP2.

Sumner, J. S. (1984). Principles of induced polarization for geophysical exploration. Amsterdam: Elsevier Science.

Sushakov, O.I. (1996) Groundwater NMR in conductive water. Geophysics, 61, 998–1006.

Swenson, S., & Wahr, J. (2002) Methods for inferring regional surface-mass anomalies from Gravity Recovery and Climate Experiment (GRACE) measurements of time-variable gravity. Journal of Geophysical Research, 113, B08410.

Taylor, K., Widmer, M., & Chesley, M. (1992) Use of transient electromagnetics to define local hydrogeology in an arid alluvial environment. Geophysics, 57, 343–352.

Telford, W. M., Geldart, L. P., & Sheriff, R. E., 1990, Applied geophysics. Cambridge: Cambridge University Press.

Turcotte D. L., & Schubert, G. (1982) Geodynamics: Applications of continuum physics to geological problems. New York: John Wiley & Sons.

Tiwari, V. M., Wahr, J., & Swenson, S. (2009) Dwindling groundwater resources in northern India, from satellite gravity observations: Geophysical Research Letters, 36(18), L18401.

Urish, D. W. (1983) The Practical application of surface electrical resistivity to detection of ground-water pollution. Ground Water, 21, 144–152.

USACOE (1995) Geophysical exploration for engineering and environmental investigations: Engineer manual. U.S. Army Corps of Engineers Manual No. 1110–1802.

Van Overmeeren, R. A. (1989) Aquifer boundaries explored by geoelectrical measurements in the coastal plain of Yemen: a case of equivalence. Geophysics, 54, 38–48.

Van Overmeeren, R. A., & Ritsema, I. L. (1988) Continuous vertical electrical sounding. First Break, 6(12), 313–324.

Viezzoli, A., Jørgensen, F., & Sørensen, C. (2013) Flawed processing of airborne EM data affecting hydrogeological interpretation. Groundwater, 51, 191–202.

Viezzoli, A., Munday, T., & Cooper, Y. L. (2012) Airborne electromagnetics for groundwater slainity mapping: case studies of coastal and inland salinisation from around the world. Bollettino di Geofisica Teorica ed Applicata, 53, 581–600.

Vouillamoz, J. M., Chatenoux, B., Mathieu, F., Baltassat, J. M., & Legchenko, A. (2007a) Efficiency of joint use of MRS and VES to characterize coastal aquifer in Myanmar. Journal of Applied Geophysics, 61, 142–154.

Vouillamoz, J. M., Baltassat, J. M., Girand, J. F., Plata, J., & Legchenko, A. (2007b) Hydrogeological experience in the use of MRS. Boletín Geológico y Minero, 118, 531–550.

Voilillamoz, J. M., Faureau, G., Massuel, S., Boucher, M., Nazoumou, Y., & Legchenko, A. (2008) Contribution of magnetic resonance sounding to aquifer characterization and recharge estimate in semiarid Niger. Journal of Applied Geophysics, 64, 99–108.

Wahr, J., Swenson, S., Zlotnicki, V., & Velicogna, I. (2004) Time-variable gravity from GRACE: First results. Geophysical Research Letters, 31, L11501.

Werkema, D. (2004) Naval Base Ventura County, Port Hueneme, California EPA characterization test cell report on electromagnetic surveys in the test cell area (EPA/600/S-04/073). Washington, DC: U.S, Environmental Protection Agency, Washington, DC,

Wilson, S. R., Ingham, M., & McConchie, J. A. (2005) The applicability of earth resistivity methods for saline interface definition. Journal of Hydrology, 316, 301–312.

Worthington, P. F. (1977) Geophysical investigation of groundwater resources in the Kalahari Basin: Geophysics, 42, 838–849.

Wynn, J. (2002) Evaluating groundwater in arid lands using airborne magnetic/EM methods: an example in the southwestern U.S. and northern Mexico. The Leading Edge, January 2002, 62–64.

Yaramanci, U. (2000) Surface nuclear magnetic resonance (MRS) – a new method for exploration of ground water and aquifer properties. Annali di Geofisica, 43, 1159–1175.

Yaramanci, U., & Müller-Petke, M. (2009) Surface nuclear magnetic resonance – a unique tool for hydrogeophysics. The Leading Edge, October 2009, 1240–1247.

Young, M. E., de Bruijn, R. G. M., & bin Salim Al-Ismaily, A. (1998) Exploration of an alluvial aquifer in Oman by time-domain electromagnetic soundings. Hydrogeology Journal, 6, 383–393.

Young, M. E., Macumber, P. G., Watts, M. D., & Al-Toqy, N. (2004) Electromagnetic detection of deep freshwater lenses in a hyper-arid limestone terrain. Journal of Applied Geophysics, 57, 43–61.

Zohdy, A. A. R. (1970) Variable azimuth Schlumberger resistivity sounding and profiling near a vertical contact. U.S. Geological Survey Bull. 1313-A.

Zohdy, A. A. R. (1974) Electrical resistivity. In A. A. R. Zohdy, G. P. Eaton & D. R. Mabey (Eds.), Application of surface geophysics to ground-water investigations (pp. 5–66). Techniques of Water-Resources Investigations of the United States Geological Survey, Book 2, Chapter D1.

Zohdy, A. A. R., Eaton, G. P., & Mabey, D. R. (1974) Application of surface geophysics to ground-water investigations. Techniques of Water-Resources Investigations of the United States Geological Survey, Book 2, Chapter D1.

Zonge, K.L. & Hughes, L.J. (1991) Controlled source audio-frequency magnetotellurics. In Nabighian, M. N. (ed.), Electromagnetic methods in applied geophysics (v. 2, pp. 713–809). Society of Exploration Geophysicists.

Chapter 12
Direct-Push Technology

Direct-push technology (DPT) is a widely adopted, low-cost method for collecting groundwater samples from unconsolidated or semi-consolidated shallow aquifers without a need for permanent monitoring wells. DPT methods are also used to install permanent small-diameter monitoring wells. DPT has the great advantage of generating minimal investigation-derived waste, which may require expensive disposal at a regulated waste facility. Direct-push technologies are increasingly being used as part of aquifer characterization programs for the installation of observation wells used in aquifer pumping tests, slug testing, electrical conductivity (resistivity) profiling, and aquifer hydraulic conductivity profiling. Hydostratigraphic profiling procedures have been developed that efficiently incorporate a series of direct-push technologies.

12.1 Introduction

Direct-push technologies involve the pushing or vibrating of a drive point (bit), screen, and drill rod into sediment or soft rock. DPT is, in essence, an outgrowth of older well-point technology, whereby a robust pipe with a screen (of various designs) is driven into shallow water-bearing strata. Well points continue to be widely used for construction dewatering and low-capacity water supply wells. In DPT, the drill bit, screen, and rod are usually driven using a hydraulic ram supplemented with vehicle weight or high-frequency percussion hammers. In shallow unconsolidated strata, the assembly may be advanced manually using a slide hammer, sledge-hammer, or hammer drill. Direct-push technologies have had their greatest use to date for water sampling. They are also being used increasingly for hydraulic testing (mini-slug tests), observation wells for pumping tests, formation sampling, and lithological characterization. The advantages of DPT over standard drilled test wells are greater speed and site accessibility, minimal generation of cuttings, and often lower costs (Butler et al. 2002). The greater speed and lower cost allow for a greater density of measurements than can affordably be obtained by

monitoring wells installed using standard drilling techniques. The terms observation wells, monitoring wells, and piezometers are commonly used interchangeably in the literature (and herein) in the sense that they are completed with a screened casing and could be used to measure water level (pressure) and/or water sampling.

At contaminated sites, investigation-derived wastes (cuttings and waste drilling fluids) may be considered under local environmental regulations to be a contaminated, or even hazardous, waste that require costly disposal in a regulated waste facility. The reduction in the costs associated with investigation-derived wastes is an important advantage of direct-push technologies.

The implementation and development of new uses for direct-push technologies accelerated in the early 1990s. Many of sampling and testing methods described herein from research papers have been refined and become commercially available through both equipment manufacturers and suppliers and as contracted services by drilling and geotechnical firms. Specific models of commercial equipment given herein are meant to provide examples of technologies available and are not an endorsement of any brand or model.

12.2   Groundwater Sampling

Direct-push technology was initially developed for groundwater sampling. For a one time sampling of groundwater at a location, such as performed as part of a contamination assessment, it is often far less expensive to use direct-push techniques, than to install a conventional monitoring well. The application of DPT for groundwater monitoring was reviewed in detail by the USEPA (2005). Groundwater samples may be collected using two broad categories of DPT methods: point-in-time samplers and DPT-installed groundwater monitoring wells.

Point-in-time samplers (also known as temporary or grab samplers) are used to collect single groundwater samples. The sampler is driven to the target depth and water flows into the sampler through an exposed screen that is generally under ambient hydrostatic pressure. Groundwater is collected from the in-place sampler using either a small-diameter bailer or an inertial or submersible pump. Alternatively, in some systems, the sampler is retracted to the surface to obtain the water sample. Once sampling is completed, the sampling equipment is removed and the boring abandoned. Point-in-time sampling is commonly used as part of contamination assessments to determine whether or not groundwater contamination is present at a location and to assess the horizontal and vertical extent of a contaminant plume. The author has used DPT point-in-time sampling to obtain salinity-versus-depth profiles. The various DPT sampling devices and their data collection capabilities were reviewed by the USEPA (2005).

DPT-installed monitoring wells typically have small diameters (e.g., 2–5 cm) and are left in place to allow for multiple groundwater sampling events. Groundwater may be collected from monitoring wells using either bailers, pumps (commonly peristaltic, inertial or bladder), or passive sampling devices. DPT-installed monitoring wells

differ from conventional monitoring wells (such as those installed using hollow-stem augers) by their smaller diameter, and either the lack of a filter pack or use of pre-packed screens. The annulus between the screen and formation is minimal and the formation is allowed to collapse against the screen.

12.3   Point-in-Time Samplers

A basic issue with the installation of either temporary or permanent screens using DPT is preventing the screen from becoming clogged as the DPT assembly is driven into the formation. For example, an exposed screen driven through clayey strata might become clogged with clay that is smeared onto the tool. It is also important that the screen not become contaminated with groundwater from the above sampling depths (i.e., cross-contamination should be avoided). A solution is to expose the screen only upon reaching the target sampling depth.

12.3.1   Sealed-Screen Samplers

Sealed-screen samplers have a coaxial design in which the screen is nested within a sealed, water-tight tool body (Fig. 12.1). The screen is not exposed as the sampler is advanced. O-ring seals between the drive tip and the tool body help to ensure that the sampler is water tight as it is advanced. The screen is also not stressed during the advancement of the assembly as the drive rods are connected to the outer steel body of the sampler, which is in contact with the drive cone. Upon reaching the target sampling interval, the protective outer rod is retracted, exposing the screen to groundwater. An example of a single-sample collection system is the HydroPunch™ and HydroPunch II™ sampling devices (Edge and Cordry 1989; Lammons et al. 1989; Cordry 1991; Smolley and Kappmeyer 1991; Zemo et al. 1995).

Sealed-screen samplers generally are limited to collecting one sample per advance of the sampler. Once the sample chamber is filled, the tool is retrieved and the sample decanted at land surface. For multi-level sampling in a single borehole, the sealed-screen samplers usually have to be retrieved and cleaned (decontaminated) before reentering the tool into hole to collect another sample.

Charette and Allen (2006) described the use of AMS™ Gas Vapor Probe Kit for groundwater sampling, which has the advantage of use of small diameter (0.625") drive cones and pipe (rods), which are driven using a slide hammer or hammer drill. The "Retract-a-tip" sampling system was used in which the screen is driven to the target depth and then exposed. The screen is connected to land surface using nylon or teflon tubing and samples are collected using a peristaltic pump. After a sample is collected, the screen may be closed (shield lowered) and the tip driven to a greater depths for collection of additional samples. In the 'dedicated-tip' system, the tips (cone and screen) are left in the ground as a permanent sample point.
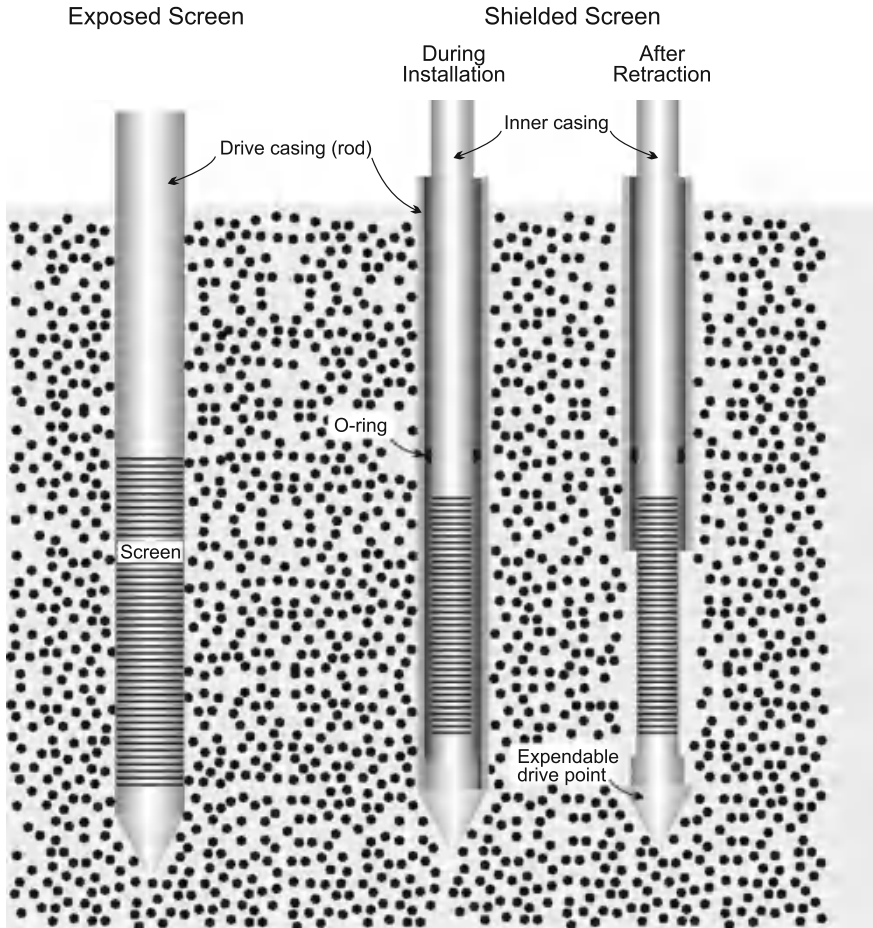
Fig. 12.1 Conceptual diagram of exposed-screen and shielded-screen direct-push groundwater samplers. The screen does not receive the driving force during advancement of shielded-screen samplers. The screen is only exposed once the target sampling depth reached by retracing the drive casing or screen shield

Burk and Cook (2015) documented another sealed-screen system for installing small diameter (15–25 mm) shallow piezometers. The piezometers are driven using a hand-held electric hammer drill, in hammer mode, equipped with a custom drive adaptor. The hammer drill is powered in the field with a portable generator. Once the drive point head and base pipe are advanced to the top of the interval to be sampled, a removable push-rod is installed and driven with the hammer drill to extend the drive point head and expose the screen. Installations were reported up to 6 m and it was noted that greater installation depths are feasible under favorable conditions.

12.3.2   Exposed-Screen Samplers

Exposed-screen (unshielded) samplers, as the names implies, have the screen open to the formation while the tool is being advanced (Fig. 12.1). Exposed-screen samplers are the basic well-point design. The primary advantage of exposed-screen samplers is that they allow for samples to be periodically (or continuously) collected as the tool is advanced. Exposed-screen samplers are an efficient means to obtain vertical profiles of groundwater chemistry. They do not require the retrieval of the screen for the collection of each sample. Manually driven exposed-screen samplers, consisting of a robust screen unit driven by a slide hammer, are an inexpensive means for sampling shallow sandy strata. They are quicker to install than monitoring wells installed by hand augering. The screen is driven to a target depth and a water sample collected using bailer or pump. The stainless steel drive point and screen unit for the Solinst® Model 615 Drive-Point Piezometer is connected to land surface using readily available polyethylene or teflon tubing that passes upward through the extension rods and out a bypass opening in the drive head. Samples are collected using a peristaltic pump. A sealed-screen version can be used in clayey strata where clogging of the screen in a concern.

Disadvantages of exposed screen samplers are a greater potential for screen clogging and cross-contamination. One solution to the clogging and cross-contamination issue is to inject clean (distilled) water out of the screen during tool advancement, which was employed for the Waterloo Ground Water Profiler (Pitkin et al. 1999). The distilled water must be completely purged from the system prior to the collection of each sample. Pitkin et al. (1999) reported that there was minimal drag-down of contamination during tool advancement. A commercial version of the University of Waterloo system is available.

12.3.3   Dual-Tube Coring and Groundwater Sampling

Dual-tube DPT methods are commonly used to obtain cores of sediments but can also be used for groundwater sampling. The basic dual-tube method involves the use of two coaxial sets of rods that are advanced together. The outer drive rod is attached to a cutting shoe and is driven down to seal off the borehole. Core samples are taken using a smaller-diameter inner set of rods that contain a core liner. Upon completion of each core interval, the inner rods and core liner are retrieved and the core removed, while the outer drive rod remains in place. The inner rods and new core liner are then reinstalled inside the outer rods and the process continued.

Water samples are obtained after the inner rod has been removed and core sample collected by either lifting the outer rod a short distance, if the formation is cohesive (i.e., the borehole will remain open), or by the installation of a temporary screen. The installation of a temporary screen also allows for slug tests to be performed to obtain hydraulic conductivity data (McCall et al. 2002).

An alternative dual-tube procedure is the use of nested (coaxial) rods consisting of an outer rod with a cutting shoe and inner rod with a drive point (instead of a core barrel). Both rods are driven together. Upon reaching the base of the target sampling zone, the inner rod is retrieved and a screen is placed at the bottom of the drill string. The outer casing is then lifted to expose the screen. After testing and sampling are completed, the screen is removed, the inner rod and drive point are reinstalled, and the rods are driven to the base of the next sampling interval (McCall et al. 2002).

12.4   Direct-Push Monitoring Wells

Important issues in the installation of DPT monitoring wells are avoiding cross-contamination, maximizing well efficiency (i.e., obtaining a good hydraulic connection with the formation), and avoiding damage to the screen. Although it is possible that contaminants may be dragged downwards during DPT monitoring well installation, the potential is less than with most other drilling methods (e.g., hollow-stem augers, mud-rotary) as there is a no (or at least a negligible) annulus between the drill rods and formation and drilling fluids are not used. Screen damage is avoided by using methods in which the screen is not driven downwards. DPT avoids much of the formation damage that occurs with other monitoring well installation methods. A good hydraulic connection with the formation can be achieved by proper well development. DPT monitoring well installation is reviewed by the USEPA (2005) and guides to their installation are provided by ASTM (2010a, 2010b).

Permanent monitoring wells are commonly installed by driving a metal casing with an expendable tip to total depth. A well casing with a screen is installed inside the metal drive casing, which is then removed. Depending upon the cohesiveness and grain size of the strata to be screened, the formation material may collapse against the screen as the drive casing is removed. Alternatively, if a filter pack is needed, then the preferred option is the use of a screen with a prepacked filter pack. Proper installation of a filter pack using the conventional method of pouring sand or gravel into the well (either directly or using a tremie pipe) from land surface is often not feasible due to the small size of the annulus between the drive casing and screen.

Annular seals and grout should be placed above the filter pack to prevent vertical flow of water into the screened interval and between intercepted aquifer layers. Either a bentonite slurry or Portland cement grout are usually used to seal the annulus, which are installed as the outer casing is being removed. The top of the filter pack should be capped with a barrier of fine sand or granular or pelletized bentonite to prevent grout infiltration.

12.5   Formation Testing

A variety of DPT methods have been developed for aquifer characterization. Dual-tube coring systems (Sect. 12.3.3) allow for the collection of formation samples that can be used for subsequent mineralogical and textural analysis, including grain size analysis. Piezometers installed using DPT are often a cost-effective means to increase the number of observation wells for aquifer pumping tests performed on shallow aquifers. Butler et al. (2002) documented that head data collected using a small diameter pressure transducer in direct-push observation wells gave hydraulic conductivity values within 4 % of the values obtained using traditional monitoring wells installed using hollow-stem augers. Aquifer hydraulic testing performed using DPT equipment is subject to the limitations of small rod and well diameters. Geophysical logging tools have been developed than can be run either during tool advancement or on completed monitoring wells. Some DPT formation testing techniques are described below. It is anticipated that new formation testing technologies will be developed because of the advantages of DPT for assessment of shallow aquifers. Walsh et al. (2011), for example, discussed the development of a slim-hole nuclear magnetic resonance (NMR) tool that is designed for DPT.

12.5.1   DPT Slug Tests

Slug tests are widely used method for determining the hydraulic conductivity of strata near a well (Sect. 8.1). Slug tests can be performed on DPT-installed wells or screens temporarily set in a formation. The conventional methods of instantaneously lowering or raising a solid slug in a well are usually impractical in DPT wells because of their small diameter. In DPT investigations, the pneumatic method is commonly used for slug testing, which involves lowering the water level in a well using pressurizing air or nitrogen gas and then rapidly releasing the pressure to cause a near instantaneously rise in water levels (Butler et al. 2002). Slug-in tests are performed by using a vacuum to cause water levels to rise in a well.

Several corrections need to be made when processing data from slug tests performed on small-diameter wells. In small-diameter wells, the cross-sectional area of the transducer cable may be a significant fraction of the cross-sectional area of well. Therefore, it is necessary to correct for the area of the cable by using the effective casing radius (r_c) rather than the nominal casing radius (r_{nc}) (Butler et al. 2002)m

$$r_c = (r_{nc}^2 - r_{cable}^2)^{1=2} \qquad (12:1)$$

where r_{cable} is the radius of the cable.

Hydraulic conductivity may be underestimated if rods with too small of a diameter are used. Butler et al. (2002) documented at the Kansas Geological Survey

test site in Lawrence, Kansas, that for hydraulic conductivity values of 180 m/day, tests performed using a tool with a 0.3 m long screen and 0.016 m inner diameter (ID) rods gave hydraulic conductivity values that were about 50 % less than the values obtained using conventional monitoring wells. No systematic biases occurred when 0.038 m ID rods were used. Butler et al. (2002) recommended using rods with an ID of greater than 0.016 m when the hydraulic conductivity of the tested strata is expected to be 70 m/d or greater. Butler et al. (2002) also documented that hydraulic conductivity is underestimated when small-diameter screens longer than 0.3 m are used. However, there are logistical and cost advantages for the use of smaller diameter rods. Butler (2002) presented a correction for the frictional head losses responsible for the lower hydraulic conductivity values obtained when using small-diameter rods.

Well development is critical for obtaining accurate results from slug tests in general. Skin effects include a variety of processes that can impede the flow of water between the formation and well, such as formation damage and the coating of the borehole wall with clays or other fine materials. Compaction of the sediment that is pushed aside during the driving of the direct-push tool can be an important skin effect. Skin effects are of particular importance in aquifer testing methods that measure the rate of flow into a well, such as slug tests. Butler (1998) provides different approaches to identify the presence of skin effects using slug test data. Skin effects are less important in observation piezometers for aquifer pump testing, particularly where the rate of water level change is slow and there is time for water levels in the piezometer to equilibrate with the formation.

Experimental results indicate that inadequate development using shielded screens could result in an underestimation of hydraulic conductivity by an order of magnitude or more (Butler et al. 2002). Henebry and Robbins (2000) presented field testing results in which the hydraulic conductivity values obtained after development were 3.2–9.6 times greater than pre-development values. Henebry and Robbins (2000) utilized a mini surge-block tool to develop direct-push wells. Butler et al. (2002) recommended two phase development including pneumatic purging and pumping.

Bartlett et al. (2004) performed a comparative study of pneumatic slug tests in high-hydraulic conductivity strata in wells with different constructions and installation methods. Both conventional monitoring wells and direct-push wells gave similar hydraulic conductivity values, provided that they are well developed and completed below the water table. The results are important in that there are cost advantages in the use of small-diameter (2 cm, 0.75 in.) direct-push wells.

12.5.2   Direct-Push Permeameter

The direct-push permeameter (DPP) provides in situ measurements of hydraulic conductivity from the pressure increase during injection. Prototype DPPs are described by Lowry et al. (1999) and Butler et al. (2007). The basic concept is that

water is injected at a constant rate from a port in the direct-push tool and the resulting change in pressure is measured at one or more transducers located on the tool either above or below the injection port or screen. The Cone Permeameter® described by Lowry et al. (1999) has five pressure ports and sensors located within 0.8 m above the center of the injection port. The direct-push permeameter described Butler et al. (2007) has a pair of ports located above the injection screen.

DPPs are based on spherical form of Darcy's law, where for an isotropic aquifer (Lowry et al. 1999; Butler et al. 2007)

$$K = Q \frac{\left(\frac{1}{r_1} - \frac{1}{r_2} \right)}{4p(Dh)} \tag{12:2}$$

where

K   hydraulic conductivity (m/s),
Q   injection rate (m^3/s),
r_1 and r_2 distances from the center of the screen to the near and far transducer, and
Dh   difference in head between the two transducers (m) under steady-shape conditions (i.e., Dh does not change over time). For anisotropic systems ($K_x = K_y = K_h \neq K_z$), the horizontal hydraulic conductivity (K_h) is equal to K (Butler et al. 2007; Liu et al. 2008).

An alternative permeameter design uses a single transducer (or only one transducer on a two transducer tool). Hydraulic conductivity for single transducer tests is interpreted using the equation

$$K = \frac{Q}{4pr_1(Dp_1)} \tag{12:3}$$

where Dp_i is the increase in pressure once steady-state conditions have been reached (Butler et al. 2007).

A fundamental premise of the DPP is that as the distance from the injection port is increased, the resulting pressure distribution will become spherical and the isobars of interest intersect the tool rod in an almost perpendicular fashion (Lowry et al. 1999). The method is also based on measurements of pressure rather than flow into the tool, and is thus less sensitive to compaction near the tool and other skin effects, than is the case for slug tests.

Comparisons of hydraulic conductivity values obtained at two experimental sites using a DPP with values obtained from slug tests indicate that for some intervals there is good agreement between the methods (Butler et al. 2007). Larger differences observed in other intervals were suggested to be due to small differences in the vertical position of the tool. In heterogeneous aquifers, large differences in hydraulic conductivity may occur over short vertical distances.

Modeling results by Liu et al. (2008) indicate that DPP tests are most sensitive to the area of the formation immediately surrounding the injection screen and most distant transducer. DPP tests provide high-resolution profiles of vertical hydraulic conductivity with little sensitivity to lateral variations further than about 0.5 m from the tool. DPP tests thus only provide information on heterogeneity in the immediate vicinity of the tool. The measured hydraulic conductivity values are the weighted average of the material between the screen and furthest transducer. In the case of the Cone Permeameter, the best estimate of hydraulic conductivity (or permeability) is obtained from the sensors located furthest from the injection port (Lowry et al. 1999). The hydraulic conductivity measurements from the furthest pair of sensors are most indicative of the actual hydraulic conductivity of the media at the location of the sensors, rather than that of the media at the injection port (Lowry et al. 1999).

Important advantages of the DPP are that the tests can be performed rapidly (more quickly than direct-push slug tests) and the method has a low sensitivity to compaction of sediment adjacent to the tool (Butler et al. 2007). Disadvantages of the method include the fragility of the transducers (which restricted testing to the use of push-drive equipment) and the potential for vertical flow channels to be developed along the pipe, which can lead to implausibly high-hydraulic conductivity values. Care must be taken in choosing injection rates that are appropriate for the tested sediments (Butler et al. 2007). In the case of clayey strata, problems may arise from the filling of pressure ports with clay and a long time required to dissipate the pressure buildup caused by rod emplacement.

12.5.3 Direct-Push Injection Logger and Hydraulic Profiling Tool

The direct-push injection logger (DPIL) is based on the principal that changes in specific injectivity (ratio of injection rate and pressure) are related to changes in hydraulic conductivity. Upon reaching a depth at which information about hydraulic conductivity is desired, advancement ceases and the injection rate and pressure are measured at land surface (Dietrich et al. 2008). Injection during tool advancement prevents clogging of the injection screen. The underlying parameter of the DPIL is the resistance to injection (R_{Total}), which is defined as (Dietrich et al. 2008)

$$R_{Total} = \frac{P_{Inj}}{Q} \qquad\qquad (12.4)$$

where
P_{inj} injection pressure (kPa)
Q injection rate (L/h)

   The unit of resistance to injection is kPa/(L·h) or, if injection pressure is expressed in meters of water and rate in m^3/d, as d/m^2. Injection pressure is the sum of the injection pressure measured at land surface (P_{trans}) and the pressure exerted by the water column (P_{WC}), which is the distance between the surface pressure transducer and water table (Dietrich et al. 2008). Resistance to injection includes the formation resistance at the screen (R_{sc}) and resistance in the injection tube (R_{tube}). The DPIL hydraulic conductivity is (Dietrich et al. 2008)

$$K_{DPIL} = \frac{1}{R_{Total} - R_{tube}} \qquad (12.5)$$

K_{DPIL} values are proportional to actual hydraulic conductivity values, and has units of flow rate divided by pressure, for example L/(hr·kPa) or L/(hr·bar). The DPIL can thus be used to generate profiles of relative hydraulic conductivity, identifying both preferential flow and confining strata (Fig. 12.2). Actual hydraulic conductivity values are obtained by calibration of the injection rate/pressure profiles against hydraulic conductivity values obtained by DPP, direct-push slug tests, or

Fig. 12.2 DPIL and HST profiles from a contaminated site in Germany. Low permeability strata that act as confining units are indicated by high HPT pressures and low DPIL values (from Kober et al. 2009)
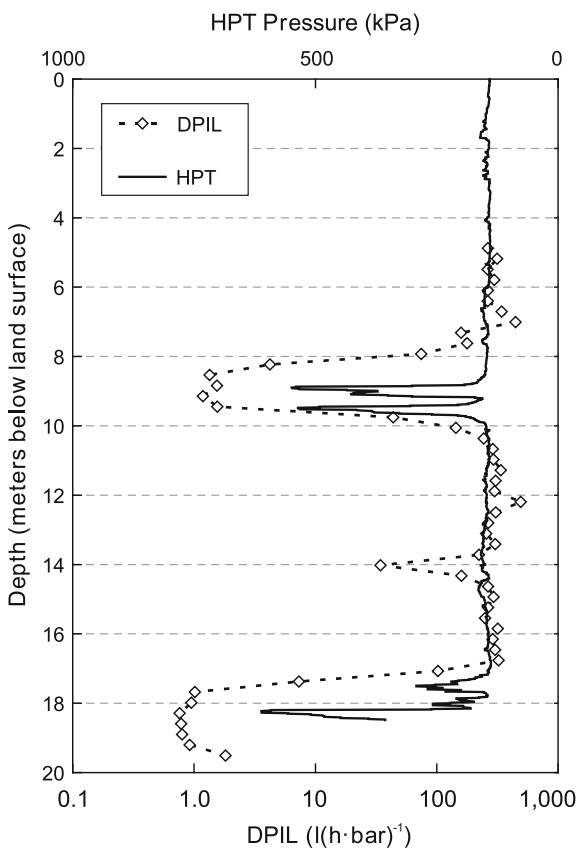
sieve analysis data (Dietrich et al. 2008; Liu et al. 2009; Lessoff et al. 2010; Dietze and Dietrich 2012). The great advantage of the DPIL is that it can provide rapid and detailed qualitative data on changes of hydraulic conductivity. Liu et al. (2009, 2012) described a prototype tool (High-resolution K Tool) that couples the DPP and DPIL into a single tool. Hydraulic conductivity values obtained from the DPP measurements may be directly used to transform high-resolution DPIL data into actual hydraulic conductivity profiles.

The DPIL measures hydraulic conductivity using the ratio of injection pressure and flow rate. The related hydraulic profiling tool (HPT) estimates hydraulic conductivity by measuring water pressure during injection at a constant rate, while continuously advancing the tool (Kober et al. 2009). Pressure is measured only downhole in the interior of the tool, which avoids the need to correct for frictional head losses within the rod. The measured pressure at the probe depends on both the hydraulic conductivity and hydrostatic pressure of the surrounding sediments. The hydrostatic water pressure is, therefore, subtracted from measured pressure for depths below the water table (Kober et al. 2009). The DPIL records pressure in a discontinuous mode (i.e., tool advancement stops to perform a reading), whereas the HPT has the advantage of providing a continuous record. The HPT could also be used to take readings in a discontinuous mode. Hydrostatic pressure is measured by terminating injection. HPT data also need to be calibrated against actual hydraulic conductivity data from other sources to provide a profile of actual hydraulic conductivity versus depth. An HPT tool is commercially available.

Kober et al. (2009) evaluated the use of advanced direct-push methods to generate an aquifer model. Data from direct-push slug tests (DPST), DPIL, and HPT were combined to generate an aquifer model that was evaluated against data from a natural-gradient tracer test. Simulated tracer breakthrough curves based on the direct-push data were compared to measured breakthrough data. The combined DPIL and DPST data were used to map high and low permeable zones in the relatively homogenous test aquifer. Model simulations considering the information from all the tools showed a good reproduction of the measured breakthrough, demonstrating the utility of the DPIL and HST methods.

McCall et al. (2009) documented the use of the HPT to develop a more refined understanding of a study site located along the Platte River in Clarks, Nebraska. The objective of the investigation was to determine the source of elevated uranium concentrations in potable-water production wells. The HPT data were used as guide for the selection of screen depths for small diameter, direct-push monitoring wells.

12.5.4   Direct-Push Flowmeter Logging

Variations in hydraulic conductivity with depth may be evaluated in screened wells by flowmeter logging. Use of direct-push wells without filter packs has the advantages of minimized formation damage and avoidance of bypass through the filter pack (Paradis et al. 2011). It is important that the formation collapses against

the screen rather than leaving an open annulus, which limits the method to wells completed in non-cohesive strata. Paradis et al. (2011) recommend that testing be performed using an electromagnetic induction tool whose diameter is slightly less than the inner diameter of the screen and casing. The tight fit avoids the need for the use of a flow diverter or packer. The flowmeter test should be performed at a maximum rate that does not result in significant head losses through the tool. Paradis et al. (2011) performed stationary reading every 6-in. (15.24 cm) after steady-state conditions were approximately achieved. Data interpretation requires an average hydraulic conductivity value for the logged interval, which could be obtained from an independent hydraulic test or from the transient time-drawdown data at the start of pumping for the flowmeter log. The hydraulic conductivity estimates from the flowmeter log are similar to the values obtained from multi-level slug tests on the same well.

12.5.5 Electrical Conductivity Logging

Direct-push electric conductivity (EC) logs are essentially small-diameter versions of borehole resistivity logs. EC logging using direct-push systems can provide high-resolution stratigraphic information, provided that the strata of interest have significant differences in conductivity and variations in the salinity (specific conductance) of the groundwater is small. EC logs may, for example, be used to distinguish between clay-rich (electrically conductive) confining strata and clean (clay-poor) aquifer sands and gravels that have a low electrical conductivity (Fig. 12.3). Similarly, direct-push EC logs could be used to evaluate vertical changes in salinity, provided that the variation in the resistivity of the rock types is not great.

Schulmeister et al. (2003) utilized an electrical conductivity probe that has four electrodes in a Wenner-type array (i.e., a collinear, evenly spaced configuration). The electrode spacing was 0.02 m, which is the approximate spatial resolution of the tool. The small electrode spacing results in a much greater vertical resolution of variations in clay content, than is provided by conventional borehole induction and gamma ray logs. The fine-scale variations in clay content detected by the direct-push electrical conductivity logs are evident in core samples from the same depth interval (Schulmeister et al. 2003).

A major limitation of the electrical conductivity logging is that it can only detect variations in lithology that have a corresponding change in the abundance of conductive materials, such as clays. Electrical conductivity logging cannot detect textural changes, such as grain size in clean sands, which can have a large effect on hydraulic conductivity. Use of direct-push technology for electrical conductivity logging has the advantages of avoiding the extraneous effects of variations in bore hole diameter and the introduction of fluids (e.g., drilling mud) into the well during drilling (Schulmeister et al. 2003).
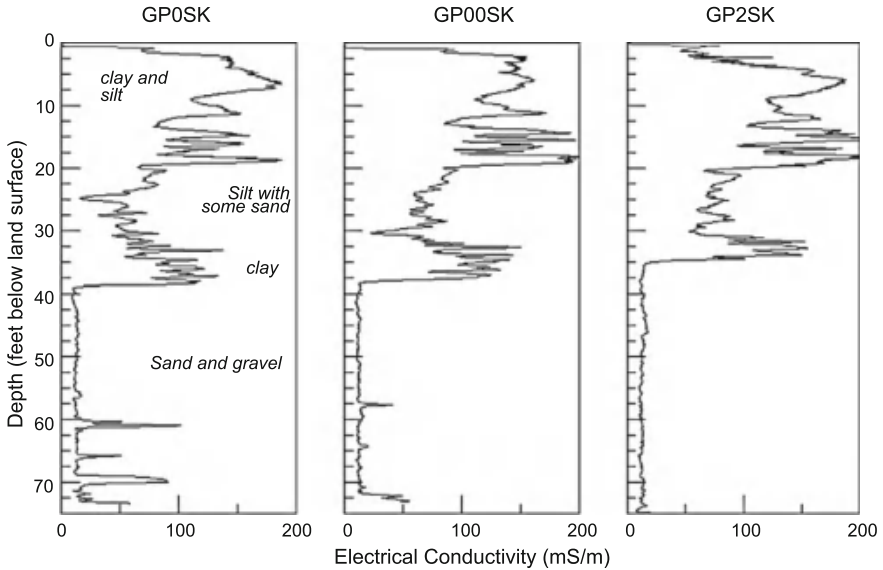
Fig. 12.3 DP electrical conductivity cross section from the Kansas Geological Survey Geohydrologic Experimental and Monitoring Site (GEMS) near Lawrence, Kansas. The cross section is approximately 46 m in length (from Butler et al. 1999)

Schulmeister et al. (2004) demonstrated the use of direct-push EC logging to identify paleosols in unconsolidated fluvial deposits, which are characterized by higher clay contents. Direct-push EC measurements allow for a great number of logs (and thus spatial coverage) to be run than is usually practicably possible using conventional cores and boreholes. However, some cores are still needed for interpretation of the EC logs. Commercial direct-push EC logging units are available.

12.5.6   Hydostratigraphic Profiling

The various direct-push formation testing technologies all have their inherent limits. The greatest value is obtained from the technologies when they are combined in an integrated investigation. EC logging is used to determine the distribution of clayey and clean (clay-poor) strata. The DPIL and HPT tools are used to generate profiles of relative hydraulic conductivity with depth. Direct-push slug tests and the DPP provide actual hydraulic conductivity data that can be used to calibrate the DPIL and HPT data.

Many of the published papers on the use of DPT for aquifer characterization focused on theory and presented results from experimental sites. Zlotnick et al. (2007) discussed some of the applied issues associated with the employment of DPT methods in a remote field site, including operational and maintenance issues.

An important consideration is optimizing the process so as to most efficiently obtain the required data. The study was an investigation of the origin of salinity in the dune-lakes in the Sand Hills of Nebraska (USA). The equipment used were a Geoprobe Systems® DP system and commercially available screen points for groundwater sampling, and slug tests, soil conductivity probes, and coring probes.

The optimized procedure developed by Zlotnick et al. (2007) was performed using three DP cycles at each site:

Cycle 1: EC profiling on the downward run to obtain basic data on hydrostratigraphy,
Cycle 2: Groundwater sampling and slug tests performed on upward run using a sheathed screen deployed and opened at the maximum target depth. Additional testing was performed during retraction of the rod string on the upward run.
Cycle 3: Core collection.

McCall et al. (2002) and Sellwood et al. (2005) described an efficient procedure for hydrostratigraphic profiling using DPT. The efficiency comes from avoiding the need to trip in and out of the hole for each analysis. The basic equipment configuration is coaxial probe rods, consisting of an outer rod with a cutting shoe and a removable inner rod fitted with a drive point and conductivity probe. The testing sequence is as follows:

- The probe rod string is driven through the entire section of strata of interest. Electrical conductivity measurements are taken at frequent intervals or continuously to obtain a profile of electrical conductivity with depth.
- Slug testing is then performed starting at the bottom of the well. The outer probe rod is retracted to just below the bottom of the target test interval, which is determined using the electrical conductivity profile data. The borehole below the casing either naturally collapses or is grouted, where the hole was driven into cohesive sediments.
- A screen of the desired length is inserted into the outer rod. The screen is positioned at the bottom of the outer rod. The outer rod is then retracted to expose the screen. The coupling at the top of the screen is caught in the cutting shoe. The probe rods and screen are retracted to position at the exact target depth interval.
- Slug testing and water sampling are performed.
- After testing and sampling are completed, the screen is retrieved and the outer rod is retracted to just below the base of the next interval to be tested.

By using the combined HPT and EC logging tool, a profile of relative hydraulic conductivity with depth is obtained during the advancement of the probe string to total depth.

12.6   Cone Penetration Test

The cone penetration test (CPT) is a widely used geotechnical procedure for soil investigations. The standard procedures for CPTs are provided by Lunne et al. (1997), Robertson and Cabal (2010), ASTM (2012), and the USDA (2012). The basic methodology is that a small-diameter (typically 10 cm^2 or 15 cm^2 area), cone-tipped rod is advanced into the ground at a set rate of 1 to 2 cm/s. CPTs are usually performed using a hydraulic ram located inside a truck. Electronic CPTs involve the measurement of three main variables, tip resistance (q_c), sleeve resistance (f_s), and pore pressure (I). CPT friction ratio is the ratio of sleeve resistance and tip resistance expressed as a percentage. CPTs provide information on subsurface stratigraphy, as the tip resistance, sleeve resistance, and pore pressure are related to lithology. Soil behavior type (e.g., clay, sand, silty sand to sandy silt) is estimated from the cone resistance and friction ratio (Fig. 12.4; Robertson 1989, 2010a). However, more complete descriptions of subsurface conditions require that CPTs be used in conjunction with conventional drilling and sampling methods.

Hydraulic conductivity can be estimated from the soil behavior type index (Robertson and Cabal 2010). The advancement of the CPT cone into saturated sediment results in a localized increase in pressure. The rate at which the excess pressure dissipates is directly related to the permeability of the sediments. Hydraulic

Zone	q_t/N		SBT
1	2		Sensitive, fine grained
2	1		Organic materials
3	1		Clay
4	1.5		Silty clay to clay
5	2		Clayey silt to silty clay
6	2.5		Sandy silt to clayey silt
7	3		Silty sand to sandy silt
8	4		Sand to silty sand
9	5		Sand
10	6		Gravelly sand to sand
11	1		Very stiff fine grained*
12	2		Sand to clayey sand*

*Over consolidated or cemented
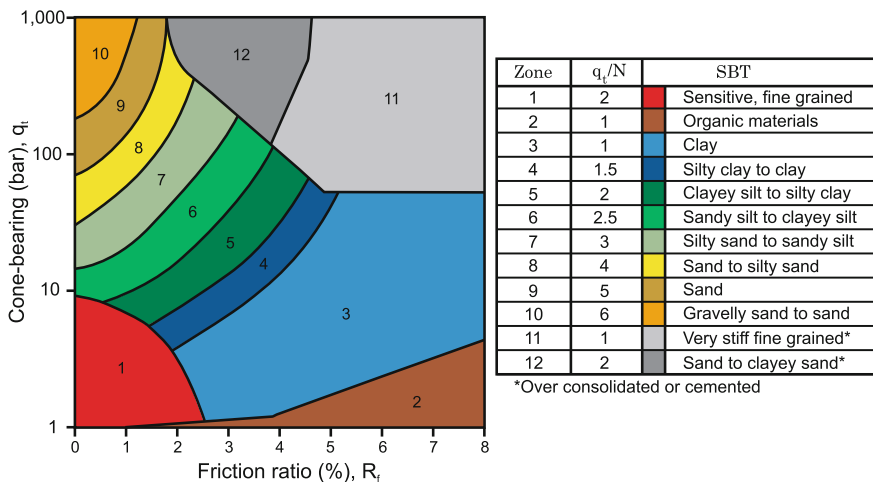
Fig. 12.4 CPT soil behavior types. The cone-bearing pressure (q_t) is the measured cone tip resistance (q_c) corrected for pore pressure effects, which are usually minor (from USDA 2012 after Robertson 1989, 2010a)

conductivity may be estimated from the dissipation time using the empirical rela-
tionship of (Parez and Faureil 1988):

$$K_h = \left(\frac{1}{251 \cdot t_{50}}\right)^{1.25} \tag{12.6}$$

where
K_h horizontal hydraulic conductivity (cm/s)
t_{50} dissipation time for the half of the excess pore pressure (s).

Robertson (2010b) cautioned that the (Parez and Faureil 1988) and other similar
simplified relationships are approximate, since the dissipation time is also a func-
tion of the soil compressibility.
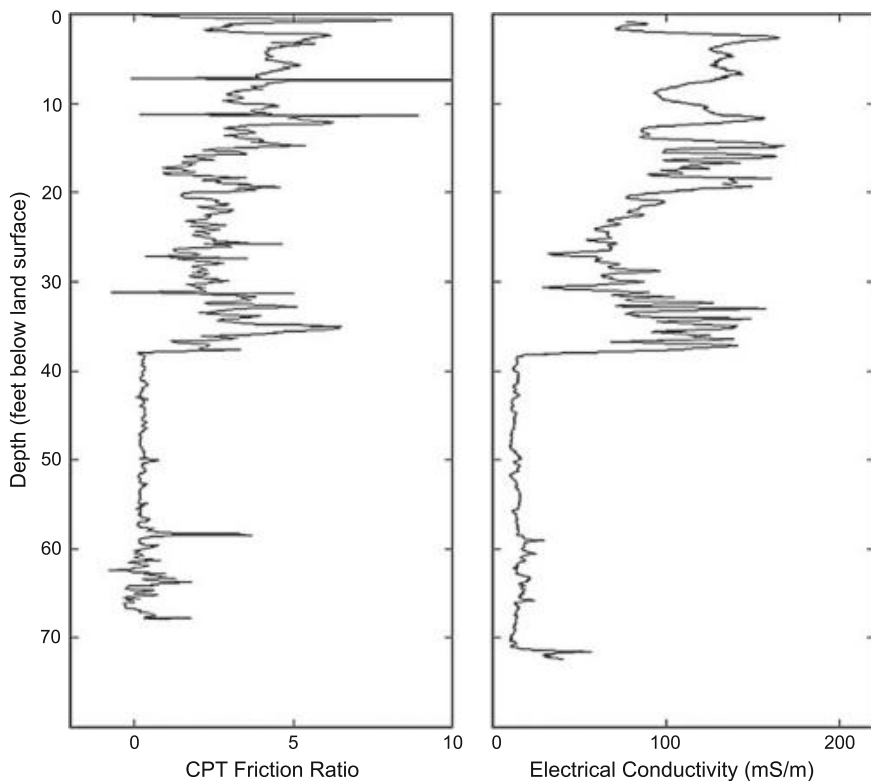
Fig. 12.5 CPT log adjacent to the locations of a DP electrical conductivity log at GEMS, which
display sand-gravel and clay-silt distributions similar to those inferred from the e-logs (from Butler
et al. 1999)

The advantages of the CPT include that (USDA 2012)

- it provides fast and continuous profiling
- equipment is economical and productive
- it generates repeatable and reliable data that are not dependent on the operator
- it can identify thin horizons of low strength
- it reduces contact between field personnel and contaminated soil
- there is a strong theoretical basis for interpretation.

The main disadvantages are that no drilling and soil samples are produced (which could be used to verify lithological interpretations), limited penetration in gravels or cemented materials, and the data are unreliable in unsaturated conditions, particularly in clayey soils (USDA 2012). Relationships between CPT parameters and hydraulic conductivity are approximate. CPTs may capture the pattern of variation in hydraulic conductivity, but the actual values may have substantial error.

Standard CPTs are not widely used for groundwater investigations. CPTs have been used to obtain information on heterogeneity in hydraulic conductivity in unconsolidated sediments. For example, Flach et al. (2005) document the use of CPT to evaluate aquifer heterogeneity at the Savannah River Site (SRS) in Georgia, United States. CPT variables were first used to determine the percent of fine-grained sediments (mud, clay, and silt) by regression analysis using the percent of fines obtained from sieve analyses of sediment samples collected from soil borings advanced near CPT points. The percent fines were then related to hydraulic conductivity. Predicted fines were used to categorize sediments into high, medium, and low hydraulic conductivity, which were then upscaled to flow model resolution using geostatistical approaches. Butler et al. (1999) demonstrate the similarity of CPT (friction ratio) and DP electric conductivity profiles in an interval of clay-rich and clay-poor alluvial sediments (Fig. 12.5).

References

ASTM (2010a) Guide for installation of direct push ground water monitoring wells, D 6724-04. West Conshohocken: ASTM International.

ASTM (2010b) Practice for direct push installation of pre-packed screen monitoring wells in unconsolidated aquifers, D 6725-04. West Conshohocken, ASTM International.

ASTM (2012) Standard test method for electronic friction cone and piezocone penetration testing of soils, D5778-12. West Conshohocken, ASTM International.

Bartlett, S. A., Robbins, G. A., Mandrick, J. D., Barcelona, M., McCall, W., & Kram, M. (2004) Comparison of hydraulic conductivity determinations in direct push and conventional wells. U.S. Naval Facilities Engineering Command, Engineering Service Center, Technical Report TR-2252-V.

Burk, L., & Cook, P.G. (2015) A simple and affordable system for installing shallow drive point piezometers. Groundwater Monitoring & Remediation, 35(3), 101–104.

Butler, J. J., Jr. (1998) The design, performance, and analysis of slug tests. Boca Raton: Lewis Publishers.

Butler, J. J., Jr. (2002) A simple correction for slug tests in small-diameter wells. Ground Water, 40, 303–307.

Butler, J. J., Jr., Dietrich, P., Wittig, V., & Christy, T. (2007) Characterizing hydraulic conductivity with direct push permeameter. Ground Water, 45, 409–419.

Butler, J. J., Jr., Healey, J.M., Zheng, L., McCall, W., & Schulmeister, M.K. (1999) Hydrostratigraphic characterization of unconsolidated alluvial deposits with direct-push sensor technology. Kansas Geological Survey Open-File Report 99-40.

Butler, J. J., Jr., Healey, J. M., McCall, G. W., Garnett, E. J., & Loehide, S. P., II (2002) Hydraulic tests with direct push equipment. Ground Water, 40, 25–36.

Charette, M. A., & Allen, M. C. (2006) Precision ground water sampling in coastal aquifers using a direct-push shielded-screen well-point system. Ground Water Monitoring & Remediation 26 (2), 87–93.

Cordry, K. E. (1991). HydroPunch™ II–The Second Generation. A New In-situ Ground Water Sampling Tool. In Proceedings of the Fifth National Outdoor Action Conference on Aquifer Restoration, Ground Water Monitoring, and Geophysical Methods (pp. 715–723). Dublin, Ohio: National Ground Water Association.

Dietrich, P., Butler, J. J., Jr., & Faib, K. (2008) A rapid method for hydraulic profiling in unconsolidated formations. Ground Water, 46, 323–328.

Dietze, M., & Dietrich, P. (2012) Evaluation of vertical variation in hydraulic conductivity in unconsolidated sediments. Ground Water, 50, 450–456.

Edge, R. W., & Cordry, K. (1989). The Hydropunch™: An in situ sampling tool for collecting ground water from unconsolidated sediments. Groundwater Monitoring & Remediation, 9(3), 177–183.

Flach, G. P., Harris, M. K., Smits, A. D., & Syms, F. H. (2005). Modeling aquifer heterogeneity using cone penetration testing data and stochastic upscaling methods. Environmental Geosciences, 12(1), 1–15.

Henebry, B.J., & Robbins, G.A. (2000) Reducing the influence of skin effects on hydraulic conductivity determination in multilevel samplers installed with direct push methods. Ground Water, 38, 882–886.

Kober, R., Hornbruch, G., Oeven, C., Tischer, L., Großmann. J., Dietrich, P., Weiß, H., & Dahmke, A. (2009) Evaluation of combined direct-push methods used for aquifer model generation. Ground Water, 47, 536–546.

Lammons, T. L., Mann, T. A., & Pelletier, A. M. (1989) An Assessment Tool for Sampling Ground Water in the Undisturbed Saturated Zone. In Proceedings of the Third National Outdoor Action Conference on Aquifer Restoration, Ground Water Monitoring, and Geophysical Methods (pp. 345–356). Dublin, Ohio: National Water Well Association.

Lessoff, S. C., Scheidewind, U., Leven, C., Blum, P., Dietrich, P., & Dagan, G. (2010) Spatial characterization of the hydraulic conductivity using direct-push injection logging. Water Resources Research, 46, W12502.

Liu, G., Bohling, G. C., & Butler, J. J., Jr. (2008) Simulation assessment of the direct-push permeameter for characterizing vertical variations in hydraulic conductivity. Water Resources Research, 44, W02432.

Liu, G., Butler, J. J., Jr., Bohling, G. C., Reboulet, E., Knobbe, S., & Hyndman, D. W. (2009) A new method for high-resolution characterization of hydraulic conductivity. Water Resources Research, 45, W08202.

Liu, G., Butler, J. J., Jr., Reboulet, E., & Knobbe, S. (2012) Hydraulic conductivity profiling with direct push methods: Grundwasser – Zeitschrift der Fachsektion Hydrogeologie, 17, 19–29.

Lowry, W., Mason, N., Chipman, V., Kisiel, K., and Stockton, J., 1999, In-situ permeability measurements using direct push techniques: Phase II topical report. Science and Engineering Associates, report prepared for the DOE Federal Energy Technology Center.

Lunne, T., Powell, J. J. M., & Robertson, P. K. (1997) Cone penetration testing in geotechnical practice. London: Blackie.

McCall, W., Butler, J.J., Jr., Healey, J. M., Lanier, A. A., Sellwood, S. M., & Garnett, E. J. (2002) A dual-tube direct-push method for vertical profiling of hydraulic conductivity in unconsolidated formations. Environmental & Engineering Geoscience, 8, 75–84.

McCall, W., Christy, T. M., Christopherson, T., & Issacs, H. (2009). Application of direct push methods to investigate uranium distributions in an alluvial aquifer. Ground Water Monitoring & Remediation, 29(4), 65–76.

Paradis, D., Lefebvre, R., Morin, R. H., & Gloaguen, E. (2011) Permeability profiles in granular aquifers using flowmeters in direct-push wells: Ground Water, 49, 534–547.

Parez, L. & Faureil, R. (1988) Le piézocône. Améliorations apportées à la reconnaissance de sols. Revue Française de Géotech, 44, 13–27.

Pitkin, S. E., Cherry, J. A., Ingleton, R.A., & Broholm M. (1999) Field demonstrations using the Waterloo Ground Water Profiler. Ground Water Monitoring & Remediation, 19(2), 122–131.

Robertson, P. K. (1989) Soil classification using the cone penetration test. Canadian Geotechnical Journal, 27, 151–158.

Robertson, P. K. (2010a). Soil behaviour type from the CPT: an update. In 2nd International Symposium on Cone Penetration Testing.

Robertson, P. K. (2010b). Estimating in-situ soil permeability from CPT & CPTu. In Memorias del 2nd International Symposium on Cone Penetration Testing, California State Polytechnic University Pomona, CA.

Robertson, P. K., & Cabal, K. L. (2010) Guide to cone penetration testing for geotechnical engineering (3rd Ed.). Signal Hill California: Gregg Drilling and Testing.

Schulmeister, M. K., Butler, J. J., Jr., Healey, J. M., Zheng, L., Wysocki, D. A., & McCall, G. W. (2003) Direct-push electrical conductivity logging for high-resolution hydrostratigraphic correlation. Ground Water Monitoring & Remediation, 23(3), 52–62.

Schulmeister, M. K., Butler, J. J., Jr., Franseen, E.K., Wysocki, D. A., & Doolittle, J. A. (2004) High-resolution stratigraphic characterization of unconsolidated deposits using direct-push electrical conductivity logging: A floodplain-margin example. In J. S. Bridge & D. W. Hyndman (Eds.), Aquifer characterization, Special Publication No. 80 (pp. 67–78). Tulsa: SEPM (Society for Sedimentary Geology).

Sellwood, S. M., Healey, J. M., Birk, S., & Butler, J. J., Jr. (2005) Direct-push hydrostratigraphic profiling: coupling electrical logging and slug tests. Ground Water, 43, 18–29.

Smolley, M., & Kappmeyer, J. C. (1991). Cone Penetrometer Tests and HydroPunch® Sampling: A Screening Technique for Plume Definition. Groundwater Monitoring & Remediation, 11(2), 101–106.

USDA (2012) Chapter 11, Cone penetrometer. Part 631 Geology, National Engineering Handbook. U.S. Department of Agriculture Natural Resources Conservation Survey.

USEPA (2005) Groundwater sampling and monitoring with direct push technologies. U.S. Environmental Protection Agency, Office of Solid Waste and Emergency Response.

Walsh, D., Turner, P., Grunewald, E., Butler, J., Knight, R., Reboulet, E., Knobbe, S., Christy, T., & McCall, W. (2011) Field demonstration of nuclear magnetic resonance (NMR) logging tools for groundwater and environmental investigations. In 24rd EEGS Symposium on the Application of Geophysics to Engineering and Environmental Problems, April, 2011.

Zemo, D. A., Delfino, T. A., Gallinatti, J. D., Baker, V. A., & Hilpert, L. R. (1995). Field Comparison of Analytical Results from Discrete-Depth Ground Water Samplers. Groundwater Monitoring & Remediation, 15(1), 133–141.

Zlotnick, V. A., Burbach, M., Swinehart, J., Bennett, D., Fritz, S.C., Loope, D. B., & Olaguera, F. (2007) Using direct-push methods for aquifer characterization in dune-lake environments of the Nebraska Sand Hills. Environmental & Engineering Geoscience, 13, 205–216.

Chapter 13
Tracer Tests

Groundwater tracer tests involve the use of existing or introduced variations in water chemistry or properties to obtain information about groundwater flow rates and directions, aquifer hydraulic and transport properties, and fluid–rock interactions. Tracer tests vary greatly in their objectives and complexity. Natural or existing anthropogenic variations in water quality may be cost-effectively taken advantage of to provide information on groundwater flow direction and rates. Key elements of tracer tests are determination of type test (e.g., natural versus forced gradient; qualitative versus quantitative), selection of tracer(s), development of a monitoring program, and data analysis. Forward numerical modeling of tests is strongly recommended to evaluate if testing objective are feasible and the optimal testing program for meeting project goals, based on plausible site hydrogeological conditions.

13.1 Introduction

Groundwater tracer tests essentially involve the use of existing or introduced variations in water chemistry to obtain information about aquifer properties. Tracer tests are most often used to obtain information on the direction and velocity of the flow of groundwater and associated contaminants, hydraulic conductivity, effective porosity, transport parameters (e.g., dispersivity values), and the presence of preferential flow paths. Tracer tests may also be used to obtain information on phase volumes, biological activity (decay constants), and cleanup efficiency (Shook et al. 2004). Tracer testing was reviewed by Davis et al. (1985), Mull et al. (1988), Käss (1998), Shook et al. (2004), Ptak et al. (2004) and Taylor and Greene (2008). The use of tracers and other means to estimate aquifer recharge was reviewed by Maliva and Missimer (2012).

Tracer tests are performed by either introducing a tracer into the investigated groundwater system or taking advantage of existing natural or anthropogenic

variations in water chemistry. The latter chemical variations are referred to as environmental tracers. Environmental tracers include atmospheric tracers (tritium, CFCs) and groundwater contamination. Applied or introduced tracers are nonnatural constituents (or constituents that are naturally present at low concentrations) that are intentionally added into a groundwater system (Divine and McDonnell 2005). Natural constituents (e.g., chloride and bromide) are introduced at concentrations markedly different from their natural or background concentration in the groundwater system. The great advantage of tracer tests is that the movement of some dyes and other nonreactive tracers almost exactly replicates the movement of water (and many dissolved solutes) through the aquifer (Taylor and Greene 2001).

Tracer tests may also have large volumes of investigation (depending upon the test type). A basic limitation of tracer tests is that the interpretation of the test data involves indirect methods and the results are not unique. Different combinations of aquifer architectures and properties can result in a given tracer test result (Shook et al. 2004). Hence, data from other aquifer characterization methods are needed for tracer test design and to constrain tracer test interpretations. Tracer movement between wells is strongly influenced by aquifer heterogeneity and may also be affected by vertical flow within wells. Borehole flowmeter logging of both tracer injection and withdrawal wells is, therefore, strongly recommended, to quantify both aquifer heterogeneity and vertical borehole flow (Riley et al. 2011; Basiricó et al. 2015). Basiricó et al. (2015) presented a detailed strategy of conducting tracer tests between boreholes that involves single-well and cross-well flowmeter logging, which was named the "Bh-flow tracer test". Flowmeter logging should be performed prior to tracer testing so that the information obtained on aquifer heterogeneity and vertical borehole flow can be used to determine optimal tracer amounts and injection and sampling points.

Tracer tests have their greatest value as one component of multiple-element aquifer characterization programs. The tests may be the primary data source when the question of concern is solute travel times between points. In other investigations, tracer tests can be used to constrain interpretations. For example, Shapiro (2011) proposed that environmental tracer concentration data be used as calibration targets in models that incorporate flow and chemical transport in both permeable fractures and rock matrix.

13.2 Tracer Tests Types—Qualitative and Quantitative Tests

A variety of tracer test types are performed in groundwater investigations with the selection of test type depending upon the data required for a given investigation and local hydrogeological conditions, which may constrain the type of tests that are practicably possible. Budgetary constraints may also limit the type of tracer testing that may be performed. For a given type of test, there are also a number of test

variables that need to be considered such as specific tracer(s) used, tracer amount and method of introduction, number and location of monitoring points, method(s) of monitoring, and test duration.

A basic distinction is between qualitative and quantitative tracer tests. Qualitative tests are used to establish if a hydrologic connection exists between two points. Qualitative tests simply involve injecting a tracer at one point in a groundwater system and looking for it at downstream locations. A common type of qualitative tracer test is to inject (or otherwise introduce) a tracer into a sinkhole and monitoring for its presence at nearby springs and other discharge points. Qualitative tests can also provide estimates of travel times and, in turn velocity. However, negative results are not necessarily diagnostic. Nondetection of a tracer could be due to its adsorption by aquifer materials (Shook et al. 2004).

Quantitative tests are used to quantify flow paths and determine aquifer hydraulic, solute-transport, and geochemical parameters. These tests require data on both tracer concentration and discharge versus time since the introduction of the tracer. The primary data from quantitative tracer tests are tracer breakthrough (e.g., dye-recovery) curves, which are plots of tracer concentration at a sampling point versus time (Fig. 13.1). Tracer concentrations may be expressed as either actual concentrations or normalized concentrations, which are the measured concentrations divided by mass of dye injected. The use of normalized concentrations allows for comparison of tests using different tracer masses or volumes.
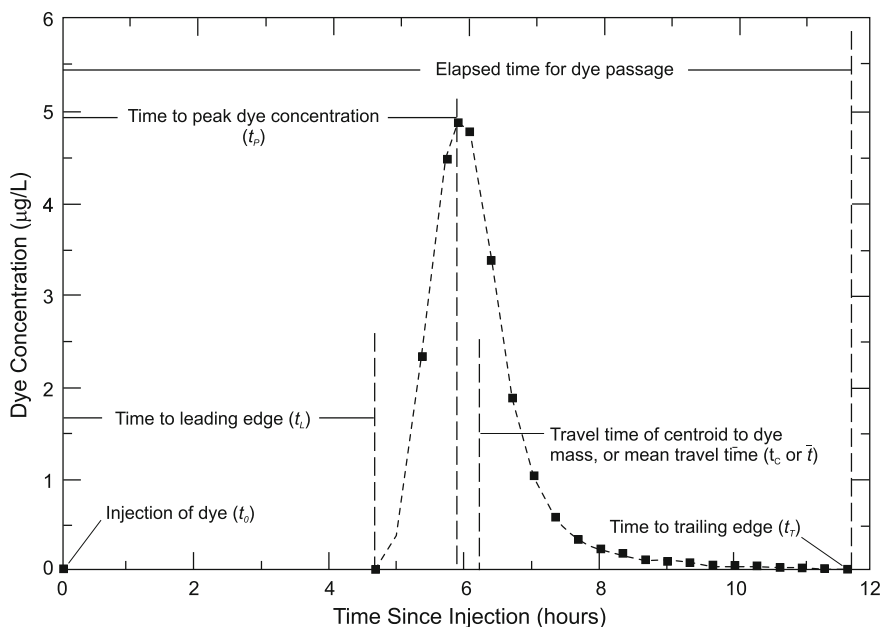
Fig. 13.1 Example of a dye breakthrough curve with key parameters (from Taylor and Greene 2001 and Mull et al. 1988)

Point sampling is critical because sampling of a large aquifer thickness (e.g., entire open-hole or screened interval of a well) gives an average value for tracer concentration, which can result in incorrectly large dispersivity values (Domenico and Schwartz 1998). Retardation of reactive tracers (e.g., sorption of susceptible tracers) can also result in incorrect large dispersivity values. Pickens et al. (1981) documented in a field experiment that dispersivity values obtained using a reactive tracer were typically a factor of about 2–5 larger than dispersivity values obtained from tests using a nonreactive tracer.

The key parts of tracer breakthrough curves are (Mull et al. 1988; Kilpatrick and Wilson 1989)

- t_L, First detection; time elapsed to arrival of the leading edge of the breakthrough curve
- t_P, Time elapsed to peak concentration
- t_c, Time elapsed to concentration centroid
- t_T, Time elapsed to the trailing end of the breakthrough curve

Mean tracer velocity is a measure of the flow rate of the centroid of the tracer mass (distance/time). The distance can be either the straight line distance or a distance corrected for sinuosity. Apparent velocity is based on the map straight line distance (Mull et al. 1988).

The shape of breakthrough curves provides information on dispersion and hydraulic properties of the conduits system. In the case of a single flow path from tracer source to measurement point, the breakthrough curve will consist of a single peak whose width is proportional to the longitudinal dispersivity. Multiple peaks may represent multiple flow routes. For example, a smaller secondary peak after the main peak may represent a subsidiary component of the total flow (and tracer transport) that traveled by a slower or more circuitous flow path (Fig. 13.2). Breakthrough curves for dye tracer tests performed in the karstic Villaneuna del Rosario system (Andalusia, Spain) indicate the passage of three tracer clouds corresponding to primary conduits, secondary conduits, and fissures (Mudarra et al. 2014).

Fig. 13.2 Diagram of a multiple peak breakthrough curve. The later secondary peak represents tracer transport from an addition slower or longer flow path
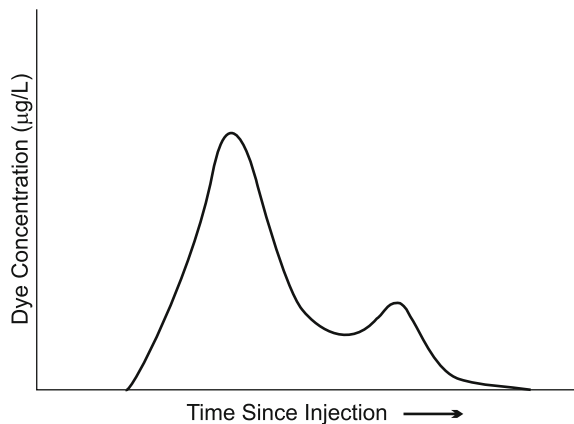
Total tracer recovery is the amount of tracer recovered at all sampling points. It requires that all relevant locations be properly monitored. Low recovery often results from improper determination of all down-gradient receptors (e.g., discharge points), or from the use of a tracer that is adsorbed or degrades during the test.

Transport parameters (dispersivity values and effective porosity) are derived through inverse modeling using numerical or analytical tools. A conceptual model is selected and model parameters are adjusted until the model-computed break-through curve matches the observed breakthrough curve (National Research Council 1996; Shook et al. 2004; Benischke et al. 2007). Forward modeling using an initial conceptual model and parameter values can be used to predict the results of different tracer test design options (Sect. 13.6).

Methods used for the interpretation of environmental tracer data in more uni-formly porous media (e.g., based on plug flow) may not be applicable to dual-porosity systems, such as fractured rock and karstic limestone (collectively referred to as fracture rock; Shapiro 2011). With respect to fractured rock, the adequacy of using simple analytical models to analyze tracer tests in fractured rock is open to question (National Research Council 1996). A realistic analysis may require a numerical model to simulate flow and transport in a heterogeneous domain, which would require intensive geological, geophysical, and hydraulic data as supportive information (National Research Council 1996). The complexities associated with interpretation of tracer data in fractured systems include (Shapiro 2011)

- diffusion between fractures and the rock matrix
- greater dispersive mixing due to the high degree of variability in velocity
- potential for mixing of waters with dramatically different velocities and flow paths.

A difficulty with parameter determination by calibration of a flow and transport model is that groundwater transport models may often induce oscillations or numerical dispersion depending upon the model mesh size, time steps, and exci-tation (Dassargues 1997). Inverse methods for calculating transport parameters also yield nonunique solution. Numerical dispersion can be evaluated by a sensitivity analysis and be reduced through the use of smaller grid cell size. Nevertheless, numerical dispersion in numerical models may still result with wide simulated tracer concentration peaks. The grid cell dimension (length in flow direction) should be no more than twice the longitudinal dispersivity (Peclet criterion). Another important issue is that dispersivity is scale dependent in heterogeneous aquifers. Transport parameters fitted during the calibration of a local-scale transport model to breakthrough data may not be appropriate for an upscaled, larger scale regional model. Multiple quantitative tests may be performed to establish the relationship between parameters (e.g., travel time, velocity, and dispersivity) with discharge (Mull et al. 1988) and to evaluate the relationship between different tracers and breakthrough curve parameters.

13.3   Tracer Tests Types—Natural- and Forced-Gradient Tests

Tracer tests can be divided into natural-gradient and forced-gradient tests. Natural-gradient tests measure the transport of tracers under the natural flow of groundwater. The prevailing groundwater flow field is not disturbed except perhaps for brief periods during tracer injection and sampling. Natural-gradient tests provide information on the direction and rate of movement of tracer under the existing hydrologic flow regime. Natural (environmental) tracers can be cost-effective tool for evaluating groundwater flow patterns and mixing. Contaminants from known sources in which the history of discharges is known provide a time-constrained marker. For example, the contaminant plume from a single-spill event can provide data on the direction and rates of groundwater flow.

Forced-gradient tests are performed in a groundwater flow field that is modified by injection or pumping (or both). Forced-gradient tracer testing in fractured-rock aquifers was reviewed by the National Research Council (1996). Forced-gradient tests are typically quicker than natural-gradient tests because of the more rapid induced groundwater flow, and have a greater recovery of tracer. Forced-gradient tests are performed primary to obtain data on aquifer transport parameters. It is important to recognize that tracer test type and conditions affect the results of forced-gradient tests, which generally underestimate longitudinal dispersivity (Ptak et al. 2004).

Several types of forced-gradient tests have been employed in groundwater investigations, which vary depending on the number of wells used and whether the tracer is introduced into a well in which water is being injected or into an observation well (Fig. 13.3). Forced-gradient test types include divergent-flow, convergent-flow, two-well, dipole, and single-well tests. Divergent-flow tests involve the injection of water into a recharge well at constant rate until a steady-state flow field is established. Tracer is then injected into the recharge well as single pulse or a stepped increase in concentration. Tracer concentration is monitored in one or more observation wells.

Convergent-flow tests are the opposite of divergent-flow tests. Water is pumped from a well until a steady-state flow field is established. Tracer is then added, ideally as a pulse, in a separate well. Tracer concentration is monitored in the pumped well and may also be monitored in one or more observation wells. Multiple tests could be simultaneously performed by injecting different tracers in separate wells.

Two-well tracer tests involve the simultaneous injection in one well and pumping from another well, if possible at the same rate. A steady-state flow field is first established, and then tracer is added as a pulsed increase in concentration. The advantage to two-well tests is efficient water management in that the test can be performed without additional water being required or water produced that requires disposal. Water from the pumped well can be piped to the injection well. However, consideration has to be given to the recycling of tracer (i.e., tracer recovered in the

Divergent flow test
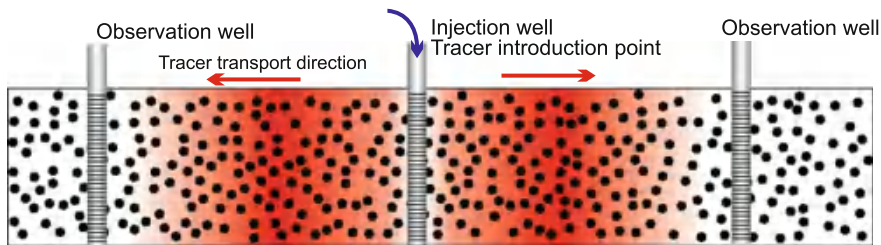
Convergent flow test
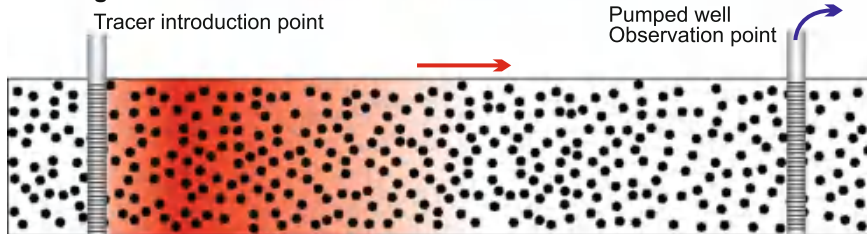
Convergent flow test (closed circulation)
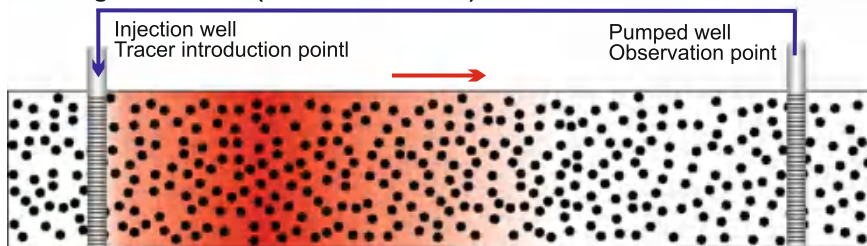
Convergent flow test (dipole test with closed circulation)
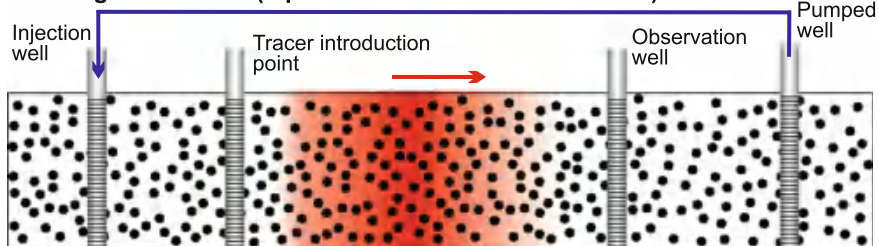
Fig. 13.3   Conceptual diagram of basic multiple-well forced-gradient test types

production well is reinjected) in long-duration tests. Two-well tracer tests have the advantage that a unidirectional flow field is established (except perhaps in a highly anisotropic aquifer), which allows for relatively rapid recovery of a large mass of the tracer.

   The dipole test is a variety of the two-well tracer test in that tracer may either be
introduced or monitored in one or more observations wells located between the
injection and pumped well. Dipole tests also have the advantage that they can be
performed with a closed circulation system. Recycling of tracer may be avoided if
the test is completed before the tracer reaches the pumped well.

   Single-well tracer tests (also referred to as single-well pulse and push-pull tests)
involve injection of the known volume of water having a known tracer concen-
tration into a well and then pumping the well to recover the tracer. The volume and
concentration of tracer in the recovered water are recorded. Tracer-dilution tests
involve releasing a tracer in a well and measuring its dilution over time to calculate
the ambient groundwater flow rate.

13.4   Single-Well Tracer Tests

Single-well tracer tests have the advantages of requiring only a single well (which
can be an existing well) and that tests can be performed to recover all of the tracer,
which may be a regulatory concern. Dispersivity values are obtained using
single-well tracer tests by injecting water containing a conservative tracer into an
aquifer and then immediately pumping the well to recover the injected water. The
data collected for the determination of the dispersivity values are the ratio of the
measured tracer concentration (C) and original tracer concentration (C_0) and the
ratio of the recovered volume of water (U_r) and the total injected volume of water
(U_i), as follows (Gelhar and Collins 1971; Pickens and Grisak 1981; Fetter 1998):

$$\frac{C}{C_0} = \frac{1}{2} \, \text{erfc} \left(\frac{(U_r - U_i) - 1}{\left\{ \frac{16}{3} (a_L = R_f)[2 - (1 - U_r = U_i)]^{1=2} [1 - (U_r = U_i)] \right\}^{1=2}} \right) \tag{13:1}$$

where
erfc   complementary error function
a_L longitudinal dispersivity (m),
R_f average front position of the injected water at the end of the injection period
       (m), which is defined as

$$R_f = \left(\frac{Qt}{pbn} \right)^{1=2} \tag{13:2}$$

where
Q   rate of injection (m^3/d),
t   total injection time (d)
b   aquifer thickness (m)
n   porosity (fractional)

Longitudinal dispersivity values are estimated by fitting the measured (C/C_0) versus (U_r/U_i) data to analytical curves generated from Eq. 13.1 using different a_L values.

Gouze et al. (2008, 2009) addressed the use of single-well injection-withdrawal (SWIS) tests to evaluate non-Fickian mass transport within immobile zones, which is manifested by a pronounced asymmetry of breakthrough curves. The CoFIS and TELog system is described, which consists of a dual-packer system (CoFIS) equipped with a high-resolution sensor (TELog) for fluorescence dye concentration monitoring. Advantages of the CoFIS and TELog system include that it avoids dispersion in the tubing, valves, and manifolds and has a very high time resolution (9 s) of measurements. A series of measurements at increasing volumes of investigation can also be readily performed.

A limitation of the use of single-well tracer tests to obtain dispersivity values is the relatively small volume of investigation of the tests. Dispersivity values obtained from the injection and recovery of a small value of water may not be accurately scaled up (Domenico and Schwartz 1998). Breakthrough curves in multiple-well tests (tracer concentrations measured in observation wells) are determined mainly by the hydraulic conductivity of the region between the injection and observation wells. Aquifer dispersivity values tend to show scale dependence due to the effects of aquifer heterogeneity with respect to hydraulic conductivity (Güven et al. 1985). In the case of single-well tests, in which water flows horizontally and radially diverges during injection and radially converges during recovery, the relative concentration versus time data at the injection and withdrawal well are primarily a function of local dispersion. During longer duration tests, vertical dispersion becomes increasingly important, causing solute in high-hydraulic conductivity layers to migrate into adjacent low hydraulic conductivity strata (Güven et al. 1985). When the advective process is accurately simulated (i.e., aquifer heterogeneity is considered), the values of longitudinal dispersivity will be small, constant, and on the order of the values measured between at individual levels (strata) on the aquifer and in the laboratory (Güven et al. 1985).

The drift and pump back test is a variation of the single-well tracer test (Hall 1993). Tracer is introduced into a test well and is allowed to move away from the wellbore under natural gradient. The tracer is then recovered by pumping. Flow velocity is calculated as a function of the pumping rate and time required to recover the center of mass of the tracer plume.

The operational (cycle) testing of aquifer storage and recovery system is in essence a large-scale single-well tracer tests when the injected water has distinct differences in composition compared to the native groundwater. If there is a

Fig. 13.4 Calibration results
of solute-transport model of
Destin Water Users ASR
system cycle test no. 1, which
was in essence a single-well
tracer test. The percent
injected water was calculated
using binary mixing equations
and conservative parameters.
Despite using very low
dispersivity values, the
simulation results still tend to
slightly underestimate
injected water percentage due
to numerical dispersion
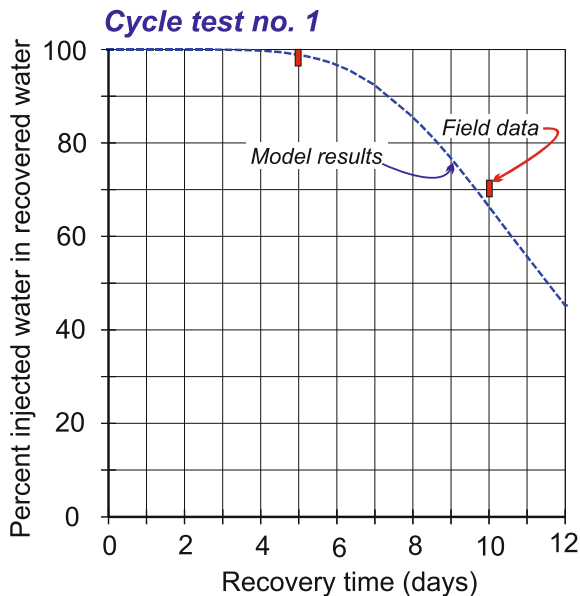
difference in concentration of a conservative species between the injected and native water (e.g., chloride), then the test data could also be used to evaluate physical mixing (dispersivity). For example, longitudinal dispersivity and effective porosity values were estimated for the storage zone of an ASR system in Destin, Florida, through the calibration of a solute-transport model for the operational cycles (Maliva et al. 2013, Fig. 13.4). The modeling was performed using the MODFLOW (McDonald and Harbough 1988) and MT3DMS (Zheng and Wang 1999) codes using salinity-related parameters (chloride and TDS) and fluoride as calibration targets. The inverse modeling results indicate that the storage zone, a sand-and-gravel aquifer, has a high effective porosity (35 %) and low longitudinal dispersivity (<0.2 m). A small grid size (0.4 m) was required in core area of the model to reduce numerical dispersion.

Operational testing data from an ASR system were used to evaluate the significance of secondary porosity (fractures) in groundwater flow at a site in Melbourne, Australia (Miotiński et al. 2011). Electrical conductivity was used as a tracer to differentiate between injected freshwater and native brackish groundwater. The operational data were simulated using an equivalent porous medium (EPM) approach and discrete fracture approach that incorporated diffusion between the matrix and fractures. Both model approaches could provide a good fit to the data, but the EPM approach required the use of a hydrogeologically unrealistically large longitudinal dispersivity value. The best fit was a simulation with 100 % of the flow in fractures.

There is great potential in the use of single-well (push-pull) tracer tests to evaluate in situ geochemical processes in aquifers. In situ tests would be expected to provide results more indicative of actual conditions than laboratory experiments in

which the samples may be disturbed and the geochemical environment differs from natural aquifer conditions. Push-pull tests have been used to estimate distribution coefficients (Pickens et al. 1981). More elaborate tests can be used to evaluate occurrence and rates of various physical and microbial reactions. The injected solution consists of a nonreactive tracer and reactive constituents (Istok et al. 1997; Haggerty et al. 1998). During the extractive phase, the concentration of tracer, reactants, and possible reaction products are measured. Istok et al. (1997) used push-pull tests to evaluate the rates of aerobic respiration, denitrification, sulfate reduction and methanogenesis in aerobic and aerobic parts of a petroleum-contaminated aquifer. Haggerty et al. (1998) provided a method for the use of push-pull tests to determine reaction rate coefficients, such as microbial denitrification in a petroleum-contaminated aquifer.

Redox reactions in some ASR systems resulted in the release of arsenic and metals that cause stored water to exceed the applicable groundwater quality standards. Single-well, push-pull, tracer tests could be an effective means of evaluating the potential for adverse reactions (Norton 2007), as well as obtaining data on aquifer transport properties. Water chemically similar to the water to be stored could be injected and the recovered water tested for arsenic and metals of concern. The single-well tests could be performed on an exploratory well, monitoring well, or existing well to determine if adverse fluid–rock interactions will be a challenge at a site in advance of construction of a pilot or full-scale system.

13.5   Tracer-Dilution Tests

Tracer-dilution tests involve the introduction of a tracer into a test well and then monitoring of its concentration over time. The basic concept is that the horizontal flow of water through a well will result in a progressive reduction in the concentration of the tracer in the well over time as water containing the tracer flows out of the well and tracer-free water flows into the well. Groundwater flow velocity is calculated as a function of the rate of dilution over time. Initial tracer-dilution tests used radioactive tracers, but fluorescent dyes, ionic tracers, or deionized water are now more commonly used (Drost et al. 1968; Lewis et al. 1966). Tracer-dilution tests can be performed in either the natural flow field or a flow field induced by local pumping or injection. The tests may be performed on either the entire open-hole or screened zone of a well or on intervals isolated using packers. Tracer-dilution testing was reviewed by Hall (1993), Palmer (1993), Cook (2003), Pitrak et al. (2007), and West and Odling (2007).

There are several variants of tracer-dilution tests. Tracer can be applied quickly and evenly distributed throughout the tested interval of a well. In a near homogenous aquifer or aquifer zone, single measurements of tracer concentration may be made to obtain an average velocity. Alternatively, the test interval can be logged (by passing a probe with a tracer detector through the tested interval) in order to detect vertical variations in tracer concentration that are related to aquifer heterogeneity. Point

dilution tests can be run with the release of a point source of tracer, which allows for the measurement of vertical movement in the well. Multiple-well dilution tests measure tracer concentrations in observation wells, while a production well is being pumped or water is injected at a constant rate. Drawdown caused by the pumping induces water and thus tracer movement in the observation well. Differences in transmissivity between flow zones (e.g., fractures) can result in differences in drawdown, which can induce vertical water flow within observation wells.

The presence of the well distorts the flow field, which needs to be considered during the analysis of the data. The basic equations for interpreting tracer-dilution tests are Hall (1993)

$$v^* = -\left(\frac{V}{At}\right)\ln\left(\frac{C_t}{C_0}\right) \tag{13:3}$$

$$v^* = vna \tag{13:4}$$

where (using consistent units)

- v^* apparent velocity of groundwater flow through and normal to the axis of the wellbore
- V   volume of the test interval (intra well)
- A   cross-section area of the test interval
- t   time
- C_t concentration at time "t"
- C_0 concentration at time t = 0
- v   seepage velocity
- n   effective porosity (unitless)
- a   flow distortion factor (dimensionless), due to the hydraulic conductivity of the well being greater than that of the formation. Hall (1993) reported a flow distortion factor of between 7 and 8, which was determined using effective porosity and net velocity from companion data from the test site

Pitrak et al. (2007) presented a similar equation (using consistent units)

$$\ln C_t = (-2v_a=pr)t + \ln C_0 \tag{13:5}$$

where r = the borehole radius and v_a is apparent filtration velocity (discharge per unit area). The word "apparent" means the velocity is affected by the borehole presence toward higher values in comparison with far field Darcy filtration velocity (Pitrak et al. 2007). Equation (13.5) can be solved using a linear plot of ln(C) versus t. To correct apparent velocity to actual filtration velocity, it is necessary to divide the computed apparent velocity by a drainage coefficient, for which the widely accepted value is 2 (Pitrak et al. 2007).

Hall (1993) documented the use of the point dilution method to create a hydraulic conductivity versus depth profile, based on the concept that flow zones will have greater dilution and thus lesser tracer concentrations. Bromide was used

as a tracer, and submersible ion-specific probe equipment was developed to obtain in situ concentration data. A key issue is to avoid mixing cause by movement of probe in well during logging. The probe diameter thus needs to small relative to casing diameter. Sampling techniques that involve removal of water samples can disturb the tracer concentrations (Lewis et al. 1966).

Pitrak et al. (2007) obtained data of heterogeneity with respect to hydraulic conductivity by performing a time series of measurements. The tested wells were periodically logged using a photometric probe with a monochromatic light source and detector sensitive to the wavelength of the adsorption maximum of the Brilliant Blue FCF food dye tracer that was used in the test.

The point dilution method assumes that the 'a' factor is constant throughout well, which may not be the case if there is significant variation in sorting. The tracer-dilution method also assumes (Moser et al. 1957; Lewis et al. 1966)

- steady-state conditions
- uniform groundwater flow and tracer distribution
- tracer concentration diminution with time is due only to horizontal groundwater flow
- no vertical flow in well.

In aquifers with very sluggish groundwater flow, diffusion of the tracer can result in significant reductions in concentration and thus over estimation of advective flow velocity. The tracer needs to be introduced evenly in the test interval and should not be introduced into the adjoining formation. A circulation system can be used in which a pump is placed near the base of the borehole with its outlet at the top of the water in the well (Cook 2003). Using this method, the tracer can be introduced and mixed without either removing or introducing water to the well.

Brainerd and Robbins (2004) presented a conceptually simple single-well tracer-dilution technique for fracture characterization. A tracer solution is injected into the bottom of the well, while water is pumped at a greater rate from the top of the well. The goal is to have a lower head in the well than in all of the fractures so that groundwater is only flowing into the well. Tracer is injected and the well is pumped until steady-state conditions are established. Discrete samples are then taken through the entire depth of the well to generate a concentration profile. The flow from each fracture can be quantified from the tracer dilution.

The transmissivity of fractures (T_f) is calculated using the Thiem solution

$$T_f = \frac{Q_f}{2pDh_f}\ln\left(\frac{r_e}{r_b}\right) \quad (13.5)$$

Dh_f change in hydraulic head experience at fracture (m of water)
Q_f fracture flow rate (m^3/d)
r_e effective radius (radius of investigation) (m)
r_b borehole radius (m)

The flow rate from individual fractures is determined from tracer dilution. The change in head at fractures (Δh_f) is the difference between the hydraulic head of the fracture (h_f) and the steady-state elevation head in the well (h_w). To determine h_f, a regression of h_w versus Q_f values from multiple pumping rates is prepared, with h_f being the value of h_w at $Q_f = 0$. A r_e value of 9.8 was used in study of fractured Gneiss at the University of Connecticut campus. A limitation of method is the need to pump significant quantities of water. The method also assumes that all fractures in the vicinity of the well are hydraulically isolated.

Tracer-dilution tests can also be performed using dissolved oxygen (DO) as a tracer in aquifers that contain anoxic or low dissolved oxygen water (Chlebica and Robbins 2013). Dissolved oxygen has the advantages that it is nontoxic, can be inexpensively increased through aeration, and is readily measured in situ using a probe. Chlebica and Robbins (2013) documented two methods for introducing dissolved oxygen. A circulation system can be used in which water is pumped from the well, aerated at land surface, and then reinjected in well. The advantage of using a circulation system is that a near uniform profile of dissolved oxygen concentration with depth can be introduced in the well. Alternatively, compressed air can be injected using a bubbler placed at the bottom of the well. The bubbler system produces a profile of increasing concentration with increasing depth. After the DO is introduced, a series of DO concentration versus depth profiles are obtained. Local greater dissipation of DO concentration is indicative of flow into the well. Depth intervals with relatively slow dissipation indicate stagnant (no flow conditions). The tests can be performed either under static conditions or with flow into or out of the well induced using a slug. Use of DO as a tracer requires an initial DO concentrations contrast with native groundwater and that the rate of flow into the well is greater than the rate of biotic and abiotic processes that consume DO (Chlebica and Robbins 2013).

Open-well dilution tests in multilayered aquifers can be used to qualitatively identify flow zones and characterize their relative permeability. Quantitative analyses can provide data on aquifer hydraulic parameters. West and Odling (2007) present an analytic solution to the advection-dispersion equation to the specific case of an aquifer system composed of two discrete permeable horizons separated by a much less permeable interval (i.e., there is no hydraulic communication between the layers).

13.6   Tracer Test Implementation

Tracer tests can provide much useful information for aquifer characterization. However, improperly designed and implemented tracer tests may fail to meet test objectives. The proverb "he who fails to plan, plans to fail" strongly applies to tracer testing. Tracer testing programs have five basic elements (Shook et al. 2004):

(1) definition of tracer test objectives
(2) tracer selection and testing
(3) development of implementation strategy
(4) field implementation
(5) test interpretation

Successful quantitative groundwater tracing studies are dependent upon (National Center for Environmental Assessment 1999; Smart 1988)

- conservative behavior of the tracer substance
- precise instrument calibration
- injection of an adequate quantity of tracer
- introduction of the tracer in a manner so that is does not disturb the flow field (in natural-gradient tests)
- sufficient monitoring frequency at all down-gradient receptor
- precise discharge measurements at down-gradient receptors
- sufficient length of monitoring period for total tracer mass recovery

Performing quantitative tracer tests usually involves considerable expense. Tracer tests using artificially introduced tracers commonly fail and the reasons are numerous. The choice of the wrong tracer is the most fundamental problem, usually due to sorption of the tracer onto solids (Davis et al. 1980). Another common source of error is an inadequate understanding of the hydrological and hydrogeological system, specifically the direction and velocity of flow, degree, and type of aquifer heterogeneity, and dispersion and dilution between the injection and sampling point (Davis et al. 1980, 1985).

Successful testing is predicated upon careful and appropriate test design, which generally requires some initial site hydrogeological information and preliminary transport modeling (Divine and McDonnell 2005). The value of forward modeling of the hydrologic system during the planning of tracer tests cannot be stressed strongly enough. Forward numerical solute-transport modeling is performed by simulating the injection of various injected tracer concentrations and volumes and the resulting travel times to and concentrations at different observation points. Multiple runs should be performed using different distributions of reasonable aquifer properties (i.e., a sensitivity analysis performed). Modeling can provide insights into potential rates of tracer movement and the potential concentrations at monitoring points, which can be used to determine whether or not tracer testing can practically provide the required data and to optimize the design of the test. Forward modeling can also provide information on the relationship between tracer mass and concentrations at observation points. Numerical modeling techniques are preferred over analytical techniques in that they inherently have the greater flexibility to incorporated aquifer heterogeneity and thus allow for more hydrogeologically realistic and thus potentially accurate simulations.

As an example of forward modeling of a hypothetical convergent tracer test, a series of synthetic tracer breakthrough curves were generated using the MODFLOW and MT3DMS codes (Fig. 13.5). The simulated test conditions are the
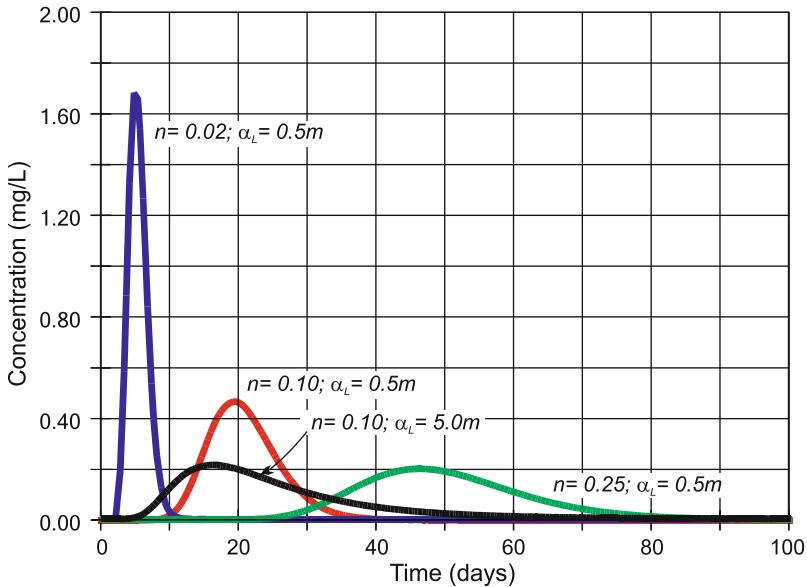
Fig. 13.5 Synthetic tracer breakthrough curves generated by numerical modeling (MODFLOW and MT3DMS) of a hypothetical convergent tracer test. Values of the effective porosity and longitudinal dispersivity were varied

introduction of 1000 g of tracer in 1 m^3 slug of water into a 5 m thick aquifer, which is pumped at a well located 50 m from the injection point. The forward modeling predicts peak tracer concentration and time to peak tracer concentration, both of which are critical for tracer test design. As would be expected, time to peak tracer concentration is highly sensitive to effective porosity. In practice, a series of predictive simulations is performed using the range of likely hydrogeological conditions to determine the envelope of potential tracer transport times and concentrations. Predicted tracer transport times are used to determine the optimal sampling program. The ratio of the introduced tracer volume and concentration to the predicted peak tracer concentrations is used to determine the optimal amount of tracer to be used, which involves consideration of analytical detection limits and natural background concentrations of the tracer.

In the case of an actual test, the model could later be used to interpret tracer test data by finding the best fit synthetic breakthrough curve(s) to the field data. Analytical solutions have long been used to interpret tracer test data. However, widely available numerical flow and solute-transport models, such as MODFLOW and MT3DMS, are suitable for interpretation of tracer test data (Peng et al. 2000). Numerical models have the great advantage that they can be used to simulate more complex hydrogeological conditions, such as layered heterogeneous aquifers. Indeed, incorporation of aquifer heterogeneity into inverse models used for tracer test evaluation is necessary to accurately interpret test data (Peng et al. 2000).

It is also recommended that a qualitative tracer be performed prior to a quantitative test to delineate groundwater flow paths (ensure that all potential dye-resurgence sites are known and sampled), and to provide guidance in selecting observation sites, determining sampling frequency and duration, and assessing possible interference of ambient fluorescent solutes with the detection and measurement of the tracer dye. The goal is to have a good understanding of the tested groundwater system in order to better design and implement the much more labor intensive quantitative tests (Mull et al. 1988; National Center for Environmental Assessment 1999; Taylor and Greene 2001; Shook et al. 2004). For major (i.e., very expensive) tracer tests, column testing using aquifer material to evaluate ion exclusion, adsorption, and geochemical incompatibility issues is recommended (Shook et al. 2004).

13.7   Tracer Selection

Tracers include natural variations in water chemistry or temperature, accidentally introduced chemicals, and intentionally introduced chemicals or materials. Water with a lower concentration of tracer than the ambient groundwater may be used as an inverse tracer. The ideal tracer is (Davis et al. 1980)

- nontoxic
- inexpensive (both cost of tracer and analyses)
- moves with the flowing water
- easy to detect in trace amounts, preferably in the field
- chemically stable for the desired length of time (duration of the test)
- not present in large amounts in the water being investigated
- not sorbed or otherwise removed during travel through the aquifer.

Unfortunately, the ideal tracer does not exist (Davis et al. 1980) and tradeoffs need to be made in tracer selection. Some of the commonly used tracers are discussed below.

13.7.1   Anionic and Cationic Tracers

A variety of cations and anions can be used as tracers. Chloride and bromide are commonly used because they are conservative in that their concentrations tend not to significantly change as a result of fluid–rock interactions. Anions are, in general, preferred for use as tracers compared to cations as the latter are more reactive with aquifer minerals, particularly clay minerals, through cation exchange (Davis et al. 1985). Anionic tracers should ideally be present at low concentrations in the tested aquifer and should have an inexpensive and accurate analytical method.

Chloride is a very inexpensive tracer as it can be introduced as common salt (sodium chloride). Chloride can also be inexpensively measured in the field by titration. Chloride is naturally present in groundwater and sufficient tracer needs to be added to be clearly detectable above background concentrations. The change in salinity associated with the chloride tracer may also be detected in the field using an electric conductivity meter or probe. A limitation of chloride is that if large amounts need to be introduced to obtain a measurable response at monitoring points, then the increase in salinity can result in density effects (Davis et al. 1980, 1985). Bromide has the advantage of normally being present at very low concentrations in natural fresh groundwater (commonly less than 1 mg/L). Bromide can also be detected at low concentrations with a specific ion electrode.

Korom and Seaman (2012) cautioned that anionic tracers, such as chloride and bromide, may not be conservative in some circumstances because as charged ions, they are subject to adsorption processes. The potential active surface charge depends upon the minerals present and pH of the groundwater. Where the aquifer materials have a negative surface charge, the ion exclusion effect may occur in which the negatively charged ions are excluded from the negatively charged surfaces. The anions accumulate towards the center of pores where there is a greater flow velocity. The transport of anions may, therefore, be more rapid than bulk water flow. On the contrary, where the surface charge of the aquifer minerals is positive, negatively charged anions are attracted to and tend to become adsorbed onto the surfaces. In this case, the transport of the anions will tend to be slower than the bulk groundwater flow (i.e., their transport retarded).

Anion exclusion and anion adsorption are most significant in materials that have relatively high surface changes. These processes are more likely to impact the transport of anions in very fine-grained sediments, which have high concentrations of clays minerals and oxides and associated high total surface areas. Chloride and bromide will behave more conservatively in carbonates and clean (low clay content) quartz sands. The general caveat applies with respect to the use of anionic tracers in that the choice of tracers and interpretation of test results should consider geochemical process that may be active in the studied aquifer.

13.7.2   Inverse Anionic and Cationic Tracers

Most tracer tests are performed by introducing a tracer at a greater concentration than the tracer occurs in groundwater. Inverse tracer tests involve the use of introduced water that has a lower concentration of the tracer than the native groundwater. For example, dilute (deionized) water can be used in tracer tests in formations in which the groundwater has high dissolved solids concentration (e.g., Tsang et al. 1990). Changes in salinity can be measured using a conductivity meter. Inverse tracers have the advantage of avoiding regulatory concerns associated with the introduction of saline water and chemicals into freshwater aquifers. However, freshwater injected into brackish or saline waters may undergo buoyancy

stratification. The inverse tracer approach may require injection of a relatively large amount of freshwater to obtain an adequate detectable signal above the analytical method error.

13.7.3   Fluorescent Dyes

Fluorescent organic dyes have the advantages of relatively low costs and toxicity and being detectable at very low concentrations. Each dye has a characteristic fluorescence peak wavelength and, therefore, multiple dyes may be used and distinguished at the same time (White 2007). The use of fluorescent dyes in tracer tests was reviewed by Smart and Laidlaw (1977).

The concentrations of dyes are measured using a fluorometer (filter fluorometer or spectrofluorometer). Excitation is provided by a light source, commonly a low-pressure mercury lamp. The light passes through a primary filter before entering the sample compartment, where it is absorbed by the dye in the sample. The light is reemitted at a greater wavelength as fluorescence, which passes through a filter opaque to the light passing through the primary filter. The amount of light passing through the secondary filter is measured using a photomultiplier. The sensitivity of fluorometric analysis depends on both the efficiency of the dye in converting excitation energy into fluorescence and the transmission of the filter combination (Smart and Laidlaw 1977). Detectability is a function of background fluorescence, which depends upon the concentrations of suspended solids and natural pigments (Smart and Laidlaw 1977). Fluorescence intensity varies inversely with temperature and pH. The pH dependence is generally not within the range of pH values normally found in groundwater. For example, the significant pH effects on rhodamine-WT fluorescence occur below a pH of 5 (Smart and Laidlaw 1977).

The concentration of dyes may decrease in surface and groundwater environments by processes other than mixing. Some dyes, such as fluorescein, have very high photochemical decay rates and are thus poor choices for surface water testing (Smart and Laidlaw 1977). Adsorptive losses are an important consideration in groundwater tests. In practice, attempts to correct dye concentrations for adsorptive losses are liable to considerable error, and a specific correction curve would be needed for each field test (Smart and Laidlaw 1977). The percent dye loss, and therefore error in flow determinations, will be higher for lower dye concentrations than for high dye concentrations in a given situation (Smart and Laidlaw 1977). Experimental losses are much greater for organic matter-rich sediments and rocks than for clean limestones, quartz sands, and clay minerals (Smart and Laidlaw 1977). Rhodamine-WT has a greater absorption onto organic matter the fluorescein. Lissamine FF and sulphorhodamine B are the most resistant to adsorption of the dyes reviewed by Smart and Laidlaw (1977). Some dyes, such as pyranine, are subject to significant losses to microbiological degradation, which is a concern for long-term tests (Goldscheider et al. 2003).

The most commonly used dyes are fluorescein (yellow green) and rhodamine-WT (orange). Both rhodamine-WT and fluorescein have low toxicities and problems should not be encountered during tracer tests because of the low concentrations used, short test durations, and low toxicities of the dyes themselves (Smart and Laidlaw 1977). Orange dye is preferred where background water has a significant fluorescence at both the green and blue wavelengths (Smart and Laidlaw 1977). Rhodamine-WT has no serious disadvantages. Lissamine FF is the recommended green dye by Smart and Laidlaw (1977) because of its low adsorption tendency, but has the disadvantage of being the most expensive of the considered dyes in terms of the cost per treatment of a volume of labeled water. Fluorescein is suitable for groundwater testing in which photochemical decay is not an issue. Goldscheider et al. (2003) used naphthionate in a tracer tests in karstic strata in Stuttgart, Germany because it is invisible under normal light, which can be an important consideration where discharge points are in populated areas.

13.7.4   Particle Tracers

Particle tracers can be used to trace the general movement of groundwater as well as the movement of suspended solids. An earlier used particle tracer is club moss (Lycopodium) spores, which have been superseded by fluorescent polystyrene microspheres (Goldscheider et al. 2008). Spore nets were used to recover the spores. Fluorescent microspheres are available with different diameters (0.05–90 l m), physical–chemical characteristics, and optical properties (Bernsichke et al. 2007).

Microspheres can be selected that mimic the size and surface properties of microorganisms of concern. The surface charge of the microspheres can be adjusted to approximately match those of microorganisms (Pang et al. 2009). For example, fluorescent microspheres have been used as surrogates for Cryptosporidium parvum oocysts (e.g., Harvey et al. 2008, 2011; Mohanram et al. 2010). Particle tracer testing was performed in Miami-Dade County, Florida, to investigate the potential for Cryptosporidium parvum oocysts to be transported from deep mine lakes into water production wells. Oocyst-sized (1.6, 2.9, and 4.9 mm diameter) carboxylated polystyrene microspheres were injected into a karstic flow zone isolated using packers and recovered from a production well located 97 m away that was open to the same flow zone (Harvey et al. 2008; Mohanram et al. 2010). The test demonstrated particle transport through a flow zone but not whether Cryptosporidium parvum-sized particles could infiltrate from a lake into a production zone. A constraint on the use of fluorescent microspheres for tracer testing is their high cost at the quantities needed for tests (Harvey et al. 2011), especially if they are to be introduced in large quantities into surface water bodies.

13.7.5   DNA Sequence-Based Tracers

DNA sequence-based tracers were reviewed by Ptak et al. (2004). The method involves the use of identical fragments of synthetic DNA molecules, which have the great advantage that they can be detected at extremely low concentrations (theoretically down to one molecule). Numerous different tracers that differ in their sequence of bases could be used in a single test. Tests could be performed with a theoretically unlimited number of tracer locations. The DNA sequence-based tracers have been field tested. The issue remains as to whether it is an economically viable technique for applied hydrogeological investigations.

13.7.6   Dissolved Gas Tracers

Dissolved gas tracers include a variety of inert or poorly reactive gases that are normally present in groundwater in only minute quantities. Tracers used include helium, neon, and other noble gases, and sulfur hexafluoride. Dissolved gases of natural and anthropogenic origin that may already be present in groundwater (i.e., are not intentionally introduced for a tracer test) can also be used for groundwater tracing and age dating.

The advantages of dissolved gas tracers are (Davis et al. 1985; Sanford et al. 1996)

- Tracer solutions can typically be saturated many orders of magnitude above background concentrations without significant changes in the chemical and physical properties of the injected water.
- Tracers can be transported to the site in pressurized containers.
- Tracer gases used are inert in hydrologic systems.
- Relatively constant source concentration can be maintained for extended periods of time with little maintenance.
- Multiple tracers can be injected and analyzed with the same equipment

The primary difficulty associated with dissolved gas tracers is that most sampling techniques are cumbersome and/or expensive (Sanford et al. 1996). Samples need to be collected and stored so that the tracer gas is not lost to the environment. Sanford et al. (1996) proposed some simpler and less expensive procedure for dissolved gas tracer experiments such as passive in situ headspace samplers and a bubbleless injection system that introduces a gas tracer by diffusion through thin-walled tubing that is permeable to the tracer gas.

Natural and introduced gas tracers were used to image the extent and travel times of water recharged into the Orange County Water District (California) surface-spreading and recharge basin system, which have been operated for more than 40 years (Clark et al. 2004). Multizone monitoring wells allowed for evaluation of both the vertical and horizontal extent of the recharged water. Radioisotope

(T/^{3}He) data allowed for the identification of large-scale flow patterns and broadly define groundwater ages. T/^{3}He data is best suited for evaluating groundwater with ages in the decades rather than the 0–2 year range (Clark et al. 2004). The introduced gas tracer experiments (SF$_6$ and Xe isotopes) defined flow patterns in detail over a short time period. The high velocities and often very different breakthrough curves from wells near recharge areas indicate preferential flow through conductive layers in the heterogeneous siliciclastic aquifer (Clark et al. 2004).

13.7.7   Heat as a Tracer

Heat can be an effective tracer and has the advantages of being inexpensive and environmentally benign, and that temperature can be accurately measured in the field (Martin and Dean 1999; Screaton et al. 2004). Temperature data are immediately available for inspection and interpretation. The application of heat as a groundwater tracer was reviewed by Anderson (2005). Heat is transferred in groundwater by advection and conduction. Heat transfer by advection is transported by the bulk movement of heated water. Heat conduction (or thermal conduction) is the flow heat within and through a body due to a thermal gradient. The steady-state heat conduction equation in one dimension has the same form as Darcy's equation

$$q = -kA\frac{du}{dx} \qquad (13.6)$$

where

q   heat flow (W, J/s)
A   cross-section area (m^2)
k   thermal conductivity (W/m °K), which is a function or mineralogy and
            porosity
du/dx   thermal gradient (°K/m)

Heat transfer in sediments is a function of several main variables (Lapham 1989) including the:

- thermal conductivity of the rock-fluid matrix
- volumetric heat capacity of the fluid and rock-fluid matrix
- density of the fluid
- wet-bulk and dry-bulk densities
- vertical fluid velocity.

Temperature for tracer testing is usually measured using some type of temperature probe and data logging systems. Self-contained units are available that automatically measure and record temperature, and simultaneously other parameters

such as electrical conductivity and water levels. Temperature profiles in a well can be measured using standard borehole logging tool. However, standard temperature and fluid conductivity logging tools have the limitation that the instrumentation can only record measurements at a single location at a given time, with the tool having to be moved upon and down the well to create a high-resolution profile (Leaf et al. 2012). Fiber optic-based distributed temperature sensing (DTS) systems can provide stationary readings along the entire length of the sensor cables at spatial intervals as fine as 1 mm or less, and at time intervals of less than 1 min (Hurtig et al. 1994; Leaf et al. 2012).

Most of the applications of heat as a tracer utilized either natural or existing anthropogenic temperature perturbations as opposed to specifically inducing a temperature perturbation for a test. For example, thermal pulses (either positive or negative) from storm events were used as a natural tracer in karst systems to calculate the travel time from recharge to discharge areas (Benderitter et al. 1993; Martin and Dean 1999; Screaton et al. 2004).

The downward propagation of temporal changes in surface water temperature can be used to determine the rate of vertical groundwater flow (Suzuki 1960; Stallman 1963). The variations in temperature may be on either an annual or shorter (e.g., diurnal) frequency. Lapham (1989) utilized temperate profile data beneath streams in Massachusetts and New Jersey that experience annual variations in temperature to evaluate vertical flow velocity and effective hydraulic conductivity. Temperature profiles were obtained from piezometers by taking multiple stepped (as opposed to continuous) readings as a temperature probe (thermistor) was slowly lowered down the well (Lapham 1989). An alternative approach is to construct a series of nested monitoring wells or piezometers at each temperature profile station and equip them with temperature probes connected to a data logging system (or use integrated probes) to provide a continuous record of temperature change over time. Lapham (1989) interpreted the data using inverse numerical modeling, which has become the most commonly used method for analyzing temperature profile data because of the inherent flexibility to simulate actual field conditions and observations.

High-resolution temperature monitoring has been used to estimate infiltration rates from the downward propagation of diurnal variations in surface water temperature into underlying sediments. Becker et al. (2013) used a fiber optic distributed temperature sensing (DTS) to measure percolation rates in a recharge basin in Orange County, California. The DTS system allowed temperatures to be measured every meter along a cable at resolutions of up to 0.02 °C. In the reported pilot project, a 150 m cross section of a basin was monitored using a cable laid at three depths (surface, 0.33 and 0.98 m). The rate of infiltration was obtained from the phase lag between the surface temperature diurnal oscillation and the correlated oscillation at the two monitored depths below the bed surface.

Streambed temperature data can provide valuable information on the pattern of stream flow, which can facilitate estimates of stream flow frequency, duration, travel time, and transmission losses (Constantz et al. 2001) and to obtain estimates of vertical hydraulic conductivity, flow velocity, and recharge rates and locations.

The basic concepts behind using of heat as a tracer of near-stream water movement are summarized by Constantz et al. (1994, 2001) and Constantz and Stonestrom (2003). Shallow surface water and surficial soils experience diurnal variations in temperature that reflect the atmospheric variations in temperature. Groundwater temperatures on the contrary are relatively constant on a diurnal time scale. Streambed temperature measurements are performed by installing temperature probes within channel sediments. Recorded changes in temperatures may reflect stream flow events (with associated infiltration) in ephemeral channels, as well as precipitation and the passing of cold fronts.

The temperature patterns associated with gaining, losing, and dry ephemeral stream conditions (Fig. 13.6) were reviewed by Constantz et al. (2001), Constantz and Stonestrom (2003), and Stewart-Deaker et al. (2007). The upwards migration of groundwater that is buffered from the temperature fluctuations at land surface during periods of gaining (i.e., discharge of groundwater to streams) is manifested by relatively constant temperatures in shallow streambed sediments and a dampening of the diurnal fluctuations. On the contrary, the downward advection of
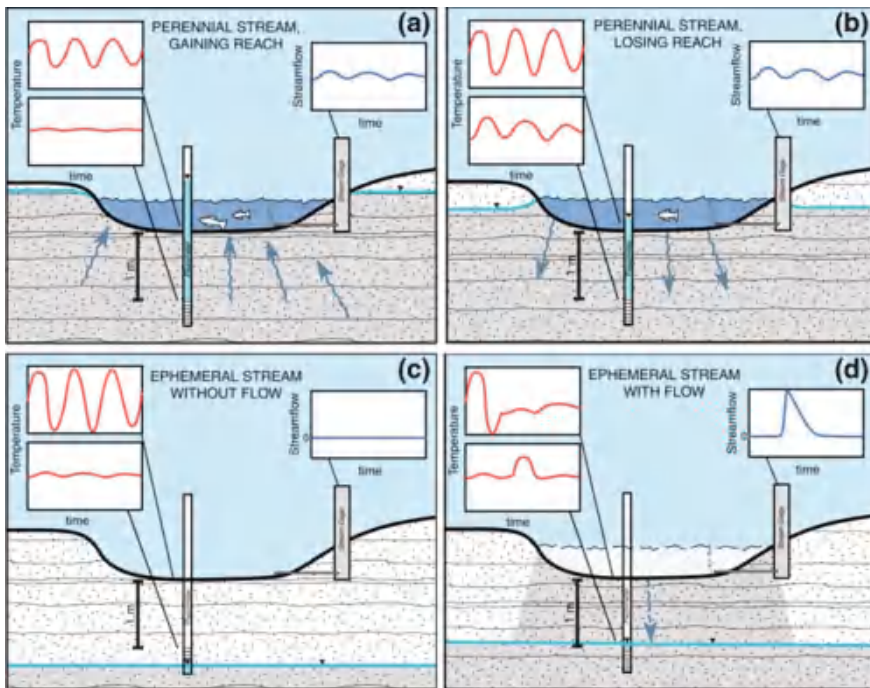
Fig. 13.6 Idealized temperature responses for four possible interactions of a stream with groundwater: a perennial stream gaining water from the underlying sediments, a perennial stream losing water to the underlying sediments, an ephemeral stream without flow, and an ephemeral stream with flow. Inset graphs show stream flow hydrographs and corresponding streambed thermographs in each case (from Constantz and Stonestrom 2003)

surface water that experiences diurnal oscillation in atmospheric temperatures results in large fluctuations in shallow sediment temperatures, which will closely follow in-stream variations. Periods of infiltration will also result in increases in the amplitude of diurnal fluctuations in temperature in deeper temperature probes.

Introduced heat was used in thermal tracer tests performed in wells completed in the Cambro-Ordovician aquifer system near Madison, Wisconsin (Leaf et al. 2012). Water was withdrawn from the wells within the casings, heated at land surface by flow through a copper coil immersed in a thermal bath, and then returned to the open-hole interval of the well. The water was heated by less than 10 °C, which was not high enough to induce significant convection. Tests were performed using both constant source and discrete-pulsed heating modes. Dilution testing using a heat as a tracer allowed for the location of flow zones and determination of ambient flow rates (Leaf et al. 2012). Leaf et al. (2012) noted that the point dilution testing is sensitive to a wider range of flows than flowmeter testing.

13.8   Tracer Volume and Introduction

Determination of tracer volume involves balancing of risks of not being able to detect the tracer, if too small a volume is used, and coloring or otherwise impacting the water, if too much tracer is used (Goldscheider et al. 2003). The normal procedure when using fluorescent tracers is to use enough tracer so that it is clearly detectable at the sampling point above background concentrations but not visible (Mull et al. 1988). Perhaps one of the best (or worst) example of a poorly planned tracer test that went awry is a 2003 test performed by the U.S. Geological Survey at the Miami-Dade Northwest Wellfield (Florida), which unintentionally dyed red the drinking for almost a million people, and had adverse impacts such as dying people's underwear pink. Determination of satisfactory tracer volumes should be based on forward modeling and experience. Solute-transport modeling that considers the range of plausible hydrogeological conditions at the test site can be used to determine the relationship between tracer mass (volume multiplied by concentration) and potential concentrations at observation points.

Käss (1998) and Worthington and Smart (2003) proposed equations for tracer masses in karst studies. The Käss (1998) equation, as follows, is simple, but requires values for two coefficients

$$M = LKB$$

where
M   mass of tracer (kg)
L   distance (km)
K   coefficient of tracer
B   factor for hydrogeological conditions

Käss (1998) and Benischke et al. (2007) provide a table of recommended values of K and B for different test conditions.

The Worthington and Smart (2003) presented two empirical equations for the tracer mass for sink to spring tracer testing in karst

$$M = 19(LQC)^{0.95}$$
$$M = 0.73(TQC)^{0.97}$$

where
M   mass of tracer (g)
Q   discharge (m^3/s)
C   target peak concentration at spring outlet (g/m^3; mg/L)
L   distance from sink to spring (m)
T   travel time (s)

Tracer volume can also be determined using the Efficient Hydrologic Tracer Test Design (EHTD) method, which is a program that calculates amount of dye required from factors such as spring discharge rate, distance from injection site to spring, conduit diameter, and tortuosity (Field 2003).

Dye concentrations are measured at concentration of parts per billion and even the slightest contamination can cause erroneous or misleading data (Mull et al. 1988). Test implementation procedures need to focus on avoiding contamination or other impacts to samples. Mull et al. (1988) provide some commonsense recommendations, such as installation of sampling equipment before dye is handled. The method of storing and transport samples is also important. Light-proof storage containers should be used to prevent photochemical decay after sample collection. Commercial dye contains a considerable amount of dilutant (i.e., dye solution or powder contains less than 100 % dye). For quantitative dye tests, the actual amount of dye injected into the aquifer must be known.

Tracer tests may be performed using continuous tracer injection or, more commonly, by the instantaneous injection of a pulse of tracer. The term 'instantaneous', implies that the duration of the injection is very short relative to the duration of the test. The instantaneous injection period may thus be minute or an hour depending upon the test. The tracer should be injected in a manner so as to not disturb the ambient flow field. In tests in which tracer is injected into a well or well zone, the tracer should be introduced in a manner so that there is a uniform concentration in the tested interval. A variety of methods are available to introduce tracer into a well. The choice of injection methods depends upon test objectives, well construction and project budget, and available resources. Davis et al. (1985), for example, documented a dedicated trailer-mounted tracer testing facility that includes packers, and tracer introduction and sampling pump systems.

For shallow wells, the tracer can be carefully poured into the wells and chased with 1 to 3 well volumes of tracer-free water (Fig. 13.7). The chase water forces the tracer into the aquifer. For deeper wells with large casing volumes, the introduction
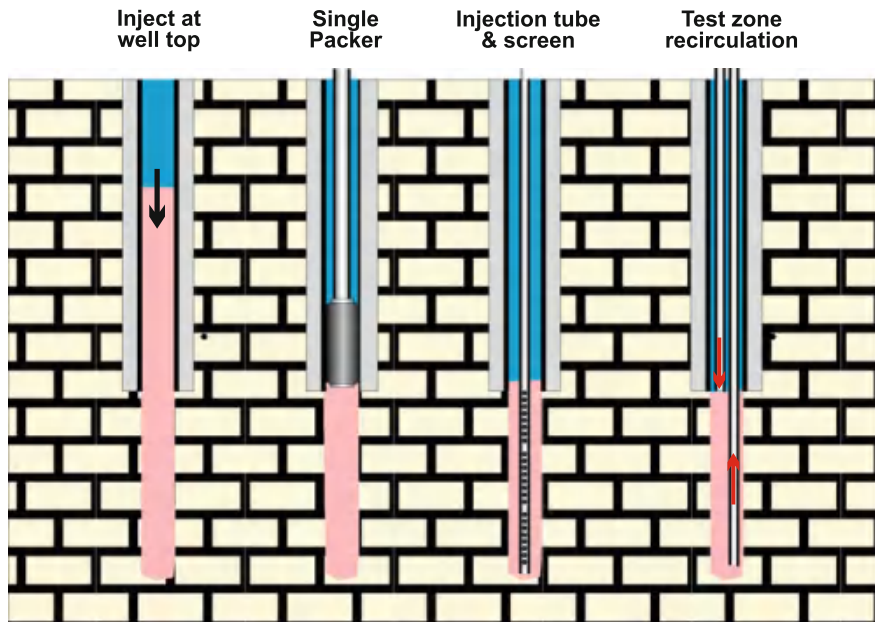
Fig. 13.7   Diagram of some tracer introduction options for a well. Tracer (pink) is poured into the well and then chased with clean water (blue). The volume of chase water can be reduced by setting a packer above the test interval and injecting the tracer through a smaller diameter tube. A more even tracer distribution in the tested interval may be achieved by injecting the tracer through a screen or perforated pipe. The top of the tested interval may be sealed off using a packer (not shown). An even tracer distribution may also be achieved by recirculating the tracer, which involves injection of the tracer at the top of the tested interval, while pumping water from the bottom of the interval at the same rate. The pumped water is reinjected into the well. A recirculation system could also be installed in an interval isolated by packers

of large volumes of chase water can impose a local flow field. Better solutions are to introduce tracer using a smaller diameter pipe, which thus requires a smaller volume of chase water. Perforations in the pipe can act to distribute the tracer throughout the tested interval. The tested interval may also be isolated using inflatable packers. Tracer may also be introduced into a deep well using perforated container that is slowly raised and lower to evenly mix the tracer in the screened or open-hole interval. In the case of karst system tests during dry weather conditions, water should first be added to wet the conduit surface. The tracer should be chased with a slug of water to flush dye into the system (Mull et al. 1988).

In heterogeneous aquifers, the manner of introduction of the tracer can impact tracer concentrations in natural-gradient and convergent forced-gradient tests. Where tracer is introduced into a well in a manner that achieves a uniform initial concentration in the tested interval of a well, over time, the tracer will preferentially enter an adjoining flow zone(s) and a large fraction of the tracer may remain behind in the well or enter the flow system very slowly (Fig. 13.8). The detected
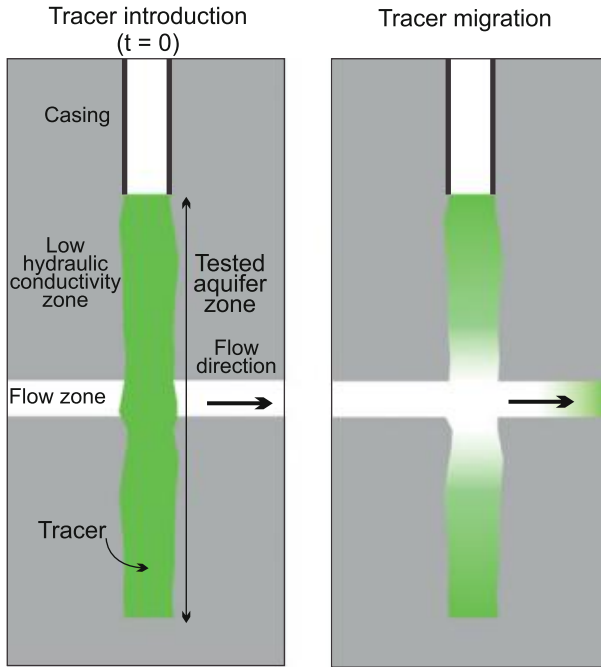
Fig. 13.8 Changes on the distribution of a tracer (green) released in a well for a natural or convergent forced-gradient test. a Tracer is introduced in manner so that the concentration in the well is near uniform in tested interval. b Tracer will preferentially enter a flow zone while remaining largely behind in depths of the borehole adjoining less conductive strata. The mass of tracer that reaches the pumped well or down-gradient production may be much less than would occur in a homogeneous aquifer in which all the tracer enters the tested interval

concentration in the pumped or down-gradient observation well will be correspondingly lower than would occur if all the tracer entered the aquifer. However, if the tracer is introduced by pumping into the well followed by chase water, then most of the tracer would enter the flow zone that accepts the majority of the water flow.

13.9   Sample Collection

Sample collection for karst systems has evolved over time, as reviewed by White (2002, 2007). Earlier test involved continuous or periodic observation and manual sample collection at discharge points, which is still common practice for pumped wells. Activated coconut charcoal packets were the first major advance for dye tracer studies, as the packets could be placed in an outlet and the charcoal would continuously sorb the dye. The tracer is later elutriated using an alkali alcohol

solution and measured. For qualitative samples, the presence of tracer may be determined from a change in color of the eluate.

Sequential automatic samplers (autosamplers) were later adopted, which allowed samples to be collected at specified time intervals. Equipment is widely available that can take up to 24 or 48 samples at programmed times. Glass bottles are recommended for fluorescent dyes as they are less likely to sorb tracers. The current state of the art is down-hole fluorometers that automatically performed high-frequency measures over the course of an entire tracer test. A disadvantage of autosamplers and field fluorometers is that they are expensive equipment and tests are often performed at unsecured sites. Theft and vandalism are a concern.

Incomplete mixing of tracer within the sampling zone can impact breakthrough curves. Details of the breakthrough curve will depend upon the location of the probe or sampling point relative to the tracer distribution along the sampled zone (e.g., open-hole or screened interval of the well) (Molz et al. 1985). The measured increase in tracer concentration versus time would be greater if the sampling point is located opposite a high-transmissivity zone. Conversely, if the down-hole fluorometer is positioned within the casing distant from a flow zone and there is minimal or no vertical flow within the well (such as may occur in an observation well that is not pumped), there could be a large lag time between the tracer first entering a well and its detection (if the tracer is detected at all). Potential impacts of fluorometer position on measured breakthrough curves will be greatest in wells with long open-hole or screened intervals.

Periodic grab samples may be obtained by pumping observation wells, but care must be taken to obtain representative samples while not materially impacting the local flow field. Pumping volumes may be reduced by using small-diameter observation wells, sampling through a small-diameter screened tubing open to the sampled interval, isolating the sampled interval using packers, or setting the pump in the sampled interval.

Down-hole grab (thief) samplers may also be used to sample non-pumped observation wells. They have the advantage of collecting small-volume samples and thus having a minimal impact on groundwater flow into and towards the well. They have the same limitation as down-hole fluorometers in that they obtain, in essence, a point sample of the sampled interval.

13.10 Tracer Test Legal Issues

Introduced tracers tests involve the introduction of chemicals, gases, or solutes to the groundwater environment. The issue arises as whether or not tracer tests result in groundwater contamination and how they are locally regulated. There are three main environmental protection issues associated with tracer tests (Holmbeck-Pelham et al. 2000):

(1) toxicity and mobility of tracers
(2) management and control of tracers, particularly the potential for their migration into water supply wells
(3) disposal of withdrawn water.

In general, properly designed and performed tracer tests present a very minor potential environment risk. Holmbeck-Pelham et al. (2000) reviewed regulation of tracer tests involving groundwater injection in the United States. Such tests fall under the jurisdiction of the U.S. Environmental Protection Agency (USEPA) and states granted primary enforcement authority (primacy), which have the mandate of prevent endangerment of underground sources of drinking water. There are no specific USEPA regulations concerning tracer tests and there are great differences in how the tests are regulated on the state levels. The regulation ranges from essentially no regulation, to an informal notification process, to a strict permit application and review process. Clearly professionals involved in tracer testing should be intimately aware of all applicable regulations that might be related to the performance of the tests at the planned locations.

13.11   Other Applications of Tracer Testing

The subject of introduced and natural (environmental) tracers is broad enough to be the subject of an entire book on its own. Followings are summaries of some other types and applications of tracer tests.

13.11.1   Surface Geophysics and Tracer Testing

Tracers are usually detected either at monitoring wells or discharge points. The movement of tracers may also be detected using surface geophysical methods, if there a significant difference in salinity that is manifested as a detected difference in resistivity. The basic test methodology is to inject a slug of water in which salt has been added and performing a time series of geophysical surveys to map the movement of the slug. Injection of freshwater into a saline aquifer could also be effective, but the technique is less sensitive to the passage of an electrically resistive slug than it is to an electrically conductive salt-water slug in freshwater (White 1988). Forward modeling is recommended to determine whether or not the tracer can be detected and to determine the optimal electrode spacing for resistivity surveys (White 1988). The tracer tests can be used to determine the direction of flow, flow velocity, and hydraulic conductivity if the aquifer effective porosity and hydraulic gradient are known.

Injected saline water was used as a tracer to evaluate groundwater flow direction and rate in an unconsolidated, unconfined aquifer in the municipality of Gray, Maine, USA (Sandberg et al. 2002). The tracer consisted of sodium chloride (table salt) added to groundwater. The movement of the tracer was successfully detected using both resistivity imaging and self-potential data. The tracer could not be satisfactorily resolved using GPR and terrain conductivity (Geonics EM-31 unit). The surface geophysical data show that the dominant flow vector contrasts with the dominant flow direction predicted from hydrogeological modeling.

Limitations of the use of surface geophysics in tracer testing is that the tracer must result in a detectable resistivity contrast and that resolution decreases with depth, particularly if a conductive layer is present near land surface. The surface resistivity signal also depends upon the thickness of the slug of saline water, which means that the method may not work in thin aquifers (White 1988). The tracer may also not be detectable in heterogeneous aquifers in which flow is concentrated in a thin flow zone. Performing tracer tests involving the injection of saline water may be construed as an illegal contamination of an aquifer. It is, therefore, important that regulatory approval be obtained (if required). The injected saline water may have to be completely recovered and properly disposed.

Borehole–surface resistivity methods can have significantly better resolution. Bevc and Morrison (1991) documented a field testing program at the University of California Richmond Field Station, in which a saline tracer was injected into an aquifer. Current source electrodes were placed in a borehole and two surface electrode configurations were tested, (1) receiver and transmitter electrodes at land surface, and (2) only receiver electrodes at land surface. The results of the tracer test suggest the presence of strong channel flow paths that could not be detected by a limited number of observation wells.

13.11.2   Borehole Flow Velocity Meter

Some borehole flow velocity meters are in essence a small-scale tracer tests. Horizontal flow velocity within the borehole is measure by the travel time of a tracer released and measured within a borehole probe. The Geoflo® meter uses a heat pulse as a tracer of groundwater flow (Kerfoot and Massard 1985; Guthrie 1986; Kerfoot et al. 1991). The tool basically consists of a central heat source surrounded by a ring of thermistors. The space between the heat source and thermistor ring is filled with glass beads. Horizontal flow velocity is calculated from the elapsed time between the emission of the heat pulse and its detection by the thermistors. The direction of groundwater flow can be determined from the tool orientation and the position of the thermistor(s) that detect the greatest magnitude temperature increase from a heat pulse.

The point velocity probe (PVP) measures flow velocity from the travel time of a conductivity pulse caused by the release of saline tracer (Labaky et al. 2009). The PVP consists of a probe that is driven or jetted in place, which contains an injector port and two detector ports on the same horizontal plane. A sodium chloride solution is released at the injector port. The detector ports consist of copper wires elements connected to a conductivity meter. Horizontal flow and flow direction are measured from the travel time from the tracer injection to its detection at the ports. The performance of in-hole flowmeters will depend on borehole skin effects and well screen design (Kerfoot and Massard 1985; Labaky et al. 2009).

Vertical flow can be measured with probes with detectors located above and below the injector port. However, density differences between injected water and native groundwater can result in vertical flow. Schillig et al. (2015) addressed the effects of density-induced tracer movement on groundwater velocity measurements using PVPs. They concluded that horizontal flow velocity measurements are unlikely to be significantly impacted by density effects. Unaccounted for buoyancy effects can affect the accuracy of vertical flow velocity measurements.

13.11.3 Partitioning Tracer Tests

Partitioning tracers have some affinity for phases other than groundwater. Partitioning tracers can be used to determine the volume of other phases present in an aquifer, such as DNAPL saturation in a contaminated aquifer (Jin et al. 1995; Annable et al. 1998; Istok et al. 2002; Shook et al. 2004). The tests are performed using both a conservative tracer and partitioning tracer. The latter should be partitioned onto the substance of interest (e.g., DNAPLs) with a predictable or measureable relationship. The conservative tracer is used to evaluate changes in concentration due to advective processes. Using DNAPLs as an example, the mixing-corrected decrease in the concentration of the portioning tracer is quantitatively related to the amount DNAPL present along the fluid flow path. Time series of partitioning tracer tests can be used, for example, to evaluate the effectiveness of cleanup activities.

13.12 Environmental Tracers

Environmental tracers are natural and anthropogenic chemicals and stable and radioactive isotopes that are already present in ground water. They can contribute to aquifer characterization programs by providing information on groundwater flow rates and flow paths, which in turn may be related to aquifer hydraulic properties. Existing natural or anthropogenic variations in water chemistry, such as from differences between recharge areas or contaminant releases, may be used to evaluate groundwater flow directions. Age-related environmental tracers, such as

chlorofluorocarbons and natural and anthropogenic radioactive isotopes, are used to date recent groundwater and, in turn, estimate groundwater flow velocity. Similarly, the rate of migration of chemicals from a discharge of known location and age (e.g., a spill that occurred on a known date or date range), can also be used to determine groundwater flow direction and rate.

A fundamental question concerning the use of environmental tracers to determine groundwater age is the significance and accuracy of calculated values. As addressed by Varni and Carrera (1998) and McCallum et al. (2015), there is a difference between the advective age of groundwater (also known as true groundwater and kinematic age) and the mean age of groundwater. The advective age is taken to be the time for a water particle to travel from recharge point to the sampling point, purely by advection. The mean age of groundwater is the average age of water molecules at a location, which is a function of the contribution of waters traveling along different flow paths and the exchange of waters between slow-moving and past-moving flow paths. The width of the age distribution represented by mean values may be great in settings where adjacent flow paths have significantly different ages and the sampling point (e.g., well screen) is open to multiple flow paths (McCallum et al. 2015). Apparent (calculated) ages may differ from actual mean ages if the concentrations of tracers were nonlinear with time (Park et al. 2002; McCallum et al. 2015).

Following is a brief overview of several environmental tracers that have been applied to groundwater investigations. All of the presented methods require specialized expertise in sample collection, analysis, and data interpretation.

13.12.1   Chlorofluorocarbons

A detailed review of the use of chlorofluorocarbons (CFCs) in groundwater hydrology is provided by the IAEA (2006). CFCs have no natural sources and their presence in groundwater is evidence that some of the water was recharged after the start of their production. Two main CFCs are of interest for determining the age of waters and thus recharge rates: CCl_3F (CFC-11, Freon-11) and CCl_2F_2 (CFC-12, Freon-12). Industrial production and atmospheric introduction of CFC-12 began in 1931 and that of CFC-11 in the 1940s. CFCs are useful as environmental tracers because they are detectable at very low concentrations, are extremely stable, and behave essentially as inert compounds (Thompson et al. 1974).

Industrial production and atmospheric measurements provide a relatively accurate CFC-11 and CFC-12 source function for the last 70 years (Ekwurzel et al. 1994). Atmospheric concentrations at the time of isolation from the vadose zone can be calculated from the measured concentration and recharge temperature, and then compared to reconstructed atmospheric CFC concentrations to determine the CFC-model age (Busenberg and Plummer 1992). The partitioning of CFCs between water and the atmosphere is a function of temperature, and can be predicted based on their Henry Law coefficient. Groundwater age can be determined from both

CFC-11 and CFC-12 data, which serves as a cross-check on the method (Ekwurzel et al. 1994). CFC sampling and analytical procedures and factors that can affect CFC concentrations in groundwater are discussed by Busenberg and Plummer (1992). A critical issue is avoiding contamination of samples with modern atmospheric CFCs during sample collection.

13.12.2 Tritium and Chlorine 39

Tritium is a radioactive isotope of hydrogen (symbol T or ^{3}H) that contains one proton and two neutrons. Inasmuch as tritium is incorporated into water molecules, it is an excellent tracer of the movement of water. The theory and applications of environmental isotopes are addressed in detail by Clark and Fritz (1997). Tritium is naturally produced in the upper atmosphere (stratosphere) by the action of cosmic radiation on atmospheric gases. Tritium occurs in nature in very small quantities. The concentration of tritium is expressed in tritium units (TU) in which one TU is equal to 1 tritium atom per 1×10^{18} hydrogen atoms.

The half-life of tritium is relatively short at 12.32 years, which results in groundwater naturally having a very low concentration of tritium. A very important source of large quantities of additional tritium to the atmosphere is the above-ground nuclear testing that was performed in the 1950s and early 1960s. The tritium released to the atmosphere entered the hydrosphere and, as a result, precipitation became enriched in tritium. The concentration of tritium in precipitation peaked in 1963.

The 1963 tritium peak provides a precise age date for water. Groundwater present above the 1963 peak can be interpreted as having been emplaced after 1963. The difficulty of using the 1963 tritium peak as a marker is that a large number of closely spaced samples are required to locate the peak. The tritium peak can also not be used as marker for dating waters younger than the middle 1960's, after the peak. An additional challenge is that the nuclear peak is progressively becoming less distinct as the concentration of nuclear testing tritium is decreasing due to radioactive decay. Instead, groundwater samples are commonly now dated using the ^{3}H/^{3}He (T/^{3}He) technique, which utilizes the daughter nuclide of tritium decay, tritogenic helium (^{3}He$_{trit}$). An advantage of ^{3}H/^{3}He dating is that it is independent of ^{3}H input because the ratio of the nuclides is considered, not the amount of each nuclide (Solomon et al. 1993; Solomon and Sudicky 1995). Isotopic analyses measure the total ^{3}He (^{3}He$_{total}$) concentration, which is the sum of ^{3}He$_{trit}$ and ^{3}He from other sources, such as the atmosphere, excess air trapped above equilibrium solubility, and mantle and nuclear (i.e., terrigenic) sources (Solomon and Sudicky 1995).

Groundwater ages determined from the ^{3}H/^{3}He ratio will approximate true groundwater travel times provided that dispersive mixing between the water table (point of water intake) and point of measurement is a weak process and the ^{3}H input has been constant over time (Solomon and Sudicky 1995). Groundwater in low recharge settings may lose significant amounts of ^{3}He$_{trit}$ through diffusion across

the water table, which could materially impact calculated ages (Schlosser et al. 1988, 1989; Ekwurzel et al. 1994). Under transient conditions where the ^3H input has varied, such as near the middle 1960s bomb testing peak, the effects of dispersion on $^3H/^3He$ ages must be examined using a specified time-dependent ^3H input function (Solomon and Sudicky 1995).

Above-ground nuclear testing also added chlorine 36 (^{36}Cl) to the atmosphere, whose peak atmospheric concentration occurred in about 1955, 8 years before the tritium peak. Chlorine-36 can provide information on the rate of movement of chloride and thus solutes in general. The primary natural source of ^{36}Cl in the atmosphere is the interaction of cosmic rays with argon. The $^{36}Cl/Cl$ ratio data can be used to date groundwater provided that (Cresswell et al. 1999)

- the only sink for ^{36}Cl in the aquifer is radioactive decay
- the only source of additional ^{36}Cl is normal deep subsurface production or that additional sources can be identified and quantified
- the production rate for ^{36}Cl now was the same at the time of recharge.

The half-life of ^{36}Cl is 301,000 years, so the method is appropriate for dating old groundwater. Chlorine-36 data were used, for example, to determine that the water in aquifers in the southwestern part of the Northern Territory, Australia, underwent substantial recharge during a favorable, wetter interglacial climatic regime (Cresswell et al. 1999). Chlorine-36 is a nonstandard analysis and thus expensive and, as a result, has seldom been used in water resources investigations.

13.12.3   Carbon-14 Dating

Carbon-14 (^{14}C) dating (also referred to a radiocarbon or carbon dating) is widely used for dating of carbonaceous material up to about 50,000–60,000 years old and is also used for the dating of dissolved inorganic carbonate (DIC) in groundwater. Radiocarbon data is discussed in detailed by Clark and Fritz (1997). Carbon-14 forms in the atmosphere by the interaction of gamma rays with ^{14}N atoms. The underlying concept of radiocarbon dating is that the ratio of ^{14}C to total carbon atoms in the atmosphere has been nearly constant. The two much more abundant nonradioactive carbon isotopes are ^{13}C and ^{12}C, with ^{12}C by far the most abundant. Once an organism dies, ^{14}C is no longer incorporated and the activity of ^{14}C starts to decrease due to radioactive decay. Similarly, once groundwater is isolated from the atmosphere, the amount of ^{14}C decreases at a rate in accordance with its half-life of 5,730 years. The time that elapsed since a sample was isolated from the atmosphere is calculated from the ratio of the original ^{14}C concentration (which is approximately known) to its current (measured) concentration.

Although radiocarbon dating is conceptually very simple, complexity lies in its details. The assumption of a constant atmosphere ^{14}C is incorrect. The atmospheric ^{14}C concentration has varied due to the addition of older carbon from the burning of

fossil fuels, the addition of ^{14}C from atmospheric nuclear weapons testing, and fluctuations in cosmic ray intensity over time. Radiocarbon dates must therefore be converted to calendar years using calibration curves that are based on radiocarbon analyses of materials of independently determined age (e.g., tree rings). Carbon 14 is fractionated during organic and inorganic phase changes and reactions, and as a result ^{14}C activities are normalized to a common $d^{13}C$ value of -25 ‰.

Radiocarbon data are subject to error by the incorporation of older, radioactively 'dead' carbon (i.e., carbon with essentially no remaining ^{14}C). The $^{14}C/^{12}C$ ratio in water (^{12}C is the predominant nonradioactive isotope) may be greatly impacted by other sources of carbon, such as soil gases, pedogenic carbon, and aquifer minerals. The carbon in aquifer minerals is typically dead with respect to ^{14}C, so any addition of mineral carbon from fluid–rock interaction tends to increase ^{14}C ages. The reservoir of carbon present as calcium carbonate ($CaCO_3$) in limestones is orders of magnitude greater than that of dissolved inorganic carbon in groundwater. Hence, ^{14}C concentration of groundwater in carbonate aquifers is highly susceptible to increase by fluid–rock interactions. Some common diagenetic processes in limestone aquifers involve the dissolution and precipitation of calcium carbonate (e.g., neomorphism of aragonite to calcite) with often minimal impact on ion concentrations.

A voluminous body of literature exists concerning correction of ^{14}C ages. The basic established practice is to use major ion and $d^{13}C$ mass balance to reconstitute the proportions of carbon from different sources (Zhu 2000; Zhu and Murphy 2000). Inverse modeling techniques, such as using the NETPATH program (Plummer et al. 1991) or PHREEQC (Parkhurst and Appelo 1999), can be used to determine the reactions or processes responsible for the changes in groundwater chemistry between the precipitation and the observation point.

A key lesson is that radiocarbon dating can be a very useful tool for evaluating groundwater age and flow, but the interpretation of the data involves a number of assumptions that may not hold for a given study area. There is no "one size fits all" formula (Zhu and Murphy 2000). Detailed knowledge of the aquifer hydrological and geochemical processes is necessary for accurate modeling and interpretation of ^{14}C data.

References

Anderson, M. P. (2005) Heat as a ground water tracer. Ground Water, 43, 951–968.

Annable, M. D., Rao, P. S. C., Hatfield, K., Graham, W. D., Wood, A. L., & Enfield, C. G. (1998). Partitioning tracers for measuring residual NAPL: Field-scale test results. Journal of Environmental Engineering, 124(6), 498–503.

Basiricò, S., Crosta, G. B., Frattini, P., Villa, A., & Godio, A. (2015). Borehole flowmeter logging for the accurate design and analysis of tracer tests. Groundwater, 53(S1), 3–9.

Becker, M. W., Bauer, B., & Hutchinson, A. (2013) Measuring artificial recharge with Fiber Optic Distributed Temperature Sensing. Ground Water, 51, 670–678.

Benderitter, Y., Roy, B., & Tabbagh, A. (1993) Flow characterization through heat transfer evidence in a carbonate fractured medium: First approach. Water Resources Research, 29, 3741–3747.

Benischke, R., Goldscheider, N., & Smart, C. (2007) Tracer techniques. In N. Goldscheider & D. Drew (Eds.), Methods in karst hydrogeology, IAH International Contributions to Hydrogeology 26 (pp. 9–23). Leiden: Taylor and Francis.

Bevc, D., & Morrison, H. F. (1991) Borehole-to-surface electrical monitoring of a salt water injection experiment. Geophysics, 56, 769–777.

Brainerd, R. J., & Robbins, G. A. (2004) A tracer dilution method for fracture characterization of bedrock wells. Ground Water, 42, 774–780.

Busenberg, E., & Plummer, L. N. (1992) Use of chlorofluorocarbons (CCl3F and CCl2F2) as hydrologic tracers and age-dating tools: the alluvium and terrace system of Central Oklahoma. Water Resources Research, 28, 2257–2283.

Chlebica, D. W., & Robbins, G. A. (2013) Altering dissolved oxygen to determine flow conditions in fractured bedrock wells. Groundwater Monitoring & Remediation, 33(4), 100–107.

Clark, I., & Fritz, P. (1997) Environmental isotopes in hydrogeology. Boca Raton: Lewis Publishers.

Clark, J. F., Hudson, G. B., Davisson, M. L., Woodside, G., & Herndon, R. (2004) Geochemical imaging of flow near an artificial recharge facility, Orange County, California. Ground Water, 42, 167–174.

Constantz, J., & Stonestrom, D. A. (2003) Heat as a tracer of water movement near streams. In D. A. Stonestrom & J. Constantz (Eds.), Heat as a tool for studying the movement of groundwater near streams (pp. 1–6). U.S. Geological Survey Circular 1260.

Constantz, J., Stonestrom, D. A., Stewart, A. E., Niswonger, R., & Smith, T. R. (2001) Analysis of streambed temperatures in ephemeral streams to determine streamflow frequency and duration. Water Resources Research, 37, 317–328.

Constantz, J., Thomas, C. L., & Zellweger, G. (1994) Influence of diurnal variations in stream temperature on streamflow loss and groundwater recharge. Water Resources Research, 30, 3253–3264.

Cook, P. G. (2003) A guide to regional groundwater flow in fractured rock aquifers. Adelaide: CSIRO.

Cresswell, R., Wischusen, J., Jacobson, G., & Fifield, K. (1999). Assessment of recharge to groundwater systems in the arid southwestern part of Northern Territory, Australia, using chlorine-36. Hydrogeology Journal, 7, 393–404.

Dassargues, A. (1997) Interpretation and modeling of multi-tracer tests in heterogeneous geological media: In Hydrochemistry (Proceedings of the Rabat Symposium, April 1997; pp. 217–225). IAHS Publication 244.

Davis, S. N., Thompson, G. M., Bentley, H. W., & Stiles, G. (1980) Ground-water tracers – A short review. Ground Water, 18, 14–23.

Davis, S. N., Thompson, G. M., Bentley, H. W., & Flynn, T. J. (1985) An introduction to ground-water tracers. Ada, Oklahoma: Robert S. Kerr Environmental Research Laboratory, U. S. Environmental Protection Agency.

Divine, C. E. & McDonnell, J. J. (2005) The future of applied tracers in hydrogeology. Hydrogeology Journal, 13, 255–258.

Domenico, P. A., & Schwartz, F. W. (1998) Physical and chemical hydrogeology (2nd Ed.): New York, John Wiley & Sons.

Drost, W., Klotz, D., Koch, A., Moser, H., Neumaier, F., & Rauert, W. (1968) Point dilution methods of investigating groundwater flow by means of radioisotopes. Water Resources Research, 4, 125–146.

Ekwurzel, B., Schlosser, P., Smethie, W. M., Plummer, L. N., Busenberg, E., Michel, R. L., Weppernig, R., & Stute, M. (1994) Dating of shallow groundwater: comparison of the transient tracers 3H/3He, chlorofluorocarbons, and 85Kr. Water Resources Research, 30, 1693–1708.

Fetter, C. W. (1998) Contaminant hydrogeology (2nd Ed.). Englewood Cliffs: Prentice-Hall.

Field, M. S. (2003) Tracer-test planning using the Efficient Hydrologic Tracer-Test Design (EHTD) Program. Washington DC, Environmental Protection Agency, Office of Research and Development, National Center for Environmental Assessment EPA/600/R-03/034.

Gelhar, L. W., & Collins, M. A. (1971) General analysis of longitudinal dispersion in nonuniform flow. Water Resources Research, 7, 1511–1521.

Goldscheider, N., Hötzel, H., Käss, W., & Ufrecht, W. (2003) Combined tracer tests in the karst aquifer of the artesian mineral springs of Stuttgart, Germany. Environmental Geology, 43, 922–929.

Goldscheider, N., Meiman, J., Pronk, M., & Smart, C. (2008) Tracer tests in karst hydrogeology and Speleology. International Journal of Speleology, 37(1), 27–40.

Gouze, P., Le Borgne, T., Leprovost, R., Lods, G., Poidras, T. & Pezard, P. (2008) Non-Fickian dispersion in porous media: 1. Multiscale measurements using single-well injection withdrawal tracer tests. Water Resources Research, 44, W06426.

Gouze, P., Leprovost, R., Poidras, T., Le Borgne, T., Lods, G., & Pezard, P. A. (2009) CoFIS and TELog: New downhole tools for characterizing dispersion processes in aquifers by single-well injection-withdrawal tracer tests. C. R. Geoscience, 341, 965–975.

Guthrie, M. (1986) Use of a Geo Flowmeter for determination of groundwater flow direction. Ground Water Monitoring and Remediation, 6(2), 81–86.

Güven, D., Falta, R. W., Motz, F. J., & Melville, J. G. (1985) Analysis and interpretation of single-well tracer tests in stratified aquifers. Water Resources Research, 21, 676–684.

Haggerty, R., Schroth, M. H., & Istok, J. D. (1998) Simplified method of "push-pull" test data analysis for determining in situ reaction rate coefficients. Ground Water, 36, 314–324.

Hall, S. H. (1993) Single well tracer tests in aquifer characterization. Ground Water Monitoring & Remediation, 13(2), 118–124.

Harvey, R. W., Metge, D. W., Shapiro, A. M., Renken, R. A., Osborn, C. L., Ryan, J. N., Cunningham, K.J., & Landkamer, L. (2008). Pathogen and chemical transport in the karst limestone of the Biscayne aquifer: 3. Use of microspheres to estimate the transport potential of Cryptosporidium parvum oocysts. Water Resources Research, 44(8), W08431.

Harvey, R., Metge, D., Sheets, R., & Jasperse, J. (2011). Fluorescent microspheres as surrogates in evaluating the efficacy of riverbank filtration for removing Cryptosporidium parvum oocysts and other pathogens. In C. Ray & M. Shamrukh (Eds.) Riverbank filtration for water security in desert countries (pp. 81–96). Amsterdam: Springer.

Holmbeck-Pelham, S. A., Rasmussen, T. C., & Fowler, L. A. (2000) Regulation of injected ground water tracers. Ground Water, 38, 541–549.

Hurtig, E., Grosswig, S., Jobmann, M., Kühn, K., & Marschall, P. (1994) Fibre-optic temperature measurements in shallow boreholes: Experimental applications for fluid logging. Geothermics, 23, 355–364.

IAEA (2006) Use of chlorofluorocarbons in hydrology: a guidebook. Vienna: International Atomic Energy Agency.

Istok, J. D., Humphrey, M. D., Schroth, M. H., Hyman, M. R., & O'Reilly, K. T. (1997) Single well, "push-pull" test for in situ determination of microbial activities. Ground Water, 35, 619–631.

Istok, J. D., Field, J. A., Schroth, M. H., Davis, B. M., & Dwarakanath, V. (2002). Single-well "push-pull" partitioning tracer test for NAPL detection in the subsurface. Environmental Science & Technology, 36, 2708–2716.

Jin, M., Delshad, M., Dwarakanath, V., McKinney, D. C., Pope, G. A., Sepehrnoori, K., & Jackson, R. E. (1995). Partitioning tracer test for detection, estimation, and remediation performance assessment of subsurface nonaqueous phase liquids. Water Resources Research, 31, 1201–1211.

Käss, W. (1998) Tracing technique in geohydrology. Rotterdam: A.A. Balkema.

Kerfoot, W. B., & Massard, V. A. (1985) Monitoring well screen influences on direct flowmeter measurements. Ground Water Monitoring and Remediation, 5(4), 74–77.

Kerfoot, W. B., Beaulieu, G., and Keily, L., 1991, Direct-reading borehole flowmeter results in field applications. In Fifth National Outdoor Action Conference on Aquifer Restoration,

Ground Water Monitoring and Geophysical Methods (pp. 1073–1084). Dublin, Ohio: National Water Well Association.

Kilpatrick, F. A., & Wilson, J. F., Jr. (1989) Measurement of time of travel in streams by dye tracing. U. S. Geological Survey Techniques of Water-Resources Investigations, Book 3, Chapter A9.

Korom, S. F., & Seaman, J. C. (2012) When "conservative" anionic tracers aren't. Ground Water, 50, 820–824.

Labaky, W., Devlin, J. F., & Gillham, R. W. (2009) Field comparison of the point velocity probe with other groundwater velocity measurement methods. Water Resources Research, 45, W00D30.

Lapham, W. W. (1989) Use of temperature profiles beneath streams to determine rates of vertical ground-water flow and vertical hydraulic conductivity. U.S. Geological Survey Water-Supply Paper 2337.

Leaf, A. T., Hart, D. J., & Bahr, J. M. (2012) Active thermal tracer tests for improved hydrostratigraphic characterization. Ground Water, 50, 726–735.

Lewis, D. C., Kriz, G. J., & Burgy, R. H. (1966) Tracer dilution sampling technique to determine hydraulic conductivity of fractured rock. Water Resources Research, 2, 533–542.

Maliva, R. G., Griswold, R. F., & Autrey, M. M. (2013) Prototype for a reclaimed water aquifer storage recovery system benefits and operational experiences. Florida Water Resources Journal, 65(3), 54–59.

Maliva, R. G., & Missimer, T. M. (2012) Arid lands water evaluation and management. Berlin: Springer.

Martin, J. B., & Dean, R. W. (1999) Temperature as a natural tracer of short residence tomes for groundwater in karst aquifers. In A. N. Palmer, M. V. Palmer & I. D. Sasowsky (Eds.), Karst modeling, Special Publication 5 (pp. 236–242). Charles Town, West Virginia: The Karst Waters Institute.

McCallum, J. L., Cook, P. G., & Simmons, C. T. (2015). Limitations of the use of environmental tracers to infer groundwater age. Groundwater, 53(S1), 56–70.

McDonald, M. G., & Harbaugh, A. W. (1988) A modular three-dimensional finite-difference ground water flow model. U.S. Geological Survey Techniques of Water-Resources Investigation Report 06-A1.

Miotiński, K., Dillon, P. J., Pavelic, P., Cook, P. G., Page, D. W., & Levett, K. (2011) Recovery of injected freshwater to differentiate fracture flow in low-permeability brackish aquifer. Journal of Hydrology, 409, 273–282.

Mohanram, A., Ray, C., Harvey, R. W., Metge, D. W., Ryan, J. N., Chorover, J., & Eberl, D. D. (2010). Comparison of transport and attachment behaviors of Cryptosporidium parvum oocysts and oocyst-sized microspheres being advected through three mineralogically different granular porous media. Water Research, 44, 5334–5344.

Molz, F. J., Melville, J. G., Güven, O., Crocker, R. O., & Matteson, K. T. (1985) Design and performance of single-well tracer tests at the Mobile site. Water Resources Research, 21, 1497–1502.

Moser, H., Neumaier, F., & Rauert, W. (1957) Die anwendung radioaktiver isotopen in der hydrologie II. Ein verfahren zur armittlung der ergiebigkeit von grundwasserstromungen: Atomkernenergie, 2(6), 225–231.

Mudarra, M., Andreo, B., Marín, A. I., Vadillo, I., & Barberá, J. A. (2014) Combined use of natural and artificial tracers to determine the hydrogeological functioning of a karst aquifer: the Villanueva del Rosario system (Andalusia, southern Spain). Hydrogeology Journal, 22, 1027–1039.

Mull, D. S., Liebermann, T. D., Smoot, J. L., Woosley, L. H., Jr., & Mikulak, R. J. (1988) Application of dye-tracing techniques for determining solute-transport characteristics of ground water in karst terranes. Atlanta: U.S. Environmental Protection Agency, Ground-Water Protection Branch, Region IV, Publication EPA 904/6–88-001.

National Center for Environmental Assessment (1999) The QTRACER program for tracer-breakthrough curve analysis for karst and fractured rock analysis. U.S. Environmental Protection Agency, Office for Research and Development, EPA/600/R-98/156a.

National Research Council (1996) Rock fractures and fluid flow. Washington, D.C.: National Academies Press.

Norton, S. B. (2007) Quantifying the near-borehole geochemical response during aquifer storage and recovery: Application of "push-pull" analytical techniques to ASR cycle testing (unpublished masters thesis). University of Florida, Gainesville.

Palmer, C. D. (1993) Borehole dilution tests in the vicinity of an extraction well. Journal of Hydrology, 146, 245–266.

Pang, L., Nowostawska, U., Ryan, J. N., Williamson, W. M., Walshe, G., & Hunter, K. A. (2009). Modifying the surface charge of pathogen-sized microspheres for studying pathogen transport in groundwater. Journal of Environmental Quality, 38, 2210–2217.

Park, J., Bethke, C. M., Torgersen, T., & Johnson, T. M. (2002). Transport modeling applied to the interpretation of groundwater ^{36}Cl age. Water Resources Research, 38(5), doi:10.1029/2001WR000399.

Parkhurst, D. L., & Appelo, C. A. J. (1999) PHREEQC (Version 2) – A computer program for speciation, batch reaction, one-dimensional transport, and inverse geochemical calculations. U.S. Geological Survey Water-Resources Investigations Report 99-4259.

Peng, W._S., Hampton, D. R., Konikow, L. F., Kambham, K., & Benegar, J. J. (2000) Can contaminant transport models predict breakthrough? Ground Water Monitoring and Remediation, Fall 2000, 104–113.

Pickens, J. F., & Grisak, G. E. (1981) Scale-dependent dispersion in a stratified granular aquifer. Water Resources Research, 17, 1191–1211.

Pickens, J. F., Jackson, R. E., Inch, K. J., & Merritt, W. F. (1981) Measurement of distribution coefficients using a radial injection dual-tracer test. Water Resources Research, 17, 529–544.

Pitrak, M., Mares, S., & Kobr, M. (2007) A simple borehole dilution technique in measuring horizontal ground water flow. Ground Water, 45, 89–92.

Plummer, L. N., Prestemon, E. C., & Parkhurst, D. L. (1991) An interactive code (NETPATH) for modeling NET geochemical reactions along a flow PATH. U.S. Geological Survey Water-Resources Investigations Report 91-4078.

Ptak, T., Peipenbrink, M., & Martac, E. (2004) Tracer tests for the investigation of heterogeneous porous media and stochastic modelling of flow and transport – a review of some recent developments. Journal of Hydrology, 294, 122–163.

Riley, M. S., Tellam, J. H., Greswell, R. B., Durand, V., & Aller, M. F. (2011). Convergent tracer tests in multilayered aquifers: The importance of vertical flow in the injection borehole. Water Resources Research, 47(7), doi 10.1029/2010WR009838.

Sandberg, S. K., Slater, L. D., & Versteeg, R. (2002) An integrated geophysical investigation of the hydrogeology of an anisotropic unconfined aquifer. Journal of Hydrology, 267, 227–243.

Sanford, W. E., Shropshire, R. G., & Solomon, D. K. (1996) Dissolved gas tracers in groundwater: Simplified injection sampling and analysis. Water Resources Research, 23, 1635–1642.

Schillig, P. C., Devlin, J. F., McElwee, C. D., Walter, K., & Gibson, B., 2015, Assessment of density-induced tracer movement in groundwater velocity measurements with point velocity probes (PVPs). Groundwater Monitoring & Remediation, 34(4), 44–50.

Schlosser, P., Stute, M., Dorr, H., Sonntag, C., & Munnich, K. O. (1988) Tritium/3He dating of shallow groundwater. Earth and Planetary Science Letters, 89, 353–362.

Schlosser, P., Stute, M., Sonntag, C., and Munnich, K.O., 1989, Tritogenic 3He in shallow groundwater. Earth and Planetary Science Letters, 94, 245–256.

Screaton, E., Martin, J. B., Ginn, B., & Smith, L. (2004) Conduit properties and karstification in the unconfined Floridan Aquifer. Ground Water, 42, 338–346.

Shapiro, A. W. (2011) The challenge of interpreting environmental tracer concentrations in fractured rock and carbonate aquifers. Hydrogeology Journal, 19, 9–12.

Shook, G. M., Ansley, S. L., & Wylie, A. (2004) Tracers and tracer testing: Design, implementation and interpretation methods. Idaho Falls: Idaho National Engineering and Environmental Laboratory (Report INEEL/EXT-03-01460).

Smart, P. L., & Laidlaw, I. M. S. (1977) An evaluation of some fluorescent dyes for water tracing: Water Resources Research, 13, 15–33.

Smart, C. C. (1988) Artificial tracer techniques for the determination of the structure of conduit aquifers. Ground Water, 26, 445–453.

Solomon, D. K., Schiff, S. L., Poreda, R. J., & Clarke, W. B. (1993) A validation of the 3H/3He method for determining groundwater recharge. Water Resources Research, 29, 2951–2962.

Solomon, D. K., & Sudicky, E. A. (1995) Tritium and helium-3 isotope ratios for direct estimation of spatial variations in groundwater recharge. Water Resources Research, 27, 2309–2319.

Stewart-Deaker, A. E., Stonestrom, D. A., & Moore, S. J. (2007) Streamflow, infiltration, and ground-water recharge at Abo Arroyo, New Mexico. In D. A. Stonestrom, J. Constantz, T. P. A. Ferré & S. A. Leake (Eds.), Ground-water recharge in the arid and semiarid southwestern United States (pp. 83–105). U.S. Geological Survey Professional Paper 1703.

Stallman, R. W. (1963) Computation of ground-water velocity from temperature data. In R. Bentall (Ed.), Methods of collecting and interpreting ground-water (pp. 36–45). U.S. Geological Survey Water-Supply Paper 1544.

Suzuki, S. (1960) Percolation measurements based on heat flow through soil with special reference to paddy field. Journal of Geophysical Research, 65, 2883–2885.

Taylor, C. J., & Greene, E. A. (2001) Quantitative approaches in characterizing karst aquifers: In E. L. Kuniansky (Ed.) U.S. Geological Survey Karst Interest Group proceedings (pp. 164–166). U.S. Water-Resources Investigations Report 01-4011.

Taylor, C. J., & Green, E. A. (2008) Hydrogeologic characterization and methods used in the investigation of karst hydrology. In. D. O. Rosenberry &, J. W. LaBaugh (Eds.) Field techniques for estimating water fluxes between surface water and ground water (pp. 75–114). U.S. Geological Survey Techniques and Methods 4-D2.

Thompson, G. M., Hayes, J. M., & Davis, S. N. (1974) Fluorocarbon tracers in hydrology. Geophysical Research Letters, 1, 177–180.

Tsang, C.-F., Hufschied, P., & Hale, F. V. (1990) Determination of fracture inflow parameters with a borehole fluid conductivity method. Water Resources Research, 26, 561–578.

Varni, M., & Carrera, J. (1998). Simulation of groundwater age distributions. Water Resources Research, 34(12), 3271–3281.

West, L. J., & Oldling, N. E. (2007) Characteristics of a multilayer aquifer using open well dilution tests. Ground Water, 45, 74–84.

White, P. A. (1988) Measurements of ground-water parameters using salt-water injection and surface resistivity. Ground Water, 26, 179–186.

White, W. B. (2002) Karst hydrology: Recent developments and open questions. Engineering Geology, 65, 85–105.

White, W. B. (2007) A brief history of karst hydrogeology: Contribution of the NSS. Journal of Cave and Karst Studies, 69(1), 13–26.

Worthington, S. R. H. & Smart, C. C. (2003) Empirical equations for determining tracer mass for sink to spring tracer testing in karst. In B. F. Beck (Ed.), Sinkholes and the engineering and environmental impacts of karst (pp. 287–295). Geotechnical Special Publication 122, American Society of Civil Engineers.

Zheng, C., & Wang, P. P. (1999) MT3DMS: a modular three-dimensional multi-species model for simulation of advection, dispersion and chemical reactions of contaminants in ground water systems: documentation and user's guide. Vicksburg, Mississippi: U.S. Army Engineer Research and Development Center Report SERDP-99-1.

Zhu, C. (2000) Estimate of recharge from radiocarbon dating of groundwater and numerical flow and transport modeling. Water Resources Research, 36, 2607–2620.

Zhu, C., & Murphy, W. M. (2000) On radioactive dating of ground water. Ground Water, 38, 802–804.

Chapter 14
Evaluation of Aquifer Storage and Aquitard Properties

Data on aquifer storage properties (storativity and specific yield) are required for transient groundwater models. Storativity is usually determined from aquifer pumping tests using the Theis method or variations thereof. Quantification of specific yield is much more challenging because of the long time required (especially in fine-grained sediments) for gravity drainage to occur to completion. Evaluation of the properties of aquitards (semi-confining units) may also be a key element of aquifer characterization and modeling investigations. Heterogeneity, particularly a strong scale effect, and very slow groundwater flow rates are the main challenges associated with aquitard characterization. Multiple methods should be employed to evaluate aquifer storage and aquitard properties with the values subject to adjustment during the model calibration process.

14.1 Aquifer Storage Parameters

Aquifer storage properties characterize the ability of an aquifer to release water from storage in response to declines in hydraulic head or increase heads in response to the addition of water. The main aquifer storage properties are storativity (storage coefficient), specific storage, and specific yield. As introduced in Chap. 1, storativity (S) is a dimensionless parameter defined as the volume of water that is released from a unit area of an aquifer under a unit decline of hydraulic head. Specific storage (S_s) is defined as the volume of water that is released from a unit volume of aquifer under a unit decline of hydraulic head. Specific storage has the units of one divided by length (e.g., m^{-1}). The storativity of a confined aquifer is the vertically integrated specific storage values, which for a homogeneous aquifer is the product of its specific storage and the thickness of the aquifer (b).

Specific yield (S_y) is the volume water that will gravitationally drain from a unit cross-sectional area of an aquifer per unit change in head. In an unconfined aquifer (or aquitard), storativity is given by

$$S = S_y + S_s b \qquad (14.1)$$

Water is produced by both gravity drainage and aquifer compaction and water expansion. The specific yield of unconfined aquifers is much greater than the storativity, and the latter is usually insignificant, especially in evaluation of the response of aquifers to long-term pumping. However, at the start of groundwater pumping, unconfined aquifers behave in the same manner as a confined aquifer and water is produced by expansion of water and compression of the aquifer (Sect. 7.3.7).

Aquifer storage properties (storativity, specific storage, and specific yield) are important parameters for transient simulations in which aquifer heads are changing over time. Storage parameters are not relevant for steady-state conditions, in which, by definition, hydraulic heads (water levels) do not change over time and there is thus no change in storage.

14.2   Evaluation of Storativity and Specific Storage

Storativity and specific storage values for aquifers are typically obtained from aquifer pumping tests. The values of these parameters may also be estimated from stress–strain relationships, particularly water level versus compaction data. Specific storage values for low-permeability confining units may be obtained from laboratory testing of core samples or analysis of relationship between stresses and water levels (e.g., from barometric efficiency data).

Specific storage is related to the compressibility of the aquifer material and water as follows (Jacob 1940)

$$S_s = q_w g(m_v + n b_w) \qquad (14.2)$$

where
q_w density of water (kg/m^3)
g gravitational acceleration (9.80665 m/s^2)
m_v coefficient of volume change, which is also called the compressibility of the bulk aquifer material (b_p, m^2 N^{-1}, Pa^{-1}, ms^2/kg)
n porosity (fractional)
b_w compressibility of water (m^2 N^{-1})

Compressibility is the change in volume (V) of water, sediment, or rock per unit of initial volume caused by a given incremental increase in pressure (P). The isothermal compressibility of water is expressed as

$$b_w = -\frac{1}{V}\left(\frac{@V}{@P}\right)_T \qquad (14\text{:}3)$$

The term $q_w g$ is called by the specific weight of water (c_w), which has the units of weight divided by volume (Nm^{-3} or $kg\ m^{-2}\ s^{-2}$). The specific weight of freshwater is approximately 9,807 N/m^3 (62.43 lbf/ft^3) at a temperature of 4 °C. Inasmuch as $m_v \gg nb_w$, Eq. 14.2 reduces to

$$S_s \cong q_w g m_v \qquad (14\text{:}4)$$

$$S_s \cong c_w m_v \qquad (14\text{:}5)$$

Aquifer and aquitard strata undergo both elastic and inelastic strain or deformation in response to changes in stress. Elastic strain, by definition, is reversible and the sediment or rock returns to its previous state after the stress has been removed. Inelastic strain or deformation is irreversible. In the case of deformation by the reorientation and change in packing of grains, the sediment does not revert back to its original looser grain packing after the stress has been released. Inelastic compaction of aquitards (semi-confining units) results in a one-time release of the 'water of compaction' (Sneed and Galloway 2000).

The deformation of sediment or rock is driven by effective stress (r'), which is defined, in one dimension, as (Terzaghi 1925)

$$r' = r - u \qquad (14\text{:}6)$$

where
r total vertical stress (Pa or psi)
u pore pressure (Pa or psi)

Effective stress is the stress carried by the solid particles. The total vertical stress acting at a point below the land surface is due to the weight of everything lying above. Reductions in pore pressure from groundwater pumping results in an increase in effective stress, which, in turn, can result in compaction and land subsidence.

The response of sediments to stress (i.e., their compressibility and thus specific storage) also depends upon the prior stress history of the sediment or rock. Deposits that were exposed to large loads in the past (e.g., due to burial by glaciers and overlying sediments and rock that were subsequently eroded) become overconsolidated (preconsolidated) and less vulnerable to further consolidation (inelastic deformation) so long as effective stress remains below the preconsolidation (historical maximum) effective stress. Inelastic compression is negligible in well-lithified rock. Preconsolidated strata and well-lithified rock still undergo elastic deformation. Once the preconsolidation effective stress is exceeded, the compressibility (and thus specific storage) of the aquifer system increases dramatically (Riley 1969; Holzer and Galloway 2005).

14.2.1 Aquifer Storativity Values from Pumping Tests

Storativity and specific storage values of confined aquifers are mostly commonly obtained from aquifer pumping tests using the Theis nonequilibrium equation or methods derived therefrom (Chap. 7). The accuracy of transmissivity and storativity values depends upon the quality of the collected data and the degree to which test conditions match the assumptions of the analytical methods used to interpret the data. Storativity values are usually obtained from multiple well pumping tests, which are preferred as these values are representative of a larger aquifer volume. Methods are available for calculating storativity values from single well pumping test data, but the values are considered less reliable than those obtained from multiple well tests (Kruseman and de Ridder 1991). Storativity values may also be estimated through inverse numerical modeling, which may be either specifically applied to interpret pumping test data or, much more commonly, employed in the calibration of groundwater models.

14.2.2 Specific Storage from Barometric Efficiency

Barometric efficiency (BE) is a measure of the degree to which changes in barometric pressure are manifested as changes in the water levels in uncapped wells completed in confined aquifers (or aquitards). Barometric efficiency is dimensionless and ranges from zero to one. The basic equation is (Jacob 1940)

$$BE = \frac{q_w g Dh}{DP_a} \text{ or } \frac{c_w Dh}{DP_a} \qquad (14{:}7)$$

where
BE   barometric efficiency (unitless)
Dh   change in piezometric water level that is caused by the barometric pressure change (m)
DP_a change in atmospheric pressure (force/area; N/m2)

The related parameter loading efficiency (LE) is the defined as the ratio of the change in aquifer head to a change in pressure loading at land surface. Loading efficiency is approximately equal to the 'tidal efficiency' defined by Jacob (1940). The sum of BE and LE is equal to one. Methods for computing barometric efficiency are presented and reviewed by Clark (1967) and Gonthier (2007). An important issue is distinguishing the component of water level changes that are due to barometric pressure change from variations in water levels that have a non-barometric origin.

Specific storage is related to barometric efficiency through the equation (Jacob 1940; Robson and Banta 1990; Geldon et al. 1997)

$$S_s = \frac{c_w b_w n}{BE} \qquad (14.8)$$

where n = porosity (fractional).

14.2.3 Storage Parameter from Field Compression Data

Storage parameters of confined aquifers can be obtained from the measured compression of aquifer strata in response to changes in pore water pressure caused, for example, by aquifer drawdowns (e.g., Robson and Banta 1990; Pavelko 2004; Pope and Burbey 2004). The vertical compressibility of a porous medium (m_v) can be determined from compression data using the equation

$$m_v = \frac{DL}{LDP_w} \qquad (14.9)$$

where
ΔL compression of the aquifer (m)
L   thickness of the aquifer (m)
ΔP_w change in pore pressure (Pa, N/m^2, kg/(ms^2))

Data on aquifer compression can be obtained using sensitive extensometers. Extensometers measure the vertical movement of land surface with respect to a fixed datum, which is typically either a steel pipe or cable that is cemented in place at the bottom of a well (Fig. 14.1). Compression and expansion of the strata between the bottom of the extensometer and land surface are measured as changes in the distance between the bottom of the well and datum at land surface. Extensometers with sensitive measuring and recording equipment can measure changes in surface elevation (and thus compression and expansion) down to a fraction of a millimeter. Estimates of compressibility and storage parameters obtained at a study site near Denver, Colorado, using aquifer pumping test, barometric efficiency, and extensometer compression data, were in good agreement with calculated storativity values ranging from 2.99×10^{-4} to 4.53×10^{-4} (Robson and Banta 1990).

Although extensometers can provide highly accurate data on compaction due to compression, they have the major limitation of being expensive to construct and are point measurements. Storage parameters have also been obtained from land surface elevation changes obtained from Global Positioning Systems (GPS) surveys and
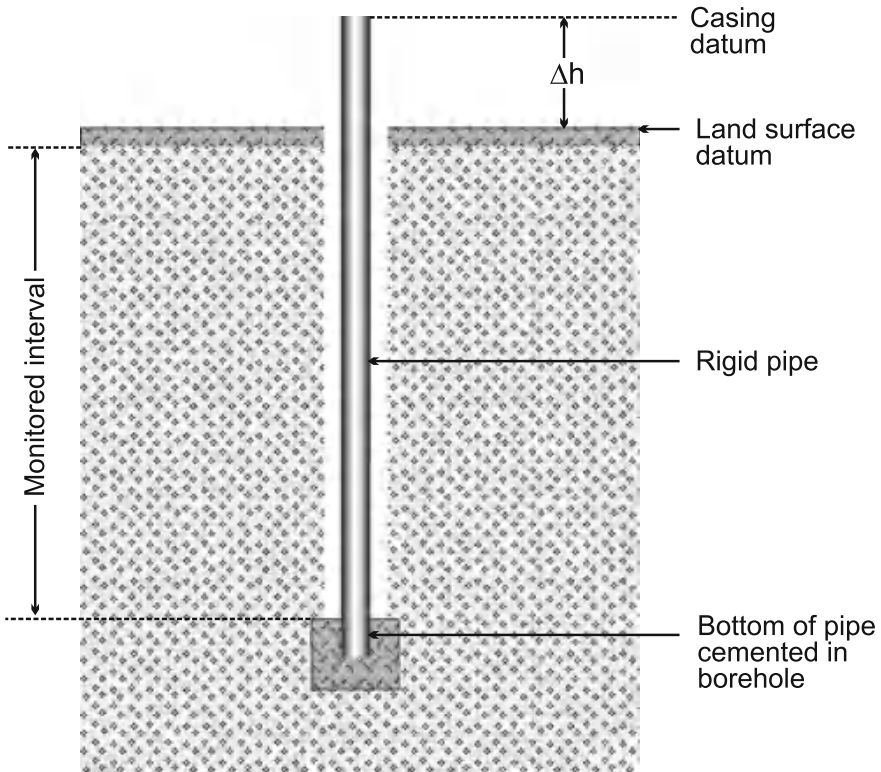
Fig. 14.1 Conceptual diagram of an extensometer. Land subsidence caused by compaction of the monitored interval is measured by the increase in distance between a datum on the pipe and land surface (Dh)

Satellite Interferometric Synthetic Aperture Radar (InSAR) interferograms (Galloway et al. 1998; Hoffmann et al. 2003; Yan and Burbey 2004). InSAR has the great advantages of providing areal coverage (as opposed to a one or limited number of point measurements) with pixels on an InSAR displacement map typically having an area of $30-90$ m^2 on the ground (Bawden et al. 2003). InSAR-measured seasonal land displacements measured in the Las Vegas Valley, Nevada, were in general agreement with borehole extensometer measurements, but were consistently greater, which was explained by InSAR measuring displacement in a greater thickness of deforming sediments (Hoffmann et al. 2001). InSAR-measured total displacement, whereas extensometers measure only compaction in the strata between the base of the extensometer and land surface. The calculated storage coefficient of 7.3×10^{-4} is within the range of values obtained from calibrated groundwater flow models and aquifer pumping tests.

14.2.4 Specific Storage from Laboratory Compressibility Data

Specific storage of low-permeability (aquitard) strata is commonly estimated on core samples by laboratory consolidation tests performed using either a consolidometer or oedometer. Consolidation tests are a basic tool in geotechnical engineering and are discussed in textbooks on the field (e.g., Holtz et al. 2010). Laboratory consolidation test results are often not representative of in situ conditions due to sample disturbance and stress changes. A review of laboratory methods for measuring specific storage by Van der Kamp (2001) indicates that laboratory measurements can give values orders of magnitude too large. The coefficient of volume change, and thus specific storage, are a function of the effective stress and are usually calculated at the existing or in situ vertical effective overburden stress (Shaver 1998).

14.2.5 Specific Storage from Geophysical Log-Derived Bulk Modulus

Specific storage is a function of the compressibility of the rock or sediment and its pore fluids. The inverse of the compressibility of materials is the bulk modulus, which can be obtained from borehole geophysical logs. In an elastic confined aquifer, neglecting a release of water from confining beds, specific storage can be calculated using the equation (Jacob 1940; Lohman 1972) with consistent units

$$S_s = nc_w \left(\frac{1}{E_w} - \frac{C}{nE_s} \right) \tag{14.10}$$

where

n   porosity (fractional)
E_w bulk modulus of elasticity of water (Pa or psi)
E_s bulk modulus of rock (solid) forming the aquifer (Pa or psi)
C   dimensionless coefficient (equal to 1 in uncemented granular matrix and 'n' in cemented aquifers)
c_w specific weight of water

Storativity is obtained by multiplying S_s by the aquifer thickness (b).
Saturated (in situ) bulk modulus E_{sat} can be calculated from the classic equation

$$E_{sat} = q_b \left(V_p^2 - \frac{4}{3} V_s^2 \right) a \tag{14.11}$$

where (with consistent units)

q_b bulk density
V_p compressional wave velocity
V_s shear wave velocity
a   constant to adjust for units

Bulk density and compressional and shear wave velocities are obtainable from density and sonic logs. E_s can be calculated from E_{sat} using a form of the Gassmann (1951) equation with known (looked up) values of the bulk modulus of the grains (minerals; E_g) and saturating fluid (water; E_w)

$$\frac{E_{sat}}{E_g - E_{sat}} = \frac{E_s}{E_g - E_s} + \frac{E_w}{n(E_g - E_w)} \qquad (14{:}12)$$

14.3   Evaluation of Specific Yield

Although conceptually simple, the accurate measurement of specific yield is quite difficult because the gravity drainage of water from pore spaces can be very slow (months or longer), especially in fine-grained sediments. Specific yield may be estimated from laboratory drainage tests, aquifer pumping tests (delayed-yield curve analysis and the volume-balance method), and using microgravimetric data. Comparison of the results of various types of specific yield measurements in sand suggests that specific yield values depend upon the type of test, the timescale of the test, and method of data analysis (Nwankwor et al. 1984). Specific yield values calculated from some pumping tests tend to be significantly lower than values obtained from laboratory methods, which raises the question as to which specific yield values are correct or, more pertinently, which values should be used in a specific groundwater model. Methods for determining specific yield values were reviewed by Johnson (1967), Nwankwor et al. (1984) and Neumann (1987).

14.3.1   Laboratory Measurement of Specific Yield

Specific yield is measured in the laboratory as the difference between the water content at saturation and the residual saturation (specific retention). The basic procedure is to fill a column with sediments, saturate the sediments with water, and then measure the volume of water that drains under gravity. Specific yield can be calculated from the sample volume and the drainage water volume. A primary difficulty in laboratory measurements of specific yield is that the time required to drain very fine-grained sediments may be extremely long. Use of suction or a centrifuge can expedite drainage, but the resulting specific yield values may not be

representative of field conditions. The water table response is usually much more rapid than gravity drainage, and specific yield values obtained from laboratory measurements may not be relevant to groundwater fluctuations in response to pumping (Neuman 1987), particularly for fine-grained sediments. Specific yield values from laboratory analyses may be appropriate for long-term evaluation of groundwater resources (Neuman 1987) in which there is ample time for gravity drainage to occur.

14.3.2   Volume-Balance Method

The volume-balance method calculates specific yield from the ratio of the volume of water pumped (V_w) to the volume of the cone of depression (V_c; Nwankwor et al. 1984):

$$Sy = \frac{V_w}{V_c} \qquad (14{:}13)$$

The methodology assumes that all of the pumped water is derived from the cone of depression. However, significant amounts of water may be released by gravity drainage outside of the observed cone of depression even though drawdowns may be imperceptible (Neuman 1987). Although drawdowns outside of the observed cone of depression are minute, they would occur over a large area. Neglecting water that originates outside of the cone of depression may result in exaggerated specific yield values (Neuman 1987). The significance of the contribution of water from outside the cone of depression was questioned by Akindunni and Gillham (1992) and Nwankwor et al. (1992). An additional source of error is incomplete drainage, which would tend to result in an underestimation of specific yield by resulting in a larger volume of the cone depression than would occur in a completely drained aquifer.

The volume-balance methods is data intensive in that numerous piezometers are required to accurately calculate the volume of the cone of depression. The cone of depression may have an irregular shape in highly heterogeneous and anisotropic aquifers, which complicates efforts to quantify its volume.

14.3.3   Aquifer Pumping Tests

Specific yield can be calculated from pumping test data using the Boulton (1963) and Neuman (1975) type-curve methods (Sect. 7.3.7). Type-curve methods performed using early test data and the volume-balance method tend to provide values that are much lower those obtained from laboratory methods (Nwankwor et al. 1984). With increasing test duration, the S_y value from pumping tests approach

laboratory determined values. The low values from early test data are attributed to a delayed drainage effect. Unsaturated zone drainage lags behind the decline of the water table. Specific yield values obtained from pumping tests should increase with increased test duration as the rate of water table decline decreases and drainage becomes essentially instantaneous (Neuman 1975; Nwankwor et al. 1984, 1992; Grimestad 2002). Test results are also influenced by partial penetration effects and drainage from the unsaturated zone (Moench 1994). Low specific yield values obtained from time-drawdown data in which delayed drainage from the unsaturated zone is not considered would underestimate the groundwater resources of an unconfined aquifer and overestimate drawdowns for a given pumping rate (Nwankwor et al. 1992).

Moench (1994) in a reanalysis of the data set used by Nwankwor et al. (1984, 1992) and Neuman (1987) concluded that analysis of pumping tests using curve-matching methods can give results consistent with the volume-balance and laboratory methods if the effects of partial penetration are included and composite plots of time-drawdown data from multiple piezometers are used with a common match point. Erroneous estimates of specific yield will also be obtained from pumping tests if there are unaccounted sources of water such as return flows of pumped water and inter-aquifer leakage (Grimestad 2002). The addition of water will reduce the rate of growth of the cone of depression for a given pumping volume. A key requirement for determining specific yield from pumping tests is that tests should have a long enough duration (several days or longer) to allow for accurate recording of the late (post-delayed yield) segment of the time-drawdown plot in which the data plot once more on the This curve (Sect. 7.3.7).

14.3.4   Microgravity

A time series of relative microgravity readings can provide information on changes in the mass, and thus volume, of water in unconfined aquifers (Sect. 11.12). Storage changes are calculated from relative gravity changes using the Bouguer slab equation, which can be simplified as follows (Pool and Eychaner 1995)

$$DS = Dg=41:9 \qquad (14:14)$$

$$S_Y = Dg=(41:9b) \qquad (14:15)$$

DS   change in storage (m)
Dg   gravity (acceleration of gravity) change (l Gal)
S_Y specific yield (dimensionless)
b   water table change (m)

For English units, a coefficient 12.77 is used instead of 41.9. Water table elevation changes are measured using monitoring wells at the same location as the

microgravity sites. Specific yield is calculated by dividing the decrease in storage by the decrease in aquifer water level (Pool and Eychaner 1995; Pool and Schmidt 1997; Pool 2008; Gehman et al. 2009).

Microgravity has the advantage of being a relative simple and inexpensive technique, but requires meticulous attention to detail by field staff (Pool and Eychaner 1995). Microgravity data can be effected by (and may need to be corrected for) earth tides, atmospheric effects, linear and nonlinear instrument drift, altitude change, and non-aquifer mass changes (Pool and Eychaner 1995). Microgravity measurements record the change in the total mass of water below the station, which includes water stored in both the unsaturated and saturated zone. Changes in the mass of the water in the unsaturated zone can impact the accuracy of specific yield values obtained from microgravity data.

14.3.5 Water Table Decline Associated with ET

Specific yield can be calculated from the decrease in the water table elevation associated with a known outflow of water from the water table aquifer. The specific yield of the water table aquifer in the Big Cypress Swamp of South Florida was determined by the U.S. Geological Survey using actual evapotranspiration (ET_a) rate data obtained from micrometeorological stations (Shoemaker et al. 2011). The ET_a rates were determined using the eddy covariance energy budget method. A specific yield value of 0.2 was obtained from the recorded decline in the elevation of the water table associated with ET_a. A specific yield of 0.2 is a commonly used value in South Florida, as determined from groundwater model calibration and other methods.

Specific yield estimation using ET_a data requires that the decline in the water table is due only to ET_a. A limitation of the application of the method is the general sparseness of data on Et_a rates. It is typically much too expensive to construct and operate a micrometeorological station solely to obtain ET_a data. However, regional ET_a rate data may be used to obtain a rough estimate of specific yield. The effects of uncertainty in ET_a rates on calculated specific yield values can be evaluated by a sensitivity analysis.

14.3.6 Water Table Rise Associated with Recharge and Water Table Fluctuations

Specific yield can be estimated from the rise of the water table associated with a recharge event such as a rainfall. Using rainfall data is operationally much simpler than the use of ET_a data, as rainfall can be measured using much less expensive and simpler rain gauges. However, recharge rates from rainfall data need to be corrected for runoff and evapotranspiration that occur during the monitoring period and

infiltrated water that does not reach the water table (i.e., increases in soil moisture; Logsdon et al. 2010). Additionally, infiltration may be impeded by air that is trapped in the unsaturated zone ahead of the wetting front. In an extreme case, air may be trapped and compressed under the wetting front resulting in abnormally high water levels in wells, which is referred to as the 'Lisse effect' (Weeks 2002). Air bubbles may also be trapped in the saturated zone during wetting, which would act to increase the water table elevation for a given amount of recharge.

On a longer duration (seasonal) and greater areal scale, specific yield has been estimated using a combination of the water table fluctuation method and groundwater basin water budget method (Maréchal et al. 2006). Specific yield is estimated from seasonal changes in aquifer water levels and water storage, with the latter determined from accurate estimates of all elements of the water budget. Detailed measurements of changes in water levels from numerous piezometers are required.

14.3.7   Inverse Modeling (Model Calibration)

In light of the difficulty of accurately measuring specific yield in the field, specific yield is commonly estimated during the numerical groundwater calibration process. The value of specific yield is adjusted to obtain a close match with observed water table elevation data. The major limitation of inverse modeling is the nonuniqueness of solutions; numerous sets of parameter values can provide the same result (e.g., same head distribution and fluxes). In practice, specific yield values are typically chosen that are hydrogeologically reasonable and consistent with historically used values for the study region. A preferred approach is to utilize one or more of the field methods to estimate specific yield to constrain the range of values considered in the model calibration process.

14.4   Evaluation of Aquitards

Low-permeability strata, referred to as aquitards or semi-confining layers, are of great importance in groundwater resources evaluation and management as they may

- protect underlying aquifers used for potable water supply from surface contamination
- divide aquifers in multiple zones
- protect aquifers from vertical migration of poorer quality (e.g., more saline) groundwater (i.e., upcoming)
- protect freshwater aquifers from upward migration of injected fluids
- be a source of water as the result of compaction
- be the primary loci for compaction and associated land subsidence

The general problem associated with characterization of low-permeability strata is the constraint of time. The slow rate of groundwater flow in low-permeability strata results in large (formation scale) responses to stresses being too long to observe (Neuzil 1986).

> In practical terms, the problem of flow in low permeability environments may be summarized as follows: How can knowledge of behavior on small scales be extrapolated to large dimensions and long periods of time? (Neuzil 1986, p. 1165).

The bulk hydraulic conductivity of aquitards may be much (orders of magnitude) greater than the hydraulic conductivity values obtained from small intact (laboratory scale) samples of aquitard materials. A greater variation in measured hydraulic conductivity values also occurs with decreasing scale of measurement.

Potential sources of the greater bulk hydraulic conductivity with increasing scale include the presence of fractures, karst features, sedimentary facies changes (discontinuities of confining strata), wells open to multiple aquifers, and other flow conduits (e.g., Herzog and Morse 1986; Mckay et al. 1993; Hanor 1993; Van der Kamp 2001; Hart et al. 2006). Where aquitard strata are unfractured (or not otherwise compromised), bulk hydraulic conductivity may be estimated by fine-scale measurements (e.g., Keller et al. 1989). Enhanced vertical flow allowed by fracture permeability can weaken the protective characteristics of aquifers, allowing for the rapid migration of contaminants. Fracture permeability in aquitards may also allow for more rapid recharge of underlying aquifers.

Methods for the determination of hydraulic conductivity of aquitards were reviewed by Keller et al. (1989), McKay et al. (1993), Döll and Scheider (1995), and Van de Kamp (2001). Each method has advantages and disadvantages. Because of the relationship between vertical hydraulic conductivity and scale, the use of multiple methods is recommended for the characterization of aquitards (Döll and Schieder 1995). It is important when developing testing programs to have knowledge of the various methods that are available, including their volume of investigations, time requirements, and other limitations.

14.4.1   Laboratory Analyses

The vertical hydraulic conductivity of confining strata can be measured by laboratory analysis of core samples. For shallow, unlithified strata, samples may be collected using thin-walled samples (e.g., Shelby tubes). Conventional coring techniques are used for lithified strata. Laboratory analytical methods used for low-permeability materials include

- steady-state flow tests
- hydraulic transient flow tests
- mechanical transient flow tests

Conventional steady-state flow analyses of low-permeability materials face the problem of long times being required to obtain steady-state flow conditions and the difficulty of generating and measuring slow rates of flow, which can be overcome using large hydraulic gradients (Neuzil 1986). Hydraulic transient flow tests commonly involve the rapid pressurization and then shut in of a reservoir on one side of sample and recording the time-dependent pressure recovery. The time pressure response of transient tests is a function of both K and S_s.

Hydraulic conductivity measurements can vary depending upon laboratory test conditions. A comparative study of the measurement of the hydraulic conductivity of two laboratory prepared clay samples indicates that the type of permeameter used (compaction mold, consolidated cell, and flexible wall) did not have a large or systematic effect on measured hydraulic conductivity values (Boynton and Daniel 1985). It is generally recognized that hydraulic defects, such as cracks, fissures, and sand lenses, control the hydraulic conductivity of fine-grained sediments. Hydraulic conductivity would be expected to increase with sample size as there would be a greater probability of encountering a defect (Boynton and Daniel 1985). In the laboratory prepared samples, there was modest sample size effect, which was not considered to be significant. The hydraulic conductivity of the largest samples was not more than twice the value obtained from the smallest samples (Boynton and Daniels 1985). Döll and Schieder (1995) documented a scale effect of increased hydraulic conductivity with core diameter and suggested that the relationship may be due to macropore flow.

14.4.2   Slug Tests

The hydraulic conductivity of low-permeability (tight) strata can be determined using conventional slug tests (Chap. 6) on wells completed entirely within the strata of interest or intervals isolated with packers. It is especially critical that the wells be properly constructed and that tight packer seals are obtained so as to avoid vertical fluid flow within the borehole. A small amount of vertical leakage may not be consequential when testing a high-transmissivity interval, which will dominate flow into the well, but can have a proportionately very large impact on the rate of change in water levels in wells completed in low-permeability strata. As is the case for slug tests in general, the results of slug tests performed in low-permeability strata can be impacted by skin effects that control the rate of flow into a well. Skin effects can be particularly problematic in wells drilled through clayey strata.

Inordinately long response times may occur during conventional slug tests performed in low-permeability strata (Neuzil 1986). It may take a year or longer for water levels to recover to static levels after both well development and during the performance of slug tests. The response rate depends upon the rate of flow from the borehole into the formation and the storage in the borehole or standpipe. An alternative method has been developed in which a well, or a packed off interval of a well, is filled with water and suddenly pressurized with additional water. The well is

shut in and the head changes caused by the pressurization are allowed to decay and are recorded (Bredehoeft and Papadopoulos 1980; Neuzil 1982).

Slug tests usually provide a measure of horizontal hydraulic conductivity. Although the volume of investigation of slug tests is greater than that of core analyses, the results may not be representative of the aquitard as a whole, particularly if zones of enhanced vertical flow (e.g., discontinuities in the aquitard) are missed. Depending up location of the tested interval with respect to fractures, slug test may reflect either the matrix permeability or fracture permeability.

14.4.3   Constant-Head Permeability Tests

Constant-head permeability tests involve monitoring the flow rate into or out of a well that is required to maintain a new constant water level. The tests yield essentially the same results are slug tests. Constant-head tests can also be performed on a large scale using trenches or excavated basins.

14.4.4   Aquifer Pumping Tests with Piezometers
in Aquitards

Neuman and Witherspoon (1972) proposed a method for estimating the hydraulic conductivity of an aquitard during an aquifer pumping test using drawdown data from piezometers completed in the aquitard. The method is based upon the ratio of drawdown in the aquitard to that measured in the aquifer at the same time and same distance from the pumped well. The solution is based on early data collected prior to the time when a discernible pressure transient reaches the adjoining unpumped aquifer and thus while the aquitard still behaves as if its thickness were infinite. The Neuman and Witherspoon (1972) solution includes six main steps (using consistent units):

(1) calculate transmissivity (T) and storativity (S) of the pumped aquifer
(2) calculate s'/s from the early test data, where s' is the drawdown measured in the aquitard and s is the drawdown measured in aquifer
(3) calculate dimensionless time (t_D),

$$t_D = \frac{Tt}{Sr^2} \qquad (14:16)$$

where r is the radial distance from pumped well and t is time since the start of the test
(4) obtain value of t_D' from a family of curves of s'/s versus t_D' for various t_D value

(5) calculate aquitard diffusivity (a′) (units L^2/T)

$$a' = \frac{t_{D'}z^2}{t} \qquad (14{:}17)$$

where z is the vertical distance from the aquitard observation point to the aquifer

6) calculate the vertical hydraulic conductivity of the aquitard (K') from the diffusivity value used a specific storage (S_s') value obtained by other means (e.g., consolidation test)

$$K' = a'S_s' \qquad (14{:}18)$$

Limitations of the Neuman and Witherspoon (1972) method are that it requires installation of monitoring wells within the aquitard and that the specific storage of the aquitard (S_s') needs to be independently determined, usually through laboratory analyses. However, laboratory analyses tend to give too large S_s' values (Van de Kamp 2001). Pressure changes within aquitards is commonly measured using simple piezometers, which have relatively high hydrodynamic lags (i.e., drawdown in piezometers is slow relative to drawdown in the aquitard). Rowe and Nadarajah (1993) provide correction factors for piezometer construction types and lengths.

14.4.5 Leakance Values from Aquifer Pumping Tests

The Hantush-Walton method is commonly used to obtain leakance values from pumping test data from semi-confined aquifers (Sect. 7.3.6). Vertical hydraulic conductivities are obtained by multiplying the leakance values by the aquitard thickness. The leakance values obtained from aquifer pumping tests with piezometers only in the pumped aquifer reflect the total leakage of water into the aquifer from both above and below. The calculated leakance may be approximately apportioned between the overlying and underlying strata based on their lithologies and thickness.

The accuracy of vertical hydraulic conductivity values obtained from aquifer pumping tests depends upon the degree to which the test conditions match the assumptions of the analytical methods. For example, is the water that leaks into an aquifer produced entirely by flow through the aquitard(s), or is there is significant component from aquitard compression? Results are most likely to be useful if the aquitard is relatively thin and the test has a sufficient duration for drawdown to penetrate through the full thickness of the aquitards and approach equilibrium. Drawdown in an aquifer may, in some tests, not be sensitive enough to quantify relatively low aquitard hydraulic conductivities (Döll and Schieder 1995)

14.4.6   Transmission of Seasonal Water Table Fluctuations

The diffusivity of aquitards can be estimated from the transmissions of sinusoidal fluctuations in pressure, such as resulting from seasonal water table fluctuations. Diffusivity is calculated from both the attenuation in the amplitude of the flow wave and from the phase shift using the basic equations for one-dimensional transient flow under homogenous conditions (Keller et al. 1989; Boldt-Leppin and Hendry 2003; Timms and Acworth 2005):

$$D = \frac{K_v}{S_s} = \frac{(z_1 - z_2)^2 p}{T_w}\left[\ln\left(\frac{a_{z1}}{a_{z2}}\right)\right]^{-2} \tag{14:19}$$

$$\frac{K_v}{S_s} = \frac{p}{T_w}\left[\frac{(z_1 - z_2)}{(d_{z1} - d_{z2})}\right]^2 \tag{14:20}$$

where

D	diffusivity (m^2/s)
K_v	vertical hydraulic conductivity (m/s)
Ss	specific storage (1/m)
z_1, z_2	measurement depths (m)
T_w	wave period (duration of one pressure cycle) (sec)
a_{z1}, a_{z2}	amplitude of wave or cycle at depths z_1 and z_2 (½ peak height measured from trough to trough)
$(d_{z1} - d_{z2})$	phase shift (radians)

   Where the upper monitoring point is located at the top of the confining unit, z_2 is equal to zero. In the field, the seasonal water level fluctuations are not perfectly sinusoidal due to the superposition of other events or processes. The seasonal water level wave or cycle can be better defined by filtering out the effects of other process on the recorded time series data (Boldt-Leppin and Hendry 2003). Harmonic data analysis can be used to decompose time series data into component single-frequency waves. For example, hydraulic heads measures in aquitards are also influenced by a secondary wave due to seasonal loading and unloading of the system caused by changes in the total mass of overlying water (Keller et al. 1989). Change in the mass of water may be due to variations in the water table elevation, surface water levels, soil moisture, and snow pack. The loading effect may be observed in piezometers that are deep enough to be practically unaffected by seasonal hydraulic head fluctuations at the upper boundary of the aquitard. The loading effect can, therefore, be corrected for by subtracting the head fluctuations from the deep piezometers from those of the shallow piezometers. If both piezometers are located within the aquitard, then the effect of loading would largely cancel out (i.e., both piezometers would experience the same loading change if they are located close together).

Piezometers with large storage volumes in very tight formations may have large response times that can cause the amplitude of observed water level fluctuations to be significantly smaller than the fluctuation in the adjoining aquitard. The actual amplitude at the piezometer intake (a_z) can be obtained by multiplying the observed amplitude by the factor (Hvorslev 1951; Keller et al. 1989)

$$\left[1 + \left(\frac{2pT_b}{T_w} \right)^2 \right]^{1=2} \tag{14:22}$$

where T_b = piezometric basic time lag.

Large piezometric response times may also affect the observed phased lag (Keller et al. 1989). Keller et al. (1989) cautioned that methods that utilize natural occurring water level or pressure changes depend upon long time series of accurate piezometric data. Drift in recording instruments and leakage into standpipes (risers) can compromise the data. The specific storage of the aquitard needs to be determined in order to obtain a value for the average vertical hydraulic conductivity of the aquitard from the calculated diffusivity values.

14.4.7 Darcy's Law-Based Methods Using Water Balance Data

The hydraulic conductivity of an aquitard can be estimated using Darcy's law from data on the discharge rate and hydraulic gradient across the unit. Hanor (1993) described application of the technique at a landfill site in Louisiana in which the study site is enclosed with berms and a subsurface slurry wall controls lateral flow off the site. The site, in essence, acts as a giant permeameter. The average K_z from the water balance calculations was four orders of magnitude greater than the K_z for laboratory testing, which was attributed to the presence of permeable sand and silt pedogenic horizons with secondary porosity and fracturing within the confining unit.

14.4.8 Tracer Testing Methods

The rate of vertical flow through an aquitard, and thus its hydraulic conductivity, can be estimated from tracer travel time through the unit. Profile from contaminant discharges may be suitable tracer datasets. Inverse modeling is used to replicate the observed profiles. Complications associated with the use of tracer data to evaluate the properties of aquitards include uncertainties associated boundary conditions, input history, and diffusion, sorption, and decay parameters, whose values are rarely accurately known. Groundwater flow through aquitards is typically much to slow for introduced tracer tests to be practical.

14.4.9   Inverse Modeling

The properties of aquitards are commonly estimated through calibration of flow models. Inverse modeling has the advantage of a very large volume of investigation. However, regional flow models may not have adequate resolution in either model grid size or calibration target locations to identify local heterogeneities that allow for enhanced vertical flow and to determine the cause of increases in vertical hydraulic conductivity with scale. Inverse modeling has the inherent limitation of the nonuniqueness of solutions.

In practice, the properties of aquitards are usually estimated first using field and laboratory testing data, with the values subsequently adjusted during the model calibration process. The effort put into characterizing aquitards depends upon their importance for a given project. For example, where the integrity of confining strata are important for preventing contamination of a potable water source, then considerable effort may be expended in characterizing aquitards, particularly their heterogeneity. Leakance values estimated from aquifer pumping tests that are adjusted during model calibration are often sufficient where the aquifer drawdowns are the primary concern.

References

Akindunni, F. F., & Gillham, R. W. (1992) Unsaturated and saturated flow in response to pumping of an unconfined aquifer: Numerical investigation of delayed drainage. Ground Water, 30, 873–884.

Bawden, G. W., Sneed, N., Stork, S. V., & Galloway, D. L. (2003) Measuring human-induced land subsidence from space. U.S. Geological Survey Fact Sheet 069-03.

Boldt-Leppin, B. E. J., & Hendry, M. J. (2003) Application of harmonic analysis of water levels to determine vertical hydraulic conductivities in clay-rich aquitards. Ground Water, 41, 514–522.

Boulton, N. S. (1963) Analysis of data from non-equilibrium pumping tests allowing for delayed yield from storage. Institute of Civil Engineers Proceedings (London), 26, 469–482.

Boynton, S. S., & Daniel, D. E. (1985) Hydraulic conductivity tests on compacted clay. Journal of Geotechnical Engineering, 111, 465–478.

Bredehoeft, J. D., & Papadopoulos, S. S. (1980) A method for determining the hydraulic properties of tight formations. Water Resources Research, 16, 233–238.

Clark, W. E. (1967) Computing the barometric efficiency of a well. Journal of the Hydraulics Division, American Society of Civil Engineers, 93(HY4), 93–98.

Döll, P., & Scheider, W. (1995) Lab and field measurement of the hydraulic conductivity of clayey silts. Ground Water, 33, 884–891.

Galloway, D. L., Hudnut, K. W., Ingebritsen, S. E., Phillips, S. P., Peltzer, G., Rogez, F., & Rosen, P. A. (1998) Detection of aquifer system compaction and land subsidence using interferometric synthetic aperture radar, Antelope Valley, Mojave Desert, California. Water Resources Research, 34, 2573–2585.

Gassmann, F. (1951). Über die elastizität poröser medien. Vierteljahrsschrift der Naturforschenden Gesellschaft in Zurich, 96, 1–23.

Gehman, C. L., Harry, D. L., Sanford, W. E., Stednick, J. D., & Beackman, N. A. (2009) Estimating specific yield and storage change in an unconfined aquifer using temporal gravity surveys. Water Resources Research, 45, W00D1.

Geldon, A. L., Earle, J. D., & Umari, A. M. A. (1997) Determination of barometric efficiency and effective porosity, boreholes UE-25 c#1, UE-25 c#2, and UE-25 c#3, Yucca Mountain, Nye County, Nevada. U.S. Geological Survey Water-Resources Investigations Report 97-4098.

Gonthier, G. J. (2007) A graphical method for estimation of barometric efficiency from continuous data – Concepts and applications to a site in the Piedmont, Air Force Plant 6, Marietta, Georgia. U.S. Geological Survey Scientific Investigations Report 2007-5111.

Grimestad, G. (2002) A reassessment of ground water flow conditions and specific yield at Borden and Cape Cod. Ground Water, 40, 14–24.

Hanor, J. S. (1993) Effective hydraulic conductivity of fractured clay beds at a hazardous waste landfill, Louisiana Gulf Coast. Water Resources Research, 29, 3691–3698.

Hart, D. J., Bradbury, K. R., & Feinstein, D. T. (2006) The vertical hydraulic conductivity of an aquitard at two spatial scales. Ground Water, 44, 201–211.

Herzog, B. L., & Morse, W. J. (1986) Hydraulic conductivity at a hazardous waste disposal site: comparison of laboratory and field-determined values. Waste Management & Research, 4(2), 177–187.

Hoffmann, J., Galloway, D. L., & Zebker, H. A. (2003) Inverse modeling of interbed storage parameters using land subsidence observations, Antelope Valley, California. Water Resources Research, 39(2), SBH 5-1–5-13.

Hoffmann, J., Zebker, H. A., Galloway, D. L., & Amelug, F. (2001) Seasonal subsidence and rebound in Las Vegas Valley, Nevada, observed by synthetic aperture radar interferometry. Water Resources Research, 37, 1551–1566.

Holtz, R. D., Kovacs, W. D., & Sheahan, T. C. (2010) An introduction to geotechnical engineering (2nd ed.). Upper Saddle River: Prentice-Hall.

Holzer, T. L., & Galloway, D. L. (2005) Impacts of land subsidence caused by withdrawal of underground fluids in the United States. In J. Ehlen, W. C. Haneberg, & R. A. Larson (Eds.), Humans as geologic agents. Reviews in Engineering Geology 16 (pp. 87–99). Boulder: Geological Society of America.

Hvorslev, J. (1951) Time lag and soil permeability in ground-water observations. Bulletin No. 36. Vicksburg, Mississippi: Waterways Experimental Station, U.S. Army Corps of Engineers.

Jacob, C. E. (1940) On the flow of water in an elastic artesian aquifer. American Geophysical Union Transactions, Part 2, 574–586.

Johnson, A. I. (1967) Specific yield – Compilation of specific yields for various materials. U.S. Geological Survey Water-Supply Paper 1662-D.

Keller, C. K., Van der Kamp, G., & Cherry, J. A. (1989) A multiscale study of the permeability of a thick clayey clayey till. Water Resources Research, 25, 2299–2317.

Kruseman, G. P. & de Ridder, N. A. (1991) Analysis and evaluation of pumping test data (Publication 47). Wageningen: International Institute for Land Reclamation and Improvement.

Logsdon, S. D., Schilling, K. E., Hernandez-Ramirez, G., Prueger, J. H., Hatfield, J. L., & Sauer, T. J. (2010). Field estimation of specific yield in a central Iowa crop field. Hydrological Processes, 24(10), 1369–1377.

Lohman, S. W. (1972) Ground-water hydraulics. U.S. Geological Survey Professional Paper 708.

Maréchal, J. C., Dewandel, B., Ahmed, S., Galeazzi, L., & Zaidi, F. K. (2006). Combined estimation of specific yield and natural recharge in a semi-arid groundwater basin with irrigated agriculture. Journal of Hydrology, 329(1), 281–293.

McKay, L. D., Cherry, J. A., & Gillham, R.W. (1993) Field experiments in a fractured clay till. 1. Hydraulic conductivity and fracture aperture. Water Resources Research, 29, 1149–1162.

Moench, A. F. (1994) Specific yield as determined by type-curve analysis of aquifer-test data. Ground Water, 32, 949–957.

Neuman, S. P. (1975) Analysis of pumping test data from anisotropic unconfined aquifers considering delayed gravity response. Water Resources Research, 11, 329–342.

Neuman, S. P. (1987) On methods of determining specific yield. Ground Water, 25, 679–684.

Neuman, S. P., & Witherspoon, P. A. (1972). Field determination of the hydraulic properties of leaky multiple aquifer systems. Water Resources Research, 8(5), 1284–1298.

Neuzil, C. E. (1982) On conducting the modified 'slug test' in tight formations. Water Resources Research, 18, 233–238.

Neuzil, C. E. (1986) Groundwater flow in low-permeability environments. Water Resources Research, 22, 1163–1195.

Nwankwor, G. I., Cherry, J. A., & Gillham, R.W. (1984) A comparative study of specific yield determinations for a shallow sand aquifer. Ground Water, 22(6), 764–772.

Nwankwor, G. I., Gillham, R.W., van der Kamp, G., & Akindunni, F. F. (1992) Unsaturated and saturated flow in response to pumping of an unconfined aquifer: field evidence of delayed drainage. Ground Water, 30, 690–700.

Pavelko, M. T. (2004) Estimates of hydraulic properties from a one-dimensional numerical model of vertical aquifer-system deformation, Lorenzi Site, Las Vegas, Nevada. U.S. Geological Survey Water-Resources Investigation Report 03–4083.

Pool, D. R. (2008) The utility of gravity and water-level monitoring at alluvial aquifer wells in southern Arizona. Geophysics, 73(6), WA49-WA59.

Pool, D. R., & Eychaner, J. H. (1995) Measurement of aquifer-storage change and specific yield using gravity surveys. Ground Water, 33, 425–432.

Pool, D. R., & Schmidt, W. (1997) Measurement of ground-water storage change and specific yields using the temporal-gravity method near Rillito Creek, Tucson, Arizona. U.S. Geological Survey Water Resources Investigations Report 97–4125.

Pope, J. P., & Burbey, T. J. (2004) Multiple aquifer characterization from single borehole extensometer record. Ground Water, 42, 45–58.

Riley, F. S. (1969) Analysis of borehole extensometer data from central California. In L. J. Tison (Ed.), Land subsidence. Publication 89 (pp. 423–431). International Association of Scientific Hydrology.

Robson, S. G., & Banta, E. R. (1990) Determination of specific storage by measurements of aquifer compression near a pumping well. Ground Water, 28, 868–874.

Rowe, R. K., & Nadarajah, P. (1993) Evaluation of the hydraulic conductivity of aquitards. Canadian Geotechnical Journal, 30, 781–800.

Shaver, R. B. (1998) The determination of glacial till specific storage in North Dakota. Ground Water, 36, 552–557.

Sneed, M., & Galloway, D. L. (2000) Aquifer-system compaction: Analyses and simulations-the Holly Site, Edwards Air Force Base, Antelope Valley, California. U.S. Geological Survey Water-Resources Investigations Report 00-4015.

Shoemaker, W. B., Lopez, C. D., & Duever, M. J. (2011) Evapotranspiration over spatially extensive plant communities in the Big Cypress National Preserve, southern Florida, 2007–2010. U.S. Geological Survey Scientific Investigations Report 2011-5212.

Terzaghi, C. (1925) Principles of Soil Mechanics. Engineering News-Record, 95, 832–836.

Timms, W. A., & Acworth, R. I. (2005) Propagation of pressure change through thick clay sequences: an example from Liverpool Plains, NSW, Australia. Hydrogeology Journal, 13, 858–870.

Van de Kamp, G. (2001) Methods for determining the in situ hydraulic conductivity of shallow aquitards – an overview. Hydrogeology Journal, 9, 5–16.

Weeks, E. P. (2002) The Lisse effect revisited. Ground Water, 40, 652–656.

Yan, T., & Burbey, T. J. (2008) The value of subsidence data in groundwater model calibration. Ground Water, 46, 538–550.

Chapter 15
Specialized Aquifer Characterization and Monitoring Methods

A wide variety of methods have been proposed or applied to groundwater investigations that are not yet widely utilized either because of limited applications, costs, or perhaps lack of widespread knowledge of their value and limitations. This chapter is a somewhat disjointed review of some specialized aquifer characterization techniques that did not fit well into the other chapters, but should still be considered in aquifer characterization investigations. Stoneley wave borehole geophysical analysis can provide information on the location of hydraulically active fractures. Advanced oil-field technologies, such as cross-well seismic tomography and wireline formation testers have potential specialized applications in groundwater investigations. Multilevel testing and monitoring systems are available that are less expensive alternatives to multiple-monitoring wells or multiple-zone wells. Remote sensing techniques have applications where aspects of subsurface hydrogeology are manifested at land surface.

15.1 Unconventional Aquifer Characterization Methods

15.1.1 Stoneley Wave Log Evaluation of Permeability

Sonic borehole geophysical logs are most often used to determine porosity from the travel times of compressional ('p') waves (Sect. 10.6). Other sonic waves can provide valuable information on aquifer properties. Stoneley waves are large-amplitude interface waves generated by a sonic tool in a borehole. Stoneley waves propagate along solid–fluid interfaces, such as along the walls of a fluid-filled borehole. They are the main low-frequency component of the signal generated by sonic sources in boreholes (Schlumberger n.d.). At low frequencies, Stoneley waves behave as a tube wave that propagates as a piston-like compression of the fluid in the borehole (Rosenbaum 1974; Algan and Toksöz 1986; Hardin et al. 1987 Brie et al. 1988;

Winkler et al. 1989; Serra 2008). In vertical seismic profiling (VSP), Stoneley waves are generated when p-waves generated by a surface seismic source interact with hydraulically active fractures that intersect the borehole (Hardin et al. 1987). When a tube waves crosses permeable strata or fractures, wave pressure pushes fluid from the borehole into the formation, which results in energy loss, and hence attenuation and slowing of the waves and the generation of reflected waves (Brie et al. 1988; Winkler et al. 1989; Serra 2008). Total fluid displacement into rock is a sum of the elastic deformation of the solid phase and the dynamic flow of fluid into the pores.

Stoneley waves are sensitive to fluid diffusivity (Algan and Toksöz 1986), which is expressed as

$$D = \frac{k}{\phi \mu c} \qquad (15.1)$$

where
D   fluid diffusivity (m^2/s)
k   permeability (m^2)
ϕ porosity (fractional)
μ   dynamic viscosity (Pa-s, kg/ms)
c   compressibility of fluid (m^2/n, Pa^{-1}, ms^2/kg)

As the diffusivity increases, the radial penetration distance increases, which is on the order of millimeters to meters (Algan and Toksöz 1986). Higher frequencies result in lower penetration distances.

The Stoneley wave method is the only technique that provides a continuous direct measurement of permeability along a well. However, the problem of extracting accurate permeability values lies in the absence of a universal empirical or simplified approach that can provide the desired level of reliability and accuracy (Brie et al. 1988; Ayan et al. 1999). Stoneley wave attenuation can be affected by factors that reduce communication between the borehole and formation, such as mudcake and formation damage (Brie et al. 1988). Changes in formation shear modulus related to increased clay content can be misinterpreted as zones of higher permeability (Ayan et al. 1999). Borehole shape and rugosity can also strongly affect the Stoneley response. The technique is a useful indicator of the presence of high permeability, hydraulically active fracture zones. However, attempts to construct a rigorous quantitative theory relating fracture hydraulic properties to tube-wave amplitude and velocity have not been successful (National Research Council 1996).

Balossino et al. (2008) investigated the use of Stoneley wave data to predict permeability in carbonate rocks from the Karachaganak Field, western Kazakstan. Log-derived permeability was validated against probe-permeability and core plug measurements. The overall shape of the Stoneley permeability curve and range of variation show a fair to good match with core data. Some of the zones of mismatch were related to borehole rugosity, breakout, local low porosities (<6 %), and layer

thicknesses of less than 1 m. Core plugs and minipermeameter measurements have different resolutions and volumes of investigation than borehole logs. The zones of mismatch could be filtered out using acoustic-image log data.

Stonely wave attenuation is not normally measured using conventional acoustic logs. The Dipole Shear Sonic Imager (DSI, mark of Schlumberger) log measures the attenuation of Stoneley wave energy that occurs between two adjacent receivers with a fixed (15 cm) spacing (Delhomme 2007). Stoneley wave logging is perhaps best considered as a supplemental method at present, which may have its greatest value as a tool for identifying hydraulically active fractures.

15.1.2   Cross-Well Seismic and Radar Tomography

A limitation of most borehole geophysical techniques is that they only provide data on the properties of the logged formation in the immediate vicinity of the borehole. The properties and continuity of strata between boreholes are evaluated by inter-polation of borehole data or inverse modeling techniques. Cross-well seismic tomography is a technique for obtaining petrophysical and stratigraphic data on the strata between boreholes. The technique is based on measurements of seismic signals transmitted from a source located in one well to a receiver array located in another neighboring well. The collected data are processed to create a profile of acoustic velocity and other acoustic properties between the wells, which can be further processed to porosity and permeability values.

There has been limited application of cross-well seismic tomographic to groundwater resources projects, and the few studies have been more of an exper-imental (test-of-concept) nature. Eldred et al. (1995) document the application of cross-well seismic tomography during the hydrogeological characterization of a proposed nuclear waste repository at the Sellafield site in the U.K. Parra et al. (2003, 2006) performed cross-well seismic tomography between two wells in South Florida completed with open holes in Eocene carbonates. The wells were con-structed as part of the Comprehensive Everglades Restoration Plan (CERP) aquifer storage and recovery project. The cross-well seismic reflection data captured changes in the velocity of compressional waves (V_p), which could be quantitatively related to porosity and permeability variations in the formation using empirical relationships from core analyses (Fig. 15.1).

The technique delineated both laterally continuous flow units and laterally dis-continuous units that are directly related to vuggy porosity development. The Parra et al. (2003, 2006) study demonstrated the importance of core data (petrophysical measurements and petrography) and conventional and advanced borehole geo-physical data (sonic and nuclear magnetic resonance logs) for the accurate and detailed interpretation of cross-well seismic tomography data.

Cross-well radar tomography combined with saline tracer tests was used on an experimental basis to characterize fractured-rock aquifers (Olsson et al. 1992;
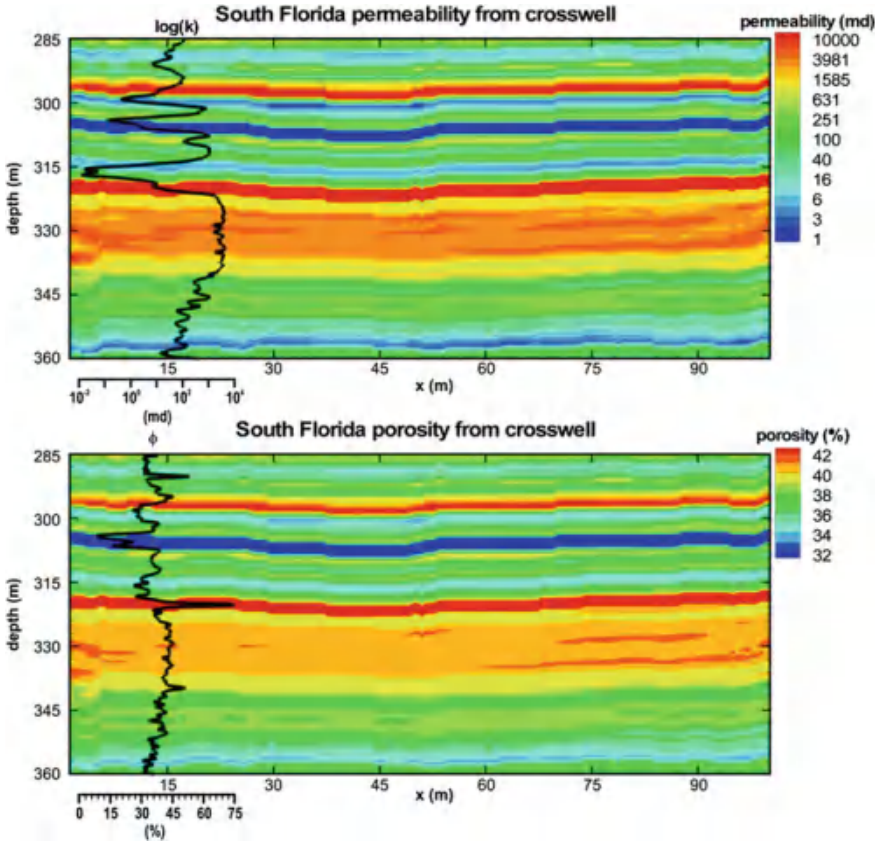
Fig. 15.1 Permeability image (top) and porosity image (bottom) computed from cross-well seismic data from the western Hillsborough aquifer storage and recovery system site, Palm Beach County, Florida. The respective well logs are superimposed on the images (from Parra et al. 2006)

Day-Lewis et al. 2003, 2006). The basic concept is that high-frequency electromagnetic waves are propagated from multiple transmitter locations in one borehole and recorded at multiple locations in a second borehole. The presence of an electrically conductive tracer serves to increase electromagnetic wave attenuation and thus illuminates permeability pathways. Time-lapsed tomograms were used to map the movement of the saline tracer. Day-Lewis et al. (2006) documented the application of the technique to a fractured metamorphic aquifer at the USGS Mirror Lake Fractured Rock Hydrology Research Site. The experiment site contained a cluster of four wells in a 10 m-sided square pattern. A basic limitation of the technique is that the inversion process used for data analysis does not lead to unique solutions. However, solutions can be constrained by other independent data. The experimental results also indicate that much of the tracer mass migrated outside of the three tomographic planes generated in the study.

Cross-well seismic and radar tomography provide data on the plane between wells, but interpolation is still required to develope three-dimensional models. The cost and technical expertise required to perform these methods will limit their application in groundwater investigations.

15.1.3   Downhole Formation Testers

Wireline tools have been developed for the oil and gas industry to efficiently obtain fluid samples and measure pressure and permeability in boreholes filled with drilling mud. The earlier Repeat Formation Tester (RFT, trademark of Schlumberger) allows for the sampling of reservoir fluids and measurement of formation pressure versus time at specific depth stations (Ahmed et al. 1991). The RFT has an electrically driven hydraulic system that can be repeatedly set and retracted to pressure test multiple zones of interest on one trip in the well. Formation fluids are allowed to flow into two chambers. Permeability is calculated from associated pressure versus time changes during drawdown and recovery (build up).

The Modular Formation Dynamics Tester (MDT, trademark of Schlumberger), as the name implies, can be run with a variety of modules that allow for different types of testing and data collection. The basic tool consists of one or more hydraulically retractable probes, each embedded in a circular packer, and two opposing pistons on the opposite side of the tool that push the probes against the formation to help achieve a good seal (Colley et al. 1992; Crombie et al. 1998). Other components or features include

- a pump out and flow control module, which can pump either to the borehole during development or to a sample chamber
- a variable rate and volume pretest chamber
- flowline fluid resistivity measurement
- temperature sensors
- pressure gauges
- an optical fluid analyzer module, which allows for the analysis of fluid composition (e.g., amount and types of oil, gas, and water) through the effects of absorption and scattering
- sample collection and transportation chambers (Modular Reservoir Multisample Module; MRMS)
- a dual-packer module that allows for drill stem and interference tests.

The related Cased Hole Dynamics Tester (CHDT, mark of Schlumberger) has the ability to drill through a cased borehole and into the formation, perform multiple pressure measurements, recover fluid samples, and then plug the hole made in the casing. The CHDT is combinable with MDT modules, and can drill and plug up to six holes and collect six samples per trip. The MDT can seal (plug) to a differential pressure of 10,000 psi.

Ayan et al. (1999) described the use of the MDT to perform local interference tests across tight zones to obtain in situ vertical and horizontal permeabilities. Water was produced between a pair of packer below the tested tight zone and a pressure probe was set above the tight zone.

Downhole formation testers are advanced technologies that are currently too expensive to run for most groundwater investigations. Potential applications where formation testers can be cost effective are deep injection well projects in which water samples and permeability data are needed from mud-filled boreholes. Other applications are where formation testing and water sampling need to be performed on existing steel-cased wells.

15.1.4 FLUTe Transmissivity Profile and Sampling System

The FLUTe (Flexible Liner Underground Technologies) hydraulic conductivity profiler involves the eversion into a well of a flexible impermeable liner composed of polyurethane-coated nylon fabric (Einarson 2006; Cherry et al. 2007; Keller et al. 2013). As the liner enters a well, it progressively seals off the borehole wall and forces water downward into the remaining open part of the well (Fig. 15.2). The
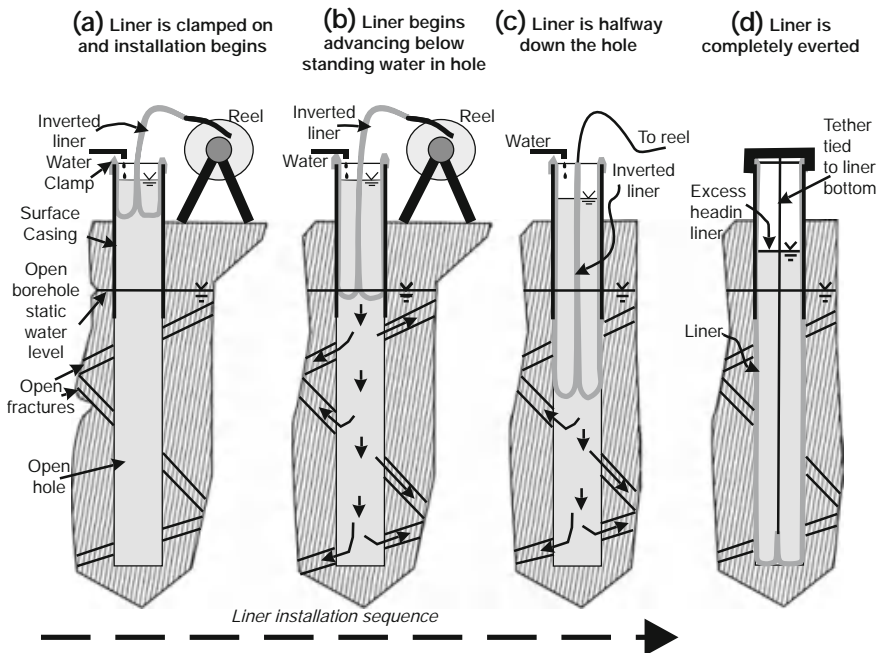
Fig. 15.2 Conceptual diagram of the FLUTe system (from Cherry et al. 2007)

eversion of the liner is performed using water pressure. The rate of liner descent is controlled by the transmissivity of the open-hole segment below the liner. As flow zones (e.g., fractures) are sealed off, the transmissivity of the open hole below the liner decreases and the velocity of the descending liner slows as back pressure increases. The raw data are the velocity of the liner eversion and the excess head in the liner versus depth, which are processed to obtain a transmissivity versus depth profile. The mapping of a borehole is reported to taken from 1 to 4 h.

After completion of the transmissivity profile, the liner is removed and the borehole is available for other uses, such as completion as a permanent monitoring well. A separately installed FLUTe multilevel groundwater sampling (MLS) system is available. The MLS liner has multiple sampling ports each connected to land surface by dedicated tubing (Cherry et al. 2007). The blank liner seals of the borehole between the sampling ports. MLS liners are custom made at the factory to customer specifications (e.g., borehole diameter and sampling port depths).

15.2 Multilevel Monitoring and Ambient Hydraulic Head Data

Multilevel monitoring involves the establishment of multiple-monitoring zones at different depths at a given site, which can be accomplished using clustered wells, nested wells, multi-zone monitoring wells, or MLS (Fig. 15.3). Nested wells consist of multiple casing strings installed inside a single borehole. Multi-zone (e.g., dual-zone or tri-zone) monitoring wells are constructed in lithified strata using multiple coaxial casing strings (Fig. 15.4). MLS systems consist of multiple sampling points within a single casing. Packer-based MLS systems include the Westbay system (Nova Metrix) and the Solinist Waterloo systems. The Westbay system consists of multiple packers installed in a single borehole that isolate selected zones of an aquifer (Fig. 15.5). The Westbay system allows for the collection of both pressure data and water samples from each discrete monitoring zone. MLS systems were reviewed by Einarson (2006), Koch and Pearson (2007), and Cherry et al. (2015).

The optimal type of multilevel monitoring system for a given project depends to a large degree upon the number of depth intervals to be monitored and their depths, and local well drilling costs and expertise. The selection between multilevel monitoring system options should also consider data quality, sample collection requirements and time, performance, reliability, and appropriateness for the site-specific hydrogeological environment.

Clustered single-zone wells are usually the least expensive option where only several shallow zones are to be monitored. Multiple-zone monitoring wells are more complicated to properly construct to ensure that the monitoring zones are hydraulically separated. Maintaining the mechanical integrity of the wells is also a concern. Some dual-zone monitoring wells used for deep injection well systems in South Florida failed due to corrosion of the inner steel tubing. The design of
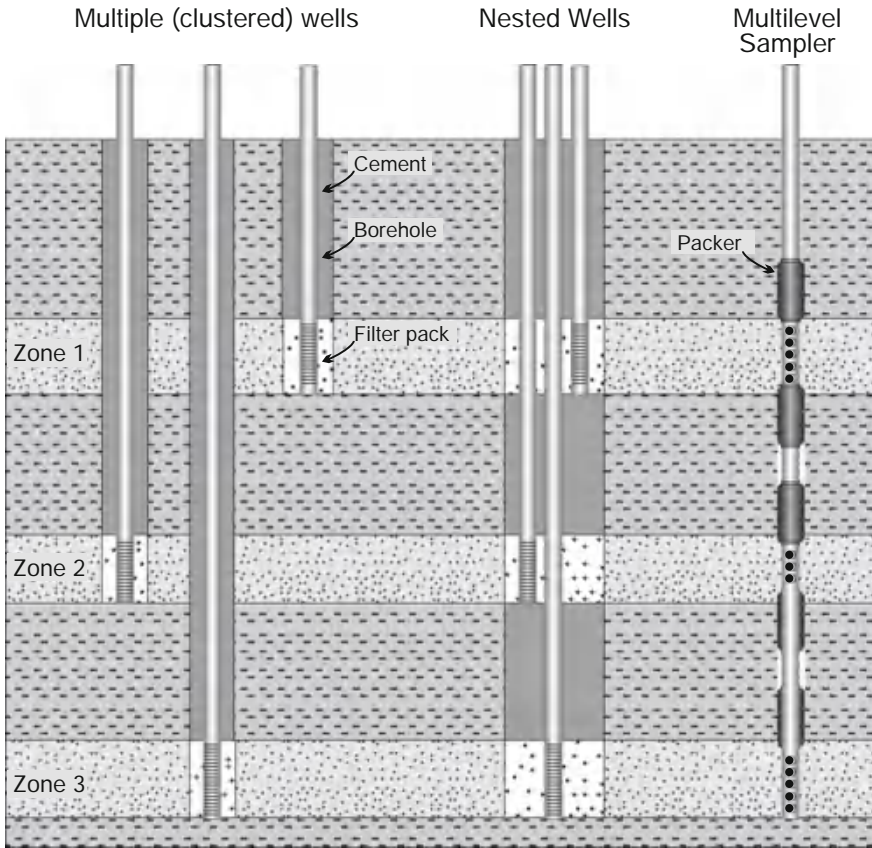
Fig. 15.3 Conceptual diagram of options for multiple-zone monitoring

subsequently constructed dual-zone monitoring wells was changed to include a fiberglass-reinforced plastic (FRP) inner tubing. Nested and coaxial multiple-zone monitoring wells need to be carefully constructed to ensure isolation of the zones. They also have the limitation of the difficulty of detecting failure of the annular seals (Cherry et al. 2015). Clustered single-zone wells have the advantage that leakage between monitoring zones due to compromised mechanical integrity of the well is least likely compared to the other design options.

As well depths increase, nested and coaxial multiple-zone wells and MLS systems become less expensive than clustered wells, with the cost 'cross-over' depth depending on construction details and local well drilling costs. MLS systems are the least expensive option when a large number of monitoring zones at different depths are required. MLS systems can be designed and constructed to establish numerous (>10) sampling points in a single well.

The primary use of MLS systems has been to obtain data on pressures and water quality from multiple aquifers, aquifer zones, and confining zones at a given

Fig. 15.4 Conceptual
diagram of triple-zone
monitoring well completed
with open holes in limestone
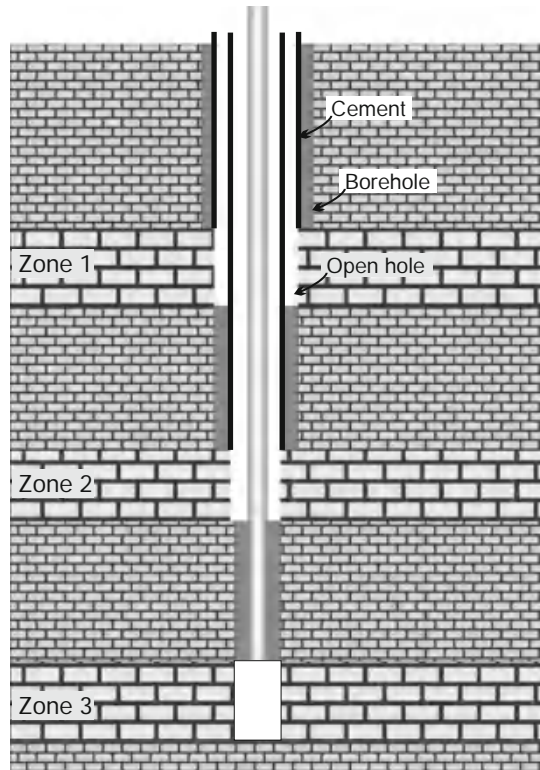
geographic location. However, multilevel monitoring can also provide important
data for aquifer characterization. For example, ambient pressure data can provide
information on the vertical and horizontal connectivity of aquifer and confining
zones. The response of different zones to groundwater pumping can provide
quantitative information on aquifer heterogeneity. Cross-well aquifer testing (hy-
draulic tomography) is a promising technology for obtaining data on the 2-D and
3-D distribution of hydraulic conductivity at hydrogeologically complex sites
(Sect. 7.6). Eldred et al. (1995) documented the application of cross-well hydraulic
testing using a 30-zone 1250 m-deep Westbay System. Primary monitoring zones
selected for the cross-well hydraulic testing were based on identified hydrogeo-
logical conductive features and zones adjacent to structural features that intercepted
the two boreholes (Eldred et al. 1995).

   Most hydraulic testing methods provide horizontally oriented data, as opposed to
data on vertical connection between hydrogeologic units (Meyer et al. 2008).
Aquifers or aquifer zones that are hydraulically well connected at a given site
should have identical or at least similar heads. Water level data from different
monitoring zones need to be converted to equivalent freshwater heads if there is a
significant difference in salinity. Differences in head between monitoring zones are

Fig. 15.5 Diagram of a
Westbay system
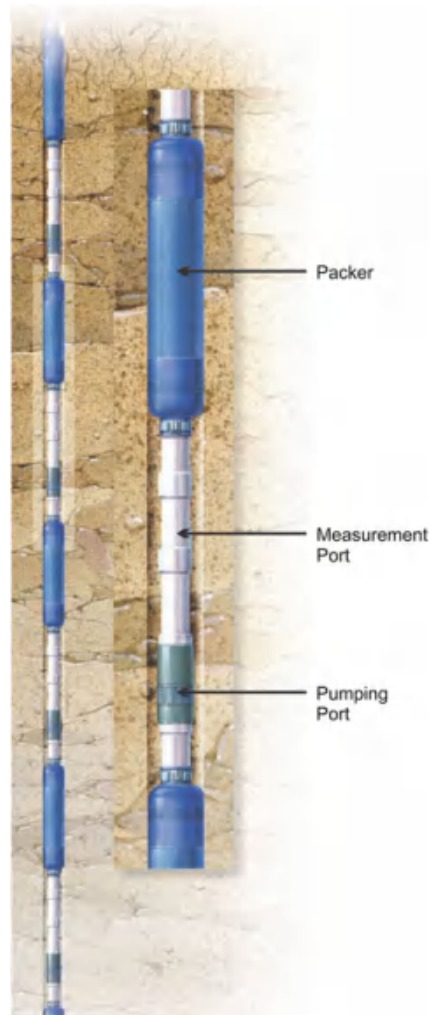
evidence that the zones are not well connected and that little flow occurs between the zones.

Meyer et al. (2008) investigated the use of a MLS system to evaluate the connection between hydrogeologic units (HGUs), which they defined to "represent partitions of the groundwater flow domain that are hydraulically consistent at a specified spatial scale." HGUs can be differentiated by hydraulic discontinuities that are generally produced by the influence of geological variability on the flow system (Meyer et al. 2008). Meyer et al. (2008) obtained a high-resolution hydraulic profile using a 36-port Westbay system at a study site in south-central Wisconsin, which is underlain by Quaternary glacial deposits and then Cambro-Ordovician sandstones, siltstones and dolostones (Fig. 15.6). Eight major head changes (inflection in the

Fig. 15.6 High-resolution
hydraulic profile of
Cambro-Ordovician strata in
south-central Wisconsin from
a 36-port Westbay system.
Major head changes indicate
that the system is divided into
multiple stacked
hydrogeologic units (HGUs)
(after Meyer et al. 2008)
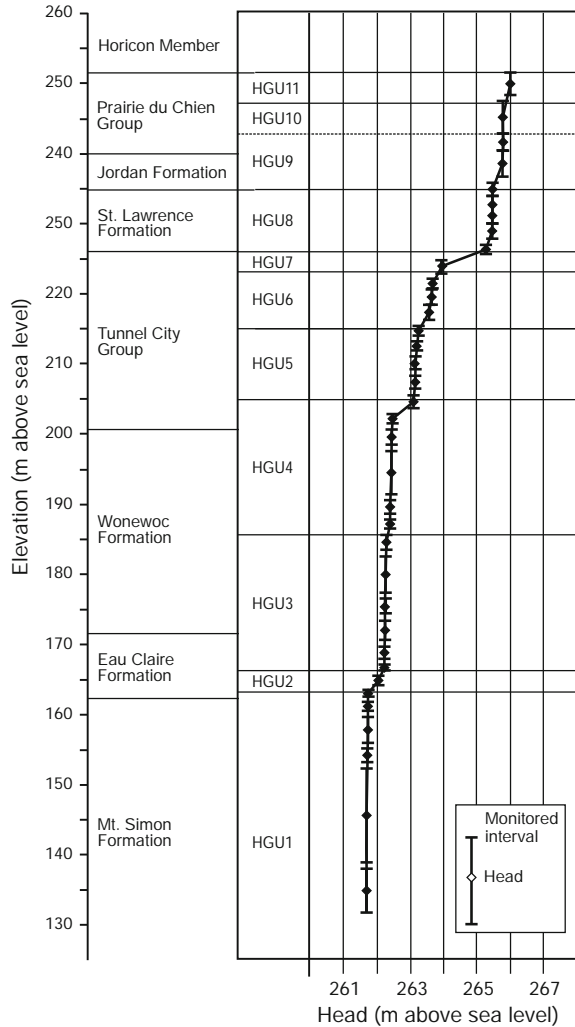
profile) were detected, which indicate that the system is not one hydraulic unit, but
is instead composed of multiple stacked HGUs

The characteristics of HGUs and specific location of the interfaces between the
monitoring intervals were evaluated using traditional techniques, such as core
descriptions, core analyses, and borehole geophysical logs. The HGUs were found
to be dominated by fracture flow, with the inflections in the hydraulic head profiles
caused by poor connection between the fracture network of adjacent units rather
than the presence of a classic aquitard (Meyer et al. 2008). The control of
groundwater flow by multiple poorly connected HGUs has great significance for
modeling contaminant migration at the study site. Meyer et al. (2014) provide the

results of a multiyear study in which head profiles with the highest, technically feasible resolution were obtained with a Westbay System to interpret vertical gradients between adjacent monitoring zones. Intervals with large vertical hydraulic gradients indicated the presence of intervening relatively low vertical hydraulic conductivity (K_v) units. The low K_v (i.e., confining or semiconfining) units were observed to be thin and were not predicted by lithostratigraphic, geophysical, or horizontal hydraulic conductivity data, thus supporting the application of MLS systems for high-resolution aquifer characterization, particularly when delineation of HGUs is critical (Meyer et al. 2014).

MLS systems were used to monitor temperature and head in the Eastern Snake River Plain (ESRP) aquifer at the Idaho National Laboratory, Idaho (Fisher and Twining 2011; Twining and Fisher 2015). The ESRP aquifer consists of interbedded basaltic lava flows and terrestrial sediments and is characterized by very high degrees of heterogeneity and anisotropy. Six Westbay systems were installed with a total of 86 sampling intervals, and temperature and head were monitored over a 2-year period. Temperature and head profiles were unique to each borehole due to the very high degree of aquifer heterogeneity. The most dramatic changes in head (greatest inflections in the hydraulic head profiles) occurred near sediment layers. However, not all sediment layers had associated head changes and it was thus difficult to predict the location of head changes based on core and geophysical data alone (Fisher and Twining 2011).

Smith and Hunt (2008) documented data from a 14-port Westbay system installed in the Edwards Aquifer and Trinity Aquifer System of central Texas. Proper groundwater management requires an understanding of hydraulic connection between the heavily utilized Edwards aquifer and Trinity aquifer system, which underlies and is adjacent to the Edwards aquifer. Large differences in head (1 to 12 m) between monitoring zones is evidence that very little vertical flow occurs between the Edwards and Trinity aquifers at the study site.

15.3   Vibrating Wire Piezometers

Aquifer water (i.e., pore) pressures are usually determined using wells or well zones that are open to the depth interval of interest. Pressure is either measured directly or, more commonly, from measured water elevations in wells. Vibrating wire piezometers (VWPs) have the advantage that they can be installed in fully grouted (cemented) boreholes and that multiple piezometers can be installed in a single borehole. The piezometer can also be installed using a sand filter method and by being pushed into soft cohesive strata using cone penetration test (CPT) equipment. The piezometers can be installed in slant and horizontal wells in addition to vertical wells. Vibrating wire piezometers are very quick to respond to pore-pressure changes and have a high reliability, which is important as they have the disadvantage of being permanently installed when grouted in place.
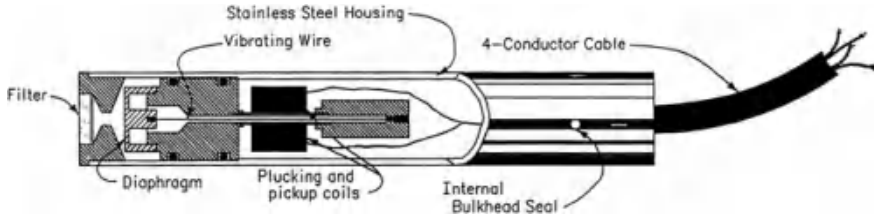
Fig. 15.7   Diagram of a vibrating wire piezometer

A vibrating wire piezometer contains the following main elements (Fig. 15.7; USBR n.d.; Zarriello 1995):

- stainless steel casing
- filter
- diaphragm
- stainless steel wire clamped under tension to the diaphragm and casing
- plucking and pick-up electromagnetic coils
- internal bulkhead seal
- cable connection

The electromagnetic coils are used to cause the steel wire to vibrate at its natural resonant frequency and to measure the vibration frequency of the wire. Changes in the fluid pressure on the diaphragm cause it to deflect, which changes the tension on the wire and its vibrational frequency. The square of the vibrational frequency is directly proportional to the pressure applied on the diaphragm. Instrument-specific calibration data are used to convert vibration frequency to pore water pressure over the design pressure range of the instrument.

Procedures for fully grouted installation were reviewed by Mikkelsen and Green (2003), Contreras et al. (2008) and the USBR (n.d.). Although it may intuitively seem that a cemented piezometer might be isolated from pore waters, both theoretical and ample empirical evidence have demonstrated that fully grouted piezometers should correctly measure the pore water pressure in the surrounding saturated sediment and rock. Grouting of the borehole is performed using a cement-bentonite grout (i.e., mixture of Portland cement and sodium bentonite). The cement-bentonite grout is permeable enough to quickly transmit pressure changes to the piezometer. A technical concern is that the grout should not be too permeable relative to the formation. Contreras et al. (2008) reported that the permeability of the grout mixtures can be up to three orders of magnitude greater than the permeability of the surrounding ground without introducing significant error.

Neels and Gray (2014) document problems observed with VWP installation using the fully grouted method in deep bores used for monitoring impacts associated with coal seam gas development in the Surat Basin, Australia. The documented problems resulted in most VWP installations for coal seam gas to be less than ideal and therefore unreliable (Neels and Gray 2014). Failure was primarily attributed to

grouting (e.g., separation, heat generation and channeling). Neels and Gray (2014) suggested that the suitability of VWPs for monitoring soil formations did not readily transfer to deeper bores used for coal seam gas monitoring.

Vibrating wire piezometers are widely used for geotechnical monitoring and in the mining and oil and gas industry, but have had a much lesser use to date for groundwater investigations. VWPs can have particular value for groundwater investigations as a cost-effective means of monitoring water pressure in multiple zones. Fully cemented piezometers might also be added during the construction of conventional monitoring wells to allow for pressure monitoring in the cemented strata above screened and open-hole intervals.

15.4   Remote Sensing and Lineament Mapping

Buried structures of hydrogeological interest may be detected by remote sensing, which was described by (Jha et al. 2007, p. 431) as the

> the observation of targets or processes from a distance (without physical contact), in contrast to in situ measurements wherein measuring devices are in touch or immersed in the observed system and/or process.

Passive remote sensing involves measurement of natural emitted energy from the target. Active remote sensing involves the transmission of artificially generated signals to the target and measuring the properties of the return signal. Radar and LIDAR (Light Detection and Ranging) are examples of active remote sensing. The great advantage of remote sensing is that it can provide spatial, spectral, and temporal data and rapid coverage of large, as well as, inaccessible, areas. Interpretation of remote sensing data requires that a link be established between surface observations and subsurface phenomena of interest (Jackson 2002).

Applications of remote sensing to water resources investigations of arid lands include (Maliva and Missimer 2012)

- location and mapping of geological features of hydrological significance, such as lineaments in hard rock terrains and buried channel deposits
- hydrogeological mapping (differentiating between different surface deposits)
- land use mapping, such as the locations and size of irrigated areas from which consumptive water use may be estimated
- land cover and vegetation mapping (both the type and density of vegetation)
- measurements of parameters important for water budgets, such as precipitation, evapotranspiration, soil moisture, snow cover, and snowmelt runoff
- mapping of groundwater discharge areas (e.g., sabkhas, playas, and streams) and their changes over time
- mapping of areas of groundwater emergence using temperature anomaly data (differences between groundwater temperature and surface temperatures)

- detailed mapping of topography
- floodplain delineation
- detection of changes in the mass of water in storage (GRACE program, Sect. 11.12.4) measurement of land subsidence

Remote sensing has perhaps the widest applications to groundwater investigations for the evaluation of surface processes, such as recharge and discharge. Applications of remote sensing for the evaluation of subsurface hydrogeology are more limited as there is usually not a surface expression of aquifer and confining unit location and properties. Remote sensing may detect shallow aquifers or aquifer features. For example, airborne radar was found to be helpful for identifying buried paleodrainage features that may have water resources importance (McCauley et al. 1982; Abdelsalam et al. 2000; El-Baz 2001; Vrba and Verhagen 2006; Robinson et al. 2007).

15.4.1   Lineament Analysis

Lineaments are linear features evident at land surface that may be an expression of an underlying geological structure. For example, erosion may be localized in zones of weakness, such as faults and fracture zones, which are evident on aerial photographs and satellite images as lineaments (Carruthers et al. 1991). Fracture zones may be the preferential site of vegetation growth (Fig. 15.8). Lineaments considered to be important include (Hobbs 1904)

- crests of ridges or the boundaries of elevated areas or depressions
- drainage lines
- coast lines
- boundaries lines of geologic formations, rock types, or lines of outcrop.

Fig. 15.8 Outcrop photograph showing preferential growth of vegetation in fracture zones, Sedona, Arizona (USA). Note hiker for scale

Mapped linear features can represent a variety of geological phenomena that do not necessarily have a geological origin and, even if so, may not necessarily mark the location of features of hydrogeological significance (Carruthers et al. 1991; Sander 2007). Linear features of hydrologic significance can be obscured by anthropogenic activities and some linear features may have to be omitted because of possible anthropogenic origins (Teeuw 1995). The translation of remote sensing and geophysically extracted properties into hydrogeological properties is thus often ambiguous (Rhén et al. 2007). Lineaments should be analyzed in the context of the hydrogeology, geological history, and structural environment of the study area (Sander et al. 1997; Sander 2007; Bisson and Lehr 2004). An initial question should be whether or not aquifer properties are likely to be influenced by geological conditions that might be detectable on land surface as lineaments. Lineament analysis is most widely applied in hardrock terrains in which groundwater flow is dominated by fractures. It is less commonly applied to sedimentary rock aquifers.

Lineaments are two-dimensional manifestations of three-dimensional features, which can be detected by a variety of remote sensing techniques including (Sander 2007)

- geophsyical data (e.g., aeromagnetic surveys)
- topographic maps
- digital elevation models (DEMs)
- radar data
- optical data from satellite images and aerial photographs.

Multispectral satellite analysis is useful because different bands may reveal surface properties indicative of underlying linear features (Vrba and Verhagen 2006). Greater confidence occurs when lineaments are resolved in multiple bands (Teeuw 1995). Surface altitude data, particularly highly detailed DEMs generated from LIDAR data can be used to detect lineaments.

The data can be analyzed both manually or using automated imaging processing software. A basic criticism of lineament analysis is a poor reproducibility between different operators and the apparent random distribution of lines without support of a proper geological understanding of the area (Mabee et al. 1994; Sander 2007). Mabee et al. (1994) reported the results of a study in which three workers evaluated the same map set. Less than 1 % of the lineaments mapped by three observers were coincident (i.e., detected by all three observers). Greater percentages of coincident lineaments and mapped linear features were reported in other studies (e.g., Sander et al., 1997). Lineaments that are most likely to be hydrogeologically significant tend to be coincident (i.e., detected by multiple workers and evident in multiple maps or images).

Automation of the lineament identification process using image-processing software may eliminate operator bias. However, the biases (i.e., professional

judgment) of experienced analysts may be beneficial in terms of identifying features of hydrological significance. As emphasized by Sander et al. (1997), professional judgment by experienced personnel is too valuable not to be included in the mapping of features for groundwater development. Although much higher degrees of technology are now used to identify and map lineaments, it is not clear whether the practical results are much better than in earlier times when lineament analyses were performed primarily manually using aerial photographs. Sander (2007, p. 73) noted with respect to lineament mapping and interpretation for water supply that

> The practical use of the results is sometimes compromised in favor of advanced image processing algorithms and numerical wizardry of mainly academic interest

Another limitation of lineament analysis is the very large number (1000's) of lineaments that can be mapped in regional studies. A lineament map for a hardrock area of New Hampshire prepared by the U.S. Geological Survey illustrates the large number of lineaments that may be identified in a relatively small area (Fig. 15.9). Therefore, it is important to be able to screen the lineaments as to whether or not they are a true surface expression of underlying geological structure that is consistent with the known tectonic fabric of the region (Bisson and Lehr 2004). Mabee et al. (1994) presented a two-step filtering process to reduce the number of lineaments to be further investigated and increase the probability of identifying features of hydrologic significance. The first step is a reproducibility filter in which overlapping linear maps prepared by different workers (or the same worker at different times) are used to identify coincident lineaments. The second step is a domain overlap analysis in which domains (areas) are identified in the field in which fractures have the same azimuths. Coincident lineaments are then screened to identify "fracture-correlated" lineaments whose orientations are coincident with the local fracture (or fault) trend.

Study area-specific investigations of the relationships between different types of lineaments and well yields are necessary to determine both whether lineament analysis is useful and, if so, how to obtain the most value from the data. A lineament itself may not be the main permeable zone. Sander et al. (1997) documented that the wells completed closest to lineaments had the lowest yields, possibly due to the presence of clay gouge, which often occurs in old, faulted environments. Wells located further away, but within 250 m (820 ft), of lineaments had a relatively higher success rate.

There is differing opinions as to the value of lineament analysis. It is clear from a review of the literature on the subject that technically rigorous lineament analysis has significant value for groundwater development in some settings (e.g., hardrock terrains) despite its limitations. However, the results from other published lineament analyses failed to make a convincing connection between observed surface feature and underlying geology. Lineament analysis is not an infallible technique for identifying productive rock for well sites, but rather, in some circumstances, can increase the success rate of well drilling (Sander et al. 1997).
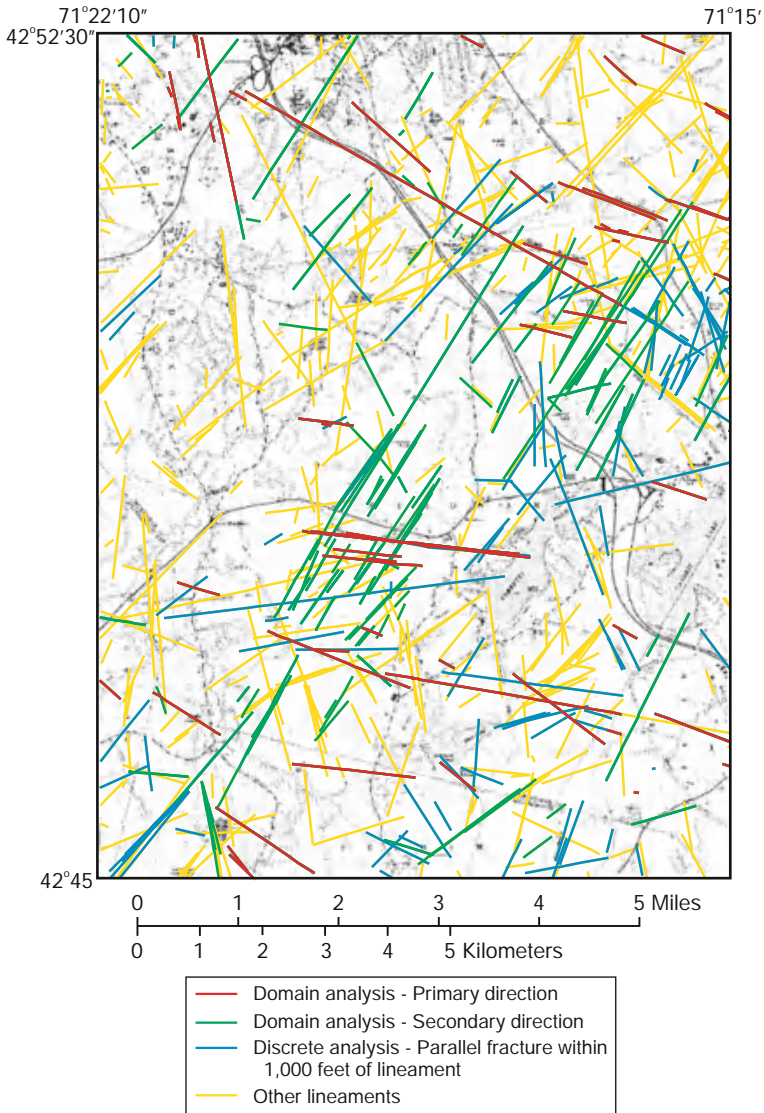
Fig. 15.9 Example of a lineament map prepared by the U.S. Geological for the Windham, New Hampshire, quadrangle (from Moore et al. 2002). A key issue is determining which of the numerous lineaments are hydraulically significant

15.4.2 Identification of Recharge and Discharge Areas

Groundwater recharge and discharge areas may be remotely sensed through differences in vegetation patterns and temperature and electrical conductivity anomalies (Batelaan et al. 1998). In arid lands, groundwater discharge areas would experience lesser water stress and more vigorous vegetation growth. Tweed et al. (2007), for example, provide an example of the use of satellite data to identify groundwater discharge areas in a basalt aquifer in southeastern Australia. The normalized difference vegetation index (NDVI) from Landsat data was used, which evaluates the amount of green vegetation locally present by differences in reflectance of visible red and infrared light by healthy green vegetation. The availability of groundwater in discharge areas allows photosynthesis to be sustained longer into the summer dry season than in recharge areas, which results in lower seasonal variability in NVDI values. Recharge areas in the site region tend to be associated with volcanic features (identified from Landsat ETM + images), are topographically high areas, and have a lesser degree of weathering of the basalts. The latter can be identified by relatively high potassium and low thorium concentrations from airborne radiometric (gamma ray spectroscopy) data (Tweed et al. 2007). Petus et al. (2013) documented how satellite-derived NVDI data could be used to evaluate changes in wetland vegetated areas associated with variations in flow from the Dalhousie Spring Complex of the Great Artesian Basin (Australia).

Münch and Conrad (2007) used remote sensing and GIS to map groundwater dependent ecosystems (GDEs) in the semi-arid Western Cape of South Africa. GDEs were identified using a combination of biomass indicators and physical wetness indicators. The latter considered factors such as the depth to water, lineament density, slope, and flow accumulation, which were evaluated using a weighted overlay function. Münch and Conrad (2007) noted that optimal image acquisition date should be at the time when GDE areas exhibit significantly different characteristics from the surrounding land cover, which usually coincides with a period of seasonal climate change and associated vegetation response. Münch and Conrad (2007) used data from shortly after the start of the onset of the winter rains in a dry period. Münch and Conrad (2007) emphasized the importance of prior knowledge of the study area, particularly the expected landscape structure and land cover and land use characteristics.

Temperature (infrared thermal analysis) data have been used to identify groundwater discharge areas and saturated soils. Shallow groundwater usually has a much narrower annual range of temperatures than land surface and surface-water bodies. Groundwater discharge areas may be detected by the difference in temperature between non-discharge areas (Becker 2006). The contrast in temperatures will be greatest at the times of the year when surface temperatures are near the ends of their annual ranges (i.e., winter and summer). Saturated soils act as heat sinks in the summer and heat sources in the winter (Becker 2006).

References

Abdelsalam, M. G., Robinson, C., El-Baz, F., & Stern, R. J. (2000) Applications of orbital imaging radar for geologic studies in arid regions: the Saharan testimony. Photoprogrammetric Engineering & Remote Sensing, 66, 717–726.

Ahmed, U., Crary, S. F., & Coates, G. R. (1991) Permeability estimation: the various sources and their interrelationships: Journal Petroleum Technology, 43(5), 578–587.

Algan, U., & Toksöz, M. N. (1986) Depth of fluid penetration into a porous permeable formation due to sinusoidal pressure source in a borehole. The Log Analyst, 11-12/1986, 30–37.

Ayan, C., Haq, S. A., Boyd, A., Schlumberger, M., El-Hamawi, H. H., & Hafez, A. D. C.O. (1999), Integration of NMR, wireline tester, core and open hole log data for dynamic reservoir properties. In Middle East Oil Show and Conference Proceedings, Society of Petroleum Engineers (SPE 53272).

Balossino, P., Pampuri, F., Bruni, C., & Ebzhasarova, K. (2008) An integrated approach to obtain reliable permeability profiles from logs in a carbonate reservoir: SPE Reservoir Evaluation & Engineering, August 2008, 726–734.

Batelaan, O., De Smedt, F. De Becker, P., & Huybrechts, W. (1998) Characterization of a regional groundwater discharge area by combined analysis of hydrochemistry, remote sensing and groundwater modelling. In P. Dillon, and I. Simmer (eds.), Shallow groundwater systems. IAH International Contributions to Hydrogeology 10 (pp. 75–85). Rotterdam: A.A. Balkema.

Becker, M. W. (2006) Potential for satellite remote sensing of ground water. Ground Water, 44, 306–318.

Bison, R. A.,& Lehr, J. H. (2004) Modern groundwater exploration: discovering new water resources in consolidated rocks using innovative hydrogeologic concepts, exploration, aquifer testing, and management methods. Hoboken: Wiley Interscience,

Brie, A., Endo, T., Johnson, D. L., & Pampuri, F. (1988) Quantitative formation permeability evaluation from Stoneley waves. SPE Annual Technical Conference and Exhibition, New Orleans, Louisiana, 27–30, 1988 (SPE 49131), pp. 389-400.

Carruthers, R. M., Greenbaum, D., Peart, R. J., & Herbert, R. (1991) Geophysical investigation of photolineaments in southeast Zimbabwe. Quarterly Journal of Engineering and Hydrogeology, 24, 437–451.

Cherry, J. A., Parker, B., Einarson, M., Chapman, S., and Meyer, J., (2015) Overview of Depth-Discrete Mutilevel Groundwater Monitoring Technologies: Focus on Groundwater Monitoring in Areas of Oil and Gas Well Stimulation in California, 11 Appendix, In Esser, B. K., et al. (eds.) Recommendations on model criteria for groundwater sampling, testing, and monitoring of oil and gas development in California, final report (LLNL-TR-669645). California State Water Resources Control Board.

Cherry, J. A., Parker, B. L., & Keller, C. (2007) A new depth-discrete multilevel monitoring approach for fractured rock. Ground Water Monitoring & Remediation, 27(2), 57–70.

Colley, N., Ireland, T., Reignier, P., Richardson, S., Joseph, J., Zimmerman, R., & Hastings, A. (1992). The MDT tool: a wireline testing breakthrough. Oilfield Review, 4(2), 58–65.

Contreras, I. A., Grosser, A. T., & and Ver Strate, R. H. (2008) The use of the fully grouted method for piezometer installation. Part 1. Geotechnical News, 26(2), 30–33.

Crombie, A., Halford, F., Haschem, M., NcNeil, R., Thomas, E. C., Melbourne, G., and Mullins, O. C. (1998) Innovations in wireline sampling. Oilfield Review (August 1998), 26–41.

Day-Lewis, F. D., Lane, J. W., & Gorelick, S. M. (2006) Combined interpretation of radar, hydraulic, and tracer data from a fractured-rock aquifer near Mirror Lake, New Hampshire, USA. Hydrogeology Journal, 14, 1–14.

Day-Lewis, F. D., Lane, J. W., Jr., Harris, J. M., & Gorelick, S. M. (2003) Time-lapse imaging of saline-tracer transport in fractured rock using difference attenuation radar tomography. Water Resources Research, 39, 1290.

Delhomme, J. P. (2007) The quest for permeability evaluation in wireline logging. In L. Chery and G. de Marsily (Eds.), Aquifer systems management: Darcy's legacy in a world of impending water shortage (pp. 55–70). London: Taylor & Francis.

Einarson, M. D. (2006) Multilevel ground-water monitoring. In D. M. Nielsen (Ed.) Practical handbook of environmental site characterization and ground-water monitoring (2nd ed.) (pp. 808–848). Boca Raton: CRC Press.

El Baz, F. (2001) Remote sensing of groundwater basins in the eastern Sahara. In Proceedings, Regional Aquifer Systems in Arid Zones – Managing Non-renewable Resources, Tripoli, Libya, 20–24 November 1999. Paris, UNESCO, IHP-V, Technical Documents in Hydrology No. 42, pp. 19–25.

Eldred, C. D., Scarrow, J. A., & Smith, A. (1995) An Integrated System for Groundwater Monitoring at Sellafield PNWR, UK. In Proceedings High-Level Radioactive Waste Management Conference, May 1–5, 1995, Las Vegas, USA, pp. 113–115.

Fisher, J. C., & Twining, B. V. (2011) Multilevel groundwater monitoring of hydraulic head and temperature in the eastern Snake River Plain aquifer, Idaho National Laboratory, Idaho, 2007–2008. U.S. Geological Survey Scientific Investigations Report 2010-5253.

Hardin, E. L., Cheng, C. H., Paillet, F. L., & Mendelson, J. D. (1987). Fracture characterization by means of attenuation and generation of tube waves in fractured crystalline rock at Mirror Lake, New Hampshire. Journal of Geophysical Research: Solid Earth (1978–2012), 92(B8), 7989–8006.

Hobbs, W. H. (1904) Lineaments of the Atlantic border region: Geological Association of America Bulletin, 15, 483–506.

Jackson, T. J. (2002) Remote sensing of soil moisture: implications for groundwater recharge. Hydrogeology Journal, 10, 40–51.

Jha, M. K., Chowdhury, A., Chowdary, V. M., Peiffer, S. (2007) Groundwater management and development by integrated remote sensing and geographic information systems: prospects and constraints. Water Resources Management, 21, 427–467.

Keller, C., Cherry, J. A., & Parker, B. L. (2013) New method for continuous transmissivity profiling in fractured rock. Groundwater, 52(3), 352–367.

Koch, R. J., & Pearson, S. G. (2007) Evaluation of sampling systems for multiple completion regional aquifer wells at Los Alamos National Laboratory (LA-UR-07-4034, August 2007, EP2007-0486). Las Alamos National Laboratory, Las Alamos, New Mexico.

Mabee, S. B., Hardcastle, K. C., & Wise, D. U. (1994) A method of collecting and analyzing lineaments for region-scale fractured-bedrock aquifer systems. Ground Water, 32, 884–894.

Maliva, R. G., & Missimer, T. M. (2012) Arid lands water evaluation and management. Berlin: Springer.

McCauley, J. F., Schaber, G. C., Breed, C. S., Grolier, M. J., Haynes, C. V., Issawi, B., Elachi, C., & Blom, R. (1982) Sub-surface valleys and geoarcheology of the Eastern Sahara revealed by shuttle radar. Science, 218, 1004–1020.

Meyer, J. R., Parker, B. L., & Cherry, J. A. (2014) Characteristics of high resolution head profiles and vertical gradients in fractured sedimentary rocks. Journal of Hydrology, 517, 493–507.

Meyer, J. R., Parker, B. L., & Cherry, J. A. (2008) Detailed hydraulic head profiles as essential data for defining hydrogeologic units in layered fractured sedimentary rocks. Environmental Geology, 56, 27–44.

Mikkelsen, P. E. & Green, G. E. (2003) Piezometers in fully grouted borehole. In Symposium on Field Measurements in Geomechanics (FMGM 2003), Olso, Norway.

Moore, R. B., Schwarz, G. E., Clark, S. F., Jr., Walsh, G. J., & Degnan, J. R. (2002) Factors related to well yield in the fractured-bedrock aquifer of New Hampshire. U.S. Geological Survey Professional Paper 1660.

Münch, F., & Conrad, J. (2007) Remote sensing and GIS based determination of groundwater dependent ecosystems in the Western Cape, South Africa. Hydrogeology Journal, 15, 9–28.

National Research Council (1996) Rock fractures and fluid flow. Washington, D.C.: National Academies Press.

Neels, B., & Gray, I. (2014) Fluid pressure monitoring in deep cement grouted boreholes, 14th Coal Operators Conference, University of Wollongong, The Australasian Institute of Mining and Metallurgy & Mine Managers Association of Australia, 2014, pp. 301–308.

Olsson, P., Falk, L., Forsund, O., Lundmark, L., & Sandberg, E. (1992) Borehole radar applied to characterization of hydraulically conductive fracture zones in crystalline rock. Geophysical Prospecting, 49, 109–142.

Parra, J. O., Hackert, C., Bennett, M., & Collier, H. A. (2003) Permeability and porosity images based on NMR, sonic, and seismic reflectivity: Applications to a carbonate aquifer. The Leading Edge, Nov. 2003, 1102–1108.

Parra, J. O., Hackert, C. L., & Bennett, M. W. (2006) Permeability and porosity images based on P-wave surface seismic data: Application to a south Florida aquifer. Water Resources Research, 42, W02415.

Petus, C., Lewis, M., & White, D. (2013). Monitoring temporal dynamics of Great Artesian Basin wetland vegetation, Australia, using MODIS NDVI. Ecological Indicators, 34, 41–52.

Rhén, I., Thunehed, H., Triumf, C.-A., Follin, S., Hartley, L., Hermansson, J., & Wahlgren, C.-H. (2007) Development of a hydrogeological model description of intrusive rock at different investigation scales: an example from south-eastern Sweden. Hydrogeology Journal, 15, 47–69.

Robinson, C. A., Werwer, A., El-Baz, F., El-Shazly, M., Fritch, T., & Kusky, T. (2007) The Nubian Aquifer in Southwest Egypt. Hydrogeology Journal, 15, 33–45.

Rosenbaum, J. H. (1974) Synthetic microseismograms: logging in porous formations. Geophysics, 39, 14–32.

Sander, P. (2007) Lineaments in groundwater exploration: a review of applications and limitations. Hydrogeology Journal, 15, 71–74.

Sander, P., Minor, T. B., & Chesley, M. M. (1997) Ground-water exploration based on lineament analysis and reproducibility tests. Ground Water, 35, 888–894.

Schlumberger (n.d.) Stoneley wave. Schlumberger oilfield glossary, http://www.glossary.oilfield.slb.com/Display.cfm?Term=Stoneley%20wave, Accessed 3/26/2012.

Serra, O. (2008) Well logging handbook. Paris: Éditions Technip.

Smith, B. A., & Hunt, B. B. (2008) Multilevel monitoring and characterization of the Edwards and Trinity aquifers of Central Texas. Gulf Coast Association of Geological Societies Transactions, 58, 833–840.

Teeuw, R. M. (1995) Groundwater exploration using remote sensing and a low-cost geographical information system. Hydrogeology Journal, 3(3), 21–30.

Tweed, S. D., Leblanc, M., Webb, J. A., & Lubczynski, M. W. (2007) Remote sensing and GIS for mapping groundwater recharge and discharge areas in salinity prone catchments, southeastern Australia. Hydrogeology Journal, 15, 75–96.

Twinning, B. V. & Fisher, J. C. (2015) Multilevel groundwater monitoring of hydraulic head and temperature in the eastern Snake River Plain aquifer, Idaho National Laboratory, Idaho, 2011–13: U.S. Geological Survey Scientific Investigations Report 2015-5042.

USBR (n.d.) Procedure for using piezometers to monitor water pressure in a rock mass (Procedure USBR 6515). Denver: U.S. Bureau of Reclamation Procedure (accessed September 10, 2015).

Vrba, J., & Verhagen, B. T. (2006) Groundwater for emergency situations. A framework document. International Hydrological Program (IHP) VI, Series on Groundwater No. 12. Paris: UNESCO.

Winkler, K. W., Liu, H.-L., & Johnson, D. L. (1989) Permeability and borehole Stoneley waves: comparison between experiment and theory. Geophysics, 54, 66–75

Zarriello, P. J. (1995). Accuracy, Precision, and Stability of a Vibrating-Wire Transducer Measurement System to Measure Hydraulic Head. Groundwater Monitoring & Remediation, 15(2), 157–168.

Chapter 16
Hydraulic Conductivity Estimation and Upscaling

Hydraulic conductivity is directly measured using Darcy's law-based methods that induce flow through a formation or sample. Indirect measures predict hydraulic conductivity from other sediment or rock properties. Methods are reviewed for obtaining profiles of permeability (hydraulic conductivity) from borehole geophysical logs, which include use of core porosity- versus-permeability transforms, porosity pore-size-permeability relationships, multivariate methods using multiple logs, and artificial neural networks. Obtaining hydraulic conductivity from geophysical logs is more complex for carbonates because of the presence of multiple pore types and the often dominance of flow by secondary porosity. Model grid cells are often one or more orders of magnitude greater than the volume of investigation of geophysical logs and other small-scale aquifer characterization methods. Upscaling is the process of assigning single equivalent values for each aquifer parameters (e.g., hydraulic conductivity) in model grid cells that results in the same modeled flow and solute transport as the original finer-scale heterogeneous values.

16.1 Introduction

Data on the two- and three-dimensional distribution of hydraulic conductivity and other aquifer parameters (e.g., storage parameters, porosity, and water quality) are needed for the development of numerical groundwater flow and solute-transport models. As are discussed in Chaps. 4–15, numerous methods are available to characterize aquifers. Hydraulic conductivity (and permeability) can be directly measured using methods that induce flow through a formation or sample. Indirect measures predict hydraulic conductivity from other sediment or rock properties. The problem of predicting hydraulic conductivity is one of selecting a model that accurately expresses hydraulic conductivity in terms of other measurable rock properties (Nelson 1994).

The selection of methods used to determine the hydraulic conductivity of aquifer and aquitard strata needs to consider volume of investigation, scale of heterogeneity, measurement environment, measurement physics, flow direction, and other variables (Ahmed et al. 1991; Helle et al. 2001). Small-volume techniques, such as core plug and minipermeameter analyses, can capture fine-scale heterogeneity in hydraulic conductivity, but provide data that are typically not representative of large-scale aquifer properties (e.g., aquifer transmissivity). Estimates of hydraulic conductivity from borehole geophysical log data are more spatially averaged than core data. Helle et al. (2001), for example, observed that the log-derived permeabilities make reservoirs look homogenous and did not detect the fine-scale heterogeneity evident in the cores. Data from pumping tests are spatially averaged to an even greater degree.

The fine-scale heterogeneity captured, for example, by core analyses and geophysical logging, is typically of too fine a scale to be incorporated into groundwater flow models, in which grid cells are usually on the order of meters to hundreds of meters in length. The fine-scale data needs to be upscaled to the model grid cell, while capturing features relevant to groundwater flow at the scale of interest. For example, fine-fractures are typically too numerous and small to be modeled as discrete features, but yet may largely control groundwater flow, and thus need to be incorporated in some manner into groundwater models.

An additional critical issue is the interpolation and extrapolation of limited point (e.g., well or borehole) data to populate the bulk of model grid areas for which data are unavailable. Various geostatistical approaches are used to interpolate and extrapolate either geological (e.g., lithofacies) or hydrogeological data (Chap. 20).

16.2   Borehole Geophysical Techniques for Evaluating Permeability

Permeability (and, in turn, hydraulic conductivity) is the most important parameter controlling groundwater flow. Permeability cannot be measured directly by borehole geophysical methods. Flowmeter logging, where possible, is the preferred logging method for evaluating medium to large (>1 m) scale heterogeneity in hydraulic conductivity because it is based on actual flow into a well. Hydraulic conductivity values can be obtained by integrating flowmeter log data on relative hydraulic conductivity with aquifer hydraulic data derived from pumping test data (Sect. 10.8.4).

Much effort has been employed in the oil and gas industry to develop techniques that can estimate permeability in wells, in which core data are not available, from other petrophysical properties, such as porosity, irreducible water saturation, mean grain diameter, and pore size distribution. Methods for estimating permeability from borehole geophysical logs were reviewed by Wendt et al. (1986), Ahmed et al. (1991), Yao and Holditch (1993), Balan et al. (1995), Ayan et al. (1999), Helle et al. (2001), and Delhomme (2007). Various empirical predictive relationships

have been established in cored wells between geophysical log data and available permeability data, which are then applied to uncored wells. Nuclear magnetic resonance (NMR) logging has the advantage that permeability estimates are based on derived total porosity and pore-size distribution data, which parameters are closely related to permeability (Sect. 10.11). However, it is commonly the case that flowmeter and NMR log data are not available, cannot be run on a given well (e.g., flowmeter logs cannot be run on mudded holes), or are cost-prohibitive due to project budgetary constraints. Hence, there is a need to develop means to extract permeability data from conventional borehole geophysical logs.

Permeability functions are equations used to calculate the expected permeability that corresponds to a given set of measurable properties, such as porosity (Balan et al. 1995). Thus, given a suite of conventional geophysical logs, permeability functions are used to generate a permeability (or hydraulic conductivity) versus depth profile. Mohaghegh et al. (1997, p. 170) cautioned that "it is an illusion that a "universal" relation between permeability and variables from wireline logs can be found." Relationships between permeability and log parameters developed in one formation are often not accurate in other formations. Empirical values for coefficients and exponents need to be calibrated against study area-specific permeability (or hydraulic conductivity) data.

Wendt et al. (1986) observed with respect to estimates of permeability from geophysical logs that

> Despite the shortcomings, both averages and variations can be predicted quite well. How good is good enough? Surprisingly, this is not easy to answer because the appropriateness of a comparison method depends upon the ultimate use of the predicted data.

Indeed, all values of aquifer hydraulic and transport parameters obtained in aquifer characterization programs should be considered best estimates and that their inherent associated uncertainty should be considered when using the data. Wendt et al. (1986) identified four potential sources of error

(1) core plug data may not be representative of the rock (sampling problem)
(2) well logs may not represent the rock (wellbore effect)
(3) wells logs are spatially averaged more than core plug data
(4) statistical predictors of permeability will better estimate mean values but tend to underestimate higher values and overestimate lower values.

16.2.1 Porosity-Permeability Transforms

Permeability correlations using well-log data are normally the least expensive way to obtain permeability profiles. An approach that is widely used in the oil and gas industry to evaluate reservoir heterogeneity is porosity-permeability transforms of core plug analysis data. Empirical porosity-permeability transforms are used to
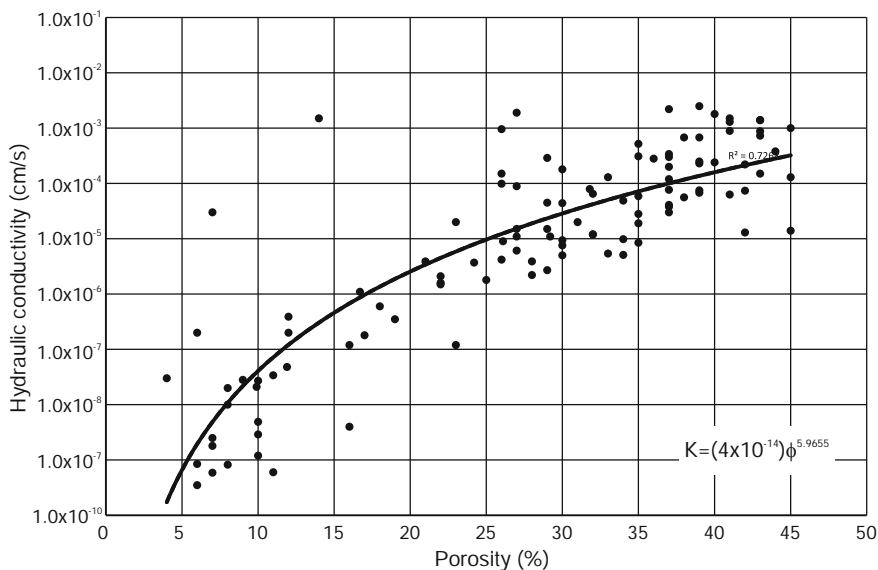
Fig. 16.1 Porosity-versus-hydraulic conductivity transform for limestones and dolostones from the Floridan Aquifer System of southeastern Florida

estimate permeability from porosity data obtained from conventional borehole geophysical logs. For example, core data from multiple deep injection well projects in southeastern Florida were used to obtain a relationship between porosity and hydraulic conductivity in limestones of the Floridan Aquifer System (Fig. 16.1). A hydraulic conductivity-versus-depth profile was then generated using sonic-log porosity data (Fig. 16.2). From the scatter evident in porosity-hydraulic conductivity transforms (e.g., Fig. 16.1), it is clear that there is a large potential error in individual predicted hydraulic conductivity values. However, the hydraulic conductivity-versus-depth profile captures larger-scale (>1 m) aquifer heterogeneity and can be upscaled to provide average values for numerical models.

Simple regression analyses relating permeability to porosity results in a distribution of predicted values that is narrower than the original dataset, and errors will be relatively large at the high and low permeability extremes (Wendt et al. 1986). Predictive equations need to be based on local geological conditions. Porosity-permeability trends can vary greatly between formations, with orders of magnitude differences in permeability occurring between rocks with the same porosity (Archie 1950). Indeed, large variations in permeability and hydraulic conductivity occur for a given porosity within a formation (e.g., Figure 16.1). The main reason for different trends between rock types is differences in pore size (Archie 1950). Granular rocks with smaller pore sizes (and thus smaller pore-throat diameters) tend to have much lower permeabilities at a given porosity than rocks with larger pores. Other factors that affect porosity-permeability relationship are
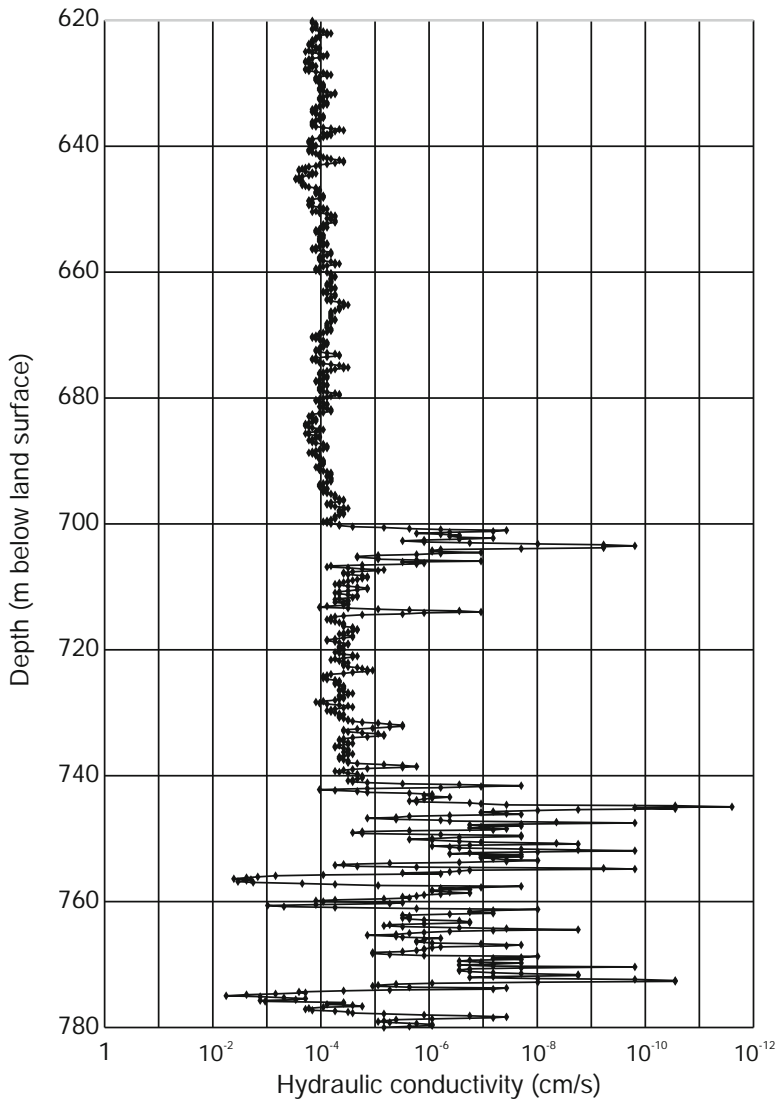
Fig. 16.2 Hydraulic conductivity obtained from a sonic porosity log and porosity-versus-hydraulic conductivity transform (Fig. 16.1), Hialeah, Florida

diagenesis and the interconnectivity of pores. Varying degrees of development of secondary porosity can result in orders of magnitude difference in permeability between rocks having the same porosity.

Simple porosity-permeability plots hold reasonably well for unconsolidated sands or formations with relatively uniform composition and diagenetic histories
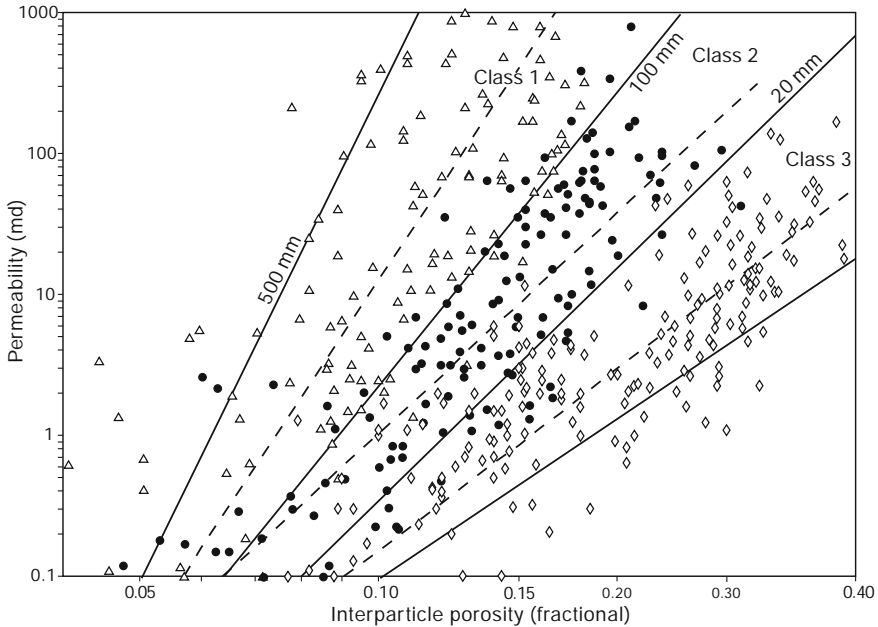
△   Class 1: Grainstones, dolograinstones, large crystalline dolostones

●   Class 2: Grain-dominated packstones, fine to medium crystalline grain-dominated
     dolopackstones, medium crystalline mud-dominated dolostone

◇   Class 3: Mud-dominated limestones and finely crystalline mud-dominated dolostone

Fig. 16.3 Composite porosity-air permeability cross plot for non-vuggy limestones and dolostones showing statistical reduced–major-axis transforms for each class (dashed lines). Modified from Lucia (1995), Copyright American Association of Petroleum Geologists

(Wendt et al. 1986). Some generic porosity-permeability transforms have been published. Lucia (1995) proposed for limestones with predominantly interparticle porosity, the following transforms relating permeability to interparticle porosity (Fig. 16.3), with reference to the limestone classification scheme of Dunham (1962):

- grainstones, dolograinstones, large crystalline dolostones:

$$k = \left(45.35 \times 10^8\right)\emptyset_{ip}^{8.537} \qquad (16.1)$$

- grain-dominated packstones, fine to medium crystalline grain-dominated dolopackstones, medium crystalline mud-dominated dolostones:

$$k = \left(2.040 \times 10^6\right)\emptyset_{ip}^{6.38} \qquad (16.2)$$

- Mud-dominated limestones and finely crystalline mud-dominated dolostones:

$$k = \left(2.884 \times 10^3\right)\emptyset_{ip}^{4.275} \tag{16.3}$$

where k is permeability (millidarcys) and $\emptyset_{ip}$ is the fractional interparticle porosity. As would be expected, Eq. 16.1 gives the highest permeability for a given porosity.

Jorgensen (1991) proposed a general equation for estimating permeability (in mD) from porosity (fractional) obtained from logs:

$$k = 84,000 \frac{\emptyset^{m+2}}{(1-\emptyset)^2} \tag{16.4}$$

where m is the cementation exponent obtained from a cross plot of log-derived porosity- versus formation resistivity. Jorgensen (1991) reported that accuracy of Eq. 16.4, using data from logs with no other prior information, is plus or minus one-half order of magnitude.

Porosity-permeability transforms applied to borehole porosity logs is a useful technique of evaluating aquifer heterogeneity, particularly in the absence of other, potentially more accurate, data. Porosity can be measured using conventional borehole geophysical logs run in both water and mud-filled boreholes. The accuracy of the predicted permeability values depends upon the degree of which core porosity-permeability relationship reflects that of the logged interval. The greatest accuracy would be expected to occur where formation-, location-, and texture-specific core and log data are used. The lowest accuracy would occur where generic relationships are used.

It is uncommon in groundwater resources investigations to have core data available, much less sufficient core plug analyses to obtain representative porosity-permeability transforms. Instead empirical relationships can be established by statistical correlation of logs with hydraulic test data (Paillet and Crowder 1996), such as obtained by flowmeter logging and packer testing. In siliciclastic strata, log-derived porosities can be corrected for clay mineral content using gamma ray log data (Paillet and Crowder 1996). Average hydraulic conductivity values obtain using other methods (e.g., aquifer pumping and packer tests) can be used to constrain log-derived data.

16.2.2   Porosity Pore-Size-Permeability Relationships

Although porosity-permeability transforms can be used to estimate permeability from porosity data obtained from geophysical logs, this method suffers from the limitation that it does not consider other factors that affect permeability. An additional factor is needed that either directly or indirectly accounts for the effect of pore

size on permeability. For example, the Kozeny-Carmen model in its present form relates permeability to porosity and specific surface area (Glover et al. 2006):

$$k_{KC} = \frac{1}{2S_{gr}^2} \frac{\emptyset^3}{(1-\emptyset)^2}$$

(16:5)

where
k_{KC} permeability (m^2),
$\emptyset$ porosity (fractional), and
S_{gr} specific surface area of rock (m^2/m^3)

Specific surface area is inversely related to grain size. All other factors (e.g., grain shape and roughness) being equal, fine-grained sediments have a greater specific surface area than coarser grained sediments. Specific surface area can be measured on samples using techniques such as gas adsorption (e.g., the Brunauer, Emmett ,and Teller (BET) method), but not directly from geophysical logs. Hence Eq. 16.5, has limited direct application to petrophysical investigations.

Glover et al. (2006) presented the RGPZ equation which relates permeability to porosity and grain size,

$$k_{RGPZ} = \frac{d^2 \emptyset^{3m}}{4am^2}$$

(16:6)

where
k_{RGPZ} permeability (m^2)
d grain diameter (geometric mean, m)
m cementation factor
a packing parameter ($\approx 8/3$ for quasi-spherical grains)

The practical limitations of Eq. 16.6 are that it requires data on grain size, which is variable within a formation. Values are also needed for two empirical factors.

Timur (1968) related permeability to irreducible or residual water saturation (S_{wi}, %) using the generalized equation

$$k_T = A \frac{\emptyset^B}{S_{wi}^C}$$

(16:7)

where
k_T permeability (md)
A, B, and C   statistically determined coefficients
$\emptyset$ porosity (fractional)

The Timur relationship for sandstones is

$$k = 0.136 \left(\frac{\emptyset^{4.4}}{S_{wi}^2} \right) \tag{16.8}$$

Irreducible water saturation (S_{wi}) is the minimum saturation that can be achieved in a sample by displacing the water by oil or gas. It consists predominantly of capillary-bound water. Irreducible water saturation is obtained in the oil and gas industry by special core analyses. In groundwater investigations, irreducible water saturation is equal to specific retention (Bear 1972), which is the water-filled porosity that is retained in a sample after gravity drainage is completed.

The Timur-Coates method (Coates et al. 1991) relates permeability to total porosity and the ratio of free fluid volume (FFV) to bound fluid volume (BFV) from nuclear magnetic resonance logs (Sec. 10.11):

$$k_{TC}\,(m^2) = 10^{-9} \left(\frac{\emptyset}{c} \right)^m \left(\frac{FFV}{BFV} \right)^n \tag{16.9}$$

$$k_{TC}\,(mD) = \left(\frac{\emptyset}{c} \right)^m \left(\frac{FFV}{BFV} \right)^n \tag{16.10}$$

where $\emptyset$ = porosity (fractional) and the sum of FFV and BFV (% or fractional) is the total porosity. The values of the coefficients c, m, and n are approximately 10 (for sandstones), 4, and 2.

Schlumberger Doll Research (SDR) equation provides permeability values from NMR log data:

$$k(mD) = a\emptyset^4 T_{2gm}^2 \tag{16.11}$$

where

T_{2gm} geometric (logarithmic) mean of the T2 (NMR transverse relaxation time) spectrum (ms),

$\emptyset$ porosity (fractional)

a empirical constant (4 mD/ms commonly used)

The limitations of the above methods is that they have coefficients whose values are ideally determined from permeability measurements for each study area (or less accurate general default values are used) and that some methods require data that are not generally or easily obtainable in groundwater studies, particularly irreducible water saturation (specific retention), grain surface areas, and grain size distribution.

16.2.3   Multivariate Borehole Geophysical Log Methods

Permeability is a function of other variables in addition to porosity, such as compaction, clay content, and cementation. More refined permeability profiles may be obtained if data from other borehole geophysical logs are considered instead of just porosity. Wendt et al. (1986) presented a workflow for permeability prediction from multiple logs using multiple regression. The study site was the Northwest Fault Block of the Prudhoe Bay Oil Field. The workflow consisted of five basic elements:

- establishment of independent variables using basic well log data (induction, density, gamma ray, and sonic)
- identification of petrological variables (e.g., percent gravel and cement) using petrographic observations and well logs
- generation of predictive equations by multiple-regression analyses. Separate equations were established for each reservoir layer. Discriminate function analysis was used to identify variables that have the greatest weights toward predicting permeability.
- computation of permeability for each foot (meter) in all wells
- comparison of predicted permeability with core permeability using graphical methods.

Yao and Holditch (1993) presented a methodology for calculating permeability in shaly sands using commonly available gamma ray, resistivity, and porosity log data. The basic form of the Yao and Holditch (1993) equation is

$$k = U \frac{\emptyset^{e1}(1 - I_{GR})^{e2} R_{ILD}^{e3}}{\left(\frac{R_{ILD}}{R_{SFL}}\right)^{e4}} \qquad (16.12)$$

where

k	permeability (mD)
U	unit conversion factor, which varies between reservoirs and mud systems
R_{ILD}	deep induction resistivity (ohm-m)
R_{SFL}	shallow focused resistivity (ohm-m)
$\emptyset$	porosity (fraction)
I_{GR}	gamma ray index (range from 0 to 1)
e1, e2, e3, and e4	empirical exponents

The gamma ray index is defined as

$$I_{GR} = \frac{GR - GR_{min}}{GR_{max} - GR_{min}} \qquad (16.13)$$

where GR = gamma ray activity (API). A multiparameter linear regression technique was used to determine the values of the unit conversion factor and exponents. Formation porosity versus-permeability data is thus required.

Khalil and Santos (2013) presented a method for estimating hydraulic conductivity from resistivity logs. The first step is the calculation of porosity from normal resistivity logs using the Archie equation, with the formation factor corrected for clay content using the Waxman and Smits (1968) method. Formation water resistivity (Rw) is determined from water samples collected from the aquifer. Hydraulic conductivity is then calculated using the Bear (1972) version of the Kozeny-Carmen equation,

$$K = \frac{(d_w g)}{I} \frac{d^2}{180} \frac{\emptyset^3}{(1 - \emptyset)^2}$$ (16:14)

where
K   hydraulic conductivity (cm/s)
d_w luid density (g/cm3)
I   dynamic viscosity of water (g/cm/s)
g   acceleration of gravity (980 cm/s)
d   medium grain diameter (cm)

The limitation of Eq. 16.14 is that data on grain size are required. Such data could be obtained from grain size analyses of samples representative of the main lithologies, which may not be practically obtainable depending upon the formation and drilling method. Khalil and Santos (2013) obtained a calculated hydraulic conductivity of 12.6 ± 1.9 m/d, which is in agreement with the value obtained from a pumping test from the same well (10.7 m/d).

Ali et al. (1999) reported the use of a gamma ray log to estimate porosity in a sandstone reservoir (Sulimar Queen), in New Mexico. An empirical correlation was obtained between gamma ray activity and core porosity,

$$\emptyset_{GR} = 0{:}334 e^{-0{:}0526(c)}$$ (16:15)

where
$\emptyset_{GR}$ porosity (percent)
c   gamma ray activity (API units)

The gamma ray response is controlled by the amount of feldspar (a framework grain). Many of the gamma ray logs available from the studied field are old and have different scales. The older gamma ray logs were first rescaled to modern API units using the available modern logs. Permeability values (in millidarcies) were estimated using from rescaled gamma ray logs using a empirical correlation with core permeability

$$Logk = -6.697 + 0.130(c) \qquad\qquad (16.16)$$

$$Logk = -1.861 + 0.2877(\emptyset_{GR}) \qquad\qquad (16.17)$$

where k = permeability (md) and $\emptyset_{GR}$ = gamma ray porosity (%).

For a given porosity, permeability of rocks can vary by several orders of magnitude. Porosity is independent of grain size, whereas permeability is strongly dependent on grain size. Within a reservoir, porosity, and permeability may be directly proportional, but there may be high and low permeability zones for a given porosity. Factors the effect the relationship between log-derived porosity and permeability include (Amaefule et al. 1993)

- presence of k-feldspars leading to apparent high Vshale (clay) contents from GR logs
- microporosity (in grains and cements) leading to high calculated apparent water saturations
- presence of siderite, pyrite, barite, and smectite, which influence resistivity, density, and neutron logs.

The porosity-permeability relationship depends rock texture, which can be inferred from mineralogy data obtained from elemental analysis logs, such as element capture spectroscopy. Herron (1987) presented a modification of the Kozeny–Carmen equation that relates permeability to porosity and mineralogy:

$$k = A_f \left(\frac{\emptyset^3}{(1 - \emptyset^2)} \right) \exp\left(\sum B_i M_i \right) \qquad\qquad (16.18)$$

where
k   permeability (mD)
Mi   weight fraction of mineral 'i'
Bi   constant for mineral 'i'
A_f feldspar dependent textural maturity factor
u   porosity (fractional)

The Herron equation is based on surface area, grain shape, and packing being directly or indirectly related to mineral composition. The porosity-permeability relationship is a function of textural maturity, which is related to mineralogical maturity and, in turn, feldspar content.

$$A_f = 4.9 + 2F_{max} \qquad\qquad (16.19)$$

where F_{max} is the maximum feldspar content over the area of interest (excluding shales), expressed as a decimal fraction.

More advanced approaches to the processing of borehole geophysical data utilize a variety of different logs to estimate key parameters such as mineralogy,

porosity, permeability, and total and irreducible water saturation. For example, DecisionXpress petrophysical evaluation system is a workflow that estimates key hydraulic parameters in siliciclastic sediments using density, neutron, resistivity, and elemental capture spectroscopy log data and formation water resistivity (R_w; Barson et al. 2005). The elemental capture spectroscopy log is used to determine elemental concentrations, mineralogy, and clay mineral volume, which, in turn, are used to estimate matrix density. Water saturation is estimated from resistivity and clay volume. Total porosity is calculated from the neutron and density logs data. Permeability is estimated from the total porosity and the ratio of pore volume to surface area, which is a function of clay mineral content. Clay minerals by far have the greatest specific surface area (surface area/mass). An advantage of DecisionXpress is that it can be used for lithological and petrophysical interpretations in real time (Barson et al. 2005).

16.2.4   Pattern Recognition and Arti*f*icial Neural Networks

Zhang and Salisch (1998) documented the use of statistical pattern recognition to characterize the conventional log response characteristics of each hydraulic unit in cored holes. The response characteristics are then used to identify hydraulic units in logged wells without cores. Various multiple-regression analysis and artificial neural network techniques have also been used to determine permeability from well logs (Mohaghegh et al. 1997; Helle et al. 2001; Balan et al. 1995; Delhomme, 2007).

Artificial neural networks (ANNs) are an alternative to semi-empirical transforms. ANNs simulate the cognitive processes of the human brain. They are nonlinear dynamic systems that learn to recognize patterns through training. The advantage of ANNs is that they are free from the constraints of a certain function form and require no underlying mathematical models. There is no assumption of linearity amongst the variables (Huang et al. 1996; Mohaghegh et al. 1997; Helle et al. 2001). A training set of data (facts) is used, which contains input values that are sent through the ANN. The difference between the calculated output and actual output from the training set is evaluated to obtain the closest solution. In the case of the Helle et al. (2001) study of the North Sea Viking Graben, the input variables were neutron porosity, density, sonic transit time, and resistivity.

Mohagheah et al. (1997) performed a comparative study of permeability determination methods from well-log data from the Granny Creek Field of West Virginia. Methods that were considered are empirical relations using published or guideline values for coefficients and exponents, multiple-variable regression analysis, and ANN. The log data used are gamma ray, density, and deep induction resistivity. The models were developed based on data from seven wells, which was used to create a permeability profile for an eighth well for which laboratory permeability data are available. The multiple-variable regression overestimated low permeabilities and under-estimated high permeabilities. The general tendency for

multiple-regression methods to average the entire data set to achieve reasonable statistical indicators is a weak point of the technique (Mogaheah et al. 1997). The relative inaccuracies of the ANN method tend to be consistent throughout the domain and results in a superior ability for pattern recognition than the multiple-regression method.

16.3   Carbonate Aquifer Characterization Methods

The greater textural diversity carbonate rocks, due to diagenesis and the often common dominance of secondary porosity on aquifer hydraulic and solute-transport parameters, adds complexity to their characterization. Primary (depositional) textures range from carbonate muds, to well-sorted ooid and bioIclast sands, to highly irregular fossiliferous limestones (reefal deposits). All of the primary textures may be altered to different degrees by various dissolution, cementation, and replacement processes. In the extreme case of karst systems, groundwater flow may be locally dominated by one or several major conduits (Chap. 18).

In carbonate rocks, there is often not a simple relationship between petrophysical properties, such as between permeability and porosity. The problems stem from heterogeneities in both rock and pore types (Kennedy 2002). Carbonate rocks typically have highly heterogeneous porosities due to the biogenic origin of grains and muds and the reorganization of pore systems during diagenesis. Intervals of carbonate rocks often contain multiple, intermingled lithologies, which have different physical properties. Multiple pore systems may be superimposed in a single sample. For example, it is not uncommon for a limestone to have intragranular microporosity, intergranular macroporosity, and secondary porosity. Hence, characterization methods developed for more uniform siliciclastic aquifers may not be appropriate or require modification for carbonate aquifers.

Permeability is related to both pore size (more particularly pore-throat size) and connectivity. A key issue in carbonate rocks is the presence of secondary macroporosity, particularly vugs and other dissolution features. Separate (isolated) vugs do not significantly contributed to permeability, whereas touching (interconnected) vugs results in enhanced permeability. Logging tools measure surrogates for permeability. Permeability of carbonates may be estimated using general techniques such as applying a core-based porosity-permeability transform to log-derived porosity. Such techniques may be suitable for strata in which there is a limited range of rock types present. However, porosity-permeability trends for carbonates vary with rock type, grain size, and pore types (Lucia 1983, 1995; Kennedy 2002). There continues to be considerable interest in developing techniques specific to carbonates.

Dorfman et al. (1990), for example, presented a method for estimating the permeability in carbonate rocks based on porosity and resistivity data. Permeability is estimated using a modification of the Carman–Kozeny equation:

$$k = \frac{\emptyset^4 \times 10^8}{2S_v(1-\emptyset)^2} \qquad (16.20)$$

where

k   permeability (Darcies)
∕   porosity (fractional)
S_v specific surface area (cm^{-1})

Specific surface area is correlated with grain size and pore size, which are related to irreducible water saturation. In water-bearing rock, S_v can be estimated using an empirical relationship based on the ratios of formation water resistivity (R_w) and true resistivity in uninvaded zone (R_t) and mud filtrate resistivity (R_{mf}) and the resistivity of the invaded zone (R_{xo}). Dorfman et al. (1999) reported that the permeability values obtained in a study site (Hanford Field, Texas) compared favorably with values obtained by core analyses.

Hassal et al. (2004) documented the results of an investigation of borehole geophysical predictors of permeability in a cored Lower Cretaceous well in Abu Dhabi. Air permeability was measured in the core using plug analyses every 1 ft (0.3 m) and minipermeameter measurements every inch (2.5 cm). The most widely used method to predict permeability in the field was a ANN using the standard gamma ray, bulk density (RHOB), neutron porosity (NPHI), and microspherically focused resistivity (MSFL) logs.

Nuclear magnetic resonance (NMR) logs (Sect. 10.11) provide data on porosity and pore size distribution, which is in turn relates to permeability. The relationship between NMR log response and permeability is much more complex in carbonate rocks than in siliciclastic sediments. The conventional equations (SDR and Timur-Coates) used for the interpretation of carbonates relate permeability to the NMR T2 distribution are (Hassal et al. 2004)

$$k_{SDR} = 0.5\emptyset^2(qT_{2LM})^2 \qquad (16.21)$$

where

k_{SDR} Schlumberger Doll Research (DSR) permeability (mD)
q   surface relaxivity (I m/sec)—adjusted to calibrate to reference permeability
T_{2LM} log mean average of T2 distribution (msec)
∕   porosity (fractional)

and

$$k_{TC} = C_T\emptyset^2\left(\frac{FFI}{V_{micro}}\right)^2 \qquad (16.22)$$

where

k_{TC} Timur-Coates permeability (mD)

C_T constant (adjustable)

FFI   free fluid index: total porosity—microporosity (V_{micro}; fractional)

The main limitations of the SDR and Timur-Coates equations, as applied to carbonate rocks, are that the SDR equation gives permeability values that are insensitive to high-permeability units, as the underlying model is based on aggregates of homogenous grains and does not apply when macroporosity dominates permeability. Timur-Coates permeability predictions are dominated by microporosity and give anomalously high-permeability spikes in intervals where microporosity approaches zero (Hassal et al. 2004). NMR can be less accurate for carbonates that are grain-supported (e.g., carbonate sands) and the grains contain significant microporosity. Diffusion between the micropore and macropores can result in merging of their T_2 peaks (Allen et al. 2000; Delhomme 2007).

Advanced petrophysicial analyses for carbonate rocks using NMR and microresistivity imaging data first partition porosity into micro-, meso-, and macroporosity components. Permeability is then estimated using specialized versions of the SDR and Timur-Coates equations depending upon which pore system classes have been identified (Hassal et al. 2004; Ahr et al. 2005). The modified SDR equation is

$$k_{SDR} = C_c \emptyset^2 (V_{macro} = (\emptyset - V_{macro}))^2 \qquad (16.23)$$

where V_{macro} is the macroporosity fraction obtained from either the NMR log or an imaging log. The modified SDR is not designed for separate vug and fractured-dominated flow systems.

Hassal et al. (2004) observed that the best estimate of permeability from log data, as assessed against core permeability, was obtained by integrating NMR log with electrical imaging data for high-resolution estimation of macroporosity. Values for exponents and coefficients used in all of the NMR-based methods must be obtained by calibration against laboratory data, spot testing from core, formation tester interpretation, or local knowledge. The values of the 'C' premultiplier and exponents can be adjusted to get a better fit to core data. Either a single or set of values can be used for the premultiplier and exponents. Ayan et al. (1999) reported that a better fit could be obtained if 'C' is modulated based on the width of the T2 distribution.

Separate vug porosity contributes only weakly to permeability and thus fluid flow. Carbonates with common separate vug porosities may give anomalously large NMR permeability values. Chang et al. (1997) documented an early study of NMR logging in a vuggy dolomitic carbonates (Permian, West Texas). Standard core and NMR laboratory analyses were performed on 27 core samples. Superior estimates of permeability were obtained using porosity with T2 < 750 ms (which excludes relatively large vuggy pores) than using total porosity values.

Westphal et al. (2005) proposed that NMR data from carbonate rocks should be evaluated in terms of dominant porosity type. The approach they used involved

- assigning samples to different groups based on the dominant pore types
- determining average T2 cutoff for bound versus movable water for each group using irreducible water saturations (S_{wirr}) measurements of core samples.
- calculation of permeability using SDR and TC methods. Best fit (optimum) values for coefficients are determined by comparing measured permeability values with estimated permeability values.

Use of dominant pore type-specific T2 cutoffs and coefficients showed an improvement over classical approach using constant values for the cutoffs and coefficients. However, carbonate rocks often have more than one pore type. The observed T2 distribution is the sum of the multiple distributions corresponding to the size distribution of the different pore types (Genty et al. 2007). The NMR T2 distributions need to be decomposed to identify and determine the contributions of the different pore types. Genty et al. (2007) proposed that the T2 distributions of carbonates are usually the sum of up to three Gaussian distributions with a specific mean, standard deviation and relative weight. Model T2 spectrums can be generated from a set of reference values for carbonate samples for which NMR and pore type evaluations were performed.

NMR logging can be a cost effective means of characterizing heterogeneity with respect to hydraulic conductivity compared to, for example, coring and core plug analyses. However, attentional needs to be paid to the rock types present and how they would impact NMR log readings and data interpretation.

16.4   Upscaling

Numerical models of groundwater flow and solute transport require the assignment of values for hydraulic and transport parameters to grid blocks or elements of a size or spacing that is orders of magnitude greater than the volume of investigations for some field data, such as cores, geophysical logs, and slug tests. Geophysical log data, for example, involves frequent (usually 0.15 m or less) measurements of petrophysical parameters, whereas model grid cell heights are often an order of magnitude or more greater. The scale-effect of the various data sources needs to be considered when utilizing field data to populate groundwater models (Sect. 5.4). Methods with small volumes of investigations may not capture features (e.g., fractures) that dominate groundwater flow. The length scale of the discretization grid is often larger than the length scale of facies–related heterogeneities in hydraulic conductivity.

Hydrofacies data may have a finer spatial scale than is practical for groundwater modeling. Models may be constructed with a very fine discretization to capture small-scale aquifer heterogeneity, but this involves a great computation cost, and thus project time and economic costs. Upscaling procedures are used to reduce the

number of grid cells while at the same time capturing the specific hydrofacies architecture. In more direct terms, "upscaling is in fact the new terminology for averaging" (de Marsily et al. 2005). The objective of upscaling is to find a single equivalent value for each aquifer parameters (e.g., hydraulic conductivity) in an aquifer block or grid cell that results in the same modeled flow and solute transport as the original finer-scale heterogeneous values. The goal is to lose as little information as possible when going from high-resolution geological data to simplified groundwater layer-type models (Quental et al. 2012).

There is a clear need for upscaling techniques that are practical (in terms of time, data requirements, and complexity) in the context of the common types of applied groundwater resources investigations. Upscaling included deterministic, stochastic, and heuristic methods (Renard and de Marsily 1997; Fleckenstein and Fogg 2008). Deterministic methods assume full knowledge of the underlying heterogeneous aquifer model. Stochastic methods account for uncertainty by taking a probabilistic approach. Heuristic methods try to derive rules to calculate plausible values of equivalent hydraulic conductivity and other parameters.

16.4.1   Representative Elementary Volume and Equivalent Porous Medium

The scale dependence of hydraulic conductivity (and other parameters) and connectivity need to be considered in the upscaling process. Flow and solute transport in groundwater systems occurs through networks of interconnected pores. It is not practically possible to explicitly simulate flow on the scale of pores in aquifer-scale models. Instead groundwater flow is necessarily simulated by considering average flow behavior over various volumes of porous media, with the volume selected depending upon project objectives. An important concept in upscaling is the representative elementary volume (REV), which was defined by Bear (1972) as the minimum volume of a porous medium for which petrophysical properties (e.g., porosity and permeability) can be represented as properties of a continuum. For volumes above the REV, the values of numerical parameters theoretically do not change as a function of the size of the investigated volume, but may have random fluctuations. The size of the REV must be large enough to include all representative heterogeneities in the medium (Yeh 1998). As a generalization, as aquifer heterogeneity increases, hydraulic conductivity values obtained from methods with smaller volumes of investigation (i.e., less than the REV) will tend to underestimate larger-scale (e.g., model grid cell size) equivalent hydraulic conductivity values.

From a practical perspective, quantitative evaluation of the size of the REV for a given problem is difficult. The REV should be larger than the scale of aquifer heterogeneities, which could be estimated, for example, from facies data or the length, spacing, and geometry of fractures and solution conduits. For relatively homogenous strata, the REV will be small, and thus data from methods with small

volumes of investigation can be upscaled to provide acceptably accurate equivalent values for a model grid scale. On the contrary, hydraulic conductivity data from methods with small volumes of investigations often cannot be upscaled to provide accurate equivalent values for parameters in highly heterogeneous aquifers. As an extreme example, core plug hydraulic conductivity data are of no value alone in determining the equivalent hydraulic conductivity of a karst aquifer in which groundwater flow is dominated by conduits.

In addition to heterogeneity related to the interspersion of different hydrofacies, aquifer heterogeneity can also results from the occurrence of dual- and multiple-porosity conditions within a given volume of rock. Secondary porosity and permeability types include fractures and flow conduits. The equivalent porous medium (EPM) approach considers volumes of aquifers as a porous medium with uniform lumped estimates of bulk hydraulic properties that result in a similar flow and solute response as the actual heterogeneous system. The EPM approach is often taken in the simulation of fractured rock and karst systems.

The main alternative approach to the EPM approach is the discrete element approach in which heterogeneity elements, such as fractures, are simulated as features with specified locations, orientations, porosities, and transmissivities. The discrete element approach is technically more rigorous, has much greater data requirements, and is computationally intensive. Very often the data requirements for the discrete element approach are far beyond that available or practically obtainable for a groundwater investigation. Aquifer hydraulic parameters obtained from methods with large volumes of investigations (e.g., aquifer pumping tests) provide information on the equivalent properties of the investigated strata. For example, transmissivity values obtained from pumping tests reflect the combined contributions from fractures and conduits and the rock matrix. An important observation is that the EPM approach works well for predicting drawdowns, but often works poorly for solute transport (Anderson 1997).

16.4.2 Connectivity and Upscaling

Interconnectedness of aquifer and aquitard strata is the key to quantifying heterogeneity for the purpose of hydrogeological investigations (Anderson 1997). Addressing connectivity is a critical issue in the simulation of aquifer heterogeneity as it can profoundly impact the results of solute-transport modeling (de Marsily et al. 2005). Transmissivity depends upon the degree to which high-and low-hydraulic conductivity units are interconnected. One or more well-connected sands among a system of otherwise disconnected sands can completely alter the groundwater flow velocity field (Ritzi et al. 1994). Uncertainty in connectivity can affect risks associated with groundwater contamination as it controls flow direction and rate (Maxwell et al. 2008). The hydraulic connection between a contamination source and well (either remediation or water supply) plays an important role in the amount of contaminants captured by the well. A well-connected high-hydraulic

conductivity flow zone (e.g., clean sand or fractured interval) could allow for much more rapid migration of contaminated water towards a sensitive receptor than anticipated based on the assumption of more homogenous conditions.

Consider two aquifer scenarios with the same proportion of a high-hydraulic conductivity (sand) facies and low-hydraulic conductivity (clay) facies (Fig. 16.4). The equivalent vertical and horizontal hydraulic conductivity will vary depending upon whether or not the facies occur in regular layers (i.e., have a 'layer-cake' geology), and are well connected, or are more randomly interspersed. The scenario in which both the high- and low-hydraulic conductivity strata are laterally connected will have a higher transmissivity and the lower equivalent vertical hydraulic conductivity (i.e., aquifer strata will be better confined). Data from a small number of boreholes would not be able to distinguish between the two scenarios.

The issue of connectivity upscaling needs to be considered during the model development process, particularly with respect to the selection of grid-size. As explained by Reilly and Harbaugh (2004).

> The size of cells determines the extent to which hydraulic properties and stresses can vary throughout the modeled region. Hydraulic properties and stresses are specified for each cell, so the more cells in a model, the greater the ability to vary hydraulic properties and stresses. If the cell size is too large, important features of the framework may be left out or poorly represented.
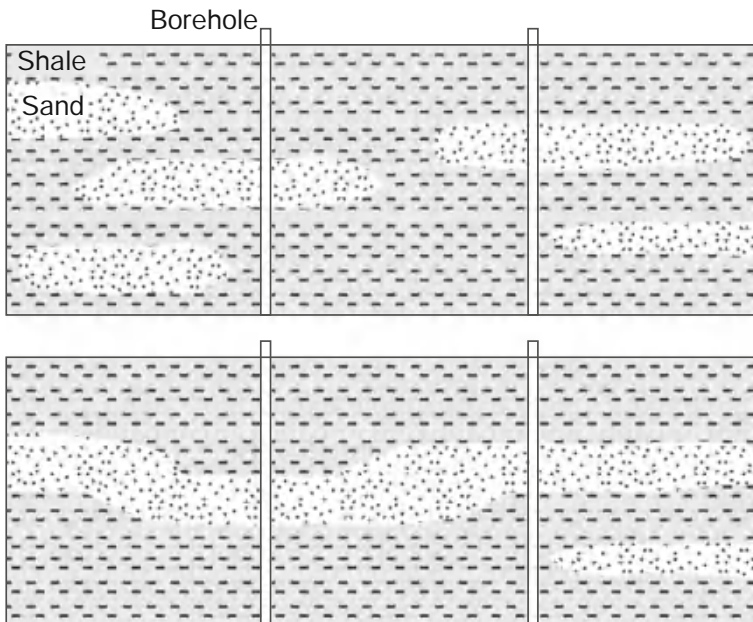
Fig. 16.4 Conceptual diagram of sand and shale systems with different degrees of connectivity of high-hydraulic conductivity sands. Aquifers with low connectivity of sand bodies (top) will have lower transmissivity than aquifers in which the sands are well connected (bottom). The degree of connectivity will not be evident in data from a small number of boreholes

Accordingly, it is important to evaluate the known (or assumed) variation of hydraulic properties and stresses of the system being simulated compared to the size of the cells.

Hence, if the connectivity high-hydraulic conductivity strata is known to dominate groundwater flow, then the model discretization should be fine enough to capture the geometry of the conductive strata.

In the simple case of horizontal uniform layers, equivalent horizontal and vertical hydraulic conductivity values (K_x, K_z, respectively) can be obtained using basic averaging equations. The equivalent horizontal hydraulic conductivity (K_x; m/d) is the arithmetic mean of the horizontal hydraulic conductivity of individual beds (using consistent units)

$$K_x = \sum_{i=1}^{n} \frac{K_{xi} b_i}{b} = \frac{\sum_{i=1}^{n} K_{xi} b_i}{\sum_{i=1}^{n} b_i} \qquad (16.24)$$

where
K_{xi} horizontal conductivity of bed 'i' (m/d)
b_i thickness of bed 'i' (m)
b total thickness (m)

The equivalent vertical hydraulic conductivity (K_z; m/d) is the harmonic mean of the vertical hydraulic conductivity of individual beds (using consistent units)

$$K_z = \frac{b}{\sum_{i=1}^{n} \frac{b_i}{K_{zi}}} = \frac{\sum_{i=1}^{n} b_i}{\sum_{i=1}^{n} \frac{b_i}{K_{zi}}} \qquad (16.25)$$

where K_{zi} = vertical hydraulic conductivity of bed 'i' (m/d).

Although some types of basic upscaling are conceptually simple, they are subject to errors. For example, transmissivity values for an aquifer can be calculated as the arithmetic average of hydraulic conductivity vertically across the aquifer thickness. The hydraulic conductivity values may be obtained, for example, from core analyses or borehole geophysical logs. However, this simple averaging process may overestimate flow rates in the horizontal plane (Dykaar and Kitanidis 1993; Desbarats and Bachu 1994). Instead use of a generalized power average has been proposed (Desbarats 1992).

$$K_B^x(x) = \frac{1}{B} \int_B K^x(x) \qquad (16.26)$$

where
$K_B(x)$ vertically average hydraulic conductivity
B total thickness
$\times$ $(1-2g_{ll})$, where g_{ll} is a geometric factor whose values in isotropic and perfectly stratified formations are 1/3 and 0, respectively

In a finite-difference model grid, a single value is assigned for each parameter. Upscaling in the horizontal direction is seldom an issue in groundwater investigations as it uncommon to have multiple borehole, cores, or other data within the area of a model grid cell. The norm is to have data for only a very small fraction of the total number of cells. Various interpolation methods are used to assign values to cells with no field data. Where multiple data points are present in a grid cell, average values of parameters may be used. In common practice, interpolation methods are used to create an 'x–y' surface of values for each parameter and each grid cell is assigned the value in the center of the cell.

Where strata are discontinuous at the scale of interest, simple averaging methods may not be appropriate. Complete characterization of the subsurface would ideally yield a site-specific three-dimensional facies model with delineation of interconnectedness of high and low connectivity zone (Anderson 1997). Evaluation of connectivity can be difficult (if not impossible) where only point (e.g., well) data are available. With respect to fluvial sandstones, Bridge (2001) cautioned that sandstone bodies at the same stratigraphic level in adjacent wells are not necessarily connected. Sandstone bodies should not be automatically correlated over the distance between two wells if this distance greatly exceeds the expected lateral extent of the channel belt (Bridge 2001). The degree of connectivity of superimposed channel belt deposits depends upon the proportion of channel deposits. If the channel deposit proportion exceeds 0.75, then the channel deposits will be connected (Bridge 2001). Facies analysis can provide valuable insights into the potential extent and direction of connectivity of aquifer strata. Considering the limited amount of spatially distributed data available in most investigations, investigators should have the mindset of trying to extract the maximum information out of all available data.

A number of studies have simulated sedimentary aquifers and demonstrated the importance of connected high-hydraulic conductivity units in channeling groundwater flow. Anderson et al. (1999) simulated groundwater flow and solute transport in braided stream aquifers using MODFLOW and a particle tracking code (PATH3D). Simulations were performed using both models developed using local field data and a synthetic, computer-generated depositional model. Both simulations showed channeling of flow in connected high-hydraulic conductivity facies.

Tracer tests and modeling results from the Macrodispersion Experiment (MADE) site, Columbus, Mississippi demonstrated that fast flow is dominated by clusters of interconnected relatively high-hydraulic conductivity sediment cells (Bianchi et al. 2011). The accumulation of tracer mass near the point of injection and extensive spreading in the direction of flow is best explained by a dual-porosity system consisting of a network of more permeable sediments embedded in a less conductive matrix (Bianchi et al. 2011). Solute travels along preferential flow paths, leaking (jumping) from one hydraulic conductivity cluster to another with transitions through low-hydraulic conductivity zones. Significant transport connectivity may not require complete connection of all zones of relatively homogenous high-hydraulic conductivity (Bianchi et al. 2011).

Connectivity is also an issue on finer scales. In rivers, clay laminae and other low permeability units are commonly present between bedding, particularly in fluvial sediments (Pryor 1973). In all deposits, boundary conditions between sedimentary packets are important features in determining the effective reservoir and aquifer characteristics of the sand packets. The effective permeability of sand packets will largely be determined by the lower permeabilities of the bounding units and hence data on the properties of the sands alone will not demonstrate their ultimate through-flow capabilities (Pryor 1973). A study of the heterogeneity of an Upper Cretaceous sandstone (Almond Formation, Wyoming) involving core and minipermeameter permeability measurements of outcrops also demonstrated the importance of bed and bedsets boundaries in controlling subsurface fluid flow (Schatzinger and Tomutsa 1999).

Several approaches that have been proposed and utilized to address aquifer connectivity are summarized below. At one end of the spectrum, connectivity can be simulated by manually mapping aquifer strata using available data, ideally guided by a conceptual facies model. At the other end, geostatistical methods may be employed to obtain geological facies and hydrofacies realizations. Facies models can give indications of the likelihood of preferential flow paths (Anderson 1997).

McFarlane et al. (1994) documented how the sedimentary architecture influences groundwater flow in the Dakota Aquifer of Kansas, which consists of fluvial, deltaic, and marine sandstones. It was noted that there is a six order of magnitude difference in hydraulic conductivity between sand aquifer units and clayey aquitards. The connectivity of sand bodies was identified as the dominant factor in assessing the water resources potential of the aquifer. Borehole geophysical logs available from the numerous oil and gas wells in the state, were used to manually correlate sand units, which act as aquifers, and clays/shales and mudstones, which act as confining units. Gamma ray logs allowed for the differentiation between clean sands and clayey confining strata. Combined neutron, density, and dual induction log data were used to determine the optimal gamma ray cutoff ($\approx$60 API) between aquifer and aquitard units.

Fogg (1986) investigated Wilcox aquifer in northeastern Texas, which consists of relatively high-hydraulic conductivity channel-fill fluvial sands and lower-hydraulic conductivity muddy interfluve deposits. The key issue is the degree of interconnection of the sand bodies. The approach taken was to map the percentage of channel sand in each model grid cell. An equivalent hydraulic conductivity was calculated from the percentage of channel-fill sands. If the percentage was less than 20 %, then it was assumed that the sands were disconnected and the equivalent hydraulic conductivity was lowered by a factor of 100 in relation to adjacent areas. The model results demonstrated how one or two interconnected sands among a system of otherwise disconnected sands could dominate the flow field.

Fleckenstein and Fogg (2008) presented an efficient upscaling technique that was used for a heterogeneous alluvial aquifer in California. Geologic heterogeneity was first characterized using transition-probability-based geostatistical simulations of hydrofacies distributions. The studied aquifer was divided into four hydrofacies,

which were assigned hydraulic conductivity values. Equivalent horizontal and vertical hydraulic conductivity values were then calculated using weighted arithmetic and harmonic averaging. It was observed that a logarithmic increase in model-domain equivalent hydraulic conductivity occurred with increasing upscaling, which was related to connectivity (interconnection of high-hydraulic conductivity flow zones).

Consider, for example, a situation where an aquifer locally contains sand and gravel bodies that are not connected. The lateral flow between sand and gravel bodies in the aquifer, as a result, will be very low. However, the upscaling process may assign cells intermediate hydraulic conductivity values, which can result in artificially enhanced connectivity between adjacent grid columns and increased modeled lateral flows (Fleckenstein and Fogg 2008). Fleckenstein and Fogg (2008) proposed application of a correction factor to the upscaled hydraulic conductivity values so that net lateral flow through the upscaled domain is the same as through the original model.

There is an on-going need for sedimentological techniques to efficiently identify and quantify connectedness among hydrofacies (Anderson et al. 1999) and then upscale the data for incorporation into numerical groundwater models. Methods used to incorporate flow features into models were reviewed by Webb and Anderson (1996) and include

- indicator statistical methods with or without conditioning using field data
- detailed field facies (hydrofacies) modeling using borehole (cutting, core, and geophysical) and surface geophysical data
- simulation of sedimentary units based on description of the general geological system and limited field data.

Cleary, the upscaling and interpolation methods selected for a given project should depend upon local hydrogeology (type and scale of aquifer heterogeneity), the available and practicably obtainable data, and project objectives. The optimal strategy, in general, may be a hybrid approach in which geological and hydrogeological data are used to condition geotatistical models. Geostatistical methods for simulating aquifer heterogeneity are further discussed in Chap. 20.

References

Ahmed, U., Crary, S. F., & Coates, G. R. (1991) Permeability estimation: The various sources and their limitations. Journal of Petroleum Technology (JPT), May 1991, 578–587.

Ahr, W. M., Allen, D., Boyd, A., Bachman, H. N., Smithson, T., Clerke, E. A., Gzara, K. B. M., Hassall, J. K., Murty, C. R. K., Zubari, H., & Ramamoorthy, R. (2005) Confronting the carbonate conundrum. Oilfield Review, 17(1), pp. 18–29.

Allen, D., Flaum, C., Ramakrishnan, T. S., Bedford, J., Castelijns, K., Fairhursts, D., Gubelin, G., Heaton, N., Minh, C. C., Norville, M. A., Seim, M. R., Pritchard, T., & Ramamoorthy, R. (2000) Trends in NMR logging. Oilfield Review, 12(3), 2–19.

Ali, M., Chawathé, A., Ouenes, A., Cather, M., & Weiss, W. (1999) Extracting maximum petrophysical and geological information from a limited reservoir database. In R. Schatzinger and J. Jordan (Ed.), Reservoir characterization – Recent advances. Memoir 1. (pp. 191–208). Tulsa: American Association of Petroleum Geologists.

Amaefule, J. O., Altunbay, M., Tiab, D., Kersey, D. G., & Keelan, D. K. (1993) Enhanced reservoirs description: Using core and log data to identify hydraulic (flow) units and predict permeability in uncored intervals/wells. In SPE Annual Technical Conference and Exhibition (pp. 205–220). Society of Petroleum Engineers (SPE Publication 26436).

Anderson, M. P. (1997) Characteriztion of geological heterogeneity. In G. Dagan and S. P. Neuman (Eds.) Subsurface flow and transport: A Stochastic Approach (pp. 23–43). Cambridge: Cambridge University Press.

Archie, G. E. (1950) Introduction to petrophysics of reservoir rocks. American Association of Petroleum Geologists Bulletin, 34, 943–961.

Ayan, C., Haq, S. A., Boyd, A., El-Hamawi, H. H., & Hafez, A. D. C. O. (1999) Integration of NMR, wireline tester, core and open hole log data for dynamic reservoir properties. In Middle East Oil Show and Conference. Society of Petroleum Engineers (SPE Publication 53272).

Balan, B., Mohaghegh, S., & Ameri, S., 1995, State-of-the-art in permeability from well log data: Part 1- A comparative study, model development: Society of Petroleum Engineers Eastern Regional Conference & Exhibition (SPE Paper 30978).

Barson, D., Christensen, R., Decoster, E., Grau, J., Herron, M., Herron, S., & Guru, U. K. (2005). Spectroscopy: the key to rapid, reliable petrophysical answers. Oilfield Rev, 17(2), 14–33.

Bear, J. (1972) Dynamics of fluids in porous media. New York: Elsevier.

Bianchi, M., Zheng, C., Wilson, C., Tick, G. R., Liu, G., & Gorelick, S. M. (2011) Spatial connectivity in a highly heterogenous aquifer: From core to preferential flow paths. Water Resources Research, 47, W-5524.

Bridge, J. S. (2001) Characterization of fluvial hydrocarbon reservoirs and aquifers: problems and solutions: AAS [Asociación Argentina de Sedimentología], 8(2), 87–114.

Chang, D., Vinegar, H., Morriss, C., & Straley, C. (1997) Effective porosity, producible fluid, and permeability in carbonates from NMR logging. The Log Analyst, March-April 1997, 60–72.

Coates, G. R., Peveraro, R. C. A., Hardwick, A., & Roberts, D. (1991) The magnetic resonance imaging log characterized by comparison with petrophysical properties and laboratory core data. In. Proceedings of the 66th Annual Technical Conference and Exhibition, Formation Evaluation and Reservoir Geology (pp. 627–635). SPE paper 22723.

Delhomme, J. P. (2007) The quest for permeability evaluation in wireline logging. In L. Chery and G. de Marsily (Eds.), Aquifer systems management: Darcy's legacy in a world of impending water shortage (pp. 55–70). London: Taylor & Francis.

de Marsily, G., Delay, F., Goncalvès, J., Renard, Ph., Teles, V., & Violette, S. (2005) Dealing with spatial heterogeneity. Hydrogeology Journal, 13, 161–183.

Desbarats, A. J. (1992) Spatial averaging of hydraulic conductivity in three-dimensional heterogeneous porous media. Mathematical Geology, 24, 249–267.

Desbarats, A. J., & Bachu, S. (1994) Geostatistical analysis of aquifer heterogeneity from the core scale to the basin scale: A case study. Water Resources Research, 30, 673–684.

Dorfman, M. H., Newey, J.-J., & Coates, G. R. (1990) New techniques in lithofacies determination and permeamability prediction in carbonates using well logs. In A. Hurst, M. A. Lovell and A. C. Morton (Eds.), Geological applications of wireline logs. Special Publication 48 (pp. 113–120). London: Geological Society.

Dunham, R. J. (1962) Classification of carbonate rocks according to depositional texture. In W. E. Ham (Ed.), Classification of carbonate rocks. Memoir 1 (pp. 108–121). Tulsa: American Association of Petroleum Geologists.

Dykaar, B. B., & Kitanidis, P. K. (1993) Transmissivity of a heterogeneous formation. Water Resources Research, 29, 985–1001.

Fleckenstein, J. H., & Fogg, G. E. (2008) Efficient upscaling of hydraulic conductivity in heterogeneous alluvial aquifers. Hydrogeology Journal, 16, 1239–1250.

Fogg, G. E. (1986) Groundwater flow and sand body interconnectedness in a thick multiple-aquifer system. Water Resources Research, 22, 679–694.

Genty, C., Jensen, J. L., & Ahr, W. M. (2007) Distinguishing carbonate reservoir pore facies with magnetic resonance measurements. Natural Resources Research, 16, 45–54.

Glover, P. W. J., Zadjali, I. I., & Frew, K. A. (2006) Permeability prediction from MICP and NMR data using an electrokinetic approach. Geophysics, 71(4), F49–F60.

Hassal, J. K., Ferraris, P., Al-Raisi, M., Hurley, N. F., Boyd, A., & Allen, D. F. (2004) Comparison of permeability predictors from, NMR, formation image and other logs in a carbonate reservoir. In In Abu Dhabi International Conference and Exhibition. Society of Petroleum Engineers (SPE publication 88683).

Helle, H. B., Bhatt, A., & Ursin, B. (2001) Porosity and permeability prediction from wireline logs using artificial neural networks: a North Sea case study. Geophysical Prospecting, 49, 431–4444.

Herron, M. M. (1987). Estimating the intrinsic permeability of clastic sediments from geochemical data. In SPWLA 28th Annual Logging Symposium. Society of Petrophysicists and Well-Log Analysts.

Huang, Z., Shimeld, J., Williamson, M., & Katsube, J. (1996) Permeability prediction with artificial neural network modeling in the Venture gas field, offshore eastern Canada: Geophysics, 61, 422–436.

Jorgensen, D. G. (1991) Estimating geohydrologic properties from borehole-geophysical logs. Groundwater Monitoring & Remediation, 11(3), 123–129.

Kennedy, M. C. (2002) Solutions to some problems in the analyses of wells in carbonate rocks. In M. Lovell & N. Parkinson (Eds.), Geological application of well logs. Memoirs in Exploration 13 (pp. 61–73).Tulsa: American Association of Petroleum Geologists.

Khalil, M. A., & Santos, F. A. M. (2013) Hydraulic conductivity estimation from resistivity logs: a case study in Nubian sandstone aquifer. Arab Journal of Geosciences, 6, 205–212.

Lucia, F. J. (1983) Petrophysical parameters estimated from visual descriptions of carbonate rocks: A field classification of carbonate pore space. Journal of Petroleum Technology, 35, 629–637.

Lucia, F. J. (1995) Rock-fabric/petrophysical classification of carbonate pore space for reservoir characterization. American Association Petroleum Geologists Bulletin, 79, 1275–1300.

Maxwell, R. M., Carle, S. F., & Tompson, A. F. B. (2008) Contamination, risk, and heterogeneity: on the effectiveness of aquifer remediation. Environmental Geology, 54, 1771–1786.

McFarlane, P. A., Doveton, J. H., Feldman, H. R., Buttler, J.J., Jr., Combes, J. M, & Collins, D. R. (1994) Aquifer/aquitard units of the Dakota Aquifer Systems in Kansas: Methods of delineation and sedimentary architecture effects on ground-water flow properties. Journal of Sedimentary Research, B64(4), 464–480.

Mohaghegh, S., Balan, B., & Ameri, S. (1997) Permeability determination from well log data. SPE Formation Evaluation, September 1997, 170–174.

Nelson, P. H. (1994) Permeability-porosity relationships in sedimentary rocks. The Log Analyst, 35(3), 38–62.

Paillet, F. L., & Crowder, R. E. (1996) A generalized approach for the interpretation of geophysical well logs in ground water studies - Theory and application. Ground Water, 34, 883–898.

Pryor, W. A. (1973). Permeability-porosity patterns and variations in some Holocene sand bodies. American Association Petroleum Geologists Bulletin, 57(1), 162–189.

Quental, P., Almeida, J. A., & Simões, M. (2012) Construction of high-resolution stochastic geological models and optimal upscaling to a simplified layer-type hydrogeological model. Advances in Water Resources, 39 18–32.

Reilly, T. E., & Harbaugh, A. W. (2004) Guidelines for evaluating ground-water flow models. U.S Geological Survey Scientific Investigations Report 2004–5038.

Renard, P., & de Marsily, G. (1997) Calculating equivalent permeability: a review. Advances in Water Resources, 20(5–6), 253–278.

Ritzi, R. W., Jr., Jayne, D. F., Zahradnik, A. J., Jr., Field, A. A., & Fogg, G. E. (1994) Geostatistical modeling of heterogeneity in glaciofluvial, buried valley aquifers. Ground Water, 32(4), 666–674.

Schatzinger, R. A., & Tomutsa, L. (1999). Multiscale heterogeneity characterization of tidal channel, tidal delta, and foreshore facies, Almond Formation outcrops, Rock Springs Uplift, Wyoming. In R. A Schatzinger and J. F. Jordan (Eds.), Reservoir characterization - Recent advances. Memoir 7. (pp. 45–56). Tulsa: American Association of Petroleum Geologists.

Timur, A. (1968) An investigation of permeability, porosity and residual water saturation relationships for sandstone reservoirs. The Log Analyst, 9(4), 8–17.

Waxman, M. H., & Smits, L. J. M. (1968) Electrical conductivities in oil bearing sands. Journal of the Society of Petroleum Engineers, 8, 107–122.

Webb, E. K., & Anderson, M. P. (1996). Simulation of Preferential Flow in Three-Dimensional, Heterogeneous Conductivity Fields with Realistic Internal Architecture. Water Resources Research, 32(3), 533–545.

Wendt, W. A., Sakurai, S., & Nelson, P. H. (1986) Permeability prediction from well logs using multiple regression. In L. W. Lake & H. B. Carroll, Jr. (Eds.) Reservoir characterization (pp. 181–221). Orlando: Academic Press.

Westphal, H., Surholt, I., Kiesl, C., Thern, H. F., & Kruspe, T. (2005) NMR measurements in carbonate rocks: Problems and an approach to a solution. Pure and Applied Geophysics, 162, 549–570.

Yeh. T.-C. J. (1998) Scale issues of heterogeneity on vadose-zone hydrology. In G. Sposito (Ed.), Scale dependence and scale invariance in hydrology (pp. 167–189). Cambridge: Cambridge University Press.

Yao, C. Y., & Holditch, S. A. (1993) Estimating permeability profiles using core and log data. In Proceedings 1993 SPE Eastern Regional Conference & Exhibition, Pittsburgh, 2–4, November, 1993 (pp. 317–322), Society of Petroleum Engineers (SPE publication 26921).

Zhang, Y., & Salisch, H. A. (1998) Evaluation of permeability from geophysical logs in the Barrow Field, Western Australia. First Break, 16(7), 243–250.

Chapter 17
Fractured Sedimentary Rock Aquifers

Fractured sedimentary rock contains two domains, the fractures and adjoining rock matrix. Fractures often provide most of the aquifer transmissivity, whereas the bulk of water and solute storage may occur in the matrix. The concentration of flow in fractures, which constitutes a very minor part of the total volume of the strata, results in greater flow velocities and travel distances than would occur in single-porosity systems. Characterization of fractured aquifers typically involves a multiple-method approach that includes identification of fractures, determination of whether or not identified fractures are hydraulically active, and determination of the hydraulic properties of the fractures and fractured zones. Fractured rock aquifers may be modeled using either a single-continuum (equivalent porous media), dual-continuum, or discrete fracture network approach.

17.1 Introduction

A fracture is defined as a crack, joint, or other break in a rock caused by mechanical failure as a result of stress. Fractures may be oriented either parallel, perpendicular, or oblique to bedding. A fault is a fracture, or a fracture zone, along which there has been displacement of the sides relative to one another and parallel to the fracture. Fractures usually provide the only porosity and permeability in aquifers that occur in otherwise impervious crystalline (igneous or metamorphic) rock. Open, hydraulically active fractures are important in sedimentary rock aquifers in that they can have a greater hydraulic conductivity than the aquifer matrix (i.e., rock between and bounded by fractures) and can thus increase the transmissivity and equivalent hydraulic conductivity (vertical and horizontal) of aquifers and aquitards. Conversely, fractures that are filled with cement, or other material, may act as barriers to groundwater flow. Spatial variation and anisotropy in hydraulic conductivity caused by a preferred fracture orientation can result in flow directions that are not perpendicular to potentiometric contours (Cook 2003).
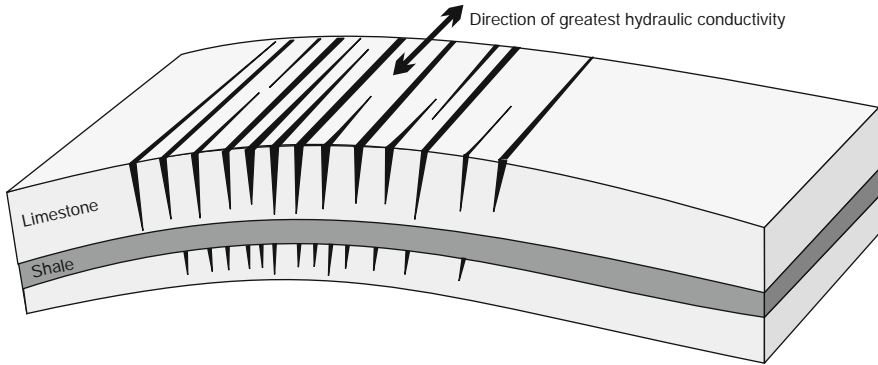
Fig. 17.1 Conceptual diagram showing a preferential orientation of fractures and associated anisotropy in transmissivity along the hinge of an anticline. Fractures would be best-developed in brittle lithologies and may be absent in clay and shale units that tend to be plastically deformed

Fractures form when a rock is stressed beyond its strength. Fracturing can be induced by both tensile and shear stresses, which can originate from processes such as tectonism, unloading (reduction in overburden), differential subsidence, collapse of underlying caverns, and changes in pore pressure and temperature. Other important factors controlling fracturing are rock strength (brittleness) and the orientation of heterogeneities in rock properties with respect to principal stress directions. A uniform stress field can result in a preferred fracture orientation and thus anisotropy in aquifer transmissivity. For example, tensile fractures may preferentially form near the hinge of anticlines (where there is the maximum tension) and have a preferred orientation parallel to the strike of the folds (Fig. 17.1). However, fracture patterns are typically more complex.

Rock types vary in their brittleness and thus susceptibility to fractures. At one extreme are soft, clay-rich strata that tend to be plastically deformed. At the other end of the spectrum, dolomites and well-cemented sandstone tend to be deformed in a brittle manner (Stearns and Friedman 1972; Nelson and Serra 1995). For example, in the Floridan Aquifer System of South Florida, dolomitic strata are often preferentially fractured compared to adjoining limestones and form high-transmissivity flow zones (Maliva and Walker 1998; Maliva et al. 2002; Reese and Richardson 2008). The same type of low-porosity dolomite strata may act as a confining unit when not fractured.

Fractured rock consists of fractures and the adjoining rock matrix, which is divided by fractures into matrix blocks. Multiple sets of fractures may be present, including a set that parallels bedding and one or more sets oriented perpendicular or oblique to bedding (Fig. 17.2). Open fracture networks, depending upon their properties, may have much greater hydraulic conductivities than the rock matrix, but constitute only a small fraction of the total porosity of the rock as a whole. The exception being where the rock matrix is essentially nonporous, such as is the case for crystalline rock. In the classic dual-porosity system model in sedimentary rocks, water flow occurs

Fig. 17.2 Fractures in an eolian sandstone at Red Rock Canyon, near Las Vegas, Nevada. Sets of fractures parallel and perpendicular to bedding are clearly evident (yellow arrows). Other perpendicular or oblique fractures with different orientations are also evident (orange arrows)

Fig. 17.3 Conceptual diagram of a dual-porosity system. Fractures (gray) have a relatively high-hydraulic conductivity but a very low porosity. The fracture-bound matrix blocks, in sedimentary aquifers, may have a low hydraulic conductivity but high porosity. The bulk of the groundwater flow occurs in the fractures but the most of water and solute storage occurs in the matrix
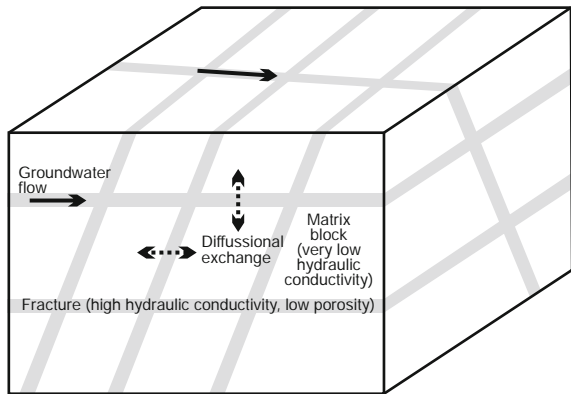
predominantly through the fracture network, whereas as the bulk of water and solute storage occurs in the rock matrix (Fig. 17.3). Fracturing is important for groundwater flow to the extent that it affects aquifer bulk hydraulic properties. The concentration of groundwater flow through fracture networks with low porosities results in much higher flow velocities under a given hydraulic gradient and transmissivity than would occur in a uniformly porous rock with a higher overall porosity.

The hydrogeology of fractured rock can be considered in terms of two end members: (1) systems dominated by a relatively few major fractures in a relatively impermeable matrix and (2) systems dominated by a network of ubiquitous, highly interconnected fractures in a relatively permeable matrix (National Research Council 1996). In the former case, the fractures essentially act as "aquifers" and the intervening unfractured rock act as "aquitards" (Gellasch et al. 2013). Key issues associated with fractured medium are the degree to which fractures contribute to local and regional groundwater flow and the amount of fluid and solute exchange between fractures and the matrix. As is the case for secondary porosity in general,

fracturing is of greatest importance in investigations involving solute (e.g., contaminant) transport as opposed to investigations considering only groundwater flow. The greater flow velocities in fractured rock results in more rapid movement, greater dispersive mixing, and larger geographic extents of contaminants in fractured rock aquifers. Similarly, fracturing is responsible for the poor performance of some aquifer storage and recovery systems, as recharged freshwater experiences rapid movement and high degrees of mixing with native, poorer-quality groundwater (Maliva and Missimer 2010). Modeling results have also demonstrated that dual-porosity conditions can result in more rapid buoyancy stratification where freshwater is injected into a brackish or saline aquifer (Guo et al. 2014).

With respect to contamination assessment and remediation, identification of preferential pathways is important for (Nativ et al. 2003)

- determination of areas likely to be impacted by contamination in the future
- selecting appropriate monitoring and remediation strategies
- reliably predicting contaminant migration rates.

Characterization and modeling of flow and solute transport in fractured rock remains one of the greatest challenges in hydrogeology. Fractured rock aquifers are characterized by extreme heterogeneity with respect to hydraulic conductivity and may also have high degrees of anisotropy. Quantification of flow and transport in fractured rock was reviewed by Neuman (2005). There has been a huge amount of research performed on quantification of flow and transport ranging in scale from an individual fracture to an entire aquifer. However, much of research is of a theoretical rather than applied nature. The applied hydrogeology of fractured rock systems is reviewed in detail by the National Research Council (1996) and Singhal and Gupta (2010). From an applied hydrogeological perspective, the key technical issues are characterizing and representing fracture systems, in which the distribution, orientation, length, and degree of interconnection of fractures are poorly constrained by field data, and quantifying the communication between fractures and adjoining matrix blocks. This information then need to be incorporated into numerical groundwater models in a manner so that flow and solute transport are simulated accurately enough to meet project-specific requirements.

17.2   Fracture Hydraulics

The hydraulic conductivity and flow rates through open fractures consisting of parallel planar plates is described using the 'cubic law', in which the flow rate under laminar conditions is proportional to the cube of the aperture height. Aperture 'height' refers to the separation distance between the 'plates'. The basic equations of the cubic law are discussed by Bear (1972) and Witherspoon et al. (1980). The general equation for flow rate through a fracture is

$$Q = -Cb^3 Dh \qquad (17:1)$$

where
Q   volumetric flow rate (m^3/s)
Dh   head difference (m)
C   constant that depends on fracture geometry and fluid properties
b   aperture height (m)

The dimensionless factor (f) is added to the general and specific equations to account for deviations from ideal conditions, such as roughness, (Witherspoon et al. 1980):

$$Q = -\frac{1}{f} wb^3 \left(\frac{qg}{12l}\right)\left(\frac{Dh}{Dl}\right) \qquad (17:2)$$

f   friction factor (dimensionless)
q   density of water (* 999.7 kg/km^3)
g   gravitation acceleration (9.8 m/s^2)
l   viscosity of water (1.307 X 10^{-3} kg/m s; Pa s)
w   fracture width (m)
Dh/Dl   hydraulic gradient (m/m)

The hydraulic conductivity (K_f) and transmissivity of fractures (T_f) is proportional to the square and cube of aperture width as follows:

$$K_f = -b^2 \left(\frac{qg}{12l}\right) \qquad (17:3)$$

$$T_f = -b^3 \left(\frac{qg}{12l}\right) \qquad (17:4)$$

Where multiple fractures are present, the aquifer transmissivity is the sum of the transmissivities of individual fractures (assuming a negligible contribution from the matrix). If the distribution of fractures is irregular, then there may be a very high variation in transmissivity. The orientation of fractures can result in high degrees of anisotropy with respect to hydraulic conductivity. In the extreme case of parallel fractures and an impervious matrix, a high-hydraulic conductivity may occur parallel to the fractures and a hydraulic conductivity of essentially zero may occur in the direction perpendicular to the fractures (Cook 2003).

Fractured rock aquifers may also show a pronounced scale effect with respect to hydraulic conductivity with hydraulic conductivity increasing with increasing volume of investigation. As volume increases, there is an increasing likelihood that large, well-interconnected fractures may be encountered. A question remains as to whether hydraulic conductivity eventually approaches a constant value at a representative elementary volume (REV; Cook 2003).

The cubic law is based on the approximation that fractures are bounded by parallel plates. However, the geometry of fractures is more complex than simple parallel planar plates. Fractures may be nonplanar (undulose), have spatial variation in aperture heights, different degrees of openness (abundance, size, and shape of asperities), and different degrees of infilling with cements and sediments. Laboratory and field studies suggest that flow and transport in rough-walled fractures tends to occur in highly variable and tortuous channels. Flow in fractures may occur mainly along narrow regions of enlarged aperture ("channels") that form, for example, at the intersection of two fractures. The remainder of the fractures contains stagnant water. The transport of solutes may be retarded by diffusion between channels and stagnant areas, and between fractures and the adjoining matrix (National Research Council 1996).

The results of percolation tests performed on unsaturated fractured chalks demonstrated that only a fraction of fractures are hydraulically active and that the active segments of fractures appear to be located at or adjacent to fracture junctions (Dahon et al. 2000). The results of a percolation test indicated that less than 20 % of the fractures in the studied unsaturated Eocene chalk transmitted most (>70 %) of the water (Dahon et al. 1999).

Witherspoon et al. (1980) concluded, based on their experimental results, that the cubic law is valid for both open and closed fractures, as deviations from ideal can be incorporated using the roughness factor. Neuman (2005) suggested, based on a literature review, that the cubic law with a correction factor holds only for fractures whose adjoining surfaces are not in contact and where fractures do not contain or are not coated with porous media.

There is much interest in determining the hydraulic conductivity and transmissivity of fractures from physical data. Alternatively, the "hydraulic" aperture of fractures can be calculated from bulk and matrix hydraulic conductivity data, and fracture spacing and orientation. For example, McKay et al. (1993) documented the use of hydraulic conductivity and fracture spacing in fractured clay till to calculate hydraulic apertures using the cubic law.

There are a number of factors that can impact hydraulic properties of fractures and fractured rock aquifers, including

- abundance (spacing) and distribution of fractures (e.g., equidistant, random, concentration into sets)
- orientation (strike and dip)
- length
- connectivity
- aperture width
- surface roughness
- presence and properties of skins.

A key issue is obtaining an accurate dataset on the geometry of fractures within the formation of interest, which may be different from the values measured in a borehole, core, or exposed surface. The release of stress associated with the

exposure of rock can open fractures. Measurements of fracture apertures, whether from a core, borehole imaging log, or exposure, need to consider the orientation of the fracture with respect to the surface and mechanical enlargement of the fracture mouth. Advanced technologies, such as computer-aided tomography (CAT) x-ray scanning have been successfully used for high-resolution imaging of fractures within cores (Keller 1997; Bertels et al. 2001). However, the reduction of pressure as cores are drilled and brought to land surface can change fracture properties, such as aperture heights. The cubic law is important for understanding fracture flow processes. Even so, cubic law-based estimation of the hydraulic properties of fractures from field measurement of fracture dimensions is usually not an accurate or practical aquifer characterization technique.

17.3   Fracture Cements and Skins

Fractures, as features with relatively high-hydraulic conductivity, are the preferential loci for groundwater flow and thus the transport of solutes. As a result, fractures may be the site of diagenetic processes, such as cementation (Fig. 17.4), dissolution, and alteration. In the case of cementation, fractures may be sealed off to become essentially impervious features, which can compartmentalize an aquifer if they are interconnected. Dissolution and precipitation can affect the dimensions and roughness or fractures and thus impact their hydraulic conductivity.

The exchange of fluids and solutes between fractures and matrix blocks can be impeded by the presence of a fracture skin. A fracture skin was defined by Moench (1984) as a thin layer of impermeable material, deposited on the surfaces of matrix blocks, that serves to impede the free exchange of fluid between the blocks and fractures. Skins form as the interconnected fissures serve as conduits for the natural circulation of mineral-charged (or geochemically active) water in aquifers and

Fig. 17.4 Mineral precipitation (white) along a fault, Lake Pleasant Regional Park, Arizona

deeper reservoirs (Moench 1984). Fracture skins have multiple origins, or contributing processes, including mineral alteration or precipitation, clay deposition, and microbiological activities (i.e., biofilm formation). The skins can strongly affect solute and colloidal transport, increasing sorption along fracture surfaces and decreasing diffusion into and out of the matrix (Sharp et al. 1996). If the skins are very well-developed, and essentially seal the surface of the matrix blocks, then little of no solute transfer may occur between the matrix and fractures.

The presence of fracture skins needs to be incorporated into solute transport models of fractured rock aquifers through a transfer function. In the case of dual-domain models, the transfer function quantifies the degree of communication between the matrix and fractures. Measurement of the properties of fracture skins remains a practical problem. Fracture skins may also change over time. Wall-rock alterations along fracture skins composed of vein fillings indicate that several episodes of fracturing healing (filling with precipitants) followed by reopening occurred in some formations. Fracture skins evident at surface outcrops may not be representative of skins at depth within aquifers because of differences in geochemical conditions and local flow regimes. Iron sulfide minerals, for example, are often oxidized to iron oxyhydroxides near land surface when exposed to the atmospheres. Degassing of carbon dioxide can cause local calcium carbonate precipitation. Biofilms may either grow or be degraded once exposed at land surface. In practice, the properties of the fracture skins are evaluated by inverse modeling. The value of transfer functions are adjusted during the model calibration process.

17.4 Fracture Distribution—Mechanical Stratigraphy

The distribution of fractures may be related to a discrete structural feature, such as a fault or fold, or to stratigraphy. Fracture distributed may be controlled by variations in the tensile strength of strata. The underlying concepts of mechanical stratigraphy were reviewed by Underwood et al. (2003) and Cooke et al. (2006). Mechanical stratigraphy refers to stratigraphic features that control fracture initiation and propagation within a sequence of sedimentary rock (Gross et al. 1995; Underwood et al. 2003; Cooke et al. 2006). The basic units of mechanical stratigraphy are mechanical units, which represent one of more stratigraphic units that fracture independently of other units, and mechanical interfaces, which are the boundary between mechanical units (Fig. 17.5). The key value of mechanical stratigraphy for aquifer characterization is that, if fractures are locally stratabound, then fracture spacing and connectivity, and thus the location and characteristics or preferential flow zones, may be predicted from lithostratigraphy. Non-stratabound (through-going) fractures may enhance vertical flow between horizontal flow units (i.e., aquifers and aquifer zones).

Beds with lower tensile strength tend to be preferentially fractured. Fractures propagate perpendicular to the direction of least principle stress until the stress concentration at the fracture tip is reduced or the fracture reaches resistant units.

Fig. 17.5 Mechanical integrity concepts. Fractures (black) terminate at mechanical interfaces, such shale (or clay) beds and other lithological contacts, which may be the location of horizontal fractures. Mechanical interfaces bound mechanical units (layers)
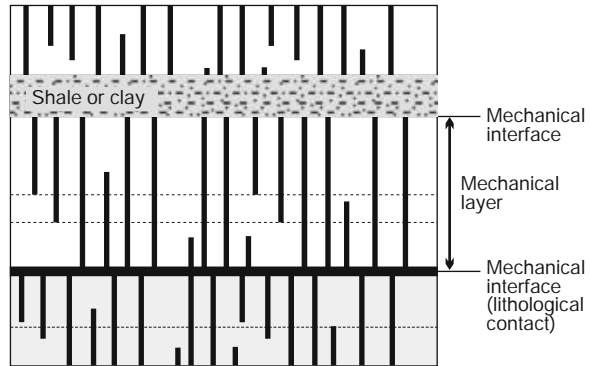
Fractures tend to terminate at ductile layers, such as shales and clays, and weak horizons that open and/or slide to prevent fracture propagation. Fractures tend to be propagated across strongly bounded horizons. Mechanical interfaces may correspond to cycle boundaries, which results in a sedimentological control over fracturing. Ductile layers, such as shales that do not fracture, can result in isolated fractured zones and highly compartmentalized flow within an aquifer (Cooke et al. 2006).

Runkel et al. (2006) documented that bedding plane fractures in the Cambrian Sandstone Aquifer System of Minnesota (USA) tended to cluster at specific stratigraphic positions that can be mapped on a regional scale. This stratigraphic correlation of fracturing has clear hydrologic importance as the bedding plane fractures are preferential flow zones. Fracturing was also observed to decrease with depth, so hydraulic properties measured in deep wells cannot be confidently extrapolated to shallow depths (and vice versa).

Mechanical stratigraphy requires outcrop data to determine the distribution and stratigraphic relationships of fractures and is thus not practical for deeply buried aquifers in which only limited borehole data are available. Nevertheless, the basic mechanical stratigraphy principles still have value for borehole-based investigations in that some general inferences on the likely distribution and extent of fractures can be made based on encountered rock types (e.g., high tensile strength versus ductile strata). For example, Underwood et al. (2003) derived the following equation relating vertical fracture density and bed thickness for Silurian dolomite in northeastern Wisconsin:

$$D = 0.8 + 0.29T \tag{17.5}$$

where D = fracture density (fractures per meter) and T = mechanical unit thickness (m). Such an empirical relationship was proposed to be useful for predicting fracture density at depth, if mechanical unit thickness could be estimated from well data (Underwood et al. 2003).

17.5   Investigation of Fractured Rock Aquifers

Characterization of fractured aquifers typically involves a multiple-element approach that includes techniques to

- identify and physically characterize fractures (e.g., caliper and imaging logs)
- determine whether or not identified fractures are hydraulically active (e.g., flowmeter logs, packer tests and tracers tests)
- quantify the hydraulic properties of fractures or fractured zones (packer and pumping tests).

Characterization of fractured sedimentary rock aquifers requires the employment of techniques with different scales or volumes of investigation. Based on the recognition that different classes of hydraulic, geological, and geophysical data are associated with different scales of investigation, Paillet et al. (1993) identified three main scales of investigation for fractured rock aquifers:

(1) Small scale—Identification of individual secondary permeability elements and their distribution. Small-scale analyses include conventional geophysical logs and recovered samples (e.g., cores).
(2) Intermediate scale—Evaluation of how secondary permeability elements are connected. Intermediate-scale analyses include straddle-packer tests (pumping, injection, and slug tests) and flowmeter logging.
(3) Large scale—Evaluation of how secondary permeability elements might be organized into large-scale flow paths and how the organization is related to known stratigraphy and structural geology. Large-scale analyses include aquifer pumping tests and remote-sensing (e.g., lineament analysis)

A limitation of fractured rock investigations is the difficulty of representative sampling of large elements of secondary permeability, which may have a disproportionately large impact on groundwater flow, from a limited number of wells. Permeability and dispersivity in fractured rock generally vary with support scale without an apparent upper limit (Neuman 2005), so fine-scale measurements would not expected to be representative of the aquifer as a whole.

Cook (2003) provided the practical recommendation that the approaches used for characterizing fractured rock aquifers should focus on measurement of the aquifer properties that are most closely related to the properties of interest. To which should be added, the scale of interest of the project. For projects in which groundwater flow rate is of primary interest, then it is preferable to measure groundwater flow directly rather than to try to infer it from indirect measurements, such as point velocity and hydraulic conductivity measurements. Similarly, investigations of groundwater flow on a site or regional scale should involve methods having a large volume of investigation.

A key issue in characterizing fractured rock aquifers is differentiating hydraulically active fractures from the total population of observed or detected fractures. Hydraulically active fractures have significantly greater transmissivity

than the adjoining matrix and are connected to other fractures. Hydraulically active fractures are thus preferential flow features. Hydraulically inactive fractures, as the term implies, do not materially contribute to groundwater flow. They may, for example, have small lengths and are not interconnected with other fractures.

Active fractures may have features that are indicative of groundwater flow, such as weathering, dissolution, mineralization, and coatings (e.g., Nativ et al. 2003). However, the above criteria are not infallible. Comparison of core observations and packer test results in Eocene chalks indicate that many fractures that have characteristics indicative of hydraulic activity are no longer active. Fractures can have characteristics that are indicative of historic groundwater flow, which terminated at some point in the past (Nativ et al. 2003). Hydraulically active fractures are typically identified by evidence of groundwater flow under ambient or stressed hydraulic conditions.

17.5.1   Cores

Cores provide a means for directly observing fractures. However, core analysis has several limitations. Most significant is that coring is expensive and provides only a small-diameter, one-dimensional profile. Intensely fractured zones that are hydraulically most important may not be recovered or may be covered as rubble zones. The coring process itself can induce fracturing. Natural fracturing may be detected by staining, alteration, or mineral precipitation on fracture surfaces. Evaluation of core of fractured rock was reviewed by Kulander et al. (1990).

An important limitation of borehole and core-based techniques is that there is a low probability of intercepting vertical and near vertical fractures. Inclined boreholes are the preferred method for intercepting vertical fractures. Wells ideally should be drilled normal to the prevailing orientation of the local fracture system. Fracture orientations and spacing measured in inclined wells or cores need to be corrected for the angle of the well or core. Drilling of non-vertical boreholes dedicated to fracture analysis may not be economically viable for most projects, particularly if the boreholes are not to be put to other uses (e.g., production or observation wells).

17.5.2   Borehole Geophysical Logging

Borehole geophysical logging is a fundamental tool for identification of fractures in the subsurface and differentiating between hydraulically active and inactive fractures. A limitation of geophysical logging is that individual fractures may be below the resolution of some logs. Fracture volumes are usually only a small fraction of the volume of investigation of the logs. Borehole geophysical logging techniques can be used to identify and characterize fractures in several manners:

- observation of the fractures (imaging logs)
- detection of associated changes in borehole diameter
- detection of changes in petrophysical rock properties
- detection of flow into or out of the well at fractures.

Borehole imaging logs (e.g., video/television survey, optical televiewer, acoustic televiewer, microresistivity imaging; Sect. 10.9) allow for the accurate location of the depths and orientation of fractures, and, in some cases, their properties (e.g., aperture height, presence of skins). Measured aperture height values depend upon tool resolution and can be impacted by wellbore effects (e.g., drilling damage).

Individual fractures or fractured horizons may be detected in conventional borehole geophysical by the following changes in petrophysical properties

- caliper log—increases (sharp spikes) in borehole diameter
- gamma ray log—increases in natural radioactivity from fracture skin minerals
- resistivity and spontaneous potential log—changes in resistivity related to waters in fractures
- sonic porosity—fractured strata may be characterized by increased transit times.

There is much interest in the oil and gas industry on the identification and characterization of fractures, because many reservoir produce mainly from fractures. Lehne (1990) compared borehole geophysical logging techniques for the detection of fractures in a North Sea chalk oil reservoir (Tommeliten Gamma Field). Fractures were detected using dipmeter, microresistivity imaging (Formation MicroScanner) and acoustic (full waveform) recording logs. The circumferential acoustic log (CALog) detects fractures by a decrease in the amplitude of circumferential Rayleigh waves and in the Echolog by the reflection of Stoneley waves. Of all the logs, the Formation MicroScanner gave the best identification of fractures although interpretation of the signal was often difficult in high-porosity zones.

A significant limitation of the use of petrophysical properties from conventional logs to identify fractures is that rock volume is much greater than the volume of the void spaces in fractures (National Research Council 1996). Log readings are an average value and the contribution of fractures may not be detectable. For borehole imaging logs, drilling effects can artificially enlarge fractures at the borehole wall. Aperture height may also vary along the width and length of fractures (Morin et al. 1997).

Conventional borehole geophysics logs (and their measured formation properties) that are used to identify hydraulically active fractures include

- flowmeter logs—flow into (or out of) the borehole at fracture depth
- fluid conductivity—changes in water salinity related to flow into the borehole at fractures
- fluid temperature—changes in water temperature related to flow into the borehole at fractures

Conventional static and dynamic flowmeter logs are an effective means of determining whether or not a fracture or set of fractures is hydraulically active and determining the transmissivity of fractures, especially where there is a pronounced difference in hydraulic conductivity between the fractures and matrix. Cross-well flowmeter logging can also be effective in detected hydraulically active fractures. Cross-well flowmeter logging basically involves the pumping of one well or interval in a well (isolated using packers) and performing flowmeter logs on other boreholes (Podgorney and Ritzi 1997). High-sensitivity (e.g., heat flow) flowmeters performed before and after the start of pumping can measure pumping-induced changes in flow across fractures and fractured intervals.

The Stonely wave sonic log (Sect. 15.1.1) can be used to locate hydraulically active fractures (e.g., Hardin et al. 1987). In theory, the Stoneley wave response could potentially provide quantitative data on the hydraulic properties of fractures. However, in current practice, it is typically used as a supplemental tool for qualitative identification of hydraulically active fractures.

Spontaneous potential (SP) logging has also been demonstrated to be a useful tool for identifying hydraulically active fractures in some formations. The flow of water through a porous medium generates an electrical field and associated spontaneous potential, which is referred to as the electrokinetic or streaming potential. Measured SP signal also reflect changes in mineralogy and water chemistry (redox state). Hydraulically active fractures may thus be identified by SP log deflections. Suski et al. (2008) demonstrated that SP signals in fractured sedimentary rock in the Swiss Alps show a good correlation with caliper, water temperature and fluid conductivity logs, which made it possible to use the SP signal to distinguish between hydraulically active and inactive fractures.

Conventional logs will not detect all fractures. Typically several logs are needed to confirm presence of fractures and to determine whether or not they are hydraulically active. A study of fracturing in the siliciclastic Passaic Formation of New Jersey (USA) provides a good generic approach for evaluation of the hydrogeology of fractured rock (Morin et al. 1997). The field investigation included the following elements

- Gamma ray and formation resistivity logs were used for stratigraphic correlation between wells and for evaluation of bedding orientation (strike and dip).
- Caliper and an imaging log (borehole acoustic televiewer) were used to identify fractures. The borehole televiewer allowed for the measurement of the orientation of fractures.
- High-frequency (3 m interval) heat pulse flowmeter log measurements and fluid temperature and electrical conductivity logs were used to identify permeable fractures amongst the identified factures.
- Flowmeter log data were used to estimate the transmissivity of each tested interval and, in turn, the transmissivity of fractures within each interval.

Gellasch et al. (2013) performed a similar multiple-method investigation of fracture connectivity in Cambrian sandstone aquifers at Madison, Wisconsin (USA). Imaging (optical borehole imager) and caliper logs (acoustic and mechanical) were used to identify fractures. The contribution of fractures to the total transmissivity was evaluated using packer slug tests and a pumping test interpreted using the Moench (1984) method. The transmissivity of fractures was estimated from the transmissivity of the packer test interval, assuming all flow was from the fractures. Wastewater indictors from leakage of the sewer system were found at a depth of 29 m at higher concentrations than in shallower monitoring zones. In particular, viable viruses were found at a depth which would require transport to have been much more rapid than would have occurred by flow through the rock using bulk hydraulic conductivity values. The conclusion of the study was the fractures were important for both the horizontal and vertical transport of sewer-derived water.

17.5.3   Surface Geophysical Methods

Surface geophysical methods are relatively low-resolution techniques, which, in some circumstances, can be used to detect fracture zones, where the fracturing and hydrochemical conditions create a sufficient contrast with unfractured strata. Water-filled fractures have a greater electrical conductivity than intact rock. The effect of fracturing is greater where the surrounding rock has a low porosity (National Research Council 1996). Directional soundings, performed by rotating a resistivity array around a center point can provide data on electrical resistivity (and in turn fracture) orientation as a function of azimuth (National Research Council 1996).

Seismic reflection and refraction can be used to differentiate between fractured and unfractured strata. Gburek et al. (1999) investigated fracturing in low porosity and permeability siliciclastic rocks in east-central Pennsylvania. Core, packer test, and seismic refraction survey data indicate that the geology of the study area can be divided into an upper fractured zone and lower poorly fractured zone, which is the regional aquifer. The former can be further subdivided into three layers, from the top down, soil and overburden, high fractured rock, and moderately fractured rock. Over 9,100 m of seismic refraction transects were run. Seismic velocity was found to be inversely proportional to the degree of fracturing, which is directly related to hydraulic conductivity. The studied watershed was modeled using a continuum approach, because of a high fracture density, using MODFLOW. Hydraulic conductivity was estimated from a steady-state model calibration and specific yield from a transient calibration. The modeling results demonstrated that the relatively high-transmissivity shallow zone has a strong influence on the pattern of groundwater flow.

The cost of surface resistivity techniques should be weighed against probability of obtaining useful data and the value of that data. Surface geophysical methods are specialized application for characterizing fractured aquifers and have limited applicability. Its greatest potential lays a supplemental tool in characterizing shallow aquifers with intense fracturing.

17.5.4 Hydraulic Testing

Aquifer test data represent the composite hydraulic response of families of fractures and solution conduits each having different hydraulic characteristics (Streltsova 1988). Typically large solution openings are connected to a smaller diffuse set of fractures. Initially water is produced from large solution conduits or fractures, which as pressure drops, are recharged from smaller conduits, fractures and the matrix. In the case of single fractures, early data are linear on log–log plots, the slope of which is related to fracture permeability (Gringarten 1982; Streltsova 1988; Gernand and Heidtman 1997). Low slopes (0.25) would be attributed to a relatively low permeability fracture, with higher values (0.5) attributed to a high-permeability fracture (Gringarten 1982). In observation wells, distant from the fracture, the entire time-drawdown data (excluding later leakage and boundary effects) may reflect radial flow (i.e., plot on the Theis curve).

The hydraulic properties of individual fractures, or fractured intervals, can be evaluated using pumping (or injection) tests and slug tests performed on either an interval of the borehole isolated with packers or the entire borehole. Both constant-rate and constant-head pumping tests are used for fracture analysis. Straddle-packer pumping tests are particularly useful for characterizing fractured aquifers because individual fractures or fractured zones may be isolated. Packer testing procedures are discussed in Sect. 8.6. Borehole geophysical log data are first used to identify fractures or fractured zones to be tested and to determine locations with suitable borehole conditions to set packers. Packer tests include conventional water-well techniques, pressure-pulse tests, and oil and gas industry-type drill-stem tests.

Injection and pumping rates should not be so large as to cause pressure changes that effect hydraulic properties. Hydraulic fracturing or opening of existing fractures occurs at high pressures. Large reductions in pressure could result in degassing with gas bubbles blocking fractures (National Research Council 1996).

There are two end-member approaches to interpreting the time-drawdown data from straddle-packer tests, the continuum approach and the discrete fracture approach. The continuum approach is based on the assumption that the hydraulic conductivity of the fractures is much greater than that of the matrix and that the test data reflect the hydraulic characteristics of the tested fracture or fractures. The discrete fracture methods (e.g., Barker and Black 1983; Dougherty and Babu 1984), requires information of the number of fractures in the tested zone, their geometry, hydraulic aperture, nature of fluid interchange between the matrix and fractures, and

specific storage, which are often not known (Barker and Black 1983; Shapiro and Hsieh 1998; Nativ et al. 2003). The continuum approach provides an equivalent hydraulic conductivity for the fractures (Nativ et al. 2003), which is usually sufficiently accurate for applied hydrogeological investigations. If the hydraulic properties of the rock matrix are known from either core analyses or tests performed on unfractured intervals, then the properties of fractures can be approximately determined from the interval average values. In the extreme case where the matrix is essentially impermeable, the interval transmissivity can be attributed entirely to fractures.

Common methods used to analyze pumping tests may not be appropriate for fractured rock because conditions may be far from the underlying assumptions of methods. The heterogeneity in hydraulic conductivity means that transmissivity values obtained from local pumping tests may not be applicable to regional flow rates estimated based on Darcy′s law. Pumping tests in fractured rock aquifers (and other dual-porosity systems) are discussed in Sect. 7.3.10. Early test data reflect water produced from fractures and should be used to evaluate the properties of fractures. Theoretical analysis by Barker and Black (1983) and Black (1985) indicates that application of standard analytical methods (i.e., Cooper and Jacob 1946) to fissured aquifers will overestimate transmissivity but by a factor unlikely to exceed three and usually less than two. Orders of magnitude larger errors may occur with estimates of specific storage. The use of conventional continuum methods that assume homogenous conditions to fissured rock is a misapplication of the techniques (Black 1985), but will continue to be used because they provide useful estimates of transmissivity. Hence, as is often the case in applied hydrogeology, imperfect methods may still provide useful data, but it is critical to consider the nature and potential magnitude of errors when using the data.

Slug tests can be performed either on the entire open-hole or screen, or a straddle-packer interval. Slug-test data are interpreted using standard methods (e.g., Bouwer and Rice and Hvorslev). Shapiro and Hsieh (1998) compared transmissivity values obtained from slug tests of 8 m to 160 m borehole intervals versus values summed from straddle-packer fluid-injection tests over the same intervals. The slug-test data were evaluated using a homogenous porous medium model (Cooper et al. 1967). The two datasets agreed within an order of magnitude (Shapiro and Hsieh 1998).

17.5.5   Tracer Testing

General tracer testing methods are reviewed in Chap. 13. Tracer tests are used to evaluate fracture connectivity in the subsurface, transport properties (kinematic porosity and dispersivity), and chemical reaction parameters (absorption distribution coefficients). Both natural- and forced-gradient tracer tests are applied to investigations of fractured rock aquifers. The basic challenge with natural-gradient tests in fractured rock is that there may not be a flow path between an injection well

and an observation well. Many observation wells may be required. Forced-gradient (or induced-gradient) tests may be the preferred option as pumping draws water from one well to another, but the fracture or fracture network still needs to connect the wells.

Qualitative force-gradient tests are used to determine whether a fracture or fracture network connects two wells. Tests can be performed using the entire completion interval of a well (i.e., entire open-hole or screened interval) or an individual fracture (or fracture horizon) that is isolated using packers. For example, a tracer solution may be injected into a fractured zone isolated with packers and monitored for in one or more observation wells, which may or may not be pumped. There is a wide variety of different tracer test configurations that can be selected from to address specific hydrogeological information requirements.

Several variations of tracer-dilution techniques (Sect. 13.5) have been developed to detect and quantify the flow from individual fracture or fracture networks. Tracer-dilution tests are used to provide qualitative information on whether or not a fracture is hydraulically active and quantitative information on the hydraulic properties of fractures. Brainerd and Robbins (2004) proposed a tracer-dilution method to quantify the flow contribution from fractures and their transmissivity. Tracer is injected into the bottom of the well at a constant rate (Q_{in}) and pumped out at the well top (Q_{out}) at a greater rate ($Q_{out} > Q_{in}$). Once steady-state flow conditions are achieved, the net flow into the well (Q_{diff}) from all fractures is calculated as follows:

$$Q_{diff} = Q_{out} - Q_{in} \tag{17:6}$$

Flow rates are adjusted so that the flow from all intersecting fractures is into the well.

The testing procedure consists of collecting at least three profiles of discrete water samples with depth at different well pumping rates. Dilution of tracer concentrations between successively shallower samples reflects the inflow of water into the well from an intervening fracture (Q_f). The transmissivity of each fracture is calculated from the tracer-dilution across the fractures using the Thiem equation. The hydraulic head of fractures is graphically estimated by extrapolating a plot of the steady-state elevation head (H_e) in a well and fracture inflow (Q_f; calculated from tracer-dilution) to the Q_f equals 0 intercept. This corresponds to the head in the well that balances the head in the fracture and thus no inflow occurs into the well.

Brainerd and Robbins (2004) suggested that tracer-dilution method may serve to compliment or supplement more conventional methods. A limitation of the method is the need to pump significant quantities of water, which can be an important consideration in contaminated aquifers in which there is significant cost for water disposal. The method also assumes that the fractures are hydraulically isolated from one another and that short-circuiting does not occur. It also assumes negligible matrix flow in the tested fractured intervals.

Tsang et al. (1990) presented a method for determination of fracture inflow parameters, which involved an inverse-tracer test. The basic methodology is to fill a borehole with deionized water and then performing a series of fluid electrical

conductivity logs while the well is pumped at a slow rate. The presence of hydraulically active fractures is indicated by the inflow of the more conductive formation waters into the well. The Tsang et al. (1990) method can be qualitatively used as a screening tool to identify hydraulically active fractures prior to hydraulic testing and water sampling. Tsang et al. (1990) also provided a quantitative interpretation method to calculate flow rates from fractures and, in turn, transmissivity values. The Tsang et al. (1990) method requires a significant conductivity difference between the water introduced into the borehole and the formation water, hence it may not be possible in aquifers containing very low-conductivity freshwater. Care must also be taken to minimize disturbance of the borehole during logging.

The 'hydrophysical' logging method is based on measuring locally induced changes in the electrical conductivity in the fluid column of a borehole (Pedler et al. 1992). The basic procedure involves performing a time series of electrical conductivity logs while deionized water is simultaneously injected at the bottom of the borehole and the well is pumped at a low flow rate. Active fractures are identified by a local increase in conductivity due to the greater salinity of the produced water relative to the deionized or diluted water in the borehole. The conductivity probe assembly can be combined with a discrete-point downhole fluid sampler (Pedler et al. 1992).

Love et al. (2007) presented a well-dilution method for estimating groundwater flow rates in fractures. The process involves creating a contrast in electrical conductivity (EC) within the well, which, in the case of the test well in the Claire Valley of South Australia, was achieved by circulating the EC-stratified water within the well. A series of EC profiles were measured until the initial, premix profile returned. Horizontal flow rate was calculated from the time required for EC to return to its premix concentration. Love et al. (2007) took advantage of existing EC variations in the well, but the test could have been performed by adding external water with a different EC than ambient values.

Hydraulically active fractures or fracture zones may also be identified using fluorescent tracers. Flynn et al. (2005) documented a method for measuring tracer concentrations in wells completed with long screens or open holes using a downhole fluorometer suspended with a programmable, motor-driven pulley system. Tracer monitoring could be performed to detect flow zones either by singe-well tracer-dilution tests or by the detection of tracer injected in another well. The fluorometer system was demonstrated to be capable of detecting fluorescent tracer in a water column with an accuracy of plus or minus 20 cm. It was proposed that by modifying the system to allow for tracer injection at a fixed separation in the well, the apparatus may be used to determine the direction and magnitude of vertical flow gradients.

Dissolved oxygen (DO) has also been used for tracer-dilution testing of fractured intervals (Chlebica and Robbins 2013). The DO concentration in boreholes is increased by either circulating water that is aerated at land surface or by using a bubbler in the well. A series of DO-versus-depth profiles are obtained by lowering a DO probe. Inflow of native groundwater that is anoxic, or has a low DO concentration, is evident by a local rapid decrease in DO concentration. The tests can be

performed either under static conditions or with flow into or out of the well induced using a slug. Use of DO as a tracer requires an initial DO concentrations contrast with native groundwater and that the rate of flow into the well is greater than the rate of biotic and abiotic processes that consume DO (Chlebica and Robbins 2013). DO has the advantages as a tracer of being non-toxic, inexpensive, and readily measurable in situ using a probe.

The practicality of tracer testing as a cost-effective applied tool for characterizing fractured aquifers depends upon the tested aquifer conditions, project time, and budgetary constraints. Water supply and disposal are important considerations, particularly for contaminated aquifers. High-resolution flowmeter logging can provide the same information as tracer-dilution methods and has the advantage that it directly measures flow. As with case of aquifer characterization methods in general, costs and benefits (i.e., information provided) need to be considered to determine the most cost-effective program that meets the data requirements of a project given budgetary constraints.

17.5.6   Water Head Data

Water elevation (head) data from wells in fractured rock terrains can be diagnostic of fracture connectedness and the relationship between fractures and the rock matrix. Differences in head between fractures in a given well (as measured by packer testing or multilevel sampling systems) or between closely spaced wells is evidence that fractures are not well connected. Water elevation changes in response to rainfall events, pumping, or other stresses may be pronounced in fracture-dominated flow systems where the matrix has a very low porosity and permeability.

17.5.7   Outcrop Investigations

Field investigations of exposed aquifer strata can provide information on the distribution and orientation of fractures. A series of measurements on the orientation (strike and dip) of fractures may reveal one or more preferred orientations, which could result in aquifer anisotropy. Field observations may also provide information on fracture density (e.g., number per meter or average spacing). Field investigations also form the basis for mechanical stratigraphy (Sect. 17.4).

There are several constraints on outcrop investigations. Most basic is that aquifer strata very often are not exposed in local study areas, with the most common exception being shallow surficial aquifers. The stress field responsible for the fracturing evident in strata at land surface may not be representative of the stress field in aquifers at depths. In general, the degree of fracturing decreases with depth. Natural and anthropogenic process responsible for rock outcrops (e.g., blasting)

may cause fracturing that is not present (or present to a lesser extent) in undisturbed areas away from the exposures. Fracture features evident at land surface, particularly aperture height, may also be greater than those present in situ at depth due to dilation and weathering (dissolution and mineral alteration). Nevertheless, it is sound practice to always take advantage of opportunities to examine aquifer and confining strata in the field where possible. Examination of outcrops can provide valuable insights into the two- or three-dimensional distribution of facies and the scale and type or aquifer heterogeneity, in addition to fracture type and distribution.

17.5.8   Lineament and Fracture Trace Analysis

Where fracturing is due to regional tectonic stresses, a resulting preferred orientation of fractures can impart aquifer anisotropy. Fractured zones may be directly observable at formation exposures at land surface or may be manifested as linear features observable using remote-sensing techniques. Examination of outcrops of aquifer strata can provide valuable insights on the type, distribution, and orientation of fractures, with the caveat that stress conditions at land surface, and thus the resulting fracture pattern, may be different from those at depth. Lineament analysis is a widely used tool for groundwater exploration in metamorphic and igneous terrains because the greatest amount of water tends to be found near fractures, which may constitute the only available porosity and permeability. Lineament analysis is discussed in Sect. 15.4.1. Weathering or erosion may be concentrated along fracture zones, which are evident on aerial photographs and satellite images as lineaments (Carruthers et al. 1991). Lineaments, if they represent fracture traces, may also mark the direction of hydraulic conductivity tensors that have an influence on regional groundwater flow (e.g., Zeeb et al. 2010).

Lineament analyses often reveal a large number of lineaments whose hydrogeological significance is uncertain. For example, a lineament analysis of South Florida, an essentially flat-lying humid region with negligible outcrops of the underlying sediment rocks, yielded numerous lineaments of varying orientations (Fig. 17.6). However, it is an unresolved question as to whether any of the mapped features are of hydrologic significance.

The hydrogeological significance of lineaments needs to be confirmed by other means. Brittle deformation zones may be identified or confirmed using geophysical signatures (Rhén et al. 2007), such as

- Magnetic lineaments. Oxidation of magnetite around fractures may reduce their magnetic susceptibility. Low magnetic linear features may thus be a sign of a flow zone.
- Electrical conductivity (resistivity) anomalies. The increased water content or clay minerals that form in fractures may be manifested by anomalies in electrical conductivity. The host nonporous crystalline rock is usually highly resistive.
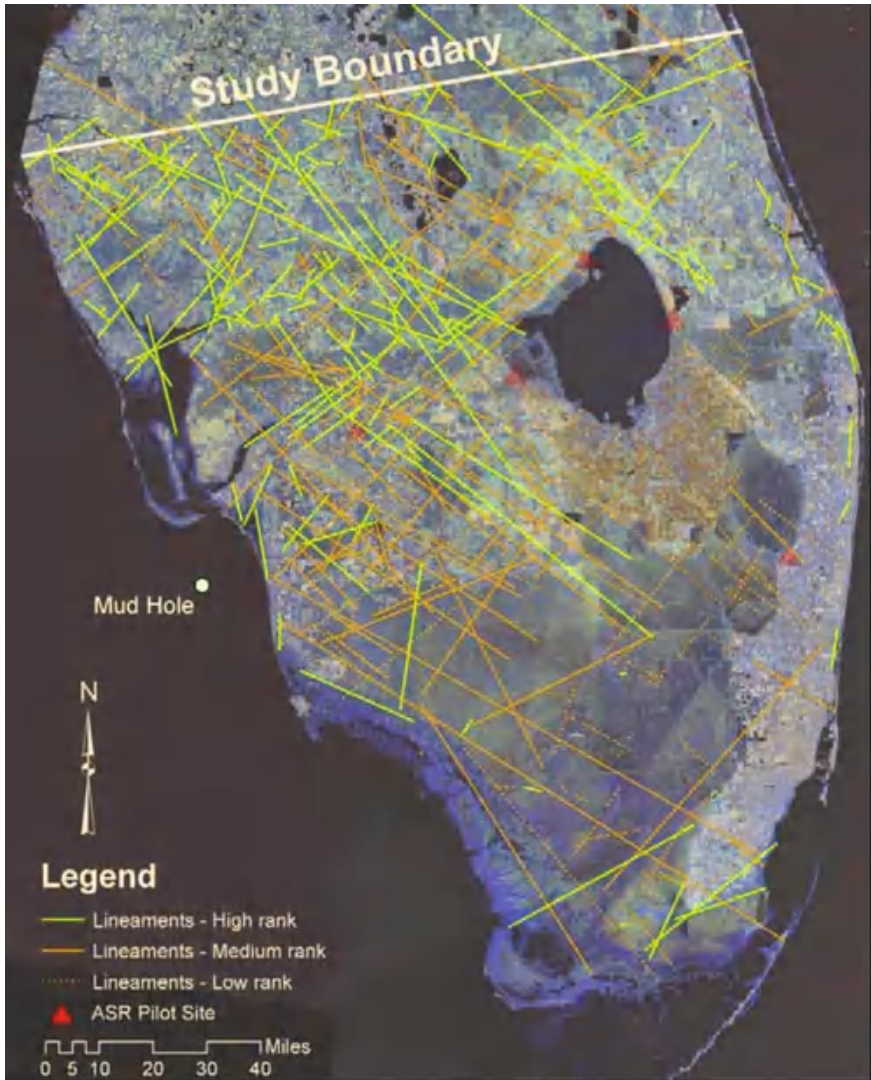
Fig. 17.6 Map showing lineaments identified in south Florida on a Landsat mosaic (Fies 2004)

- Reduced seismic velocities and diffracted or scattered patterns on seismic reflection profiles. Fracturing results in greater porosities, slower seismic velocities, and wave scattering.

Lineament analysis has its greatest value where aquifer transmissivity is likely impacted by faults or large-scale fracture zones whose presence might be evident at land surface. Its greatest application is on shallow fractured-bedrock aquifers.

17.6 Fractured Rock Modeling

Both fractured rock and karstic aquifers have two (or more) porosity (media) domains with different properties. The secondary (macropore) porosity typically has the greatest hydraulic conductivity and thus dominates groundwater flow. The matrix has a lesser hydraulic conductivity but often greater storage volume. Solute transport between the secondary pores and matrix is typically mainly due to diffusion driven by concentration gradients. Modeling of solute transport in dual-porosity aquifers thus requires simulation of the simultaneous advection through the secondary porosity and solute exchange between the secondary pores and matrix. Flow within the matrix may also be significant and may need to be considered in simulations.

Key questions for modeling fractured rock system are (National Research Council 1996)

- Does the conceptual model provide an adequate characterization of the flow system?
- Is the database adequate to estimate parameters in the numerical model with sufficient precision to produce reliable predictions for the intended applications?

It is useful to start a discussion of characterization of fractured rock by considering how fractures may be incorporated into numerical groundwater models. There are three main approaches to the modeling of fractured rock systems, (1) single-continuum or equivalent porous media approach (2) dual-continuum approach, and (3) discrete fracture network approach (Long et al. 1982; National Research Council 1996; Cook 2003; Muldoon and Bradbury 2005; Neuman 2005). In the selection of a modeling approach, it is important to consider the geology (fracture abundance, distribution, and connectivity) of the strata of interest, the scale of interest, data availability, and the purpose to which the model is being developed (National Research Council 1996). Fracture systems may be highly interconnected on a large scale, but dominated by a relatively few large fractures when viewed on a smaller scale.

As is the case for groundwater modeling in general, the modeling process should start with the development of a conceptual model. Conceptual models should consider (National Research Council 1996)

- identification of the most important features in the fracture system
- identification of the location (distribution and orientation) of the most important fractures in the rock mass
- determination of whether or not, and to what extent, the identified structures conduct water

Not all features are equally important and connectivity is a critical issue. Fracturing has its greatest impact on groundwater flow and solute transport when the fractures are well connected and form preferred fluid flow pathways. Understanding of the genesis of fractures and how it relates to geological history of

the strata under investigation can provide insights into the hydrological properties of the rock mass (National Research Council 1996).

Continuum approaches in a deterministic framework have been the most common practice for modeling fractured rock (National Research Council 1996). The single-continuum (or equivalent continuum or equivalent porous medium) approach does not considered individual fractures (and other flow conduits) and treats the aquifer as a homogenous porous medium in which bulk hydraulic and transport parameters are adequate to characterize water flow and solute transport. Primary and secondary porosity and hydraulic conductivity distribution are replaced by an equivalent porous medium having equivalent hydraulic properties. The key parameters for modeling groundwater flow are transmissivity and storativity. For solute transport, key additional variables are effective porosity and the three dispersivities (longitudinal, lateral, and transverse). The effects of a preferred orientation of fractures can be introduced by assigning anisotropy to transmissivity values.

The single-continuum approach may be satisfactory for groundwater flow modeling, but may not be appropriate for modeling solute transport. The main challenges associated with the equivalent continuum approach are defining equivalent effective porosity and dispersive properties (Cook 2003). The values of hydraulic and solute transport parameters can be obtained from aquifer hydraulic and tracer testing, but the scale-dependency of variables still remains as an issue (National Research Council 1996).

The dual-continuum (or dual-porosity) approach considers two overlapping continuum: the fracture network and the rock matrix. There are several variations of the dual-continuum approach. The simplest approach is to treat the rock matrix as a non-conducting storage reservoir (immobile domain) and the fractures as a conducting medium with negligible storage capacity (mobile domain). Solute and fluid transport between the fractures and matrix is linearly proportional to the concentration or pressure difference (Neuman 2005). In more complex models, both the matrix and fractures conduct fluids and solute. Models may also account for solute diffusion through matrix blocks and effects of skins that retard fluid flow between fractures and matrix blocks. Solute exchange between the two porosity (mobile and immobile) domains is controlled in models using an empirical mass transport coefficient, whose value is estimated and subsequently adjusted (if needed) during the calibration process.

The discrete fracture network (DFN) approach involves characterization of properties of discrete fractures and their incorporation into models The DFN modeling approach is based on the assumption that fluid flow behavior can be predicted from knowledge of fracture geometry and data on the transmissivity of individual fractures (National Research Council 1996). The goal behind most real-world DFN applications has been to capture the intricacies of flow and transport in discrete fractures in a way that is consistent with available site data (Neuman 2005). Clearly, the DFN approach is much more data-intensive than both the single- and dual-continuum approaches, particularly where fractures are abundant. Spatial statistics associated with a fracture network (including transmissivity) can be measured with considerable effort, and these statistics can be used to generate

realizations of fracture networks with the same properties (National Research Council 1996). Unless the location(s) of specific major fracture(s) or fault(s) are known and can be mapped, either an arbitrary or stochastically generated fracture network is used.

Neuman (2005) opined that site-specific hydrogeological models for flow and transport in fractured rock are more robust when based directly on measurable flow and transport properties, rather than on properties derived from fracture geometric models. It is thus advisable to focus of bulk properties rather that the properties of individual fractures or matrix blocks. Neuman (2005) also noted that it may be possible to incorporate a limited number of site-specific features, such as major fracture zones and faults, explicitly into a hydrogeological model, but is it not necessary or advisable to do the same for a large number of small-scale features. It is thus critical to have an accurate conceptual understanding of the aquifer system of interest.

Two basic issues arise when selecting modeling approaches for fractured rock aquifers (and also karst aquifers; Chap. 18). First is whether or not there is sufficient data on fracture abundance, size, location and properties to attempt either a dual-continuum or DFN approach (or the practical opportunity to collect additional data). Second, is whether or not an equivalent porous medium properties can be defined for the modeled system. Long et al. (1982) noted that the characterization of fractures is complete if each fracture is described in terms of effective or hydraulic aperture, orientation, location, and size. Clearly, any attempt to fully characterize a fractured aquifer is destined to be far from successful. It may not be possible to rigorously define equivalent homogenous properties for inherently heterogeneous systems. A fractured rock behaves as an equivalent porous medium when (Long et al. 1982)

- insignificant change in the value of the equivalent permeability occurs with a small addition or subtraction to the test volume
- an equivalent permeability tensor exists, which provides the correct flux when the direction of a constant gradient changes

For a continuum approach, a representative elementary volume (REV; Bear 1972) must be defined, which can be considered to be a volume of a formation at which the average permeability (or value of other parameter) does not significantly change with the addition of subtraction of a small volume of rock. Size of REVs is large compared to fracture length in order to provide a good statistical sample of fracture population. Fractured rock approaches an equivalent porous medium when (Long et al. 1982)

- fracture density is increased
- apertures are constant rather than distributed
- fracture orientation are distributed rather than constant
- larger samples sizes are tested
- there is a high density of fractures and non-uniform orientation distribution

Where a fractured aquifer does not meet the above criteria, which could be the case where groundwater flow is dominated by a one or more large fractures or a fracture network with a preferred orientation, then additional aquifer testing may be required to adequately characterize the fractures to allow them to be incorporated into a model as discrete features. Accurate data on the values of hydraulic and solute transport properties of fractures are typically not practicably obtainable, and estimated values are used or adjusted through inverse-modeling in the DFN approach as part of the model calibration process.

Several studies compared the different approaches for modeling fractured sedimentary rock. Blessent et al. (2014) performed a modeling investigation that simulated the vertical transport of the pesticide Mecoprop in fractured clayey till near Havdrup, Denmark, using the single-continuum, dual-porosity (continuum) and discrete fracture network approaches. All three types of models could be equally well calibrated to reproduce observed contaminant concentrations. However, several orders of magnitude differences in concentration can result when the boundary conditions are changed. A model calibrated to one set of conditions may not adequately predict contaminant (solute) concentration distributions resulting from spatial to temporal boundary conditions that are different from those used for calibration. Discrete fracture network codes were concluded to provide better representation of governing mass transport processes and have a greater robustness for a wider range of boundary conditions (Blessent et al. 2014).

Muldoon and Bradbury (2005) compared the continuum and discrete fracture approaches for simulating solute transport in fractured Silurian dolostones in southeastern Wisconsin. Hydraulic conductivity values determined using the continuum approach analysis of open-hole pumping tests data predicted the lower end of the measured tracer velocity data. Hydraulic conductivity values obtained using the discrete fracture approach from short-interval packer test data are more appropriate for prediction of the faster tracer velocities. Hydraulic conductivity values from open-hole pumping tests are average values, which do not predict the rapid groundwater travel times through the fracture network. A key conclusion is that the continuum approach may underestimate contaminant transport rates.

The DFN modeling approach can allow for more accurate models as it allows for the explicit incorporation of features that dominate groundwater flow but suffers from a greater data requirement. In applied practice, the DFN approach might be considered when the single- and dual-continuum approaches are found to give inadequate results. For example, a suspected discrete feature (fracture or fault) might be added to a model in an attempt to obtain a better model calibration to field data (e.g., match to mapped contaminant concentration), with the properties of the feature adjusted during model calibration. If a DFN modeling approach is contemplated, then an aquifer characterization program should focus on obtaining the required hydrogeological data on fracture locations, orientations, and properties, recognizing that complete characterization of fracture systems is not practically possible.

References

Barker, J. A. & Black, J. H. (1983) Slug tests in fissured aquifers. Water Resources Research, 19, 1558–1564.

Bear, J. (1972) Dynamics of fluids in porous media. New York: Elsevier.

Bertels, S. P., DiCarlo, D. A., & Blunt, M. J. (2001) Measurement of aperture distribution, capillary pressure, relative permeability, and in situ saturation in a rock fracture using computed tomography scanning. Water Resources Research, 37(3), 649–662.

Black, J. H. (1985) The interpretation of slug tests in fissured rock. Quarterly Journal of Engineering Geology, 18(2), 161–171.

Blessent, D., Jørgenesen, P. R., & Therrien, R., (2014) Comparing discrete fractures and continuum models to predict contaminant transport in fractured porous media. Groundwater, 52, 84–95.

Brainerd, R. J., & Robbins, G. A. (2004) A tracer dilution method for fracture characterization of bedrock wells. Ground Water, 42, 774–780.

Carruthers, R. M., Greenbaum, D., Peart, R. J., & Herbert, R. (1991) Geophysical investigation of photolineaments in southeast Zimbabwe. Quarterly Journal of Engineering and Hydrogeology, 24, 437–451.

Chlebica, D. W., & Robbins, G. A. (2013) Altering dissolved oxygen to determine flow conditions in fractured bedrock wells. Groundwater Monitoring & Remediation, 33(4), 100–107.

Cook, P. G. (2003) A guide to regional groundwater flow in fractured rock aquifers. Adelaide: CSIRO.

Cooke, M. L., Simo, J. A., Underwood, C. A., & Rijken, P. (2006) Mechanical stratigraphic controls on fracture patterns within carbonates and implications for groundwater flow. Sedimentary Geology, 184, 225–239.

Cooper, H. H., Jr., & Jacob, C. E. (1946) A generalized graphical method for evaluating formation constants and summarizing well-field history. Transactions American Geophysical Union, 27, 526–534.

Cooper, H. H., Jr., Bredehoeft, J. D., & Papadopulos, I. S. (1967) Response of a finite-diameter well to an instantaneous charge of water. Water Resources Research, 3, 263–269.

Dahon, O., Nativ, R., Adar, E. M., Berkowitz, B., & Romen, Z. (1999) Field observation of flow in a fracture intersecting unsaturated chalk. Water Resources Research, 35, 3315–3326.

Dahon, O., Nativ, R., Adar, E. M., Berkowitz, B., & Weisbrod, N. (2000) On fracture structure and preferential flow in unsaturated chalk. Ground Water, 38, 444–451.

Dougherty, D. E., & Babu, D. K. (1984) Flow to a partially penetrating well in a double-porosity reservoir. Water Resources Research, 20, 1116–1122.

Fies, M. W. (2004) Lineament analysis South Florida region. Aquifer storage and recovery regional study. Jacksonville, U.S. Army Corps of Engineers.

Flynn, R. M., Schnegg, P.-A., Costa, R., Mallen, G., & Zwahlen, F. (2005) Identification of zones of preferential groundwater tracer transport using a mobile downhole fluorometer. Hydrogeology Journal, 13, 366–377.

Gburek, W. J., Folmor, G. J., & Urban, J. B. (1999) Field data and ground water modeling in a layered fractured aquifer. Ground Water, 32, 175–185.

Gellasch, C. A., Bradbury, K. R., Hart, D. J., & Bahr, J. M. (2013) Characterization of fracture connectivity in a siliciclastic bedrock aquifer near a public water supply well (Wisconsin, USA). Hydrogeology Journal, 21, 383–399.

Gernand, J. D., & Heidtman, J. P. (1997) Detailed pumping test to characterize a fractured bedrock aquifer. Ground Water, 35, 632–637.

Gringarten, A. C. (1982) Flow-test evaluation of fractured reservoirs. Geological Society of America Paper 189, 237–263.

Gross, M. R., Fischer, M. P., Engelder, T., & Greenfield, R. J. (1995) Factors controlling joint spacing in interbedded sedimentary rocks: interpreting numerical models with field models from the Monterey Formation, USA. In Ameen, M. S., (Ed.) Fractography; fracture

topography as a tool in fracture mechanics and stress analysis. Special Publication 92 (pp. 215–233). Boulder: Geological Society of America.

Guo, W., Coulibaly, K., & Maliva, R. G. (2014) Simulated effects of aquifer heterogeneity on ASR system performance. Environmental Earth Sciences, 73, 7803–7809.

Hardin, E. L., Cheng, C. H., Paillet, F. L., & Mendelson, J. D. (1987). Fracture characterization by means of attenuation and generation of tube waves in fractured crystalline rock at Mirror Lake, New Hampshire. Journal of Geophysical Research: Solid Earth (1978–2012), 92(B8), 7989–8006.

Keller, A. A. (1997). High resolution CAT imaging of fractures in consolidated materials. International Journal of Rock Mechanics and Mining Sciences, 34(3), 155.e1–155.e16.

Kulander, B. R., Dean, S. L. & Ward, B. J., Jr. (1990) Fractured core analysis: interpretation, logging, and use of natural and induced fractures in core. Methods in Exploration Series, No. 8. Tulsa: American Association of Petroleum Geologists.

Lehne, K. A. (1990) Fracture detection from logs of North Sea chalk. In A. Hurst, M. A. Lovell & A. C. Morton (Eds.) Geological applications of wireline logs. Special Publication 48 (pp. 263–271). London: Geological Society.

Long, J. C. S., Remer, J. S., Wilson, C. R., & Witherspoon, P. A. (1982) Porous media equivalents for networks of discontinuous fractures. Water Resources Research, 18, 645–658.

Love, A., Simmons, C. t., Cook, P., Harrington, G. A., Herczeg, A., & Halihan, T. (2007) Estimating groundwater flow rates in fractured metasediments: Claire Valley, South Australia. In J. Krásný & J. M. Sharp, Jr. (Eds.), Groundwater in fractured rocks. Selected papers from the Groundwater in Fractured Rocks International Conference, Prague, 2003 (pp. 364–477). Leiden: Taylor & Francis.

Maliva, R. G., Kennedy, G. P., Martin, W. K., Missimer, T. M., Owosina, E. S., & Dickson, J. A. D. (2002) Dolomitization-induced aquifer heterogeneity: Evidence from the Upper Floridan Aquifer, Southwest Florida. Geological Society America Bulletin, 114, 419–427.

Maliva, R. G., & Walker, C. W. (1998) Hydrogeology of deep-well disposal of liquid wastes in Southwestern Florida, U.S.A. Hydrogeology Journal, 6, 538–548.

Maliva, R. G., & Missimer, T. M. (2010) Aquifer storage and recovery and managed aquifer recharge using wells: Planning, hydrogeology, design, and operation. Houston: Schlumberger Water Services.

McKay, L. D., Cherry, J. A., & Gillham, R. W. (1993) Field experiments in a fractured clay till. 1. Hydraulic conductivity and fracture aperture. Water Resources Research, 29, 1149–1162.

Moench, A. F. (1984) Dual-porosity models for a fissured groundwater reservoir with fracture skin. Water Resources Research, 20, 831–846.

Moore, R. B., Schwarz, G. E., Clark, S. F., Jr., Walsh, G. J., & Degnan, J. R. (2002) Factors related to well yield in the fractured-bedrock aquifer of New Hampshire. U.S. Geological Survey Professional Paper 1660.

Morin, R. H., Carleton, G. B., & Poirer, S. (1997) Fractured-aquifer hydrogeology from geophysical logs: The Passaic Formation, New Jersey. Ground Water, 35, 328–338.

Muldoon, M., & Bradbury, K. R. (2005) Site characterization in densely fractured dolomite: Comparison of methods. Ground Water, 43, 863–876.

National Research Council (1996) Rock fractures and fluid flow. Washington, D.C.: National Academy Press.

Nativ, R., Adar, E., Assaf, L., & Nygaard, E. (2003) Characterization of the hydraulic properties of fractures in chalk. Ground Water, 41, 532–543.

Nelson, R. A., & Serra, S. (1995) Vertical and lateral variations in fracture spacing in folded carbonate sections and its relation to locating horizontal wells. Journal of Canadian Petroleum Technology, 34(6), 51–56.

Neuman, S. P. (2005) Trends, prospects and challenges in quantifying flow and transport through fractured rock. Hydrogeology Journal, 13, 124–147.

Pedler, W., Head, C. L., & Williams, L. L. (1992) Hydrophysical logging: A new wellbore technique for hydrogeologic and contaminant characterization of aquifers. In Proceedings 6th

National Outdoor Action Conference (pp. 701–715). Dublin, Ohio: National Ground Water Association.

Paillet, F. L., Kay, R. T., Yeskis, D., & Pedler, W. (1993) Integrating well logs into a multiple-scale investigation of a fractured sedimentary aquifer. The Log Analyst, 1 24–40.

Podgorney, R. K., & Ritzi, R. W., Jr. (1997) Capture zone geometry in a fractured carbonate aquifer. Ground Water, 35, 1040–1049.

Reese, R. S., & Richardson, E. (2008) Synthesis of the hydrogeologic framework of the Floridan Aquifer System and delineation of a Major Avon Park permeable zone in central and southern Florida. U.S. Geological Survey Scientific Investigations Report 2007–5207.

Rhén, I., Thunehed, H., Triumf, C.-A., Follin, S., Hartley, L., Hermansson, J., & Wahlgren, C.-H. (2007) Development of a hydrogeological model description of intrusive rock at different investigation scales: an example from south-eastern Sweden. Hydrogeology Journal, 15, 47–69.

Runkel, A. C., Tipping, R. G., Alexander, E. C., Jr., & Alexander, S. C. (2006) Hydrostratigraphic characterization of intergranular and secondary porosity in part of the Cambrian sandstone aquifer system of the cratonic interior of North America: Improving predictability of hydrogeologic properties. Sedimentary Geology, 184, 281–304.

Shapiro, A. M., & Hsieh P.A. (1998) How good are estimates of transmissivity from slug tests in fractured rock? Ground Water, 36, 37–48.

Sharp, J. M., Kreisel, I., Milliken, K. L., Mac, R. E., & Robinson, N. I. (1996). Fracture skin properties and effects on solute transport: Geotechnical and environmental implications. In 2nd North American Rock Mechanics Symposium. American Rock Mechanics Association.

Singhal, B. B. S., & Gupta, R. P. (2010) Applied hydrogeology of fractured rocks. Dordrecht: Springer.

Stearns, D. W., & Friedman. M. (1972) Reservoirs in fractured rock: Geologic exploration methods. In R. E. King (Ed.), Stratigraphic oil and gas fields: classification, exploration methods, and case histories. Memoir 16 (pp. 82–106). Tulsa: American Association of Petroleum Geologists.

Streltsova, T. D. (1988) Well testing in heterogeneous formations. New York: John Wiley.

Suski, B., Ladner, F., Baron, L., Vuataz, F.-D., Philippossian, F., & Holliger, K. (2008) Detection and characterization of hydraulically active fractures in a carbonate aquifer: results from self-potential, temperature and fluid electrical conductivity logging in the Combioula hydrothermal system in the southwestern Swiss Alps. Hydrogeology Journal, 16, 1319–1328.

Tsang, C.-F., Hufschied, P., & Hale, F. V. (1990) Determination of fracture inflow parameters with a borehole fluid conductivity method. Water Resources Research, 26, 561–578.

Underwood, C. A., Cooke, M. L., Simo, J. A., & Muldoon, M. A. (2003) Stratigraphic controls on vertical fracture patterns in Silurian dolomite, northeastern Wisconsin. American Association of Petroleum Geologists Bulletin, 87(1), 121–142.

Vrba, J., & Verhagen, B. T. (2006) Groundwater for emergency situations. A framework document. International Hydrological Program (IHP) VI, Series on Groundwater No. 12. Paris: UNESCO.

Witherspoon, P. A., Wang, J. S. Y., Iwai, K., & Gale, J. E. (1980) Validity of cubic law for fluid flow in a deformable rock fracture. Water Resources Research, 16, 1016–1024.

Zeeb, C., Göckus, D., Bons, P., Al Ajmi, H., Rausch, R., & Blum, P. (2010) Fracture flow modelling based on satellite images of the Wajid Sandstone, Saudi Arabia. Hydrogeology Journal, 18, 1699–1712.

Chapter 18
Karst

Karst aquifer systems are characterized by often extreme heterogeneity as flow is dominated by secondary porosity, which includes fractures and solution conduits of multiple scales. Karst aquifers cannot be fully characterized using conventional hydrogeological methods alone, such as potentiometric surface mapping and well pump testing. A basic limitation of borehole-based methods in karst aquifers is that boreholes usually do not intersect flow-dominating conduits. Greater emphasis needs to be placed on identification of subsurface flow paths, hydrologic boundaries, recharge sources, and distribution and properties of flow conduits. Karst systems are studied using techniques that have large volumes of investigation, such as tracer tests, rainfall-runoff relationships (e.g., spring hydrograph analysis), water balance analysis, and input and output chemical data analyses, in addition to general (non-karstic) aquifer characterization techniques.

18.1 Introduction

The term 'karst' has been variously defined in the literature. Karst specifically refers to a type of geomorphology. Karst also refers to a type or style of hydrogeological systems. As Vacher and Mylroie (2002) noted, the term 'karst' includes the plumbing as well as the landscape. The U.S. Geological Survey (n.d.) defined karst as

> a terrain with distinctive landforms and hydrology created from the dissolution of soluble rocks, principally limestone and dolomite. Karst terrain is characterized by springs, caves, sinkholes, and a unique hydrogeology that results in aquifers that are highly productive but extremely vulnerable to contamination.

Virtually all carbonate rock exposed at land surface experiences some dissolution and associated secondary porosity development because rainwater is undersaturated with respected to calcite. In karst aquifers, dissolutional secondary porosity dominates groundwater flow.

The term 'paleokarst' refers to karst systems that are hydrologically decoupled from the contemporary hydrological system (Ford and Williams 1989). Paleokarst systems may still be hydrologically important as high-transmissivity flow zones. The similar term 'relict karst' is defined as karst systems that still exist within the contemporary system, but are removed from the situation in which they were developed (Ford and Williams 1989). For example, a major lowering of base level may result in some conduit systems no longer being active.

The hydrogeology of karst systems was reviewed by Mull et al. (1988), White (1988), Ford and Williams (1989) and Goldscheider and Drew (2007). Karst hydrogeology is typified by a network of interconnected fissures, fractures, and conduits emplaced in a relatively low-permeability rock matrix. The hydraulic conductivity contrast between conduits and adjoining matrix could be as high as 5–7 orders of magnitude (Teutsch and Sauter 1991). Most of the groundwater flow and transport occurs through the network of conduits, while most of the groundwater storage occurs in the matrix. The key hydrogeological characteristics of karst systems are a very high degree of aquifer heterogeneity and anisotropy, a strong scale-effect of aquifer heterogeneity, and rapid and variable flow velocities (Goldscheider et al. 2007). Failure to recognize the potential for very rapid groundwater flow velocities can result in rapid transport of contaminants to water supply wells, which was the case in the May 2010 'Walkerton Tragedy' in Ontario, Canada. Previously undocumented karst conditions allowed pathogenic bacteria to rapidly reach a public water supply well, resulting in contamination of the potable supply that caused 2,300 people to become ill and seven fatalities (Goldscheider et al. 2007).

The extreme heterogeneity of karst systems creates great challenges for aquifer characterization. Groundwater flow is independent of topography, hence surface water catchments or drainage basins do not necessarily correspond to groundwater basins. Karst aquifers cannot be fully characterized using conventional hydrogeological methods alone, such as potentiometric surface mapping and well pump testing. Greater emphasis needs to be placed on identification of subsurface flow paths, hydrologic boundaries, recharge sources, and distribution and properties of flow conduits (White 1993; Taylor and Greene 2008). Quantitative hydrologic data obtained from selected points in the systems tend to be representative of the immediate surroundings and can rarely be extrapolated to the average function of the system as a whole (Padilla et al. 1994). Karst systems thus tend to be studied using techniques that have large volumes of investigation, such as tracer studies and analyses of spring hydrograph data.

18.2 Karst Hydrogeology Basics

The hydrogeology of karst systems is complex and is an important discipline unto itself. Hence any chapter on the characterization of karst systems will necessarily be cursory. The objective of this chapter is to provide a general introduction on the

hydrogeology of karst systems and methods used for their characterization. Karst systems are characterized by three main vertical zones, three main porosity types, and three main flow types.

18.2.1   Karst Zones

The karst landscapes are divided into (Goldscheider and Andreo 2007) the exokarst, epikarst, and endokarst zones and output (Fig. 18.1). The exokarst zone consists of features found at land surface either directly or indirectly related to dissolution. Small-scale dissolution features, which are referred to as karren, include a wide variety of structures such as flutes, ridges, runnels, and clints and grikes. Exposed limestones on Caribbean Islands are often sculpted by biological dissolution to form sharp fluted and pitted surfaces, which is called 'phytokarst' (Fig. 18.2a). Clints are limestone slabs that are separated by grikes, which are deep fissures formed by solution widening of fractures (Fig. 8.2b). Type examples of limestone pavements made up of clints and grikes occur in the Burren of western Ireland and the Yorkshire Dales of northern England. Large-scale exokarst features are solution depressions of various sizes.

The epikarst zone (also referred to as the subcutaneous zone) occurs immediately below the soil-bedrock interface. It is part of the vadose zone and consists of weathered limestone that is characterized by well-developed dissolution features and high permeabilities. Epikarst is defined as (Jones et al. 2004; Jones 2013)

> the heterogeneous interface between unconsolidated material, including soil, regolith, sediment and vegetative debris, and solutionally altered carbonate rock that is partially saturated with water and capable of delaying or storing and locally rerouting vertical infiltration to the deeper regional, phreatic zone of the underlying karst aquifer.
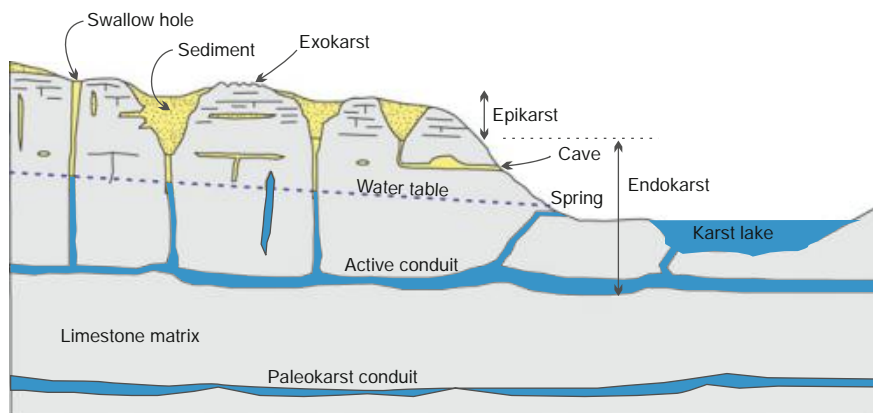
Fig. 18.1 Karst system diagram

Fig. 18.2 Examples of
karren landforms.
a Sharp-edged phytokarst
common along parts of the
coast of Aruba. b Clints
(flat-topped slabs) and grikes
(solution-widened fissures) in
Carboniferous limestones in
the Yorkshire Dales, near
Malham, England (bottom)
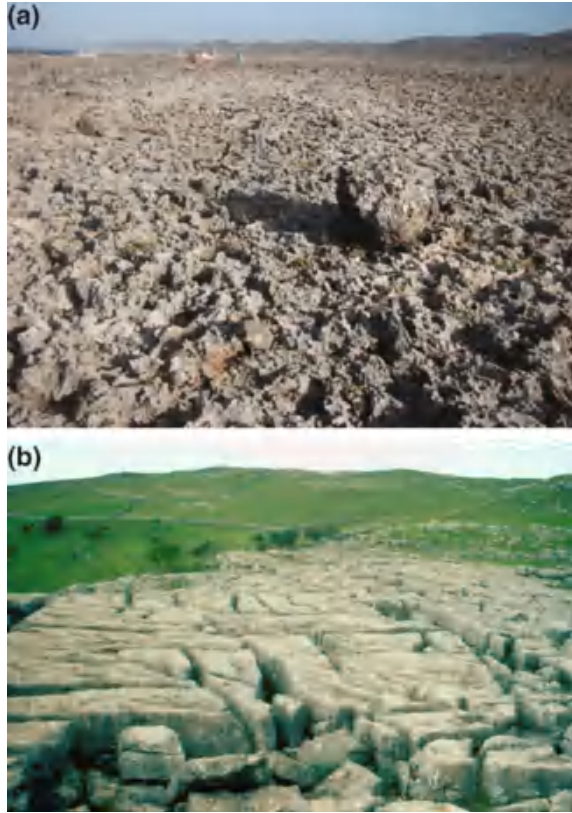
The role of the epikarst zone in karst hydrogeology was reviewed by Williams
(1983), Ford and Williams (1989), Jones et al. (2004), Klimchouk (2004), Williams
(2008), and Jones (2013). A key attribute of the epikarst zone is that it serves a
storage function. The permeability of the epikarst zone is less than that of the
underlying aquifer, which creates a bottleneck for the downward percolation of
water (i.e., water infiltrates into the zone more easily than it percolates out of the
zone). A perched aquifer may form at the base of the epikarst zone after a major
rainfall event or a wet period or season. The epikarst zone detains recharge,
moderates floods, and attenuates discharge, which often results in the year-round
release of water to the underlying endokarst zone.

The endokarst zone constitutes the main part of the karst system and includes
various types of conduits and caves. It includes both the lower vadose zone (per-
colation or transmission zone) and phreatic zone. In contrast to the epikarst zone,
the vadose part of the endokarst zone provides minimal storage. The boundary
between the epikarst and endokarst zones is typically marked by a downward
decrease in porosity. The outputs of karstic groundwater basin are typically con-
centrated into one or several springs, which may form the headwaters of streams of
various sizes (Fig. 18.3) or feed lakes.

Fig. 18.3 Blue Springs, Florida. In addition to its scenic and recreational values, Blue Springs is an important cold-weather sanctuary for the endangered Florida manatee because of its near constant annual water temperature

Paleokarst (Sect. 18.5) features may be identical to endokarst features but are not a significant part of the current shallow groundwater flow system. Paleokarst features may be modified to varying degrees by subsequent compaction and diagenetic processes, such as dissolution and cementation. Paleokarst includes both buried intact remnants of conduit systems and breccias formed by their collapse.

18.2.2   Porosity Types

Three porosity and permeability components occur in karst aquifers: matrix, fractures, and dissolutional voids (Ford and Williams 1989; White 1999, 2002, 2006, 2007; Worthington 1999). Matrix porosity is the intergranular and intercrystalline porosity within the rock itself. Matrix porosity varies greatly depending upon the age, diagenetic, and burial history of the rock. Young limestones may have matrix porosities of 40 % or greater, whereas the matrix porosity of limestones that have been deeply buried or have undergone extensive diagenesis may be only several percent or less.

Karst limestone may have one or more generations of fractures, which may arise from structural geological processes (e.g., tectonism), reductions in stress caused by the removal of overlying rock mass by erosion (unloading), collapse of dissolution features (e.g., caverns), and differential compaction. Conduits are defined as relatively large dissolution voids, although there is not an agreement as to the size threshold for a void to become a conduit. In some usage, conduits may include all voids greater than 10 mm in diameter (White 1999), but another classification scheme places them between the arbitrary limits of 100 mm–10 m (USEPA 2002). The term conduit also implies that a void is elongate and that it now or in the past contained flowing water. The term 'cave' is usually reserved for conduits that are

large enough for human entry. Conduits commonly have non-Darcian behavior due high flow periods due to turbulent flow.

Conduits have low resistance to flow (very high permeabilities) and thus allow water in them to short circuit the matrix or fracture permeability of the aquifer (White 2002). Conduits constitute only a minute fraction of the total volume of an aquifer, but may completely dominate the flow behavior of an aquifer (White 2002). Conduits may constitute less than 1 % of the porosity but more than 95 % of the permeability of karst aquifers (Taylor and Greene 2008).

18.2.3   Karst Aquifer Flow Types

White (1967), in a classic paper, described three end-member types of flow in karst aquifers (Table 18.1). Free flow or mature karst systems are characterized by solution being concentrated to form a well-developed subsurface drainage network. Integrated conduit systems form that may be either perched (near or above base level) or deep (below base level). Groundwater flow tends to be convergent toward major springs. Flow is often rapid, flashy, and in the turbulent regime, particularly under high flow conditions. High flow velocities allow for the transport of sediment.

Diffuse flow is characteristic of immature karst systems and systems in relatively low solubility rock. Caves are rare and, if present, are small, poorly formed, and irregular. Karstic flow conduits are often little more than solution-widened joints and bedding planes. Flow tends to be slow and non-flashy.

Confined flow systems are those in which some sort of geological boundaries (e.g., confining strata), rather than simple hydraulics, are the flow-rate limiting factors. Examples of confined flow systems, provided by White (1967), are artesian systems in which tilted confining strata force water downwards, and aquifers sandwiched between overlying and underlying confining strata. Retarded flow occurs in confined aquifers in which stratigraphic conditions force groundwater flow to be confined to relatively thin beds. Network cave patterns may form in which solution occurs along many available joints. The key feature is that hydrodynamic forces are dampened by external controls.

Table 18.1   Karst aquifer flow types (after White 1967)

Type	Hydrological controls	Associated cave type
Diffuse flow	Gross lithology, less soluble rock	Caves are rare, small, and irregular
Free flow	Thick massive soluble rock	Groundwater flow is localized to form well-integrated cave systems
Confined flow	Structural and stratigraphic control	Two- or three-dimensional cave networks, in which solution is concentrated along many joints

18.2.4   Eogenetic and Telogenetic Karst

The term 'eogenetic karst' is used for systems that were never deeply buried and retain high intergranular porosity (Vacher and Mylroie 2002). Choquette and Pray (1970) applied the term 'eogenetic' to karst in which the rocks are undergoing early burial and meteoric diagenesis (chemical alteration). Examples of eogenetic karst are the Biscayne Aquifer of South Florida (Cunningham et al. 2009), the Floridan Aquifer of central Florida (Lane 1986; Knochenmus and Robinson 1996; Tihansky and Knochenmus 2001), and the surficial Plio-Pleistocene limestones on Caribbean islands and in Yucatan, Mexico (Fig. 18.4).

Telogenetic karst forms in typically older rocks that are, or were, buried and altered, and thus have low intergranular matrix porosity. Examples of telogenetic karst are the caves systems in the Cambro-Ordovician, Devonian, and Carboniferous limestones in the Appalachians and mid-continent of the United States (e.g., Mammoth Cave system; White and White 1989) and western Ireland and northern England (Fig. 18.5).

The large difference in matrix porosity and permeability between eogenetic and telogenetic karsts controls their ability to temporarily store water. In very low-porosity telogenetic karsts, matrix storage is minimal and recharged water flow is predominantly through conduits. The dominance of conduit flow in telogenetic karst results in 'flashiness' in which discharge at springs has a pronounced and often rapid response to rainfall events (White 1988; Ford and Williams 1989; Martin and Dean 2001; Florea and Vacher 2006). If all or part of a conduit system is flooded, rising head at the upstream end of the system will cause or increase discharge at the downstream end as the result of the rapid transmittal of the pressure pulse (Atkinson 1977; White 2007). In eogenetic karst systems in which matrix flow dominates conduit flow, there is a low degree of temporal variation in discharge, particularly in response to rainfall events (Martin and Dean 2001; Florea and Vacher 2006).

Fig. 18.4 Eogenetic karst exposed on Curacao

Fig. 18.5 Telogenetic karst
cave, Mammoth Caves
National Park, Kentucky
(source U.S. National Park
Service)

18.3 Karst Formation

Karst terrains and flow systems form by the dissolution of soluble rock, mainly
carbonate rocks (especially limestone). The development of karst systems requires
two essential conditions:

(1) geochemical conditions that allow for the dissolution of carbonate minerals
(2) flowing groundwater, which requires both a source of water (e.g., precipita-
     tion) and a hydraulic gradient to drive groundwater flow.

Geochemical conditions for carbonate mineral dissolution are widespread as
rainwater is undersaturated with respect to carbonate minerals (calcite, aragonite,
and dolomite). The pH of infiltrating water may decrease (and thus increase its
ability to dissolve carbonate minerals) as the result of the addition of carbon dioxide
from the decomposition of organic matter in the soil zone. Dissolution, and at least
incipient karst development, will occur virtually anywhere limestone is exposed at
land surface and there is some rainfall. The amount of limestone dissolution
depends largely upon the solutional capacity of rainwater (and groundwater flowing
into a given basin), amount of rainfall, degree to which surface water flow (runoff)
is focused, infiltration rate, and time. The dissolution rate depends upon the degree
of undersaturation of the water with respect to carbonate minerals and the kinetics
of the dissolution reaction (Palmer 1991).

Dissolution processes tend to be concentrated at discontinuities, such as frac-
tures, joints, or bedding planes, that tend to focus groundwater flow. The conduit
network pattern reflects the pattern of discontinuities, the magnitude of the
hydraulic gradient, and the orientation of the hydraulic gradient with respect to the
discontinuities (Bakalowicz 2005). Positive feedbacks are an important driver of
karst development (Ford and Williams 1989; Palmer 1991; Worthington 1999). The

focusing of the flow of water undersaturated with respect to calcite by permeability contrasts concentrates dissolution along these features, thus accentuating the permeability contrasts and further concentrating flow. The more transmissive conduits may capture flow from the less transmissive ones, resulting in more dissolution of the conduit walls and an associated further increase in transmissivity.

The permeability contrasts that influence groundwater flow in eogenetic karsts include planar and cross bedding, dissolution vugs (e.g., molds after aragonitic fossils) and burrows (Vacher and Mylroie 2002). Flow and dissolution tend to be focused at fractures in telogenetic karst (Lattman and Parizek 1964; Ford and Williams 1989; Vacher and Mylroie 2002). Dissolution may also be concentrated along lithological interfaces and zones of weakness. Joint and fracture patterns, in turn, are controlled by structural geology (e.g., location of areas of extensional and shear stress), reductions in stress caused by removal of overlying rock mass by erosion, rock hardness (brittleness), and bed thickness (Domenico and Schwartz 1998; Goldscheider and Andreo 2007).

Karst processes develop conduit networks in a hierarchial way comparable to the organization of flow in a surface river system. Smaller tributaries converge into large conduits or caves, which discharge at land surface as a spring (Atkinson 1977; Worthington 1999; Bakalowicz 2005). Mapping of cave systems has documented that they consist of arrays of intersecting passages whose patterns show a great degree of variability. Depending upon the cave type, preexisting geological conditions (e.g., fracture distribution) may impart some regularity to the morphology of cave systems. The conditions or features that control cave morphology are (Palmer 1991)

- distribution of soluble rocks and recharge and discharge points
- mode of groundwater recharge
- geologic structure, distribution of vadose and phreatic zone flow, and geomorphic history.

The development of karst systems is also influenced by changes in base level due to tectonic uplift or eustatic sea level changes. Multistory cave systems can form in response to base level changes (Bakalowicz 2005). Palmer (1991) identified four cave patterns, which are viewed as end members or types

- branchwork caves—dendritic pattern consisting of tributaries that converge into higher order passages.
- network caves—network pattern formed by the widening of an angular grid of intersecting fractures
- anastomotic caves—braided pattern with many closed loops
- spongiform caves—connected caves of varied sized in a seemingly random three-dimensional pattern.

Branchwork caves are by far the most common type and are analogous to surface water river systems in which flow is concentrated to fewer channels and eventually one main channel.

18.4   Hydrogeology of Karst Aquifers

Karst systems should be considered in terms of drainage basins delineated by groundwater divides. Drainage basins are the capture areas of springs or local spring clusters (White 2002). Karst drainage basins may not coincide with surface water drainage basins. Geological variables that distinguish one karst drainage basin from another include (Ford and Williams 1989; White 2007)

- thickness of karstic rock units
- position of karstic rocks with respect to non-karstic rocks and their location within the drainage basin
- bulk lithology (limestone, dolomite, or gypsum)
- detailed lithology and properties (e.g., dense micritic limestone, shaley limestone, porous fossiliferous limestone)
- stratigraphy, including bedding thickness and orientation, lithological variations, and the presence and location of shale or sandstone confining units
- large-scale structure, such as faulting and folding
- small-scale structures including the density and connectivity of vertical joints, bedding plane partings.

A characteristic feature of karst systems is relatively rapid groundwater flow from recharge to discharge areas. The sources of recharge for karstic aquifers include (White 1999)

- allogenic recharge—surface water that enters aquifers at the swallets of sinking streams
- internal runoff—overland storm flow into closed depressions where it enters the aquifer through sinkhole drains
- diffuse infiltration (diffuse autogenic)—precipitation onto the land surface and its subsequent infiltration through soils and epikarst
- recharge from perched catchments.

Most karst recharge is diffuse autogenic, as is the case for many non-karst hydrogeologic settings (Taylor and Greene 2008). Discharge is usually from a small number of large springs. However, some aquifer discharge is through thick alluvium, lakes, and the sea, so that the exact location of springs may be very difficult to detect (Worthington 1999).

Groundwater flow may be quite complex in karst networks and vary depending upon flow rates. Some parts of conduit systems may only receive flow during major flow events, as evident, for example, by dry or normally low-flow cave systems that are explored by cavers. The dominance of conduit flow is responsible for very high flow velocities that occur at times in karst systems. At high flow velocities, groundwater flow becomes turbulent and Darcy's law is no longer valid.

Laminar flow through fractures is expressed by the cubic law, where for a given hydraulic gradient, the flow rate is proportional to the cube of fracture aperture.

$$Q = -\frac{1}{f} wb^3 \left(\frac{qg}{12g}\right) \frac{dh}{dL} \tag{18:1}$$

where

f	friction factor (dimensionless)
Q	flow rate (m^3/s)
w	fracture width (m)
b	aperture of fracture (m)
q	density of water (* 999.7 kg/km^3)
g	gravitational acceleration (9.8 m/s^2)
η	viscosity of water (1.307×10^{-3} Pa · s)
dh/dl	hydraulic gradient (m/m)

The dimensionless factor (f) is added to account for deviations from ideal conditions, such as roughness (Witherspoon et al. 1980):

Conduit flow rate is related to conduit radius through the Hagen–Poisenville equation for laminar flow

$$Q = \frac{pqgr^4}{8g} \frac{dh}{dL} \tag{18:2}$$

and the Darcy–Weisbach equation for turbulent flow in a pipe

$$Q = 2p\left(\frac{g}{f}\right)^{0:5} r^{2:5} \left(\frac{dh}{dL}\right)^{0:5} \tag{18:3}$$

where

r   conduit radius (m)
f   Darcy–Weisbach friction factor (empirical)

As indicated by the cubic law, small increases in fracture apertures have a much greater proportional impact on flow rates. Similarly, small increases in the radii of conduits will also have a disproportionately large impact on groundwater flow rates. Modeling by White and White (2005) demonstrate, as would be expected, that where fractures are common, fracture flow will dominate matrix flow. If the fractures are enlarged by solution, then they will eventually form conduits that completely dominate the flow system. Large, flow-dominating conduits develop where geological conditions focus flow into one or several conduits and fracture enlargement does not continue to occur. Conduit flow systems can be quite complex. For example, Atkinson (1977) documented a situation in a karst system in the Mendip Hills of England in which karst conduits crossed each other without mixing.

Conduit systems act as low-resistance drains that create a flow field in the surrounding matrix and fracture systems toward the conduit (White 1993, 1999).

Large conduits act as drains whose locations are marked by troughs in the water table (White 1999, 2002). The effectiveness of coupling conduits and fractures, combined with matrix and fracture hydraulic conductivity, control the movement of water into and out of conduits (White 1999). Potentiometric surface maps generated from observation well data are often not indicative of hydraulic conditions in the conduit network (Bakalowicz 2005).

The direction of the hydraulic gradient may be reversed during storm events (White 1999). The interaction between allogenic (focused) recharge and diffuse recharge in karst systems also varies with recharge rates. The Santa Fe Sink and Rise System in the Upper Floridan Aquifer of northeastern Florida is a well-studied example of the relationships between allogenic and diffuse recharge and flow between conduits and matrix in a karst system. The sink and rise are about 5 km apart and are connected by approximately 15 km of mapped conduits (Martin and Dean 2001; Langston et al. 2012). A comparison of river flows into and out of the system, hydraulic gradient data, and water quality (specific conductance) data reveals that the direction of flow between conduit and matrix changes depending upon the river flow rate (Martin and Dean 2001; Screaton et al. 2004; Langston et al. 2012). During low-flow periods, there is greater flow out of the rise and the water has a greater specific conductance, which is evidence for the drainage of more mineralized water from the Upper Floridan Aquifer into the conduit system. Diffuse recharge occurs with water flow, and associated limestone dissolution, occurring along the water table and locally downwards into the conduit. On the contrary during high flow periods, water flows from the conduit into the limestone, with dissolution occurring around the conduit. The flow of water into the Upper Floridan Aquifer elevates the water table, broadening the zone of dissolution at the water table directly above the conduit. Mitrofan et al. (2015) similarly used tracer data to document changes in the direction of flow between a karst conduit and adjacent porous rock in the Hercules spring, Carpathian Mountains, Romania.

The direction of groundwater flow between conduits and matrix has important implications for water management as it affects the susceptibility of an aquifer to contamination (Martin and Dean 2001). If surface water flows rapidly through conduit systems and the direction of flow is from the matrix into the conduits, then there is a low potential for contaminants present in the conduits to enter the matrix. Contamination problems may occur rapidly and environmental impacts to water quality in the outflow springs will be high magnitude, but the duration of the contamination will tend to be brief (Screaton et al. 2004). On the contrary, where conduit flow is slow and the water flows from conduits into the adjoining limestone matrix, there is greater susceptibility for contaminants that reach the conduit system to enter the regional groundwater flow system and impact groundwater quality in downstream production wells (Martin and Dean 2001; Screaton et al. 2004). The dominance of conduits in karst groundwater flow results in rapid flows and short residence times.

Another important attribute of karst groundwater systems is a very high degree of macrodispersive mixing. Macrodispersion is mechanical mixing resulting from variations in velocity associated with the large-scale heterogeneities present in

aquifers. The heterogeneities include the tortuosity, branching, and interfingering of pore channels. Extreme heterogeneities in hydraulic conductivity and flow paths are characteristic features of karst systems. In complex conduits systems, conduits divide and rejoin and have different flow paths and travel velocities.

Environmental and legal issues associated with karst areas are reviewed by LaMoreaux et al. (1997). The range of environmental problems associated with karst are diverse. Human, animal, industrial, and municipal wastes may locally disappear underground and then reappear at a great distance from their source. Systems respond rapidly to spill events and are vulnerable to far reaching contamination. However, there may also be a rapid flushing of contaminants from the system (Bakalowicz 2005). Dewatering of karst systems can induce sinkhole formation through the following triggering mechanisms

- loss of buoyant support
- increased hydraulic gradient and thus groundwater velocity
- water-level fluctuations
- induced recharge.

18.5   Paleokarst

Recent karst accessible at land surface has received the most attention. Ancient karst systems (i.e., paleokarst) may form high-transmissivity flow zones that are important for groundwater flow. Paleokarst features include (Maslyn 1977) fossil caves, which may be either open or filled with sediment, and sinkholes that formed by the collapse of the roofs of caverns. The location of the water table influences the development of conduits. The majority of common cave systems have different levels in which the major conduits were created in response to changes in the elevation of springs and the associated water table (Ford 1999). Conversely, the development of conduit systems can change the position (typically lowering) of the water table (Ford 1999). Upper galleries of cave systems may become totally inactive (relict) or may convey water only during large flood events. Paleokarst may also form as the result of regional changes in the water table elevation related to global changes in sea level. For example, relict conduits and caves that formed during Pleistocene sea level low stands are occasionally encountered over 100 m below the water table in central Florida (Fig. 18.6). Deformation associated with paleokarst may occur long after the karst dissolution.

The collapse of caverns can result in a variety of types of deformation. Collapse of the cavern roof may affect all overlying strata resulting in a topographic depression. Caverns may survive the formative karst processes, and collapse at a much later time due to pressure from overlying rock. The effects of cavern collapse may extend 700 m or more above the collapsed cavern but not reach land surface (Maslyn 1977; Loucks 2007). Cavern collapse may be manifested by the sagging and fracturing of the overlying strata or the formation of steep-sided breccia pipes.

Fig. 18.6 Downhole video
photograph of a paleokarst
cavern, City of Sanford,
Florida ASR exploratory well.
Cavern is located
approximately 127 m (418 ft)
below land surface and 116 m
below sea level

Collapse caverns have two main zones, a lower breccia zone consisting of a col-
lapsed roof and walls, and an upper zone of strata that are deformed to varying
degrees by the collapse and compaction of the underlying paleocave-bearing strata
(Loucks 2007).

Ancient caves can be either flow zones or relatively impermeable zones
depending upon whether or not they are open and, if filled, the nature of the fill
material. Karst breccias may also be important flow features if they are not
cemented. Conversely, karst surfaces may be the preferred site for mineralization
and could act as a flow boundary.

Paleokarst zones may thus represent long-term flow regimes close to the water
table and can be used for paleo-hydrology reconstruction (Laskow et al. 2011).
Laskow et al. (2011) used borehole geophysical logs (gamma ray, resistivity,
caliper, and acoustic) to identify fractured zones of suspected paleokarst origin in
the Yarkon-Taninim aquifer of Israel. The karstic nature of some geophysical
horizons was confirmed through borehole videos and reported losses of circulation.
Laskow et al. (2011) related the presence of paleokarst horizons to the proximity of
paleo-canyons (former spring sites), which were in turn related to tectonic uplift and
sea level changes in the Mediterranean Sea.

18.6   Characterization of Karst Aquifers

18.6.1   Characterization Objectives and Methods

The presence of multiple pore systems, especially conduits, adds an extra element
of complexity to the characterization of karst aquifers. It is important to start with
the understanding that at least some local dissolutional enhancement of perme-
ability occurs in virtually all limestones present near land surface. Hence the term

karst aquifer includes a broad spectrum of degrees of permeability modification, from strata in which some dissolutional enlargement of fractures occurred, to aquifers in which groundwater flow is dominated by one or several caves. In the former case, karst aquifers can be characterized and modeled using an equivalent porous medium approach. In the latter case, accurate simulation of karst aquifers often requires that the cave system be simulated as a discrete feature.

The main difficulties associated with simulating karst networks are a determination of (Bakalowicz 2005; Taylor and Greene 2008)

- whether or not conduit or cave networks locally exist
- where networks are located
- what role networks play in the function of the system
- storage capacity of the system
- the extent and overall effects of conduit-dominated flow
- the discrete inputs and outputs (e.g., recharge and discharge points)
- temporal variability in recharge, drainage, and storage.

Karst systems need to be considered in the terms of the length-scale of the flow or transport domain (groundwater basin), the length-scale of flow-dominating heterogeneities (e.g., conduits), and the length or averaging scale of the detection method used (e.g., drawdown cone during a pumping test; Teutsch and Sauter 1991). Detection methods with large averaging volumes will produce parameter fields that appear to be almost homogenous, whereas methods with small averaging volumes will produce highly heterogeneous parameter fields. Methods with small averaging volumes are better able to capture heterogeneity that impacts local groundwater flow and solute transport, provided that there is a sufficiently high density of measurements to intercept or otherwise detect the local heterogeneity elements that control flow.

The characterization of karst aquifers may involve the following tools (Ford and Williams 1989)

- rainfall-runoff relationships—spring hydrograph analysis
- water balance analysis
- input and output chemical data
- tracer testing
- borehole data
- cave exploration
- surface geophysics.

Data collection and analysis of the three flow components (matrix, fracture, and channel) can give an overall understanding of how a carbonate aquifer functions (Worthington 1999). Matrix hydraulic conductivity can be evaluated through core analyses. Hydraulic conductivity values from pumping tests tend to be a measure of the fracture permeability near the wellbore (White 2002). Direct measurement of the permeability of conduit systems is much more difficult, particularly in the common situation where the layout of the conduit system is poorly known or unknown.

Direct mapping of caves and large conduits is generally not practically possible. The speleological approach, which involves direct exploration of caves, mostly describes abandoned conduits (Bakalowicz 2005). The primary speleological data source remains the compass and tape measurements and notebook sketches and photographs of cave explorers (White 2007). Radio location is now commonly used to map the location of cave divers from land surface. The speleological approach is labor intensive and dangerous, and cannot be applied to conduits that may be too small for human exploration, but still have a major impact on local groundwater flow.

Surface geophysical methods are used to locate large-scale karst features, such as caverns and sinkholes that are located close to (usually within 30 m of) land surface (Hoover 2003). Large air- or water-filled cavities may be detected by a difference in resistivity from saturated rock, a lesser mass, and a sharp change in acoustic impedance. Hence, the primary and secondary surface geophysical methods used in karst investigations are gravity, resistivity-based methods (DC-resistivity and frequency-domain electromagnetic induction), ground-penetrating radar (GPR) and seismic reflection surveys (Butler 1984; Hoover 2003; ASTM 2011; Vadillo et al. 2012). Surface geophysical methods, to date, have had their greatest value in geotechnical investigations of karst areas (e.g., assessment of the existence of a sinkhole on a property prior to construction) and in detecting large-scale deformation associated with recent and paleokarst collapse (e.g., Evans et al. 1994; Hardage et al. 1996; Kindinger et al. 2000).

The methods used to evaluate karst aquifers include methods commonly used to evaluate non-karstic aquifers. A basic limitation of borehole data in the characterization of karst aquifers is that boreholes usually do not intersect major conduits. Therefore, it is difficult to directly measure properties using wells. Borehole geophysical methods that are used to locate conduits and to determine whether or not they are hydraulically active are essentially the same methods used to evaluate fractured aquifers (Sect. 17.5.2). Particular care needs to be taken in the interpretation of aquifer pumping test data from karst aquifers, as test conditions may greatly vary from the underlying assumptions of the commonly used analytical methods. Karst aquifers may have extreme heterogeneities and anisotropies in transmissivity. The transmissivity in the principal direction of the conduits system may be orders of magnitude greater than the transmissivity normal to the conduit system.

The time-drawdown data represents the composite hydraulic response of often multiple families of fractures and conduits having different hydraulic characteristics (Streltsova 1988). Kresic (2007) provides an overview of pumping tests in karst aquifers. The tests should have a sufficient duration so as to detect dual-porosity conditions. As is the case for fractured aquifers, time-drawdown curves may have multiple segments that reflect the contributions of different pore systems. For example, the initial test data may reflect water production from conduits or fractures intersected by the well, whereas late time data may reflect water production from the matrix. There is no rigorous, widely accepted method for the interpretation of pumping test data from karst aquifers (Kresic 2007). Nevertheless, hydrogeologist

still use standard methods to interpret pumping test data in karst aquifers and the results of such analyses should be viewed as general estimates whose accuracies are unknown (Bakalowicz 2011). Estimates of aquifer hydraulic properties obtained from analytical solutions may be used as initial estimates for numerical model calibration. Data on the properties of conduit systems can be more directly obtained from tracer tests and spring hydrograph analysis.

18.6.2   Karst Tracer Tests

Tracer tests are a fundamental tool for the analysis of flow in karst terrains. General tracer testing methods are discussed in Chap. 13. Tracer tests are used in karst investigations to (Goldscheider et al. 2008)

- delineate catchment areas
- identify active conduit networks
- determine flow velocity
- resolve conduit networks in more detail
- determine solute (contaminant) transport parameters (dispersivity, retardation, degradation),

Qualitative tracer testing is performed to evaluate whether or not there is a direct connection between a recharge point and discharge point. For example, tracer may be introduced into a swallow hole and monitored for at springs and other suspected discharge locations. Qualitative tracer tests can also provide information on the travel time between two points. Quantitative tracer concentration data are used with simultaneous measurements of discharge to deduce the flow geometry (structure) of the flow system, including input, tributary, distributary and maximum discharges in the system, and the volume of the underground conduits (Atkinson et al. 1973).

The basic data for quantitative tracer tests are breakthrough curves, which are plots of tracer concentration versus time. The form of breakthrough curves depend upon (Smart 1988)

- character of tracer—some tracer may be lost through decay, photodecomposition, sorption, and natural background
- prevailing flow conditions (steady vs. unsteady)
- structure of aquifer
- sampling frequency

Aquifer structural issues that can affect breakthrough curves include

- the presence of dead-zone storage along the flow routes,
- divergence and convergence of flow distribution—recombination of tracer clouds can produce a bimodal breakthrough curve
- dilution with water entering from dye-free tributaries.

Karstic conduits are conceptualized as containing two components; a mobile region and an immobile region in which flow is stagnant relative to the mobile phase (Field and Pinsky 2000; Geyer et al. 2007). The tracer mass may be delayed by eddies and zones of slow flow and may be slowly released with time. The behavior and configuration of the active aquifer can vary dramatically with discharge (Smart 1988). Tracer breakthrough curves may have long tails, which are due to parallel flow paths of different velocities, immobile regions in karst conduits, and diffusion between matrix and conduits (Field and Pinsky 2000; Geyer et al. 2007).

Multitracer tests using both conservative and reactive tracers can provide useful information on reactive transport processes that cannot be obtained from single tracer tests (Geyer et al. 2007). Geyer et al. (2007) present the result of a modeling investigation of a multitracer test performed in a karst system in Germany. The modeling was performed using CXTFIT, a uniaxial two-region nonequilibrium transport model, which assumes that the liquid phase in a conduit can be divided into a mobile and immobile fluid region. The conservative tracer transport model was found to be highly sensitive to average velocity (v) and the fraction of mobile water (θ_m). Calibration of the conservative tracer model provides estimates of v and θ_m, which are necessary for estimation of reactive transport parameters. A key result of the modeling is that the tracer-rock interactions responsible for the retardation of reactive tracers preferably occur in the immobile region, although the immobile fraction may constitute only a small percentage of the total conduit system.

Natural or environmental tracers can be used to provide information on the source of water in karst systems. Major and minor ion concentrations, stable isotope ratios, and the concentrations of natural and anthropogenic organic compounds can be used to determine the contribution of waters from different sources, provided that there are distinct chemical differences between the different potential source waters. The saturation state of groundwater with respect to carbonate minerals has long been used to estimate residence time of water in the subsurface and whether flow is predominantly diffuse or through conduits (Martin and Dean 1999, and references therein). Temperature has also been used as a tracer in karst systems. Delays in the arrival of temperature maxima and minima from sink to rise reflect the residence time of water in the subsurface. Martin and Dean (1999) documented the use of temperature data to evaluate the residence time of water in the Santa Fe River sink/rise system of west-central Florida.

18.6.3   Spring Hydrographs

A karst spring is like a perfectly placed well in other aquifers. Water discharging from a spring carries an imprint of everything upstream in the aquifer (White 2002, p. 97).

Hydrographs are plots of flow rates versus time (Fig. 18.7). Spring hydrographs show the overall response of aquifers to precipitation events. They offer important

Fig. 18.7 Conceptual stream hydrograph illustrating periods of quickflow, mixed flow, and baseflow during recession after a rainfall event (from Taylor and Greene 2008)
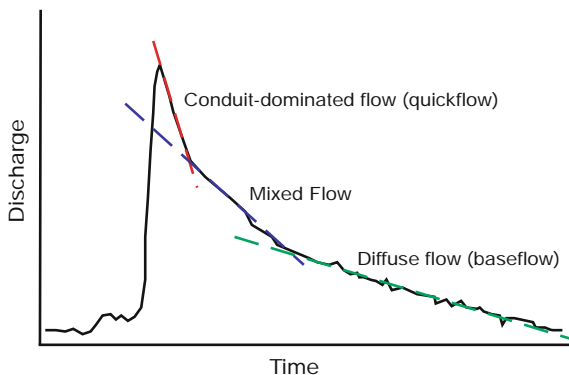
tools for probing the interior workings of karst aquifers (Groves 2007). Spring response to precipitation events depends upon (White 2002):

- the contributions of allogenic recharge and internal runoff
- carrying capacity and internal structure of the conduit system
- area of the groundwater basin

Two basic types of spring flow occur, quickflow and baseflow (Atkinson 1977). Quickflow is the short-term, rapid response to rainfall events. Baseflow is the delayed flow of water mainly out of storage. The form of hydrographs is a function of the geometry and size of the aquifer system and is highly influenced by the contributions to the total flow of quickflow through conduits and baseflow through porous media and small factures.

The mechanics of data collection for hydrographs is reviewed by Grove (2007). The basic requirement is accurate measurement of discharge with as high a temporal resolution as possible. Flow can be measured using methods, such as stage height using rating curves, current meters, weirs and flumes, tracer dilution, and noncontact flow measurement methods (Grove 2007). As discussed by Padilla et al. (1994), the shape of the recession curve of hydrographs can be quantitatively analyzed to determine the contribution of quickflow and baseflow. The quickflow and baseflow periods are separated by a period of mixed flow of varying duration (Fig. 18.8).

As would be expected, quickflow-dominated systems have steep recession curves, reflecting the rapid flow of water through conduit systems. Baseflow-dominated systems have a more gradual recession, due to the moderation of flow by the unsaturated zone and porous-saturated zone. Spring discharge reflects processes that occur within the karst aquifer and groundwater basin, including recharge, storage, discharge, and conduit flows. Numerous papers and book chapters have been published on recession curve analysis including review or method papers by Hall (1968), Bonacci (1993), Arnold et al. (1995), Tallaksen (1995), and Amit et al. (2002). A step-by-step process for recession curve analysis is provided by Kresic (1997). The recession of groundwater discharge over time can be expressed as an exponential equation (Taylor and Greene 2008)
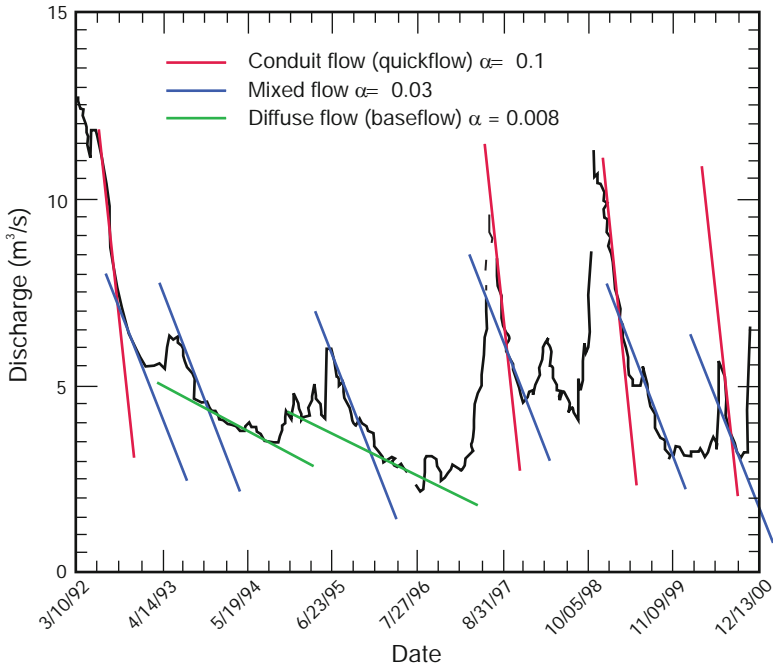
Fig. 18.8 Hydrograph for San Marcos Spring, Texas showing quick flow, mixed flow, and base
flow regimes (from Taylor and Greene 2008)

$$Q_t = Q_0^{a(t-t_o)}$$

where
Q_t discharge at time "t"
Q_0 discharge at time of beginning of recession
t_0 time at beginning of recession (usually 0)
t any time since the beginning of recession for which discharge was calculated
a regression constant (slope) that expresses both the storage and transmissivity
        properties of the aquifer

18.7   Modeling of Karst Systems

One of the most important challenges in modeling karst aquifers is that hydraulic
conductivity is highly scale dependent (White 2007). White (2007, p. 21) cautioned
that

> any attempt to reduce the aquifer to a single value of hydraulic conductivity can best be
> described as nonsense.

The basic modeling approach for karst systems involves

- delineation and characterization of the function and structure of the system from the results of field investigations, which commonly include tracer tests and monitoring data (e.g., precipitation and spring flow)
- development of a conceptual model of the system
- quantitative model development starting with the selection of the modeling approach.

The three main approaches to the modeling of fractured rock systems (Sect. 17.6) are applicable to karst systems, (1) single-continuum (equivalent porous medium) approach, (2) dual-continuum approach, and (3) discrete fracture (conduit) network approach. The limitation of the discrete conduit approach is the usual absence of sufficient data on the location and properties of conduits. It is usually not possible to deterministically map or otherwise predict the layout of conduit systems (White 1999). Hence, a stochastic approach is typically required for the discrete fracture network approach.

Teutsch and Sauter (1991) suggest that the dual-continuum porous equivalent (CDPE) approach is preferred because it does not require the detailed geometrical information needed for the discrete conduit approaches. Clearly data availability practically limits the type of modeling that is possible and technically defendable. The purpose of the modeling should also dictate modeling approach. If the primary goal of model development is to predict solute transport, then aquifer heterogeneity needs to be included in greater detail and accuracy, then would be necessary if the objective is to just predict aquifer heads. A dual-continuum approach may be the best solution to model solute (e.g., contaminant) transport, while an equivalent porous medium approach may be sufficient to simulate aquifer water levels.

Equivalent porous media (EPM) models work best for aquifers in which karst flow paths are dispersed and consist mainly of solution-widened fractures. It is assumed that fractures and small conduits are abundant enough so that the aquifer can be modeled as a single equivalent porous medium using programs, such as MODFLOW (Worthington 1999). The EPM approach is also suitable for large-scale (regional) models of groundwater flow. The equivalent porous media approach works least well for aquifers with well-developed large conduits systems (White 2007) and for modeling local solute transport. The equivalent porous media approach has been successfully used for regional groundwater flow (groundwater elevations) models in many limestones aquifers, such as the Floridan Aquifer System (e.g., Sepulveda 2002; and water planning models developed by the U.S Geological Survey and state water management districts) and the Edwards aquifer of Texas (Scanlon et al. 2003). A hybrid strategy incorporating the single-continuum approach and conduit network approach is to simulate major conduit features as high-transmissivity zones embedded in the mesh of finite-difference and finite-element models (Taylor and Greene 2008). The effects of known or suspected conduit systems are incorporated into equivalent porous medium models by

assigning the cells in the conduit areas high-transmissivity values. This approach requires some information on the location and properties of conduit zones.

Quinn et al. (2006) presented a method for using the drain package of MODFLOW to simulate karst conduits in mixed (diffuse and conduit) flow systems. A series of drains are assigned to adjacent model cells to simulate conduits that connect the upstream end of flow paths to discharge points. The locations of intermediate points are determined from flow paths inferred from surface characteristics (e.g., lineaments) and the results of surface geophysical surveys. Total discharge from the modeled drains is the sum of discharges from each cell. Drain elevations at the downstream terminus were determined from the elevation of associated springs or levels in surficial receiving water. Upstream water elevations were estimated from drilling logs and potentiometric surface maps of shallow groundwater systems. High conductance values (100 m/d) were used to simulate the ready flow of water into the conduits from the matrix.

The MODFLOW Conduit Flow Process (CFP) module (Shoemaker et al. 2008) allows for simulation of turbulent flow as either a discrete network of cylindrical pipes (mode 1), as a high hydraulic layer that can switch between laminar and conduit flow (mode 2), or a combination of both (mode 3). Mode 1 is data intensive requiring information on the location and properties of conduits. Other modeling codes (e.g., FeFlow®) also allow for modeling of discrete elements. In the absence of adequate field data on the geometry and properties of conduit networks, stochastic methods have been developed to simulate karst conduit networks (e.g., Jaquet et al. 2004; Borgi et al. 2012; Pardo-Igúzquiza et al. 2012). The objective is to generate three-dimensional karst networks connecting inlets and outlets that are statistically similar to observed (studied) karst conduit networks. The models may be conditioned with field data and modified by inverse modeling. On a large scale, a model-generated network that is statistically similar to the actual network could produce acceptably accurate predictions. However, large local errors may occur where groundwater flow and transport depend upon the proximity and properties of actual conduits. Stochastic methods are not a substitute for detailed aquifer characterization as there is still a large data requirement for model conditioning.

References

Amit, H., Lyakhovsky, V., Katz, A., Starinsky, A., & Burg, A. (2002) Interpretation of spring recession curves. Ground Water, 40, 543–551.

Arnold, J. G., Allen, P. M., Muttiah, R., & Bernhardt, G. (1995) Automated base flow separation and recession analysis techniques. Ground Water, 33, 1010–1018.

ASTM (2011) Standard guide for selecting surface geophysical methods (D6429–99(2011)e1). West Conshohocken: ASTM International.

Atkinson, T. C., Smith, D. I., Lavis, J. L, & Whitaker, R. J. (1973) Experiments in tracing underground waters in limestone. Journal of Hydrology, 10, 323–349.

Atkinson, T. C. (1977) Diffuse flow and conduit flow in limestone terrain in the Meddip Hills, Sommerset (Great Britain). Journal of Hydrology, 35, 93–110.

Bakalowicz, M. (2005) Karst groundwater: a challenge for new resources. Hydrogeology Journal, 13, 148–160.

Bakalowicz, M. (2011) Karst management. In P. E. Van Beynern (Ed.) Karst management (pp. 263–282). Dordrecht: Spinger.

Bonacci, O. (1993) Karst springs hydrographs as indicators of karst aquifers. Hydrological Sciences Journal, 38, 51–62.

Borghi, A., Renard, P., & Jenni, S. (2012). A pseudo-genetic stochastic model to generate karstic networks. Journal of hydrology, 414, 516–529.

Butler, D. K. (1984). Microgravimetric and gravity gradient techniques for detection of subsurface cavities. Geophysics, 49(7), 1084–1096.

Choquette, P. W., & Pray, L. C. (1970) Geologic nonemclature and classification of porosity in sedimentary carbonates. American Association of Petroleum Geologists Bulletin, 54, 207–250.

Cunningham, K. J., Sukop, M. C., Huang, H., Alvarez, P. F., Curran, H. A., Renken, R. A., & Dixon, J. F. (2009). Prominence of ichnologically influenced macroporosity in the karst Biscayne aquifer: Stratiform "super-K" zones. Geological Society of America Bulletin, 121, 164–180.

Domenico, P. A., & Schwartz, F. W. (1998) Physical and chemical hydrogeology (2nd Ed.). New York: John Wiley & Sons.

Evans, M. W., Snyder, S. W., & Hine, A. C. (1994). High-resolution seismic expression of karst evolution within the upper Floridan Aquifer system: Crooked Lake, Polk County, Florida. Journal of Sedimentary Research, 64(2), 232–244.

Field, M. S., & Pinsky, P. F. (2000) A two-region non-equilibrium model for solute transport in solution conduits in karstic aquifers. Journal of Contaminant Hydrology, 44, 329–351.

Florea, L. J., & Vacher, H. L. (2006) Springflow hydrographs: Eogenetic vs. telogenetic karst: Ground Water, 44, 352–361.

Ford, D. C., & Williams, P. W. (1989) Karst geomorphology and hydrology. London: Chapman and Lewis.

Ford, D. C. (1999) Perspectives in karst hydrogeology and cave genesis. In A. N. Palmer, M. W. Palmer & I. D. Sasowsky (Eds.), Karst Modeling (Special Publication No. 5, pp. 17–29). Charlestown, West Virginia: The Karst Water Institute.

Geyer, T., Birk, S., Licha, T., Liedl, R., & Sauter, M. (2007) Multitracer test approach for characterize reactive transport in karst aquifers. Ground Water, 45, 36–45.

Goldscheider, N., Drew, D., & Worthington, S. (2007) Introduction. In N. Goldscheider & D. Drew (Eds.), Methods in karst hydrogeology. IAH International Contributions to Hydrogeology 26 (pp. 1–8). Leiden: Taylor and Francis.

Goldscheider, N., Meiman, J., Pronk, M., & Smart, C. (2008) Tracer tests in karst hydrogeology and speleology. International Journal of Speleology, 37(1), 27–40.

Goldscheider, N., & Drew, D., (Eds,) (2007) Methods in karst hydrogeology. IAH International Contributions to Hydrogeology 26. Leiden: Taylor and Francis.

Goldscheider, N., & Andreo, B. (2007) The geological and geomorphological framework. In N. Goldscheider & D. Drew (Eds.), Methods in karst hydrogeology. IAH International Contributions to Hydrogeology 26 (pp. 9–23). Leiden: Taylor and Francis.

Groves, C. (2007) Hyrological models. In N. Goldscheider & D. Drew (Eds.), Methods in karst hydrogeology. IAH: International Contributions to Hydrogeology 26 (pp. 48–64). Leiden: Taylor and Francis.

Hall, F. R. (1968) Base-Flow Recessions—A Review. Water Resources Research, 4(5), 973–983.

Hardage, B. A., Carr, D. L., Lancaster, D. E., Simmons Jr, J. L., Elphick, R. Y., Pendleton, V. M., & Johns, R. A. (1996). 3-D seismic evidence of the effects of carbonate karst collapse on overlying clastic stratigraphy and reservoir compartmentalization. Geophysics, 61, 1336–1350.

Hoover, R. A. (2003, December). Geophysical Choices for Karst and Mine Investigations. In 3rd International Conference on Applied Geophysics (pp. 529–38).

Jaquet, O., Siegel, P., Klubertanz, G., & Benabderrhamane, H. (2004). Stochastic discrete model of karstic networks. Advances in Water Resources, 27(7), 751–760.

Jones, W., Culver, D., & Herman, J., (Eds.) (2004) Epikarst. Charles Town, West Virginia: Karst Waters Institute Special Publication 9.

Jones, W. K. (2013) Physical structure of the epikarst. Acta Carsologica, 42, 311–314.

Kindinger, J. L., Davis, J. B., & Flocks, J. G. (2000) Subsurface characterization of selected water bodies in the St. Johns River Water Management District, Northeast Florida: US Geological Survey Open-File Report 00-180.

Klimchouk, A. (2004) Towards defining, delimiting and classifying epikarst: Its origin, processes and variants of geomorphic evolution. Speleogenesis and Evolution of Karst Aquifers, 2(1), 1–13.

Knochenmus, L. A., & Robinson, J. L. (1996) Descriptions of anisotropy and heterogeneity and their effects on groundwater flow and areas of contribution to public supply wells in a karst carbonate aquifer system. U.S. Geological Survey Water-Supply Paper 2475.

Kresic, N. (1997) Quantitative solutions in hydrogeology and groundwater modeling. Boca Raton: CRC Lewis.

Kresic, N., 2007, Hydraulic methods, In N. Goldscheider & D. Drew (Eds.), Methods in karst hydrogeology. IAH International Contributions to Hydrogeology 26 (pp. 65–95). Leiden: Taylor and Francis.

LaMoreaux, P. E., Powell, W. J., & LeGrand, H. E. (1997) Environmental and legal aspects of karst areas. Environmental Geology, 27(1/2), 23–35.

Lane, E. (1986) Karst in Florida. Florida Geological Survey Special Publication 29.

Langston, A. L., Screaton, E. J., Martin, J. B., & Bailly-Comte, V. (2012) Interaction of diffuse and focus allogenic recharge in an eogenetic karst aquifer (Florida, USA). Hydrogeology Journal, 20, 707–781.

Laskow, M., Gendler, M., Goldberg, I., Gvirtzman, H., & Frumkin, A. (2011) Deep confined karst detection and paleo-hydrology reconstruction at a basin-wide scale using new geophysical interpretation of borehole logs. Journal of Hydrology, 406, 158–169.

Lattman, H. L., & Parizek, R. R. (1964) Relationship between fracture traces and the occurrence of ground water in carbonate rocks. Journal of Hydrology, 2, 73–96.

Loucks, R. G. (2007) A review of coalesced, collapses-paleocave systems and associated suprastratal deformation. Acta Carsologica, 36(1), 121–132.

Martin, J. B., & Dean, R.W. (1999) Temperature as a natural tracer of short residence tomes for groundwater in karst aquifers. In A. N. Palmer, M. V. Palmer & I. D. Sasowsky (Eds.), Karst modeling (Special Publication No. 5. pp. 236–242). Charles Town, West Virginia: The Karst Waters Institute.

Martin, J. B., & Dean, R.W. (2001) Exchange of water between conduits and matrix in the Floridan aquifer. Chemical Geology, 179: 145–165.

Maslyn, R. M. (1977) Recognition of fossil karst features in the ancient record: A discussion of several common fossil karst forms. In H. K. Veal (Ed.) Southern and Central Rockies exploration frontiers: Rocky Mountains Associations of Geologists Guidebook (pp. 311–319).

Mitrofan, H., Marin, C., & Povară, I. (2015). Possible conduit-matrix water exchange signatures outlined at a karst spring. Groundwater, 53(S1), 113–122.

Mull, D. S., Liebermann, T. D., Smoot, J. L., Woosley, L. H., Jr., & Mikulak, R. J. (1988) Application of dye-tracing techniques for determining solute-transport characteristics of ground water in karst terranes. Atlanta: U.S. Environmental Protection Agency, Ground-Water Protection Branch, Region IV.

Padilla, A., Pulido-Bosch, A., & Mangin, A. (1994) Relative importance of baseflow and quickflow for hydrographs for karst springs. Ground Water, 32, 267–277.

Palmer, A. N. (1991) Origin and morphology of limestone caves. Geological Society of America Bulletin, 103, 1–21.

Pardo-Igúzquiza, E., Dowd, P. A., Xu, C., & Durán-Valsero, J. J. (2012). Stochastic simulation of karst conduit networks. Advances in Water Resources, 35, 141–150.

Quinn, J. J., Tomasko, P., & Kuiper, J. A. (2006) Modeling complex flow in a karst aquifer. Sedimentary Geology, 184, 343–351.

Scanlon, B. R., Mace, R. E., Barrett, M. E., & Smith, B. (2003) Can we simulate regional groundwater flow using equivalent porous media models? Case Study, Barton Springs, Edwards aquifer, USA. Journal of Hydrology, 276, 137–158.

Screaton, E., Martin, J. B., Ginn, B., & Smith, L. (2004) Conduit properties and karstification in the unconfined Floridan Aquifer: Ground Water, 42, 338–346.

Shoemaker, W. B., Kuniansky, E. L., Birk, S., Bauer, S., & Swain, E.D. (2008) Documentation of a Conduit Flow Process (CFP) for MODFLOW-2005. U.S. Geological Survey Techniques and Methods, Book 6, Chapter A24.

Smart, C. C. (1988) Artificial tracer technique for the determination of the structure of conduit aquifers. Ground Water, 26, 445–453.

Sepulveda, N. (2002). Simulation of ground-water flow in the intermediate and Floridan aquifer systems in peninsular Florida. U.S. Geological Survey Water-Resources Investigations Report 02-4009.

Streltsova, T. D. (1988) Well testing in heterogeneous formations. New York: John Wiley and Sons.

Tallaksen, L. M. (1995). A review of baseflow recession analysis. Journal of hydrology, 165(1), 349–370.

Taylor, C. J., & Greene, E. A. (2008) Hydrogeologic characterization and methods used in the investigation of karst hydrology. In D. O. Rosenberry & J. W. LaBaugh (Eds.), Field techniques for estimating water fluxes between surface water and ground water (pp. 75–114). U.S. Geological Survey Techniques and Methods 4-D2.

Teutsch, G., & Sauter, M. (1991) Groundwater modeling in karst terranes: Scale effects, data acquisition and field validation. In Proceedings Third Conference on Hydrogeology, Ecology, Monitoring, and Management of Ground Water in Karst Terranes (pp. 17–35). Dublin, Ohio: National Ground Water Association.

Tihansky, A. B., & Knochenmus, L. A. (2001). Karst features and hydrogeology in west-central Florida—a field perspective. In Kuniansky, E. L. (Ed.), U.S. Geological Survey Karst Interest Group proceedings. U.S. Geological Survey Water-Resources Investigations Report 01-4011 (pp. 198–211).

USEPA, 2002, A lexicon of cave and karst terminology with special reference to environmental karst hydrology. Washington, D.C: Office of Research and Development, U.S. Environmental Protection Agency (EPA/600/R-02/003).

U.S. Geological Survey (n.d.) What is Karst? http://water.usgs.gov/ogw/karst/pages/whatiskarst (accessed July 19, 2012).

Vacher, H. L., & Mylroie, J. E. (2002) Eogenetic karst from the perspective of an equivalent porous medium. Carbonates and Evaporites, 17(2): 182–196.

Vadillo, I., Benavente, J., Neukum, C., Grützner, C., Carrasco, F., Azzam, R., & Reicherter, K. (2012). Surface geophysics and borehole inspection as an aid to characterizing karst voids and vadose ventilation patterns (Nerja research site, S. Spain). Journal of Applied Geophysics, 82, 153–162.

White, W. B. (1967) Conceptual models for carbonate aquifers. Ground Water, 7(3), 15–21.

White, W. B. (1988) Geomorphology and hydrology of karst terrains. New York: Oxford University Press.

White, W.B. (1993) Analysis of karst aquifers. In W. M. Alley (Ed.), Regional ground-water quality (pp. 471–489). New York: Van Nostrand.

White, W. B. (1999) Conceptual models for karstic aquifers. In A. N. Palmer, M. V. Palmer & I. D. Sasowsky (Eds.), Karst modeling. Special Publication No. 5 (pp. 11–16). Charles Town, West Virginia: The Karst Waters Institute.

White, W. B. (2002) Karst hydrology: Recent developments and open questions. Engineering Geology, 65, 85–105.

White, W. B. (2006) Fifty years of karst hydrology: 1953–2003. In R. S. Harmon & C. M. Wicks (Eds.), Perspectives on karst geomorphology, hydrology, and geochemistry. Special Paper No. 404 (pp. 139-152). Boulder: Geological Society of America.

White, W.B., 2007, A brief history of karst hydrogeology: Contribution of the NSS: Journal of Cave and Karst Studies: 69(1): 13–26.

White, W. B., and White, E. L., (eds.) (1989) Karst hydrology: Concepts from the Mammoth Cave area. New York: Van Nostrand Reinhold.

White, W. B., & White, E. L. (2005) Ground water flux distribution between matrix, factures, and conduits: constraints of modeling. Speleogenesis and Evolution of Karst Aquifers, 3(2), 1–6.

Williams, P. W. (1983) The role of the subcutaneous zone in karst hydrology. Journal of Hydrology, 61, 45–67.

Williams, P. W. (2008) The role of the epikarst in karst and cave hydrogeology: a review. International Journal of Speleology, 37(1), 1–10.

Witherspoon, P. A., Wang, J. S. Y., Iwai, K.,& Gale, J. E. (1980) Validity of cubic law for fluid flow in a deformable rock fracture. Water Resources Research, 16, 1016–1024.

Worthington, S. R. H. (1999) A comprehensive strategy for understanding flow in carbonate aquifer. In A. N. Palmer, M. V. Palmer & I. D. Sasowsky (Eds.), Karst modeling. Special Publication No. 5 (pp. 30–37). Charles Town, West Virginia: The Karst Waters Institute.

Chapter 19
Groundwater Model Development

Aquifer characterization programs are usually performed with the objective of obtaining the data required to develop numerical groundwater models. Groundwater modeling starts with the development of a conceptual model, which is followed by the selection of a modeling code and model discretization. Initial values for the hydraulic and transport properties are then assigned to each model cell or element, which are subject to adjustment during the model calibration process. Predictive simulations are performed to evaluate the response of the aquifer to various stresses (e.g., groundwater pumping scenarios). A deterministic approach has been taken for most groundwater models, in which the goal is to obtain a single solution that represents a 'best' estimate of future conditions. The alternative stochastic approach involves running a large number of simulations in a probabilistic framework to explore the range of possible future conditions. The basic premise of stochastic modeling is that due to an incomplete knowledge of the spatial variability of parameters, the decision is made to analyze all (or least numerous) plausible representations of the aquifer. Stochastic modeling has high data requirements and is not a substitute for a robust aquifer characterization program.

19.1 Introduction

The primary goal of aquifer characterization programs is usually to obtain the data required to develop numerical groundwater models, which are used for predictive simulations. The simulations may be performed to predict, for example, future aquifer responses to ongoing or new stresses (e.g., well-field pumping and changes in land use or cover), the effectiveness of groundwater recharge options, the rate of migration of contaminants toward production wells, and the effectiveness of remediation systems to capture contaminant plumes. Groundwater modeling can also be an important element of the characterization of an aquifer through the calibration process. Model calibration is essentially inverse modeling in which data

from measurements of observable parameters (e.g., aquifer heads) are used to infer the values of the aquifer hydraulic and transport parameters. Inverse modeling is particularly valuable for aquifer characterization because it has a very large volume of investigation, which, on a broad scale, consists of the entire model domain and, on a finer scale, the area in the vicinity of observation points (e.g., monitoring wells or piezometers).

Numerical groundwater modeling is a specialized discipline. Considerable expertise and experience are required to build technically defendable models. The development of pre- and post-processing software with user-friendly graphical user interfaces (GUIs) has facilitated groundwater modeling but has had the effect of allowing unexperienced and poorly trained personal to perform groundwater modeling with often dubious quality. The focus of this chapter is to introduce some fundamental modeling concepts, particularly with respect to their relationship to the aquifer characterization process in terms of both data required and information provided. It is by no means a guide to performing modeling. Although not all groundwater professionals need to be able to perform groundwater modeling, they should have a firm understanding of the modeling process if they are to use the result of models or contribute to their development through the aquifer characterization process.

19.2   Modeling Approach

The classical approach to modeling was summarized by de Marsily et al. (1998) and consists of the three elements:

- A conceptual model of the groundwater system of interest is first developed, which is decomposed into aquifer and aquitard (confining) layers.
- The schematic conceptual model is next discretized into a numerical grid and a set of parameter values is assigned to each cell, element, or node. Local parameter values, obtained from pumping tests and other aquifer characterization data sources, are interpolated and extrapolated to other cells in the grid for which data are not available.
- The values of parameters are adjusted through the model calibration process, which can be performed either manually or using automated inverse procedures.

The Anderson and Woessner (1992) proposed a nine element protocol for groundwater modeling, which explicitly incorporates all the main tasks involved in the design and evaluation of a model. The following sequence of elements is largely based on the Anderson and Woessner (1992) protocols

(1) statement of purpose and modeling objectives
(2) conceptual model development
(3) code selection
(4) design and construction

(5)   calibration and sensitivity analysis
(6)   verification
(7)   predictive simulations
(8)   reporting
(9)   post-audit.

19.2.1   Statement of Problem and Modeling Objectives

An important first step in any activity should be to have a clear understanding of the reasons for performing the activity, the objectives of the activity, and the likelihood that the activity under consideration will achieve the objectives. In the case of modeling projects, the goal is often to predict some future conditions of the aquifer under investigation. A key question is whether there are sufficient data to construct and populate a numerical model that can make the desired predictions with an acceptable degree of accuracy.

19.2.2   Conceptual Model Development

A conceptual model is a pictorial representation of the groundwater flow system, which necessarily is a simplification of the field system (Anderson and Woessner 1992). Bredehoeft (2005) described the conceptual model as 'the basic idea, or construct, of how the system or process operates.' Conceptual design includes identification of the boundaries of the model, and defining hydrostratigraphic units and the general flow system. The latter includes the sources and sinks of water (discharge and recharge sources and rates) and expected flow directions. The conceptual model should also include consideration of the likely type, extent, and distribution of aquifer heterogeneity, which may involve consideration of the depositional history of the aquifer and (semi)confining strata. A conceptual model is a general guide as to how the numerical model will be constructed. It should normally be documented in no more than a several page document with planar and cross sections.

   A conceptual model is the foundation of a numerical model. If the conceptual model does not accurately represent the basic hydrogeological conditions of the study area, then the numerical model built upon the conceptual model cannot be expected to provide reliable results. Bredehoeft (2005) defined 'surprise' as 'the collection of new information that renders one's original conceptual model invalid.' A surprise might be, for example, the discovery of a hitherto unexpected high-transmissivity fracture zone in the modeled study area that that has a major influence on groundwater flow. Of even greater concern than surprises, are major flaws in conceptual models that are never discovered. Hydrogeological conditions may exist at a site whose presence is not suggested by the available data. A numerical based on a flawed conceptual model

may be adequately calibrated through the adjustment of model parameters but give inaccurate predictions (Refsgaard et al. 2012). Conceptual model uncertainty is particularly important for cases where the predicted variables are not used for calibration (Højberg and Refsgaard 2005; Trolborg et al. 2007; Konikow 2011), such as where water quality is predicted using a model calibrated to aquifer heads.

Surprises that can result in a complete paradigm shift are more frequent (perhaps 20 to 30 % of models) than is commonly realized (Bredehoeft 2005). The uncertainty associated with conceptual models is typically greater than the estimated uncertainty in models due to parameter values (Poeter 2007). The possibility of major surprises can be reduced through a more thorough aquifer characterization and remaining open to fact that an initial conceptual model may be incorrect. Uncertainty in conceptual models can be evaluated by constructing and testing numerical models based on alternative conceptual models (Poeter 2007). Identification of possible alternative conceptual models involves a thorough investigation of the hydrogeology of the study area to evaluate the types of hydrogeological features or conditions that might be present (e.g., whether the presence of faults or fracture zones is plausible), imagination, and intuition. All alternative conceptual models will not have an equal probability of being correct. Once a set of alternative conceptual models is developed, then a means is needed to evaluate their plausibility. However, the optimal method to evaluate the probability of different conceptual models remains an unresolved issue. Ultimately, evaluation of potential alternative conceptual models may be a matter of professional judgment by experts with knowledge of the project site.

Conceptual and numerical model development should be an iterative process in which a conceptual model is continuously reformulated and updated (Bredehoeft 2005). Although evaluation of alternative conceptual models is necessary to more accurately evaluate uncertainty in model predictions, it is typically not put into practice (Bredehoeft 2005). Reasons for not considering an adequate number of conceptual models are (1) practical limitations (time and costs), (2) hydrogeologist′s inadequate imagination, and (3) that conceptual models cannot account for unknown information (i.e., available data provide no suggestion of a potential alternative model; Refsgaard et al. 2012). Bredehoeft (2005) noted that there is no ready remedy to conceptual surprise other than to collect as much data as possible and to be open to the fact that there are alternative conceptualizations and that a model can change dramatically.

19.2.3   Choice of Model Code

The model code (software) selected for a project should be capable of performing the type of simulation required to meet project objectives. Considerations in the selection of the model code for a specific project include

- finite-difference versus finite-element discretization
- whether or not surface water–groundwater interaction needs to be simulated
- whether or not solute transport or density-dependent solute transport needs to be simulated
- model acceptability and defensibility
- availability and cost of the model code
- modeler expertise, experience, and personal preferences.

The selected model code must meet the technical requirements of the project and also the requirements of the project owner, regulatory agencies, and other groups or professionals that may use or review the model. Governmental agencies may prefer widely used, open-source codes, such as MODFLOW (McDonald and Harbaugh 1988). Project owners tend to prefer that widely available codes are used so that they have the option of having other modelers review or, in the future, build upon the models. In some instances, models using proprietary (not open source) codes may not be admissible in courts of law. The choice of model code is often based on the personal preferences of the modeler. Groundwater modelers usually have one or more codes that they personally prefer, use more frequently, and with which they are particularly proficient.

In the United States, the U.S. Geological Survey MODFLOW family of codes is very commonly used because they are open access, widely accepted, have been extensively tested, and have the capability to simulate a wide range of hydrogeo-logical conditions and processes. Codes that have been developed upon, or utilize the outputs of, MODFLOW include MODPATH (Pollock 1994; particle tracking), MT3DMS (Zheng and Wang, 1999, solute transport), SEAWAT (Guo and Langevin 2002, density dependent solute transport), PHT3D (Prommer et al. 2003, reactive solute transport), and SEAWAT Version 4, which includes heat transport (Langevin et al. 2008).

The proprietary FEFLOW code (Diersch 1998) is also widely used, especially in Europe. ECLIPSE™ (Schlumberger n.d.) is a proprietary reservoir simulation software developed by Schlumberger Limited for the oil and gas industry that has advanced capabilities to simulate complex features or conditions including well and near well bore conditions, non-vertical wells, dual-porosity and permeability systems, chemical reactions, complex reservoir geologies, and multiple-phase systems.

There are many other, less commonly used, groundwater modeling software that have broad or specialized capabilities (e.g., vadose zone and integrated surface water and groundwater simulations) that are not discussed herein. Their omission is not a statement as to their quality or capabilities but rather due to space limitations. Professional modelers should be aware of the various softwares available and be able to select the one most suitable for any given groundwater investigation.

19.2.4   Model Design and Parameterization

Model development includes the selection of the grid design, boundary and initial conditions, and initial values of the aquifer parameters. Grid design includes the method of discretization (finite difference versus finite element), numbers of model layers, and the grid cell size or node spacing. The finite-difference method subdivides the aquifer into rectangular grid blocks. In block-centered, finite-difference models, hydraulic heads are calculated at nodes located in the center of the grid blocks (Fig. 19.1). Finite-element grids are divided into elements (commonly triangular) whose shapes are determined by typically irregularly distributed nodes. The finite-element grid has greater flexibility to simulate irregularly shaped features. Most geological and hydrogeological features do not have an orthogonal geometry, so the flexibility of the finite-element grid is advantageous in incorporating irregularly shaped model boundaries. However, finite-difference codes are mathematically simpler and more stable.

MODFLOW employs the block-centered finite-difference discretization. Greater spatial resolution can be achieved in finite-difference models by decreasing the grid size, which comes at an increased computation cost. Local grid refinement (LGR) methods for MODFLOW, reviewed by Mehl et al. (2006), allow for the reduction in grid size in the area of models that is of most interest, while maintaining a coarser grid elsewhere. As the computational speed of personal computers progressively increases, the time 'penalty' for inefficient models with great numbers of cells decreases. Computation horsepower can overcome inefficient model designs.

A new version of MODFLOW, called MODFLOW-USG (for UnStructured Grid; Panday et al. 2013), which is largely based on the finite-volume method, has been developed to support a wide variety of structured and unstructured grid types,

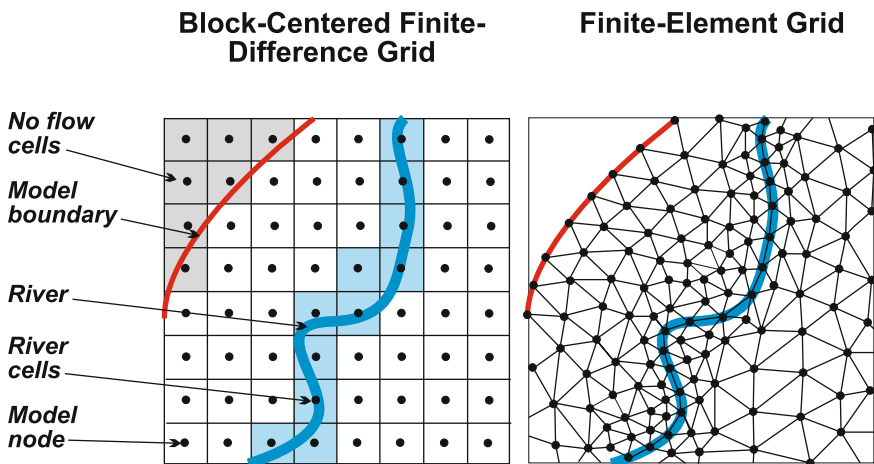**Block-Centered Finite-Difference Grid**   **Finite-Element Grid**

Fig. 19.1   Block-centered finite-difference and finite-element discretization

including nested grids and grids based on prismatic triangles, rectangles, hexagons, and other cell shapes. Flexibility in grid design can be used to focus resolution along rivers and around wells, for example, or to subdiscretize individual layers to better represent hydrostratigraphic units. However, it is expected that the original version of MODLOW with its rectilinear grid will continue to be primarily used for some time because of the availability of GUIs and numerous modules, and its capability of handling most modeling needs.

Values for the various hydraulic parameters must be assigned to all cells or nodes in the model grid. Typically, actual data are available for a very small fraction of the total number of cells or nodes in a model. Parameterization, as it is most commonly applied, involves the subdivision of a model domain into zones that are assigned a constant value for the parameter in question. The traditional approach used in groundwater models is to divide the domain into a relative small number of zones with uniform parameter values inferred from hydrogeological knowledge of the system (Anderson and Woessner 1992; Eaton 2006). Parameter values are preferably obtained from site-specific aquifer testing. In the absence of site-specific data, data from regional models or best estimates based on aquifer lithologies may be used. A variety of geostatistical methods are available for populating model grids utilizing available field data, including facies analyses (Chap. 20). Preprocessing software packages are available that can perform basic interpolation and extrapolation (e.g., kriging) between data points (e.g., wells) in the model grid.

A fundamental question in groundwater modeling is what is the optimal level of parameterization (Hunt et al. 2007). Hunt et al. (2007, p. 254) observed that

> there appears to be a diminishing return whereby some level of parameter complexity improves our simulation capabilities, but too much leads to instability, nonuniqueness, long run times, and increased potential for predictive error.

Long run (execution) times can preclude performing the numerous model runs needed to understand system dynamics, test models against data, and thus hamper model refutability and transparency (Hill 2006). A more detailed model is not necessarily a better (more accurate) model.

Parsimony is interpreted as striving for simplicity and has been proposed as an important criterion in the development of useful models (Hill 2006). Hill (2006) recommends starting with simple models and adding complexity carefully as supported by the available data and as important to predictions. The key issue is whether the observations available for model calibration support increased parameterization. Gómez-Hernández (2006, p. 783) noted that the

> issue is not so much the degree of complexity but, rather, how to address the uncertainty associated with model predictions due to lack of knowledge″, and that ″the debate should center of the selection of the model that can best approximate aquifer behavior, with the smallest uncertainty possible.

19.2.5   Model Calibration and Sensitivity Analysis

Model calibration is an inverse process in which observed measurements are used to obtain information on the distribution of hydraulic and other parameters in the model domain of interest. Groundwater model calibration was reviewed by Anderson and Woessner (1992) and Hill and Tiedeman (2006). Values of model inputs (e.g., hydraulic parameters, boundary conditions, and stresses) are adjusted so that the model output better matches observed data. The observed data, referred to as calibration targets, may include static (single value) or time series of

- water elevations or heads (measured in wells)
- drawdowns
- discharge rates (e.g., spring flows)
- surface water body elevations and flows
- water quality data (e.g., salinity) measured in wells or pumped water.

Calibration to a greater number of targets over a longer time period in general increases confidence in a model. Model calibration is evaluated by analysis of the residuals (errors), which are the difference between simulated and observed values. With respect to aquifer heads, the residual (r_i) at a given target (i) is defined as the difference between the measured or observed head (h_m) and the simulated head (h_s) in units of length:

$$r_i = h_m - h_s \tag{19.1}$$

Alternatively, residual head is sometimes defined as ($h_s - h_m$). The basic calibration statistics include

- mean error (ME),
- mean absolute error (MAE),
- root mean square error (RMSE), and
- weighted root-mean-squares error (WRMSE)
- standard deviation of residuals (SDR)

ME, MAE, RMSE, WRMSE, and SDR are defined with respect to heads as

$$ME = \frac{1}{n} \sum_{i=1}^{n} (h_m - h_s)_i \tag{19.2}$$

$$MAE = \frac{1}{n} \sum_{i=1}^{n} |h_m - h_s|_i \tag{19.3}$$

$$RMSE = \left[\frac{1}{n} \sum_{i=1}^{n} (h_m - h_s)_i^2 \right]^{0.5} \tag{19.4}$$

$$\text{WRMSE} = \left[\frac{1}{n} \sum_{i=1}^{n} w_i (h_m - h_s)_i^2 \right]^{0.5} \tag{19.5}$$

$$\text{SDR} = \left(\frac{1}{(n-1)} \sum_{i=1}^{n} (r_i - \text{ME})^2 \right)^{0.5} \tag{19.6}$$

where
n   number of calibration targets
w_i weighting factor (dimensionless, from 0 to 1)

Mean error is sensitive to the direction of errors (i.e., whether simulated values are greater or less than the measured values). An ME of close to zero suggests that there is no overall bias in the model in that the sum of errors greater than and less than calibration target (measured) values cancel out. MAE and RMSE are not functions of the direction of error and provides a measure of the closeness of predicted values to measured valued. WRMSE (and weighted versions of the statistical functions) includes a weighting factor, which reflects the expected measurement error (i.e., observation data that may have great errors or variance are given a lower weight) or proportional importance allocated to specific targets. Areas of greatest interest in a model domain are given greater weight.

The objective of the calibration procedure is to reduce the residuals so that the calibration statistics approach predetermined thresholds. Model calibration may be performed either manually or using an automated process (or sometimes a combination of both). Manual calibration is performed using a systematic trial and error process. The values for a model parameter in model zones are adjusted either upward or downward in increments to try to obtain a better fit (lower residuals) to the calibration targets. An understanding of the hydrogeological system in question and the response of models to changes in the various parameters allows the process to be efficiently performed. A key component of the calibration process is knowledge regarding the real range of the parameter values within the model domain. Calibration using unrealistic parameter values, that are outside of the realistic range of variation, can ultimately lead to large model predictive errors. Some parameters may be known with a high degree of certainty and should be modified only slightly or not at all during calibration (Anderson and Woessner 1992).

Software is available that automatically performs model calibration. The PEST parameter estimation and optimization software program (Doherty and Hunt 2010) is increasingly being used for model calibration. The PEST program takes control of the model and automatically performs as many model runs as it needs, while adjusting the parameter values, until the weighted least squares residual is reduced to a predetermined minimum value. There is still debate as to whether manual or automated calibration provides better results. Automated calibration has the advantages of being quicker and less subjective than manual calibration. However, subjectivity based on a sound understanding of the modeled system can bring great value to the model

calibration process. Model calibration does not result in a unique solution as there are multiple ways to match a given set of calibration target. However, because of the nonuniqueness of model calibration, the best fit solution may not necessarily result in the most accurate predictive model, particularly where the predictive simulation scenario differs significantly from the model calibration conditions.

A criticism of automated calibration, expressed by experienced modelers, is that it commonly results in very well-calibrated models whose results are not hydrogeologically reasonable (i.e., are contrary to what is known about the study site). If this is the case, then additional conditioning may be required to constrain the calibration process. On the other hand, automated calibration may provide a result that reveals that the underlying conceptual model may be wrong (i.e., some unknown feature may be present or not adequately represented that is impacting observational data). Hence, it must be stressed that automated calibration is a tool that is subject to abuse if applied without a firm understanding of site hydrogeology and a careful evaluation and understanding of the results.

A sensitivity analysis is a critical component of the model calibration process as it can provide approximate error bars for the model results. Sensitivity analyses are performed by running predictive simulations in which the values of hydraulic parameters are adjusted by fixed amounts (e.g., upward and downward by 50 %). The goal of the sensitivity analysis is to quantify the effects of the inherent uncertainty in the values of hydraulic parameters on model results. If the results of the sensitivity analysis show only a minor change in predictions, then a higher degree of confidence can be placed on the model. Conversely, if a modest adjustment in the value of a hydraulic parameter, whose value is uncertain, causes a substantial change in simulation results, then a large uncertainty (error bars) exists for the simulation results.

A well-calibrated model is considered to better represent the structure and properties of a studied aquifer than a less well-calibrated model. However, a parallel issue is the relationship between the true hydraulic properties and those estimated through the calibration process (Moore and Doherty 2006). The reality is that the parameter value assigned to a given point is unlikely to be equal to the true value of the hydraulic property at that point. Estimated values of a hydraulic property at any point within a model domain is, in fact, a weighted average of the true hydraulic properties over a much greater area (Moore and Doherty 2006). For example, transmissivity values calculated from pumping test data reflect the hydraulic conductivity throughout the cone of depression, rather than only the value at the pumped well or an observation well.

In all but the most homogenous of hydrogeological environments, solutions to the groundwater inverse problem are inherently non-unique (Moore and Doherty 2006). Numerous sets or fields of values of hydraulic parameters can produce a given set of measured data (e.g., heads). There is always more spatial property variability than observational data can constrain. The envelope of potential solutions to an inverse problem can be constrained by hydrogeological data. A critical issue with calibration (inverse modeling) is that the parameter values should be reasonable. Modelers may accept greater discrepancies in the match between field

observations and model results to maintain reasonable model parameters. The use of unreasonable values to calibrate a model can ignore important information about the system, particularly that the underlying conceptual model may be wrong (Poeter and McKenna 1998).

The hydrogeological detail that can be captured in a calibrated model is related to the number of calibration points. As less data are available for calibration, there is a greater reduction in the ability of the calibrated field to reproduce the spatial detail existing in the true field. If a model is used to make predictions that are dependent on system detail beyond that which can be captured by the calibration process, then the consequences of using the calibrated field to make predictions can be serious (Moore and Doherty 2006).

19.2.6   Calibration Using Pilot Points

Doherty (2003) presented a model calibration procedure that involves the use of pilot points in conjunction with a nonlinear parameter estimation software that incorporates an advanced regularization functionality (e.g., PEST). The basic concept is that hydraulic parameters are assigned to a set of points (i.e., pilot points) distributed throughout the model domain, rather than directly to the model grid or mesh elements (Fig. 19.2). Property values are assigned throughout the model

Fig. 19.2 Set of pilot points (crosses) and observation bores (circles) used to calibrate a groundwater flow model of an industrial facility (from Doherty 2003, copyright National Groundwater Association)

domain by spatial interpolation and extrapolation methods from the pilot points to the model grid or mesh elements. Doherty (2003) used kriging but noted that other spatial interpolation methods could also be used. Pilot points should be placed throughout the model domain with an increased spatial density in areas of suspected heterogeneity and where measurement density is high. Model calibration is performed by adjusting the values of the pilot points using PEST until a satisfactory calibration is achieved, as quantified using a 'measurement objective function.' PEST allows for bounds to be placed on parameter value in order to 'listen to the data' (Doherty 2003). Fixed (hard) pilot points may be used whose values are not changed during the calibration run. Fixed points may be used for locations in which there is confidence in the measured parameter value (e.g., pumping test locations).

The pilot points technique is well suited to stochastic uncertainty analysis through the assignment of stochastically generated multiplier values to the pilot points. A secondary property field is generated by multiplying the primary field by a multiplier or 'warping' field. Respect for conditioning data can be retaining by placing pilot points at conditioning points and fixing their multiplier value at unity (Doherty 2003). Nonuniqueness of inverse model techniques may be addressed by recruiting additional information to constrain the solution (e.g., Poeter et al. 1997; Bohling and Butler 2010).

Regularization describes the process that makes a function more regular or smooth. It can broadly be defined as any method that helps provide an approximate and meaningful answer to an ill-posed problem (Hunt et al. 2007). An ill-posed problem has a number of parameters greater than the number of observations. Regularization may involve definition of preferred system conditions based on hydrogeological knowledge. Hunt et al. (2007) discussed regularized inversion using pilot points, which is proposed to allow for better calibration through the introduction of spatial variability into key parameters (hydraulic conductivity and porosity). They suggest that a case can be made that regularized inversion provides a more rigorous and subjective method for calibration than do traditional zone-based approaches. Hunt et al. (2007) introduced a hydrid Tikhonov—truncated single value decomposition (TSVD) regularized inversion, in which numerical stability and numerical (computational) burden is reduced through the exclusion of insensitive and highly correlated parameters from the solution space. The calibration is reformulated so that calibration is performed in a subspace of important parameter combinations (i.e., 'super parameters'). The use of super parameters allows for the benefits of highly parameterized inversion with a comparatively small run-time burden.

19.2.7   Model Verification and Validation

The purpose of model verification and validation (the terms are often used interchangeably) is to establish greater confidence in a calibrated model by performing additional simulations using new stress conditions and observational data that were

not used in the model calibration (Anderson and Woessner 1992). For example, a hypothetical model might be calibrated for a two-year period, and then a verification simulation is performed using data for a third year. If there is a good match between the simulated and observed data for the third year, then greater confidence may be placed in the ability of the model to adequately represent real conditions.

The term verification means the establishment of truth by demonstration. It is not possible to verify or validate any numerical model in the sense that the veracity of a model is established (Konikow and Bredehoeft 1992; Oreskes et al. 1994). Due to the nonuniqueness of model calibration, even if a model is satisfactorily calibrated and subsequently found to provide a good match to an additional data set, it has been correctly noted that it still has not been 'verified' that the model will provide accurate predictions of the future. These arguments are in some respects pedantic as it is understood that there is always some uncertainty in modeling future conditions. Instead the burden on a modeler is to demonstrate the degree of correspondence between the model and the material world it seeks to represent and to delineate the limits of that correspondence (Oreskes et al. 1994).

This demonstration may be met by providing technical justification (e.g., from field data) for the conceptual model and parameter values used, sensitivity analysis results, and verification simulation results.

19.2.8 Predictive Simulations and Reporting

Once a model has been calibrated and verified (accepting the limitations of the verification process), then the next step is to perform the actual predictive simulations. Predictive simulations are usually performed to evaluate the response of aquifers to future conditions. An important part of projects is the preparation of a final report that documents the entire modeling process. The report should document

- the objectives of the modeling
- conceptual model(s) including its technical basis
- model code used and the rationale for its selection
- summary of the model design and sources of data used
- model calibration process including calibration statistics and sensitivity analysis results
- model verification including calibration statistics
- results of predictive simulations
- sources of uncertainty in model and their impacts on predictions
- archival of the model files

Model files should be labeled and archived in a manner so that they are readily identifiable as to their corresponding model run and are recoverable by future authorized users.

19.2.9 Post-audits

Post-audits are performed after the modeling has been completed. They involve a comparison of model predictions to what actual happened (i.e., subsequently collected monitoring data) in order to confirm that the model does indeed provide an acceptable representation of real-world conditions and to obtain insights into future possible model enhancements (Anderson and Woessner 1992). If there is a significant discrepancy between predicted and observed data, then the source of the discrepancy should be identified. A discrepancy between predicted and observed water levels could be due to input conditions (e.g., recharge rate and well-field withdrawals) being different than those simulated, rather than a problem with the model itself. If the problem lies within the model (e.g., conceptual model or parameter errors), then the model should be refined and recalibrated. Models should also be revaluated and refined, as necessary, as new hydrogeological data become available, particularly if it does not support the conceptual model of the study area.

Post-audits are perhaps the most neglected part of groundwater modeling. It has been the author's experience that after the completion of a project (e.g., well-field design and construction), the modeling results are seldom revisited. In the applied hydrogeology and engineering realm, once a project is completed, the project is 'closed' and there is usually no funding for additional data collection and modeling work. The value of models as an ongoing water management tool is not realized. At a minimum, predictions of concern (e.g., aquifer water levels or the salinity of produced water) should be regularly compared against field data, which requires only a modest effort.

19.3 Stochastic Groundwater Modeling

The deterministic model calibration approach is to obtain a single solution that represents a 'best' estimate. The alternative is running a large number of simulations in a probabilistic framework to explore the range of possible future conditions (Anderson 1997; Webb and Davis 1998; Zhang 2003; Hunt et al. 2007). A stochastic model is a tool for estimating probability distributions of potential outcomes by allowing for random variation in one or more inputs over time. The term 'stochastic' is understood to apply to any method that requires estimates of uncertainty in parameter values and yields ranges of heads or concentrations (Anderson 1997). The aquifer structure is captured, with varying degrees of accuracy, using geostatistical methods, which are discussed in Chap. 20.

From a water management perspective, stochastic modeling may be used to predict the probability of various outcomes rather than predicting a single, presumed most likely, outcome with an unquantified uncertainty. Consider, as an example, the impacts of groundwater pumping on the flow rate of an environmentally sensitive spring. A deterministic modeling approach would produce a

single predicted spring flow rate for a given set of input conditions. A stochastic approach might predict that spring flow would be maintained above a target rate and frequency with a 95 % confidence level (Sepúlveda and Doherty 2015).

The basic premise of stochastic modeling is that, due to a lack of knowledge of the spatial variability of parameters, the decision is made to analyze all plausible representations of the aquifer, which only exist in our imagination and of which only one best represents the real aquifer (Gómez-Hernández 2006). The plausibility of realizations is generally measured by two controls: (1) how well do the values of parameter variables (direct conditioning) and state (e.g., head) variables (inverse conditioning) of the realization match observed values and (2) how some predetermined structure about the heterogeneity of the aquifer is preserved in the realization.

The development of stochastic simulations was driven by the realization that hydrogeological environments are exceeding heterogeneous, and that even in locations where considerable data are available, the exact spatial variations of the heterogeneous elements can never be uncovered (Smith 1981; Gelhar 1986). Stochastic approaches have the perceived advantage that complete aquifer characterization is not necessary and thus the data burden is lighter (Phillips et al. 1989). However, Phillips et al. (1989) noted that a 'data paradox' occurs in that stochastic methods avoid the need for detailed investigation of aquifer heterogeneity, but very large amounts of data are still needed for parameterization of stochastic transport models. Binley et al. (2010) similarly observed that "stochastic models require even more data that traditional deterministic models, as an estimate of the underlying spatial statistical structure of the governing parameters is needed."

19.3.1 Probability Density Functions

Probability density functions (pdfs) are theoretical probability distributions for continuous variables. The most important probability density function in natural sciences is the normal or Gaussian probability density distribution (Fig. 19.3), which is expressed by the equation:

$$f(x) = \frac{1}{r\sqrt{2p}} e^{-\frac{(x-1)^2}{2r^2}} \tag{19.7}$$

where
f(x) frequency of x (height of ordinate)
x   variable
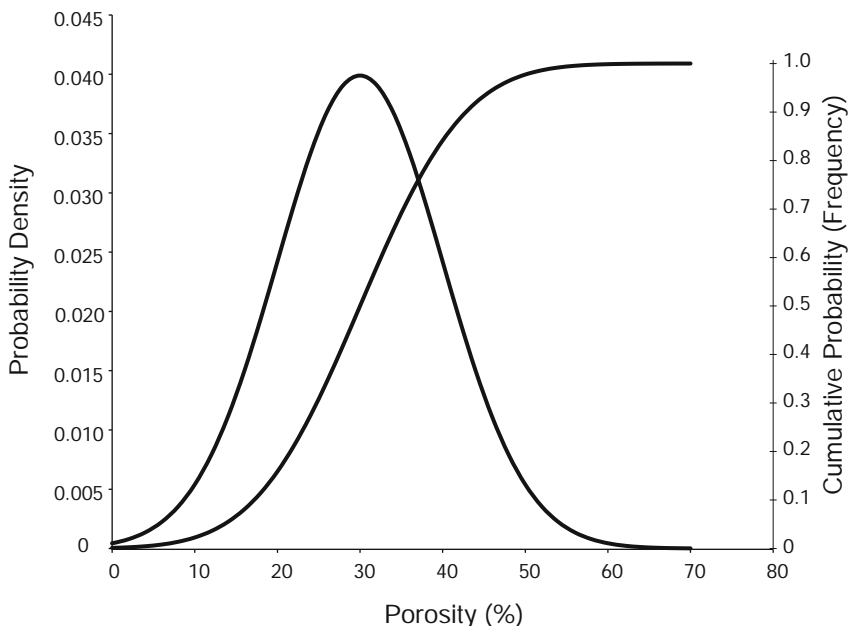l   mean
r   standard deviation

Fig. 19.3 Normal probability distribution and cumulative probability or frequency curves for a mean porosity of 30 % and standard deviation of 10 %

The shapes of normal probability distribution functions are controlled by the mean and standard deviation of the variable in question. The mean controls the position of the distribution on the x-axis of the plot and the standard deviation controls the spread of the distribution. Normal distributions are symmetric about the mean. The mean plus and minus one standard deviation contains 68.28 % of the distribution. When the frequencies are normalized (divided by the total number of values), the sum of the relative frequencies (i.e., area under the curve) is equal to 1. The expected frequencies of observations between two values (limits) are represented by the area under the curve.

Cumulative frequency plots (Fig. 19.3) give the total frequency from negative infinity to any x value (point of the abscissa). The cumulative probability of any normal distribution plots on a straight line when plotted on normal probability paper. For some variables, such a hydraulic conductivity, the raw data may not have a normal distribution. Normal distributions may be obtained, or approached, by transforming the data. With respect to hydraulic conductivity, a log transformation is often used;

$$x = \log(x) \tag{19:8}$$

Data that has a normal distribution after a log transformation is said to have a log-normal distribution.

The great practical value of the normal probability distribution is that once a normal distribution is fitted to the experimental field data (from the mean and standard deviation of the sample data), the probability and expected frequency of different values can be predicted. Whether or not data are normally distributed can be evaluated using statistical methods, such as the Kolmogorov–Smirnov goodness-of-fit test.

19.3.2   Basic Stochastic Modeling Approach

There is a variety of different types of stochastic models. The general approach includes the following steps:

(1) Development of a conceptual model, including discretization.
(2) Probability distribution functions (pdf) are obtained for the parameters and boundary conditions.
(3) Simulations are performed with values assigned to the model cells, elements, and nodes from the pdfs using a Monte Carlo method.
(4) The plausibility of each realization (simulation results) is evaluated using calibration criteria. If the realization does not meet calibration (and model structure) criteria, then it is considered to be unrealistic.
(5) Predictive simulations are performed using the realistic realizations.
(6) The results of realistic simulations are aggregated and the probability (and uncertainty) of given events are determined.

The essential feature of Monte Carlo simulations, as applied to groundwater modeling, is that a large number of equally probable hydrogeological model realizations are generated and solved. Typically, the realizations are generated by combining random instances of parameter values from probability density and covariance functions or by the use of transition probability geostatistical methods (Yeh 1992; Jones et al. 2005). The results are analyzed to get probabilities of different outcomes. Monte Carlo simulations can be conditioned to known data by keeping parameter values constant at measurement points.

Monte Carlo methods vary, but tend to follow a general pattern

(1) definition of a domain of possible inputs
(2) generation of inputs (realization) from a probability distribution or covariance function over the domain using a pseudorandom number generator
(3) performance of a simulation for each realization
(4) compilation and analysis of the results.

A very simple example of a Monte Carlo approach involves the division of a model layer into a limited number of hydraulic conductivity zones and assignment of initial values based on aquifer pumping testing results and geological knowledge or intuition. A five zone hydraulic conductivity grid generated by the U.S.

Geological Survey for a watershed in California is illustrated in Fig. 19.4. The commonly used procedure employed in this investigation was to adjust parameter values for the zones during the model calibration process, which can be performed either manually or using automatic calibration software. For stochastic simulations, a hydraulic conductivity pdf is needed for each of the five zones, which ideally is obtained from study area-specific field testing data. For each of, for example, 200 realizations, a hydraulic conductivity value is obtained for each zone from its respective pdf. For realizations in which there is an acceptable calibration, based on a minimum threshold value for calibration functions, a predictive simulation is performed. The results from all the accepted realizations are then used to determine the frequency distribution of the output of concern, which depending upon the model, could be spring or streams flows, groundwater level in wetlands, or aquifer water levels. The challenges for real-world problems are obtaining a reasonable accurate spatial patterns of the zones and pdfs for the properties of each zone.
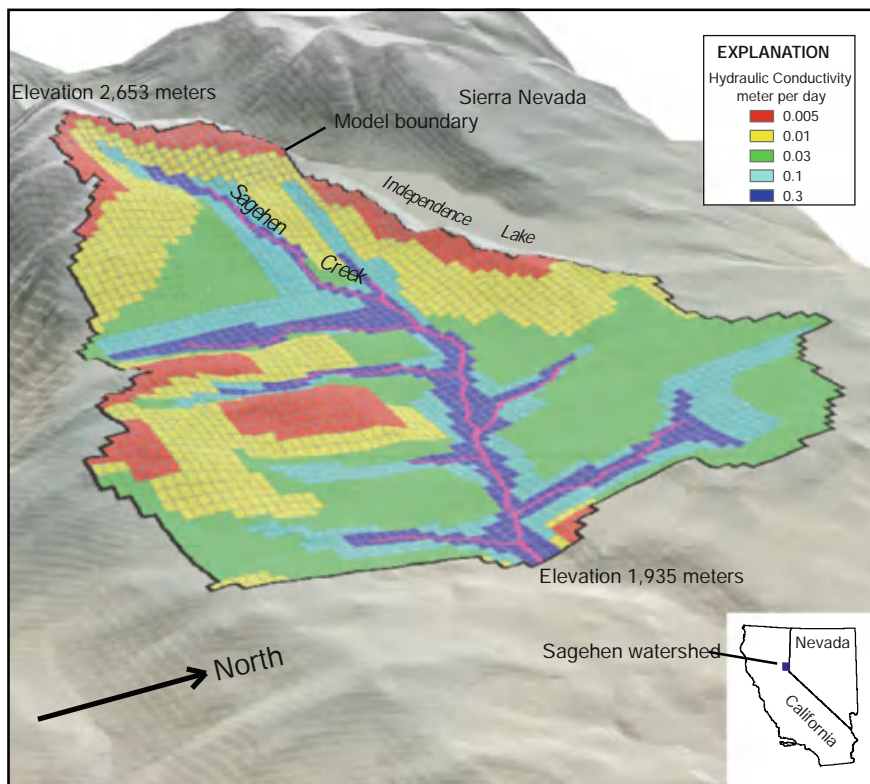

Fig. 19.4 Hydraulic conductivity zonation for a single layer model of the Sagehen watershed, located on the eastern slope of the northern Sierra Nevada, near Truckee, California. Grid cells have lengths and widths of 90 m (from Niswonger et al. 2006)

Sepúlveda and Doherty (2015) analyzed uncertainty in predicted water levels and spring flows in east-central Florida. The uncertainty analysis focused on parameter uncertainty and did not consider conceptual model uncertainty. Parameters considered are the horizontal hydraulic conductivity of aquifer layers, the vertical hydraulic conductivity of confining layers, recharge rates, and local conductance affecting spring flow. Spatial variability of parameters was represented using both pilot points, zones, and spatially uniform layers. The results of this regional (multicounty) modeling using the 'Null Space Monte Carlo' method indicate that the capacity of the model to predict water levels changes resulting from increased pumping was greater than the capability to predict changes in spring flow.

According to the law of large numbers, as the number of simulations approaches infinity, the relative frequency distribution of the Monte Carlo realizations will approach the true probability distribution, provided that correct hypotheses have been made (Gómez-Hernández and Gorelick 1989). The Monte Carlo approach is computationally expensive and the results may be biased because of incorrect assumptions in the numerical model (Gómez-Hernández and Gorelick 1989).

The need for probability functions for the various parameters means that stochastic models have a high data requirement. Stochastic modeling is not a means to avoid field investigations. Stochastic modeling requires 100 s or 1,000 s of model runs, which in the past meant that it would take a prohibitively long time for most studies. Run time varies greatly depending upon on the size and complexity of the model, including whether or not solute transport is simulated. However, with progressively increasing available computational power, stochastic simulations are becoming more viable as an applied tool.

19.3.3 Stochastic Versus Deterministic Modeling

Deterministic modeling typically provides a best estimate prediction, based on the use of what are judged to be the most appropriate conceptual model and the most likely parameter values based on aquifer characterization results. The potential uncertainty in the predictions is often evaluated through sensitivity analyses based on professional judgment of the potential range of parameter values. Stochastic modeling has the advantage that it can be used to quantitatively evaluate the probability of a potential future event. For example, with respect to the movement of a contaminant, predictive simulations using a deterministic model might indicate that a given contaminant is expected to migrate a given distance over a given time frame. A sensitivity analysis would provide information on the possible range of contaminant migration distances. A stochastic analysis might be used to evaluate the probability that contamination may reach a given point (sensitive receptor) and its likely travel distance over a given period of time and the confidence limits of the predictions.

The number of academic papers on stochastic approaches to modeling spatial heterogeneity increased exponentially since the publication of the pioneering work on the subject by Freeze (1975) (Dagan 1986). Gelhar (1986, p. 144S) noted that

> During the last decade there has been a revolutionary change in the way that we conceptualize fluid transport processes in natural permeable earth materials. This stochastic approach has produced research results which establish a sound quantitative basis for predicting the large-scale behavior of subsurface flow systems.

Yet over 25 years later, stochastic methods are still largely in realm of academic research and are uncommonly used in applied hydrogeology.

A number of workers (Freeze 2004; Renard 2007; Pappenberger and Beven 2006; Winter 2004) reviewed the reasons why stochastic methods are not more widely used in applied hydrogeology. One reason put forward is that there is an aversion to uncertainty in preference for the perceived certainty of the deterministic world. For example, there is often a preference for concluding that modeling results based on the best available data indicate that a contaminant will not reach a production well after 10 years, as opposed to concluding that there is a 0.1 % probability the contaminant will reach the production wells within 10 years. Acknowledging that a bad result is a possibility (albeit very low) is construed (often correctly) as giving project opponents support for their arguments. Indeed, it is well documented that the general public tends to overestimate the risks from low-probability events. Nevertheless, the main advantage of stochastic techniques is their ability to quantify uncertainty (Winter 2004; Renard 2007), which is the technically correct approach.

One the greatest impediments to the increased implementation of stochastic and other geostatistical techniques are that many professionals and parties that would rely upon the data are unfamiliar with or simply do not understand the techniques. Technical literature presenting geostatistical methods are very commonly 'dense' equation-full papers that are unintelligible to most non-geostatisticians. Academic publications on geostatistics are typically written for other geostatisticians. In a legal or regulatory setting, the parties involved (e.g., a judge, regulators, and stakeholders) need to understand the procedures that are used to derive conclusions. If one's methods cannot be clearly explained to a nonexpert, then they may not be accepted.

A major misconception is that stochastic modeling is a substitute for the data collection required for deterministic models. Stochastic models require a lot of data in part because they are most appropriate in settings that are hard to characterize. Geostatistical estimates of system parameters must be representative of the strata under investigation, which usually requires a fairly large sample population (Winter 2004). Stochastic approaches that have large data requirements have limited their usefulness for practical applied problems. For example, methods that were employed in several year-long doctoral theses are often not practical for applied projects that have much more limited time frames. In the absence of sufficient study area-specific data, either assumed or perhaps rock-type-specific 'default' pdfs might be used, but such an approach introduces a large uncertainty element that negates the principle advantage of stochastic methods as a means of quantifying uncertainty.

Regulatory interest invariably focuses on the tails of such distributions, which are likely to be the least reliable parts of a stochastic prediction. A tail of a distribution, might be the probability of a very high contaminant concentration at, or much faster travel time to, a sensitive receptor than indicated by predictions based on most likely (median or mean) parameter values.

The deterministic alternative to stochastic evaluation of uncertainty is worst-case design (Winter 2004; Renard 2007). For example, if a model indicates that the salinity of water produced in a planned coastal well field is sensitive and positively correlated to production zone transmissivity, then a predictive simulation could be performed using a worst-case large transmissivity value (i.e., a value beyond the likely range of values based on aquifer characterization). The water treatment plant would be designed using this worst-case value, with the anticipation that the design includes a substantial safety factor and actual salinities will be less than the values used in the design.

References

Anderson, M. P. (1997) Characterization of geological heterogeneity. In G. Dagan & S. P. Neuman (Eds.) Subsurface flow and transport: a stochastic approach (pp. 23–43). Cambridge: Cambridge University Press.

Anderson, M. P., & Woessner, W. W. (1992). Applied groundwater modeling: simulation of flow and advective transport. New York: Academic Press.

Binley, A., Cassiani, G., & Deiana, P. (2010) Hydrogeophysics: opportunities and challenges. Bollettino di Geofisica Teorica ed Applicata, 51, 267–284.

Bredehoeft, J. (2005) The conceptualization model problem—surprise. Hydrogeology journal, 13 (1), 37–46.

Bohling, G. C., & Butler, J. J., Jr. (2010) Inherent limitations of hydraulic tomography. Ground Water, 48, 809–824.

Dagan, G. (1986) Statistical theory of groundwater flow and transport: Pore to laboratory, laboratory to formation, and formation to regional scale. Water Resources Research, 22(9), 120S to 134S.

de Marsily, G., Delay, F., Teles, V., & Schafmeister, M. T. (1998) Some current methods to represent heterogeneity of natural media in hydrogeology. Hydrogeology Journal, 6, 115–130.

Diersch, H. J. (1998) FEFLOW: Interactive, graphics-based finite-element simulation system for modeling groundwater flow, contaminant mass and heat transport processes. User's Manual Version 4.6: Berlin, Germany; WASY, Institute for Water Resources Planning and System Research Ltd.

Doherty, J. (2003) Ground water model calibration using pilot points and regularization. Ground Water, 41, 170–177.

Doherty, J. E., & Hunt, R. J. (2010). Approaches to highly parameterized inversion: A guide to using PEST for groundwater-model calibration. US Department of the Interior, US Geological Survey.

Eaton, T. T. (2006) On the importance of geological heterogeneity for flow simulation. Sedimentary Geology, 184, 187–201.

Freeze, R. A. (1975) A stochastic-conceptual analysis of one-dimensional groundwater flow in nonuniform homogeneous media. Water Resources Research, 11, 725–741.

Freeze, R. A. (2004) The role of stochastic hydrogeological modeling in real world engineering applications. Stochastic Environmental Research and Risk Assessment, 18, 286–289.

Gelhar, L. W. (1986) Stochastic subsurface hydrology from theory to applications. Water Resources Research, 22(9), 135S-145S.

Gómez-Hernández, J. J. (2006) Complexity. Ground Water, 44, 782–785.

Gómez-Hernández, J. J., & Gorelick, S. M. (1989) Effective groundwater model parameter values: Influence of spatial variability of hydrulaulic conductivity, leakance, and recharge. Water Resources Research, 25, 405–491.

Guo, W., & Langevin, C. D. (2002) User's guide to SEAWAT: a computer program for simulation of three-dimensional variable-density ground-water flow. U.S. Geological Survey Open-File Report 01–434.

Hill, M. C. (2006) The practical use of simplicity in developing ground water models. Ground Water, 44, 775–781.

Hill, M. C., & Tiedeman, C. R. (2006) Effective groundwater model calibration: with analysis of data, sensitivities, predictions, and uncertainty. Hoboken: John Wiley & Sons.

Højberg, A. L., & Refsgaard, J. C. (2005) Model uncertainty – parameter uncertainty versus conceptual models. Water Science & Technology, 52(6), 177–186.

Hunt, R. J., Doherty, J., & Tonkin, M. J. (2007) Are models too simple? Arguments for increased parameterization. Ground Water, 45, 254–262.

Jones, N. L., Walker, J. R., & Carle, S. F. (2005) Hydrogeologic unit flow characterization using transition probability geostatistics. Ground Water, 43, 285–289.

Konikow, L. F. (2011) The secret of successful solute-transport modeling. Ground Water, 49, 144–159.

Konikow, L. F., & Bredehoeft, J. D. (1992). Ground-water models cannot be validated. Advances in Water Resources, 15(1), 75–83.

Langevin, C. D., Thorne, D. T., Jr., Dausman, A. M., Sukop, M. C., & Weixing, G. (2008) SEAWAT version 4: A computer program for simulation of multi-species solute and heat transport. U.S. Geological Survey Techniques and Methods Book 6, Chapter A22.

McDonald, M. G., & Harbaugh, A. W. (1988) A modular three-dimensional finite-difference ground water flow model. U.S. Geological Survey Techniques of Water-Resources Investigation Report 06-A1.

Mehl, S., Hill, M. C., & Leake, S. A. (2006). Comparison of local grid refinement methods for MODFLOW. Groundwater, 44, 792–796.

Moore, C., & Doherty, J. (2006) The cost of uniqueness in groundwater model calibration. Advances in Water Resources, 29, 605–623.

Niswonger, R. G., Prudic, D. E., & Regan, R. S. (2006) Documentation of the Unsaturated-Zone Flow (UZF1) Package for modeling unsaturated flow between the land surface and the water table with MODFLOW-2005. U.S. Geological Survey Techniques and Methods 6-A19.

Oreskes, N., Shrader-Frechette, K., & Belitz, M. (1994) Verification, validation, and confirmation of numerical models in the Earth Sciences. Science, 263, 641–646.

Panday, S., Langevin, C. D., Niswonger, R. G., Ibaraki, M. & Hughes, J. D. (2013) MODFLOW–USG version 1: An unstructured grid version of MODFLOW for simulating groundwater flow and tightly coupled processes using a control volume finite-difference formulation. U.S. Geological Survey Techniques and Methods, Book 6, Chap. A45.

Pappenberger, F., & Beven, K. J. (2006) Ignorance is bliss: Or seven reasons not to use uncertainty analysis. Water Resources Research, 42, W05302.

Phillips, F. M., Wilson, J. L., & Davis, J. M. (1989) Statistical analysis of hydraulic conductivity distributions: A qualitative geological approach. In Proceedings Conference of New Field Techniques for Quantifying the Physical and Chemical Properties of Heterogeneous Aquifers (pp. 19–31). Dublin, Ohio: National Water Well Association.

Poeter, E. (2007). "All models are wrong, how do we know which are useful?" - Looking back at the 2006 Darcy Lecture tour. Ground Water, 45, 390–391.

Poeter, E. P., & McKenna, S. A. (1998) Combining geologic information and inverse parameter estimation to improve groundwater models. In G. S. Fraser & J. M. Davis (Eds.), Hydrogeologic models of sedimentary aquifers. Concepts in Hydrogeology and Environmental Geology No. 1 (pp. 171–188). Tulsa: SEPM.

Poeter, E. P., Wingle, W. S., & McKenna, S. A. (1997) Improvising groundwater project analysis with geophysical data. The Leading Edge, 16, 1675–1681.

Pollock, D .W. (1994) User's guide for MODPATH/MODPATH-PLOT version 2: A particle tracking post-processing package for MODFLOW, the U.S. Geological Survey finite-difference ground-water flow model. U.S. Geological Survey Open-File Report 94-464.

Prommer, H., Barry, D. A., & Zheng, C. (2003) MODFLOW/MT3DMS based reactive multi-component transport modeling. Ground Water, 41, 347–257.

Refsgaard, J. C., Christensen, S., Sonnenborg, T. D., Seifert, D., Højberg, A. L., & Troldborg, L. (2012) Review of strategies for handling geological uncertainty in groundwater flow and transport modeling. Advances in Water Resources, 36, 36–50.

Renard, P. (2007) Stochastic hydrogeology: What professions really need? Ground Water, 45(5), 531–541.

Schlumberger (n.d.) ECLIPSE industry reference reservoir simulator. Retrieved from http://www.software.slb.com/products/foundation/Pages/eclipse.aspx.

Sepúlveda, N, & Doherty, J. (2015) Uncertainty analysis of a groundwater flow model in east-central Florida. Groundwater, 53(3), 464–474.

Smith, L. (1981) Spatial variability for flow parameters in a stratified sand. Mathematical Geology, 13(1), 1–21.

Trolborg, L., Refsgaard, J. C., Jenson, K. H., & Engesgaard, P. (2007) The importance of alternative conceptual models for simulation of concentrations in multi-aquifer. Hydrogeology Journal, 15, 843–860.

Winter, C. L., 2004, Stochastic hydrology: practical alternatives exist. Stochastic Environmental Research and Risk Assessment, 18, 271–273.

Webb, E. K., & Davis, M. (1998) Simulation of the spatial heterogeneity of geologic properties: An overview. In G. S. Fraser & J. M. Davis (Eds.), Hydrogeologic models of sedimentary aquifers. Concepts in Hydrogeology and Environmental Geology No. 1 (pp. 1–24). Tulsa: SEPM.

Yeh, T. -C., J. (1992) Stochastic modeling of groundwater flow and solute-transport in aquifers. Hydrological Processes, 6, 369–395.

Zhang, D. (2003) Stochastic methods for flow in porous media: Coping with uncertainties. San Diego: Academic Press.

Zheng, C., & Wang, P. P. (1999) MT3DMS: a modular three-dimensional multi-species model for simulation of advection, dispersion and chemical reactions of contaminants in ground water systems: documentation and user's guide. Report SERDP-99-1.Vicksburg, Mississippi: U.S. Army Engineer Research and Development Center.

Chapter 20
Geostatistical Methods and Applications

Geostatistical analysis techniques are used to predict the values of parameters between data points. Geostatistical methods are only valid for spatially dependent (i.e., nonrandom) data. The basic method is to first identify and quantify the spatial structure of the variables of concern and then to interpolate or estimate the values of variables from neighboring values taking into account their spatial structure. Conditioning is the incorporation of hard or soft data into a model to reduce uncertainty. Hard data, by definition, has negligible uncertainty (e.g., direct measurements of property of interest), whereas soft data (inferred properties) have significant uncertainty. Geostatistical methods have been used to obtain realizations of sedimentary facies distributions, which typically require upscaling to a groundwater model grid, and assignment of hydraulic parameters values. A promising approach is hybrid methodologies that combine facies models and other soft geological information with geostatistical methods. Geostatistical techniques, when properly applied, are data intensive and are not a substitute for detailed field investigations and hydrogeological knowledge.

20.1 Introduction

Geostatistics is perhaps the most important subject of this book as it ties together the other chapters on aquifer characterization methods and modeling. Data on aquifer properties collected during a field program need to be incorporated into a numerical groundwater model in a manner that captures as much of their information as practically possible. The basic aquifer characterization and modeling workflow is illustrated diagrammatically in Fig. 20.1.

A variety of approaches are used to assign values for hydraulic and transport parameters to a model domain, which is referred to as parameterization. Geostatistics consist of techniques used to estimate or interpolate parameter values in space where sampling data are not available (Yeh 1992). Geostatistical methods
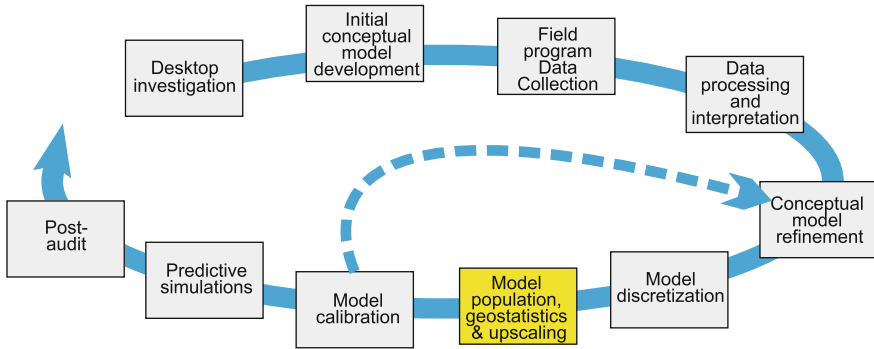
Fig. 20.1 Aquifer characterization workflow

are only valid for spatially dependent (i.e., nonrandom data) data. The basic premise of geostatistics, as applied to groundwater investigations, is that probability distributions of sediment of rock properties are dependent on location. The properties of sediment or rock at two points in a study area are likely to be more similar if the points are located close together. Similarly, as the distance between two points in a study area increases, eventually a distance is reached at which there is no longer a spatial correlation in properties between the points.

In random data, there is no spatial relationship in rock properties within the study area regardless of the distance between points. The properties of an aquifer at any two points independently vary regardless of their geographic separation. It is clear from facies analyses that the distribution of rock and sediment types, and thus their properties, is not random. Hence, the goal of geostatistics with respect to sedimentary rock aquifers is to capture as much of the underlying sedimentological structure of aquifers in groundwater models as practically possible.

The parameterization process provides an initial value for parameters, which are subject to adjustment during model calibration process. Parameterization methods commonly used in numerical groundwater models are

- Parsimonious uniform distribution
- Poorly structured interpolated distribution
- Pilot points
- Advanced geostatsical methods

Parsimonious uniform distribution methods involves assigning all cells (or nodes) in a layer of the model domain either a uniform value or dividing the layer into a number of discrete subunits or zones that are each assigned a uniform value. For example, if there are only one or two data points for a parameter (e.g., storativity) in a model layer, then there is no technical basis for a fine-scale parameterization. Where data are sparse, an entire layer may be assigned a single value, unless there is hydrogeological data available that suggest geographic variation in the parameter value is justified. The division of a layer into subunits is sometimes performed by simply defining zones as polygons centered around data points (e.g.,

wells from which pumping tests are available), which is a reasonable, default approach if there is insufficient data for a more structured approach. The preferred strategy is to define the shape and locations of zones based on a conceptual geological and hydrogeological model to the degree possible. For example, a zone representing a high transmissivity channel sand unit would encompass the best estimate of the channel location and orientation based on the available field data. The values assigned to the zones are adjusted during model calibration and additional zones may be added or the zonation pattern modified during calibration, if needed, to obtain a better local calibration.

Poorly structured interpolated distribution involves the assignment of values to cells or nodes by interpolation of observed values. The interpolation could be a simple linear interpolation between point values or basic geostatistical methods may be employed, such as kriging using assumed geostatistical parameters. Interpolation methods assume that there is a gradation in values between data points and do not recognize sharp discontinuities. Poorly structured interpolated distribution is a widely used method and most modeling software packages include this option.

Pilot parametrization and inverse modeling are introduced in Sect. 19.2.6. Instead of defining zones with assigned parameter values, pilot points are strategically placed throughout the model domain, which are assigned initial values that may be either subject to change (soft points) or fixed (hard points) during the calibration of the model. The values of the parameters in the areas of the model between the pilot points are interpolated from pilot points. Model calibration is performed by adjusting the values of the pilot points. The model can be conditioned (hydrogeological data and interpretations incorporated) through the pilot point pattern and by the use hard pilot points and pilot points whose values that can be adjusted by a only prescribed maximum amount.

Advanced geostatistical methods attempt to capture aquifer heterogeneity through the detailed modeling of lithofacies and hydrofacies distributions. These methods have become fundamental tools for the modeling of hydrocarbon reservoirs but, to date, have had been applied much less frequently to groundwater investigations.

20.2 Geostatistics Basics

Geostatistics is a complex discipline and a number of dedicated books have been published on the subject (e.g., Isaaks and Srivastava 1989; Kitanidis 1997; Rubin 2003; Olea 2009). Following is a brief discussion of basic concepts to illustrate potential applications for aquifer characterization. Geostatistical methods have two basic elements (Yeh 1992):

(1) identification and quantification of the spatial structure of the variable of concern
(2) interpolation or estimation of the values of spatially distributed variables from neighboring values taking into account the spatial structure of the variables.

Geostatistical approaches include the use of continuous random functions (e.g., hydraulic conductivity values) and indicator-based methods for categorical variables, such as distribution of facies. A simple example of an indicator statistical application is to categorize a model domain as containing cells that either represent coarse-grained channel sands (assigned a value of 1) or fine-grained flood plain deposits (assigned a value of 0).

Geostatistical methods have various assumptions concerning the statistical properties of the data, which need to be understood before the methods are applied. Most of the commonly used geostatisical methods are based on the assumption of stationarity. There are several types or orders of stationarity. Strong or strict stationarity implies that the statistics of the variables in question are invariant with location. In practice, 2nd order or weak stationarity is employed in applied geostatistics. Weak stationarity assumes that the mean and covariance do not vary with location. Covariance only varies with the distance between points. Intrinsic stationarity assumes that the mean does not change with location and variance depends only on the distance and direction separating any two locations. Various methods are available to detrend nonstationary data. As noted by Henley (1981), most authors accept that data sets rarely approach stationarity and suggest that departures from stationarity are not significant as local stationarity can be assumed (although there is no general proof of this). The effects of departures from stationarity of data in groundwater investigations are likely much less than the impacts of typically inadequate geostatistical data, especially in the horizontal directions.

20.2.1   Semivariogram

The semivariogram is a key element of spatial statistics, which expresses the spatial correlation of parameters. Experimental (empirical or sample) semivariance is defined as:

$$c(h) = \frac{1}{2n(h)} \sum_{i=1}^{n(h)} [z(s_i) - z(s_i + h)]^2 \qquad (20:1)$$

where

h	lag (distance between samples; m)
$c(h)$	semivariance at lag 'h' (unit is square of the variable unit)
$n(h)$	number of sample pairs with a lag of 'h'
$z(s_i)$	value of variable at site 'i'
$z(s_i + h)$	value of variable at a site lag distance 'h' from site 'i'

Lag in the above equation is a scalar quantity defined by magnitude. Lag can alternatively be defined as a vector quantity that has both magnitude and direction.

The term $z(s_i)$ is referred to as the "tail" variable and $z(s_i + h)$ as the "head" variable, as they are located at the tail and head of the lag vector "h."

The related function covariance $C(h)$ is defined as

$$C(h) = \frac{1}{n(h)} \sum_{i=1}^{n(h)} [(z(s_i)z(s_i + h)] - [m(s_i)m(s_i + h)] \qquad (20.2)$$

where

$$m(s_i) = \frac{1}{n(h)} \sum_{i=1}^{n(h)} z(s_i) \qquad (20.3)$$

where $m(s_i)$ and $m(s_i + h)$ are the mean values of the head and tail.

Semivariograms are plots of semivariance versus lags for sets of data (Fig. 20.2). In practice, because of the limited number and irregular distribution of wells and other data points, there will be few pairs of data values with the exact same lag. Average semivariance values are calculated for unevenly spaced observations using distance "bins," which requires consideration of (Kaluzny et al. 1998).

- the appropriate lag increment (i.e., distances at which the semivariogram is calculated)
- the tolerance of the lag increment (i.e., bin distances for lag increments)
- the number of lag increments over which the semivariogram will be calculated

Omni-directional semivariograms are nondirectional. Directional semivariograms are commonly used, particularly in the horizontal and vertical directions or in two horizontal (x and y) and one vertical (z) directions. In the case of a fluvial system, for example, the semivariogram parallel to the channel trend would be expected to differ from that perpendicular to the channel trend.

Fig. 20.2 Semivariogram diagram. The range is the lag (distance) for which there is a spatial correlation of the parameter of interest
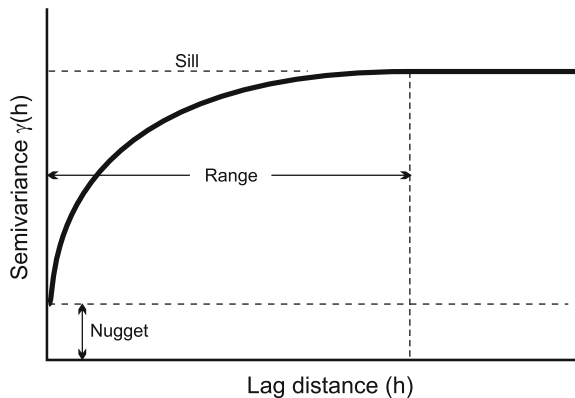
Semivariograms have three defining parameters, the nugget (c_0), range (a), and sill (c). The nugget (or nugget effect) is the value of $c(h)$ at $h = 0$. The nugget effect reflects measurement error or microscale variation. The range is the distance (lag) at which the data are no longer spatially correlated and the semivariogram levels off to constant value referred to as the sill. The range is related to the dimensions of the hydrofacies.

Semivariograms can also be prepared using for binary indicator functions (also referred to as indicator random variables), $I(x)$, where

$I(x) = 1$ for all elements of x that are A
$I(x) = 0$ for all elements of x that are not A

Indicators may be lithofacies or hydrofacies types, or may be specified by threshold values for continuously varying parameters. Where data are continuous, indicator values can be assigned based on whether or not a variable is less than or equal to a specified threshold value. Indicator statistics are particularly well-suited to characterizing and modeling sedimentary architecture, as sedimentary facies can be coded using integers (Proce et al. 2004). For example, facies can be divided into sand and gravel (i.e., aquifer units) and clayey units (i.e., confining strata). The empirical indicator semivariogram equation is:

$$c(h) = \frac{1}{2n(h)} \sum_{i=1}^{n(h)} [I(s_i) - I(s_i + h)]^2 \tag{20.4}$$

In practice, the empirical semivariograms are obtained using the following process

- calculation of the squared difference (lag) between all pairs of measurements at different locations
- group pairs into 'bins' with similar distances (or distances and directions for vector data)
- calculate average semivariance for each bin
- plot average semivariance versus distance

After an empirical semivariogram model is created, the next step to fit a semivariogram model to the data. There are a variety of semivariogram models including, linear, exponential, spherical, and Gaussian. For example, the exponential and spherical semivariogram models are

$$c(h) = c_0 + (c - c_0)\left[1 - e^{\left(\frac{3h}{a}\right)}\right] \tag{20.5}$$

$$c(h) = c_0 + (c - c_0)\left[\frac{3h}{2s} - \frac{h^3}{2a^2}\right] \tag{20.6}$$

Statistical software packages are now typically used to process the data, generate experimental semivariogram plots, and select and fit semivariogram models.

Semivariograms vary with direction in anisotropic aquifers, both in the horizontal direction (x vs. y anisotropy) and, to a much greater degree, between the vertical and horizontal directions. Areal anisotropy can be evaluated by mapping semivariograms in azimuthal steps in all directions. For example, directional semivariograms in glaciofluivial valley-fill aquifers in eastern Ohio indicate a maximum principal direction (i.e., greatest spatial correlation) occurred in a NE-SW direction that subparallels the trend of the bedrock valley (Ritzi et al. 1995). Facies analysis can provide insights into the type of spatial trends likely present in the data. As another example, beach sand units would be expected so have greater spatial correlation parallel to the paleoshoreline

The basic challenge with geostatistical methods lies in accurately estimating spatial correlation functions (e.g., semivariograms). Study area-specific empirical semivariograms can be generated if data are abundant. However, where data are very abundant, it is often sufficient to map heterogeneity by simple deterministic techniques. Collection of statistically significant semivariance data required to construct semivariograms is data intensive. Estimation of correlation scale using semivariogram methods requires data at spacings appropriate to the scale of the problem (Phillips and Wilson 1989). Typically in groundwater investigations, vertical data are more readily available as multiple measurements may be made in a single borehole. Semivariograms are typically poorly defined in the horizontal direction due to fewer data points (e.g., wells) and much larger spacings (Fogg 1989). The borehole spacing is often larger than the correlation range (Poeter et al. 1997).

The alternative to the generation of synthetic semivariograms from experimental semivariograms is to synthesize semivariograms from field data and some knowledge of the expected spatial pattern in permeability between data points (Fogg 1989). In other words, a conditional simulation is performed in which geological interpretation is incorporated within the semivariogram. For example, to obtain a horizontal range, assumed reasonable values may be used based on geological models of facies dimensions, if hydraulic conductivity is indeed related to facies (Fogg 1989). General geometric scaling relationships based on field studies can be used to infer the unknown dimensions of hydrofacies (Rubin et al. 2006; Sun et al. 2008). Facies data may form the basis of estimates of lateral–vertical ratios of mean length, geologically plausible juxtapositional tendencies, and the proportions of facies (Jones et al. 2005). Semivariograms obtained from outcrop studies may also be applied to geologically similar aquifers.

Walther's law has been applied to geostatistical analyses, which states that facies adjacent to one another in a continuous vertical sequence also accumulated adjacent to one another horizontally. Thus, the semivariances observed in a vertical section should also be observed horizontally over larger length scales (Desbarats and Bachu 1994). There are definite limitations to the application of Walther's law, particularly in that it does not apply to sections with unconformities and diachronous boundaries.

Various soft data can be used to estimate or constrain horizontal semivariograms. Cross-well seismic tomography can provide information on hydraulic conductivity and facies distributions between wells (McKenna and Poeter 1995), but is an expensive method and thus impractical for most investigations. Surface

geophysical data (e.g., GPR) can provide data on the directional continuity of strata (Knight et al. 1997). However, GPR has a much greater attenuation in saturated sediments and thus a limited depth of investigation.

20.2.2 Kriging

Interpolation algorithms, such as kriging, estimate the value of a variable at a given unsampled location as a weighted sum of data values at surrounding locations. Usually, both the expected value and variance are computed for every unsampled location within a region. Kriging incorporates a family of methods whose appropriateness for a given project depends on the characteristics of the data and the type of spatial model desired. Commonly used kriging methods are

- ordinary kriging
- simple kriging
- universal kriging

Ordinary kriging is the most frequently used kriging method. It is based on the assumption that the mean is constant but unknown over the entire region of interest. In simple kriging, the mean is known and constant throughout the study region. Universal kriging is used when the mean varies in a linear manner in the region of interest and can be modeled by simple functions.

The ordinary kriging process includes three basic steps:

(1) construction of an experimental semivariogram from field data
(2) selection of an appropriate semivariogram model
(3) estimation of the values at unsampled locations using the weighted average of neighboring samples.

The basic ordinary kriging equation is

$$z^*(s_0) = \sum_{i=1}^{n} k_i(z(s_i)) \tag{20.7}$$

where
$z^*(s_0)$ estimated value at location s_0,
n number of observations
$z(s_i)$ value of variable $z(s)$ at location 'i'
k_i weight for location 'i' (the sum of all the weighting factors used is equal to one)

In the case of inverse distance-weighted interpolations, the value of k_i is a function of distance, with the value decreasing with increasing distance. The key element of the kriging process is that the weighting factors are optimized (i.e.,

estimation error variance minimized) using a semivariogram or covariance model. Ordinary kriging assumes that the data are stationary. For nonstationary data, large-scale trends can be identified and removed from the data (i.e., the data is detrended). Kriging predictions are also more accurate if the input data is Gaussian. Transformation of the data may be required to obtain a Gaussian distribution.

Kriging is very commonly used in a deterministic manner to obtain a single best estimate of the distribution of the parameter of interest. In laterally heterogeneous aquifers, which are the norm rather than the exception, interpolation techniques such as kriging tend to overestimate continuity and create unrealistically smooth spatial patterns of hydraulic conductivity (Fogg 1989). Delhomme (1979, p. 271) observed that

> Kriging is an optimal estimation procedure, but an estimator, even an optimal one, cannot restore details that have not been surveyed. Thus a kriged map is inevitably smoother than the 'true' one.

Kriging can be performed using indicator statistics. In the case of binary indicator kriging, field data, for example, might be assigned as I(x) = 1 for sand (permeable) units and I(x) = 0 for nonsand (e.g., low-permeable clayey) units. The lithology at unsampled locations is assigned based on whether or not the values calculated for each location is less than or equal to a specified cut off value (Johnson and Dreiss 1989). For example, Johnson and Dreiss (1989) and Johnson (1995) in a study of alluvial fan deposits in the Santa Clara Valley, California, used a binary division of the sediments into high- and low-permeability indicator values based on the Unified Soil Classification System (USCS). Sediments were classified from borehole data at 0.6 m (2 ft) intervals. The three-dimensional structure was described with two near horizontal variograms (parallel to stratigraphic layers) and one vertical variogram. Three-dimensional kriging using indicator variogram models was used to evaluate the probability that sediments at a particular location are relatively high permeability. The location of the 0.5 indicator contour was used as the approximate boundary between high- and low-permeability sediments (Johnson and Dreiss 1989).

Ritzi et al. (1994) used an indicator function to differentiate between wells in which a low-permeability zone is present in a glaciofluvial aquifer system and wells in which a low-permeability zone are absent. Ordinary point kriging was used to compute the best unbiased estimation of the expectation of I(x) and thus the probable occurrence of the low-permeability facies. Cut-off values of 0.50 and 0.66 were used to delineate facies boundaries. The 0.66 cut-off value corresponds to wells in which the low-permeability unit is present. Appropriate hydraulic parameters values were then assigned to the mapped facies.

Ouellon et al. (2008) presented "imbricated" kriging as an alternative to indicator kriging for the estimation of three-dimensional hydraulic conductivity fields. The method is based on the proportion of hydrofacies within a model grid cell. Hydrofacies were first defined and their relationship to hydraulic conductivity determined using core and slug test data. Thirty-nine geological facies were identified based on lithofacies description, which were grouped into four hydrofacies.

The hydrofacies proportions over 5-m intervals was then determined from borehole logs. Approximately, 1350 data points were generated.

Three-dimensional interpolation of hydrofacies was next performed using variography and imbricated kriging. Imbricated kriging was performed in three steps in which hydrofacies proportions were successively interpolated so that each variography and kriging step considers the results of the previous interpolation. The process was started with the better-structured hydrofacies (in terms of horizontal and vertical ranges) being kriged first. The proportion of the final (fourth) hydrofacies was the residual from the first three krigings. Finally, the vertical and hydraulic conductivity of each grid cell was calculated from the facies proportions at the center of each grid element. Hydraulic conductivities were calculated from the proportion of each hydrofacies and their associated hydraulic conductivity values.

20.2.3   Markov Chain

Markov chain is a transition statistical method in which the probability of 'k' occurring at location 'x + h' is only dependent upon what happens at location 'x'. In the case of facies analysis, the probability that a given facies is present at another location with respect to a given point, depends upon the facies at that point. The analysis can be conditioned by using a fixed facies assignment for cells in which field data are available (Carle and Fogg 1996, 1997).

Proce et al. (2004) provides a good example of the application of indicator statistics and Markov chain models to simulation the location of high-permeability sand and gravel units within a glaciofluvial aquifer in North Dakota. Aquifer heterogeneity and interconnectivity were considered on two main scales. First is on the scale of facies assemblages, of which three assemblages were considered: broad aquifer (multiple channel system), narrow aquifer (single channel system), and interaquifer. Each facies assemblage is in turn composed mud and diammicton (m) facies and sand and gravel (s) facies.

The Markov Chain framework is built upon the probability of transitioning from one assemblage type to another with translation. It does not involve the use of variograms. Given that assemblage type j exists at point x, the transition probability t_{jk} (x, x′) gives the probability that assemblage type k exists at location x′ (Proce et al. 2004). For three assemblage types (1, 2, and 3) the basic three-component transition probability matrix is (Proce et al. 2004):

$$T(h_\emptyset) = \begin{bmatrix} t_{11}(h_\emptyset) & t_{12}(h_\emptyset) & t_{13}(h_\emptyset) \\ t_{21}(h_\emptyset) & t_{22}(h_\emptyset) & t_{23}(h_\emptyset) \\ t_{31}(h_\emptyset) & t_{32}(h_\emptyset) & t_{33}(h_\emptyset) \end{bmatrix} \tag{20:8}$$

where $h_/$, which is defined as a vector with a tail at x and head x′ in the direction / with a magnitude h/ (Proce et al. 2004). Transition probability matrices may be calculate in multiple directions (e.g., vertical and two normal horizontal directions).

The transition probability at all lags can be modeled as a continuous Markov chain (Proce et al. 2004):

$$T(h_U) = \exp(R_U h_U) \tag{20.9}$$

where R_U is a transition rate matrix and $r_{ij,/}$ is the rate of transition from j to k in direction $/$

$$R_\emptyset = \begin{bmatrix} r_{11;\emptyset} & r_{12;\emptyset} & r_{13;\emptyset} \\ r_{21;\emptyset} & r_{22;\emptyset} & r_{23;\emptyset} \\ r_{31;\emptyset} & r_{32;\emptyset} & r_{33;\emptyset} \end{bmatrix} \tag{20.10}$$

and

$$\exp(R_{/} h_\emptyset) = \sum_{i=1}^{3} \exp(k_i h_i) z_i$$

where k_i and z_i denote the eigenvalues and spectral component matrices, respectively, of $R_{/}$ (Proce et al. 2004).

An advantage of the transition probability/Markov chain (TP/MC) method is that it can incorporate geological information such as the mean lengths and orientation of lithofacies (Carle and Fogg 1996, 1997; Ye and Khaleel 2008). The basic limitation is often the unavailability of adequate data to accurately estimate TP/MC parameters in the x, y, and z directions

Elfeki and Dekking (2007) applied a coupled Markov chain approach to simulate a confining layer in an unconfined aquifer located in the central Rhine-Meuse delta in The Netherlands. The coupled Markov chain approach described the sequence of lithologies in the vertical and horizontal directions using two coupled chains in which the state in cell (i, j) depends on the state of the cells at the top $(i, j - 1)$ and on the left $(i - 1, j)$ of the current cell (Elfeki and Dekking 2001, 2007). The method requires horizontal and vertical transition probability matrices obtained from boreholes.

20.3 Conditioning

Conditioning is the incorporation of hard or soft data into a model to reduce uncertainty. Hard data, by definition, has negligible uncertainty (e.g., direct measurements of property of interest), whereas soft data have significant uncertainty. Conditioning can be employed in forward modeling, in which measured values of aquifer parameters are honored, or in inverse modeling, in which system responses (e.g., heads or tracer concentrations) are honored (Scheib and Chen 2003). The degree to which conditioning improves model predictions depends upon the type of information, its quantity and quality, and its observation scale (Scheib and Chen 2003).

The data requirements for geostatistical methods can be reduced by the introduction of soft information into classical geostatistics (Journel 1986). Soft information may include data on the dimensions and distribution of sedimentary units. Types of soft information include (Zhu and Journel 1993; McKenna and Poeter 1995; Poeter et al. 1997)

- values based in imprecise measurements (e.g., estimates from geophysics)
- recognized bounds of a value without information of the distribution of values between bounds (e.g., relative differences in properties)
- prior data on the probability distribution of a variable (e.g., hydraulic conductivity data from previous studies).

Mixed or hybrid approaches (Webb and Davis 1998, p. 2) can be defined as methods that

> distill the essential geologic elements from knowledge of geologic processes and the resulting patterns of heterogeneity acquired through many years of careful evaluation.

These essential elements are then incorporated into quantitative models of aquifer heterogeneity. Hybrid models (Gómez-Hernández 2006) may involve the generation of realizations of aquifer architecture (e.g., hydrofacies distribution) with each hydrofacies populated in model using a stochastic approach. Pattern matching approaches are also used in which a "training image" of the aquifer structure is selected based on knowledge of the aquifer system, and each stochastic realization of built ensuring that the pattern of the training image is mimicked. The emphasis of hybrid methods is on capturing facies heterogeneity rather than on capturing heterogeneity within facies.

A very promising approach for simulating geological heterogeneity is the use of indicator statistics and conditional stochastic simulation (Anderson 1997). Geological information is used to help define units of similar hydraulic conductivity (hydrofacies). Facies models and other soft geological information are combined with indicator geostatistical methods to simulate the distribution of hydrofacies (Anderson 1997). Values for hydraulic parameters are assigned to the hydrofacies zones either stochastically or deterministically. The data may require upscaling to the model discretization scale. Hydraulic parameter values are subject to adjustment during model calibration.

20.4 Applied Geostatistical Approaches

The primary objective of applying advanced geostatistical methods to groundwater investigations is to develop numerical models that better capture aquifer heterogeneity and thus more accurately simulate groundwater flow and solute transport. Geostatistical methods are widely used to develop reservoir models in the oil and

gas industry and advanced workflow software (e.g., Petrel), have the built-in capabilities to perform advanced, conditioned geostatistical simulations and upscaling of the geological data into a numerical groundwater model grid. From an applied perspective, the selected method or methods must be compatible with project resources in terms of data availability, schedule, and budget. Following are summaries of some groundwater investigations in which advanced geostatistical methods have been applied. The intent is to present examples of the range of methods that are available and have actually been applied.

Ritzi et al. (1994) documented the use of stochastic conditional indicator geostatistics to map the distribution of a low permeability zone in a glaciofluvial aquifer system. The data were also deterministically analyzed by indicator point kriging. The basic procedure employed was to use semivariograms to estimate the probability of indicator types at each node. The probabilities were ordered in a conditional probability distribution function with a probability scale of 0 to 1. A random number (q) is then drawn and the interval in which q falls determines whether the simulated facies (e.g., the low-permeability zone) is present at a particular location. The simulation procedures provide many equiprobable realizations that are a more realistic representation of the facies distribution in a global sense (Ritzi et al. 1994).

Poeter and Townsand (1994) took a similar conditional multiple stochastic simulation approach to a 2-D simulation of the shallow aquifers at the Hanford site in Washington State (USA). Geophysical log, descriptive core logs, and grain size analysis data were used to classify sediments into four categories (hydrofacies). The cumulative probability that a given facies (indicator) exists at a location represented by a grid block was determined using the data surrounding the location, weighted on the basis of distance using a semivariogram model. The main advantages of this method is that it honors available data and accounts for uncertainty associated with hydrofacies interpretations. Hydraulic conductivity values for each hydrofacies were obtained from testing data previously performed by other workers. Each realization was used to determine the distribution of aquifer properties in flow and transport models. The values of aquifer parameters can be subsequently adjusted for each realization through the model calibration process. Poeter and Townsend (1994) proposed that the calibration process could be used to evaluate the validity of the realizations. If calibration proves to be impossible using a reasonable range of parameter values, then the geological configuration can be considered implausible.

McKenna and Poeter (1995) incorporated soft data into conditional stochastic simulations. Noteworthy is the use of cross-borehole seismic tomography to derive soft-data estimates of hydrofacies between wells. Stochastic indicator simulations of facies distribution were performed using both hard data and combined soft and hard data. Forward modeling was then performed using estimates of hydraulic conductivity of the hydrofacies from field testing. Realizations using combined hard and soft data yielded smaller head residuals than realizations generated using hard data alone. However, average absolute head errors obtained from forward modeling were still substantial, even after incorporation of the soft information into the zonation process. Inverse modeling was then used to estimate hydraulic conductivity values for each facies given the plausible zonation patterns based on the

geophysical, geological, and hydrological information. The McKenna and Poeter (1995) study demonstrates how data fusion constrains the solution to a greater degree than can be achieved through refined analysis and interpretation of any single data source.

The value of conditioning on the accuracy of forwards predictions of solute transport was evaluated by Scheib and Chen (2003) for a tracer test performed at a highly investigated site in Oyster, Virginia. Available conditioning data includes slug and pump tests, borehole flowmeter measurements, laboratory permeability measures, GPR, and cross-borehole radar tomography data. Six types of simulations were performed:

Deterministic

(1) homogenous
(2) layered with homogenous layers
(3) kriged heterogeneous conditioned to borehole flowmeter data

Stochastic

(4) stochastic indicator simulation with no conditioning
(5) stochastic indicator simulation conditioned to borehole flowmeter data
(6) stochastic indicator simulation conditioned to tomographic interpretation

A surprising result is that conditioning to a large number of small-scale hydraulic conductivity measurements did not significantly improve model simulations. Conditioning to geophysical interpretation with a large spatial support (i.e., cross-borehole radar tomography) did significantly improve model accuracy.

Sequential indicator simulation (Goovaerts 1997) is a commonly used technique for the geostatistical simulation of facies distribution in hydrocarbon reservoirs and aquifers. The similar sequential Gaussian simulation (SGS) is used for the modeling of continuous variables, such as hydraulic conductivity. The basic SIS approach is as follows:

(1) condition the model by assigning data values (from field data) to the closest grid nodes (or cells).
(2) establish a random path through all the grid nodes, visiting each node only once (skip over nodes that already have a value)
(3) at each node

   (a) find the nearest data and previously simulated grid nodes
   (b) construct a complementary cumulative distribution function (CCDF) by kriging
   (c) draw a simulated value from the CCDF (using a pseudo-random number generator)
   (d) assign the simulated value to the grid node
   (e) proceed to the next node and repeat steps (a) through (d)

Proce et al. (2004) performed a three-dimensional sequential indicator simulation using a rate matrix in a two-step procedure consisting of indicator simulation using

cokriging and simulated quenching. Geological information was imposed on the
Markov chain model (Weissman et al. 1999), specifically that the mean length of
facies assemblages are greater in the dip (stream gradient) direction than in the strike
direction. The simulations were also performed to honor conditioning data (i.e.,
observed well data). The continuous Markov chain analysis was used to generate
realizations of the distribution of facies. The facies assemblage was conceptualized
as having only two facies, 'm' and 's'. Because only two facies were considered,
autotransition probabilities could be used to completely define the system (Proce
et al. 2004). Field data were used to determine the autotransition probabilities, i.e., to
quantify the probability of the transition from one facies to the same facies as a
function of lag distance. A conditional sequential indicator simulator code was then
used to calculate separate three-dimensional realizations for the facies within each
facies assemblage. Simulated interconnection of the high-permeability sand and
gravel units (Fig. 20.3), and thus the creation of high-permeability pathways, was
found to be consistent with the interconnectivity suggested by prior hydraulic and
geochemical studies of the regional system (Proce et al. 2004).

Optimal value for existing data may be obtained by a combined deterministic
and stochastic approach. Were field data are available to sufficiently map large-scale
features than a deterministic approach is applied. Stochastic approaches may then
be used to model fine-scale features for which sufficient data are unavailable for
deterministic modeling. A multiple-scale, combined deterministic and stochastic
approach was applied to alluvial fan deposits in California (Weissmann and Fogg
1999; Weissmann et al. 2002). Large-scale features, such as unconformity bounded
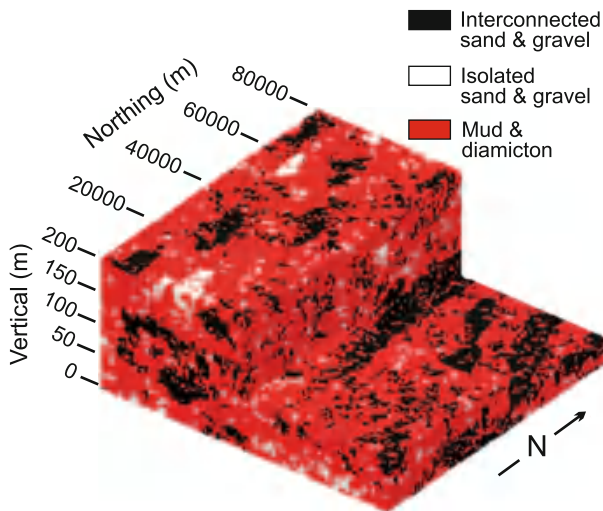sequences, was deterministically modeled since they could typically be correlated

Fig. 20.3 Facies distribution for a glaciofluvial aquifer in North Dakota (Spiritwood Aquifer
Region) simulated using the modified Markov chain model. Simulations show interconnectivity of
sand units suggested by the field data (from Proce et al. 2004, copyright National Groundwater
Association)

between wells. Intermediate scale features, such as facies assemblages (e.g., channel and overbank assemblages) were stochastically modeled through the application of transition probability statistics. Small-scale features were modeled through the use of appropriate dispersivity tensors. The workflow includes the following main elements:

- development of a deterministic model of the stratigraphic framework
- development of a Markov chain model of each stratigraphic unit (i.e., unconformity bounded sequence)
- application of Markov chain model to sequential indictor simulation and simulated annealing to produce separate realizations for each stratigraphic unit
- combination of the realizations for each stratigraphic unit into a final realization.

The above approach assumes that there was no correlation across sequence boundaries. A basic constraint on geostatistical methods is inadequate data on the lateral spatial distribution of facies. Weissmann et al. (1999) documented the use of soil survey data from alluvial faces to obtain data on the spatial distribution of facies. Jones et al. (2005) presented a similar method for stochastic modeling of a heterogeneous aquifer. A transition probability indicator simulation approach was combined with the hydrogeologic unit flow (HUF) package of MODFLOW 2000. The Transition Probability Geostatistical Software (T-PROG; Carle 1999) was used to generate a specific number of arrays of indicator values, where each value specifies the material identification (facies) for the corresponding MODFLOW grid cell. A complexity that was addressed is that the background geostatistics grid is typically orthogonal (equidimensional cells), whereas geological and model (e.g., MODFLOW) grid may not be (e.g., top and bottom elevations vary). Upscaling may also be required to calculate vertical and horizontal hydraulic conductivity values for coarse grid size.

TPROG was used in investigations of the San Joaquin Valley of central California by Phillips et al. (2007) and Traum et al. (2014). Hydraulic properties were estimated on the basis of sediment textures or facies derived from driller's logs. Traum et al. (2014) discretized the driller's log data by 1 foot (0.3 m) intervals and interpreted each interval as one of four facies; gravel, sand, muddy sand, or clay. The horizontal cell dimension is 0.125 miles (201 m) by 0.125 miles. The study area was divided into four separate domains (geological settings). The relations between vertical transitional probabilities and lag (distance) for the San Joaquin Proximal domain is provided in Fig. 20.4. Information on the horizontal lengths of facies is sparse and boreholes are too far apart to make reasonable correlations. Phillips et al. (2007) used scaling factors of 200 and 100 times in the dip and strike directions, respectively, to obtain lateral mean facies lengths from vertical lengths measured in boreholes. For the proximal facies, Traum et al. (2014) used mean lateral lengths from a previous study in a similar setting. Lateral mean facies lengths for the other three domains were obtained using the values for the proximal facies scaled by the ratio of the measured vertical mean facies lengths (vertical length in domain/vertical length in the proximal domain). The combined sediment texture distribution derived using TPROGS is shown in Fig. 20.5.
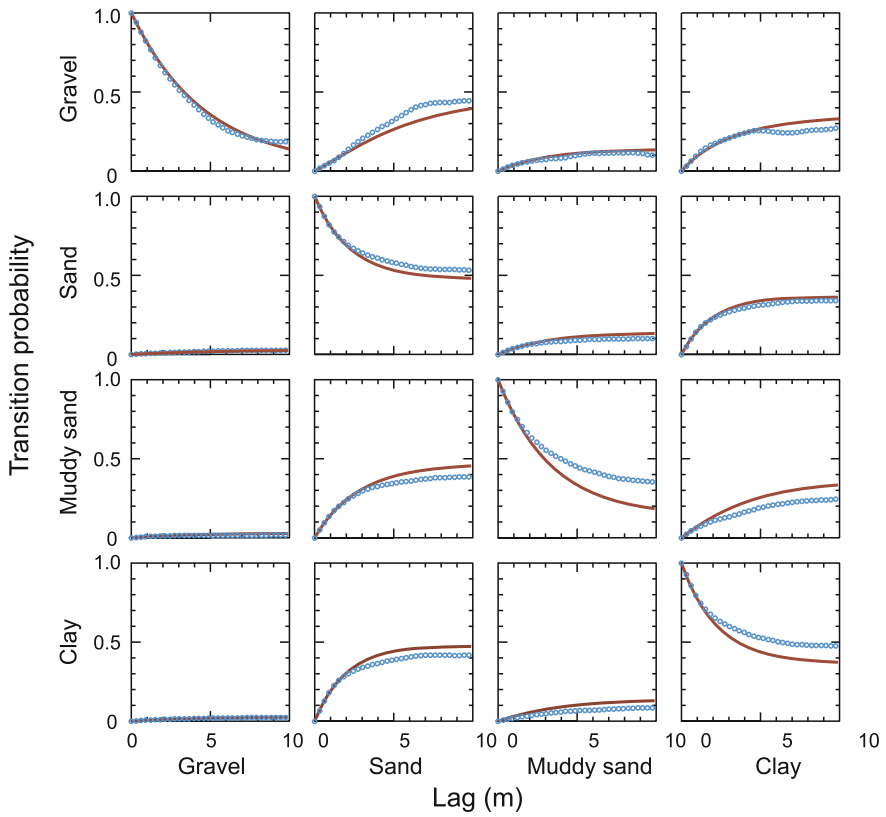
Fig. 20.4 Relation between vertical transitional probabilities and lag (transiograms) for the San Joaquin Proximal domain (California) measured using borehole data (blue) and simulated using Markov chain models (maroon). From Traum et al. (2014)
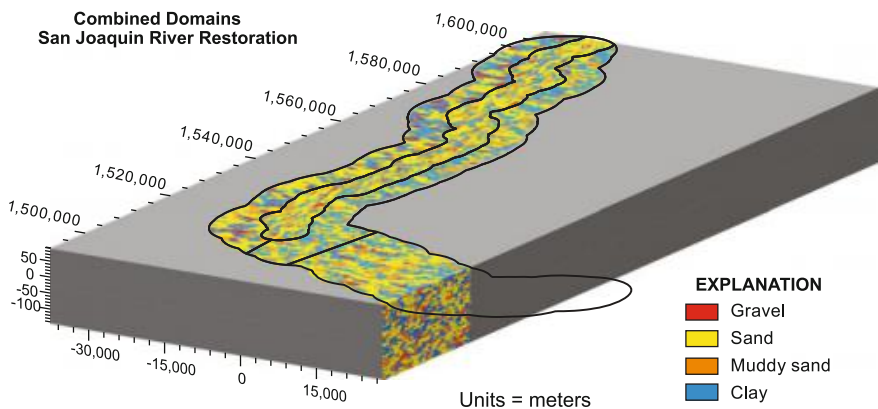

Fig. 20.5 Sediment texture derived from TPROGS simulation of the four domains of the San Jaoquin Valley, California (from Traum et al. 2014)
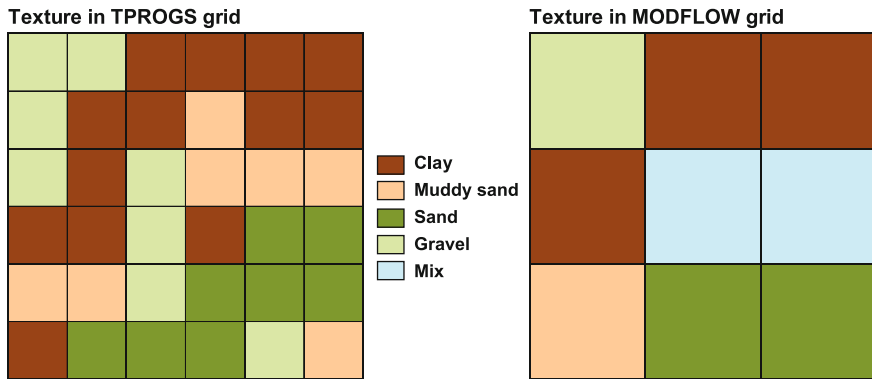
Texture in TPROGS grid   **Texture in MODFLOW grid**

Clay
Muddy sand
Sand
Gravel
Mix

Fig. 20.6 Example of horizontal combination of TPROGS geology grid cells into groundwater flow model grid cells (San Joaquin River Restoration groundwater flow model, from Traum et al. 2014)

The finer sediment–texture distribution grid from TPROGS was upscaled to the coarser grid of the MODFLOW model (Fig. 20.6). There are 35 possible combinations of the four TPROGS textural classes in each horizontal MODFLOW model cell, which were binned into 5 classes of aquifer materials (Traum et al. 2014). For example, a gravel MODFLOW cell contains at least 2 gravel and less than 2 muddy sands or clays TPROG cells.

The limited data on hydraulic conductivity can be addressed by using more frequent secondary parameters (soft data). For example, Ye and Khaleel (2008), in a vadose zone study, transformed more frequent soil-moisture data into soil classifications to facilitate characterization of the geometry of four identified soil textural classes (hydrofacies) and estimation of transition probability statistics. High soil-moisture concentrations correspond to finer soil textures. The T-PROG program was used to generate realizations of soil class geometry for a Monte Carlo simulation.

Blouin et al. (2013) performed a two-step, nested stochastic simulation of groundwater flow and solute transport in a glacial and deltaic sediment aquifer located 30 km NW of Quebec City, Canada. Multiple-point geostatistics (MPG) were used to generate equiprobable simulations of heterogeneity at a hydrofacies scale, particularly the connectivity of units. Hydrogeologic hard data were incorporated in the model through the training image. Sequential Gaussian simulations was next used to generate multiple realizations of hydraulic conductivity for each hydrofacies realization. The hydrofacies simulations provided information on preferential flow paths and the hydraulic conductivity realizations provided information that has an important impact on dispersion. Five hundred simulations of hydraulic conductivity were generated of which 50 were kept for solute transport modeling based on the degree to which they honored observed heads. The stochastic modeling results allowed for calculations of the probability of solute concentration exceeding a threshold criteria.

Felletti et al. (2006) used field mapping of an outcrop on a 0.21 m square grid scale to model a sandy gravel braided glaciofluvial aquifer in northern Italy. The field data were used to determine semivariograms and transition probabilities. The 3D facies distribution was simulated using SIS. Each facies was assigned a hydraulic conductivity value adopted from field data and literature data on analogous sediments. The data were upscaled to calculate equivalent hydraulic conductivity tensors for cubic blocks with side lengths of 13 m. At this scale, the medium is almost homogeneous but anisotropic with the lowest hydraulic conductivity values in the vertical direction and greatest values along the direction of elongation of sedimentary units. A subsequent study evaluated three geostatistical methods on the same data set (dell′Arciprete et al. 2010, 2012):

- sequential indicator simulation (SISIM), which is based on indicator variograms for the different facies
- transition probability geostatistical simulation (T-PROGS), which utilizes the Markov chain method
- multiple-point simulation (MPS), which is a pixel-based simulation technique that utilizes training images of the heterogeneity to be reproduced.

A training image can be a picture of the geology that provides a surrogate for an exhaustive field data set. Kessler et al. (2013) similarly used transition probability-based methods and MPS to model the distribution of sand and gravel lenses in low-hydraulic conductivity glacial tills in eastern Denmark. Comparison of the simulations (Fig. 20.7) indicates that the methods yield different images of the facies architecture (dell′Arciprete et al. 2012). MPS was found to be effective in mapping the geometry of the most-represented facies, whereas SISIM and T-PROGS can better account for the distribution of the less represented facies. MPS has the capability of reproducing complex facies geometries (Kessler et al. 2013).

Geological models that represent the distribution of different rock types may have too fine a discretization than is efficient for hydrogeological models used in flow simulations. Models with too numerous grid cells have excessively long run times, which is a particularly problem for stochastic simulations in which numerous realizations are run. Quental et al. (2012) presented an example of a basic three-step approach for flow model development. The initial step is spatial analysis of hydrofacies and calculation of single and multiple phase semivariograms. High-resolution, three-dimensional stochastic models of rock types and hydrofacies are next generated using a version of sequential indicator simulation (SIS; Goovaerts 1997). The high-resolution geological model can capture key aspects of aquifer heterogeneity such as connectivity and honors available field data. The final step is simplification (upscaling) of the high-resolution geological model using a simulated annealing (SA) optimization procedure with the goal of loosing as little information as possible.

The effects of lithofacies data on the resolution of aquifer heterogeneity was evaluated by Sakaki et al. (2009) using a synthetic sand model and corresponding numerical reference model that includes the heterogeneity incorporated into the synthetic model. The synthetic and reference models contain five sand lithofacies.
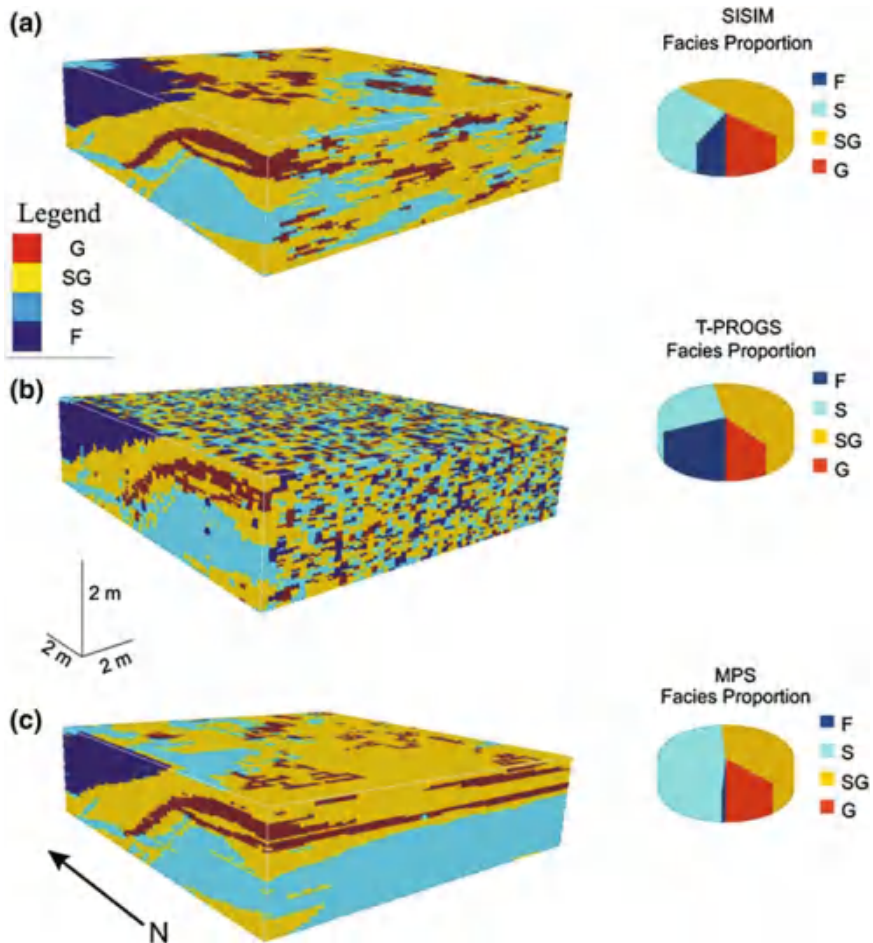
Fig. 20.7 Comparison of the results in simulations using the sequential indicator simulation (SISIM), transition probability geostatistical simulation (T-PROGS), and multiple-point simulation (MPS) methods on the same dataset (from dell'Arciprete et al. 2012)

Lithofacies realizations generated using a transition probability/Markov chain approach utilizing lithofacies distributions where compared to the actual known lithofacies distribution. Similarly, data from simulated pumping tests using the realizations of the reference model were compared to measured data from the synthetic model. As would be expected, increasing the amount of lithofacies data improved the accuracy of the groundwater flow model. However, Sakaki et al. (2009) concluded that

> while using more lithofacies data in a stochastic framework always yields improvement as compared to simple deterministic models of heterogeneity, lithofacies data could be too sparse to provide significant constraints on the estimation of the heterogeneous distribution of lithofacies in the subsurface.

Indeed, it is commonly the case that lithofacies data is too sparse within a groundwater model domain to adequately constrain models of aquifer heterogeneity, with perhaps the rare exception of some intensely monitored experimental and contaminated sites.

20.5   Conclusions

Basic geostatistical methods, such as kriging, are routinely used in groundwater investigations to interpolate limited point data. Kriging is typically performed using default or assumed semivariograms, because of insufficient project-specific experimental (i.e., empirical or field) data. Advanced geostatistical methods are frequently employed in the reservoir simulations in the oil and gas industry, but have had limited penetration into groundwater investigations outside of academic research. Advanced geostatistical techniques have considerable potential for the development of numerical models that better capture aquifer heterogeneity, but implementation is hindered by the general low-level of technical expertise in the methods in the applied hydrogeology realm, and the considerable data, time, and effort requirements. As is the case for technology in general, utilization of advanced geostatistical tool will accelerate once it becomes realized that their benefits exceed their costs. Advanced geostatistical techniques should also not be viewed and employed as a substitute for detailed field investigations and hydrogeological knowledge. Different geostatistical methods applied on the same data set may give significantly different realizations. Hence, professional judgement is required both in the selection of the methods and evaluation of the results. Geostatistical methods, when properly employed, are also data intensive. Hydrogeological knowledge and intuition, such as derived from facies analyses, provide valuable soft information to constraint geostatistical models.

References

Anderson, M. P. (1997) Characterization of geological heterogeneity. In G. Dagan & S. P. Neuman (Eds.), Subsurface flow and transport: A stochastic approach (pp. 23–43). Cambridge: Cambridge University Press.

Blouin, M., Martel, R., & Gloaguen, E. (2013) Accounting for aquifer heterogeneity from geological data to management tools. Groundwater, 51, 421–431.

Carle, S. F. (1999) T-PROGS: Transition probability geostatistical software (v. 2.1). Davis, University of California, Davis.

Carle, S. F., & Fogg, G. E. (1996) Modeling of spatial variability using one- and multidimensional Markov chains. Mathematical Geology, 28, 453–476.

Carle, S. F., & Fogg, G. E. (1997) Transition probability-based indicator geostatistics. Mathematical Geology, 29, 891–918.

Delhomme, J. P. (1979) Spatial variability and uncertainty in groundwater flow parameters: A geostatistical approach. Water Resources Research, 15(2), 269–280.

Dell'Arciprete, D., Bersezio, R., Felletti, F., Giudici, M., & Vassena, C. (2010) Simulation of heterogeneities in a point-bar/channel aquifer analogue. Memorie Descriitive Carta Geologica d'Italia, 90, 85–96.

Dell'Arciprete, D., Bersezio, R., Felletti, F., Giudici, M., Comunian, A., & Renard, P. (2012) Comparison of three geostatistical methods for hydrofacies simulation: a test on alluvial sediments. Hydrogeology Journal, 20, 299–311.

Desbarats, A.J., & Bachu, S. (1994) Geostatistical analysis of aquifer heterogeneity from the core scale to the basin scale: A case study. Water Resources Research, 30, 673–684.

Elfeki, A. M. M., & Dekking, F. M. (2001) A Markov chain model for subsurface characterization: theory and applications. Mathematical Geology, 33, 569–589.

Elfeki, A. M. M., & Dekking, F. M. (2007) Reducing geological uncertainty by conditioning on boreholes: the couple Markov chain approach. Hydrogeology Journal, 15, 1439–1455.

Felletti, F., Bersezio, R., & Giudici, M. (2006) Geostatistical simulation and numerical upscaling, to model ground-water flow in a sandy-gravel, braided river, aquifer analogue. Journal of Sedimentary Research, 76, 1215–1229.

Fogg, G. E. (1989) Emergence of geological and stochastic approaches for characterization of heterogeneous aquifers. In Proceedings R.S. Kerr Environmental Research Lab (EPA) Conference on New Field Techniques for Quantifying the Physical and Chemical Properties of Heterogeneous Aquifers.

Gómez-Hernández, J. J. (2006) Complexity. Ground Water, 44, 782–785.

Goovaerts, P. (1997) Geostatistics for natural resources evaluation. Oxford: Oxford University Press.

Henley, S. (1981) Nonparametric geostatistics. Barking, England: Elsevier.

Isaaks, E. H., & Srivastava, R. M. (1989) An introduction to applied geostatistics. New York: Oxford University Press.

Johnson, N. M. (1995). Characterization of alluvial hydrostratigraphy with indicator semivariograms. Water Resources Research, 31(12), 3217–3227.

Johnson, N. M., & Dreiss, S. J. (1989) Hydrostratigraphic interpretation using indicaor geostatistics. Water Resources Research, 15, 2501–2510.

Jones, N . L., Walker, J. R., & Carle, S. F., 2005, Hydrogeologic unit flow characterization using transition probability geostatistics. Ground Water, 43, 285–289.

Journel, A. G. (1986). Constrained interpolation and qualitative information—the soft kriging approach. Mathematical Geology, 18(3), 269–286.

Kaluzny, S. P., Vega, S. C., Cardoso, T. P., & Shelly, A. A. (1998) S + SpatialStats: User's Manual for Windows® and UNIX®. New York: Springer.

Kessler, T. C., Comunian, A., Orani, F., Renard, P., Nilsson, B., Klint, K. E., & Berg, P. L. (2013) Modeling fine-scale geological heterogeneity – examples of sand lenses in tills. Groundwater, 51, 692–705.

Kitanidis, P. K (1997) Introduction to geostatistics: applications in hydrogeology. Cambridge: Cambridge University Press.

Knight, R., Tercier, P., & Jol, H. (1997) The role of ground penetrating radar and geostatistics in reservoir description. The Leading Edge, 16(11), 1576–1582.

McKenna, S. A., & Poeter, E. P. (1995) Field example of data fusion is site characterization. Water Resources Research, 31, 3229–3240.

Olea, R. A. (2009) A practical primer on geostatistics. U.S. Geological Survey Open-File Report 2009-1103.

Ouellon, T., Lefebvre, R., Marcotte, D., Boutin, A., Blais, V., & Parent, M. (2008) Hydraulic conductivity heterogeneity of a local deltain aquifer system from the kriged 3D distribution of hydrofacies from borehole logs, Valcartier, Canada. Journal of Hydrology, 351, 71–86.

Phillips, F. M., & Wilson, J. L. (1989) An approach to estimating hydraulic conductivity spatial correlation scales using geological characteristics. Water Resources Research, 25, 141–143.

Phillips S. P., Green, C. T., Burow, K. R., Shelton, J. L., & Rewis, D. L. (2007) Simulation of multiscale ground-water flow in part of the northeastern San Joaquin Valley, California. U.S. Geological Survey Scientific Investigations Report 2007–5009.

Poeter, E. P., & Townsend, P. (1994) Assessment of critical flow path for improved remediation management. Ground Water, 32, 439–447.

Poeter, E. P., Wingle, W. S., & McKenna, S. A. (1997) Improvising groundwater project analysis with geophysical data. The Leading Edge, 16(11), 1675–1681.

Proce, C. J., Ritzi, R. W., Dominic, D. F., & Dai, X. (2004) Modeling multiscale heterogeneity and aquifer interconnectivity. Ground Water, 42, 658–670.

Quental, P., Almeida, J. A., & Simões, M. (2012) Construction of high-resolution stochastic geological models and optimal upscaling to a simplified layer-type hydrogeological model. Advances in Water Resources, 39, 18–32.

Ritzi R. W., Jr., Dominic, D. F., Brown, N. R., Kausch, K. W., McAlenney, P. J., & Basial, M. J. (1995) Hydrofacies distribution and correlation in the Miami Valley aquifer system. Water Resources Research, 31, 3271–3281.

Ritzi, R. W., Jr., Jayne, D. F., Zahradnik, A. J., Jr., Field, A. A., & Fogg, G. E. (1994) Geostatistical modeling of heterogeneity in glaciofluvial, buried valley aquifers. Ground Water, 32, 666–674.

Rubin, Y. (2003) Applied stochastic hydrogeology. New York: Oxford University Press.

Rubin, Y., Lunt, A. I., & Bridge, J. S. (2006) Spatial variability in river sediments and its link with river channel geometry. Water Resources Research, 42, W06D16.

Sakaki, T., Frippiat, C. C., Komatsu, M., & Illangasekare, T. H. (2009) On the value of lithofacies data for improving groundwater flow model accuracy in a three-dimensional laboratory-scale synthetic aquifer. Water Resources Research, 45, W11404.

Scheib, T. D., & Chen, Y.-J. (2003) An evaluation of conditioning data for solute transport prediction. Ground Water, 41(2), 128–141.

Sun, A. Y., Ritzi, R. W., & Sims, D. W. (2008) Characterization and modeling of spatial variability in a complex alluvial aquifer: implications on solute transport. Water Resources Research, 44, W04402.

Traum, J. A., Phillips, S. P., Bennett, G. L., Zamora, C., & Metzger, L. F. (2014) Documentation of a groundwater flow model (SJRRPGW) for the San Joaquin River Restoration Program study area, California. U.S. Geological Survey Scientific Investigations Report 2014–5148.

Webb, E. K., & Davis, M. (1998) Simulation of the spatial heterogeneity of geologic properties: An overview. In G. S. Fraser & J. M. Davis (Eds.) Hydrogeologic models of sedimentary aquifers. Concepts in Hydrogeology and Environmental Geology No. 1 (pp. 1–24). Tulsa: SEPM.

Weissmann, G. S., Carle, S. F., & Fogg, G. E. (1999) Three-dimensional hydrofacies modeling based on soil survey and transition probability geostatistics. Water Resources Research, 35(6), 1761–1770.

Weissman, G. S., & Fogg, G. E. (1999) Multi-scale alluvial fan heterogeneity modeled with transition probability geostatistics in a sequence stratigraphic framework. Journal of Hydrology, 226, 48–65.

Weissmann, G. S., Yong, Z., Fogg, G. E., Blake, R. G., Noyes, C. D., & Maley, M. (2002) Modeling alluvial fan aquifer heterogeneity in multiple scales through stratigraphic assessment In Proceedings of the International Groundwater Symposium: Bridging the gap between measurement and modeling in heterogeneous media (pp. 25–28). Berkley, California: Lawrence Berkeley National Laboratory.

Ye, M., & Khaleel, R. (2008) A Markov chain model for characterizing medium heterogeneity and sediment layering structure. Water Resources Research, 44, W09427.

Yeh, T.-C., J. (1992) Stochastic modeling of groundwater flow and solute-transport in aquifers. Hydrological Processes, 6, 369–395.

Zhu, H., & Journel, A. G. (1993) Formatting and integrating soft data: Stochastic imaging via the Markov-Bayes algorithim. In A. Soares (Ed.) Geostatistics Troia '92, Quantitative geology and geophysics (pp. 1–12). Norwell, Mass: Kluwer.